FABAD

JOURNAL of PHARMACEUTICAL SCIENCES

ISSN 1300-4182 e-ISSN: 2651-4648 www.fabad.org.tr

Volume: 50 • Issue: 2 • August 2025

An Official Journal of The Society of Pharmaceutical Sciences of Ankara (FABAD)



The Society of Pharmaceutical Sciences of Ankara (FABAD) FABAD Journal of Pharmaceutical Sciences Volume: 50 Issue: 2 August 2025



Publisher

Sevgi AKAYDIN (Gazi University, Department of Biochemistry, Ankara, Turkey)

Editor in Chief

Nesrin Gökhan KELEKCİ (Hacettepe University, Department of Pharmaceutical Chemistry, Ankara, Turkey)

Co-Editors

Selen ALP (Ankara University, Department of Pharmaceutical Chemistry, Ankara, Turkey)

Selin Seda TİMUR (Hacettepe University, Department of Pharmaceutical Technology, Ankara, Turkey)

Aylın ELKAMA (Gazi University, Department of Pharmaceutical Toxicology, Ankara, Turkey)

Technical Editors

Gökçen TELLİ (Hacettepe University, Department of Pharmacology, Ankara, Turkey)
Vahap Murat KUTLUAY (Hacettepe University, Department of Pharmacognosy, Ankara, Turkey)

Biostatistics Editor

Hatice Yağmur ZENGİN Hacettepe University, Faculty of Medicine, Department of Biostatistics, Ankara, Turkey

Editorial Board

Almira RAMANAVİČİENĖ Alper GÖKBULUT Vilnius University, Nanotechnology and Material Sciences Center, Vilnius, Latvia Ankara University, Department of Pharmacognosy, Ankara, Turkey Ashok K. SHAKYA Aygin EKİNCİOĞLU Al Ahliyya Amman University, Department of Pharmaceutical Chemistry, Amman, Jordan Hacettepe University, Department of Clinical Pharmacy, Ankara, Turkey Ayşe KURUÜZÜM UZ Hacettepe University, Department of Pharmacognosy, Ankara, Turkey Bharat JHNAWAR Lovely Professional University, Pharmaceutical Sciences, Punjap, India Bülent KIRAN Ege University, Department of Pharmacy Management, İzmir, Turkey Ceyda Tuba ŞENGEL TÜRK Chia-Yi TSENG Ankara University, Department of Pharmaceutical Technology, Ankara, Turkey Chung Yuan Christian University, Biomedical Engineering, Taoyuan, Taiwan Didem DELİORMAN ORHAN Gazi University, Department of Pharmacognosy, Ankara, Turkey Emel Öykü ÇETİN UYANIKGİL Ege University, Department of Pharmaceutical Technology, Izmir, Turkey Filiz BAKAR ATEŞ Ankara University, Department of Biochemistry, Ankara, Turkey Francesco EPIFANÓ G. D'Annunzio" University, Department of Pharmaceutical Chemistry, Chieti-Pescara, Italy Gerard LIZARD University of Burgundy, French Institute for Medical and Health Research, Dijon, France Gökçe CİHAN ÜSTÜNDAĞ Istanbul University, Department of Pharmaceutical Chemistry, Ankara, Turkey Gökçen EREN Gazi University, Department of Pharmaceutical Chemistry, Ankara, Turkey Hande GÜRER ORHAN Ege University, Department of Pharmaceutical Toxicology, Izmir, Turkey Hasan Abougazar YUSUFOĞLU King Saud University, Department of Pharmacognosy, Riyadh, Saudi Arabia Yeditepe University, Department of Pharmacognosy, Istanbul, Turkey University of Missipsippi, National Center for Natural Product Research, USA. Hasan KIRMIZIBEKMEZ Ikhlas KHAN Işıl ÖZAKCA GÜNDÜZ Ankara University, Department of Pharmacology, Ankara, Turkey Karadeniz Technical University, Department of Pharmaceutical Chemistry, Trabzon, Turkey Anadolu University, Department of Pharmaceutical Chemistry, Eskisehir, Turkey İnci Selin DOĞAN Leyla YURTTAŞ Hacettepe University, Department of Pharmacology, Ankara, Turkey Ankara University, Department of Pharmaceutical Chemistry, Ankara, Turkey Melike H. ÖZKAN Meltem ÜNLÜSOY University of Health Sciences, Department of Pharmaceutical Toxicology, Ankara, Turkey Merve BACANLI Afyonkarahisar University of Health Sciences, Department of Pharmaceutical Toxicology, Afyonkarahisar, Turkey Merve BECİT Mesut SANCAR Ming-Wei CHAO Marmara University, Department of Clinical Pharmacy, Istanbul, Turkey Chung Yuan Christian University, Department of Bioscience Technology, Taoyuan, Taiwan Muharrem ÖLÇER Natalizia MICELI Afyonkarahisar University of Health Sciences, Department of Pharmaceutical Technology, Afyonkarahisar, Turkey University of Messina, Department of Chemistry and Biology, Messina, Italy Özlem Nazan ERDOĞAN Istanbul University, Department of Pharmacy Management, Ankara, Turkey Hacettepe University, Department of Pharmaceutical Technology, Ankara, Turkey Sevda ŞENEL Sevtap AYDIN DİLSİZ Hacettepe University, Department of Pharmaceutical Toxicology, Ankara, Turkey Suryakanta SWAIN The Assam Kaziranga University, Department of Pharmaceutical Sciences, Assam, India Şükrü BEYDEMİR Anadolu University, Department of Pharmaceutical Microbiology, Ankara, Turkey Tuba İNCEÇAYIR Gazi University, Department of Pharmaceutical Technology, Ankara, Turkey Tuğba TÜYLÜ KÜÇÜKKİLINÇ Tuğçe YEŞİL Hacettepe University, Department of Biochemistry, Ankara, Turkey Marmara University, Department of Pharmaceutical Toxicology, Istanbul, Turkey Uğur TAMER Gazi University, Department of Analytical Chemistry, Eskisehir, Turkey Hanoi University of Pharmacy, Department of Analytical Chemistry and Toxicology, Hanoi, Vietnam Vu Dang HOANG Wolfgang SCHUHLY University of Graz Institute of Pharmaceutical Sciences, Department of Pharmacognosy, Graz, Austria

The FABAD Journal of Pharmaceutical Sciences is published three times a year by the Society of Pharmaceutical Sciences of Ankara (FABAD)

All expressions of opinion and statements of supposed facts appearing in articles and / or advertisiments carried in this journal are published on the responsibility of the author and / or advertiser, and are not to be regarded those of the Society of Pharmaceutical Sciences of Ankara. The manuscript submitted to the Journal has the requirement of not being published previously and has not been submitted elsewhere. Manuscript should bu prepared in accordance with the requirements specified as in the back cover. The submission of the manuscript to the Journal is not a condition for acceptance; articles are accepted or rejected on merit alone. This Journal is published electronically and it is an open-access journal without publication fee. All rights reserved. Neither this work nor any part may be reproduced or transmitted in any form or by any means, electronic or mechanical, microfilming and recording, or by any information storage and retrieval systems without written permission from FABAD Journal of Pharmaceutical Sciences.

The FABAD Journal of Pharmaceutical Sciences is indexed in Chemical Abstracts,

Analytical Abstracts, International Pharmaceutical Abstracts, Excerpta Medica (EMBASE), Scopus and TR Index

CONTENTS

Research Articles

227 Exploration of Nanoparticulate *In Situ* Gel of Moxifloxacin Hydrochloride in Ophthalmic Delivery

Janani PRAKASH*, Preethi SUDHEER**o

243 Leiotrametes lactinea (Berk.) Induces Sperm Dysmorphogenesis and Testicular Damage Via Oxidative and Inflammatory Pathways in Mice

Ayomide ADEDAMOLA AJIBEWA*, Deborah IFEOLUWA SOLADEMI**, Tolulope BLESSING OLOWOPOROKU***, Precious ULONNAM EZURIKE****, Chinwe BRIDGET OFUDI*****, Oyindamola OLAJUMOKE ABIODUN******

259 Effects of Epigallocatechin-3-Gallate in Preventing 5-Fluorouracil-induced Liver Injury in AML-12 Cell Line

Melek AKINCI*°, Çağatay OLTULU**, Elvan BAKAR***, Zatiye Ayça ÇEVİKELLİ YAKUT****

271 Mechanistic Insights into *Uncaria gambir* Ethanol Extract's Modulation of Cytoglobin and ECM Protein in Keloid Fibroblasts

Sri Widia A. JUSMAN*°, Maftuhatun Fista AMALIA**, Raisa NAULI***, Reni PARAMITA****, Sri NINGSIH*****, Radiana Dhewayani ANTARIANTO******

283 Cytotoxic Potential and Apoptotic Mechanism of Digigrandifloroside: A Cardioactive Glycoside Targeting Caspase 3/7

Vahap Murat KUTLUAY*°, İclal SARAÇOĞLU**

- Optimization of a Spray Dried Dispersion Powder of Ritonavir with HPMCAS-L Ayse Nur OKTAY*°, James E. POLLI**
- 311 Bivariate and Multivariate Calibration Approach for the Spectrophotometric Analysis of Two-Component Drugs in Real Tablets

Erdal DİNÇ*°, Asiye ÜÇER**, Zehra Ceren ERTEKİN***, Ömer Faruk GÜZEL****

319 Development of Innovative Microemulsion-based Gelatine Capsules of Ondansetron Hydrochloride

Sreehari S. NAIR*, Dhanashree P. SANAP***, Kisan R. JADHAV***

329 Antifungal Activity of Ethanol Extract of *Desmanthus virgatus* (L.) Leaves *In Silico* and *In Vitro*

Lilik FARKHIYAH*, Marshellia GHINANDA DEWISTAMARA**, Tukiran TUKIRAN***

- Development and Characterization of Indomethacin Quantum Dot Loaded Hydrogel Gamze ÇAMLIK*°, Gökçe KARAOTMARLI GÜVEN**, Besa BİLAKAYA***, Emre Şefik ÇAĞLAR****, Tuğçe BORAN*****, Neslihan ÜSTÜNDAĞ OKUR*****,İsmail Tuncer DEĞİM******
- 355 Comparative Evaluation of Kollidon®VA64, SoluPlus®, and Aquasolve™ Hpmcas H-L Polymers: Impacts on Oral Spray Dried Powders

Ayse Nur OKTAY *°, James E. POLLI **

371 Quantitative Estimation of Dexketoprofen and Paracetamol in Effervescent Tablets by Chemometrics-Assisted Spectrophotometry

Zehra Ceren ERTEKİN*°, Erdal DİNÇ**

- Clinical Pharmacist in Palliative Care Unit: A Retrospective Study

 Özgenur GERİDÖNMEZ *,** °, Kamer TECEN ***
- 395 Development and Validation of an UPLC-MS/MS Method for Quantification of Glyphosate in Urine

Göksel KOÇ MORGİL*, Ismet ÇOK ***

- Evaluation of Antioxidant and Enzyme Inhibitory Activities of Some Daphne Species Semih BULUT**, Hüseyin FAKİR**
- 417 In Vitro and Bioinformatic Studies on The Phytochemical Constituent of Selected Zingiberaceae Plants Targeting Inhibitor Lipoxygenase (LOX)

Nur Amalia CHOIRONI*°, Asep Gana SUGANDA**, Kusnandar ANGGADIREDJA***

Review Articles

- 429 Bioavailability File: Bicalutamide
 Nihal Tugce OZAKSUN**, Tuba INCECAYIR**
- A Comprehensive Review on The Phytochemical Profile, Ethnobotanical Uses and Pharmacological Activities of *Cuscuta reflexa* Roxb.: An Asiatic Parasitic Vine

 Rosy AHMED*, Akramul ANSARY**, Abhilash BHARADWAJ***, Koushik Nandan DUTTA****, Bhargab Jyoti SAHARIAH*****, Nilutpal Sharma BORA*******
- Nuclear Imaging Modalities and Radiopharmaceuticals in Veterinary Medicine Elif Tugce SARCAN*, Asuman Yekta ÖZER***
- 493 A New Perspective on The Treatment of Brain Diseases: Plant-Derived Exosome-Like Nanovesicles

Meric A. ESMEKAYA*, Burhan ERTEKIN***

Exploration of Nanoparticulate *In Situ* Gel of Moxifloxacin Hydrochloride in Ophthalmic Delivery

Janani PRAKASH*, Preethi SUDHEER**°

Exploration of Nanoparticulate In Situ Gel of Moxifloxacin Hydrochloride in Ophthalmic Delivery

SUMMARY

Moxifloxacin hydrochloride, an ophthalmic solution, treats bacterial eye infections but suffers from rapid lachrymal drainage and poor corneal penetration. This study aims to enhance corneal penetration by combining nanoparticles with an in-situ gelling system. Chitosan nanoparticles were synthesized using the ionotropic gelation method, guided by a 'Custom experimental design' approach. Key parameters, including drug entrapment efficiency, particle size, and drug release profiles, were evaluated, and the model's fit was analyzed using ANOVA. Characterization of the formulations included particle size analysis, SEM, DSC, and FTIR. Sodium alginate nanoparticle gels were analyzed for gelling capacity, viscosity, and drug diffusion and permeation studies. Sixteen formulations were created, with drug entrapment efficiency ranging from 70.9 ± 0.08% to 89.7 ± 0.09% and diffusion profiles between 67.3 ± 0.03% and 90.6 ± 0.08%. The most influential formulation had an average particle size of 497nm, and SEM revealed slightly agglomerated particles with uneven surfaces. This formulation exhibited a onefold increase in permeability coefficient and a twofold increase from the nanoparticulate in situ gel compared to marketed drops (0.5% w/v) and the pure drug in situ gel indicating its potential to penetrate deeper eye layers. The eye irritation study reports no irritation. The developed formulation also showed enhanced antimicrobial activity against E. coli and S. aureus compared to commercial samples. The Moxifloxacin hydrochloride nanoparticulate in situ gel offers a promising strategy to improve ocular penetration, prolong retention time, and potentially increase ocular bioavailability.

Key Words: Moxifloxacin hydrochloride, nanoparticle, in situ, gel, ophthalmic.

Oftalmik Uygulamada Moksifloksasin Hidroklorür Nanopartikül In Situ Jelinin Araştırılması

ÖZ

Oftalmik bir solüsyon olan moksifloksasin hidroklorür, bakteriyel göz enfeksiyonlarını tedavi eder, ancak hızlı lakrimal drenaj ve zayıf kornea penetrasyonundan muzdariptir. Bu çalışma, nanopartikülleri yerinde jelleştirme sistemiyle birleştirerek kornea penetrasyonunu artırmayı amaçlamaktadır. Kitosan nanopartikülleri, 'Özel deneysel tasarım' yaklaşımının rehberliğinde iyonotropik jelleşme yöntemi kullanılarak sentezlendi. İlaç tutulma verimliliği, parçacık boyutu ve ilaç salım profilleri gibi temel parametreler değerlendirildi ve modelin uyumu ANOVA kullanılarak analiz edildi. Formülasyonların karakterizasyonu partikül boyut analizi, SEM, DSC ve FTIR'ı içeriyordu. Sodyum aljinat nanopartikül jelleri, jel oluşturma kapasitesi, viskozite ve ilaç difüzyonu ve geçirgenlik çalışmaları açısından analiz edildi. İlaç tutulma etkinliği %70.9 ± 0.08 ile %89.7 ± 0.09 arasında ve difüzyon profilleri %67.3 ± 0.03 ile %90.6 ± 0.08 arasında değişen on altı formülasyon oluşturuldu. En etkili formülasyonun ortalama partikül boyutu 497 nm idi ve SEM, pürüzlü yüzeylere sahip, hafif kümelenmiş parçacıkları ortaya çıkardı. Bu formülasyon, pazarlanan damlalara (%0.5 a/h) ve saf ilaç in situ jeline kıyasla geçirgenlik katsayısında bir kat artış ve nanopartiküllü in situ jelde iki kat artış sergiledi; bu, daha derin göz katmanlarına nüfuz etme potansiyelini göstermektedir. Göz tahrişi çalışması herhangi bir tahriş rapor etmemektedir. Geliştirilen formülasyon ayrıca ticari numunelerle karşılaştırıldığında E. coli ve S. aureus'a karşı gelişmiş antimikrobiyal aktivite gösterdi. Moksifloksasin hidroklorür nanopartikül in situ jel, oküler penetrasyonu iyileştirmek, tutulma süresini uzatmak ve potansiyel olarak oküler biyoyararlanımı artırmak için umut verici bir strateji sunmaktadır.

Anahtar Kelimeler: Moksifloksasin hidroklorür, nanopartikül, in situ, jel, oftalmik.

Received: 27.06.2024 Revised: 26.11.2024 Accepted: 14.03.2025

ORCID: 0000-0002-7041-8993, Department of Pharmaceutics, Nitte College of Pharmaceutical sciences. Nitte (Deemed to be University), Bengaluru campus P.B No. 6429, NITTE Campus, Yelahanka, Bengaluru - 560064

[&]quot;ORCID: 0000-0003-3864-7830, Department of Pharmaceutics, Nitte College of Pharmaceutical Sciences, Bangalore- 560035, India

INTRODUCTION

Ocular drug delivery remains challenging, with noninvasive methods predominantly addressing anterior eye segment disorders. Targeting the anterior region, sustaining optimal drug levels, and prolonging residence time pose significant challenges in designing an effective drug delivery system to the eye. Conventional eye drops, like solutions and ointments, suffer from poor bioavailability due to rapid tear drainage and limited contact time. Overcoming these challenges is crucial for achieving successful ocular drug delivery and ensuring prolonged efficacy in treating eye disorders. Incorporating nanocarriers offers advantages such as controlled and continuous drug release, longer retention time at the target site, thus improved penetration, and enhanced bioavailability (Maharjan et al., 2019; Raj et al., 2020).

The strategies adopted in increasing drug penetration via cornea include viscosity enhancers, mucoadhesive systems, in situ gels, prodrugs, and colloidal carriers like nanoparticles and liposomes. New approaches for the eye using polymers are milestones in the delivery of drugs to the pre and intraocular tissues. In situ gels show promise as a practical approach to prolong corneal retention time and alter ocular bioavailability (Bhatia et al., 2013; Gote et al., 2019; Irimia et al., 2018).

In situ gel systems consist of polymers that exhibit sol-to-gel phase transitions with specific physicochemical responses such as pH, temperature, and ionic concentration. Consequently, the extended residence time of the system will result in a sustained drug release, enhance the ocular bioavailability, and reduce the frequent dosing regimen of the medications, resulting in improved patient compliance (Majeed & Khan, 2019; Wu et al., 2019; Yu et al., 2015).

Drug-loaded nanoparticles (DNPs) target the drug to the frontal part of the eye with enhanced bio-availability. Biocompatible-biodegradable polymers from poly(lactide-coglycolide) (PLGA), chitosan, poly lactic acid (PLA) act as permeation enhancers, thus enhancing the cellular uptake and reduced tissue

clearance, and therefore offering a sustained drug delivery (Ahmed & Aljaeid, 2017; Clemens et al., 2019; Wani, et al., 2020).

Moxifloxacin hydrochloride (MOX), an 8-methoxy fluoroquinolone antibiotic, is employed in the treatment of susceptible microorganisms such as bacterial conjunctivitis. The two bacterial enzymes, topoisomerase II and topoisomerase IV involved bacterial replication translation, repair, and even recombination of deoxyribonucleic acid. The drug acts by binding to the gyrase, thus blocking the action of these enzymes (Gupta et al., 2019; Miller, 2008).

Research on MOX in situ gel systems has explored various formulations. One study incorporated MOX-loaded Eudragit RL100 nanoparticles into a gellan gum-based in situ gelling system, which exhibited prolonged ocular retention (Kesarla et al., 2016). Other investigations have examined MOX in situ gel formulations using different gelling polymers, such as sodium alginate, gellan gum, and carbopol(Shashank Nayak et al., 2012) both individually and combined with mucoadhesive polymers. Additionally, researchers have studied diverse nanosystems, including nano-emulsions in mucoadhesive gel formulations (Youssef et al., 2022). MOX niosomes have also been evaluated for their potential in controlled ophthalmic drug delivery (Kaur & Pawar, 2015).

MOX, being a hydrophilic substance, is anticipated to have restricted passage through the corneal membrane. Chitosan, a naturally occurring polymer, exhibits antibacterial qualities, forms gels, and possesses mucoadhesive characteristics. Furthermore, scientific literature has documented its ability to enhance penetration across biological membranes.

Considering the characteristics of both the drug and polymer, a decision was made to develop a nanoparticulate system of MOX using chitosan. This approach offers several advantages. The unique adhesive properties of chitosan allow for proximity to the corneal membrane, enabling penetration into deeper corneal layers in cases of severe bacterial infections. Additionally, the gradual release of the drug

from nanoparticles may result in prolonged therapeutic effects. Combining nanoparticles with an in-situ gel-forming polymer can enhance penetration by maintaining close contact between the nanoparticles and the ocular surface. Furthermore, utilizing an ion-sensitive in situ polymer can address precorneal clearance issues and extend drug action through the controlled release of nanoparticles from the gel matrix.

Thus, to achieve an optimal drug concentration and therapeutic potential, we combined a nanoparticulate chitosan system with in situ gels to deliver moxifloxacin hydrochloride. This approach enhances drug permeation through the chitosan-based nanosystem and increases the corneal retention time through the sol-gel system, thereby ensuring higher ocular bioavailability.

MATERIAL AND METHODS

Materials

_ . . . _

MOX was obtained from Yarrow Chemicals Pvt Ltd, Mumbai, India; chitosan (>85% deacetylated, (molecular weight of 161.16 kDa) was obtained from Indian Fine Chemicals India; Sodium tripolyphosphate and sodium alginate were obtained from Loba Chemie Pvt Ltd, Mumbai, India. The animal study was approved by protocol (Institutional Animal Eth-

ics Committee (IAEC) (Ref No: KCP/IAEC/PCOL/PCEU/62/2020).

Preparation of nanoparticles by ionotropic gelation method

Firstly, the polymer chitosan was dissolved in 1% v/v acetic acid, then the drug was added under magnetic stirring and continued stirring for one h. The required crosslinking agent STPP solution was added to the chitosan solution, homogenized (Polytron Homogenizer) for 30 min to get nano-sized particles, and continued stirring. The product was transferred into a centrifuge tube and centrifuged at 3000 rpm for 30 minutes. From the supernatant, the particles were filtered and washed with three 10 ml portions of water. The particles were then dried to obtain nanoparticles (Mohammadpour Dounighi et al., 2012; da Silva Furtado et al., 2020)

Experimental design

Custom design using Design Expert software 13 was used to optimize the trials. The concentration of chitosan (%) and STPP (%) were continuous factors. Stirring speed (rpm) and stirring time (h) were used as categorical factors, which were chosen as independent variables on the responses as given in Table 1(Elmizadeh et al., 2013), and the experimental layout is shown in Table 2.

Tabl	e 1.	Experimental	l design witl	n tactors and	l responses
------	------	--------------	---------------	---------------	-------------

Factors	Values		
	Low level	High level	
Chitosan (%)	0.25	1	
STPP (%)	0.5	1	
Stirring speed (rpm)	7500	15000	
Stirring time (h)	6	24	
Responses	Goal		
Particle size (nm)	100	500	
Drug entrapment efficiency (%)	80	90	
Drug release (%) (24h)	80	90	

	0 1			
Formulation code	Chitosan (%)	STPP (%)	Stirring speed (rpm)	Stirring time (h)
T1	0.69625	0.64	7500	6
T2	1	1	7500	24
Т3	0.25	0.5	7500	6
T4	0.2575	0.64	15000	6
T5	0.8575	0.5454	15000	6
Т6	1	0.5	7500	6
T7	0.55	0.9955	15000	24
Т8	0.7	0.5	7500	24
Т9	1	1	15000	6
T10	0.25	1	7500	6
T11	0.6962	0.5	15000	6
T12	0.992	0.46	15000	24
T13	0.3856	0.554	15000	24
T14	0.2575	0.6355	7500	24
T15	0.69625	0.64	7500	6
T16	0.25	0.5	15000	24

Table 2. Custom Design Experimental Runs

Evaluation of nanoparticles

Drug content

The amount of moxifloxacin in nanoparticles was assayed by solubilizing the nanoparticles (10 mg) in 1% acetic acid, diluted suitably, and drug concentration was determined by UV spectrophotometrically (Shimadzu) analytical India at 293 nm (Desai, 2016).

Drug entrapment efficiency

The free drug concentration of a 10 mg formulation was determined after dissolving the free drug by centrifugation at 2500 rpm. The spectrophotometric determination of the supernatant was carried out at 293 nm after suitable dilution using water as blank. The following formula calculates entrapment efficiency (Shelake et al., 2018; Yurtdaş-Kirimlioğlu et al., 2018).

$$EE = \frac{Total \ drug - free \ drug}{Total \ drug} x100$$
Particle size analysis

The Horiba SZ-100 nanoparticle dynamic light

scattering (DLS) system determined the mean particle size and size distribution. The particle size was analyzed after a suitable dilution in double distilled water at a scattering method at 90° at 25.2 °C (Mahor et al., 2016; Mahmood et al., 2017).

Drug diffusion studies from nanoparticles

A specially designed glass cylinder, open at both ends, had one end fitted with a pre-soaked dialysis membrane (pore size of 70). This setup was immersed in 50 ml of receiver fluid maintained at $37.0^{\circ}\text{C} \pm 0.2^{\circ}\text{C}$ and stirred magnetically at 100 rpm. The volume of the diffusion medium withdrawn hourly over 24-hours period was replaced with an equal volume under sink conditions. After appropriate dilution, the drug concentration was analyzed spectrophotometrically at a \lambdamax of 293 nm (Gadad et al., 2016).

Preparation of in situ gel

Polymeric solutions were prepared by dispersing the necessary amount of sodium alginate until it dissolved. The polymeric solution was examined to assess the impact of concentration on gelling behavior in the presence of simulated tear fluid (Nanjawade et al., 2007).

Physical evaluation of gels

Two parameters, transparency and clarity, were assessed. Clarity was evaluated by visually inspecting the samples under appropriate lighting against a dark background. After gently shaking, the samples were examined for particle presence. The pH of the formulations was measured using a calibrated digital pH meter to ensure compatibility with the ocular environment (Nanjawade et al., 2007).

Viscosity of gel

The viscosity measurements describe the drop's retention time in the eye. A Brookfield viscometer is used at different angular velocities, 10-100 rpm 37 °C, to record the viscosity (Gadad et al., 2016)

Gelling capacity

Considering that the volume of fluid retained in the non-blinking eye is about 30 μ l, 3 ml of simulated tear fluid was used to study the gelling capacity. A 0.5 ml freshly prepared gel was mixed with a 3 ml volume of simulated tear fluid at 37°C. Time for solgel conversion is noted (Mandal et al., 2012).

Preparation of nanoparticulate gel system

Weighed quantity of drug-loaded optimized nanoparticles formulation equivalent to the prescribed dose of (MOX Equivalent to 0.5% w/v) in commercial ophthalmic drops) was taken and dispersed into an in-situ gel (1% w/v sodium alginate solution). The formulation was further scaled up to obtain the same concentration to form a nanoparticle-loaded in-situ gel (Ahmed & Aljaeid, 2017; Anish Wani et al.,2020).

Compatibility study by FT-IR Spectra

An ATR-FTIR was employed to study the compatibility of MOX, chitosan, tripolyphosphate, and sodium alginate. Using an IR spectrophotometer (Alpha-II (Bruker)), samples were examined in the 4000-400cm⁻¹ range. The same study was extended to formulation in the later stage (Gadad et al., 2016).

Zeta potential

Zeta potential was carried out for optimum formulation, approximating their surface charge. Zeta potential was determined using Horiba SZ-100, which utilizes an electrophoretic light scattering method, where specific electrodes contain cuvettes at 20 μ g/ml concentrations. The measurements were carried out after diluting with distilled water at 25°C at a 90° angle

(Mahmood et al., 2017).

Scanning electron microscopy (SEM)

The surface topography of optimum formulation was studied using SEM Jeol Japan functioned 15KV acceleration voltage. After gold sputtering the surface photographs were captured (Mahor et al., 2016).

Differential scanning calorimetry (DSC)

The heat transition behavior of pure drug, excipients, and the optimum formulation was deliberated by weighing 5mg of the MOX, excipients, and drug equivalent formulations into a non-hermetically sealed aluminium pan of the calorimeter (Perkin Elmer 4000) and crimped. It was melting transitions and changes in heat capacity of the drug and polymers performed under nitrogen at a 50 mL/min flow rate at 50-300 °C with an increased rate of 10 °C (Gadad et al., 2016).

Ex- vivo permeation studies

An isolated goat cornea (from a previously stored eyeball at four °C in saline) sample (n=3) was used to assess the nanoparticle gel's permeation characteristics. The cornea and a thin layer of sclera tissue were isolated, and the nanoparticulate gel formulation was instilled on the cornea that was mounted on a diffusion cell assembly (diffusional area of 3.39cm⁻²). A one ml volume of simulated tear fluid wets the donor compartment. In comparison, phosphate buffer pH 7.4 (100 ml) was used as the receiver medium, and its temperature was regulated at 350C. The assembly was magnetically stirred at 50 rpm. The sample concentration in the receiver fluid was determined at regular time intervals using spectroscopic analysis. A similar procedure was performed using commercially available MOX drops and a pure drug-loaded gel. Both the permeability coefficient and flux were calculated from the permeation profiles (ElMeshad & Mohsen, 2016). The results of the ex vivo permeation studies were subjected to statistical analysis using one-way ANOVA to understand the results to understand the level of significance.

Ocular irritancy

All animal experiments complied with the Committee for the Purpose of Control and Supervision of Experiments on Animals (CPCSEA) guidelines and were carried out under the Prevention of Cruelty to Animals (PCA) Act, 1960. This study used male New Zealand white rabbits ((Ref. No. KCP/IAEC/PCOL/ PCEU/62/2020), weighing 1.5 and 2 kg from the institutional animal facility. The experimental animals were familiarized for four days before beginning the study. One eye of each rabbit was used to administer the drops, whereas the other eye served as a control to evaluate the extent of irritation. After administering the nanoparticulate in situ drops into the eye cul-desac, the eyes were monitored at 1, 24, 48, and 72 h and continued to be observed for up to 7 days. Parameters such as eye-watering, redness, mucosal discharge, and swelling were evaluated at these time intervals and throughout the week (Gadad et al., 2016).

Stability studies

International conference on harmonization. (ICHQ1 A R_2) guidelines, assisted stability conditions at 25°C±2° //65%± 5% RH (40°C ±2°C 75%± 5% RH) for six months. The formulations were stored in glass vials and evaluated after six months for physical nature, viscosity, and gelling capacity (Gupta et al., 2019).

Antimicrobial studies

The antimicrobial study utilized Mueller Hinton agar medium using the agar cup method, where S. aureus and *E. coli* were incubated in broth media to gain their colony. The medium, after sterilization, was transferred to Petri plates. The medium was allowed to solidify under aseptic conditions; after solidifying the medium, the lawn was made with 0.1ml microorganisms, both strains, in separate Petri plates. After preparing cups using a sterile borer, nanoparticulate gel, and marketed moxifloxacin drops (0.1 ml) were added and incubated for 48 h at 37°C. The zone of inhibition was measured for both formulations (Swain et al., 2019).

RESULTS AND DISCUSSION

The custom design assisted in optimization trials utilized concentration of chitosan (%), STPP (%) was chosen as continuous factors, stirring speed (rpm), and stirring time (h) as categorical factors, for the responses such as drug entrapment efficiency (%), particle size (nm), drug release (%). The design generated 16 experimental trials.

The drug entrapment ranged between 70.9±0.08 to 89.7±0.09 %, as shown in Table 3. The NPs comprised chitosan and STPP; the coexistence of these two provides high loading efficiency. The pH of the STPP solution of about 9 provides OH- and phosphoric ions, which may react with cationic NH3+ groups of chitosan, resulting in cross-linking at acidic conditions. The OH- groups responsible for CS deprotonation compete with TPP. A higher concentration of TPP disclosed a significant effect on drug entrapment efficiency (> 85%.) Similarly, a lower concentration of TPP reduced the drug entrapment within the nanoparticles by < 70%. However, chitosan concentration had a variable effect on drug entrapment efficiency values. We could not conclude the effect of chitosan on drug entrapment efficiency, as it was invariably different according to the conditions performed. The drug release ranged between 67.3±0.03 to 90.6±0.08% (Figure 1.) and was affected by the structure of nanoparticles, concentration of chitosan, and STPP. As seen in T2 and T9, where the concentration of chitosan and crosslinker is higher, the dug release was maximum. Formulation with higher cross-linking capacity showed significant swelling; therefore, the drug release greatly depended on the extent of cross-linking. The lowest drug release was observed for T11, for which all factors except stirring speed were at the highest level. Perhaps we can say that the responses are contributed by permutation and combination effects. The particle size of the formulations ranged from 350-647 nm. In all the formulations, except T1, T2, T7, and T13, the particle size was > 500nm. The properties and concentrations of polymer, cross-linking agents, and processing

parameters greatly affected the particle size. A lower concentration yielded a low viscosity and thus might have promoted smaller particles' formation. Hence, a

cross-linking agent, especially STPP, offers the additional effect of avoiding aggregation of the fine particles.

Table 3. Results of responses

Formulation code	Average Particle size (nm)	Drug release at 24 h (%)	Drug entrapment efficiency (%)
T1	430.5±2.24	84.6±0.6	80.5±0.4
T2	350.7±1.89	90.6±0.08	89.4±0.05
Т3	597.1±1.4	78±0.01	75.7±0.1
T4	553.3±2.09	77.7±0.8	85.7±0.02
T5	589.3±3.12	77.3±0.06	83.3±0.06
Т6	506.8±1.45	84.3±0.01	70.9±0.8
T7	420.5±3.11	81.6±0.05	89.7±0.09
Т8	647.3±2.12	85.8±0.9	72±0.02
Т9	542.8±2.12	86±0.06	88±0.03
T10	592.8±1.89	80.5±0.07	88.3±0.07
T11	570.2±1.45	67.3±0.3	76.9±0.0
T12	600.2±1.34	74.4±0.06	79±0.05
T13	433.2±1.90	78.1±0.04	85±0.02
T14	580.3±1.11	83.4±0.09	86±0.08
T15	530.2±1.89	84.8±0.01	88±0.4
T16	430.5±1.09	70.6±0.05	78±0.01

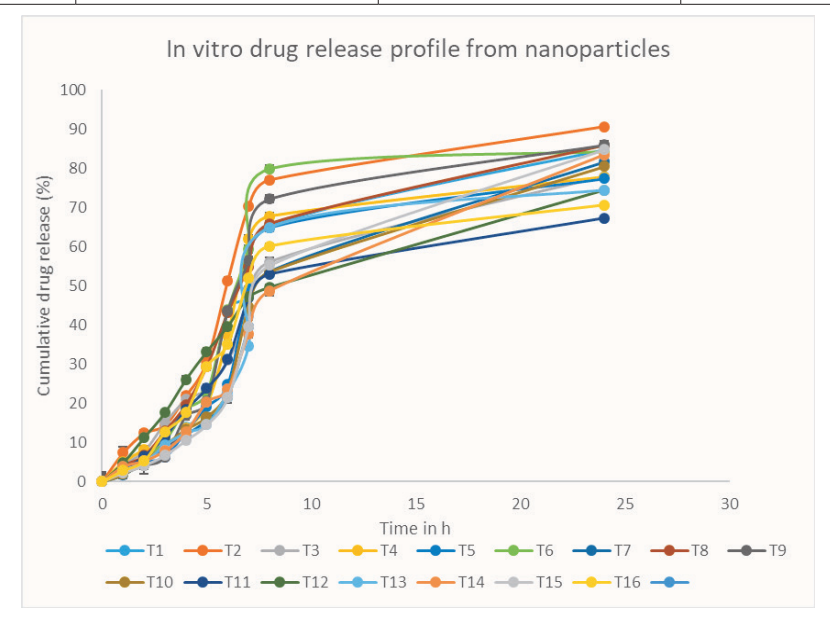


Figure 1. In vitro drug release profile from nanoparticles (T1-T16)

A custom design is an experimental approach that addresses various challenges within a structured framework. Fit statistics suggest (Table 4) 2FI for particle size and drug release and a linear model for drug entrapment efficiency. A summary of the responses is shown in Table 5.

Table 4. Fit Summary of the Responses

Parameter	Source	Sequential P-value	Lack of Fit P-value	Adjusted R ²	Predicted R ²	Model suggested
Particle Size	2FI	0.0073	0.9970	0.8496	0.8109	Suggested
Drug Entrapment	Linear	< 0.0001	0.9878	0.8632	0.8073	Suggested
Drug Release	2FI	0.0022	0.0971	0.9745	0.8130	Suggested

 Table 5. Statistical Evaluation of the responses

Source				p-v	alue			
	Partic	ele Size	Drug release (%)			Drug Entrapment Efficiency (%)		
Model	0.0114	Significant	Model	0.0002	Significant	Model	< 0.0001	Significant
A-Chitosan conc	0.6303	NS	A	0.0034	S	A	0.0548	NS
B-TPP	0.0053	S	В	< 0.0001	S	В	< 0.0001	S
C-Stirring speed	0.8743	NS	С	< 0.0001	S	С	0.2117	NS
D-Stirring time	0.3789	NS	D	0.0541	S	D	0.9329	NS
AB	0.0207	S	AB	0.0868	NS			
AC	0.0030	S	AC	0.0029	S			
AD	0.0693	NS	AD	0.1564	NS			
ВС	0.1091	NS	ВС	0.0003	S			
BD	0.0431	S	BD	0.0397	S			
CD	0.0238	S	CD	0.0337	S			
Residual			Residual					
Lack of Fit	0.9970	Not significant	Lack of Fit	0.0971	Not significant	Lack of Fit	0.9878	Not significant
		S=Significant				NS: Non-s	significant	

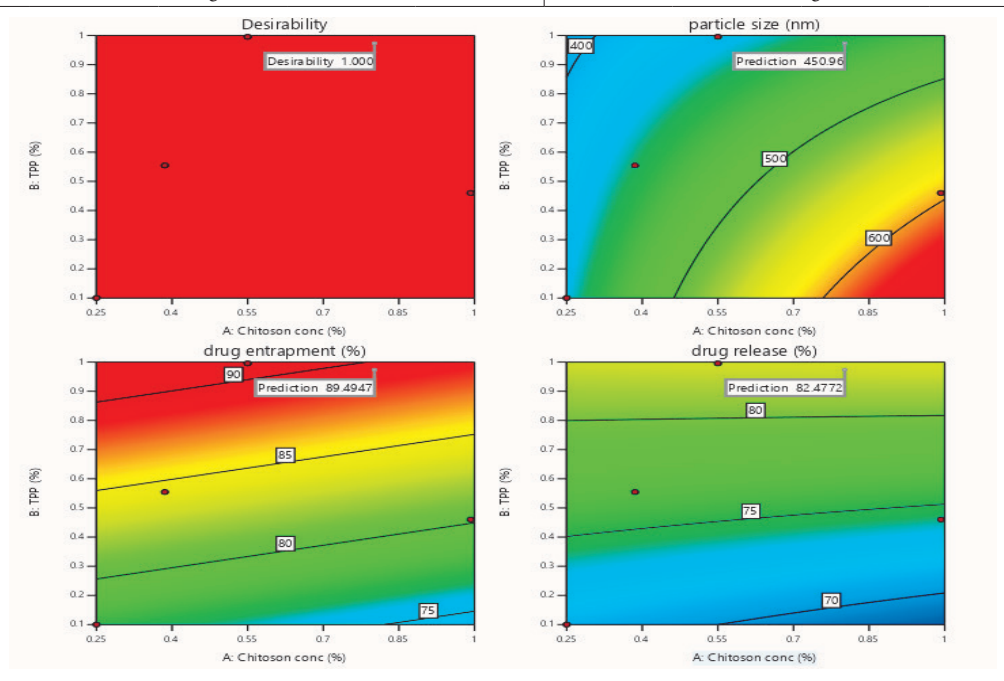


Figure 2. Predication profiler for the experimental runs

As per the surface response graphs (Figure 2), the chitosan concentration positively affected the particle size. Meanwhile, with a higher concentration of TPP, particle size was low and gradually increased as the concentration increased, with an additional curvature effect from high-order interactions. However, drug entrapment efficiency was a linear factor of TPP concentration, and chitosan concentration had a reverse effect. A similar response was observed in the drug release profile; an increase in the concentration of chitosan resulted in a decrease of this parameter;

however, the interactive effect of the cofactor, chitosan concentration, had a noteworthy impact on drug entrapment efficiency.

The desirability approach specifies how to deal with multiple response processes and how the ranges are close to the optimum, which has values of zero to one. At a maximum desirability value of 1, the optimized formulation exhibited a particle size, zeta potential, and in vitro drug release profile of 503.1nm, -41.6mV, and 90.7%± 1.01%, respectively.

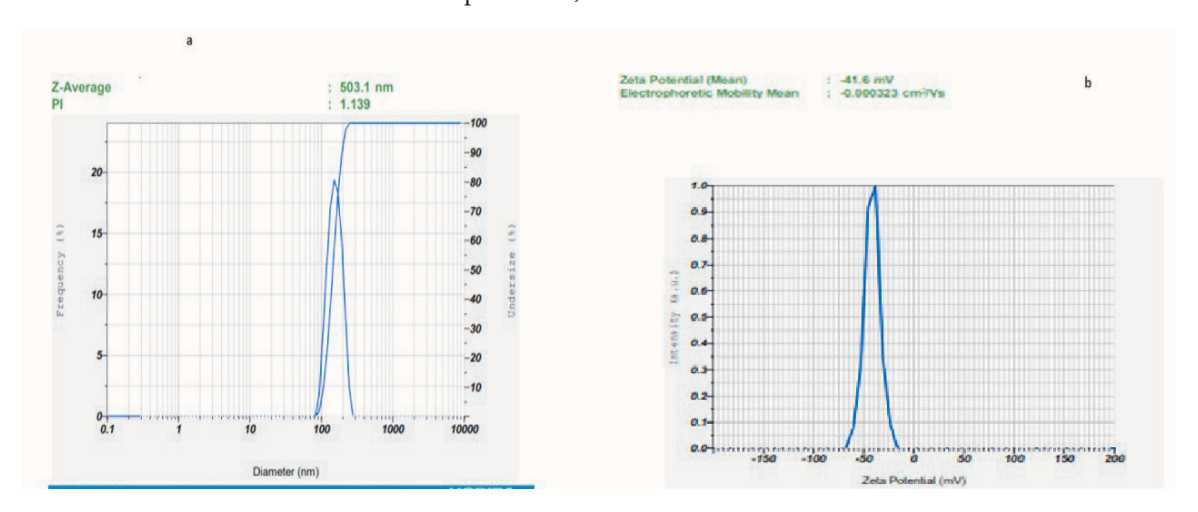


Figure 3. a) Particle size distribution of optimum formula b) Zeta potential

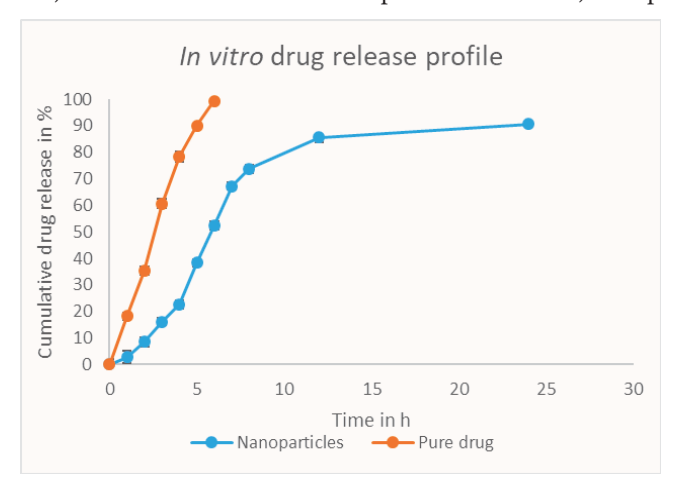


Figure 4. Comparative in vitro drug release profile of pure drug vs Nanoparticles

A comparative drug release profile of optimum nanoparticle formulation (Figure 4) against marketed drops (Moxicip) showed a rapid drug release from marketed drops and 99.34±1.8% drug release in 6 h compared to a sustained drug release from optimised

nanoparticle formulation. It took 24 hours for 90.7±1.6% of the drug to get released. The delay in drug release suggests a crosslinked form of chitosan, which may require time to deprotonate and release the drug from the networks.

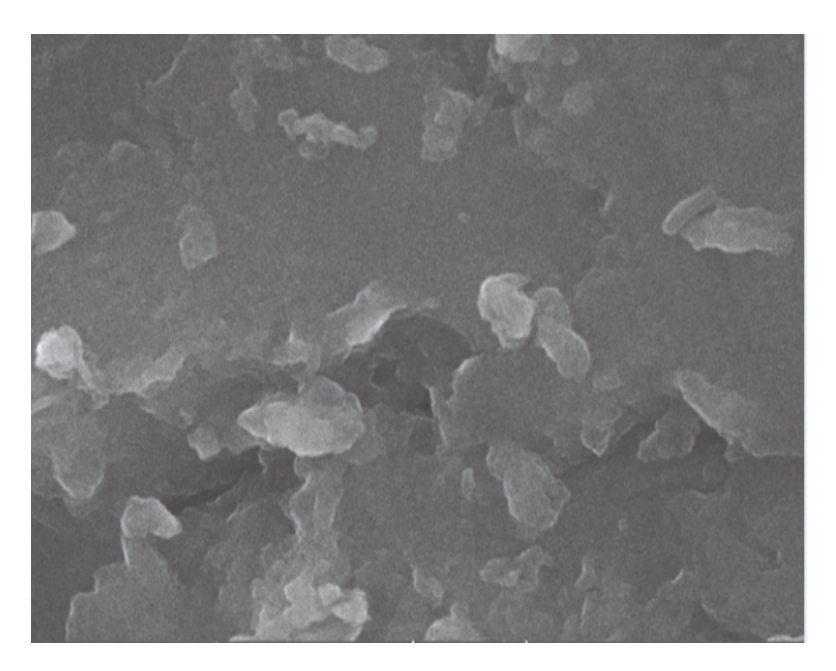


Figure 5. Surface photograph of optimized formulation

The surface photograph of the nanoparticles in Figure 5 reveals slightly distorted particles with uneven surfaces. The high stirring speed may have

disoriented the structure of the chitosan, contributing to this unevenness.

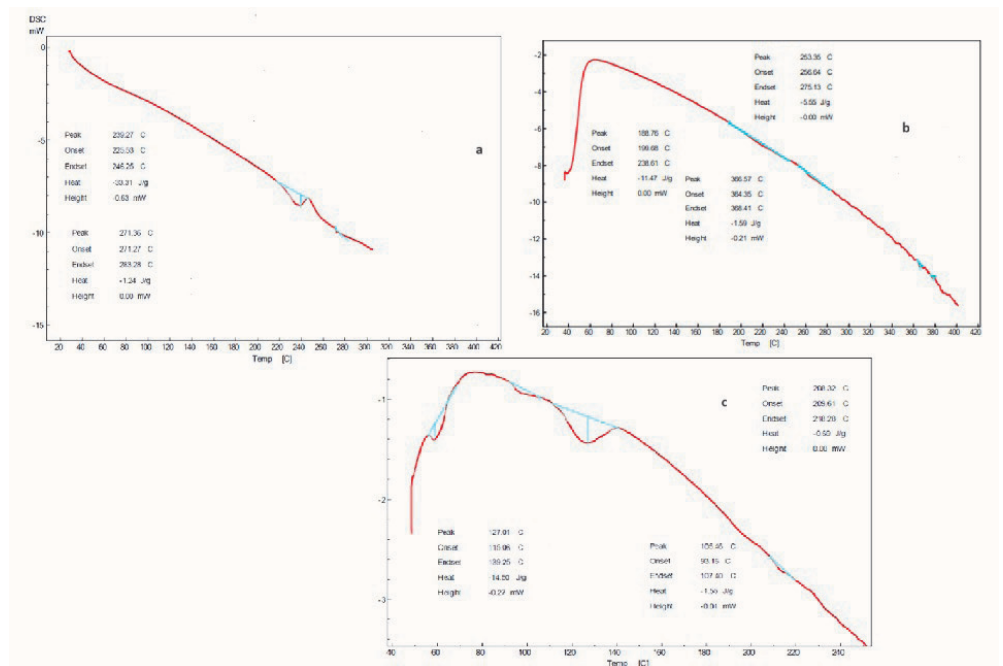


Figure 6. DSC thermogram of a) Pure drug, b) Physical Mixture c) Optimized NP formulation

The thermal behavior of Moxifloxacin hydrochloride (MH) and its nanoparticles (NP) is directed to the heat impact on both the polymer and MH. The DSC thermogram of MH displays an 236

endothermic peak at 239°C, while in the physical mixture, the peak shifts slightly to 259°C. An endothermic peak appears at 208°C for the optimized formulation, as optimized Figure 6. These results

suggest that in nanoparticle form, the drug's solubility decreases due to chitosan, a solubilizing agent, contributing to MH's melting point. Consequently, this promotes the retention of the drug within the polymer matrix. Upon contact with an aqueous medium (pH 7.4), the drug release increases due to the reversal of these effects.

Polymer solutions (0.5%, 1%, and 1.5% w/v) were studied for their gelling, physical, and viscosity. The 0.5% w/v concentration remained liquid under physiological conditions, whereas the 1% w/v concentration exhibited good gelling action. The

1.5% w/v concentration showed high viscosity under the studied conditions, as detailed in Table 6. Sodium alginate is an ion-responsive polymer. It contains monomeric sugar units such as mannuronic acid (M moiety) and guluronic acid (G moiety), with gelation depending on the ionic interaction between the cation and the carboxyl functional group of the G moiety. In the presence of divalent calcium ions, the sodium alginate solution undergoes a sol-to-gel conversion, which is ion and concentration-dependent. The gelling properties were evaluated using scores: (+: slow), (++: immediate and short-time effect), (+++: immediate and extended period).

Table 6. Evaluation of *In Situ* Gel

Sl.no	Concentration %	Clarity	pН	Viscosity (Cp)	Gelling capacity
1.	0.5	Clear	7.4±0.04	15.2	+
2.	1	Clear	7.4±0.07	34.8	+++
3.	1.5	Turbid	7.4±0.02	59.3	++

Note: + Gelled slowly and lost its consistency immediately, +++, Spontaneous gelling retained its consistency up to 8.5 h, ++ Spontaneous gelling, retained its consistency up to 5 h.Optimized nanoparticle-loaded in situ gel formulation was studied for its clarity, pH, drug content, and viscosity to know the extent of drug retention on the eye. The nanoparticulate gel (1w/w alginate gel base) was clear without any gritty particles by visual observation, had a pH of 7.4 \pm 0.04, and drug content of 87.5 \pm 0.2%. The viscosities of the gel formulation before and after the addition of STP at various angular velocities are given in Figure 7. As seen, in the absence of STF, the viscosity was increased by increasing the rpm, whereas after combing with STF, there was a decrease in viscosity with an increase in rpm.

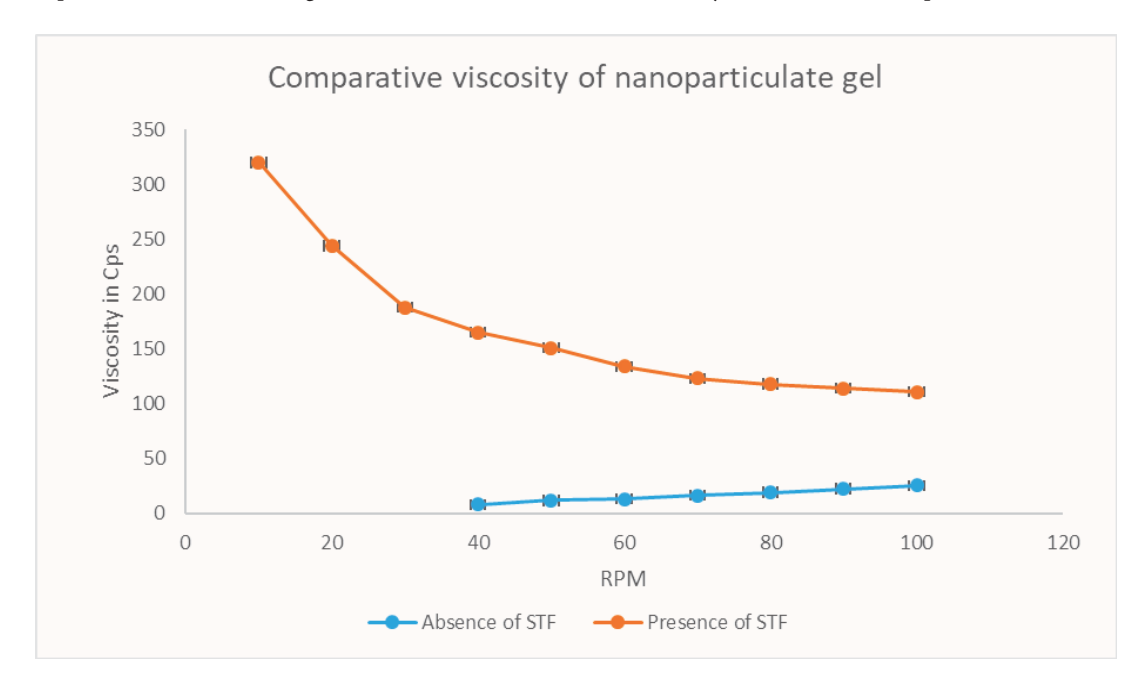


Figure 7. Comparative viscosities of nano particulate gel in the presence and the absence of SNF

The drug permeation rate from the NP in situ gel was 91.5 \pm 0.02%, compared to 70.4 \pm 0.05% for the pure drug-loaded gel and 69.12 \pm 0.7% for the marketed Moxicip drops (0.5%) over a 24-hour release study, as illustrated in Figure 8. The NP gel formulation showed sustained activity for up to 24 hours, with a peak at six hours, indicating prolonged action of the in-situ gel. While both the marketed formulation and the pure drug gel achieved a maximum drug permeation of approximately 70%, the developed NP in situ gel demonstrated a faster onset of action, comparable to the marketed drops. The *ex-vivo* permeation results showed a higher flux of 3.02 \pm 0.3 cm/h x 10^3, a permeability coefficient of 0.73cmh⁻¹10³. and rapid permeation for the NP in situ gel. In comparison, the

pure drug gel had a flux of 0.64 ± 0.04 , a permeability coefficient of 0.30, and the marketed Moxicip drops had a flux of 1.64 \pm 0.08 μ g/cm²/h and a permeability coefficient of 0.60. ANOVA results shows that there was statistical difference between the permeation profiles of the three formulations studied p>0.05). The significant mucoadhesive properties of chitosan, due to electrostatic interactions and hydrogen bonding with anionic mucin, prolong corneal residence time. The pH-responsive nature of the polymer can also help control drug delivery and extend drug release. chitosan's Additionally, permeation-enhancing properties and the colloidal size contribute to its effectiveness.

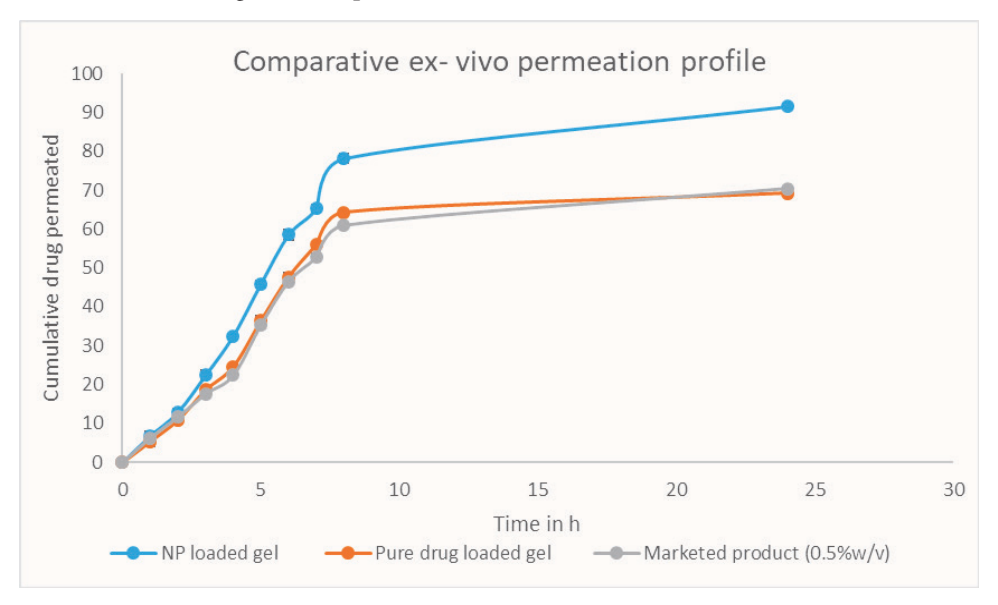


Figure 8. Ex-vivo permeation profile of NP-loaded gel, pure drug-loaded gel and marketed product

The optimum MOX-loaded gel formulation (OF) was subjected to short-term stability studies for 3 m at 25°C \pm 2°CRH and 40°C \pm 2°CRH. The result of physical appearance shows that there was no change at

different storage conditions. No notable changes were observed in viscosity and gelling capacity at both storage conditions, as shown in Table 7.

Table 7. Stability Studies

CIN-	Physical appearance		7	Viscosity (cps)			Gelling capacity (min±SD)			
SLNo	Days	OF	25±2°C	40±2°C	OF	25±2°C	40°±2°C	OF	25±2°C	40°±2°C
1	0	Free-flowing and clear			111±1.1			0.5±0.03		
2	180	Free-flowing and clear		111±1.1	145±1.9	200±2.2	0.5±0.03	0.5±0.07	0.6±0.02	

The FTIR of the drug, drug/excipients, and the optimum formula are given in Figure 9. Compatibility studies showed that there is no interaction between drugs and excipients used. Peaks for drug and excipients were observed within the stretching range 1500-1700 for carboxylic Acid (C=O), 1550-1500 for nitro compound N-O, 840-790 for aromatic

Substitution C, 1400-1000 for fluoro compound C. The observed ranges for optimum formulation were within the stretching range 3550-3200 for Alcohol O-H, 2000-1650 for Aromatic compound C-H, 1550-1500 for Nitro compound N-O, and 1400-1000 for Fluoro compound C-F.

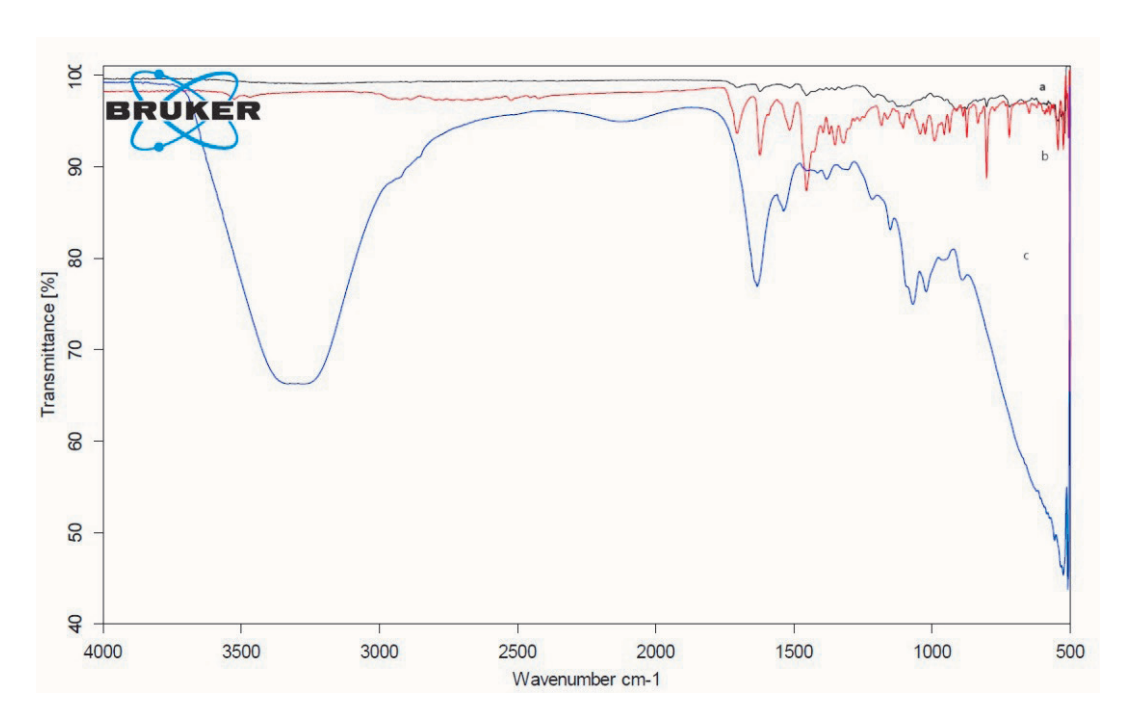


Figure 9. FTIR spectrum of NP formulation

The optimum MOX-loaded was studied for its irritation on rabbit eye against as a control—seven days to see the eye's irritation and redness (Figure 10). There were no signs of watering or inflammation.



Figure 10. *In vivo* eye irritation study (a) Control, (b) Normal rabbit eye, before instillation of the drops, (c) Instillation of optimum formulation, (d) After instillation, observation for 7 days.

Table 8. Antimicrobial Study

Oncomican	Zone of Inhibition*(mm)				
Organism	Marketed Formulation	Developed formulation			
S aureus	34.6±0.4	38.6±0.4			
E coli	38±0.8	45.6±0.9			

The antimicrobial study indicates that MOX retained its antimicrobial property when formulated into nanoparticle-loaded in situ gel, as shown in Table 8. Also, the study showed that the developed formulation reflected more antimicrobial activity

compared to the marketed formulation, as shown in (Figure 11) this may be due to the combined effect of polymer, gel, and the drug and because of its more penetration power

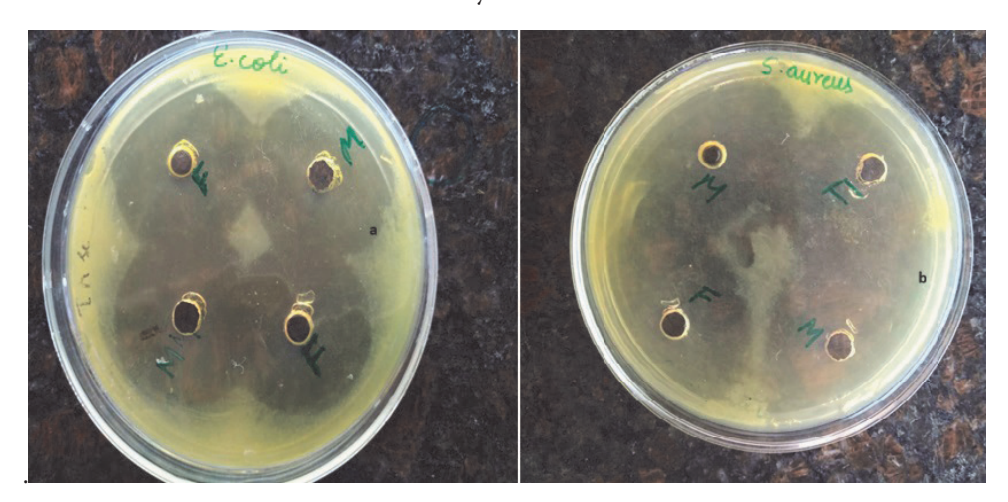


Figure 11. Zone of inhibition of (a) organism E. Coli (b) Organism S. aureus, (F): Developed formulation (M): Marketed formulation.

CONCLUSION

The study aimed to develop a colloidal carrier-based in situ gel for ophthalmic delivery of moxifloxacin hydrochloride to treat deep corneal infections. Chitosan-MX nanoparticles, prepared through experimental design, were incorporated into a sodium alginate in situ gel. The *ex vivo* permeation profile demonstrated that the optimized formulation provided higher permeation and extended drug action compared to the marketed eye drop (Moxicip - 0.5% w/v). The formulation exhibited superior antimicrobial activity against both gram-positive and gram-negative bacteria, comparable to that of marketed formulations, and was non-irritating to the eye. The combination of chitosan nanoparticles-

loaded in situ gel showed enhanced ocular bioavailability, increased corneal retention time, and reduced frequency of drug administration, thereby improving patient compliance. Additionally, this approach offers clinicians a new, cost-effective, safe, and efficient option for ocular drug delivery.

AUTHOR CONTRIBUTION STATEMENT

PS: Concept, Design, Supervision and Manuscript Writing

JP: Literature Search, Data Collection, and Processing

CONFLICT OF INTEREST

The authors declare that there is no conflict of interest.

REFERENCES

- Ahmed, T. A., & Aljaeid, B. M. (2017). A potential in situ gel formulation loaded with novel fabricated poly(Lactide-co-glycolide) nanoparticles for enhancing and sustaining the ophthalmic delivery of ketoconazole. *International Journal of Nanomedicine*, 12, 1863–1875. https://doi.org/10.2147/IJN.S131850
- Bala, H.B., Ajay, S., Anil, B. Studies on Thermoreversive Mucoadhesive Ophthalmic in Situ Gel of Azithromycin. (2013). 3(5),106–109.
- Bhatia, HB., Sachan, A., Bhandari, A. (2013) studies on thermoreversive mucoadhesive ophthalmic in situ gel of azthromycin. Journal of Drug Delivery and Therapeutics, 3(5), 106-109.
- da Silva Furtado, G. T. F., Fideles, T. B., de Cassia Alves Leal Cruz, R., de Lima Souza, J. W., Barbero, M. A. R., & Fook, M. V. L. (2020). Chitosan/NaF Particles Prepared Via Ionotropic Gelation: Evaluation of Particles Size and Morphology. *Materials Research*, 21(4). https://doi.org/10.1590/1980-5373-MR-2018-0101
- Desai, K. G. (2016). Chitosan nanoparticles prepared by ionotropic gelation: An overview of recent advances. *Critical Reviews in Therapeutic Drug Carrier Systems*, 33(2), 107–158. https://doi.org/10.1615/CritRevTherDrugCarrierSyst.2016014850
- ElMeshad, A. N., & Mohsen, A. M. (2016). Enhanced corneal permeation and antimycotic activity of itraconazole against Candida albicans via a novel nanosystem vesicle. *Drug Delivery*, 23(7), 2115–2123. https://doi.org/10.3109/10717544.2014.942811
- Elmizadeh, H., Khanmohammadi, M., Ghasemi, K., Hassanzadeh, G., Nassiri-Asl, M., & Garmarudi, A. B. (2013). Preparation and optimization of chitosan nanoparticles and magnetic chitosan nanoparticles as delivery systems using Box-Behnken statistical design. *Journal of Pharmaceutical and Biomedical Analysis*, 80, 141–146. https://doi.org/10.1016/j.jpba.2013.02.038
- Gadad, A. P., Wadklar, P. D., Dandghi, P., & Patil, A. (2016). Thermosensitive in situ gel for ocular delivery of lomefloxacin. *Indian Journal of Pharmaceutical Education and Research*, 50(2), S96–S105. https:// doi.org/10.5530/ijper.50.2.24

- Gote, V., Sikder, S., Sicotte, J., & Pal, D. (2019). Ocular drug delivery: Present innovations and future challenges. *Journal of Pharmacology and Experimental Therapeutics*, 370(3), 602–624. https://doi.org/10.1124/jpet.119.256933
- Gupta, C., Juyal, V., & Nagaich, U. (2019). Formulation, optimization, and evaluation of in-situ gel of moxifloxacin hydrochloride for ophthalmic drug delivery. *International Journal of Applied Pharmaceutics*, 11(4), 147–158. https://doi.org/10.22159/ijap.2019v11i4.30388
- Irimia, T., Ghica, M. V., Popa, L., Anuţa, V., Arsene, A. L., & Dinu-Pîrvu, C. E. (2018). Strategies for improving ocular drug bioavailability and cornealwound healing with chitosan-based delivery systems. *Polymers*, 10(11). https://doi.org/10.3390/polym10111221
- Kaur, V., & Pawar, P. (2015). Formulation and Evaluation of Moxifloxacin Hydrochloride Niosomes for Controlled Ophthalmic Drug Delivery. *Journal* of Pharmaceutical Technology, Research and Management, 3(1), 11–28. https://doi.org/10.15415/ jptrm.2015.31002
- Kesarla, R., Tank, T., Vora, P. A., Shah, T., Parmar, S., & Omri, A. (2016). Preparation and evaluation of nanoparticles loaded ophthalmic in situ gel. *Drug Delivery*, 23(7), 2363–2370. https://doi.org/10.3109/ 10717544.2014.987333
- Maharjan, P., Cho, K. H., Maharjan, A., Shin, M. C., Moon, C., & Min, K. A. (2019). Pharmaceutical challenges and perspectives in developing ophthalmic drug formulations. *Journal of Pharmaceutical Investigation*, 49(2), 215–228. https://doi.org/10.1007/s40005-018-0404-6
- Mahmood, S., Mandal, U. K., Chatterjee, B., & Taher, M. (2017). Advanced characterizations of nanoparticles for drug delivery: Investigating their properties through the techniques used in their evaluations. *Nanotechnology Reviews*, 6(4), 355–372. https://doi.org/10.1515/ntrev-2016-0050

- Mahor, A., Prajapati, S. K., Verma, A., Gupta, R., Iyer, A. K., & Kesharwani, P. (2016). Moxifloxacin loaded gelatin nanoparticles for ocular delivery: Formulation and in-vitro, in-vivo evaluation. *Journal of Colloid and Interface Science*, 483, 132–138. https://doi.org/10.1016/j.jcis.2016.08.018
- Majeed, A., & Khan, N. A. (2019). Ocular in situ gel: An overview. *Journal of Drug Delivery and Therapeutics*, 9(1), 337–347. https://doi.org/10.22270/jddt. v9i1.2231
- Mandal, S., Prabhushankar, G., Thimmasetty, M., & Geetha, M. (2012). Formulation and evaluation of an in situ gel-forming ophthalmic formulation of moxifloxacin hydrochloride. *International Journal of Pharmaceutical Investigation*, *2*(2), 78. https://doi.org/10.4103/2230-973x.100042
- Miller, D. (2008). Review of moxifloxacin hydrochloride ophthalmic solution in the treatment of bacterial eye infections. *Clinical Ophthalmology*, *2*(1), 77. https://doi.org/10.2147/opth.s1666
- Mohammadpour Dounighi, N., Damavandi, M., Zolfagharian, H., & Moradi, S. (2012). Preparing and characterizing chitosan nanoparticles containing hemiscorpius lepturus scorpion venom as an antigen delivery system. *Archives of Razi Institute*, *67*(2), 145–153.
- Nanjawade, B. K., Manvi, F. V., & Manjappa, A. S. (2007). In situ-forming hydrogels for sustained ophthalmic drug delivery. *Journal of Controlled Release*, 122(2), 119–134. https://doi.org/10.1016/j.jconrel.2007.07.009
- Raj, V. K., Mazumder, R., & Madhra, M. (2020). Ocular drug delivery system: Challenges and approaches. *International Journal of Applied Pharmaceutics*, 12(5), 49–57. https://doi.org/10.22159/ijap.2020v12i5.38762
- Shashank Nayak, N., Sogali, B. S., & Thakur, R. S. (2012). Formulation and evaluation of pH triggered in situ ophthalmic gel of Moxifloxacin hydrochloride. *International Journal of Pharmacy and Pharmaceutical Sciences*, 4(2), 452–459.

- Shelake, S. S., Patil, S. V., Patil, S. S., & Sangave, P. (2018). Formulation and evaluation of fenofibrate-loaded nanoparticles by precipitation method. Indian Journal of Pharmaceutical Sciences, 80(3), 420–427. https://doi.org/10.4172/pharmaceutical-sciences.1000374
- Swain, G. P., Patel, S., Gandhi, J., & Shah, P. (2019). Development of Moxifloxacin Hydrochloride loaded in-situ gel for the treatment of periodontitis: In-vitro drug release study and antibacterial activity. *Journal* of Oral Biology and Craniofacial Research, 9(3), 190– 200. https://doi.org/10.1016/j.jobcr.2019.04.001
- Wani, M., Jagdale, S., Khanna, P., Gholap, R., Baheti, A. (2020). Formulation, and evaluation of ophthalmic In-situ gel using moxifloxacin coated silver nanoparticles. Research J. Pharm. and Tech., 13(8), :3623-3630. 10.5958/0974-360X.2020.00641.1%0A
- Wu, Y., Liu, Y., Li, X., Kebebe, D., Zhang, B., Ren, J., Lu, J., Li, J., Du, S., & Liu, Z. (2019). Research progress of in-situ gelling ophthalmic drug delivery system. Asian Journal of Pharmaceutical Sciences, 14(1), 1–15. https://doi.org/10.1016/j.ajps.2018.04.008
- Youssef, A.A.A., Thakkar, R., Senapati, S., Joshi, P.H., Dudhipala, N., Majumdar, S. (2022). Design of Topical Moxifloxacin Mucoadhesive Nanoemulsion for the Management of Ocular Bacterial Infections. Pharmaceutics, 14(6), 1246. https://doi.org/10.3390/ pharmaceutics14061246
- Yu, S., Wang, Q. M., Wang, X., Liu, D., Zhang, W., Ye, T., Yang, X., & Pan, W. (2015). Liposome incorporated ion sensitive in situ gels for opthalmic delivery of timolol maleate. *International Journal* of *Pharmaceutics*, 480(1–2), 128–136. https://doi. org/10.1016/j.ijpharm.2015.01.032
- Yurtdaş-Kirimlioğlu, G., Özer, S., Büyükköroğlu, G., & Yazan, Y. (2018). Formulation and in vitro evaluation of moxifloxacin hydrochloride-loaded polymeric nanoparticles for ocular application. *Latin American Journal of Pharmacy*, 37(9), 1850–1862.

Leiotrametes lactinea (Berk.) Induces Sperm Dysmorphogenesis and Testicular Damage Via Oxidative and Inflammatory Pathways in Mice

Ayomide ADEDAMOLA AJIBEWA*, Deborah IFEOLUWA SOLADEMI**, Tolulope BLESSING OLOWOPOROKU***, Precious ULONNAM EZURIKE****, Chinwe BRIDGET OFUDI*****, Oyindamola OLAJUMOKE ABIODUN******

Leiotrametes lactinea (Berk.) Induces Sperm Dysmorphogenesis and Testicular Damage Via Oxidative and Inflammatory Pathways in Mice

SUMMARY

Leiotrametes lactinea (Berk.) had antioxidant, antimicrobial, antitumor and anti-ulcer activities. However, little has been reported on its safety in the male reproductive system, if used for these therapeutic potentials. Thus, this study evaluated the safety profile of ethanol extract of Leiotrametes lactinea (EELL) on the reproductive system of male Swiss mice. For acute toxicity study, 15 mice were grouped into 5 (n = 3). Each group received a single dose of EELL at 500, 1000, 2000, 5000 mg/kg or distilled water (10 mL/kg) and were observed for 14 days for toxicity signs or mortality. Subsequently, twenty-four mice were grouped into four (n = 6) for a sub-acute toxicity study to receive distilled water or graded doses of EELL (50, 100, and 200 mg/kg) for 30 days. Thereafter, under anesthesia, the testes, epididymis, and blood were collected from the animals. Hormonal, and biochemical parameters were assayed. With no death recorded in the acute toxicity study, the median lethal dose was assumed to be >5000 mg/kg. However, subacute toxicity study showed significant alterations in sperm parameters, decreased testicular catalase, superoxide dismutase and glutathione levels while malondialdehyde level increased. Similarly, inflammatory markers (tumor necrosis factor-alpha and interleukin-6) were significantly elevated. Serum testosterone level significantly reduced at 200 mg/kg dose and testicular histology was disrupted at all doses with evidence of infiltration of inflammatory cells. Sub-acute administration of EELL induces reproductive toxicity in male Swiss mice at the tested doses via induction of oxidative stress and inflammation.

Key Words: Leiotrametes lactinea, reproductive toxicity, sperm parameters, toxicity.

Leiotrametes lactinea (Berk.) Farelerde Oksidatif ve İnflamatuar Yollarla Sperm Dismorfogenezine ve Testis Hasarına Neden Olur

ÖZ

Leiotrametes lactinea (Berk.)'nın antioksidan, antimikrobiyal, antitümör ve antiülser aktiviteleri bulunmaktadır. Ancak bu terapötik potansiyeller için kullanıldığında erkek üreme sistemindeki güvenilirliğine dair çok az rapor bulunmaktadır. Bu nedenle bu çalışmada Leiotrametes lactined'nın (EELL) etanol ekstresinin İsviçre erkek farelerinin üreme sistemi üzerindeki güvenlik profili değerlendirildi. Akut toksisite çalışması için 15 fare 5'e (n = 3) ayrıldı. Her gruba 500, 1000, 2000, 5000 mg/kg veya distile su (10 mL/kg) dozunda tek doz EELL verildi ve toksisite belirtileri veya ölüm oranı açısından 14 gün boyunca gözlemlendi. Daha sonra, yirmi dört fare, 30 gün boyunca distile su veya kademeli dozlarda EELL (50, 100 ve 200 mg/kg) almak üzere subakut toksisite çalışması için dörde (n = 6) ayrıldı. Daha sonra anestezi altında hayvanlardan testisler, epididim ve kan toplandı. Hormonal ve biyokimyasal parametreler ölçüldü. Akut toksisite çalışmasında ölüm kaydedilmediğinden, ortalama öldürücü dozun >5000 mg/kg olduğu varsayılmıştır. Ancak subakut toksisite çalışmasında sperm parametrelerinde anlamlı değişiklikler, testiküler katalaz, süperoksit dismutaz ve glutatyon düzeylerinde azalma, malondialdehit düzeyinde ise artış olduğu görüldü. Benzer şekilde inflamasyon belirteçleri (tümör nekroz faktörü-alfa ve interlökin-6) de anlamlı derecede yüksekti. Serum testosteron düzeyi 200 mg/kg dozunda önemli ölçüde azaldı ve tüm dozlarda testis histolojisi bozuldu ve inflamatuar hücre infiltrasyonu kanıtlandı. EELL'nin subakut uygulanması, test edilen dozlarda erkek İsviçre farelerinde oksidatif stres ve inflamasyon yoluyla üreme toksisitesine neden olmaktadır.

Anahtar Kelimeler: Leiotrametes lactinea, üreme toksisitesi, sperm parametreleri, toksisite.

Received: 10.09.2024 Revised: 9.03.2025 Accepted: 18.03.2025

ORCID: 0009-0002-3243-9555, Department of Pharmacology and Toxicology, Faculty of Pharmacy, University of Ibadan, Ibadan, Oyo State, Nigeria.

[&]quot;ORCID: 0009-0004-7761-0883, Department of Pharmacology and Therapeutics, Faculty of Basic Medical Sciences, College of Medicine, University of Ibadan, Ibadan, Oyo State, Nigeria.

[&]quot;" ORCID: 0009-0009-1612-1484, Department of Pharmacology and Therapeutics, Faculty of Basic Medical Sciences, College of Medicine, University of Ibadan, Ibadan, Oyo State, Nigeria.

[&]quot;" ORCID: 0000-0002-7380-1584, Department of Biochemistry, College of Natural Sciences, Michael Okpara University of Agriculture, Umudike, Abia State, Nigeria.

ORCID: 0009-0004-9161-5285, Department of Pharmacology and Toxicology, Faculty of Pharmacy, University of Ibadan, Ibadan, Oyo State, Nigeria.

[&]quot;"" ORCID: 0000-0002-6629-3016, Department of Pharmacology and Therapeutics, Faculty of Basic Medical Sciences, College of Medicine, University of Ibadan, Ibadan, Oyo State, Nigeria.

INTRODUCTION

Leiotrametes lactinea, a type of wood-rotting fungus is synonymous with Trametes lactinea a kind of polypore that sprouts from decaying wood. Trametes lactinea is widely distributed in Africa (Nigeria), South Asia (Malaysia, Indonesia, Sri Lanka, Pakistan, India, and Philippines), Australia and East Asia (Tiwari et al., 2013). Antioxidant as well as antimicrobial activities of L. lactinea and other species of Leiotrametes have been documented (Awala and Oyetayo, 2015; Adeyelu et al., 2016, Noraswati, 2010). Trametes lactinea extracts have been reported to effectively restore impaired memory and learning in rats with cerebral ischemia (Wang et al., 2019). Trametenolic acid B (TAB) isolated from Trametes lactinea has been shown to suppress gastric and breast cancer cells, in addition to inhibiting H+/K+ ATPase activity as the mechanism of anti-peptic ulcers effect (He et al., 2018, Zhang et al., 2014).

Although there are reports on the therapeutic activities of *Leiotrametes lactinea*, data that reveals its safety profile in the male reproductive system is scarce. Thus, given the acclaimed therapeutic benefits of the mushroom, its safety ought to be ascertained, thus this study focused on elucidating the effect of ethanol extract of *Leiotrametes lactinea* (EELL) on the male reproductive system of Swiss mice.

MATERIAL AND METHODS

Collection and Presumptive Identification of Mushroom

Growing mushroom samples were randomly picked from the University of Ibadan environment. Mushroom samples were identified morphologically by looking out for the features described by Okon et al., 2022 and thereafter kept in a sterile paper bag and stored at -4° C.

Molecular Identification of the Mushroom Samples

Genomic DNA Extraction, Amplification, Purification, Sequencing and Alignment

The genomic DNA of the collected mushroom samples was extracted with the Plant/ Fungi DNA Isolation Kit of Norgen Biotek Corporation (Thorold, Ontario, Canada), using the procedure described by the kit manufacturer. The extracted DNA was stored at -20°C until required for the next process. Polymerase chain reaction (PCR) was used to amplify the isolated DNA using primers ITS 1 (TCCGTAGGTGAACCTGCGG) and 4 (TCCTCCGCTTATTGATATGC) (Abiodun al., 2022). The PCR products were sequenced and aligned using CLUSTAL W (Thompson et al., 1997) and a dendrogram tree plotted using Molecular Evolutionary Genetics Analysis (MEGA) 4 software (Version 7.0) (Figure 1).

Sample (Mushroom) Ethanol Extraction

One thousand one hundred and sixty-eight grams (1168 g) of the mushroom sample was freezedried and extracted with 70% ethanol for 3 days after which it was filtered, and rotary evaporator was used to separate the solvent from the main extract at 40°C under reduced pressure thus concentrating the extract. The extract yielded on concentration was dried in vacuo and stored at -4°C until needed.

Experimental Animals

Healthy and sexually matured male Swiss mice (within 6-8 weeks from birth) procured from the University's animal house (University of Ibadan, Ibadan) were kept in standard cages. They were fed with mouse cubes (ACE* Feeds Nigeria Limited) and clean water *ad libitum*. They were allowed to acclimatize to their new environment for a week before commencing the study. Ethical approval for the use and care of animals was sought and obtained from the University of Ibadan Animal Care and Use Research Ethics Committee (UI-ACUREC/051/2022A).

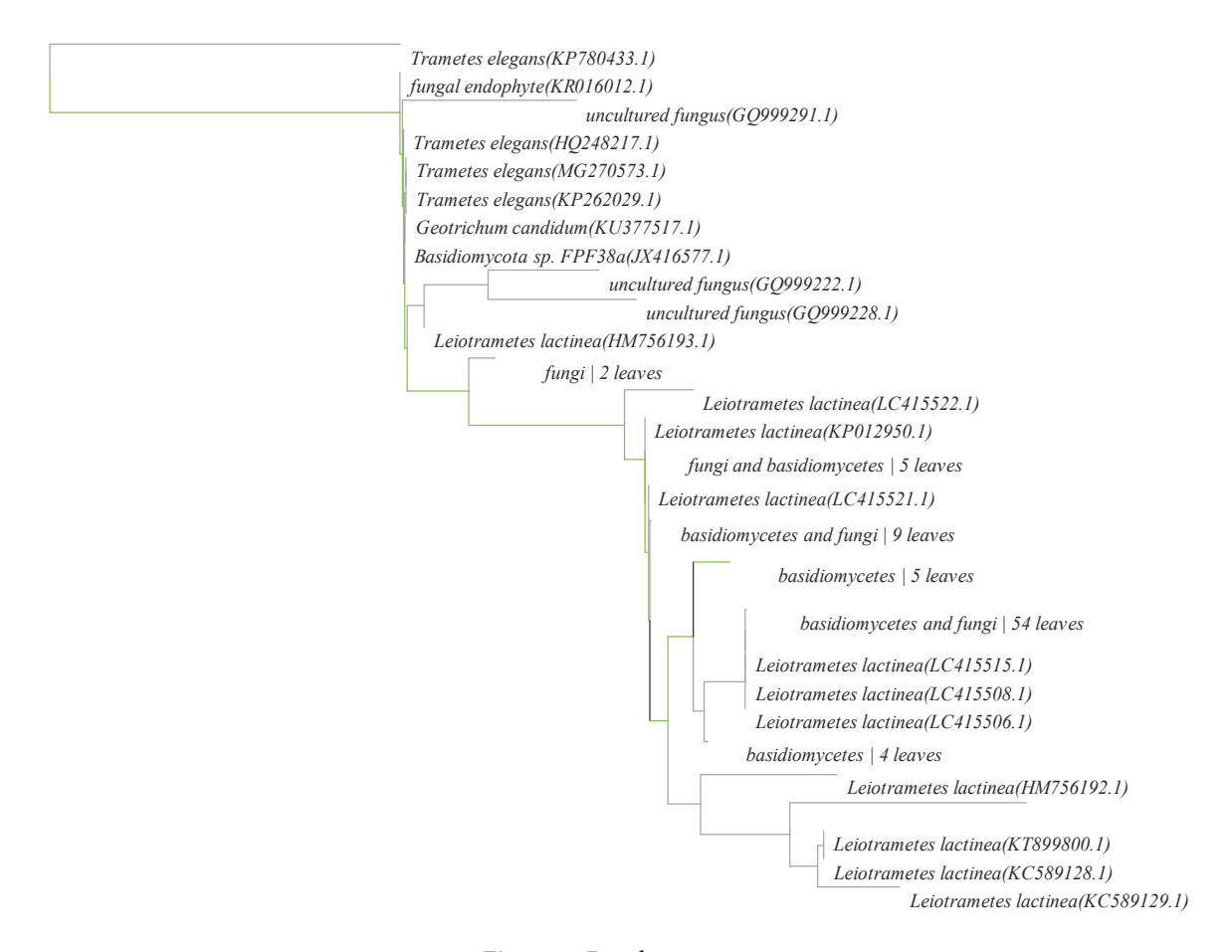


Figure 1. Dendogram tree

Acute Oral Toxicity Study

Slightly revised OECD 423 (Organization for Economic Cooperation and Development) guidelines were followed (OECD, 2001). Five groups were formed from fifteen nulliparous male Swiss mice (n=3) to receive 500, 1000, 2000, and 5000 mg/kg EELL or distilled water (10 mL/kg) orally. The study animals were deprived of food for about 3 hours before EELL administration and about 1-2 hours after administration, but water was made available ad libitum. Signs of toxicity, behavioral change or, mortality were monitored for 24 hours and thereafter, daily for 14 days after treatment.

Sub-Acute Toxicity Study

Using OECD Guidelines 407 (OECD, 2008), a total of 24 sexually mature male Swiss mice were grouped into 4 (n=6) to receive orally, distilled water

(10 mL/kg) as control or EELL (50, 100, or 200 mg/kg; respectively) for 30 consecutive days daily. The change in weight of each experimental animal was monitored weekly and food and water intake as well as signs of toxicity were monitored daily.

Samples Collection and Preparation for Sperm, Biochemical, and Histological Evaluation

After 30 days of daily dosing, the weight of each animal was recorded after which they were anaesthetized using ketamine/diazepam (75/0.5 mg/kg). Sperm was quickly extracted from the left cauda of the excised epididymis to assess motility, morphology, viability, and count. The gonadosomatic index for each animal was also calculated by removing and weighing the two testes and relating it to the individual body weight. Blood samples were collected into plain bottles and centrifuged for 10 minutes at

4°C and 3000 rpm. The clear supernatants (serum) were obtained and stored at -20°C for hormonal (testosterone) assay. The right testes were put in 10% formalin for histological purposes while the left testes were homogenized in phosphate buffer (0.1 M, pH 7.4) under cold temperature. The homogenized tissue samples were centrifuged, and the supernatants were stored in aliquots at -20°C for biochemical and proinflammatory cytokines assay.

Sperm Analysis

The cauda epididymis harvested from the animals were cut to release sperm samples on a glass slide. The sperm motility of each mouse was immediately evaluated microscopically and expressed as a percentage of the total number of counted sperm (Linder et al., 1986). The percentage of live spermatozoa (sperm viability) in all sperm samples was determined using an eosin-nigrosin stain (Acharya et al., 2008). The percentage viability was recorded. Sperm concentration (count) was verified using the Neubauer hemocytometer and expressed in millions (Feustan et al., 1989). Change in sperm morphology was observed under the microscope. The results were expressed in percentage of overall abnormal form (Feustan et al., 1989).

Biochemical Assessment

Jollow et al., (1974) procedure was followed to quantify the testicular level of reduced glutathione (GSH) while the extent of testicular lipid peroxidation (malondialdehyde; MDA) was determined using Varshney and Kale (1990) procedure. Superoxide dismutase (SOD) and catalase (CAT) activity in the testes samples were evaluated as described by Misra and Fridovich (1972) and Beer and Sizer (1952) respectively. Two markers of inflammation, tumor necrosis factor (TNF-α) and interleukin-6 (IL-6) were assayed for in the testicular tissues using the enzyme-linked immunosorbent assay kits (ELISA MAXTM Deluxe Set Mouse TNF-α and IL-6) ordered from BioLegend (San Diego, USA) with product Cat. No: 430904 and Cat. No: 431304 respectively.

The instructions provided by the manufacturer were followed. Serum testosterone level was measured using Melsin* mouse testosterone ELISA kit (Cat. No: EKMOU-0375) following the manufacturer's instructions.

Histological Studies (H & E Staining)

The tissues placed in 10% formalin were dehydrated in ethanol and clarified in xylene. Thereafter, the tissues were then processed using the hematoxylin and eosin (H & E) staining method as reported by Romanucci *et al.*, 2018. The photomicrographs of histological examination of mice testis stained with H & E were captured (x 400).

Statistical Analyses

Values were expressed as Mean ± SEM and multiple comparison of data was carried out using one-way analysis of variance (ANOVA), then a post-hoc test (Dunnett's). p < 0.05 is considered as statistically significant.

RESULTS

Acute and Sub-acute Oral Toxicity Effect of Ethanol Extract of *Leiotrametes lactinea* (EELL)

There was an absence of observable signs of toxicity and death in all the treatment groups, throughout the 14 days of the acute oral toxicity study. It can thus be inferred that the median lethal dose ($\rm LD_{50}$) of the extract might be greater than 5000 mg/kg. Two deaths were recorded during the 30 days of sub-acute toxicity study; firstly, on day 18 in the group that was administered 200 mg/kg of EELL, then on day 23 in the group that was administered 100 mg/kg of EELL.

Effect on Weight Gain, Gonadosomatic Index (GSI), Average Daily Feed and Water Intake in Male Swiss Mice

After 30 days of EELL administration, weight gain reduces with increasing extract dose (50 mg/kg; 4.28 \pm 0.85 g and 200 mg/kg; 3.38 \pm 0.68 g). The control group has the best weight gain (7.21 \pm 0.87 g), Figure 2A.

The average daily feed intake also decreased in treated groups (6.82 - 8.41; 50 to 200 mg/kg) as compared to the control group (10.01 \pm 0.48 g) (Figure 2B). Also, there was a decrease in the average daily water intake in animals that took EELL compared to the control group (Figure 2C). However, the decrease

was significant at the dosage level of 200 mg/kg (4.75 \pm 0.09 mL).

The difference in the gonadosomatic index of the treated animals showed no level of significance (0.90 \pm 0.021 - 0.98 \pm 0.03) when related to the control group (0.84 \pm 0.02) as represented in Figure 2D.

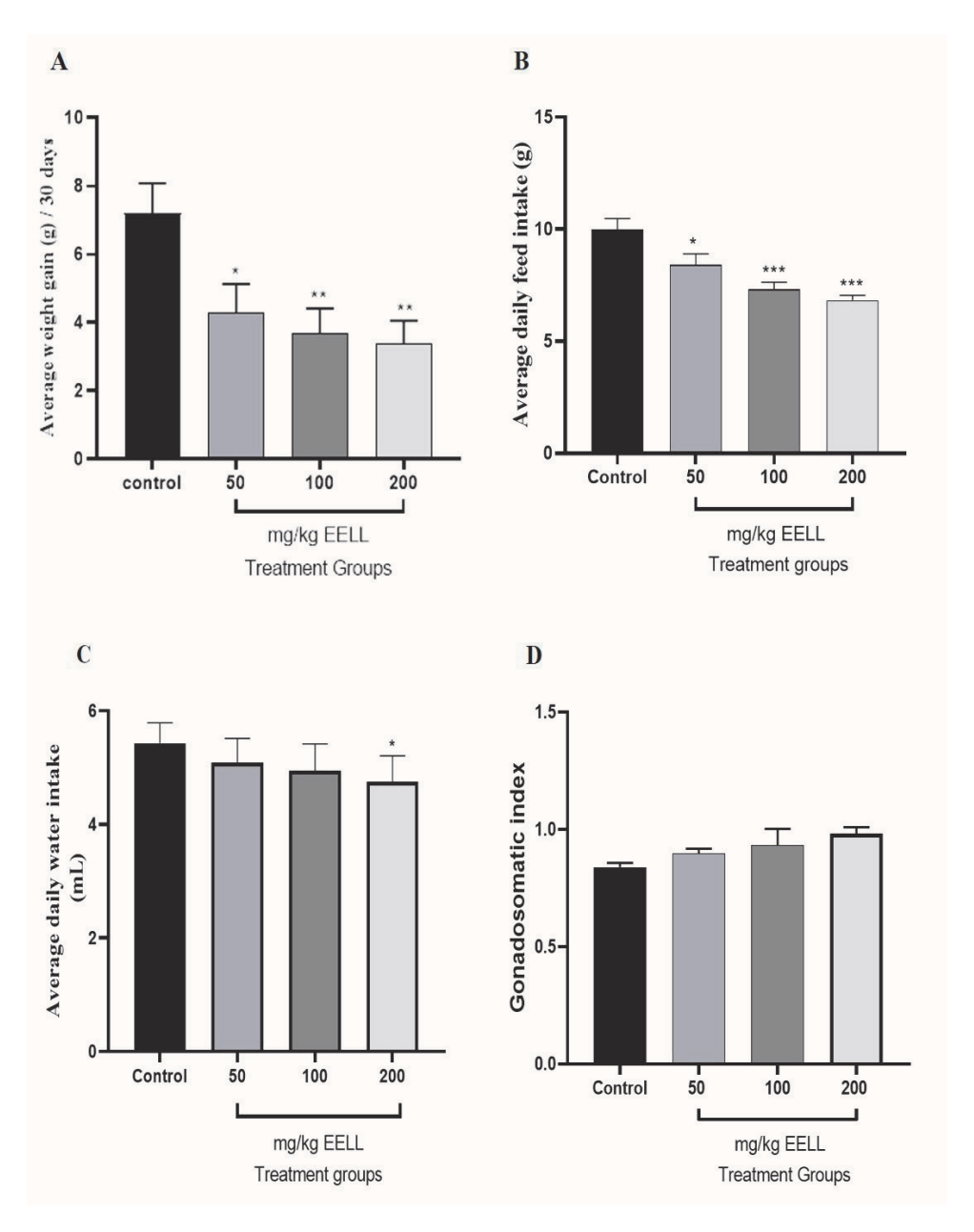


Figure 2. Effects of EELL on some physiological parameters in male Swiss mice. The data are expressed as mean \pm SEM, n = 6. Level of significant difference from the control group: *p<0.05, **p < 0.005, ***p < 0.001 (One-way ANOVA followed by Dunnett's multiple comparisons test).

Effects of EELL on Sperm Parameters

The percentage sperm motility of animals in the EELL treatment groups ranging from 56% (200 mg/kg) to 70% (50 mg/kg) (p<0.001) was decreased significantly compared to the control group (88%) (Figure 3A). The sperm count significantly decreased

with increasing EELL dose (Figure 3B). Furthermore, the decrease in the percentage of live to dead sperm cells in the groups treated with 100 and 200 mg/kg EELL (88.33 \pm 2.11%, p = 0.004 and 84.83 \pm 2.06 %, p < 0.001) was significant when related to the control group (97.0 \pm 0.63%) (Figure 3C).

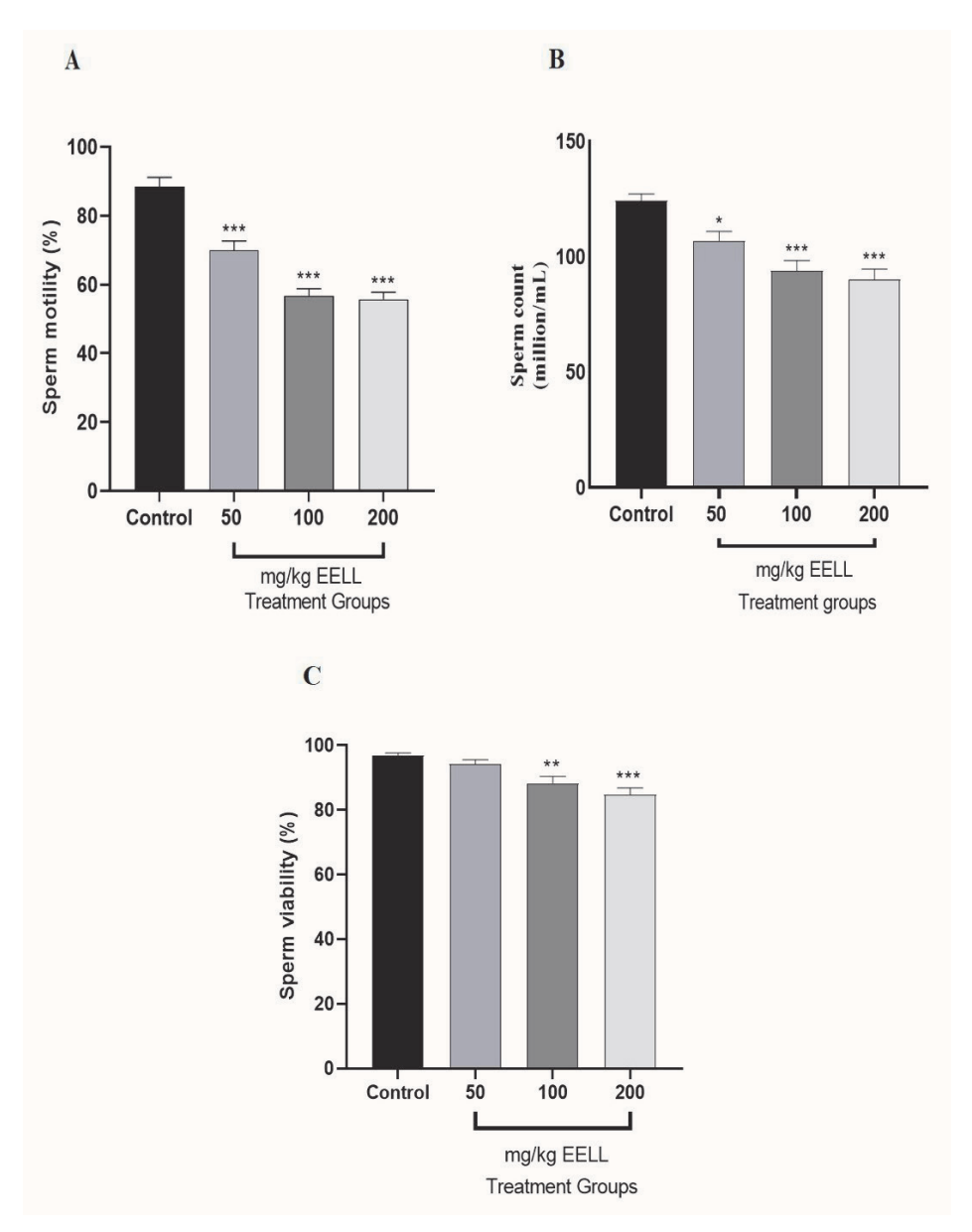


Figure 3. Effects of EELL on sperm quality (parameters) of male Swiss mice. The data are expressed as mean \pm SEM, n = 6. Level of significant difference from the control group: *p < 0.05, **p < 0.005, ***p < 0.001 (One-way ANOVA followed by Dunnett's multiple comparisons test).

The overall population of abnormal sperm cells in EELL-treated groups was significantly increase in comparism with the control group (Table 1).

Table 1. Effect of selected doses of ethanol extract of *Leiotrametes lactinea* on sperm morphology of male Swiss mice

	Control group		Treatment groups (mg/kg	(;)
Parameters	Control	50	100	200
Tail-less head	4.33 ± 0.49	4.63 ± 0.42	5.14 ± 0.26	5.29 ± 0.42
Headless tail	4.67 ± 0.29	4.714 ± 0.29	4.83 ± 0.30	5.13 ± 0.30
Rudimentary tail	2.00 ± 0.27	2.43 ± 0.30	2.43 ± 0.20	2.50 ± 0.34
Bent tail	8.67 ± 0.56	9.63 ± 0.18	10.00 ± 0.58	11.57 ± 0.37**
Curved tail	8.33 ± 0.42	$9.88 \pm 0.30^*$	$10.00 \pm 0.49^*$	11.29 ± 0.42***
Curved mid-piece	7.67 ± 0.33	$9.38 \pm 0.42^*$	9.71 ± 0.36**	11.29 ± 0.52***
Bent mid-piece	8.67 ± 0.56	9.50 ± 0.46	$10.14 \pm 0.34^*$	11.14 ± 0.34**
Looped tail	2.00 ± 0.37	1.75 ± 0.31	2.14 ± 0.26	1.57 ± 0.30
% NABS	11.44 ± 0.21	12.87 ± 0.28**	13.50 ± 0.24***	$14.84 \pm 0.15***$
% NNS	88.39 ± 0.21	87.13 ± 0.28**	86.50 ± 0.24***	85.16 ± 0.15***
TNC (million/mL)	405.00 ± 1.83	403.125 ± 1.32	402.86 ± 1.01	402.86 ± 1.49

The data are expressed as mean \pm SEM, n = 6. Level of significant difference from the control group: *p < 0.05, **p < 0.01, ***p < 0.001 (One-way ANOVA followed by Dunnett's multiple comparisons test). %NABS = % number of abnormal spermatozoa; %NNS = % number of spermatozoa; TNC = Total number of cells; Control = distilled water (10 mL/kg).

Effects of EELL on Biochemical Markers

Testicular indicators of oxidative stress (MDA, GSH, SOD, and CAT), inflammatory markers (TNF- α and IL-6), and serum testosterone levels were used to evaluate the effects of EELL on the reproductive system of male Swiss mice (Figure 4). The treatment groups expressed lowered GSH levels (199.02 \pm 0.20 to 108.71 \pm 7.13 μ mol) (Figure 4A). Furthermore, a significant decline in catalase activity in the groups that took 100 and 200 mg/kg EELL (30.39 \pm 2.56 and 18.25 \pm 2.78 μ mol/min/mg protein; p < 0.001) was observed in comparison with the control group (53.60 \pm 2.40 μ mol/min/mg protein) (Figure 4C). The superoxide dismutase (SOD) activity in the treated group also decreased significantly with increasing

dose of EELL (35.51 \pm 1.92 to 15.31 \pm 0.99 U/min/mg protein; p < 0.001) compared to the control group (48.56 \pm 1.78 U/min/mg protein) (Figure 4D). In addition, the groups treated with 100 and 200 mg/kg EELL (28.03 \pm 1.96 and 36.33 \pm 1.15 μ mol/mg protein; p < 0.001) expressed a significant increase in malondialdehyde level when related to that of the control group (16.22 \pm 0.57 μ mol/mg protein) (Figure 4B). Treatment with EELL brought about a dose-dependent increase in testicular levels of TNF- α and IL-6 relative to the control group (Figure 4E & 4F). In addition, the serum testosterone level was observed to reduce at a significant level in mice that received 200 mg/kg EELL (0.26 \pm 0.01 ng/mL; p = 0.05) relative to the control group (0.29 \pm 0.01 ng/mL) (Figure 4G).

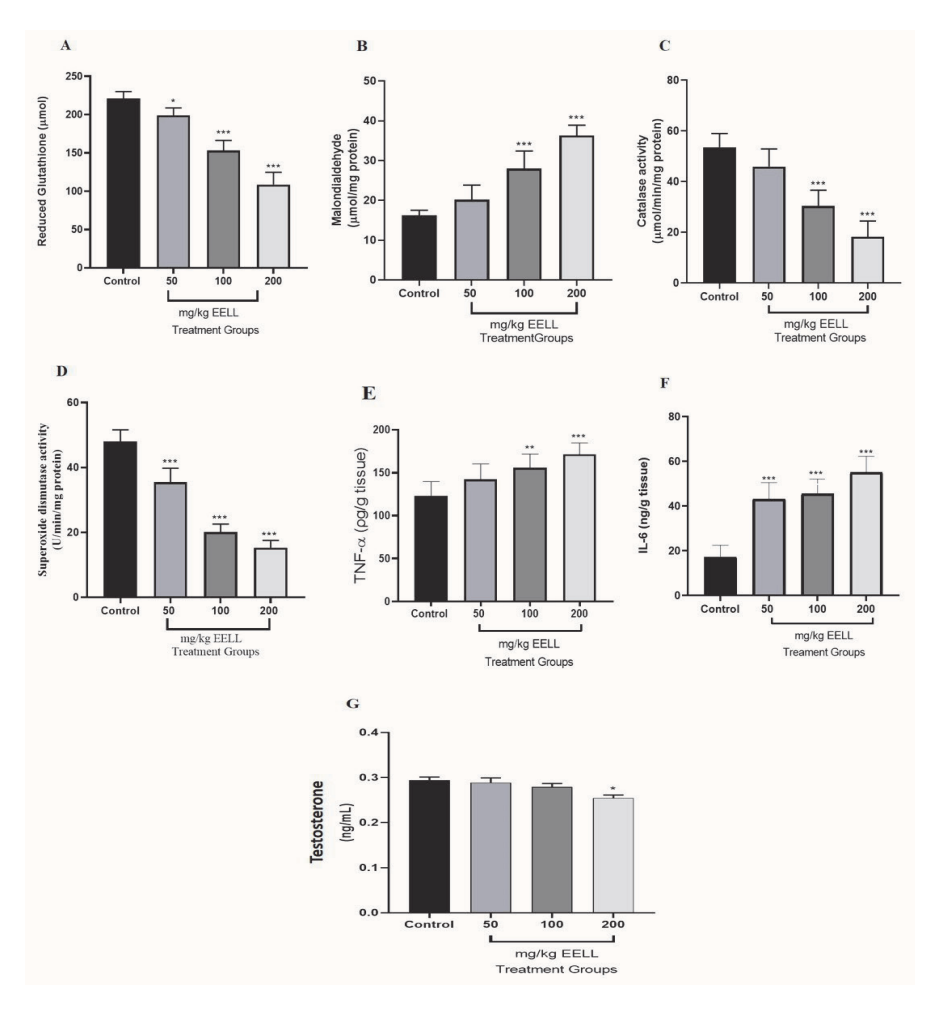


Figure 4. Effects of varying doses of EEGL on biochemical parameters in the testes or serum of male Swiss mice. The data are expressed as mean \pm SEM, n = 6. Level of significant difference from the control group: *p < 0.05, **p < 0.005, ***p < 0.001 (One-way ANOVA followed by Dunnett's multiple comparisons test).

Effects of EELL on Testes Histology of Swiss Mice

Figure 5A is a photomicrograph of a testicular section of a mouse in control group which showed normal testicular structure with spermatozoa in the lumen of the seminiferous tubules at maturation stages (white arrow). The spermatogonia as well as the Sertoli cells showed normal structure. The Leydig cells appear normal within the interstitial space (black slender arrow). In Figure 5B, the photomicrograph of a testicular section of a mouse treated with 50 mg/kg EELL showed normal seminiferous tubules (white arrow) with normal and fully developed germinal cells. However, some tubules have sloughed germinal

cells within their lumen. The figure however shows Leydig cells hyperplasia within the interstitial space (red slender arrow). Furthermore, Figure 5C depicts the photomicrograph of the testicular section of mice treated with 100 mg/kg EELL. It shows seminiferous tubules (red arrow) containing sloughed germinal cells. The interstitial spaces showed Leydig cells, and the tunica albuginea moderately infiltrated by inflammatory cells (blue slender arrow). In Figure 5D, the photomicrograph of a testicular section of experimental mice treated with 200 mg/kg EELL showed immature, degenerated seminiferous tubules (blue arrow).

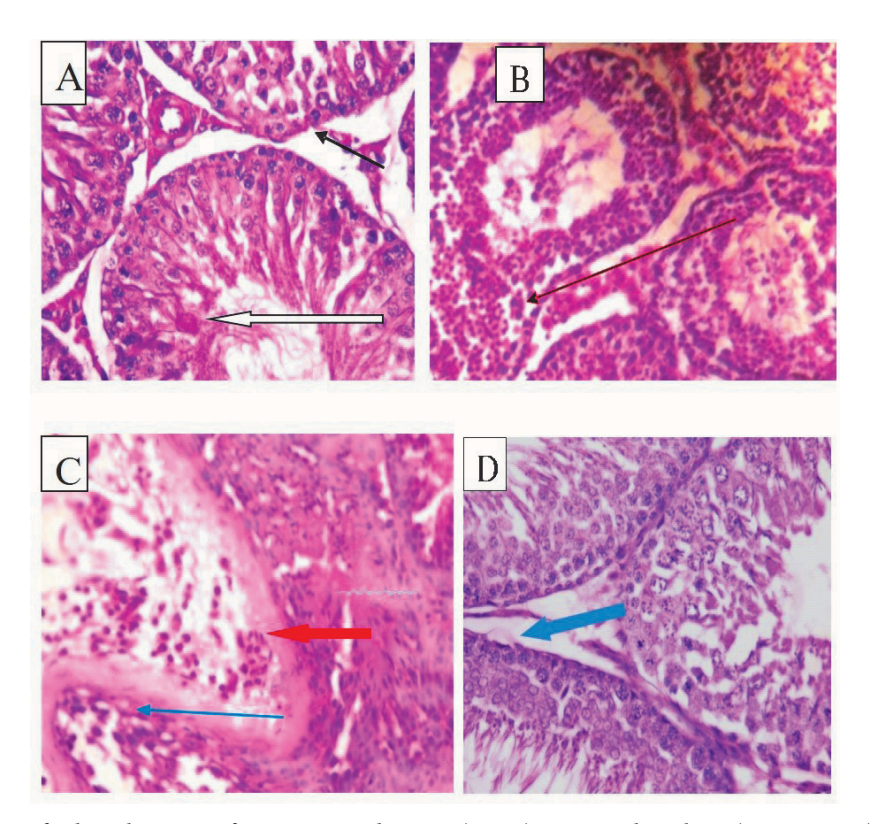


Figure 5. Effects of Ethanol extract of *Leiotrametes lactinea* (EELL) on testes histology (H & E x 400) of Swiss mice. A-Control (distilled water); B-50 mg/kg EELL; C-100 mg/kg EELL; D-200 mg/kg EELL.

DISCUSSION

In evaluating the toxicity potential of medicinal products, determining the 50% lethal dose (LD50) through acute toxicity testing is a routine initial step (Mansouri *et al.*, 2021). In the acute toxicity test performed in this study, no sign of toxicity or death was recorded even at the highest dose (5000 mg/kg) administered. It can thus be inferred that the LD $_{50}$ of ethanol extract of *Leiotrametes lactinea* (EELL) is >5000 mg/kg which appears to be relatively safe according to (OECD, 2001). However, 16.7% of death was recorded with 30 days daily dosing of 100 and 200 mg/kg.

Body and organ weight are important biomarkers used in determining toxicity (Kong et al., 2014). The decline in weight gain observed in the treated animals can be attributed to the corresponding decrease in average daily feed and water intake that was observed as well. This is in line with the reports from various studies on rodents (Myers et al., 2017). Additionally,

evaluating relative organ weight is a means of detecting potential organ or tissue damage either by atrophy or hypertrophy (Ashafa et al., 2012). The relative organ weight of the reproductive system may be influenced by the inflammatory changes that occur in these organs due to the buildup of toxic mediators as well as reduction in hormone level, especially testosterone. Thus, different factors are considered when interpreting changes in relative organ weight (Azenabor et al., 2015). However, the reduction in the relative organ weight of the testes (gonadosomatic index) following 30 days of administration of EELL was insignificant.

In reproductive toxicity studies, sperm motility, morphology, viability, and count are important parameters that can be evaluated to determine sperm quality (Dev et al., 2013). Sperm motility, among all other parameters is regarded as a highly reliable indicator of male reproductive potential because it is essential in the fertilization process as it has to

do with the migration of sperm cells to the oocyte after ejaculation for fertilization (Vicram et al., 2022). Thus, the decline in sperm motility can affect fertility (Toman et al., 2014). The decline in sperm motility recorded in the EELL-treated group appears to be a sign of toxicity which correlates with the previous findings of Orazizadeh et al., (2016). Sperm morphology is a result of the maturation process of the sperm cells, and it is a crucial biomarker of testicular functions (Jayachandra and AnnGie, 2013). The head, mid-piece and tail are important parts of the sperm cell that enhance its motility and any abnormality in them contributes to impaired motility which is linked to infertility (Trivedi et al., 2009; Svalheim et al., 2015). Thus, a measure of sperm normality and abnormality is a suitable method for male reproductive toxicity evaluation in rodents (Ramachandran and Singh, 2017). Increased sperm cell abnormalities following administration of EELL at the two highest doses was observed. Additionally, both the live/dead sperm count, and total sperm count were significantly lowered in mice treated with EELL. The decrease in sperm motility observed in this study was consistent with the decline in sperm viability. This could be because of the extract's toxic impact on the maturing and matured spermatozoa within the epididymis (Nikolaidis, 2017). These anomalies discovered in sperm parameters of the EELL-treated groups may suggest direct damage caused by prolonged/continuous treatment with higher doses of the extract.

Hormone measurement gives insights into the effects of reproductive toxicants (Creasy and Chapin 2018). Testosterone is the major and essential androgenic steroid in males that functions in the development of secondary sexual characteristics, spermatogenesis, sperm quality, sperm maturation and sperm release (Smith and Walker, 2014). The significantly reduced serum testosterone in the treatment group that received the highest dose of EELL can be attributed to various physiological factors one of which is the decrease in the number of luteinizing

hormone (LH) binding sites in the Leydig cell (site for testosterone production) (Xiayan et al., 2021) since it was previously reported that testosterone is produced when there is release and binding of LH to its receptor site in the Leydig cell (Corradi et al., 2016).

Oxidative stress sets in when there is an imbalance between free radicals generation and the scavenging antioxidant system (Darbandi et al., 2016). The antioxidants are defense systems that protect cells and macromolecules from ROS-induced damaging on the reproductive system (Tousson et al., 2020). Sperm cells are highly susceptible to ROS due to their poor antioxidant system, lack of DNA repair mechanism in the mature sperm cells, as well as the presence of high levels of plasma membrane and cytoplasmic poly unsaturated fatty acids (Sabeti et al., 2016). Reactive oxygen species when at a moderate level regulate various intracellular signaling pathways, immunological and mitogen responses (Kruk et al., 2019). However, they trigger damage to proteins, lipids and nucleic acids at higher levels thus facilitating tissue damage and cell death (Majzoub and Agarwal, 2018). As previously reported, ROS can have deleterious effects on sperm count, motility, and morphology, thus, leading to a decrease in sperm fertilization potential (Dutta et al., 2019). Thus, the observed reduction in sperm count and quality may have resulted from the imbalance in ROS generation and clearance following the administration of EELL. Also, the intrusion of inflammatory cell into the testicular tissue of the treated mice noticed in the histology of the testes may have resulted from a rise in ROS level as noticed by the decreased level of antioxidants and increased MDA level. This is consistent with the report of Dobrakowski et al., (2017). Although previous studies reported the antioxidant activity of the extract in vitro, the opposite was the case in this study. This may be because in vitro studies occur outside the host influence or factors while in in vivo study, pharmacokinetic factors such as metabolism may influence the treatment outcome. Increased metabolism or first-pass effect could affect the bioavailability of the extract. The extract might be metabolised to secondary metabolites that lack antioxidant activity. As the extract caused increased lipid peroxidation this will overwhelm the antioxidant system of the mice.

Tumor necrosis factor-alpha (TNF-α) is a proinflammatory cytokine generated and released by mononuclear phagocytes and macrophages (Leisegang et al., 2016) and is crucial in the onset of inflammatory response (Azenabor et al., 2015). Calcium ion signaling is reported to control the activity of mouse sperm flagella (Lesich et al., 2012). However, by reducing plasma membrane permeability to Ca^{2+} , the large concentration of TNF- α may affect intracellular calcium ion homeostasis (Carrasquel et al., 2013). Increase in TNF-α level as observed in the EELL-treated groups may be a contributing factor to the decrease observed in sperm motility and abnormal morphology relative to the findings reported by Pascarelli et al., (2016). There exists a noticeable rise in the IL-6 level of the EELL-treated animals when compared to that of the control. Interleukin-6 levels has been reported to be elevated in cases of decreased functional competence of the spermatozoa (Micheli et al., 2019). At a particular threshold, the testicular structure experiences pathological changes in the presence of oxidative stress (Owagboriaye et al., 2017). Consequently, inflammation of the reproductive tract tightly integrates oxidative stress and creates vicious pathways that damage the structural and functional integrity of male reproductive tissues (Dutta et al., 2022). This results in an increase in cellular damage and chronic disorders, such as disturbance of the tissues of the male reproductive system that affects male fertility (Agarwal et al., 2020). The rise in cytokine level may lead to an increase in OS level (Dobrakowski et al., 2017) which may not only impact spermatozoa but may also result in a systemic reaction by lowering the level of testosterone hormone (Leisegang and Henkel, 2018).

In this study, the repeated administration of EELL disrupted the histological architecture of the

testes. These observed testicular changes may be linked to the observed increased abnormalities in the spermatozoa of the EELL-treated groups (Song et al., 2019). Degeneration of seminiferous tubules and maturation arrest observed in groups treated with 200 mg/kg EELL is a significant sign of interference in spermatogenesis as reported by Thakur et al., (2014). Leydig cell is the site for testosterone production in the seminiferous tubules of the testes (Yan et al., 2022). Leydig cell hyperplasia (hypertrophy) and inflammatory cell infiltration were observed in the testes of sample mice that received 50 and 100 mg/kg EELL respectively which may be a result of the EELL interference (decrease) in Leydig cell responsiveness through prolactin inhibition since prolactin stimulates LH receptors in the Leydig cell (de Mattos et al., 2023).

CONCLUSION

Continuous use at doses ≥ 50 mg/kg may pose a reproductive toxicity concern by affecting sperm quantity and quality (reducing sperm motility, viability and sperm count), reduce antioxidant activities and increase the extent of testicular tissue polyunsaturated fatty acids' peroxidation.

ACKNOWLEDGEMENTS

This research work did not at any time receive a specific grant from funding agencies in the public, commercial, or not-for-profit sectors.

AUTHOR CONTRIBUTION STATEMENT

A.A Ajibewa: experimenting, statistical analysis, interpretation of data, preparing the study text, literature search. D.I Solademi: experimenting & technical support, reviewing text. T.B Olowoporoku: experimenting & technical support, reviewing text P.U Ezurike: reviewing the text & literature search. C.B Ofudi: reviewing the text & technical support. O.O Abiodun: developing the hypothesis, preparing the study text, statistical analysis & reviewing the text.

CONFLICT OF INTEREST

Authors declare that there is no conflict of interest.

REFERENCES

- Abiodun, O. O., Alege, A.M., Ezurike, P. U., Nkumah, A., Adelowo, O., & Oke, T. A. (2022). *Lentinus squarrosulus* (Mont.) mushroom: Molecular identification, in vitro anti-diabetic, anti-obesity, and cytotoxicity assessment. *Turk. J. Pharm. Sci.*, 19(6), 642-648. doi: 10.4274/tjps.galenos.2021.72798
- Acharya, U. R., Mishra, M., Patro, J., & Panda, M. K. (2008). Effect of vitamins C and E on spermatogenesis in mice exposed to cadmium. *Reproductive Toxicology*, 25, 84-88. DOI: 10.1016/j.reprotox.2007.10.004
- Adeyelu, A. T., Oyetayo, V. O., & Awala, S. I. (2016). Evaluation of the anti-candidal property of a wild macrofungus, *Trametes lactinea*, on clinically isolated Candidia species. *Annals of Complementary and Alternative Medicine*, 1(1), 4-8. Retrieved at: https://www.researchgate.net/publication/303383151
- Agarwal, A., & Sengupta, P. (2020). Oxidative stress and its association with male infertility. In Male Infertility. Berlin/Heidelberg, Germany; Springer, 57–68.
- Ashafa, A. O. T., Orekoya, L. O., & Yakubu, M. T. (2012). Toxicity profile of ethanolic extract of Azadirachta indica stem bark in male Wistar rats. *Asian Pacific Journal of Tropical Biomedicine*, *2*(10), 811–817. doi: 10.1016/S2221-1691(12)60234-2
- Awala, S. I., & Oyetayo, V. O. (2015). Molecular Identity and Antimicrobial Profile of Trametes species collected from the Teaching and Research Farm of the Federal University of Technology, Akure, Nigeria. *Journal of Advances in Medical and Pharmaceutical Sciences*, 4(3), 1-14. doi:10.9734/JAMPS/2015/20059
- Azenabor, A., Ekun, A. O., & Akinloye, O. 2015. Impact of Inflammation on male reproductive tract. *Journal of Reproduction and Infertility, 16*, 123–129. PMID: 26913230; PMCID: PMC4508350.

- Beers, R. F. (Jr) & Sizer, I. W. (1952). A spectrophotometric method for measuring the breakdown of hydrogen peroxide by catalase. *Journal of Biological Chemistry*, 195, 133-140. https://doi.org/10.1016/S0021-9258(19)50881-X
- Carneiro, A. A. J., Ferreira, I. C. F. R., Due nas, M., Barros, L., da Silva, R., Gomes, E., & Santos-Buelga, C. (2013). Chemical composition and antioxidant activity of dried powder formulations of Agaricus blazei and Lentinus edodes. *Food Chemistry*, *138*(4), 2168-2173. https://doi.org/10.1016/j. foodchem.2012.12.036
- Carrasquel, G., Camejo, M. I., Michelangeli, F., & Ruiz, M. C., (2013). Effect of tumor necrosis factor-α on the intracellular Ca2+ homeostasis in human sperm. American Journal of Reproductive Immunology, 70, 153–161. doi: 10.1111/aji.12106
- Chang, S. T., & Miles, P. G. (2008). Mushrooms: Cultivation, Nutritional, Medicinal Effect, and Environmental Impact (2nd ed.). Boca Raton, Fla, USA: CRC Press.
- Chatterjee, S., Sarma, M. K., Deb, U., Steinhauser, G., Walther, C., & Gupta D. K. (2017). Mushrooms: from nutrition to mycoremediation. *Environmental Science and Pollution Control*, 24, 19480-19493. https://doi.org/10.1007/s11356-017-9826-3
- Chen, J., Xu, H., He, D., Li, Y., Luo, T., Yang, H., & Lin, M. (2019). Historical logging alters soil fungal community composition and network in a tropical rainforest. *Forest Ecology and Management*, 433, 228–239. https://doi.org/10.1016/j.foreco.2018.11.005
- Corradi, P. F., Corradi, R. B., & Greene, L. W. (2016). Physiology of the hypothalamic pituitary gonadal axis in the male. *Urologic Clinics*, 43(2), 151-162. DOI: 10.1016/j.ucl.2016.01.001

- Creasy, D., Bube, A., deRijk, E., Kandori, H., Kuwahara, M., Masson, R.,..., & Whitney, K. (2012). Proliferative and Nonproliferative Lesions of the Rat and Mouse Male Reproductive System. *Toxicolology Pathology*, 40(6), 40–121. https://doi.org/10.1177/0192623312454337
- Creasy, D. M., & Chapin, R. E. (2018). The measurement of male reproductive hormones in laboratory animals. *Toxicologic Pathology*, 40, 1063-1078. https://doi.org/10.1016/B978-0-12-809841-7.00017-4
- Darbandi, S., & Darbandi, M. (2016). Lifestyle modifications on further reproductive problems. *Cresco Journal of Reproductive Science*, *1*(1), 1–2. http://crescopublications.org/pdf/cjrs/CJRS-1-001.
- de Mattos, K., Pierre, K. J., & Tremblay, J. J. (2023). Hormones and Signaling Pathways Involved in the Stimulation of Leydig Cell Steroidogenesis. *Endocrines*, 4, 573-594. https://doi.org/10.3390/ endocrines4030041
- Dev, K. R., Yadamma, K., & Reddy, K. D. (2013). Protective effects of curcumin in cyclophosphamide induced sperm head abnormalities in male mice. *International Journal of Pharmacy and Biological Sciences*, 4(1), 1131-1137. Retrieved from: https://www.researchgate.net/publication/286338049
- Dobrakowski, M., Kasperczyk, S., Horak, S., Chyra-Jach, D., Birkner, E., & Kasperczyk, A. (2017). Oxidative stress and motility impairment in the semen of fertile males. *Andrologia*, 49(10), e12783. doi: 10.1111/and.12783
- Dutta, S., Majzoub, A., & Agarwal, A. (2019). Oxidative Stress and Sperm Function: A Systematic Review on Evaluation and Management. *Arabian Journal of Urology*, *17*(2), 87-97. doi: 10.1080/2090 598X.2019.1599624
- Dutta, S., Sengupta, P., & Chakravarthi, S. (2022). Oxidant-Sensitive Inflammatory Pathways and Male Reproductive Functions. Advance Experimental and Medical Biology, 1358, 165-180. doi: 10.1007/978-3-030-89340-8

- Erg, B., Ergonul, P. G., Akata, I., & Kalyoncu, F. (2013). "Fatty acid compositions of six wild edible mush-room species. *The Scientific World Journal*, *2013*, 4. https://doi.org/10.1155/2013/163964
- Feustan, M. H, Bodnai, K. R., & Kerstetter, S. L. (1989). Reproductive toxicity of 2-methoxy ethanol applied dermally to occluded and no-occluded sides in male rats. *Toxicology and Applied Pharmacology,* 23, 45-65. https://doi.org/10.1016/0041-008X(89)90098-7
- Finimundy, T. C., Gambato, G., Fontana, R., Camassola, M., Salvador, M., Moura, S.,..., & Roesch-Ely, M. (2013). Aqueous extracts of Lentinula edodes and Pleurotus sajor-caju exhibit high antioxidant capability and promising in vitro antitumor activity. *Nutrition Research*, *33*(1), 76-84. https://doi.org/10.1016/j.nutres.2012.11.005
- He, N., Tian, L., Zhai, X., Zhang, X., & Zhao, Y. (2018).
 Composition characterization, antioxidant capacities and anti-proliferative effects of the polysaccharides isolated from *Trametes lactinea* (Berk.)
 Pat. *International Journal of Biological Macromolecules*, 115, 114-123. https://doi.org/10.1016/j.ijbiomac.2018.04.049
- Jayachandra, S., & AnnGie, N. (2013). Possible toxic effect of antihypertensive drug Olmesartan on male reproductive system of rat. *International Journal of Basic Clinical Pharmacology*, 2(1), 83-88. doi:10.5455/2319-2003.ijbcp20130116
- Jollow, D. J., Mitchell, J. R., Zampaglione, N., & Gillete, J. R. (1974). Bromobenzene induced liver necrosis: Protective role of glutathione and evidence for 3, 4-bromobenzene oxide as hepatotoxic metabolite. *Journal of Pharmacology*, 1, 151-169. doi: 10.1159/000136485
- Kong, L., Tang, M., Zhang, T., Wang, D., Hu, K., Lu, W., Wei, C., Liang, G., & Pu, Y. (2014). Nickel nanoparticles exposure and reproductive toxicity in healthy adult rats. *International Journal of Molecular Science*, 15(11), 21253-21269. doi: 10.3390/ijms151121253

- Kruk, J., Aboul-Enein, H. Y., Kładna, A., & Bowser, J. E. (2019). Oxidative Stress in Biological Systems and its Relation with Pathophysiological Functions: The Effect of Physical Activity on Cellular Redox Homeostasis. *Free Radical Research*, 53(5), 497–521. doi: 10.1080/10715762.2019.1612059
- Kumar, P., Singh, S., Sharma, A., Singh, N., & Singh, A. N. (2021). Arundo donax L.: An overview on its traditional and ethnomedicinal importance, Phytochemistry and Pharmacological aspects. *Journal of herbmed Pharmacology*, 10, 269-280. doi:10.34172/jhp.2021.31
- Leisegang, K., Bouic, P. J., & Henkel, R. R. (2016). Metabolic syndrome is associated with increased seminal inflammatory cytokines and reproductive dysfunction in a case-controlled male cohort. *American Journal of Reproductive Immunology*, 76(2), 155–163.
- Lesich, K. A., Kelsch, C. B., Ponichter, K. L., Dionne, B. J., Dang, L. & Lindemann, C. B. 2012. The calcium response of mouse sperm flagella: role of calcium ions in the regulation of dynein activity. *Biology of Reproduction*, 86, 105. https://doi.org/10.1111/aji.12529
- Linder, R. E., Strader, L. F. & McElroy, W. K. (1986). Measurement of epididymal sperm motility as a test variable in the rat. Bulletin of Environmental Contamination and Toxicology, 36, 317–324. doi: 10.1007/BF01623514
- Majzoub, A., & Agarwal, A. (2018). Systematic Review of Antioxidant Types and doses in Male Infertility: Benefits on Semen Parameters, Advanced Sperm Function, Assisted Reproduction and Live-Birth Rate. *Arabian Journal of Urology*, *16*(1), 113–124. doi: 10.1016/j.aju.2017.11.013
- Mansouri, K., Karmaus, A. L.,..., & Fitzpatrick. J. (2021). CATMoS: Collaborative Acute Toxicity Modeling Suite. *Environ Health Perspect.*, *129*(4), 47013. doi: 10.1289/EHP8495.

- Micheli, L., Collodel, G., Cerretani, D., Menchiari, A., Noto, D., Signorini, C., & Moretti, E. (2019). Relationships between ghrelin and obestatin with MDA, proinflammatory cytokines, GSH/GSSG ratio, catalase activity and semen parameters in infertile patients with leukocytospermia and varicocele. Oxidative Medicine and Cellular longevity, 2019, 7261842. doi: 10.1155/2019/7261842
- Misra, H. P., & Fridovich, I. (1972). The role of superoxide anion in the autooxidation of epinephrine and a simple assay for superoxide dismutase. *Journal of Biological Chemistry*, 247, 3170-3175.
- Myers, C. E., Hoelzinger, D. B., Truong, T. N., Chew,
 L. A., Myles, A., Chaudhuri, L., & Cohen, P. A.
 (2017). Chemotherapy can induce weight normalization of morbidly obese mice despite undiminished ingestion of high fat diet. *Oncotarget*,
 8, 4526-5438. https://doi.org/10.1016/S0021-9258(19)45228-9
- Nikolaidis, E. (2017). Relevance of animal testing and sensitivity of endpoints in reproductive and developmental toxicity. In: Reproductive and Developmental Toxicology (2nd ed.). Gupta RC, San Diego CA: Elsevier, Academic Press, 211–224.
- Noraswati, M. N. R. (2010). Diversity and antioxidant activity of Trametes fr. In Malaysia. Retrieved from:https://docslib.org/doc/1505621/diversity-and-antioxidant-activity-of-trametes-fr-in-malaysia
- Okon, O. G., Okon, J. E., Antia, U. E., Sam, S. M, Udoh, L. I, Usen, E. N., & Ibanga, I. A. (2022). Species richness, morphological features and inventory of wild macrofungi found in Akwa Ibom State, Nigeria. *European Journal of Biology and Biotechnology*, 3(4), 390. doi:10.24018/ejbio.2022.3.4.390
- Orazizadeh, M., Khorsandi, L., Absalan, F., Hashemitabar, M., & Daneshiand, E. (2014). Effect of beta-carotene on titanium oxide nanoparticles-induced testicular toxicity in mice. *Journal of Assisted Reproduction and Genetics*, *31*, 561-568. https://doi.org/10.1007/s10815-014-0184-5

- Organization for Economic Cooperation and Development (OECD). (2001). Guideline 423: Acute Oral Toxicity- Acute Toxic Class Method. 470 adopted by the council on 17th, December 2001. OECD Test Guideline 423
- Organization for Economic Cooperation and Development (OECD). (2008). Test No. 407: Repeated dose 28-days oral toxicity study in rodents, OECD Guidelines for the testing of Chemicals, Organization for Economic Cooperation and Development, Paris, France, 2008. Test No. 407: Repeated Dose 28-day Oral Toxicity Study in Rodents | OECD
- Owagboriaye, F. O., Dedeke, G. A, Ademolu, K. O., Olujimi, O. O., Ashidi, J. S. & Adeyinka, A. A. (2017). Reproductive toxicity of Roundup herbicide exposure in male albino rat. *Experimental and Toxicologic Pathology*, 69, 461–468. https://doi.org/10.1016/j.etp.2017.04.007
- Pascarelli, N. A., Fioravanti, A., Moretti, E., Guidelli, G. M., Mazzi, L., & Collodel, G. (2016). The effects in vitro of TNF-alpha and its antagonist 'etanercept' on ejaculated human sperm. *Reproduction, Fertility and Development*, 29, 1169–1177. https://doi.org/10.1071/rd16090
- Ramachandran, N., & Singh, N. P. (2017). Effect of management systems and seasons on sperm abnormalities in Jamunapari bucks semen. *Indian Journal of Animal Research*, *51*, 1138-1143. doi:10.18805/ijar.v0iOF.7808
- Romanucci, V., Agarwal, C., Agarwal, R., Pannecouque, C., Iuliano, M., De Tommaso, G.,...,& Zarrelli, A. (2018). Silibinin phosphodiester glyco-conjugates: synthesis, redox behavior and biological investigations. *Bioorg Chem.*, 77, 349-359. https://doi.org/10.1016/j.bioorg.2018.01.026
- Sabeti, P., Pourmasumi, S., Rahiminia, T., Akyash, F., & Talebi, A. R. (2016). Etiologies of sperm oxidative stress. *International Journal of Reproductive Biomedicine*, *14*(4), 231–240. Etiologies of sperm oxidative stress PubMed

- Smith, L. B., & Walker, W. H. (2014). The regulation of spermatogenesis by androgens. *Seminars in Cell* and *Developmental Biology*, 30, 2-13. https://doi. org/10.1016/j.semcdb.2014.02.012
- Song, X., Zhang, F., Chen, D., Bian, Q., Zhang, H., Liu, X., & Zhu, B. (2019). Study on systemic and reproductive toxicity of acetochlor in male mice. *Toxicological Research*, 8, 77. https://doi.org/10.1039/ c8tx00178b
- Svalheim, S., Sveberg, L., Mochol, M., & Taubøll, E. (2015). Interactions between antiepileptic drugs and hormones. *Seizure*, *28*, 12-17. doi: 10.1016/j. seizure.2015.02.022
- Thakur, M. Gupta, H. Singh, D., Mohanty, I. R., Maheswari, U., Vanage, G. & Joshi, D. S. (2014). Histopathological and ultra-structural effects of nanoparticles on rat testis following 90 days (Chronic study) of repeated oral administration. *Journal of Nanobiotechnology*, 12, 42–46. https://doi.org/10.1186/s12951-014-0042-8
- Tiwari, C. K., Parihar, J., &. Verma, R. K. (2010). Additions to wood decaying fungi of India. *Journal of Threatened Taxa*, *2*(6), 970-973. Additions to wood decaying fungi of India
- Toman, R., Hluchy, S., Massanyi, R., Lukac, N., Adamkovicova, M., Cabaj, M. & Hajkova, Z. (2014). Selenium and Cadmium Tissue Concentrations and the CASA Sperm Motility Analysis after Administration to Rats. American Journal of Animal and Veterinary Sciences, 9(4), 194-202. doi: 10.3844/ ajavssp.2014.194.202
- Tousson, E., Hafez, E., Zaki, S., Gad, A., & Elgharabawy, R. M. (2020). Evaluation of the testicular protection conferred by damiana (Turnera diffusa Willd.) against amitriptyline-induced testicular toxicity, DNA damage and apoptosis in rats. *Biomedicine and Pharmacotherapy, 132*, 110819. doi: 10.1016/j.biopha.2020.110819

- Trivedi, P. P., Kushwaha, S., Tripathi, D. N., & Jena, G. B. (2010). Evaluation of male germ cell toxicity in rats: correlation between sperm head morphology and sperm comet assay. *Mutation Research*, 703(2), 115-121. https://doi.org/10.1016/j.mrgentox.2010.08.005
- Vashney, R., & Kale, R. K. (1990). Effects of calmodulin antagonist. *International Journal of Radiation Biology*, 58, 733-743. http://dx.doi.org/10.1080/09553009014552121
- Vicram, S., Rohini K., Anbarasu, K, Nibedita, D., Palanivelu, J., Thanigaivel, S., Isaac, P. K., & Arockiaraj, J. (2022). Semonogelin, a coagulum macromolecule monitoring factor involved in the first step of fertilization: A prospective review. *Inter*national Journal of Biological Macromolecules, 209a, 951-962. https://doi.org/10.1016/j.ijbiomac.2022.04.079
- Wang, J., Wang, A., He, H., She, X., He, Y., Li, S.,..., & Zou, K. (2019). Trametenolic acid B protects against cerebral ischemia and reperfusion injury through modulation of microRNA-10a and PI3K/Akt/mTOR signaling pathways. *Biomedicine & pharmacotherapy*, 112, 108692. doi: 10.1016/j.bio-pha.2019.108692.
- Welti, S., Moreau, P., Pierre, A., Favel, A., Courtecuisse, R., Haon, M.,..., & Lesage, M. L. (2012). Molecular phylogeny of Trametes and related genera, and description of a new genus Leiotrametes. *Fungal Diversity*, 55(1), 47-64. doi:10.1007/s13225-011-0149-2

- World Health Organization (2012). "WHO laboratory manual for the examination and processing of human semen (6th Ed.). World Health. Retrieved from Publication Item
- World Health Organization (2017). WHO manual for the standardized investigation and diagnosis of the infertile couple.
- Xiayan, Z., Miner, H., Haosen, J., Tongliang, H., Ren-Shan, G., & Yiyan, W. (2021). Exposure to di-n-octyl phthalate during puberty induces hypergonadotropic hypogonadism caused by Leydig cell hyperplasia but reduced steroidogenic function in male rats. *Ecotoxicology and Environ*mental Safety, 208, 0147-6513. doi: 10.1016/j.ecoenv.2020.111432
- Yan, Q., Zhang, Y., Wang, Q., & Yuan, L. (2022). Autophagy: A Double-Edged Sword in Male Reproduction. *International Journal of Molecular Science*, 23(23), 15273. https://doi.org/10.3390/ijms232315273
- Zhang, Q. Y., Wang, J. Z., He, H. B., Liu, H. B. Yan, X. M., & Zou, K. (2014). Trametenolic acid B reverses multidrug resistance in breast cancer cells through regulating the expression level of P-glycoprotein. *Phytotherapy Research*, 28(7), 1037-1044. doi: 10.1002/ptr.5089

Effects of Epigallocatechin-3-Gallate in Preventing 5-Fluorouracil-induced Liver Injury in AML-12 Cell Line

Melek AKINCI^{**}, Çağatay OLTULU^{**}, Elvan BAKAR^{***}, Zatiye Ayça ÇEVİKELLİ YAKUT^{****}

Effects of Epigallocatechin-3-Gallate in Preventing 5-Fluorouracil-induced Liver Injury in AML-12 Cell Line

SUMMARY

This study evaluates the potential of epigallocatechin-3-gallate (EGCG) to mitigate 5-fluorouracil (5-FU)-induced hepatotoxicity using the AML-12 cell line. The AML-12 cell line is divided into four groups: control, 5-FU, EGCG, and 5-FU+EGCG. IC50 (Inhibitory Concentration 50) values are determined using the MTT assay. The mRNA expression levels of antioxidant systemrelated genes, including SOD, CAT, and GSH, are analyzed via RT-qPCR. Additionally, the expression levels of apoptosis-related genes such as Caspase-9 (Cas-9), Apaf-1, Caspase-3 (Cas-3), Bcl-2, and Bax, as well as p53 and SMAC/DIABLO, are evaluated. Coadministration of EGCG with 5-FU results in a significant increase in GSH, SOD, and CAT mRNA expression levels. Treatment with 5-FU alone significantly increases the expression levels of SMAC/ DIABLO, Bax, Apaf-1, Bcl-2, and Cas-3 mRNA by inducing apoptosis. Furthermore, co-administration of EGCG and 5-FU leads to a significant elevation in the mRNA expression levels of Cas-9, Bax, Apaf-1, p53, Cas-3, and SMAC/DIABLO, indicating the elimination of damaged structures through apoptosis. In conclusion, our findings demonstrate that EGCG exerts a hepatoprotective effect against 5-FU-induced damage through its antioxidant properties. Moreover, EGCG enhances the anticancer efficacy of 5-FU by promoting apoptosis and facilitating the removal of damaged cells. These results suggest a potential therapeutic synergy between EGCG and 5-FU in treating liver damage and cancer.

Keywords: 5-Fluorouracil, epigallocatechin-3-gallate, hepatoprotective effect, oxidative stress, apoptosis.

AML-12 Hücre Hattında 5-Florourasil Kaynaklı Karaciğer Hasarının Önlenmesinde Epigallokateşin-3-Gallat'ın Etkileri

ÖZ

Bu çalışmada, AML-12 hücre hattı kullanılarak epigallokateşin-3gallat'ın (EGCG), 5-florourasil (5-FU) kaynaklı hepatotoksisiteyi azaltma potansiyeli değerlendirilmiştir. AML-12 hücre hattı, kontrol, 5-FU, EGCG ve EGCG+FU olmak üzere dört gruba ayrılmıştır. IC50 (İnhibitör Konsantrasyon 50) değerleri, MTT testi kullanılarak hesaplanmıştır. SOD, katalaz ve GSH gibi antioksidan sistemle ilişkili genlerin mRNA ekspresyon düzeyleri RT-qPCR yöntemiyle analiz edilmiştir. Ayrıca, apoptozla ilişkili Kaspaz-9 (Cas-9), Apaf-1, Kaspaz-3 (Cas-3), Bcl-2 ve Bax genlerinin ekspresyon düzeyleri ile birlikte p53 ve SMAC/DIABLO gen ekspresyonları da değerlendirilmiştir. EGCG'nin, 5-FU ile birlikte uygulanması sonucunda, GSH, SOD ve CAT mRNA ekspresyon düzeylerinde anlamlı bir artış tespit edilmiştir. 5-FU uygulamasının, apoptozu uyararak SMAC/ DIABLO, Bax, Apaf-1, Bcl-2 ve Cas-3 mRNA ekspresyon düzeylerini istatistiksel olarak anlamlı şekilde artırdığı gözlenmiştir. EGCG'nin, 5-FU ile birlikte uygulanması ise Cas-9, Bax, Apaf-1, p53, Cas-3 ve SMAC/ DIABLO mRNA ekspresyon düzeylerinde anlamlı artışa neden olmuş, bu durumun hasarlı yapıların apoptoz yoluyla ortadan kaldırıldığını gösterdiği anlaşılmıştır. Sonuç olarak, bulgularımız EGCG'nin antioksidan özellikleri sayesinde 5-FU kaynaklı hasara karşı hepatoprotektif etkiler sağladığını göstermektedir. Ayrıca, EGCG'nin apoptozu teşvik ederek hasarlı hücrelerin ortadan kaldırılmasını kolaylaştırdığı ve 5-FU'nun antikanser etkinliğini artırdığı ortaya konmuştur. Bu sonuçlar, karaciğer hasarı ve kanser tedavisinde EGCG ve 5-FU arasında potansiyel bir terapötik sinerji bulunduğunu düşündürmektedir.

Anahtar Kelimeler: 5-Florourasil, epigallokateşin-3-gallat, hepatoprotektif etki, oksidatif stres, apoptoz.

Received: 31.10.2024 Revised: 24.01.2025 Accepted: 20.03.2025

^{*} ORCID: 0000-0003-3879-4232, Department of Pharmacology, Faculty of Pharmacy, Trakya University, Edirne, Turkey.

[&]quot;ORCID: 0000-0002-6051-3479, Department of Pharmaceutical Toxicology, Faculty of Pharmacy, Trakya University, Edirne, Turkey.

[&]quot;ORCID: 0000-0001-5703-3469, Department of Basic Phamaceutical Sciences, Faculty of Pharmacy, Trakya University, Edirne, Turkey.

[&]quot;" ORCID: 0000-0002-6697-6781, Department of Pharmacognosy, Faculty of Pharmacy, Trakya University, Edirne, Turkey. Department of Pharmacology, Faculty of Pharmacy, Marmara University, Istanbul, Turkey.

INTRODUCTION

Cancer comprises a collection of prevalent diseases marked by unregulated cellular proliferation. Surgery, radiation, and chemotherapy are widely utilized as cancer treatment options (Cleeland et al., 2012; Herrmann et al., 2020; Dongsar et al., 2023). Chemotherapy is essential in cancer treatment, targeting the eradication or suppression of cancer cell proliferation. However, chemotherapy resistance remains a significant obstacle, impairing the effectiveness of treatment and reducing its therapeutic potential. Contemporary cancer therapies, aside from their exorbitant expense, engage with signaling pathways, leading to a diverse array of side effects with differing severities and classifications. These side effects depend on the dosage of chemotherapeutic drugs and the patient's sensitivity to the medications. Due to their non-selective nature, chemotherapeutic drugs damage healthy tissues and cells alongside tumor cells (Wang et al., 2023).

Cytotoxic drugs, which represent an important class of chemotherapy, demonstrate high efficacy in cancer treatment. 5-fluorouracil (5-FU) is a prominent cytotoxic drug (Ranjit et al., 2023). It permanently inhibits thymidylate synthase (Yu et al., 2015). 5-FU-based therapies are widely utilized as a key component in various chemotherapy regimens for cancer treatment. However, 5-FU is associated with hepatoxicity, including hepatitis, steatohepatitis, and hepatic sinusoidal obstruction syndrome (Vauthey et al., 2006; Robinson et al., 2012; Hubert et al., 2013). Hepatocellular damage is reported to intensify due to elevated aminotransferases in 5-FU-induced liver cirrhosis (Momiyam et al., 2015).

Certain phytochemicals, such as epigallocatechin gallate (EGCG), enhance sensitivity to chemotherapy and mitigate chemotherapy-induced toxic side effects (Wang et al., 2023). EGCG exhibits various health advantages (Alam et al., 2022). Depending on its dosage, EGCG is reported to exhibit either antioxidant or pro-oxidant properties (Yang et al., 2022). It also

exhibits antioxidant, anti-inflammatory, anti-allergic, anti-angiogenesis, vasodilator, and anti-carcinogenic effects (Liczbiński et al., 2022).

This study investigates the impact of EGCG on 5-FU-induced hepatotoxicity. The study investigates the mRNA levels of key antioxidant enzymes, such as glutathione (GSH), catalase (CAT), and superoxide dismutase (SOD). Furthermore, it explores the gene expression profiles related to apoptosis, including SMAC/DIABLO (Second Mitochondria-Derived Activator of Caspases/Direct IAP Binding Protein with Low pI), Bcl-2 (B-cell lymphoma 2), Caspase-9 (Cas-9), Apaf-1 (Apoptotic Protease-Activating Factor 1), p53 (tumor suppressor protein 53), Caspase-3 (Cas-3), and Bax (Bcl-2-associated X protein). The effects of pathways involved in the apoptotic process are analyzed to elucidate their influence on gene expression.

MATERIALS AND METHODS

Groups

This study includes four experimental groups: control, 5-FU, EGCG, and 5-FU+EGCG.

Cell culture

AML-12 cells (ATCC*, CRL-2254 TM) are cultured in flasks containing a nutrient medium composed of 10 mg/ml streptomycin, 100 IU/ml penicillin, 1% L-glutamine, and 5% heat-inactivated fetal bovine serum. The medium is prepared in a 1:1 ratio of Dulbecco's Modified Eagle's Medium, HAMS F12, and Eagle's Minimum Essential Medium. The study uses cells between the 5th and 12th passages (5% CO₂, 37°C).

Determination of EGCG and 5-FU Dosages

The dosages of EGCG and 5-FU are determined based on prior studies. In vitro research indicates a wide range of IC50 (Inhibitory Concentration 50) values for 5-FU, varying with cell line and experimental conditions. For example, the IC50 of 5-FU is approximately 13 µg/ml in SW620 colon cancer cells (Gao et al., 2014) and ranges from 0.25

 μM to 1.5 μM in MCF7 breast cancer cells when used with β-escin (Mazrouei et al., 2019). Similarly, EGCG at a concentration of 20 μM has been shown to augment the apoptotic effects of 5-FU in MCF7 cells (Zhang et al., 2016). Based on these findings and the requirements of the experimental design, 5-FU and EGCG are administered at concentrations between 1.25 and 20 μM in this study, enabling a comprehensive evaluation of their effects on the AML-12 cell line.

Determination of IC50 doses by the MTT assay

Percent viability is calculated using the Thiazolyl Blue Tetrazolium Bromide (MTT) assay, and IC50 values are determined via probit analysis (Turker and Bakar, 2023). A total of 180 µL of 1x106 cells are inoculated into each well of 96-well plates, with four replicates studied. At the end of the 24 hours of incubation (37°C, 5% CO₂) 20 μL of the agents indicated for each group are applied and incubated for an additional 24 hours. An aqueous solution containing 0.01% dimethyl sulfoxide (DMSO) was added to the control group. Aqueous solutions of 5-FU (Sigma F6627) and EGCG (Sigma 1236700), each containing 0.01% DMSO, are prepared separately. 5-FU and EGCG are combined in a 1:1 (v/v) ratio and administered simultaneously to the treatment groups. All substances, except in the control group, are applied at varying doses of 1.25, 2.5, 5, 10, and 20 µM, with a total volume of 20 μ L. The cells in all groups are exposed to the substances for a total duration of 24 hours. Thereafter, 20 µL of MTT solution (5 mg/ mL) is introduced into the wells, and the plates are left to incubate (3 hours). 200 μL of 0.01% DMSO is added to dissolve the resultant formazan crystals. Absorbance values are recorded at 492 nm using a microplate reader. The viability of cells in the control group is assumed to be 100%, and the IC50 doses are determined using probit analysis.

RNA isolation and cDNA synthesis

The AML-12 cell line is plated in culture dishes with 3x10⁶ cells allocated to each well and maintained under incubation for 24 hours. Subsequently, the chemical compounds are applied to the cells at their determined IC50 values and left to incubate (24 hours). Following treatment, RNA is extracted from the cells using the PureLink RNA Mini Kit. The quality and amount of RNA obtained are evaluated using a Nanodrop spectrophotometer. cDNA synthesis is subsequently carried out using the High Capacity cDNA Reverse Transcription Kit.

RT-qPCR analysis

Real-time Quantitative polymerase chain reaction (RT-qPCR) analysis is conducted using the method described by Akıncı et al. (Akıncı et al., 2023). Primer sequences are provided in Table 1. This analysis assesses the expression levels of antioxidant enzymes, such as SOD, CAT, and GSH, as well as genes associated with apoptosis, such as Apaf-1, SMAC/DIABLO, Bax, Cas-9, Bcl-2, p53, and Cas-3. mRNA expression is evaluated through the comparative cycle threshold method ($2^-\Delta\Delta$ Ct) (Akıncı et al., 2023). Gene expression levels are analyzed relative to the control group and standardized using glyceraldehyde 3-phosphate dehydrogenase (GAPDH) mRNA as a reference.

Table 1. Primer sequences of the genes used for RT-qPCR analysis

Gene	Primer sequences (Forward/Reverse)		
SOD	5'-AGCTGCACCACAGCAAGCAC-3' (Tam et al. 2023) 5'-TCCACCACCCTTAGGGCTCA-3'		
CAT	5'-TCCGGGATCTTTTTAACGCCATTG-3' (Dkhil et al. 2016) 5'-TCGAGCACGGTAGGGACAGTTCAC-3'		
GSH	5'-ACTTGGCACTCCTCTGA-3' (Akıncı et al. 2023) 5'-AGGCACTAGAACCTGCTGGA-3'		
Cas-3	5'-GGTATTGAGACAGACAGTGG-3' (Oltulu et al. 2022) 5'-CATGGGATCTGTTTCTTTGC-3'		
Cas-9	5'-GAGTCAGGCTCTTCCTTTG-3' (Oltulu et al. 2022) 5'-CCTCAAACTCTCAAGAGCAC-3'		
Apaf-1	5'-GATATGGAATGTCTCAGATGGCC-3' (Yakovlev et al. 2001) 5'-GGTCTGTGAGGACTCCCCA-3'		
Bax	5'-TTCATCCAGGATCGAGCAGA-3' (Oltulu et al. 2022) 5'-GCAAAGTAGAAGGCAACG-3'		
Bcl-2	5'-ATGTGTGGGAGAGCGTCAA-3' (Oltulu et al. 2022) 5'-ACAGTTCCACAAAGGCATCC-3'		
p53	5'-CACGAGCGCTGCTCAGATAGC-3' (Oltulu et al. 2022) 5'-ACAGGCACAAACACGCACAAA-3'		
SMAC/DIABLO	5'-CTCTGTGGCTGAGGGTTGAT-3' (Tokatlı et al. 2020) 5'-TTGTAGATGCCCACAGG -3'		
GAPDH	5'-GTCTCCTCTGACTTCAACAGCG-3' (Bednarz-Misa et al. 2020) 5'-ACCACCCTGTTGCTGTAGCCAA-3'		

Statistical analysis

IC50 values were determined by probit analysis using MTT assay data. The AML-12 cell line is subsequently treated with the IC50 doses of EGCG and 5-FU, which are calculated as 0.38 μ M for EGCG and, 4.78 μ M for 5-FU respectively, for 24 hours. The relative fold-change values of gene expressions are analyzed using one-way *ANOVA* followed by post hoc *Tukey's test*, with statistical significance set at p < 0.05. Probit analysis and *ANOVA* tests are performed using SPSS 20 software (IBM).

RESULTS

MTT Assay

The MTT assay evaluates the effects of 5-FU, EGCG, and their combination (5-FU+EGCG) on the viability of AML-12 cells. The cells are incubated for 24 hours before the MTT assay. The results indicate a dose-dependent decline in cell viability across all treatment groups (5-FU, EGCG, and 5-FU+EGCG) compared to the control group (Figure 1). The IC50 values are presented in Figure 1.

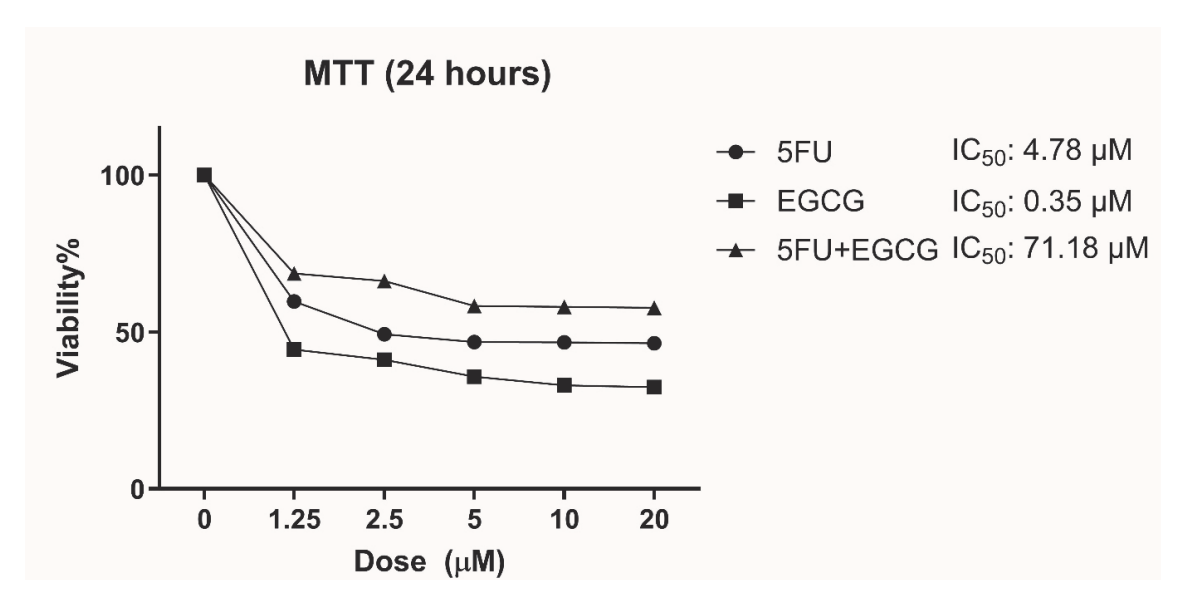


Figure 1. MTT assay results. The standard deviation is shown by vertical bars. (mean \pm std dev.) (The percentage of viability is calculated using the formula: (average absorbance of the sample/average absorbance of the control) \times 100.).

Antioxidant Gene mRNA Expression

CAT, SOD, and GSH are analyzed. SOD mRNA expression significantly increases in all treatment groups (EGCG, 5-FU, and 5-FU+EGCG) against the control group, with the combination group (5-FU+EGCG) exhibiting the highest expression levels (Figure 2A). Similar trends are observed for

CAT and GSH mRNA expression levels, where the combination group reveals a considerable improvement over the control and single-treatment groups (Figures 2B and 2C). These findings indicate that the combined application of EGCG and 5-FU enhances the antioxidant defense mechanism.

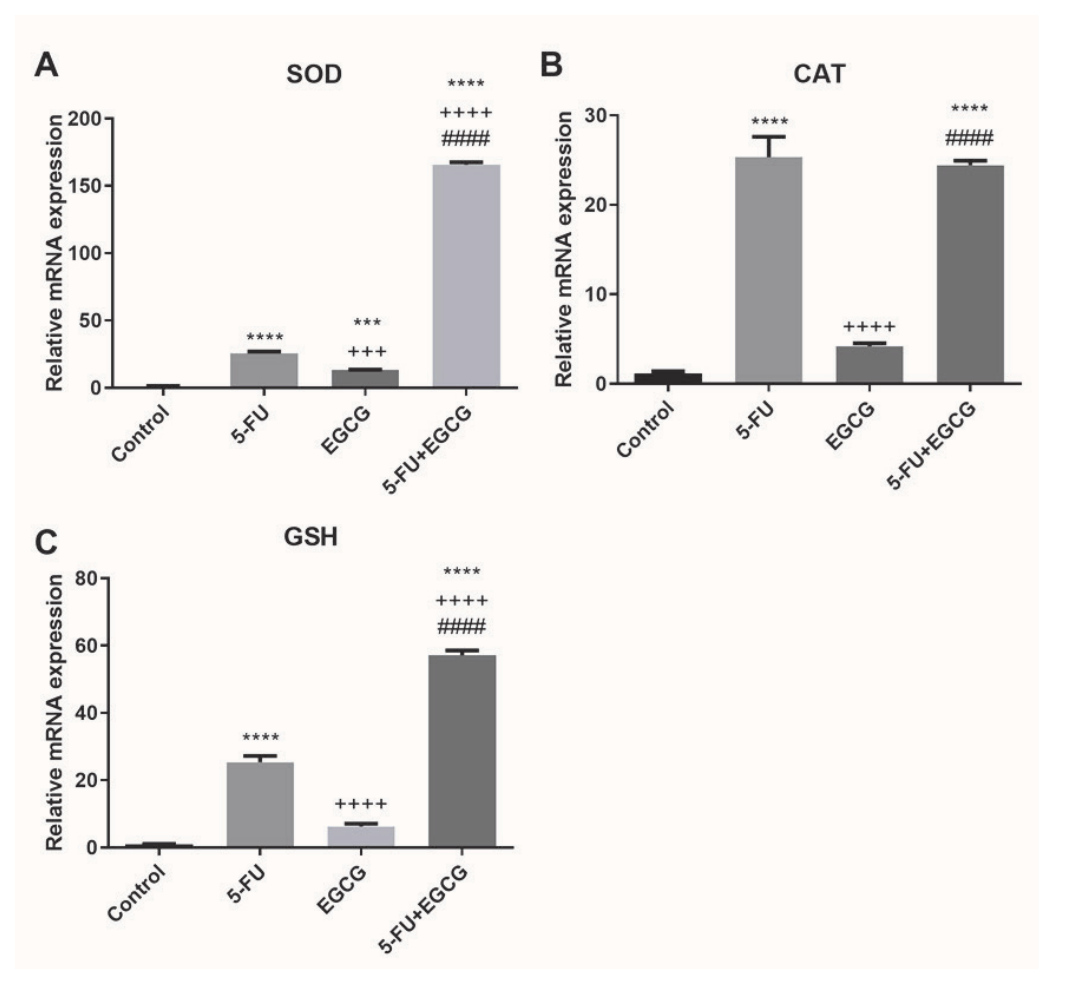


Figure 2. SOD (A), CAT (B), GSH (C) Relative mRNA Expression. **** p<0.0001, *** p<0.001 compared to control group, ++++ p<0.0001, +++ p<0.001 compared to 5-FU group, #### p<0.0001, ### p<0.001 compared to EGCG group.

Apoptosis-Related Gene mRNA Expression

The expression levels of apoptosis-related genes Bax, Apoptotic protease-activating factor 1 (Apaf-1), Bcl-2, Cas-9, p53, Cas-3, and SMAC/DIABLO are evaluated. Treatment with 5-FU significantly increases the expression of pro-apoptotic genes (Cas-3, SMAC/DIABLO, Cas-9, Bax, and Apaf-1), while anti-apoptotic Bcl-2 expression decreases against

the control group (Figure 3). Co-administration of EGCG and 5-FU leads to further upregulation of pro-apoptotic genes and p53 expression, suggesting enhanced apoptosis in the combination group (Figures 3A-3G). These findings imply that EGCG amplifies the apoptotic effects of 5-FU by regulating both anti- and pro-apoptotic pathways.

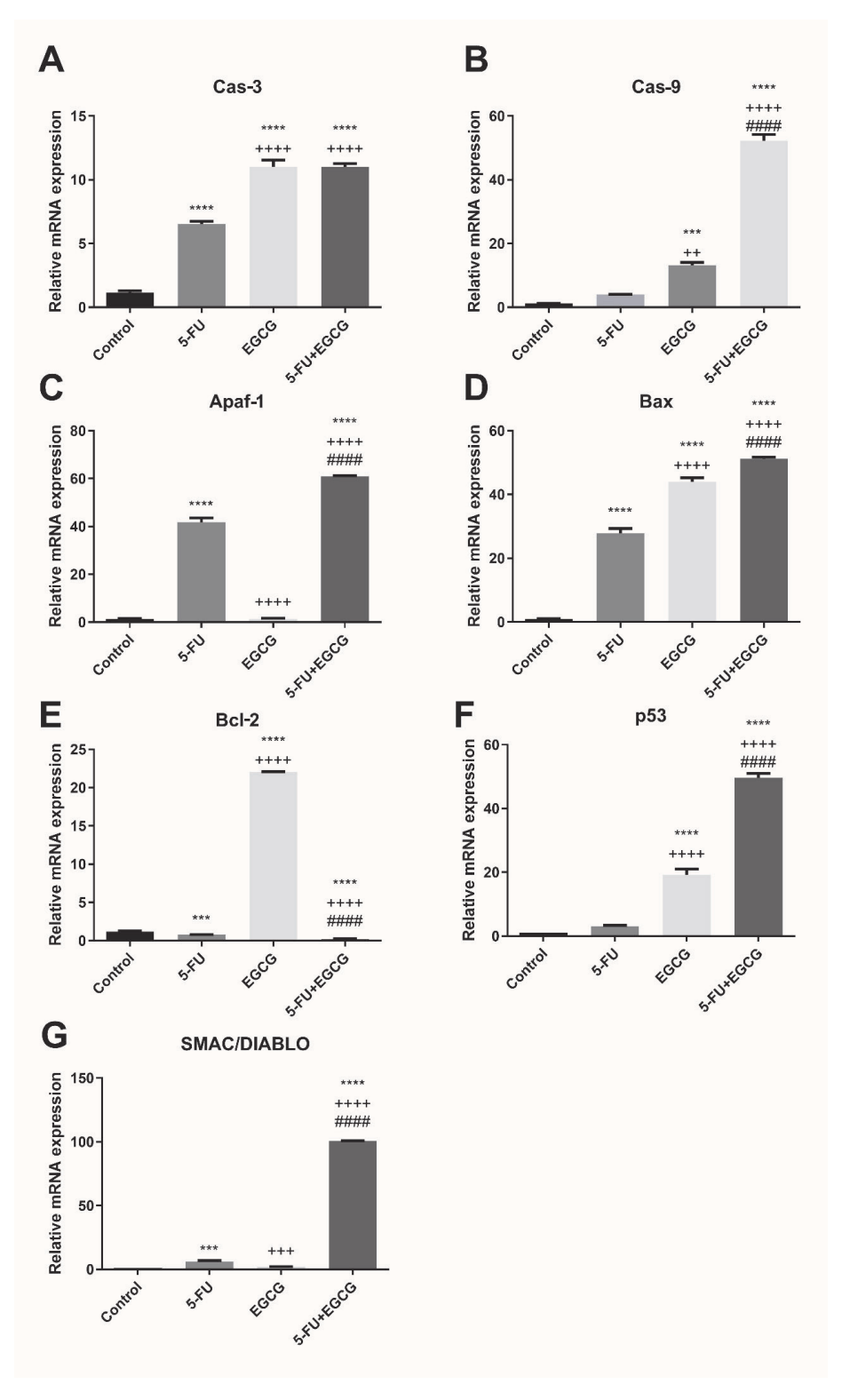


Figure 3. Cas-3 (A), Cas-9 (B), Apaf-1 (C), Bax (D), Bcl-2 (E), p53 (F), SMAC/DIABLO (G) Relative mRNA Expression. **** p<0.0001, *** p<0.001 comparing to control group, ++++ p<0.0001, +++ p<0.001 comparing to 5-FU group, #### p<0.0001 comparing to EGCG group.

DISCUSSION

The liver constitutes a vital organ responsible for maintaining health and homeostasis. It performs critical roles in numerous biochemical processes, including growth, disease defense, nutrient provisioning, and energy production. The primary functions of the liver include carbohydrate, protein, and fat metabolism, bile secretion, vitamin storage, and detoxification. A healthy liver is therefore indispensable for overall well-being. Hepatotoxicity denotes liver injury induced by various chemicals. Certain medications, particularly at high doses or in predisposed individuals, induce hepatotoxicity. Examples of hepatotoxins include acetaminophen and alcohol, along with herbal products and industrial chemicals. These agents damage hepatocytes, leading to dysfunction and potentially causing hepatitis, jaundice, liver fibrosis, or alcoholic liver disease. The liver injury induced by the drug is estimated to represent around 5% of all hospital admissions for acute liver failure (Pandit et al., 2012).

5-FU is commonly used in the treatment of various cancers. It is used either as monotherapy or in conjunction with other medications (Pujari and Bandawane, 2021). 5-FU, classified as an antimetabolic $drug, influences \, the \, synthesis \, of \, RNA \, and \, DNA \, in \, both$ tumor and normal cells. The predominant portion of 5-FU undergoes detoxification via the liver, with only a minor quantity excreted through the kidneys (Gelen et al., 2018). Toxic intermediates responsible for liver injury are produced during 5-FU metabolism. Studies demonstrate that 5-FU treatment induces oxidative stress in the liver, resulting in structural and functional abnormalities in hepatocytes, as observed in both in vitro and in vivo investigations (Tam et al., 2003). In response to 5-FU, increased activity levels of ALP (Alkaline Phosphatase), lactate dehydrogenase, and AST (Aspartate Aminotransferase) are observed (Gelen et al., 2018).

Traditional medicines have historically been used to treat liver ailments. The hepatoprotective benefits of

these remedies are often ascribed to their antioxidative characteristics and their ability to stimulate the body's innate antioxidative defense system. Given the role of oxidative stress in nearly all forms of liver damage, the antioxidative properties of these substances likely play a significant role in their hepatoprotective effects. Increasing data indicates that the therapeutic activity of natural substances is attributable to pharmacological qualities beyond antioxidative mechanisms (Domitrović and Potočnjak, 2016).

EGCG, the primary flavonoid in tea, is shown in numerous studies to mitigate drug-induced liver injury, although its precise mechanism of action remains unclear. For instance, in an experimental study conducted by Lin et al. in rats, EGCG demonstrates antioxidant activity that reduces acetaminopheninduced liver damage (Lin et al., 2021). This study focuses on EGCG's ability to prevent 5-FU-induced liver damage.

The increase in antioxidant enzyme mRNA expression levels (SOD, CAT, and GSH) observed in our study aligns with findings from Gelen et al. (Gelen et al., 2018), which demonstrate the depletion of these enzymes under 5-FU-induced oxidative stress. By enhancing their expression, EGCG appears to counteract the oxidative damage induced by 5-FU, consistent with the hepatoprotective effects reported by Lin et al. in acetaminophen-induced liver injury (Lin et al., 2021).

Recent findings reveal that 5-FU-induced liver and kidney damage is associated with elevated ROS levels. Antioxidant levels, such as SOD, CAT, and GSH, are shown to decrease in liver and kidney tissues following 5-FU administration. Furthermore, serum malondialdehyde (MDA) levels increase significantly. Studies in experimental animals indicate that 5-FU administration lowers SOD and GSH levels, accelerates lipid peroxidation, and significantly elevates serum ALT (Alanine Aminotransferase), AST, and ALP activity, leading to hepatotoxicity (Gelen et al., 2018).

EGCG, known for its anti-inflammatory and antioxidant activities, exhibits anticancer properties in animal studies. EGCG inhibits the proliferation of hepatocellular carcinoma cells and promotes apoptosis (Yang et al. 2012). Yang et al. (2012) demonstrate that EGCG enhances the suppression of cell proliferation induced by 5-FU in hepatocellular carcinoma cells. EGCG enhances the susceptibility of hepatocellular carcinoma cells to the anticancer properties of 5-FU. Moreover, EGCG and 5-FU exhibit a synergistic effect on chemoresistant cancer cells (Moracci et al., 2022). This study demonstrates that co-administration of EGCG with 5-FU significantly increases the mRNA expression levels of SOD, CAT, and GSH, supporting the antioxidant defense system.

Apoptosis, a physiological process that selectively eliminates undesirable cells, plays a pathological role in cases of cell injury. Cytotoxic or chemotherapeutic drug exposure induces oxidative stress, causing cell damage. Cancer progression can be mitigated by eliminating damaged cells through apoptosis (Coşkun and Özgür, 2011). DNA damage activates p53, a transcription factor that allows time for DNA repair while suppressing anti-apoptotic factors and promoting pro-apoptotic factors (Gökhan et al., 2020). Anti-apoptotic effectors like Bcl-2 are downregulated, while pro-apoptotic effectors such as Bax are released. Bax/Bak proteins oligomerize and translocate to the mitochondria, promoting outer membrane permeabilization. This facilitates the cytoplasmic translocation of pro-apoptotic proteins such as cytochrome c and SMAC/DIABLO. Cytochrome c and Apaf-1 form the apoptosome, which activates Cas-9 and subsequently Cas-3 (Pradhan et al., 2023). The upregulation of pro-apoptotic genes (SMAC/ DIABLO, Bax, Apaf-1, Cas-3, and Cas-9) and the downregulation of anti-apoptotic Bcl-2, observed upon 5-FU treatment, are consistent with apoptosis induction mechanisms described by Coşkun and Özgür (Coşkun and Özgür, 2011) and Pradhan et al. (Pradhan et al., 2023). The enhanced apoptotic response when EGCG is co-administered highlights its role in amplifying chemotherapeutic efficacy, as similarly demonstrated by Moracci et al. (Moracci et al., 2022) in chemoresistant cancer cells.

Our study builds upon the existing literature by providing comprehensive data on the dual role of EGCG in mitigating 5-FU-induced hepatotoxicity while enhancing its anticancer activity. Previous research has demonstrated the antioxidant properties of EGCG in preventing oxidative stress-induced liver damage (Lin et al., 2021) and its ability to enhance the cytotoxic effects of 5-FU in cancer models (Yang et al., 2012; Moracci et al., 2022). However, the precise mechanisms underlying these effects, particularly in the context of apoptosis and antioxidant gene modulation, remain poorly understood.

Our findings provide novel insights into the molecular pathways involved, demonstrating significant upregulation of key antioxidant enzymes (SOD, CAT, and GSH) and pro-apoptotic genes (SMAC/DIABLO, Bax, Apaf-1, Cas-9, and Cas-3) when EGCG is co-administered with 5-FU. This suggests that EGCG not only mitigates oxidative damage but also promotes the removal of damaged cells through apoptosis, thereby reducing the hepatotoxic effects of 5-FU and potentially enhancing its therapeutic efficacy.

By targeting both oxidative stress and apoptotic pathways, EGCG demonstrates a dual protective and synergistic effect when combined with 5-FU. These findings advance our understanding of the therapeutic synergy between natural compounds like EGCG and conventional chemotherapeutics such as 5-FU. They also validate the role of natural compounds in mitigating drug-induced toxicities, while emphasizing their potential to enhance cancer treatment outcomes. This study thus provides a foundation for future in vivo investigations and clinical trials to evaluate EGCG as a promising adjuvant therapy in cancer treatment.

CONCLUSION

The findings of this study demonstrate that EGCG protects the liver from 5-FU-induced damage through its antioxidant effects. Additionally, EGCG enhances the anticancer efficacy of 5-FU by inducing apoptosis, thereby facilitating the elimination of cells damaged by 5-FU. These results suggest that further in vivo studies and clinical research are warranted to evaluate the potential of EGCG in mitigating hepatotoxicity and enhancing cancer treatment outcomes.

ACKNOWLEDGEMENTS

This study was supported by the Trakya University Scientific Research Project Fund with the grant number 2018/274.

AUTHOR CONTRIBUTION STATEMENT

Concept, Design, Supervision, Resources, Materials, Data Collection and Processing, Analysis and Interpretation, Literature Search, Writing, Reviews (MA), Concept, Design, Resources, Materials, Data Collection and Processing, Analysis and Interpretation, Literature Search, Critical Reviews (ÇO), Concept, Design, Resources, Materials, Data Collection and Processing, Analysis and Interpretation, Literature Search, Critical Reviews (EB), Analysis and/or Interpretation, Literature Search, Writing, Critical Reviews (ZAÇY).

CONFLICT OF INTEREST

The authors declare that there is no conflict of interest.

REFERENCES

- Akıncı, M., Oltulu, C., Bakar, E., & Cevikelli Yakut, Z. A. (2023). Puerarin protects from methotrexate induced hepatotoxicity in AML-12 cells. *Nam Kem Medical Journal*, *11*(3), 193–201. https://doi.org/10.4274/nkmj.galenos.2023.27147
- Alam, M., Ali, S., Ashraf, G. M., Bilgrami, A. L., Yadav,
 D. K., & Hassan, M. I. (2022). Epigallocatechin
 3-gallate: From green tea to cancer therapeutics.
 Food Chemistry, 379, Article 132135. https://doi.org/10.1016/j.foodchem.2022.132135

- Bednarz-Misa, I., Neubauer, K., Zacharska, E., Kapturkiewicz, B., & Krzystek-Korpacka, M. (2020). Whole blood ACTB, B2M and GAPDH expression reflects activity of inflammatory bowel disease, advancement of colorectal cancer, and correlates with circulating inflammatory and angiogenic factors: Relevance for real-time quantitative PCR. Advances in Clinical and Experimental Medicine, 29(5), 547–556. https://doi.org/10.17219/acem/118845
- Cleeland, C. S., Allen, J. D., Roberts, S. A., Brell, J. M., Giralt, S. A., Khakoo, A. Y., & Skillings, J. (2012). Reducing the toxicity of cancer therapy: Recognizing needs, taking action. *Nature Reviews Clinical Oncology*, *9*(8), 471–478. https://doi.org/10.1038/nrclinonc.2012.99
- Coşkun, G., & Özgür, H. (2011). Apoptoz ve nekrozun moleküler mekanizması. *Arşiv*, *20*, 145.
- Dkhil, M. A., Moneim, A. E. A., & Al-Quraishy, S. A. (2016). Indigofera oblongifolia ameliorates lead acetate-induced testicular oxidative damage and apoptosis in a rat model. *Biological Trace Element Research*, 173, 354–361. https://doi.org/10.1007/s12011-016-0689-0
- Domitrović, R., & Potočnjak, I. (2016). A comprehensive overview of hepatoprotective natural compounds: Mechanism of action and clinical perspectives. *Archives of Toxicology*, *90*, 39–79. https://doi.org/10.1007/s00204-015-1580-z
- Dongsar, T. T., Dongsar, T. S., Gupta, N., Almalki, W. H., Sahebkar, A., & Kesharwani, P. (2023). Emerging potential of 5-fluorouracil-loaded chitosan nanoparticles in cancer therapy. *Journal of Drug Delivery Science and Technology*, Article 104371. https://doi.org/10.1016/j.jddst.2023.104371
- Gao, L., Shen, L., Yu, M., Ni, J., Xiao, D., Zhou, Y., & Wu, S. (2014). Colon cancer cells treated with 5-fluorouracil exhibit changes in polylactosaminetype n-glycans. *Molecular Medicine Reports*, 9(5), 1697–1702. https://doi.org/10.3892/ mmr.2014.2008

- Gelen, V., Şengül, E., Yıldırım, S., & Atila, G. (2018). The protective effects of naringin against 5-fluorouracil-induced hepatotoxicity and nephrotoxicity in rats. *Iranian Journal of Basic Medical Sciences*, 21(4), 404–410. https://doi.org/10.22038/IJBMS.2018.27510.6714
- Gökhan, A., Kılıç, K. D., Gülle, K., Uyanıkgil, Y., & Çavuşoğlu, T. (2020). Apoptotic pathways and targeted therapies. *Medical Journal of SDU, 27*(4), 565–573. https://doi.org/10.17343/sdutfd.619417
- Herrmann, J. (2020). Vascular toxic effects of cancer therapies. *Nature Reviews Cardiology*, *17*(8), 503–522. https://doi.org/10.1038/s41569-020-0347-2
- Hubert, C., Sempoux, C., Humblet, Y., van den Eynde, M., Zech, F., Leclercq, I., & Gigot, J. F. (2013). Sinusoidal obstruction syndrome (SOS) related to chemotherapy for colorectal liver metastases: Factors predictive of severe SOS lesions and protective effect of bevacizumab. HPB, 15(11), 858–864. https://doi.org/10.1111/hpb.12047
- Liczbiński, P., & Bukowska, B. (2022). Tea and coffee polyphenols and their biological properties based on the latest in vitro investigations. *Industrial Crops and Products*, 175, Article 114265. https:// doi.org/10.1016/j.indcrop.2021.114265
- Lin, Y., Huang, J., Gao, T., Wu, Y., Huang, D., Yan, F., & Weng, Z. (2021). Preliminary study on hepatoprotective effect and mechanism of (-)-epigallocatechin-3-gallate against acetaminophen-induced liver injury in rats. *Iranian Journal of Pharmaceutical Research*, 20(3), 46–56. https://doi.org/10.22037/ijpr.2020.112727.13918
- Mazrouei, R., Raeisi, E., Lemoigne, Y., & Heidarian, E. (2019). Activation of p53 gene expression and synergistic antiproliferative effects of 5-fluorouracil and β-escin on MCF7 cells. *Journal of Medical Signals & Sensors*, 9(3), 196–202. https://doi.org/10.4103/jmss.jmss_44_18

- Momiyam, K., Nagai, H., Ogino, Y., Mukozu, T., Matsui, D., Matsui, T., & ... (2015). Glutathione for hepatotoxicity in patients with liver cirrhosis and advanced hepatocellular carcinoma receiving hepatic arterial infusion chemotherapy. *Clinical Cancer Drugs*, *2*(1), 54–60. https://doi.org/10.1007/s00280-014-2564-z
- Moracci, L., Sensi, F., Biccari, A., Crotti, S., Gaio, E., Benetti, F., Traldi, P., Pucciarelli, S., & Agostini, M. (2022). An investigation on [5 fluorouracil and epigallocatechin-3-gallate] complex activity on HT-29 cell death and its stability in gastrointestinal fluid. *Oncotarget*, 13, 476–489. https://doi.org/10.18632/oncotarget.28207
- Oltulu, C., Akıncı, M., & Elvan, B. (2022). Antitumor activity of etoposide, puerarin, galangin and their combinations in neuroblastoma cells. *International Journal of Life Sciences and Biotechnology*, *5*(3), 407–423. https://doi.org/10.38001/ijlsb.1089164
- Pandit, A., Sachdeva, T., & Bafna, P. (2012). Druginduced hepatotoxicity: A review. *Journal of Applied Pharmaceutical Science*, 2(5), 233–243. https://doi.org/10.7324/JAPS.2012.2541
- Pradhan, A., Sengupta, S., Sengupta, R., & Chatterjee, M. (2023). Attenuation of methotrexate induced hepatotoxicity by epigallocatechin 3-gallate. *Drug* and Chemical Toxicology, 46(4), 717–725. https:// doi.org/10.1080/01480545.2022.2085738
- Pujari,R.,&Bandawane,D.D.(2021).Hepatoprotective activity of gentisic acid on 5-fluorouracil-induced hepatotoxicity in Wistar rats. *Turkish Journal of Pharmaceutical Sciences*, *18*(3), 332–338. https://doi.org/10.4274/tjps.galenos.2020.95870
- Ranjit, S., Anjleena, M., & Ranju, B. (2023). Synthetic cytotoxic drugs as cancer chemotherapeutic agents. In P. C. Acharya & M. Kurosu (Eds.), *Medicinal chemistry of chemotherapeutic agents* (pp. 499–537). Academic Press. https://doi.org/10.1016/B978-0-323-90575-6.00015-5

- Robinson, S. M., Wilson, C. H., Burt, A. D., Manas, D. M., & White, S. A. (2012). Chemotherapy-associated liver injury in patients with colorectal liver metastases: A systematic review and meta-analysis. *Annals of Surgical Oncology*, *19*, 4287–4299. https://doi.org/10.1245/s10434-012-2438-8
- Tam, N. N. C., Gao, Y., Leung, Y. K., & Ho, S. M. (2003). Androgenic regulation of oxidative stress in the rat prostate involvement of NAD(P) H oxidases and antioxidant defense machinery during prostatic involution and regrowth. American Journal of Pathology, 163(6), 2513–2522. https://doi.org/10.1016/S0002-9440(10)63606-1
- Tokatlı, C., Doğanlar, O., & Doğalar, Z. B. (2020). Meriç Delta balıklarında çevre kirliliğinin genotoksik etkileri: Antioksidan savunma, ısı şok protein sinyali ve DNA hasar-onarım mekanizmaları. Journal of Limnology and Freshwater Fisheries Research, 6(1), 14–24.
- Turker, N. P., & Bakar, E. (2023). Effects of L-dopa and p-coumaric acid combination on oxidative stress, DNA damage, and mitochondrial apoptosis in neuroblastoma cells. *Bangladesh Journal of Pharmacology, 18*(2), 49–57. https://doi.org/10.3329/bjp.v18i2.65531
- Vauthey, J. N., Pawlik, T. M., Ribero, D., & ... (2006). Chemotherapy regimen predicts steatohepatitis and an increase in 90-day mortality after surgery for hepatic colorectal metastases. *Journal of Clinical Oncology, 24*(13), 2065–2072. https://doi.org/10.1200/JCO.2005.05.3074
- Wang, L., Li, P., & Feng, K. (2023). EGCG adjuvant chemotherapy: Current status and future perspectives of radiopharmaceuticals in China. *European Journal of Medicinal Chemistry*, 250, Article 115197. https://doi.org/10.1007/s00259-021-05615-6

- Yakovlev, A. G., Ota, K., Wang, G., Movsesyan, V., Bao, W. L., & Yoshihara, K. (2001). Differential expression of apoptotic protease-activating factor-1 and caspase-3 genes and susceptibility to apoptosis during brain development and after traumatic brain injury. *The Journal of Neuroscience*, 21(19), 7439–7446. https://doi.org/10.1523/JNEUROSCI.21-19-07439.2001
- Yang, L., Jia, L., Li, X., Zhang, K., Wang, X., He, Y., & ... (2022). Prooxidant activity-based guideline for a beneficial combination of (–)-epigallocatechin-3-gallate and chlorogenic acid. *Food Chemistry*, 386, Article 132812. https://doi.org/10.1016/j. foodchem.2022.132812
- Yang, X. W., Wang, X. L., Cao, L. Q., Jiang, X. F., Peng, H. P., Lin, S. M., Xue, P., & Chen, D. (2012). Green tea polyphenol epigallocatechin-3-gallate enhances 5-fluorouracil-induced cell growth inhibition of hepatocellular carcinoma cells. *Hepatology Research*, 42(5), 494–501. https://doi. org/10.1111/j.1872-034X.2011.00947.x
- Yu, H., Liu, Y., Pan, W., & Shen, S. (2015).
 Polyunsaturated fatty acids augment tumoricidal action of 5-fluorouracil on gastric cancer cells by their action on vascular endothelial growth factor, tumor necrosis factor-alpha and lipid metabolism related factors. Archives of Medical Science, 11(2), 282–291. https://doi.org/10.5114/aoms.2015.50962
- Zhang, X., Wang, J., Hu, J., Huang, Y., Wu, X., Zi, C., & Sheng, J. (2016). Synthesis and biological testing of novel glucosylated epigallocatechin gallate (EGCG) derivatives. *Molecules*, 21(5), Article 620. https://doi.org/10.3390/molecules21050620

Mechanistic Insights into *Uncaria gambir* Ethanol Extract's Modulation of Cytoglobin and ECM Protein in Keloid Fibroblasts

Sri Widia A. JUSMAN*°, Maftuhatun Fista AMALIA**, Raisa NAULI***, Reni PARAMITA****, Sri NINGSIH******, Radiana Dhewayani ANTARIANTO******

Mechanistic Insights into Uncaria gambir Ethanol Extract's Modulation of Cytoglobin and ECM Protein in Keloid Fibroblasts

SUMMARY

Keloids are benign tumors that result from abnormal wound healing. These growths may cause cosmetic and functional problems, especially when they grow in the joint area. Although the pathogenesis is not fully understood, stimulated fibroblasts cause excess collagen deposition in the extracellular matrix, leading to keloid formation. They also synthesize cytoglobin, the overexpression of which can protect against the fibrotic process. At present, keloid therapy remains unoptimized, primarily because keloids often experience recurrence after treatment. Therefore, studies to find keloid therapy are still being carried out. This study explored the effect of ethanol extract of Uncaria gambir (EG) on the expression of cytoglobin, elastin, desmosine, and collagen type I, and III of keloid fibroblasts. Fibroblasts were isolated from keloid and non-keloid skin tissues using primary culture techniques. An enzyme-linked immunosorbent assay (ELISA) method was used to determine the expression of cytoglobin, elastin, and desmosine. Meanwhile, immunocytochemistry was used to determine collagen I and III expression. The results showed that EG increased the expressions of cytoglobin, elastin, and desmosine while reducing the expression of collagen types I and III. EG is likely to have potential as an anti-keloid.

Key Words: Cytoglobin, extracellular matrix, fibroblast, keloid, Uncaria gambir.

Uncaria gambir Etanol Ekstresinin Keloid Fibroblastlarda Sitoglobin ve ECM Proteininin Modülasyonuna İlişkin Mekanik İçgörüler

ÖZ

Keloidler, anormal yara iyileşmesi sonucu oluşan iyi huylu tümörlerdir. Özellikle eklem bölgesinde büyüdüklerinde kozmetik ve fonksiyonel sorunlara neden olabilmektedir. Patogenezi tam olarak anlaşılmamış olsa da uyarılmış fibroblastlar, ekstraselüler matrikste aşırı kollajen birikimine neden olarak keloid oluşumuna yol açmaktadir. Ayrıca, aşırı eksprese edilmesi fibrotik sürece karşı koruma sağlayabilen sitoglobini de sentezlerler. Günümüzde keloid tedavisi hala optimize edilememiştir, çünkü keloidler genellikle tedaviden sonra sıklıkla tekrarlar. Bu nedenle, keloid tedavisini bulmaya yönelik araştırmalar devam etmektedir. Bu çalışmada, Uncaria gambir (EG) etanol ekstresinin keloid fibroblastlardaki sitoglobin, elastin, desmosin ve tip I ve III kollajen ekspresyonu üzerindeki etkisi araştırılmıştır. Fibroblastlar, primer kültür teknikleri kullanılarak keloid ve keloid olmayan deri dokularından izole edilmiştir. Sitoglobin, elastin ve desmosin ekspresyonunu belirlemek için enzim bağlantılı immünosorbent testi (ELISA) yöntemi kullanılmıştır. Öte yandan, kollajen I ve III ekspresyonunu belirlemek için immünositokimya kullanılmıştır. Sonuçlar, EG'nin sitoglobin, elastin ve desmosin ekspresyonunu artırırken, kollajen tip I ve III ekspresyonunu azalttığını göstermiştir. EG'nin anti-keloid potansiyele sahip olduğu düşünülmektedir.

Anahtar Kelimeler: Sitoglobin, hücre dışı matris, fibroblast, keloid, Uncaria gambir.

Received: 20.11.2024 Revised: 19.03.2025 Accepted: 14.04.2025

ORCID:0000-0002-8169-6825, Department of Biochemistry and Molecular Biology, Faculty of Medicine, Universitas Indonesia, Jakarta 10430, Indonesia, Center of Hypoxia and Oxidative Stress Studies, Faculty of Medicine Universitas Indonesia, Jakarta 10430, Indonesia

[&]quot;ORCID: 0000-0001-5992-6359, Master's Programme in Biomedical Sciences, Faculty of Medicine, Universitas Indonesia, Jakarta 10430, Indonesia

[&]quot;ORCID: 0009-0001-5390-4551, Master's Programme in Biomedical Sciences, Faculty of Medicine, Universitas Indonesia, Jakarta 10430, Indonesia

[&]quot;**ORCID: 0000-0003-2968-3629, Department of Biochemistry and Molecular Biology, Faculty of Medicine, Universitas Indonesia, Jakarta 10430, Indonesia, Center of Hypoxia and Oxidative Stress Studies, Faculty of Medicine Universitas Indonesia, Jakarta 10430, Indonesia, Master's Programme in Biomedical Sciences, Faculty of Medicine, Universitas Indonesia, Jakarta 10430, Indonesia

[&]quot;" ORCID: 0000-0002-6139-7625, Health Research Organization, Research Center for Pharmaceutical Ingredient and Traditional Medicine, National Research and Innovation Agency (BRIN), LAPTIAB Building No. 610, PUSPIPTEK Serpong Area, South Tangerang, Banten 15314, Indonesia

^{······} ORCID:0000-0002-8578-7505, Department of Histology, Faculty of Medicine, Universitas Indonesia, Jakarta 10430, Indonesia

[°] Corresponding Author; Sri Widia A. Jusman Email: sriwidiaaj@gmail.com

INTRODUCTION

During wound healing, neutrophils and macrophages release transforming growth factor (TGF)-1 and platelet-derived growth factor (PDGF), activating fibroblasts to differentiate into myofibroblasts, which produce extracellular matrix (ECM) components, primarily collagen (Andrews et al., 2016). Myofibroblasts express α-SMA and nonmuscle myosins, enhancing contractility (Shinde et al., 2017). Under normal conditions, they undergo apoptosis, regulated by interleukin-1 (IL-1), fibroblast growth factor-1 (FGF-1), and prostaglandin E2 (PGE2). However, failed apoptosis leads to prolonged myofibroblast activity, disrupting ECM composition and contributing to keloid formation (Cohen et al., 2017; Hinz & Lagares, 2020). Collagen provides structural strength, while elastin, rich in desmosine (DES) and other amino acids, maintains skin elasticity (Baumann et al., 2021; Leiva et al., 2018; Schräder et al., 2018).

Excess ECM deposition characterizes keloids, leading to persistent fibrotic growth beyond the original wound margins (Andrews et al., 2016; Nangole & Agak, 2019). Studying keloid pathology in vivo is challenging, as keloids do not develop in experimental animals, making in vitro fibroblast cultures a widely accepted alternative for investigating keloid-associated cellular and molecular mechanisms. Previous studies have demonstrated that fibroblasts isolated through primary culture retain their phenotype according to the tissue sources, supporting the relevance of this model (Deng et al., 2021; Ningsih et al., 2024; Qin et al., 2021). To provide a comparative baseline, non-keloid fibroblasts (NKFs) from surrounding skin are used as controls, as previous studies have shown that they offer a reliable reference for assessing fibroblast behavior and ECM composition in keloid research (Ningsih et al., 2024; Qin et al., 2021).

Fibroblasts expressed cytoglobin (CYGB), a vertebrate globin protein expressed in various tissues (Burmester et al., 2002; Nakatani et al., 2004). While its function remains unclear, CYGB is regulated by the

hypoxia-inducible-factor-1α (HIF-1α) protein, which enhances its expression under hypoxia. Inhibiting HIF-1α with ibuprofen reduced CYGB expression in keloid fibroblast (KF) (Jusman et al., 2019), and siR-NA-mediated CYGB inhibition impaired mitochondrial biogenesis and function in KFs (Jusman et al., 2021). CYGB is also involved in oxygen distribution and free radical scavenging under hypoxic conditions (Guo et al., 2007; Jusman et al., 2014; Mathai et al., 2020; Xu et al., 2006). Furthermore, CYGB overexpression exhibits antifibrotic effects in the liver, kidney, and ocular tissues (Mimura et al., 2010; Wei et al., 2019; Xu et al., 2006).

Keloids frequently recur despite available treatments, highlighting the need for alternative therapies (Sutheno, 2021). Gambir (Uncaria gambir [W.Hunter] Roxb.), a plant rich in polyphenolic compounds, is widely cultivated in West Sumatra and possesses anti-lipid peroxidation, antibacterial, antiseptic, and antioxidant properties (Dewi & Pratiwi, 2018; Fasrini & Lipoeto, 2021; Jusman et al., 2022; Melia et al., 2015; Ningsih et al., 2014). Recent studies suggest its therapeutic potential. Ethanolic extract of gambir (EG) has hepatoprotective effects in a carbon tetrachloride (CCl₄) induced liver injury (Fahrudin et al., 2015) and prevents bleomycin-induced pulmonary fibrosis by inhibiting nuclear factor kappa beta (NFκB), transforming growth factor beta (TGF-β), tissue inhibitor metalloproteinase (TIMP)-1, and collagen type-I (COL I) formation (Desdiani et al., 2022). Additionally, the in-silico analysis revealed that gambirin A1, procyanidin B2, and neooxygambirtanninecomponents found in EG-can bind to PDGF-A, potentially inhibiting its activity (Jusman et al., 2022). These findings provide insight into possible molecular mechanisms of EG in modulating keloid fibroblast proliferation. This study examines the effects of EG on CYGB and ECM components (elastin, desmosine, collagen I/III) in keloid fibroblasts. While CYGB is not an established fibrosis marker, it has been reported to have antifibrotic potential, particularly through oxidative stress regulation. Investigating its expression in response to EG may provide new insights into keloid pathophysiology. ECM markers were selected as they are key indicators of fibrosis progression (Deng et al., 2021; Limandjaja et al., 2020).

MATERIAL AND METHODS

Study design

The study adopted an experimental design using KFs as the primary culture. We obtained keloid tissues from three women at the Tanjung Priok Hospital in Jakarta, Indonesia, whose previous Caesarean section wounds had developed keloids and who had undergone another Caesarean section procedure. The KFs were divided into an untreated control group and groups treated with different concentrations of EG. This study also used the normal keloid fibroblasts (NKFs) cultured in a complete medium without EG as an additional control. The NKFs used in this study were isolated from normal tissue around keloid wounds. All the keloid tissues were acquired with the patient's consent. The study was conducted from June 2021 to February 2022 at the Department of Biochemistry and Molecular Biology and the Department of Histology, Faculty of Medicine, Universitas Indonesia. The Faculty of Medicine Universitas Indonesia Research Ethics Commission approved this study's ethics evaluation with the number 472/UN2. F1/ETIK/2016.

Uncaria gambir extraction

The ethanol extract of gambir used in this study was obtained from Dr. Sri Ningsih of the Health Research Organization, Research Center for Pharmaceutical Ingredients and Traditional Medicine (BRIN). The gambir, sourced from a community product in West Sumatra, Indonesia, was identified at the Biology Department of the Indonesian Institute of Sciences (LIPI) Cibinong, Indonesia, and herbarium specimen has been deposited at LIPI with the reference number 1085/IPH.1.02./If.8/VI/2013.

To prepare the extract, the whole part of the *Uncaria gambir* plant was steamed and then pressed to

obtain the sap. The sap was left overnight, dried in an oven at 45–50°C, and further ground. A 25 g dried gambir sap was soaked in ethanol and shaken for 24 hours before filtration. The resulting filtrates were then separated and evaporated under a vacuum at 45°C until a semisolid mass was formed. To obtain the dried extract, all samples were further dried in an oven at 40°C for 24 hours.

Fibroblast isolation

We isolated the KFs and NKFs using explant cultures, as described in our previous study (Ningsih, et al., 2024; Siregar et al., 2019). All the isolation procedures were conducted in a biological safety cabinet (BSC) II. Keloid and nonkeloid tissues were chopped into smaller fragments (1 \times 1 \times 1 mm) before being cultured in a 24-well plate with a complete culture medium consisting of low glucose DMEM (Cat No. 11885084, Gibco, New York, USA), 10% FBS (Cat No. A4766901, Gibco, New York, USA), 1% amphotericin (Cat No. 15290026, Gibco, New York, USA), and 1% penicillin-streptomycin (Cat No. 15140122, Gibco, New York, USA). The tissues were incubated at 37°C with 5% CO2. Cells that reached 80% confluence were harvested using Tryple Select (Cat No. 12563029, Gibco, New York, USA) and counted using an automated LUNA cell counter. Flow cytometry with CD73+, CD105+, and CD90+ marker antibodies (BD Stemflow, New Jersey, USA) was used to examine the fibroblast population. The fibroblasts used in this study were from passages 4 to 6.

EG treatment of KF cultures

The EG was dissolved in ethanol at a concentration of 1000 ppm. The working concentrations of EG for KF treatment were determined based on the IC $_{50}$ test from our previous study (Jusman et al., 2022), which were 12.5 and 50 μ g/mL. Before application, the extract was diluted in a complete culture medium to achieve the final working concentration, ensuring that the ethanol concentration remained at a level that did not affect cell viability. The KFs were grown in culture at a density of $3x10^5$ cells/well in a complete me-

dium. They were incubated for 24 hours at 37°C with 5% CO₂. After that, the cells were treated with EG at 12.5 and 25 µg/mL for another 24 hours. The total protein from each group of cells was isolated and then analyzed for research parameters such as All analyses of CYGB [Cat No. MBS2533318, Mybiosource, San Diego, USA], ELN [Cat No. MBS2021199 Mybiosource, San Diego, USA], and DES [Cat no. MBS730011, San Diego, USA] were performed using sandwich ELISA according to the manufacturer's protocol.

Isolation of proteins from KFs and NKFs

For total protein analysis, KF cells treated with various concentrations of EG and nonkeloid fibroblast cells were extracted and isolated using a mammalian protein extraction reagent (Cat No. 78505, Thermo-Fisher, Rockford, IL, USA). The total protein concentration was measured using a Bradford assay (Cat No. 5000006, Bio-Rad, CA, USA).

Immunocytochemistry analysis of COL I and COL III

COL I and COL III were measured using an immunocytochemistry method based on that used in our previous study (Nauli et al., 2023). First, at a density of 1.5 x 103 cells/well, KFs and NKFs were cultured in a complete medium for 72 hours at 37° C with 5 % CO₂. After 72 hours, the KF cells were treated with EG at different concentrations for 24 hours. The cells were incubated with a 1:100 diluted primary antibody of COL I (Invitrogen, Catalog No. PA1-2604, Rockford, USA) and COL III (Cat No. PA1-28870, Invitrogen, Rockford, USA) for 2 hours. After that, the cells were incubated for 1 hour in a 1:400 dilution of IgG-HRP antibody (Cat No. A1949, Sigma-Aldrich, Saint Louis, USA). Along with hematoxylin, 3,3'-diaminobenzidine (DAB) was used to stain the cells. Microphotographs of each group were documented using Optilab Viewer 3.0.

Statistical analysis

The data obtained were analyzed using GraphPad Prism version 10.1.0. We presented the data from triplicate experiments in mean and standard deviation (SD) values. We used a one-way analysis of vari-

ance (ANOVA) followed by least significant differences (LSD) as a post hoc test for normally distributed data. Statistical significance was set to $\alpha = 5\%$, a 95% confidence interval (CI), and a *P*-value of < 0.05.

RESULTS

Cytoglobin concentration

CYGB concentrations were significantly lower in KFs (176 \pm 10.1 pg/mg protein) than in NKFs (639 \pm 9.44 pg/mg protein) (Figure 1). The addition of EG 12.5 µg/mL (212 \pm 10.5 pg/mg protein) and 25 µg/mL (235 \pm 8.73 pg/mg protein) significantly increased CYGB concentration in keloid fibroblasts compared to the absence of EG (176 \pm 10.1 pg/mg protein). Similarly, CYGB concentrations were significantly higher in fibroblasts treated with EG 25 µg/mL than EG 12.5 µg/mL. The result indicated that CYGB concentration in KFs rose as the EG concentration increased (ANO-VA, LSD test, p < 0.05).

Elastin concentration

The addition of EG 12.5 μ g/mL (140 \pm 1.021 pg/mg protein) and 25 μ g/mL (157 \pm 1.074 pg/mg protein) to KFs increased ELN protein concentration significantly compared to EG-untreated KFs (120 \pm 0.972 pg/mg protein). ELN concentrations in fibroblasts treated with EG 25 μ g/mL were significantly higher than those treated with EG 12.5 μ g/mL. Like CYGB, the concentration of ELN in KFs increased with the rising concentration of EG used (Figure 2). Nevertheless, ELN concentrations in all KF treatment groups remained significantly lower compared to the NKF group.

Desmosine concentration

Significant differences in DES concentration were found between all groups, demonstrating that KF contained substantially less DES than NKF (Figure 3). When EG 12.5 μ g/mL (173 \pm 3.85 pg/mg protein) and 25 μ g/mL (207 \pm 6.14 pg/mg protein) were added to keloid fibroblast cultures, DES levels increased significantly compared to KF without EG addition (157 \pm 2.21 pg/mg protein) (ANOVA, LSD test, p < 0.05).

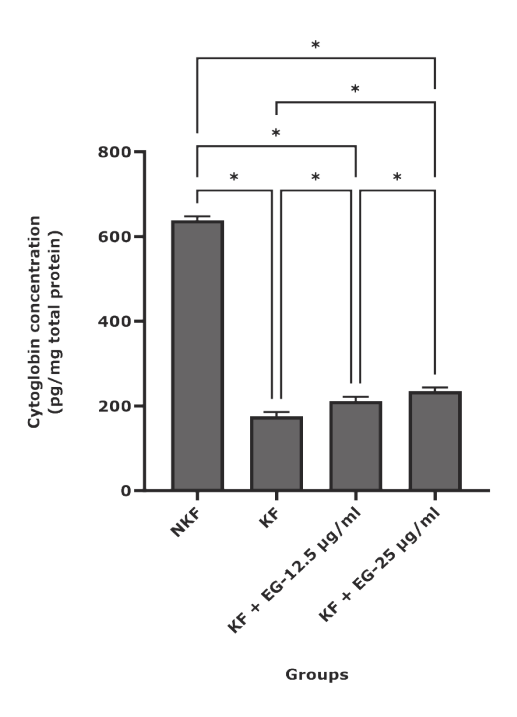


Figure 1. Cytoglobin concentrations in nonkeloid (NKF) and keloid fibroblasts (KF) without and with the addition of various concentrations of EG (ANO-

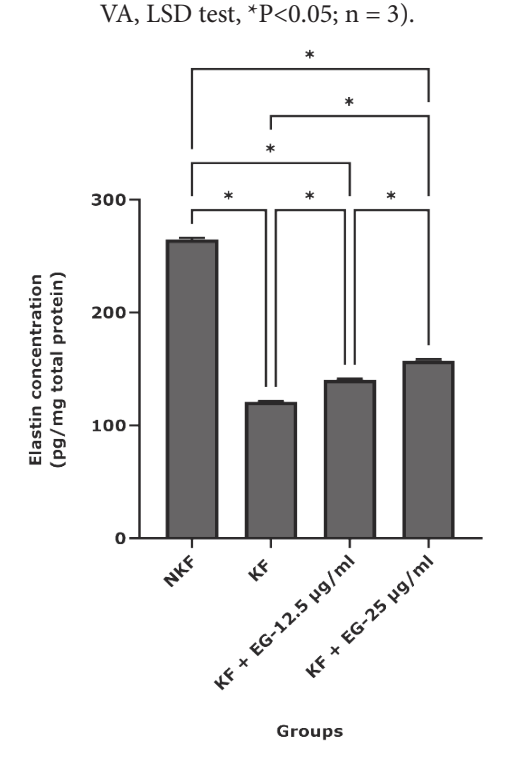


Figure 2. Concentrations of elastin in nonkeloid (NKF) and keloid fibroblasts (KF) with and without the addition of EG at various concentrations (ANO-VA, LSD test, P<0.05; n=3).

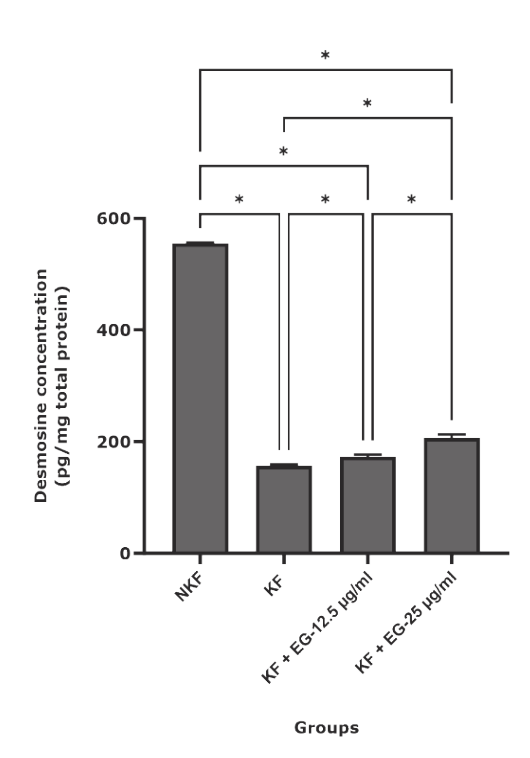


Figure 3. Desmosine concentrations in nonkeloid (NKF) and keloid fibroblasts (KF) in the absence and presence of varying concentrations of EG. (ANOVA, LSD test, $^*P<0.05$; n=3).

COL I and COL III distribution

In the NKF, each fibroblast expressed COL I, indicated by the brownish granular appearance of the cell membrane and adjacent extracellular areas (Figure 4A). These results were also found in the KFs (Figures 4B–D). The COL I expression patterns in the EG-treated groups (at both 12.5 μ g/mL and 25 μ g/mL concentrations) were different from those observed in the untreated group, and the EG-treated groups showed predominantly intracytoplasmic COL I expression (Figures 4C and 4D). COL I expression in KF treated with 12.5 μ g/mL EG distinctly showed more prominent COL I (Figure 4C) than in KF treated with 25 μ g/mL EG (Figure 4D).

In the NKF cultures, fibroblasts expressed COL III, indicated by the brownish granular appearance of the cytoplasm, membrane, and adjacent extracellular areas (Figure 4E). These results were also found in KF, which expressed COL III predominantly in the extracellular area (Figures 4F–H). COL III expression

in the EG-treated groups showed different expression levels at 12.5 μ g/mL and 25 μ g/mL concentrations. The 12.5 μ g/mL EG-treated group showed intracytoplasmic COL III expression (Figure 4G), while the 25 μ g/mL EG-treated group showed minimal to no

COL III expression (Figure 4H). Based on the result, KF treated with 12.5 μ g/mL EG clearly showed more prominent COL III (Figure 4G) compared to KFs treated with 25 μ g/mL EG (Figure 4H).

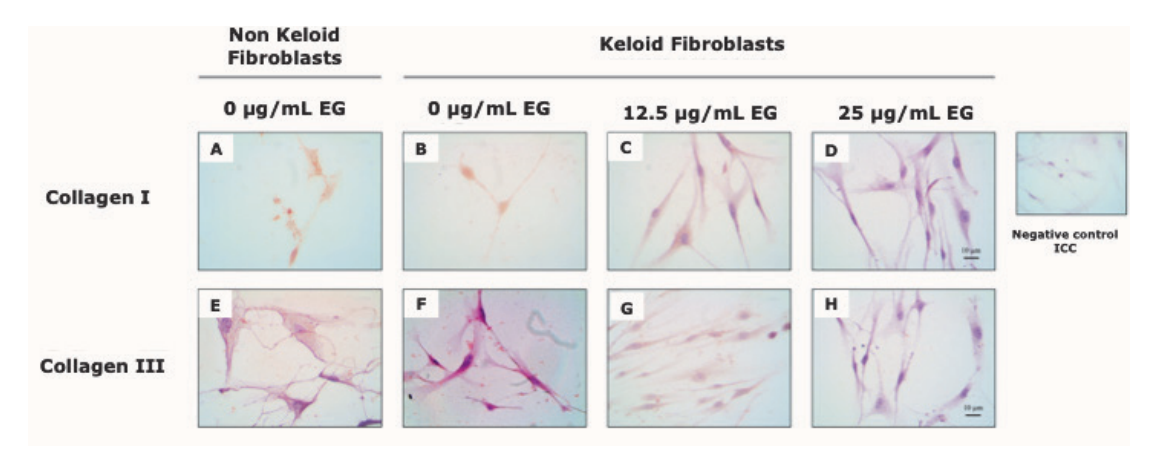


Figure 4. Immunocytochemistry of COL I and III from nonkeloid fibroblast culture (A &E); keloid fibroblast culture without treatment (B&F); keloid fibroblast culture treated with 12.5 μ g/mL EG (C&G); and keloid fibroblast culture treated with 25 μ g/mL EG (D&H). These microphotographs were taken as representative microphotographs from each group random five high power field microphotographs using Optilab. The scale bar represents 10 μ m. Negative control is shown in the right upper side.

Discussion

This study examined the effect of EG on KFs and found that EG at 12.5 and 25 μ g/mL increased CYGB levels in KFs compared to untreated KFs, although levels remained lower than in NKFs. CYGB, known for its antifibrotic properties, reduces ROS, leading to decreased α -smooth muscle expression and COL I levels (Dat et al., 2021; Hieu et al., 2022; Lv et al., 2018; Okina et al., 2020). CYGB's antioxidant role helps lower oxidative stress, as shown by reduced kidney nitrotyrosine accumulation with CYGB overexpression (Mimura et al., 2010).

In keloids, increased activation and proliferation of fibroblasts cause elevated ROS, leading to excessive collagen production, inflammation, and fibrosis (Desdiani et al., 2020; Siregar et al., 2019). EG may help reduce ROS and fibrosis in keloids by increasing CYGB expression, which has ROS-scavenging properties. Our previous study showed that CYGB expression has a negative correlation with ROS levels in KFs (Siregar et al., 2019). EG's effect on CYGB expression may involve 276

the TGF- β signaling pathway. Okina et al. found that TGF- β reduced CYGB expression in hepatic stellate cells through the pSMAD2/SP-3 M1 pathway, leading to oxidative stress and liver fibrosis (Okina et al., 2020). In silico studies by Desdiani et al. showed that components of *U. gambir* (e.g., (+)-catechin, epigallocatechin gallate, procyanidin B3) had strong binding affinities with TGF- β , potentially blocking its receptor (Desdiani et al., 2020). Thus, EG may prevent TGF- β from binding to its receptor, increasing CYGB expression (Desdiani et al., 2020). Therefore, the presence of EG components may prevent TGF- β from binding to its receptor and cause increased CYGB expression.

The results showed that EG treatment (12.5 and 25 μ g/mL) increased ELN expression in KFs compared to untreated KFs. The mechanism behind this increase is unclear but may involve the inhibition of fibroblast activation into myofibroblasts, leading to higher matrix metalloproteinase (MMP) activity, particularly MMP-9. This stabilizes ELN in the extracellular matrix, as MMP-9 is known to degrade ELN. The study also found that DES amino acid expression increased

with ELN, as DES is a key component of ELN (Ozsvar et al., 2021). DES forms cross-links with other amino acids like AA, IDES, and LNL to create ELN. According to Ozsvar et al., tropoelastin, an ELN precursor, cross-links with lysine and DES through the action of lysyl oxidase (LOX), which is crucial for ECM renewal (Ozsvar et al., 2021).

Immunocytochemistry revealed differences in COL I and III distribution in KFs, suggesting that EG may inhibit the secretion of COL I from the cytoplasm to the extracellular matrix. Higher EG concentrations (12.5 and 25 μ g/mL) showed greater inhibition of COL I and III expression. This may be due to EG's ability to inhibit the TGF- β signaling pathway, which regulates ECM components like collagen (Tong et al., 2019). EG components may bind to TGF- β receptors, thus influencing collagen expression (Desdiani et al., 2020).

Additionally, EG may reduce collagen deposition by inhibiting the PDGF-α/PDGFR-α signaling pathway. A previous *in silico* study showed that EG components like gambirin A1, procyanidin B2, and neooxygambirtannine could bind to PDGFA, potentially inhibiting PDGF activity (Jusman et al., 2022). Since fibrosis involves excessive ECM formation and deposition (Klinkhammer et al., 2018), and PDGF/PDG-FR signaling plays a key role in fibrosis development (Olson & Soriano, 2009), inhibiting this pathway may help prevent fibrosis.

Overall, EG (12.5 and 25 μ g/mL) significantly increased CYGB, ELN, and DES expression while reducing COL I and III secretion in KFs. These ECM changes, along with CYGB upregulation, may contribute to fibrosis modulation, suggesting EG's potential as a treatment for keloid fibrosis. However, this study has several limitations. The collagen secretion was assessed using immunocytochemistry, which provides localization data but lacks precise quantification. Future studies should incorporate biochemical validation of EG's active compounds and quantitative protein analysis to further clarify its antifibrotic mechanisms. The proposed mechanism of *U. gambir* ethanol extract in inhibiting keloid in this study is illustrated in Figure 5.

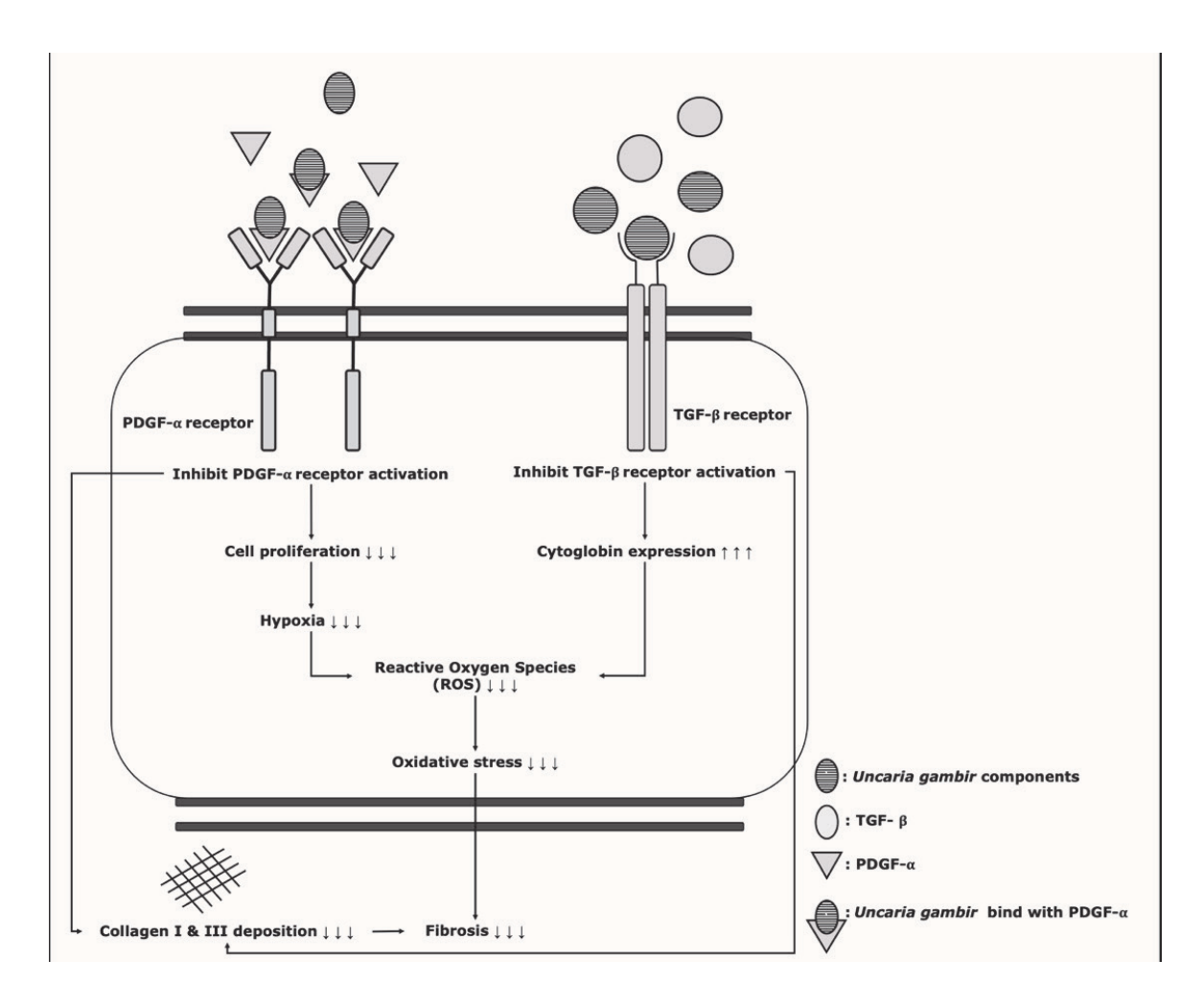


Figure 5. The proposed mechanism of *Uncaria gambir* inhibits fibrosis in keloid through PDGF and TGF-β

CONCLUSION

Treatment with 12.5 μ g/mL and 25 EG significantly increased CYGB, ELN, and DES expression in KFs but decreased COL I and COL III secretion from the cytoplasm to extracellular areas in KFs. Therefore, EG is a potential candidate for the future treatment of keloids.

ACKNOWLEDGMENTS

Many thanks to the Research Center for Medicinal Raw Materials and Traditional Medicines-BRIN, Indonesia, for the ethanol extract of gambir (*Uncaria gambir* (Hunter) Roxb.), and to dr. Jimmy Panji Wirawan, Sp.OG from Tanjung Priok Regional General Hospital, North Jakarta for the keloid tissue. We also express our gratitude to the Ministry of Research 278

and Technology of the Republic of Indonesia / National Research and Innovation Agency of the Republic of Indonesia for funding this study (Hibah Penelitian Dasar Unggulan Perguruan Tinggi (PDUPT) No. NKB 140/UN2.RST/HKP.05.00/2021).

AUTHOR CONTRIBUTION RATE STATE-MENTS

SWAJ: Study concept and design, analysis and interpretation of data, critical revision of the manuscript for important intellectual content, contributing to the completion of the manuscript, obtained funding, study supervision; MFA: Acquisition of data, analysis, and interpretation of data, drafting the manuscript, statistical analysis, contributing to the completion of the manuscript; RN: Acquisition of data, analysis, and

interpretation of data, critical revision of the manuscript, technical and administrative support, contributing to the completion of the manuscript; RP: Technical support, contributing to the completion of the manuscript, study supervision; SN: Material support, contributing to the completion of the manuscript; RDA: Technical and material support, study supervision; contributing to the completion of the manuscript.

CONFLICT OF INTEREST

Authors declare that there is no conflict of interest.

REFERENCES

- Andrews, J. P., Marttala, J., Macarak, E., Rosenbloom, J., & Uitto, J. (2016). Keloids: The paradigm of skin fibrosis Pathomechanisms and treatment. *Matrix Biology*, *51*, 37–46. https://doi.org/10.1016/j.matbio.2016.01.013
- Baumann, L., Bernstein, E. F., Weiss, A. S., Bates, D.,
 Humphrey, S., Silberberg, M., & Daniels, R. (2021).
 Clinical Relevance of Elastin in the Structure and
 Function of Skin. *Aesthetic Surgery Journal Open Forum*, 3(3), ojab019. https://doi.org/10.1093/as-jof/ojab019
- Burmester, T., Ebner, B., Weich, B., & Hankeln, T. (2002). Cytoglobin: A Novel Globin Type Ubiquitously Expressed in Vertebrate Tissues. *Molecular Biology and Evolution*, 19(4), 416–421. https://doi.org/10.1093/oxfordjournals.molbev.a004096
- Dat, N. Q., Thuy, L. T. T., Hieu, V. N., Hai, H., Hoang,
 D. V., Thi Thanh Hai, N., ... Kawada, N. (2021).
 Hexa Histidine-Tagged Recombinant Human
 Cytoglobin Deactivates Hepatic Stellate Cells and
 Inhibits Liver Fibrosis by Scavenging Reactive
 Oxygen Species. Hepatology, 73(6), 2527–2545.
 https://doi.org/10.1002/hep.31752

- Deng, Z., Subilia, M., Chin, I. L., Hortin, N., Stevenson, A. W., Wood, F. M., ... Fear, M. W. (2021). Keloid fibroblasts have elevated and dysfunctional mechanotransduction signaling that is independent of TGF-β. *Journal of Dermatological Science*, 104(1), 11–20. https://doi.org/10.1016/j.jdermsci.2021.09.002
- Desdiani, D., Rengganis, I., Djauzi, S., Setiyono, A., Sadikin, M., Jusman, S. W. A., ... Eyanoer, P. C. (2022). Fibropreventive and Antifibrotic Effects of Uncaria gambir on Rats with Pulmonary Fibrosis. *Evidence-Based Complementary and Alternative Medicine*, 2022, 1–11. https://doi.org/10.1155/2022/6721958
- Desdiani, D., Rengganis, I., Djauzi, S., Setiyono, A., Sadikin, M., Jusman, S. W. A., ... Fadilah, F. (2020). In vitro Assay and Study Interaction of Uncaria gambir (Hunter) Roxb. as Anti-fibrotic Activity Against A549 Cell Line. *Pharmacognosy Journal*, 12(6), 1232–1240. https://doi.org/10.5530/pj.2020.12.172
- Dewi, S. R. P., & Pratiwi, A. (2018). The Effect of Gambier Extracts (Uncaria gambir [Roxb]) as Antiseptic on Gingival Wound in Rats. 5(1), 80–88.
- Fahrudin, F., Solihin, D. D., Kusumorini, N., & Ningsih, S. (2015). Isolasi Efektifitas Ekstrak Gambir (Uncaria gambir (Hunter) Roxb.) sebagai Hepatoprotektor pada Tikus (Rattus norvegicus L.) yang Diinduksi CCl4. 13(2), 115–122.
- Fasrini, U., & Lipoeto, N. (2021). Gambir catechins modulates amyloid-β concentration in cerebrospinal fluid of Alzheimer's model rat. *IOP Con*ference Series: Earth and Environmental Science, 741(1), 012068. https://doi.org/10.1088/1755-1315/741/1/012068
- Guo, X., Philipsen, S., & Tan-Un, K.-C. (2007). Study of the hypoxia-dependent regulation of human CYGB gene. *Biochemical and Biophysical Research Communications*, 364(1), 145–150. https://doi. org/10.1016/j.bbrc.2007.09.108

- Hieu, V. N., Thuy, L. T. T., Hai, H., Dat, N. Q., Hoang, D. V., Hanh, N. V., ... Kawada, N. (2022). Capacity of extracellular globins to reduce liver fibrosis via scavenging reactive oxygen species and promoting MMP-1 secretion. *Redox Biology*, *52*, 102286. https://doi.org/10.1016/j.redox.2022.102286
- Hinz, B., & Lagares, D. (2020). Evasion of apoptosis by myofibroblasts: a hallmark of fibrotic diseases. *Nature Reviews Rheumatology*, *16*(1), 11–31. https://doi.org/10.1038/s41584-019-0324-5
- Jusman, Sri W.A, Iswanti, F. C., Suyatna, F. D., Ferdinal, F., Wanandi, S. I., & Sadikin, M. (2014).
 Cytoglobin expression in oxidative stressed liver during systemic chronic normobaric hypoxia and relation with HIF-1α. *Medical Journal of Indonesia*, 23(3), 133–138. https://doi.org/10.13181/mji. v23i3.1025
- Jusman, Sri W.A, Sari, D. H., Ningsih, S. S., Hardiany, N. S., & Sadikin, M. (2019). Role of Hypoxia Inducible Factor-1 Alpha (HIF-1α) in Cytoglobin Expression and Fibroblast Proliferation of Keloids. 65(1), E10-18.
- Jusman, Sri Widia A., Amalia, M. F., Paramita, R., Ningsih, S., & Fadilah, F. (2022). Structure-based screening of inhibitor platelet-derived growth factor from ethanol extract of Uncaria gambir (Hunter) Roxb. as an antifibrotic in keloid fibroblast cells. *Journal of Applied Pharmaceutical Science*. https://doi.org/10.7324/JAPS.2023.59304
- Jusman, Sri Widia A, Azzizah, I. N., Sadikin, M., & Hardiany, N. S. (2021). Is the Mitochondrial Function of Keloid Fibroblasts Affected by Cytoglobin? Malaysian Journal of Medical Sciences, 28(2), 39–47. https://doi.org/10.21315/mjms2021.28.2.4
- Klinkhammer, B. M., Floege, J., & Boor, P. (2018).
 PDGF in organ fibrosis. Molecular Aspects of Medicine, 62, 44–62. https://doi.org/10.1016/j. mam.2017.11.008

- Leiva, O., Leon, C., Kah Ng, S., Mangin, P., Gachet, C., & Ravid, K. (2018). The role of extracellular matrix stiffness in megakaryocyte and platelet development and function. *American Journal of Hematology*, 93(3), 430–441. https://doi.org/10.1002/ ajh.25008
- Limandjaja, G. C., Niessen, F. B., Scheper, R. J., & Gibbs, S. (2020). The Keloid Disorder: Heterogeneity, Histopathology, Mechanisms and Models. Frontiers in Cell and Developmental Biology, 8, 360. https://doi.org/10.3389/fcell.2020.00360
- Lv, W., Booz, G. W., Fan, F., Wang, Y., & Roman, R. J. (2018). Oxidative Stress and Renal Fibrosis: Recent Insights for the Development of Novel Therapeutic Strategies. *Frontiers in Physiology*, 9, 105. https://doi.org/10.3389/fphys.2018.00105
- Mathai, C., Jourd'heuil, F. L., Lopez-Soler, R. I., & Jourd'heuil, D. (2020). Emerging perspectives on cytoglobin, beyond NO dioxygenase and peroxidase. *Redox Biology*, 32, 101468. https://doi.org/10.1016/j.redox.2020.101468
- Melia, S., Novia, D., & Indri, J. (2015). Antioxidant and Antimicrobial Activities of Gambir (Uncaria gambir Roxb) Extracts and Their Application in Rendang. 14(12), 938–941.
- Mimura, I., Nangaku, M., Nishi, H., Inagi, R., Tanaka, T., & Fujita, T. (2010). Cytoglobin, a novel globin, plays an antifibrotic role in the kidney. *American Journal of Physiology-Renal Physiology*, 299(5), F1120–F1133. https://doi.org/10.1152/ajprenal.00145.2010
- Nakatani, K., Okuyama, H., Shimahara, Y., Saeki, S., Kim, D.-H., Nakajima, Y., ... Yoshizato, K. (2004). Cytoglobin/STAP, its unique localization in splanchnic fibroblast-like cells and function in organ fibrogenesis. *Laboratory Investigation*, 84(1), 91–101. https://doi.org/10.1038/labin-vest.3700013

- Nangole, F. W., & Agak, G. W. (2019). Keloid pathophysiology: fibroblast or inflammatory disorders? *JPRAS Open*, 22, 44–54. https://doi.org/10.1016/j.jpra.2019.09.004
- Nauli, R., Wanandi, S. I., Sadikin, M., Antarianto, R. D., & Jusman, S. W. A. (2023). Inhibition of ALA dehydratase activity in heme biosynthesis reduces cytoglobin expression which is related to the proliferation and viability of keloid fibroblasts. *Journal of Clinical Biochemistry and Nutrition*, 73(3), 185–190. https://doi.org/10.3164/jcbn.23-25
- Ningsih, S., Fachrudin, F., Rismana, E., Purwaningsih, E. H., Sumaryono, W., & Jusman, S. W. A. (2014). Evaluation Of Antilipid Peroxidation Activity Of Gambir Extract On Liver Homogenat In Vitro. 6(3), 982–989.
- Ningsih, S. S., Jusman, S. W. A., Syaidah, R., Nauli, R., & Fadilah, F. (2024). Efficient protocol for isolating human fibroblast from primary skin cell cultures: application to keloid, hypertrophic scar, and normal skin biopsies. *Biology Methods and Protocols*, *9*(1), bpae082. https://doi.org/10.1093/biomethods/bpae082
- Okina, Y., Sato-Matsubara, M., Matsubara, T., Dai-koku, A., Longato, L., Rombouts, K., ... Kawada, N. (2020). TGF-β1-driven reduction of cytoglobin leads to oxidative DNA damage in stellate cells during non-alcoholic steatohepatitis. *Journal of Hepatology*, 73(4), 882–895. https://doi.org/10.1016/j.jhep.2020.03.051
- Olson, L. E., & Soriano, P. (2009). Increased PDGFRα Activation Disrupts Connective Tissue Development and Drives Systemic Fibrosis. *Developmental Cell*, *16*(2), 303–313. https://doi.org/10.1016/j. devcel.2008.12.003

- Ozsvar, J., Yang, C., Cain, S. A., Baldock, C., Tarakanova, A., & Weiss, A. S. (2021). Tropoelastin and Elastin Assembly. *Frontiers in Bioengineering and Biotechnology*, *9*, 643110. https://doi.org/10.3389/fbioe.2021.643110
- Qin, H., Liu, R., Nie, W., Li, M., Yang, L., Zhou, C., ... Zhang, G. (2021). Comparison of Primary Keloid Fibroblast Cultivation Methods and the Characteristics of Fibroblasts Cultured from Keloids, Keloid-surrounding Tissues, and Normal Skin Tissues. *International Journal of Morphology*, 39(1), 302–310. https://doi.org/10.4067/S0717-95022021000100302
- Schräder, C. U., Heinz, A., Majovsky, P., Karaman Mayack, B., Brinckmann, J., Sippl, W., & Schmelzer, C. E. H. (2018). Elastin is heterogeneously cross-linked. *Journal of Biological Chemistry*, 293(39), 15107–15119. https://doi.org/10.1074/ jbc.RA118.004322
- Shinde, A. V., Humeres, C., & Frangogiannis, N. G. (2017). The role of α-smooth muscle actin in fibroblast-mediated matrix contraction and remodeling. *Biochimica et Biophysica Acta (BBA) Molecular Basis of Disease*, *1863*(1), 298–309. https://doi.org/10.1016/j.bbadis.2016.11.006
- Siregar, F. M., Hardiany, N. S., & Jusman, S. W. A. (2019). Negative Correlation between Cytoglobin Expression and Intracellular ROS Levels in Human Skin Keloid Fibroblasts. *The Indonesian Biomedical Journal*, 11(1), 48–51. https://doi. org/10.18585/inabj.v11i1.488
- Sutheno, A. (2021). Keloid after orthopedic surgery: prevention, current therapy modalities, and emerging therapies modalities. *Bali Medical Journal*, *10*(1), 225–228. https://doi.org/10.15562/bmj. v10i1.2264

- Tong, T., Park, J., Moon, Y., Kang, W., & Park, T. (2019). α-Ionone Protects Against UVB-Induced Photoaging in Human Dermal Fibroblasts. *Molecules*, 24(9), 1804. https://doi.org/10.3390/molecules24091804
- Wei, H., Lin, L., Zhang, X., Feng, Z., Wang, Y., You, Y., ... Hou, Y. (2019). Effect of cytoglobin overexpression on extracellular matrix component synthesis in human tenon fibroblasts. *Biological Research*, 52(1), 23. https://doi.org/10.1186/s40659-019-0229-4
- Xu, R., Harrison, P. M., Chen, M., Li, L., Tsui, T., Fung, P. C. W., ... Farzaneh, F. (2006). Cytoglobin Overexpression Protects against Damage-Induced Fibrosis. *Molecular Therapy*, 13(6), 1093–1100. https://doi.org/10.1016/j.ymthe.2005.11.027

Cytotoxic Potential and Apoptotic Mechanism of Digigrandifloroside: A Cardioactive Glycoside Targeting Caspase 3/7

Vahap Murat KUTLUAY**, İclal SARAÇOĞLU**

Cytotoxic Potential and Apoptotic Mechanism of Digigrandifloroside: A Cardioactive Glycoside Targeting Caspase 3/7

SUMMARY

Cardioactive glycosides (CGs) have been used mainly for their positive inotropic effects. However, recent studies on CGs showed their antitumor potential in several cancers. Cytotoxicity of a CG digigrandifloroside was tested against MCF-7 and HeLa cancer cells by the MTT method. Lanatoside A-C, and digitonin were also tested for comparison. To determine the role of apoptosis via caspase 3 and 7, the Caspase-Glo 3/7 test was used. The predicted biological activities of the compounds were also evaluated via the PASSONLINE database. IC50 values for cytotoxic activity of digigrandifloroside against MCF-7 and HeLa cells were found as<100 nM and 252.1 nM, respectively. Digigrandifloroside at 100 nM increased enzyme levels, 1.29 and 2.35 fold, compared to the control cells for MCF-7 and HeLa cells, respectively. These findings suggest the role of apoptosis. Digitonin, a steroidal saponin, showed relatively lower cytotoxicity when compared to CGs on both cells. According to the results obtained from the PASSONLINE database, the potential biological activities of the compounds were reported as, anticarcinogenic activity, antineoplastic activity in lung and breast cancer, caspase 3 and 8 stimulant activity, tp53 expression enhancer activity, together with anti-inflammatory activity, and chemopreventive potential. Digigrandifloroside has an activating effect on caspase 3; this has been proved with the help of biological activity testing. Digigrandifloroside IC50 found for MCF-7 cells is higher than for HeLa cells. It is a well-known fact that MCF-7 cells do not have caspase 3. That is why the higher IC50 found for MCF-7 cells can be connected with the tend to caspase 3 stimulation of digigrandifloroside.

Key Words: Cardioactive glycosides, Digitalis, Cytotoxicity, MCF-7, HeLa

Dijigrandiflorozitin Sitotoksik Potansiyeli ve Apoptotik Mekanizması: Kaspaz 3/7'yi Hedefleyen Bir Kardiyoaktif Glikozit

ÖZ

Kardiyoaktif glikozitler (KG'ler) esas olarak pozitif inotropik etkileri için kullanılmıştır. Bununla birlikte, KG'ler üzerinde yapılan son çalışmalar, çeşitli kanserlerde antitümör potansiyellerini göstermiştir. Bir KG olan dijigrandiflorozit'in sitotoksisitesi, MTT yöntemi ile MCF-7 ve HeLa kanser hücrelerine karşı test edilmiştir. Karşılaştırma için lanatozit A-C ve dijitonin de test edilmiştir. Kaspaz 3 ve 7 yoluyla apoptozisin rolünü belirlemek için, Kaspaz-Glo 3/7 testi kullanılmıştır. Bileşiklerin öngörülen biyolojik aktiviteleri de PASSONLINE veritabanı üzerinden değerlendirilmiştir. Dijigrandiflorozit'in MCF-7 ve HeLa hücrelerine karşı sitotoksik aktivitesi için İC50 değerleri sırasıyla <100 nM ve 252,1 nM olarak bulunmuştur. 100 nM'deki dijigrandiflorozit, MCF-7 ve HeLa hücreleri için kontrol hücreleriyle karşılaştırıldığında enzim seviyelerini sırasıyla 1,29 ve 2,35 kat artırmıştır. Bu bulgular apoptozisin rolünü göstermektedir. Steroidal bir saponin olan dijitonin, her iki hücrede de KG'lerle karşılaştırıldığında nispeten daha düşük sitotoksisite göstermiştir. PASSONLINE veritabanından elde edilen sonuçlara göre, bileşiklerin potansiyel biyolojik aktiviteleri antikarsinojenik aktivite, akciğer ve meme kanserinde antineoplastik aktivite, kaspaz 3 ve 8 uyarıcı aktivite, tp53 ekspresyon arttırıcı aktivite, anti-inflamatuar aktivite ve kemopreventif potansiyel olarak bildirilmiştir. Dijigrandiflorozit, kaspaz 3 üzerinde aktive edici bir etkiye sahiptir; bu, biyolojik aktivite testi yardımıyla kanıtlanmıştır. MCF-7 hücreleri için bulunan Digigrandifloroside IC50 değeri, HeLa hücrelerine göre daha yüksektir. MCF-7 hücrelerinin kaspaz 3'e sahip olmadığı iyi bilinen bir gerçektir. Bu nedenle MCF-7 hücreleri için bulunan daha yüksek IC50, dijigrandiflorozitin kaspaz 3'ü uyarma eğilimiyle bağlantılı olabileceği değerlendirilmiştir.

Anahtar Kelimeler: Kardiyoaktif glikozitler, Digitalis sitotoksisite, MCF-7, HeLa

Received: 8.12.2024 Revised: 8.04.2025 Accepted: 17.04.2025

ORCID: 0000-0003-4135-3497, Department of Pharmacognosy, Faculty of Pharmacy, Hacettepe University, Ankara, Türkiye.

[&]quot; ORCID: 0000-0003-0555-6262, Department of Pharmacognosy, Faculty of Pharmacy, Lokman Hekim University, Ankara, Türkiye.

INTRODUCTION

The genus *Digitalis* has 27 species mainly distributed in northwest Africa, Europe, and Anatolia. They are known as "foxglove" due to their flower shape named in Latin. (Kreis, 2017). The genus *Digitalis* belongs to the Plantaginaceae family (Albach, Meudt, & Oxelman, 2005). Phenylethanoids, terpenoids, saponins, anthraquinones, flavonoids, and some other compounds have been reported from the genus so far (Kutluay, Ishiuchi, Makino, & Saracoglu, 2019a). *Digitalis* species is well known for its CG content and has been used in the treatment of cardiac diseases for a long while in history (Kreis, 2017).

The first use of cardiac glycosides (CG) as medicine to treat cardiac diseases such as heart failure was reported by William Withering as an extract of *Digitalis purpurea* in 1785 (Prassas & Diamandis, 2008).

In addition to being composed of molecules that are similar in structure, CGs are also a group that exhibits comparable pharmacological effects. Historically, they have been used as arrow poison for hunting and war in Africa, Asia, and South America. Throughout history, it has also been used as an emetic, diuretic, and heart tonic (Morsy, 2017).

These structures are distributed in several genera in some families, such as Apocynaceae (Adenium, Acokanthera, Strophanthus, Apocynum, Cerbera, Tanghinia, Thevetia, Nerium, Carissa, and Urechites), Asclepiadaceae (Gomphocarpus, Calotropis, Pachycarpus, Asclepias, Xysmalobium, Cryptostegia, Menabea, and Periploca), Liliaceae (Urginea, Bowiea, Convallaria, Ornithogalum, and Rohdea), Ranunculaceae (Adonis and Helleborus), Moraceae (Antiaris, Antiaropsis, Naucleopsis, Maquira, and Castilla), Cruciferae (Erysimum and Cheiranthus), Sterculiaceae (Mansonia), Tiliaceae (seeds of Corchorus), Celastraceae (Euonymus, Lophopetalum), Leguminosae (Coronilla) and Plantaginaceae (Digitalis) (Evans, 2002).

Epidemiological studies reported that people who use CGs as a treatment have a lower rate of death risk

of cancer (Prassas & Diamandis, 2008). After the first studies held in the second half of the 20th century, researchers have reported so many findings for the anticancer activity of CGs (Ainembabazi, Zhang, & Turchi, 2023). Among cancer, breast, lung, colorectal, prostate and stomach leads in the number of diagnosed patients (Sung et al., 2021).

CGs have been shown to inhibit Na+/K+-ATPase and induce the immune system to show anticancer activity. CGs block the Na+/K+-ATPase pump, causing elevated levels of intracellular calcium that are sufficient to lead to cell death in cancer cells (Prassas & Diamandis, 2008; Skubník, Pavlícková, & Rimpelová, 2021). Even though Na+/K+-ATPase is accepted as one of the mechanisms of action for CGs the whole process has not been elucidated yet. In a study by Gupta et al., they reported that CGs were 100-fold cytotoxic to human cells when compared with rodent cells. Rodent Na+/K+-ATPase activity was shown to be inhibited in higher concentrations of CGs (Gupta, Chopra, & Stetsko, 1986). In the past few years, many studies have revealed that cardiac glycosides show anticancer activity by blocking different signal transduction pathways implicated in cell proliferation and cell survival. Digoxin, digitoxin, lanatoside C, oleandrin, and some other CGs were studied in detail to decipher the effects and mechanism of action of these compounds (Duan et al., 2021; Durmaz et al., 2016; Karakoyun et al., 2021; Yang et al., 2022).

Digigrandifloroside (13- epidigoxigenin 3-O- β - glucopyranosyl (1 \rightarrow 4) digitoxopyranoside), is a CG that was isolated from *D. grandiflora* Miller, an endemic plant for Balkan region. Digigrandifloroside was reported to show promising results on the HEp-2 cell line (Kutluay, Makino, Inoue, & Saracoglu, 2019b).

In this study, we aimed to compare the cytotoxicity potential of the compound with other well-known CGs such as lanatosides A-C and a saponin called digitonin which was previously isolated by *Digitalis* species. For this purpose the potential biological activities were evaluated and experimentally tested.

MATERIAL AND METHOD

Compounds

Digigrandifloroside was obtained from our previous isolation studies (Kutluay, Makino, et al., 2019). Lanatosides A-C (Fluka, AG, Buchs, Germany) and digitonin (Merck, Germany) were used in biological activity assays. MEM's Earle medium and Fetal bovine serum were obtained from Sigma Aldrich. Penicillin-streptomycin and trypsin (Biowest, France), Caspase 3/7 Glo assay kit (Promega Corporation, Madison, WI, USA), MTT (Sigma Aldrich), dimethylsulfoxide (Merck, Germany) were purchased.

Biological activity prediction

Using the PASSONLINE database (https://www.way2drug.com/PASSOnline/index.php), the biological activities of digigrandifloroside, lanatosides A–C, and digitonin were predicted (Filimonov et al., 2014). This extensive database offers information on the possible actions of substances in over 4,000 biological processes. The Pa (probability to be active) and Pi (probability to be passive) values are used to express the results. If a compound's Pa value is higher than its Pi value, suggesting a higher probability of biological action, it is deemed potentially active.

Cytotoxic activity

For cytotoxic activity assays, HeLa (human cervical carcinoma), and MCF-7 (human breast adenocarcinoma), cell lines were employed. A volume of 100 μ L of cells was seeded into a 96-well plate at a density of 3×10⁴ cells/mL for HeLa and 8×10⁴ cells/mL for MCF-7. MEM's Earle medium was used to culture cells. The cells were maintained in media supplemented with 10% FBS and 1% penicillin-streptomycin solution in a humidified atmosphere containing 5% CO₂ at 37 °C for 24 h. Subsequently, the cells were exposed to various concentrations of samples (0.1-10 μ M) for an additional 48 h. Following incubation, the cells were washed and the medium was replaced with fresh media. To each well, 10 μ L of MTT solution (5 mg/mL in

phosphate-buffered saline) was added and incubated for 4 h. Then, $100~\mu L$ of dimethylsulfoxide was added to dissolve the formazan crystals produced by viable cells. Absorbance was measured at 570/620~nm using a microplate reader. The results were presented as the percentage of inhibition in treated cells compared to untreated control cells (Saracoglu, Inoue, Calis, & Ogihara, 1995). The averages of three independent tests were calculated.

Determination of caspase 3/7 activity

HeLa (ATCC: CCL-2) and MCF-7 (ATCC: HTB-22) cell lines were cultured in their respective growth media, which were supplemented with 10% fetal bovine serum (FBS) and 1% penicillin-streptomycin, and maintained in a humidified incubator at 37°C with 5% CO₂. For the Caspase-Glo 3/7 assay (Promega Corporation, Madison, WI, USA), cells were seeded into 96-well white-walled plates at a density of cells 3×10⁴ cells/mL for HeLa and 8×10⁴ cells/mL for MCF-7 and allowed to adhere through 24-h incubation. After that test compounds were added to the cells; control wells received an equivalent volume of vehicle. Following the 48 h treatment, the Caspase-Glo Reagent was brought to room temperature, and an equal volume of this reagent was subsequently added into each well. The plates were subsequently incubated in the dark at room temperature and gently shaken using a plate shaker for 30 seconds. We assayed luminescence using a plate-reading luminometer (BioTek Instruments, Winooski, VT, USA), with the signal indicative of caspase-3/7 activity. All luminescence readings of treated wells were divided by the average control well to calculate relative caspase-3/7 activity that was plotted as percent control.

RESULTS and DISCUSSION

Compounds; 4 CG named digigrandifloroside, lanatoside A-C, and a steroidal saponin digitonin were selected for evaluation and comparison of their role in selected cancer cells (Figure 1). One of the compound selection criteria was to compare the aglycone of CGs. Lanatosides A-C has all the same sugar moiety but

different types of aglycones. Lanatoside A has digitoxigenin, Lanatoside B has gitoxigenin, Lanatoside C has digoxigenin skeleton. Digigrandifloroside has

epidigoxigenin skeleton. To compare the cytotoxicity profile of CGs with a steroidal saponin which was also isolated from the *Digitalis* genus previously used.

Figure 1. The chemical structures of the compounds tested in the study

Biological activity prediction of selected compounds

To assess the potential targets before *in vitro* and *in vivo* studies, there are some tools used for biological activity prediction. PASS (Prediction of Activity Spectra for Substances) is one of the applications that is used often in research studies. This software provides predictions of various types of biological activities. This biological activity can consist of pharmacotherapeutic effects, biochemical mechanisms, toxicity, metabolism, and gene expression regulation (Filimonov et al., 2014). All selected compounds were applied to the software and results were obtained. The probabil-

ity of the results is given as the probability of being active 'Pa' and the probability of being inactive 'Pi'. Results with higher values of Pa than 0.7 were selected as a threshold. Predicted biological activities are given in Supplementary Table 1 and Figure 2. Cancer is a complex disease with underlying several mechanisms. The potential biological activities of the compounds were elucidated. Anticarcinogenic activity, antineoplastic activity in lung and breast cancer, caspase 3 and 8 stimulant, tp53 expression enhancer activity, together with anti-inflammatory activity, and chemopreventive potential were reported as potential biological activities of these compounds related to cancer.

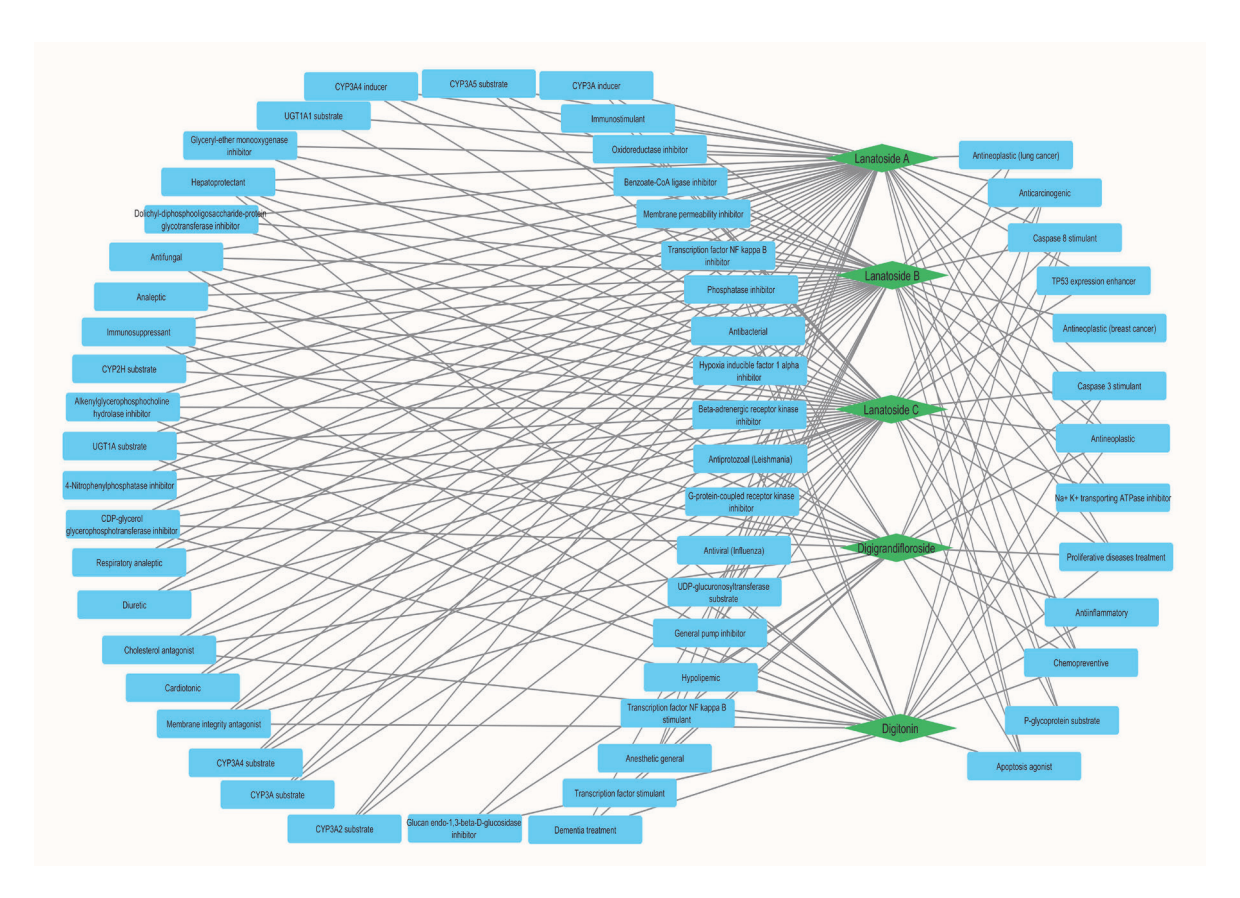


Figure 2. The predicted biological activities of digigrandifloroside, lanatosides A-C, and digitonin. Blue nodes represent the biological activity green nodes represent the compounds.

Previous studies on CGs show their potential for chemopreventive activity. People who use CG as a treatment clinically were reported to have a lower prevalence of death risk from cancer (Prassas & Diamandis, 2008). From these predicted biological activities, breast cancer, and caspase 3 levels were experimentally evaluated in our study. Experimental validation was performed testing the cytotoxicity of compounds on MCF-7 and HeLa cell lines and determination of caspase 3/7 levels.

Cytotoxic activity of CGs and digitonin

To evaluate the cytotoxicity of the compounds MCF-7 and HeLa cancer cell lines were selected. Compounds digigrandifloroside, lanatosides A-C, and digitonin were tested at 0.1-10 μ M. CGs showed higher cytotoxicity when compared with digitonin. The IC value of digitonin against MCF-7 and HeLa cells were found as 1,12 μ M and 0,66 μ M, respectively (Table 1).

Table 1. IC.	values of extr	act and comp	ounds against	HeLa and	MCF-7 cell lines

Compounds	Cell lines			
	HeLa	MCF-7		
Digigrandifloroside	252.1 nM	<100 nM*		
Lanatoside A	<100 nM*	<100 nM*		
Lanatoside B	<100 nM*	<100 nM*		
Lanatoside C	<100 nM*	<100 nM*		
Digitonin	662,6 nM	1120.1 nM		

^{*} The IC $_{\!\scriptscriptstyle{50}}$ value was lower than the tested minimum concentration of 100 nM

Tested CGs showed higher cytotoxicity on MCF7 cells, whereas digitonin was more cytotoxic on the HeLa cell line (Figures 3 and 4.). The cell viability was decreased by under 40% in both cells with even 0.1

 μM lanatosides A-C application. Digigrandifloroside showed similar cytotoxicity on the MCF-7 cell line but it decreased the cell viability to 60% at 0.1 μM concentration (Figure 4.).

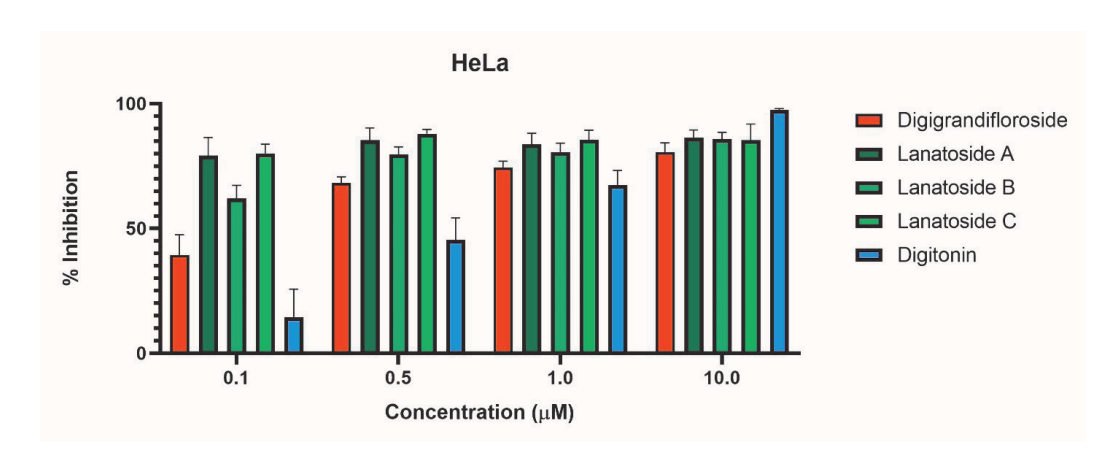


Figure 3. Cytotoxic activity of CGs and digitonin on HeLa cell line using MTT method. Results are given as inhibition %, and expressed as mean \pm S.D. (n=3)

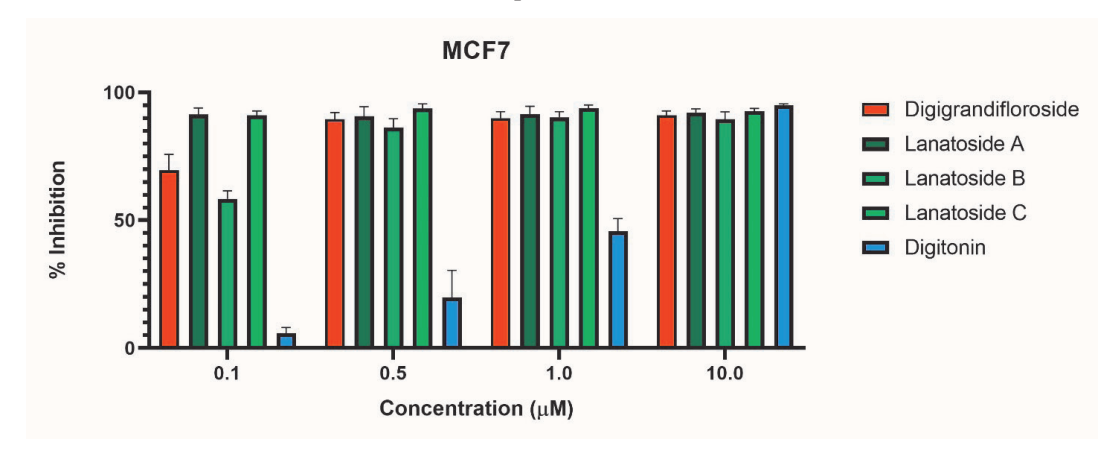


Figure 4. Cytotoxic activity of CGs and digitonin on MCF-7 cell line using MTT method. Results are given as inhibition % and expressed as mean \pm S.D. (n=3)

When we compare different aglycon types of CGs via Lanatosides A-C, the results showed that both digitoxigenin and digoxigenin type CGs showed higher cytotoxicity than gitoxigenin. Also, epimerisation from C-13 of digoxigenin might have a role in the decrease in cytotoxic activity as Lanatoside C showed higher cytotoxic activity than digigrandifloroside. But in this comparison, the sugar units of the compounds are also different but the potential bioactivity of CGs depends on their structure of aglycon.

There are several reports of lanatoside C against cancer in the literature (Chao et al., 2017; Duan et al., 2021; Durmaz et al., 2016; Hu et al., 2018; Reddy, Kumavath, Ghosh, & Barh, 2019). In a previous study on lanatoside C, Reddy et al. reported the IC₅₀ value as 0.4 µM on the MCF-7 cell line and suggested the potential mechanisms as arresting G2/M phase through blocking MAPK/Wnt/PAM signaling pathways and stimulating apoptosis via inhibition of PI3K/AKT/ mTOR signaling pathways (Reddy et al., 2019). In a study on hepatocellular carcinoma lanatoside C induced apoptosis through protein kinase activation (Chao et al., 2017). Lanatoside C was also reported to induce cell cycle arrest at the S and G2/M phases. In the same study lanatoside C was also reported to inhibit JAK-2-STAT6 signaling and induce apoptosis (Duan et al., 2021). Studies on lanatoside C indicate that it can both induce intrinsic or extrinsic pathways of apoptosis and is one of the most studied compound among the group of CGs (Schneider, Cerella, Simoes, & Diederich, 2017). The only study on digigrandifloroside reported the cytotoxicity of the compound on HEp-2 cells. In the same study, it was found that digigrandifloroside showed cytostatic activity on normal cell line L929 where it was cytotoxic on cancer cell line Hep-2 at the same concentrations. The selectivity of the compound between cancer and non-cancerous cells was reported (Kutluay, Makino, et al., 2019).

The other compound tested in our studies was digitonin, a spirostan saponin, reported to have a hemolytic effect and a role in membrane permeabilization (Korchowiec, Janikowska-Sagan, Kwiecinska, Stachowicz-Kusnierz, & Korchowiec, 2021). Digitonin is also reported for its anticancer activity and enhancing other secondary metabolites' cytotoxicity. The effect on the cell membrane causes an increase in cell membrane permeability and helps polar cytotoxic compounds to enter through the cell membrane (Eid, El-Readi, & Wink, 2012).

Determination of caspase 3/7 activity

Caspase 3/7 levels were measured for digigrandifloroside on MCF-7 and HeLa cells. Apoptosis involves the roles of caspases 3 and 7. Caspase 3 regulates apoptosis's morphological alterations and DNA fragmentation. When caspase-3 is present, cell death occurs more effectively. Caspase 7 is involved in both inducing apoptosis and releasing cells from the extracellular matrix. It is well known that MCF-7 cells lack caspase 3 (Laffin, Chavez, & Pine, 2010). Taking into consideration this situation, our results support this. Caspase 3/7 levels increased 1.29-fold in MCF-7 cells and 2.35-fold in HeLa cells. The results showed that digigrandifloroside has increased caspase levels in both cells (Figure 5.). The 1.29-fold increase is upon the induction of caspase 7 but not caspase 3 in MCF-7 cells.

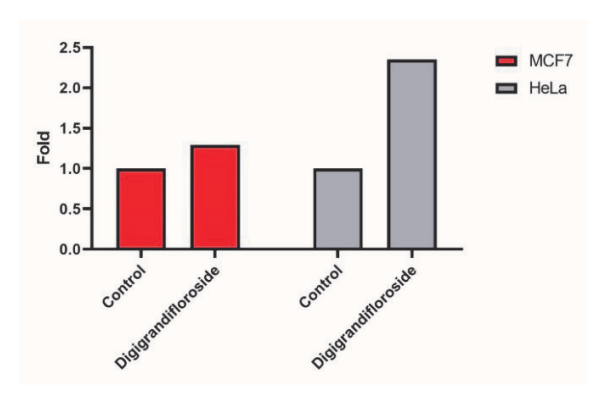


Figure 5. Caspase 3/7 activity of digigrandifloroside in the MCF-7 and HeLa cell lines

CONCLUSION

Overall, the diverse actions of cardiac glycosides in cancer treatment highlight their canonical role in this space and consequently emphasize. Researchers focus on CGs to determine their role and the mechanisms against several cancers. Na+/K+-ATPase inhibition is one of the major mechanisms in the cytotoxicity of this group of compounds. In addition, they induce cell cycle arrest at different stages, and induce apoptosis via several protein kinases and caspases. In our study an unusual CG, digigrandifloroside, with an aglycone of 13-epidigoxigenin was tested on 2 different cancer cells, and caspase 3/7 levels were evaluated. The study showed that digigrandifloroside might induce apoptosis via both caspase 3 and 7. The biological activity prediction studies performed in our research showed that digigrandifloroside has a caspase 3 stimulatory effect which was validated by in vitro assays in our study. The IC_{50} value of digigrandifloroside is found to be higher in MCF-7 cells when compared to HeLa cells. MCF-7 cells are known to be lack of caspase 3. This might explain the higher IC₅₀ value and caspase 3 stimulation of digigrandifloroside.

Digoxigenin and digitoxigenin-type CGs demonstrated more cytotoxicity than gitoxigenin when we compared the various aglycon of CGs using Lanatosides A–C. Furthermore, as digoxigenin's C-13 epimerization exhibited a lower cytotoxic activity than digigrandifloroside, this could potentially account for the drop in cytotoxic activity. Although the compounds' sugar units differ, the aglycon structure of CGs determines their potential bioactivity.

These findings might be useful for future studies and mechanisms underlying the cytotoxicity of these compounds should be investigated further.

AUTHOR CONTRIBUTION STATEMENT

Developing hypothesis (VMK), experimenting (VMK), preparing the study text (VMK), reviewing the text (VMK, İS), analysis and interpretation of the data (VMK, İS), literature research (VMK)

CONFLICT OF INTEREST

The authors declare that there is no conflict of interest.

ACKNOWLEDGEMENT

Lanatosides A-C and digitonin were a kind gift from the Department of Pharmacognosy, Faculty of Pharmacy, Hacettepe University. Authors are thankful to the Department of Pharmacognosy, Faculty of Pharmacy Hacettepe University, Türkiye. Authors are also thankful to Prof. Dr. L. Ömur Demirezer and Assoc. Prof. Nadire Özenver for Caspase 3/7 Glo kit.

REFERENCES

- Ainembabazi, D., Zhang, Y. W., & Turchi, J. J. (2023). The mechanistic role of cardiac glycosides in DNA damage response and repair signaling. *Cellular and Molecular Life Sciences*, 80(9). doi:10.1007/s00018-023-04910-9
- Albach, D. C., Meudt, H. M., & Oxelman, B. (2005). Piecing together the "new" Plantaginaceae. *American Journal of Botany*, 92(2), 297-315. doi:DOI 10.3732/ajb.92.2.297
- Chao, M. W., Chen, T. H., Huang, H. L., Chang, Y. W., HuangFu, W. C., Lee, Y. C., . . . Pan, S. L. (2017). Lanatoside C, a cardiac glycoside, acts through protein kinase Cδ to cause apoptosis of human hepatocellular carcinoma cells. *Scientific Reports*, 7. doi:10.1038/srep46134
- Duan, Y. C., Chen, L., Shao, J., Jiang, C., Zhao, Y. M., Li, Y. Y., . . . Yu, M. H. (2021). Lanatoside C inhibits human cervical cancer cell proliferation and induces cell apoptosis by a reduction of the JAK2/STAT6/SOCS2 signaling pathway. *Oncology Letters*, 22(4). doi:10.3892/ol.2021.13001
- Durmaz, I., Guven, E. B., Ersahin, T., Ozturk, M., Calis, I., & Cetin-Atalay, R. (2016). Liver cancer cells are sensitive to Lanatoside C induced cell death independent of their PTEN status. *Phytomedicine*, 23(1), 42-51. doi:10.1016/j.phymed.2015.11.012
- Eid, S. Y., El-Readi, M. Z., & Wink, M. (2012). Digitonin synergistically enhances the cytotoxicity of plant secondary metabolites in cancer cells. *Phytomedicine*, *19*(14), 1307-1314. doi:10.1016/j. phymed.2012.09.002

- Evans, C. W. (2002). *Trease and Evans Pharmacognosy* (16 ed.). London: Saunders and Company Ltd.
- Filimonov, D. A., Lagunin, A. A., Gloriozova, T. A., Rudik, A. V., Druzhilovskii, D. S., Pogodin, P. V., & Poroikov, V. V. (2014). Prediction of the Biological Activity Spectra of Organic Compounds Using the Pass Online Web Resource. *Chemistry of Heterocyclic Compounds*, 50(3), 444-457. doi:10.1007/s10593-014-1496-1
- Gupta, R. S., Chopra, A., & Stetsko, D. K. (1986).
 Cellular Basis for the Species-Differences in Sensitivity to Cardiac-Glycosides (Digitalis). *Journal of Cellular Physiology*, 127(2), 197-206. doi:DOI 10.1002/jcp.1041270202
- Hu, Y. D., Yu, K. K., Wang, G., Zhang, D. P., Shi, C. J., Ding, Y. H., . . . Qian, F. (2018). Lanatoside C inhibits cell proliferation and induces apoptosis through attenuating Wnt/β-catenin/c-Myc signaling pathway in human gastric cancer cell. *Biochemical Pharmacology*, 150, 278-290. doi:10.1016/j. bcp.2018.02.023
- Karakoyun, Ç., Küçüksolak, M., Bilgi, E., Dogan, G., Çömlekçi, Y. E., & Bedir, E. (2021). Five new cardenolides transformed from oleandrin and nerigoside by 1E1BL1 and 1E4CS-1 and their cytotoxic activities. *Phytochemistry Letters*, *41*, 152-157. doi:10.1016/j.phytol.2020.12.003
- Korchowiec, B., Janikowska-Sagan, M., Kwiecinska, K., Stachowicz-Kusnierz, A., & Korchowiec, J. (2021). The role of cholesterol in membrane activity of digitonin: Experimental and theoretical model studies. *Journal of Molecular Liquids*, 323. doi:10.1016/j.molliq.2020.114598
- Kreis, W. (2017). The Foxgloves (Digitalis) Revisited. *Planta Medica*, 83(12-13), 962-976. doi:10.1055/s-0043-111240

- Kutluay, V. M., Ishiuchi, K., Makino, T., & Saracoglu, I. (2019a). Cytotoxic phenylethanoid glycosides from Digitalis davisiana Heywood: Evaluation of structure activity relationships and chemotaxonomical significance of isolated compounds. *Fitoterapia*, *135*, 90-98. doi:10.1016/j.fitote.2019.04.009
- Kutluay, V. M., Makino, T., Inoue, M., & Saracoglu, I. (2019b). New knowledge about old drugs; a cardenolide type glycoside with cytotoxic effect and unusual secondary metabolites from Digitalis grandiflora Miller. *Fitoterapia*, 134, 73-80. doi:10.1016/j.fitote.2019.02.001
- Laffin, B., Chavez, M., & Pine, M. (2010). The pyrethroid metabolites 3-phenoxybenzoic acid and 3-phenoxybenzyl alcohol do not exhibit estrogenic activity in the MCF-7 human breast carcinoma cell line or Sprague-Dawley rats. *Toxicology*, 267(1-3), 39-44. doi:10.1016/j.tox.2009.10.003
- Morsy, N. (2017). Cardiac Glycosides in Medicinal Plants. In *Aromatic and Medicinal Plants Back to Nature*.
- Prassas, I., & Diamandis, E. P. (2008). Novel therapeutic applications of cardiac glycosides. *Nature Reviews Drug Discovery*, 7(11), 926-935. doi:10.1038/nrd2682
- Reddy, D., Kumavath, R., Ghosh, P., & Barh, D. (2019).
 Lanatoside C Induces G2/M Cell Cycle Arrest and Suppresses Cancer Cell Growth by Attenuating MAPK, Wnt, JAK-STAT, and PI3K/AKT/mTOR Signaling Pathways. *Biomolecules*, 9(12). doi:10.3390/biom9120792
- Saracoglu, I., Inoue, M., Calis, I., & Ogihara, Y. (1995). Studies on constituents with cytotoxic and cytostatic activity of two Turkish medicinal plants Phlomis armeniaca and Scutellaria salviifolia. *Biol Pharm Bull*, *18*(10), 1396-1400. doi:10.1248/bpb.18.1396

- Schneider, N. F. Z., Cerella, C., Simoes, C. M. O., & Diederich, M. (2017). Anticancer and Immunogenic Properties of Cardiac Glycosides. *Molecules*, 22(11). doi:10.3390/molecules22111932
- Skubník, J., Pavlícková, V., & Rimpelová, S. (2021).
 Cardiac Glycosides as Immune System Modulators. *Biomolecules*, 11(5). doi:10.3390/biom11050659
- Sung, H., Ferlay, J., Siegel, R. L., Laversanne, M., Soerjomataram, I., Jemal, A., & Bray, F. (2021). Global cancer statistics 2020: GLOBOCAN estimates of incidence and mortality worldwide for 36 cancers in 185 countries. *Ca-a Cancer Journal for Clinicians*, 71(3), 209-249. doi:10.3322/caac.21660
- Yang, H. Y., Chen, Y. X., Luo, S. W., He, Y. L., Feng, W. J., Sun, Y., . . . Gao, K. (2022). Cardiac glycosides from Digitalis lanata and their cytotoxic activities. *Rsc Advances*, *12*(36), 23240-23251. doi:10.1039/d2ra04464a

Optimization of a Spray Dried Dispersion Powder of Ritonavir with HPMCAS-L

Ayse Nur OKTAY**, James E. POLLI**

Optimization of a Spray Dried Dispersion Powder of Ritonavir with HPMCAS-L

SUMMARY

Ritonavir (RTN) is frequently administered as a drug metabolism inhibitor to "boost" other drugs, such as nirmatrelvir to treat COVID-19. However, like many orally administered drugs, RTN has low water solubility. Hence, RTN is formulated as an amorphous solid dispersion (ASD). The objective was to prepare an optimal RTN spray-dried dispersion (SDD) via spray drying. Using the polymer HPMCAS-L, an optimal spray drying condition was identified, where aspirator rate, spray gas flow, and solution feed rate were varied in a 23 (3 repeated) full factorial design. Yield %, moisture %, and Carr index were assessed. Optimal spray drying conditions were an aspirator rate of 38 m³/h, spray gas flow rate of 742 L/h, and solution feed rate of 6mL/min, resulting in the highest yield %, lowest moisture %, and lower Carr index. Next, optimal spray drying conditions were applied to fabricate RTN SDDs using HPMCAS-L, at each 70 and 140 °C inlet temperatures. Particle size, drug content %, DSC, yield %, moisture %, bulk density, tapped density, Hausner ratio, and Carr index of each SDD were assessed or conducted. Solubility, stability, and dissolution studies were also carried out. Both SDD were stable for three months and exhibited improved solubility, compared to unprocessed RTN and physical mixtures. SDD using HPMCAS-L polymer provided rapid RTN release. Overall, an optimal RTN SDD was achieved and employed HPMCAS-L rather than PVP-VA, which is used in several commercial forms of RTN, albeit using hot melt extrusion.

Key Words: Ritonavir, hpmcas-l, spray drying, design of experiment, optimization.

Ritonavirin HPMCAS-L ile Püskürterek Kurutulmuş Dispersiyon Tozunun Optimizasyonu

ÖZ

Ritonavir (RTN), COVID-19'u tedavi etmek için kullanılan nirmatrelvir gibi diğer ilaçları "desteklemek" amacıyla ilaç metabolizma inhibitörü olarak sıklıkla uygulanmaktadır. Ancak, oral yoldan uygulanan birçok ilaç gibi, RTN'nin de suda çözünürlüğü düşüktür. Bu nedenle, RTN amorf katı dispersiyon (ASD) olarak formüle edilmektedir. Amaç, püskürterek kurutma aracılığıyla optimum RTN- püskürterek kurutulmuş dispersiyonu (SDD) hazırlamaktır. HPMCAS-L polimeri kullanılarak, aspiratör hızı, sprey gaz akış hızı ve çözelti besleme hızının değiştirildiği 23 (3 tekrarlı) tam faktöriyel tasarımda optimum püskürterek kurutma koşulu belirlenmiştir. % Verim, % nem ve Carr indeksi değerlendirilmiştir. Optimum püskürterek kurutma koşulları olan aspiratör hızı 38 m³/sa, sprey gaz akış hızı 742 L/sa ve çözelti besleme hızı 6mL/dk ile en yüksek % verim, en düşük % nem ve daha düşük Carr indeksi sağlanmıştır. Daha sonra, HPMCAS-L kullanılarak 70 °C ve 140 °C giriş sıcaklıklarında RTN SDD'leri üretmek için optimum püskürterek kurutma koşulları uygulanmıştır. Her SDD'nin partikül boyutu, % etkin madde içeriği, DSC, % verim, % nem, küme dansitesi, sıkıştırılmış dansite, Hausner oranı ve Carr indeksi değerlendirilmiştir. Çözünürlük, stabilite ve çözünme hızı çalışmaları gerçekleştirilmiştir. SDD'ler üç ay boyunca stabil bulunmuştur, ve işlem görmemiş RTN ve fiziksel karışımlarla karşılaştırıldığında çözünürlük iyileştirilmiştir. HPMCAS-L polimeri kullanılan SDDler, RTN'nin hızlı salımını sağlamıştır. Genel olarak, optimum RTN SDD elde edilmiştir ve sıcak eriyik ekstrüzyonu kullanılmasına rağmen, çeşitli ticari RTN formlarında kullanılan PVP-VA yerine HPMCAS-L kullanılmıştır.

Anahtar Kelimeler: Ritonavir, hpmcas-l, püskürterek kurutma, deneysel tasarım, optimizasyon.

Received: 20.12.2024 Revised: 7.03.2025 Accepted: 17.04.2025

^{*} ORCID ID: 0000-0002-6465-6450, Department of Pharmaceutical Technology, Gulhane Faculty of Pharmacy, University of Health Sciences, Ankara, Turkey.

[&]quot;ORCID ID: 0000-0002-5274-4314, Department of Pharmaceutical Sciences, University of Maryland, Baltimore, U.S.A.

INTRODUCTION

Ritonavir (RTN) is an anti-HIV protease inhibitor, although is mostly used as a drug metabolism inhibitor to "boost" other drugs, such as nirmatrelvir (in PAXLOVID) to treat COVID-19. Nirmatrelvir/ ritonavir received Emergency Use Authorization by the U.S. Food and Drug Administration (FDA) to treat COVID-19 in adults and pediatric patients. Nirmatrelvir effects by binding the SARS-CoV-2 3CL protease, which ultimately causes viral replication to stop. RTN is a potent CYP3A4 inhibitor, and it acts as a boosting agent to slow the metabolism of nirmatrelvir, thus increasing the concentration of nirmatrelvir. RTN was selected here as a model drug, in light of its importance as a drug and "boosting" agent, as well as it being a prototypical poorly water-soluble drug (~1 μg/ml). Because of its low aqueous solubility, Norvir (ritonavir) includes amorphous solid dispersions of RTN prepared with the hot melt extrusion (HME) method. Crystalline RTN intrinsic dissolution rate is too slow (0.03 mg/cm²/min at pH 1 (0.1 N HCl)) (Law et al., 2001). It is a high lipophilic active substance (log P = 5.6) (Yu, Yu, Lane, McConnachie, & Ho, 2020). Due to low solubility and dissolution rate, crystalline RTN oral bioavailability is poor. After a single oral 600mg dose of amorphous RTN to healthy volunteers, the pharmacokinetic parameters are: Maximum plasma concentration (C_{max}) is 11.2 μg/ mL; plasma elimination half-life $(t_{1/2})$ is 3–5 h. The absolute bioavailability of RTN in human subjects has not been determined, although the fraction dose absorbed at 600 mg was estimated to be 60 to 80% (Hsu, Granneman, & Bertz, 1998; Karakucuk, Teksin, Eroglu, & Celebi, 2019; Kempf et al., 1995). Also, the oral bioavailability of RTN differs between fed and fasting conditions. The maximum blood concentration of RTN in the fasted state is 23-49% lower than the moderate-fat and high-fat conditions (AbbVie, 2017; Klein et al., 2008). Solubility enhancement methods comprise a wide range of approaches, including chemical and physical methods, as well as innovative technologies such as co-crystals, cyclodextrin complexes, nanosuspensions, nanoemulsions, supercritical fluid technology, solid dispersions (SD) and amorphous solid dispersions (ASD). The selection of methods depends on the specific physicochemical properties of the drug and the desired formulation characteristics, as well as available equipment.

Over the last decade, solid dispersion technology has been one of the most widely accepted solubility enhancement strategies in the pharmaceutical industry and academia. SDs provide higher membrane flux due to drug supersaturation and so, improve bioavailability. It offers various excipient/ processing options and provides increased flexibility in developing oral drug formulations of drugs, especially poorly soluble drugs (BCS Class II and IV). ASD is a solid dispersion in which the active substance is dispersed within an excipient matrix in a substantially amorphous form. It combines the advantages of the amorphous structure and solid dispersion. The amorphous structure of the drug is essential for increasing its solubility and dissolution, because no energy is required to break the drug's crystal lattice. ASDs have a higher wettability through hydrophilic polymers. There has been an increase in the number of ASDs under development and have been marketed (Bhujbal et al., 2021; Jermain, Brough, & Williams III, 2018; Moseson, Tran, Karunakaran, Ambardekar, & Hiew, 2024; Stegemann, Leveiller, Franchi, De Jong, & Lindén, 2007; Van den Mooter, 2012; Williams et al., 2013).

RTN was selected as a model drug for ASD formulations, due to RTN having a relatively high glass transition temperature (T_g) (~ 52.43 °C) and is generally stable in the amorphous state (Chiou & Riegelman, 1971; Law et al., 2001; Oktay & Polli, 2024; Zhou, Zhang, Law, Grant, & Schmitt, 2002). Currently, there are numerous ASD fabrication methods such as hot melt extrusion, spray drying, solvent casting, rotary evaporator, KinetiSol, and freeze-drying. Compared to the other methods, the

spray drying method has the advantages of being less energy intensive, a continuous and commercially scalable drying process in a single operation with no handling (Bhujbal et al., 2021; Mujumdar, 2006; Ogawa et al., 2018; Singh & Van den Mooter, 2016). In addition to the solubility and dissolution enhancement, spray drying provides uniform and controllable spherical particle size. Lower bulk density and lower powder flow are potential limitations for tablet manufacturing. The ASD that results from spray drying is denoted as a spray-dried dispersion (SDD). Spray drying provides a large surface area for heat and mass transfer by atomizing the liquid into small droplets. The spray drying process involves the following steps sequentially. Liquid is sprayed into a stream of hot air, so that each droplet dries to a solid particle. The drying chamber can be described as the cyclone ensuring good air circulation, facilitating heat and mass transfer, and separating dried particles by centrifugal action. However, the inherently complex nature of this process needs an optimized process and formulation parameters. So, this study assesses the effects of critical process parameters of spray drying on the critical quality attributes of RTN SDD. The inlet temperature included temperatures above and below the melting point of RTN.

MATERIALS AND METHODS

Materials

Ritonavir was purchased from ChemShuttle (Blue Current Inc; Hayward, USA). HPMCAS-L was provided by Ashland (Ashland Inc., Covington, USA).

Solvents were purchased from Fischer Scientific (Fischer Scientific; Hampton, NH) and Sigma Aldrich (Sigma-Aldrich; St. Louis, MO).

Methods

Figure 1 illustrates the overall study design and flow of experiments. The drug was RTN, and the polymer was HPMCAS-L. Briefly, stage 1 involved a full factorial design to elucidate the impact of three spray drier critical process parameters (CPP) on three critical quality attributes (CQA). The experimental design was a 23-full factorial design (3-repeated). The CPPs were aspirator rate, spray gas flow rate and solution feed rate. The CQAs were yield % of spray drying, moisture % of SDD, and Carr index of SDD. Twenty-four batches (or runs) were manufactured. Of note, the spray dryer inlet temperature was 70°C. In stage 2, the optimum spray drying parameters that provided SDD powder with the highest yield, lowest moisture, and lowest Carr index were then used in a study to examine the impact of spray dryer inlet temperature. Using the optimum spray drying parameters, the SDD of RTN was fabricated using the same parameters that were applied with inlet temperatures of 70 °C and 140 °C, to comparatively assess the effect of inlet temperatures below and above the melting point of RTN, which is 128°C. Each SDD was characterized in terms of crystalline or amorphous content, bulk and tapped densities, Carr index and Hausner ratio, moisture content, yield, particle size, stability, drug solubility, and drug dissolution.

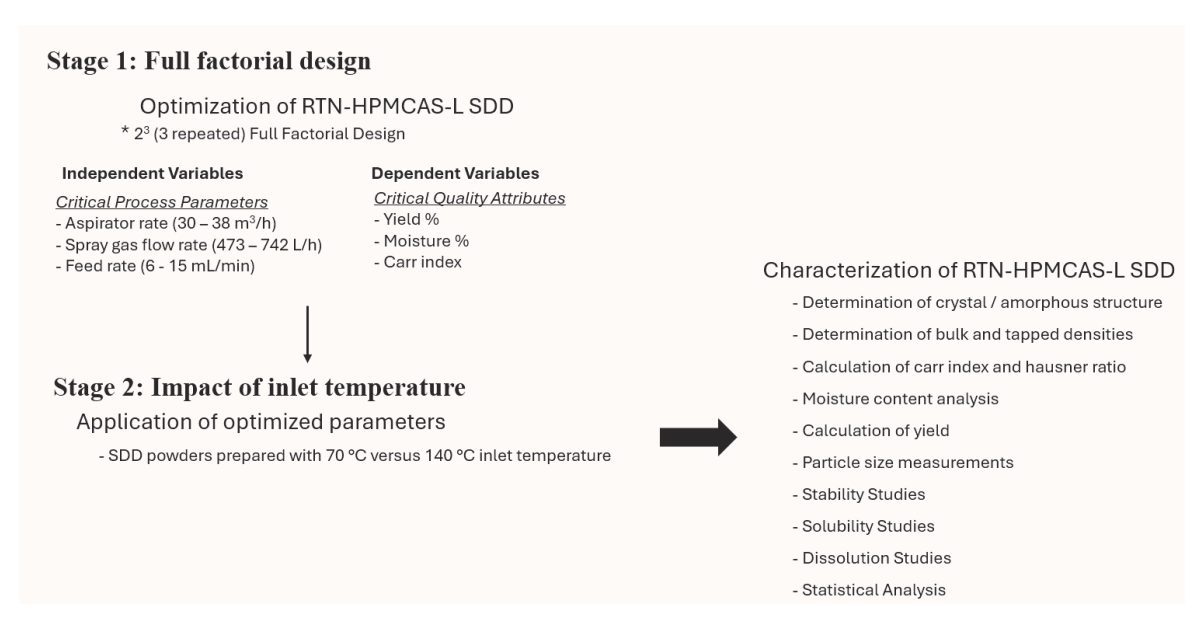


Figure 1. Flow chart of the studies. Stage 1 involved a full factorial design to elucidate the impact of three spray drier critical process parameters on three critical quality attributes. In stage 2, the optimum spray drying parameters were then used to examine the impact of the spray drier inlet temperature.

Stage 1: Full factorial design

From prior studies using film casting, organic solvent was a 2:1 ratio of dichloromethane: methanol, solid content ratio of 10% (w/w), and polymer: drug ratio was 20:80 (Oktay & Polli, 2024). These spray drier solution parameters were fixed here and not changed, since they provided a solution of both drug and polymer. For the preparation of RTN SDD, a Buchi B-290 spray dryer (BUCHI Corporation; New Castle, DE) in closed-loop mode was used. The polymer was dissolved in an organic solvent and then ritonavir powder was added to the polymer solution. To obtain the homogenous system, the solutions were mixed using a magnetic stirrer. A design of experiment (DoE) approach with 2³ full factorial design (3-repeated) was performed to investigate the effect of process parameters on the critical quality attributes (CQA), reflecting a Quality-by-Design (QbD) approach. In general, spray drying process parameters are pressure, temperature (inlet/outlet temperature), properties of the feed solution, feed rate, the flow rate of atomizing gas (i.e. spray gas flow rate), atomizing gas type, atomizer type, air flow model and dryer gas flow model. While some parameters can be changed, 296

others cannot, depending on the type of spray dryer, or in terms of interrupting the process. Here, the aspirator rate (30-38 m³/h via 75-100% setting), spray gas flow rate (473-742 L/h via 40 mm and 60 mm height pump setting), and feed rate of solution (6-15 mL/min via 20-50% setting) were determined as critical process parameters (CPP) (Table 1). Each CPP was studied at two levels (i.e. high and low). The effects of these parameters on the CQAs of the formulation were evaluated, which were yield %, moisture %, and Carr index. The inlet temperature was kept constant at 70°C. After the evaluation of the spray dryer process parameters with an inlet temperature of 70°C, the same parameters were applied in stage 2 with an inlet temperature of 70 °C and 140 °C, to assess the effect of an inlet temperature which is higher than RTN melting point (128°C). Per Table 1, the solution was pumped into the atomizer at the rate of 6-16 g/min, via a pump setting of 20% and 50%, respectively. The inlet temperature was 70°C. The spray (atomizing) gas flow settings were adjusted as 40mm and 60mm height for 473 and 742 L/h rates, respectively. The collected SDDs were dried for an additional 12 h at 40°C and stored in a desiccating cabinet (RH < 5%).

	_		
Parameter	Low (-)	High (+)	Unit
Aspirator rate	30	38	m³/h
Spray gas flow rate	473	742	L/h
Feed rate	6	15	L/min

Table 1. The processing variables used in factorial design

Stage 2: Impact of inlet temperature

In stage 2, the optimum spray drying parameters from stage 1 were then used to examine the impact of the spray drier inlet temperature. In one case, the inlet temperature was 70 °C, below the RTN melting point of 128°C. In the other case, the inlet temperature was 140 °C, above the RTN melting point. Each SDD was characterized in terms of crystalline or amorphous content, bulk and tapped densities, Carr index and Hausner ratio, moisture content, yield, particle size, stability, drug solubility, and drug dissolution. For reference, unprocessed RTN powder, as well as a physical mixture of RTN and HPMCAS-L, were also characterized.

Characterization of SDD powders

Determination of crystal / amorphous structure

Differential Scanning Calorimetry (DSC) analyses were conducted to characterize the internal structure of the prepared RTN SDDs. Samples (5-10 mg) were loaded into Tzero pans and analyzed using a Discovery DSC 2500 (TA Instruments; New Castle, DE). To evaporate the possible water content in the SDD powder, the heat/cool/heat method was applied under the nitrogen gas flow (50 ml/min). The melting point was observed on the first heating process to 200°C at 10°C/ min. Then the system was cooled to 30°C at 10°C/ min and reheated to 200°C at 10°C/min. After the confirmation of the amorphous transformation, the glass transition (T_g) temperature of the polymer and SDD powders (20% of drug with 80% of polymer) was determined from the secondary heating cycle. These observed T_g values were compared to the predicted T_g values from the Fox equation (1).

Fox Equation:
$$\frac{1}{T_g} = \frac{W_1}{T_{g1}} + \frac{W_2}{T_{g2}}$$
 (1) where the W_p , W_2 , and T_{g1} and T_{g2} are the weight

fractions and T_g 's of the RTN and the polymer, respectively. Literature value for the T_g of amorphous RTN was 52.43°C (Wagner et al., 2012).

Determination of bulk and tapped densities

Bulk and tapped densities of all SDD powders were determined. The bulk density of powder was measured by pouring 1.5 gr of powder through to funnel into a graduated cylinder. After filling it, the volume of powder (V_B) was determined. The tapped density was determined by placing the graduated cylinder in a Stampf volumeter JEL STAV 2003 jolting volumeter (J. Engelsmann AG; 98 Ludwigshafen, Germany) and tapped 250, 500, 900, 1250 ,and 1500 times. The V_{1500} is the tapped volume (V_T) if the difference between V_{500} and V_{1500} is less than 2 mL (United States Pharmacopeia). The final volume (V_T) was recorded at the determined tapped times and no further reduction in volume was observed.

Calculation of Carr index and Hausner ratio

The Carr index (CI) and Hausner ratio (HR) of the powders, which are related to powder flowability, were determined as follows:

$$CI = 100 \cdot \left(\frac{V_B - V_T}{V_R}\right) \tag{2}$$

Where V_B is the volume occupied by a given mass of powder before tapping, and V_T is the volume occupied by the same mass of powder after tapping. The flowability is determined using the USP standard (Pharmacopeia). A CI value above 26 indicates poor flowability.

Hausner ratio (HR) was determined as follows:

$$HR = \left(\frac{V_B}{V_T}\right) \tag{3}$$

Hausner's ratio between 1.00–1.11 anticipates excellent flow properties (Patel, Patel, & Shah, 2023).

Moisture content analysis

Loss on drying (LOD) was measured on the 0.5 gr of SDD powders using a Mettler Toledo Moisture Analyzer HB43 (Mettler-Toledo; Columbus, OH). Three readings were obtained for each sample.

Calculation of Yield

The % yield was calculated over the total weight of the solid in the solution (W_i) and the weight of spray dry powder obtained after the spray drying method (W_s) (Pongsamart, Limwikrant, Ruktanonchai, Charoenthai, & Puttipipatkhachorn, 2022).

$$\% production \ yield = \left(\frac{W_s}{W_T}\right) \tag{4}$$

Particle size measurements

Particle size values of spray-dried solid dispersions (SDD) were measured by using a laser scattering analyzer (LA-910 Laser Scattering Particle Size Distribution Analyzer; HORIBA, Inc. Irvine-CA, USA) and by using a Master Sizer-2000 optical laser diffraction system (Malvern Panalytical; Malvern, UK). For the Master Sizer-2000 optical laser diffraction system, the measurement time was set to 12 s. The dispersive air pressure was set to 1 bar with a 50 % vibrational feeding rate. The Mie model was used and a refractive index of 1.33 was used for particle analysis. The measurements were repeated three times, and the results reported the mean and standard error mean (mean±SEM) of these three measurements.

Stability Studies

Short-term chemical stability studies were performed to evaluate the effect of HPMCAS-L and inlet temperatures on the stability of SDD powder. SDD powders were subjected to stability studies using the Caron environmental chamber (Marietta, OH). Accelerated stability studies were conducted as per the ICH guidelines (40 °C \pm 2°C and 75 \pm 5% RH), for 3 months. Drug content of the SDD powders were measured on the day of production, 1, 7, 14, 30 days, and 3 months of storage at 25°C \pm 2°C / 60 \pm 5% relative humidity (RH) and 40 \pm 2°C / 75 \pm 5% RH. RTN contents of the SDD powders were determined by HPLC. The SDD powders were dissolved in methanol and samples were filtered using a 0.22 μm

membrane filter before analysis. % Drug content was calculated by considering the initial amount of RTN (20% of drug load). The results were statistically analyzed.

Quantification method of ritonavir

HPLC method was used to determine the concentration of RTN. Samples were analyzed by the Waters 2489 HPLC system (Waters Corporation; Milford, MA), using a UV-vis detector. The UVvis detector was set to 240 nm. An isocratic mobile phase consisting of acetonitrile (47%) and 0.05 M phosphoric acid (53%) solution was used, with a 25.0 μL injection volume and a flow rate of 1 mL/min. A 4.6×150 -mm Zorbax C18 5- μ m HPLC column was used. The retention time of RTN was 9-10 min, with a 13 min run time. A calibration curve containing 50, 25, 12.5, 6.25, 3.125, 1.56, 0.78, 0.39, 0.195, 0.098 µg/mL RTN was run in triplicate with each analysis $(r^2 = 0.9999)$. For the solubility studies (below), the calibration curves were obtained for 50 mM maleic acid (pH 5.8) with 60 mM polyoxyethylene 10 lauryl ether (POE10). The standard samples were obtained from the stock solution of RTN in methanol (1 mg/ mL) by diluting a 1:9 ratio with the solubility media. The obtained standard solutions were diluted with mobile phase to prepare the 0.78, 1.56, 3.125, 6.25, 12.5, 25 and 50 μg/mL concentrations.

Solubility Studies

Solubility of the RTN-SDD powders which are prepared HPMCAS-L was evaluated in 50 mM MA with 60 mM polyoxyethylene 10 lauryl ether (POE10). The solubility studies were performed with coarse powder, physical mixture of RTN with HPMCAS-L polymer (20:80%) and with amorphous solid dispersion.

Dissolution of the powders

The powders which were prepared at 70 °C and 140 °C were subjected to USP II dissolution testing, using a USP II apparatus (SR8PLUS, Hanson Research; Chatsworth CA). A single dissolution medium was purposely applied across all formulation. USP II dissolution testing on each formulations (n=3) used 900 ml of 50 mM maleic acid buffer including 60 mM polyoxyethylene 10 lauryl ether (POE) (pH 5.8) at

37°C at 100 rpm for 6 hr. 2 ml of the samples were taken at the determined time points (0, 5, 10, 20, 30, 45, 60, 90, 120, 180, 240 and 360 min) and then filtered through a 0.45 mm Millipore filter. 2 ml of fresh dissolving solution was added to the mixture to keep the volume consistent. USP II dissolution testing yielded a mass dissolved profile. The drug was quantified using HPLC as previously described.

Statistical analysis

The data obtained was analyzed using SPSS software (Version 16). The statistical analysis of variance (ANOVA) was carried out to determine the significance of the main effects and their interactions at the 95% confidence level (0.05 level of probability; p < 0.05). Results were given as the mean \pm standard error mean (SEM) (n = 3).

RESULTS

Optimization of spray-dryer process with HPMCAS-L: results from full factorial design

Table 2 shows yield %, moisture %, and Carr index results from each of the 24 runs that composed the 2³ full factorial design. Yield % ranged from 62.5 to 81.5. Moisture % ranged from 2.57 to 4.19. Carr index ranged from 22.45 to 35.25.

From multivariate analysis of these 2^3 experimental designs, the main effects of all three process parameters (i.e. spray gas flow rate, feed rate ,and aspirator rate) were significant (p \leq 0.05) on each yield, moisture, and Carr index values. Table 3 lists the p-values of the main effects, as well as two-factor and three-factor interactions. The r^2 square value of the model was higher than the 0.85 for yield % (r^2 : 0.8846), moisture % (r^2 : 0.8772), and Carr index (r^2 : 0.9041), indicating the robustness of statistical analysis.

Table 2. 2³ Full factorial design to the effect of process parameters on spray-dried ritonavir powders

	Factor 1	Factor 2	Factor 3	Response 1	Response 2	Response 3
Run	A: Spray Gas Flow Rate	B: Feed Rate	C: Aspirator Rate	Yield	Moisture	Carr Index
	L/h	L/min	m³/h	%	%	%
1	473	6	30	68.5	3.34	25.474
2	473	15	38	73.3	3.58	25.143
3	742	6	30	73.5	3.38	23.077
4	742	6	38	84	2.96	23.043
5	742	6	38	80.8	2.98	23.167
6	473	6	38	78.5	3.2	24.429
7	742	6	30	73.8	3.2	24.815
8	473	6	38	79.5	3.18	23.73
9	473	6	38	75	3.12	22.56
10	742	6	38	81.5	2.57	22.451
11	742	15	30	69.5	3.47	29.667
12	473	6	30	70	3.37	27.727
13	473	15	30	65	4.16	35.25
14	473	15	38	73.3	3.54	29.63
15	742	15	30	69	3.46	27.05
16	742	15	38	76.3	2.97	25.225
17	473	15	30	62.5	3.76	34.33
18	473	15	38	73.8	3.57	27.33
19	742	6	30	84	2.96	23.043
20	473	15	30	64.5	4.19	32.412
21	742	15	38	76.8	3.19	26.343
22	742	15	38	77.3	3.3	26.688
23	473	6	30	68	3.32	28.5
24	742	15	30	70	3.42	27.391

Table 3. Multivariate analysis results from 2³ full factorial design of the impact of process parameters on yield, moisture, and Carr index

Source	Yield % Moisture %		ure %	Carr Index		
	F-value	p-value	F-value	p-value	F-value	p-value
Model	17.51	< 0.0001	16.32	< 0.0001	21.55	< 0.0001
A- Spray Gas Flow Rate	29.25	< 0.0001	35.58	< 0.0001	27.88	< 0.0001
B-Feed Rate	30.35	< 0.0001	45.05	< 0.0001	69.20	< 0.0001
C-Aspirator Rate	59.06	< 0.0001	26.67	< 0.0001	35.51	< 0.0001
AB	0.9431	0.3459	4.06	0.0610	1.85	0.1924
AC	2.27	0.1513	0.0016	0.9686	12.08	0.0031
BC	0.5428	0.4720	1.00	0.3318	3.64	0.0745
ABC	0.1752	0.6811	1.89	0.1883	0.6630	0.4274
R ²	0.8846		0.8772		0.9041	

The effect of process parameters on the yield % of the spray-dried powder

The yield is one of the most important parameters for spray-dried powders. To increase yield, the effects of the spray gas flow rate, aspirator rate, and the feed rate were evaluated. The yield was 60-84% for all formulations. Yield increased when the spray gas flow rate and aspirator rate increased, and the feed rate decreased. Two-way interactions of these factors were also evaluated. In Figure 2, 3D surface graphs showed yield% increased when the spray gas flow rate increased and the feed rate was decreased at the constant aspirator rate (panel a). At the constant feed rate, yield% increased when the spray gas flow rate and aspirator rate were increased (panel b). Yield also increased with the combination of low feed rate and high aspirator rate at the constant spray gas flow (panel c). Predicted and observed values were similar (panel d).

Overall, yield% was increased with high aspirator rate, a high spray gas flow rate ,and low feed rate.

These results agreed with the literature. The powder recovered with a high aspirator rate and high spray gas flow rate has a low moisture content as compared to powder recovered at a low aspirator rate and spray gas flow rate. So, the yield is higher due to the powders with high moisture content were challenging to scrape from the collector, or tended to accumulate on the cyclone during the process (Gu, Linehan, & Tseng, 2015; Magri, Franzé, Musazzi, Selmin, & Cilurzo, 2019). A low feed rate causes less liquid for evaporation within the chamber thus, the temperature rises in the spray-drying glassware (LeClair, Cranston, Xing, & Thompson, 2016; Maa, Costantino, Nguyen, & Hsu, 1997). When the temperature increases in the glassware, it can provide a higher yield, since there is a positive correlation between temperature and yield. With the higher temperature, the solution is dried more by the heated air in the drying chamber, resulting in a greater collection of powders (Gu et al., 2015).

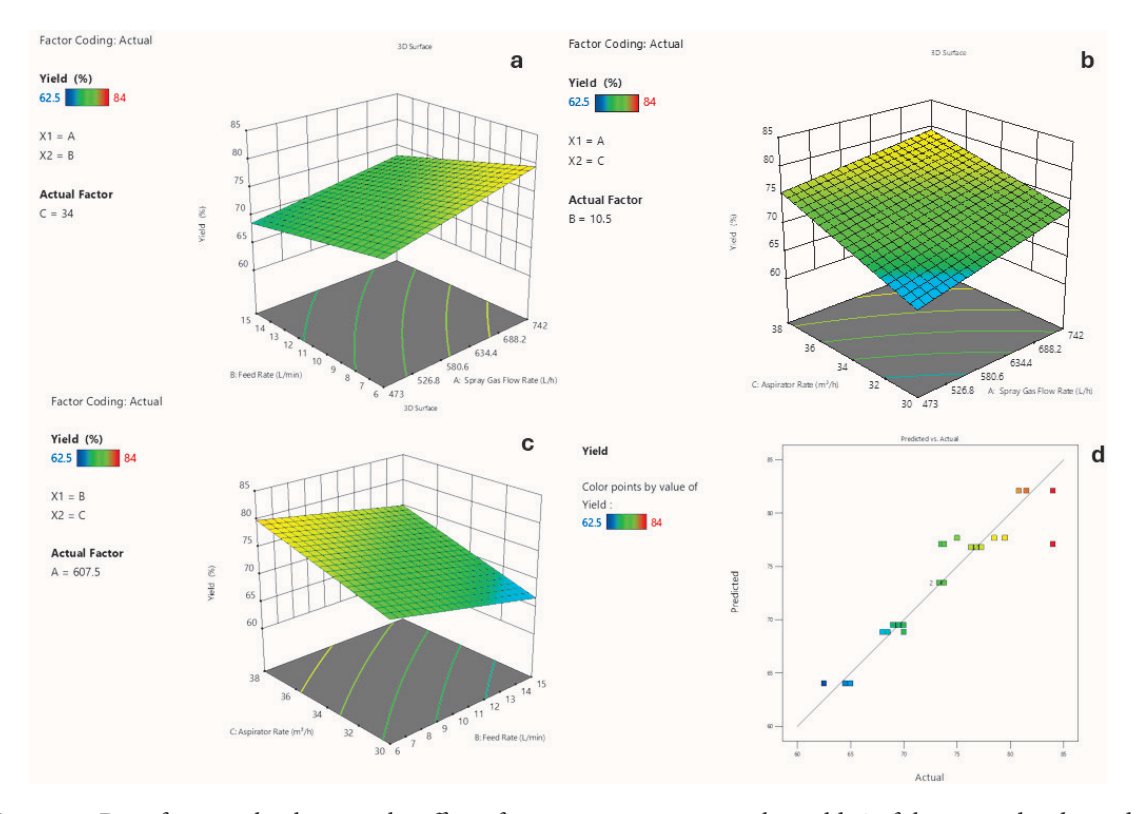


Figure 2. 3D surface graphs showing the effect of process parameters on the yield % of the spray-dried powder

The effect of process parameters on the moisture % of the spray-dried powder

Moisture content is a key parameter that has a high effect on the long-term physical stability of spray-dried powders. The moisture content of the formulation affects the particle size and crystalline state of the powder due to the plasticization of the amorphous phase during storage (Focaroli et al., 2019). In Figure

3, 3D, surface graphs showed moisture % decreased when the spray gas flow rate was increased and feed rate was decreased, at a constant aspirator rate (panel a). When the feed rate kept constant, lower moisture content resulted with the high spray gas flow rate and high aspirator rate (panel b). Moisture content was also decreased with a high aspirator rate and low feed rate, at a constant spray gas flow rate (panel c).

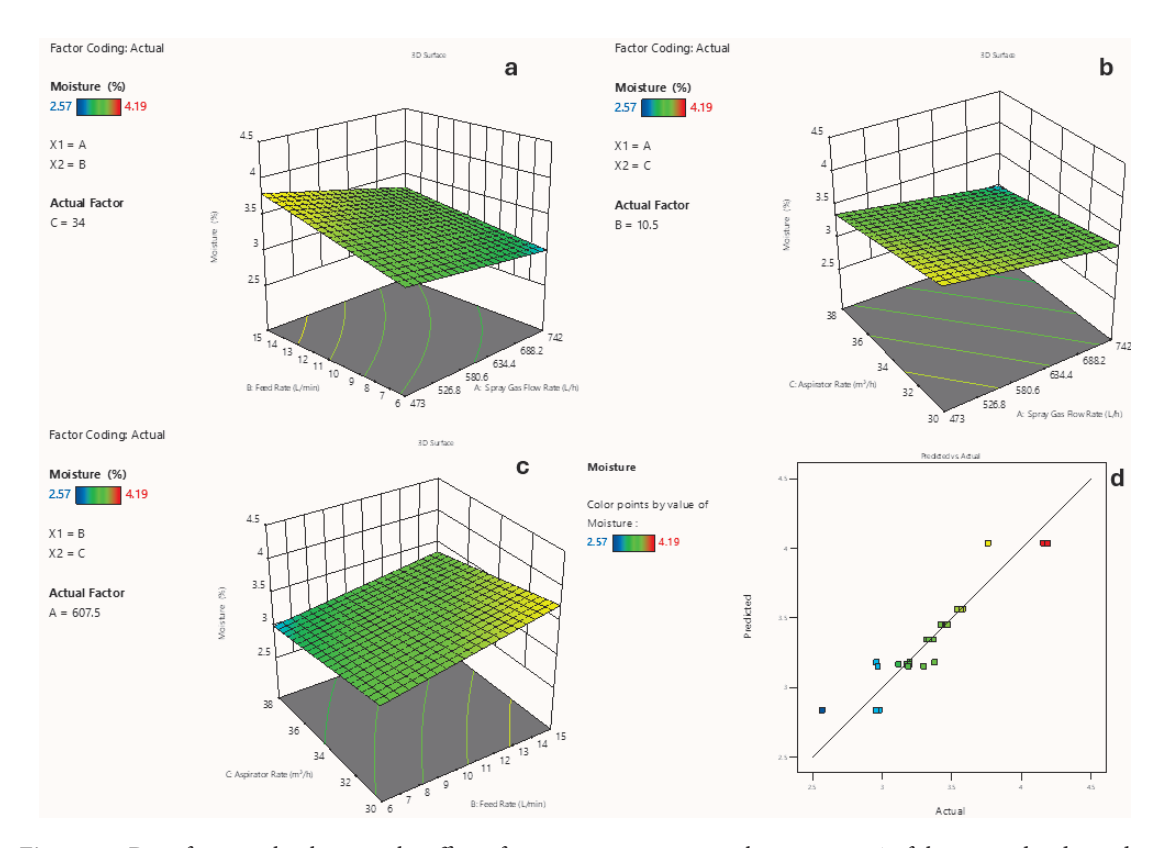


Figure 3. 3D surface graphs showing the effect of process parameters on the moisture % of the spray-dried powder

moisture content of the spray-dried powders varied with spray gas flow rate and feed rate, in agreement with the literature. Gu et al, 2015 mentioned that a lower spray rate caused a decrease in drying efficiency (i.e. higher moisture content) (Gu et al., 2015). Focaroli et al, 2019 observed that powders produced with the lowest feed rate resulted in lower moisture content (Focaroli et al., 2019). Muzaffar and Kumar also indicated higher feed rate caused a short contact time between the drying air and feed, providing less heat transfer and higher moisture content in the powder (Muzaffar, Dinkarrao, & Kumar, 2016). It has also been shown that powder moisture content decreased when the aspirator rate increased from 50% to 100%. This can be explained by the high energy available for evaporation leading to the high amount of drying air so a higher aspirator rate has a positive effect on drying efficiency (Thirugnanasambandham & Sivakumar, 2017).

The effect of process parameters on the Carr index of the spray-dried powder

A lower Carr index generally provided better power flow. The Carr index was always lower than the 30, indicating fair flowability. In Figure 4, at the constant aspirator rate, the Carr index decreased with a low feed rate and low spray gas flow rate (panel a). The Carr index also decreased with a higher spray gas flow rate and higher aspirator rate at the constant feed rate (panel b). Better flowability was observed with a lower feed rate and a higher aspirator rate when the spray gas flow rate was kept constant (panel c). These results can be explained by the lower moisture contents of the powders at a high aspirator rate, high spray gas flow rate ,and low feed rate. Several studies have investigated the effect of the moisture or water content on the flowability of the powder. It was showed that the flowability decreases significantly as the moisture content increases for moisture contents between 3.5%-9%, 6%-32%, and 10%-20%, respectively (Aviara, Power, & Abbas, 2013; Chinwan & Castell-Perez, 2019; Guiling, Xiaoping, Cai, Pan, & Changsui, 2017; Kalman, 2021).

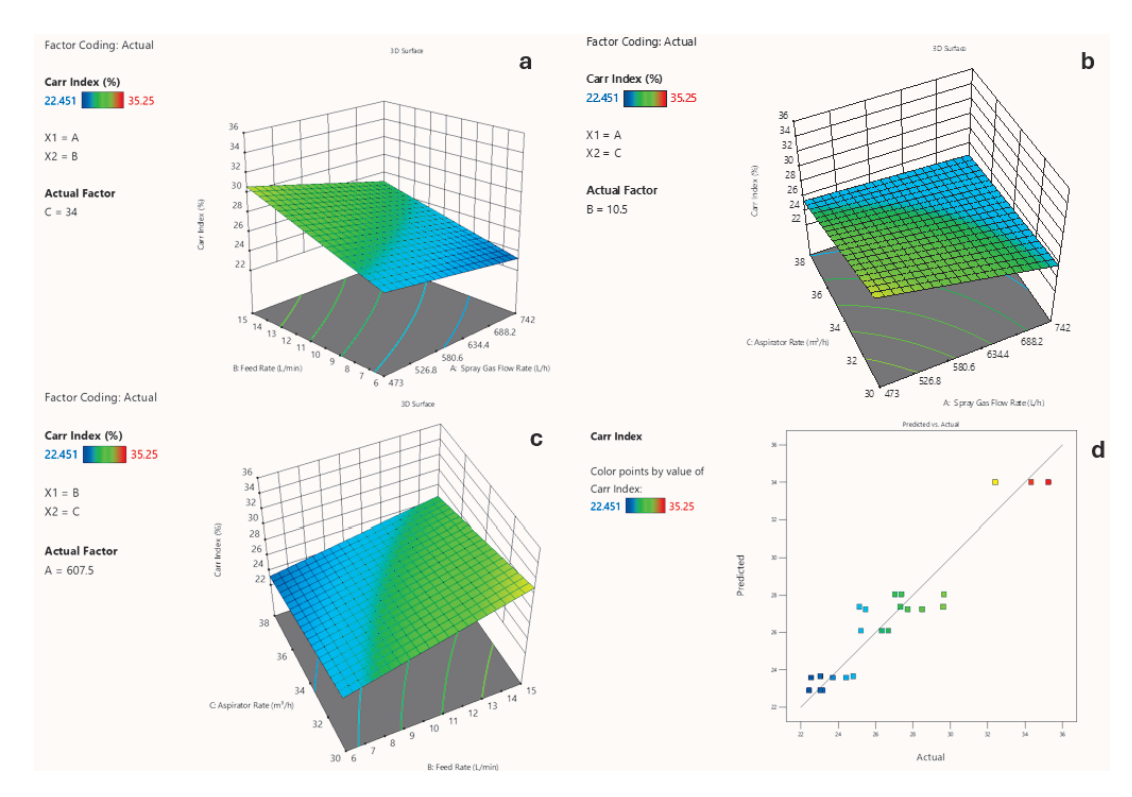


Figure 4. 3D surface graphs showing the effect of process parameters on the Carr index of the spray-dried powder

Results from 2³ full factorial design were subjected to modeling, in the form:

$$Y = a_0 + a_1 X_1 + a_2 X_2 + a_3 X_3 + a_{12} X_1 X_2 + a_{13} X_1 X_3 + a_{23} X_2 X_2 + a_{11} X_1^2 + a_{22} X_2 + a_{23} X_3 X_3 + a_{23} X_3 +$$

Where Y is the dependent variable or response (i.e. Yield %, Moisture % ,or Carr index); a_0 is the arithmetic mean response of the 24 experiments ,and a_i is the estimated coefficient for the factor X_i . X_1 , X_2 ,and X_3 are the coded main effects for spray gas flow

rate, feed rate and aspirator rate, respectively. The main effects represent the average results of changing one factor at a time from its low to high value. The interaction terms (X_1X_2) show how the response changes when two factors are simultaneously changed and X_1^2 and X_2^2 represent the polynomial terms.

Table 4 listed the resulting model equations for yield %, moisture % ,and Carr index.

Table 4. Models for the impacts of spray drying variables on Yield %, Moisture % and Carr index

Response variable	Expression with coded equation	
Yield %=	+73.68+2.69A-2.74B+3.82C-0.4833AB-0.7500AC+0.3667BC+0.2083ABC	(5)
Moisture %=	+3.34-0.1863A+0.2096B-0.1613C-0.0629AB+0.0013AC-0.0312BC+0.0429ABC	(6)
Carr index=	+26.60-1.44A+2.27B-1.62C-0.3711AB+0.9477AC-0.5202BC+0.2220ABC	(7)

^{*}Independent variables: A-Spray Gas Flow Rate; B-Feed Rate; C-Aspirator Rate

Overall, the optimum process parameters were determined to be 742 L/h of spray gas flow rate (i.e. 60 mm height of pump setting), 6 mL/min of feed rate (i.e. 20% of setting) ,and 38 m³/h of aspirator rate (i.e. 100% of setting). These optimum parameters provided

the powder with the highest yield, lowest moisture, and lowest Carr index. Predicted values were similar to observed values which were $82.1\pm0.971\%$ for yield%, $2.84\pm0.133\%$ for moisture% ,and 23.89 ± 0.22 for Carr index.

Characterization of optimum spray-dried powder using different inlet temperatures

In stage 2 here, the optimum spray drying parameters from stage 1 above were then used to examine the impact of spray drier inlet temperature. In one case, the inlet temperature was 70 °C, below RTN melting point of 128°C. In the other case, inlet temperature was 140 °C. The SDD powder properties were compared. For reference, unprocessed RTN powder, as well as a physical mixture of RTN and HPMCAS-L, were also characterized.

Particle size values of spray-dried powders

The mean particle size (d_{50}) of unprocessed ritonavir powder was $36.3\pm10.1~\mu m$ (mean±SEM). The d_{50} values of the physical mixture of RTN with HPMCAS-L was $185.9\pm15.7~\mu m$. As expected, spray drying reduced particle sizes. D_{50} values of the SDD were $15.28\pm0.59~\mu m$ and $28.62\pm6.75~\mu m$ for $70~^{\circ}C$ and $140~^{\circ}C$ of inlet temperatures, respectively. Higher inlet temperature led to larger particle size. Honick et al. prepared SDD powders of itraconazole with HPMCAS-L, HPMCAS-M and HPMCAS-H. D_{50} of the SDD powders with HPMCAS-L and HPMCAS-H were $14.30\pm0.92~\mu m$ and $9.84\pm0.33~\mu m$, using $100~^{\circ}C$ inlet temperature; D_{50} of the itraconazole physical mixture with HPMCAS-L was $193.3\pm7.8~\mu m$

(Honick et al., 2020). HPMCAS-L has d_{50} = 204 µm. (Carina Hubert; Honick et al., 2020). Osei-Yeboah et al. prepared celecoxib-PVP-VA amorphous solid dispersions, and the particle sizes of SDD powders varied in a narrow range of 1.9 – 3.0 µm (d_{10}); 8.6 – 14.2 µm (d_{50}); 32.8 – 40.2 µm (d_{90}) respectively (Osei-Yeboah & Sun, 2023). Hofman et al. determined by microscopy that the particle size of the SDD powder and physical mixture with SoluPlus were in the range of 2-35 µm and 10-100 µm, respectively, for 10% drug load (Hofmann, Harms, & Mäder, 2024).

Evaluation of crystal / amorphous structure

DSC analyses were conducted to examine the effect of the spray drying method on the internal structure of the prepared RTN solid dispersions. The melting point of crystalline RTN was determined as 128.21 °C, with a T_g value of 52.43 ± 1.2 °C. HPMCAS-L polymer was in an amorphous state, and T_g was 123.56 °C. The spray-dried powder was also amorphous. T_g values were 93.64 °C and 90.23 °C for 20:80 % (w/w) RTN: HPMCAS-L spray-dried powders prepared at 70 °C and 140 °C inlet temperatures, respectively (Figure 5). Hence, there was not a large difference in T_g from using two different inlet temperatures. Observed T_g was also close to the predicted value from the Fox equation, which was 97.19 °C.

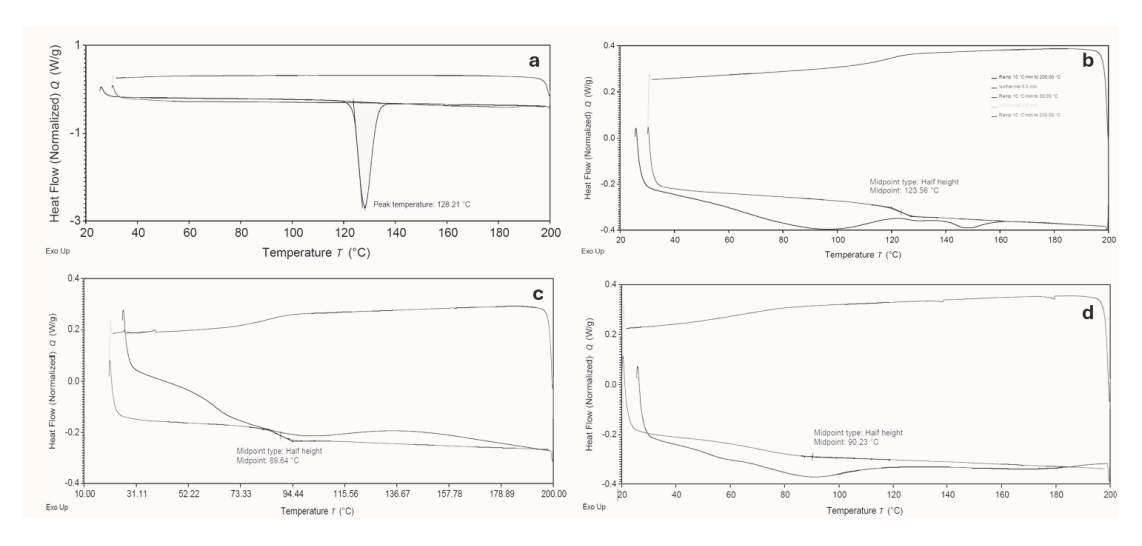


Figure 5. DSC profiles of coarse powder of RTN (a), HPMCAS-L (b) ,and SDDs of RTN-HPMCAS-L at 70 °C (c) and 140 °C (d) of inlet temperatures

Evaluation of bulk and tapped densities, Hausner ratio ,and Carr index

Table 5 lists bulk and tapped densities, Carr index ,and Hausner ratios for SDD powder from 70 °C and 140°C inlet temperatures. The bulk density of the RTN-SDD powder prepared at 140 °C (0.082±0.002 g/cm³) was markedly lower than the powder prepared at 70 °C (0.251±0.003 g/cm³). Similarly, tapped density from 140 °C (0.119±0.003 g/cm³) was markedly lower than that from 70 °C (0.344±0.029 g/cm³).

The Carr index and the Hausner ratio are indicators of the flowability of bulk solids. Each was calculated from bulk and tapped densities, to assess the inlet temperature effect on SDD powder flowability and compressibility. The Hausner ratios were 1.37±0.10 and 1.45±0.005 for powders prepared with 70 °C and 140°C inlet temperatures, respectively. The Carr index was 25.96±5.76% and 31.051±0.259% for 70 °C and 140 °C, respectively. These values indicate that the powder from 70 °C has moderate flowability, and higher inlet temperature resulted in poor flowability.

Table 5. The bulk and tapped densities, Hausner ratio ,and Carr index values of RTN SDD powders prepared with HPMCAS-L at 70 °C and 140 °C inlet temperatures (mean±SEM).

Polymer	Inlet temperature	Bulk density (gr/cm ³)	Tapped Density(gr/cm³)	Hausner Ratio	Carr Index (%)
HPMCAS-L	70 °C	0.251±0.003	0.344±0.029	1.366±0.099	25.962±5.756
HPMCAS-L	140 °C	0.082±0.002	0.119±0.003	1.450±0.005	31.051±0.259

Evaluation of moisture %, yield % and drug content %

The moisture %, yield %, and drug content % are listed in Table 6. For the compression of tablets, the moisture content is an important factor due to its effect on flowability. The moisture % of the powder prepared with high inlet temperature (1.197±0.018 %) was significantly lower than that from the low temperature (2.835±0.243 %), as expected. Higher inlet temperature also provided a higher yield (88.067±0.961 %) compared to the lower inlet

temperature (82.227±0.191 %). However, the drug contents decreased from 95.2+0.6 % to 92.9+0.1 % when the inlet temperature increased from 70 °C to 140 °C (Table 6). When the inlet temperature increased from 70 °C to 140 °C, and while the moisture decreased and yield increased, drug content significantly decreased. Results reflect that RTN melted at a higher inlet temperature, causing the drug to stick to the surface of the cyclone. Hence, it is concluded that the lower temperature (i.e. below drug melting temperature) was the better option.

Table 6. The moisture content %, yield %, and drug content % of the spray dried powders

Polymer	Polymer Inlet temperature (°C)		Yield (%)	Drug content (%)
HPMCAS-L	70	2.835±0.243	82.227±0.191	95.177±0.558
HPMCAS-L	140	1.197±0.018	88.067±0.961	92.870±0.137

Solubility Studies

The effect of fabricating RTN into an SDD with HPMCAS-L on RTN solubility was evaluated in the 50 mM maleic acid buffer (MA) (pH 5.8) with 60 mM polyoxyethylene 10 lauryl ether (POE10). Solubility studies were also performed with unprocessed RTN powder. Solubility results are given in Table 7. The solubility of unprocessed RTN in POE10 medium was

198.6 μ g/mL. Meanwhile, RTN solubility from SDD powders was 2797.8 and 3126.4 μ g/mL for 140 °C and 70 °C inlet temperatures, respectively. Overall, there was no significant difference between the SDD powders from the different inlet temperatures, as their solubility increase was about 15-fold higher than from unprocessed RTN. Meanwhile, the physical mixture provided an almost 2-fold increase.

Table 7. Solubility results of unprocessed RTN powder and SDD powders of RTN

Sample	Solubility in POE10 (μg/mL, mean ±SEM)
RTN coarse powder	201.778±2.423
RTN-HPMCAS-L PM powder	363.563±28.007
RTN- HPMCAS-L SDD powder – 70 °C	3126.4±84.34
RTN- HPMCAS-L SDD powder – 140 °C	2797.8±108.90

Stability of SDD powders

Drug content (i.e. chemical stability) of the SDD powders at the end of the three months was determined (Table 8). Drug content (%) was 95.027±0.524 and 92.713±0.101 for 70 °C and 140 °C inlet temperatures,

respectively, after the storage at room temperature for 3 months. These values were practically identical to drug content at the start. Similar results were obtained after storage at 40 °C. RTN was chemically stable in both SDDs for three months.

Table 8. Drug contents of the SDD powders prepared with HPMCAS-L and two levels of inlet temperatures after storage at room temperature and at 40 °C for three months.

	Drug content (%) after storage at room temperature								
Polymer	Inlet temperature	initial	1 st day	7 th day	14 th day	1 st month	3 rd month		
HPMCAS-L	70°C	95.177±0.558	95.148±0.559	95.126±0.524	95.103±0.532	95.060±0.531	95.027±0.524		
HPMCAS-L	140°C	92.870±0.137	92.840±0.247	92.802±0.211	92.787±0.058	92.737±0.064	92.713±0.101		
Drug content (%) after storage at 40°C									
		Dr	ug content (%) a	fter storage at 40)°C				
Polymer	Inlet temperature	initial	ug content (%) a	ofter storage at 40	14 th day	1st month	3 rd month		
Polymer HPMCAS-L						1st month 94.830±0.636	3 rd month 94.767±0.664		

Dissolution of SDD powders

The dissolution profiles of RTN from the SDD powders were determined in POE10 medium having pH 5.8. In Figure 6, at 360 min, release was 100% from SDD powder prepared at 70°C and 140 °C. At 10 min,

the drug release was 97.32 %, from 70 °C and 97.62% from 140 °C inlet temperature. The dissolution profiles of the SDD powders prepared at 70 °C were similar to an SDD powder at 140 °C. There was no significant difference in dissolution profiles (p>0.05).

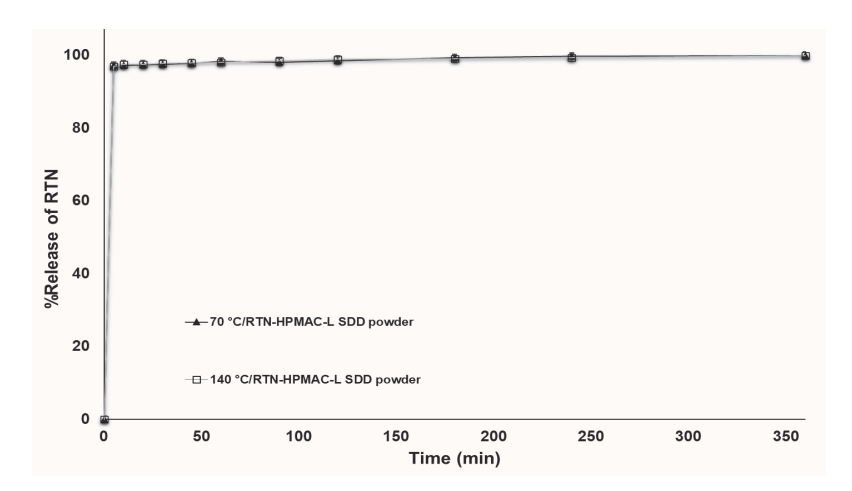


Figure 6. Dissolution profiles of the SDD powders prepared with 70 °C and 140 °C inlet temperatures

CONCLUSION

A DoE approach with 23 full factorial design (3-repeated) was performed to investigate the effect of process parameters on three CQAs. Ritonavir amorphous solid dispersions having low moisture content, better flowability, lower particle size, and high yield were successfully prepared via the spray dryer method. Short-term chemical stability studies supported that the RTN SDD powders were stable for three months. The solubility of the unprocessed crystalline RTN was significantly increased through the spray-dried powders, as well as compared to the physical mixture of ritonavir and HMPCAS-L. Dissolution studies showed that the SDDs from both inlet temperatures showed rapid drug release. Overall, an optimal RTN SDD was achieved and employed HPMCAS-L rather than PVP-VA, which is used in several commercial forms of RTN, albeit using hot melt extrusion.

ACKNOWLEDGEMENTS

This research was supported by the Scientific and Technological Research Council of Turkey (BIDEB 2219 (Project code: 1059B192000617)

AUTHOR CONTRIBUTION STATEMENT

Writing – review & editing, Writing – original draft, Methodology, Investigation, Funding acquisition, Conceptualization (Ayse Nur Oktay). Writing – review & editing, Resources, Conceptualization (James E. Polli).

CONFLICT OF INTEREST

Authors declare that there is no conflict of interest.

REFERENCES

AbbVie. (2017). Ritonavir (package insert). https://www.accessdata.fda.gov/drugsatfda_docs/label/2017/209512lbl.pdf, (accessed 18 March 2024).

Aviara, N. A., Power, P. P., & Abbas, T. (2013). Moisture-dependent physical properties of Moringa oleifera seed relevant in bulk handling and mechanical processing. *Industrial Crops and Products*, 42, 96-104.

Bhujbal, S. V., Mitra, B., Jain, U., Gong, Y., Agrawal, A., Karki, S., . . . Zhou, Q. T. (2021). Pharmaceutical amorphous solid dispersion: A review of manufacturing strategies. *Acta Pharmaceutica Sinica B*, *11*(8), 2505-2536.

Carina Hubert, T. C., Verena Geiselhart, Nils Rottmann Influence of the particle size of copovidone and crospovidone on tablet characteristics. https://www.pharmaexcipients.com/wp-content/uploads/2019/08/Influence-of-the-particle-size-of-copovidone-and-crospovidone-on-tablet-characteristics.pdf, (accessed 25 November 2024)

- Chinwan, D., & Castell-Perez, M. E. (2019). Effect of conditioner and moisture content on flowability of yellow cornmeal. *Food science & nutrition*, *7*(10), 3261-3272.
- Chiou, W. L., & Riegelman, S. (1971). Pharmaceutical applications of solid dispersion systems. *Journal of pharmaceutical sciences*, 60(9), 1281-1302.
- Focaroli, S., Mah, P., Hastedt, J., Gitlin, I., Oscarson, S., Fahy, J., & Healy, A. (2019). A Design of Experiment (DoE) approach to optimise spray drying process conditions for the production of trehalose/leucine formulations with application in pulmonary delivery. *International Journal of Pharmaceutics*, 562, 228-240.
- Gu, B., Linehan, B., & Tseng, Y.-C. (2015). Optimization of the Büchi B-90 spray drying process using central composite design for preparation of solid dispersions. *International Journal of Pharmaceutics*, 491(1-2), 208-217.
- Guiling, X., Xiaoping, C., Cai, L., Pan, X., & Changsui, Z. (2017). Experimental investigation on the flowability properties of cohesive carbonaceous powders. *Particulate Science and Technology*, 35(3), 322-329.
- Hofmann, N., Harms, M., & Mäder, K. (2024). ASDs of PROTACs: Spray-dried solid dispersions as enabling formulations. *International Journal of Pharmaceutics*, 650, 123725.
- Honick, M., Das, S., Hoag, S. W., Muller, F. X., Alayoubi, A., Feng, X., . . . Polli, J. E. (2020). The effects of spray drying, HPMCAS grade, and compression speed on the compaction properties of itraconazole-HPMCAS spray dried dispersions. *European journal of pharmaceutical sciences*, 155, 105556.
- Hsu, A., Granneman, G. R., & Bertz, R. J. (1998).
 Ritonavir: clinical pharmacokinetics and interactions with other anti-HIV agents. *Clinical pharmacokinetics*, 35, 275-291.

- Jermain, S. V., Brough, C., & Williams III, R. O. (2018). Amorphous solid dispersions and nanocrystal technologies for poorly water-soluble drug delivery–an update. *International Journal of Pharmaceutics*, 535(1-2), 379-392.
- Kalman, H. (2021). Effect of moisture content on flowability: angle of repose, tilting angle, and Hausner ratio. *Powder Technology*, 393, 582-596.
- Karakucuk, A., Teksin, Z. S., Eroglu, H., & Celebi, N. (2019). Evaluation of improved oral bioavailability of ritonavir nanosuspension. *European journal of* pharmaceutical sciences, 131, 153-158.
- Kempf, D. J., Marsh, K. C., Denissen, J. F., McDonald,
 E., Vasavanonda, S., Flentge, C. A., . . . Kong, X.P. (1995). ABT-538 is a potent inhibitor of human immunodeficiency virus protease and has high oral bioavailability in humans. *Proceedings of the National Academy of Sciences*, 92(7), 2484-2488.
- Klein, C., Chiu, Y., Awni, W., Ng, J., Cui, Y., Morris, J., . . . Bernstein, B. (2008). The effect of food on ritonavir bioavailability following administration of ritonavir 100 mg film-coated tablet in healthy adult subjects. *Age (years)*, 30(10.9), 20-55.
- Law, D., Krill, S. L., Schmitt, E. A., Fort, J. J., Qiu, Y., Wang, W., & Porter, W. R. (2001). Physicochemical considerations in the preparation of amorphous ritonavir–poly (ethylene glycol) 8000 solid dispersions. *Journal of pharmaceutical sciences*, 90(8), 1015-1025.
- LeClair, D. A., Cranston, E. D., Xing, Z., & Thompson, M. R. (2016). Optimization of spray drying conditions for yield, particle size and biological activity of thermally stable viral vectors. *Pharmaceutical research*, 33(11), 2763-2776.
- Maa, Y.-F., Costantino, H. R., Nguyen, P.-A., & Hsu, C. C. (1997). The effect of operating and formulation variables on the morphology of spray-dried protein particles. *Pharmaceutical development and technology*, 2(3), 213-223.

- Magri, G., Franzé, S., Musazzi, U. M., Selmin, F., & Cilurzo, F. (2019). Data on spray-drying processing to optimize the yield of materials sensitive to heat and moisture content. *Data in brief, 23*, 103792.
- Moseson, D. E., Tran, T. B., Karunakaran, B., Ambardekar, R., & Hiew, T. N. (2024). Trends in amorphous solid dispersion drug products approved by the US Food and Drug Administration between 2012 and 2023. *International Journal of Pharmaceutics: X*, 100259.
- Mujumdar, A. S. (2006). *Handbook of industrial drying*: CRC press.
- Muzaffar, K., Dinkarrao, B. V., & Kumar, P. (2016). Optimization of spray drying conditions for production of quality pomegranate juice powder. *Cogent food & agriculture*, 2(1), 1127583.
- Ogawa, N., Hiramatsu, T., Suzuki, R., Okamoto, R., Shibagaki, K., Fujita, K., . . . Yamamoto, H. (2018). Improvement in the water solubility of drugs with a solid dispersion system by spray drying and hot-melt extrusion with using the amphiphilic polyvinyl caprolactam-polyvinyl acetate-polyethylene glycol graft copolymer and d-mannitol. *European journal of pharmaceutical sciences*, 111, 205-214.
- Oktay, A. N., & Polli, J. E. (2024). Screening of Polymers for Oral Ritonavir Amorphous Solid Dispersions by Film Casting. *Pharmaceutics*, *16*(11), 1373.
- Osei-Yeboah, F., & Sun, C. C. (2023). Effect of drug loading and relative humidity on the mechanical properties and tableting performance of Celecoxib–PVP/VA 64 amorphous solid dispersions. *International Journal of Pharmaceutics*, 644, 123337.
- Patel, K., Patel, J., & Shah, S. (2023). Development of Delayed Release Oral Formulation Comprising Esomeprazole Spray Dried Dispersion Utilizing Design of Experiment As An Optimization Strategy. AAPS PharmSciTech, 24(7), 186.

- Pharmacopeia, U. S. <1174>PowderFlow. https://www.usp.org/sites/default/files/usp/document/harmonization/gen-chapter/20230428HSm99885.pdf, (accessed 25 November 2024)
- Pongsamart, K., Limwikrant, W., Ruktanonchai, U. R., Charoenthai, N., & Puttipipatkhachorn, S. (2022). Preparation, characterization and antimalarial activity of dihydroartemisinin/β-cyclodextrin spray-dried powder. *Journal of Drug Delivery Science and Technology*, 103434.
- Singh, A., & Van den Mooter, G. (2016). Spray drying formulation of amorphous solid dispersions. *Advanced drug delivery reviews*, 100, 27-50.
- Stegemann, S., Leveiller, F., Franchi, D., De Jong, H., & Lindén, H. (2007). When poor solubility becomes an issue: from early stage to proof of concept. *European journal of pharmaceutical sciences*, 31(5), 249-261.
- Thirugnanasambandham, K., & Sivakumar, V. (2017). Influence of process conditions on the physicochemical properties of pomegranate juice in spray drying process: Modelling and optimization. *Journal of the Saudi Society of Agricultural Sciences*, 16(4), 358-366.
- United States Pharmacopeia. <616>Bulk Density
 Of Powder., https://www.usp.org/sites/default/
 files/usp/document/our-work/referencestandards/20240927HSm99375.pdf (accessed 25
 November 2024)
- Van den Mooter, G. (2012). The use of amorphous solid dispersions: A formulation strategy to overcome poor solubility and dissolution rate. *Drug Discovery Today: Technologies*, 9(2), e79-e85.
- Wagner, C., Jantratid, E., Kesisoglou, F., Vertzoni, M., Reppas, C., & Dressman, J. B. (2012). Predicting the oral absorption of a poorly soluble, poorly permeable weak base using biorelevant dissolution and transfer model tests coupled with a physiologically based pharmacokinetic model. European Journal of Pharmaceutics and Biopharmaceutics, 82(1), 127-138.

- Williams, H. D., Trevaskis, N. L., Charman, S. A., Shanker, R. M., Charman, W. N., Pouton, C. W., & Porter, C. J. (2013). Strategies to address low drug solubility in discovery and development. *Pharmacological reviews*, 65(1), 315-499.
- Yu, J., Yu, D., Lane, S., McConnachie, L., & Ho, R. J. (2020). Controlled solvent removal from antiviral drugs and excipients in solution enables the formation of novel combination multi-drugmotifs in pharmaceutical powders composed of lopinavir, ritonavir and tenofovir. *Journal of pharmaceutical sciences*, 109(11), 3480-3489.
- Zhou, D., Zhang, G. G., Law, D., Grant, D. J., & Schmitt, E. A. (2002). Physical stability of amorphous pharmaceuticals: importance of configurational thermodynamic quantities and molecular mobility. *Journal of pharmaceutical sciences*, 91(8), 1863-1872.

Bivariate and Multivariate Calibration Approach for the Spectrophotometric Analysis of Two-Component Drugs in Real Tablets

Erdal DİNÇ*, Asiye ÜÇER**, Zehra Ceren ERTEKİN***, Ömer Faruk GÜZEL****

Bivariate and Multivariate Calibration Approach for the Spectrophotometric Analysis of Two-Component Drugs in Real Tablets

SUMMARY

This study presents a novel and simple spectrophotometric method for simultaneously quantifying rosuvastatin (ROS) and amlodipine (AML) in tablet formulation. Due to their overlapping absorption spectra, traditional spectrophotometric techniques were inadequate for analyzing these two drugs. To address this challenge, bivariate and multivariate calibration techniques were employed for the simultaneous determination of ROS and AML. Regression equations were generated using known concentrations and corresponding absorbance values of ROS and AML across different wavelengths, specifically between 224 and 371 nm. A total of 22 different regression equations were computed to establish the bivariate calibration method. The slope values from these equations were utilized to create sensitivity matrices, and the determinant of each sensitivity matrix was calculated for various wavelength pairs. An optimal wavelength pair was selected using Kaiser's technique, and a corresponding set of equations was constructed based on this chosen pair. The effectiveness of the proposed methods was validated through the analysis of synthetic mixtures and standard addition samples. Ultimately, the methods demonstrated a successful application for quantitatively analyzing ROS and AML in tablets.

Key Words: Amlodipine, bivariate calibration method, multivariate calibration method, quantitative determination of tablets, rosuvastatin, spectrophotometric analysis.

Gerçek Tabletlerdeki İki Bileşenli İlaçların Spektrofotometrik Analizi İçin İki Değişkenli ve Çok Değişkenli Kalibrasyon Yaklaşımı

ÖZ

çalışma, tablet formülasyonunda rosuvastatin (ROS) ve amlodipin (AML) için eş zamanlı olarak tayin etmek için yeni ve basit bir spektrofotometrik yöntem sunmaktadır. Çakışan absorbans spektrumları nedeniyle, geleneksel spektrofotometrik teknikler bu iki ilacı analiz etmek için yetersizdir. Bu zorluğun üstesinden gelmek için, ROS ve AML'nin eş zamanlı tayini için iki değişkenli ve çok değişkenli kalibrasyon teknikleri kullanıldı. Regresyon denklemleri, bilinen konsantrasyonlar ve farklı dalga boylarında, özellikle 224 ile 371 nm arasında ROS ve AML'nin karşılık gelen absorbans değerleri kullanılarak oluşturuldu. İki değişkenli kalibrasyon yöntemini oluşturmak için toplam 22 farklı regresyon denklemi hesaplandı. Bu denklemlerden elde edilen eğim değerleri duyarlılık matrisleri oluşturmak için kullanıldı ve her duyarlılık matrisinin determinantı cesitli dalga boyu ciftleri için hesaplandı. Kaiser tekniği kullanılarak optimum bir dalga boyu çifti seçildi ve bu seçilen çifte karşılık gelen bir denklem seti oluşturuldu. Önerilen yöntemlerin etkinliği, sentetik karışımların ve standart ekleme örneklerinin analizi aracılığıyla doğrulandı. Sonuç olarak, yöntemlerin tabletlerdeki ROS ve AML'nin kantitatif analizinde başarılı bir şekilde uygulanabileceği ortaya konmuştur.

Anahtar Kelimeler: Amlodipin, çift değişkenli kalibrasyon yöntemi, çok değişkenli kalibrasyon yöntemi, tabletlerin kantitatif tayini, rosuvastatin, spektrofotometrik analiz.

Received: 21.01.2025 Revised: 14.03.2025 Accepted: 18.04.2025

° Corresponding Author; Prof. Dr. Erdal Dinç E-mail: dinc@ankara.edu.tr

ORCID: 0000-0001-6326-1441, Department of Analytical Chemistry, Faculty of Pharmacy, Ankara University, 06560 Yenimahalle, Ankara, Turkey.

[&]quot;ORCID: 0000-0002-9286-3211, Department of Analytical Chemistry, Faculty of Pharmacy, Ankara Yıldırım Beyazıt University, 06010 Etlik, Keçiören, Ankara, Turkey.

[&]quot;" ORCID: 0000-0002-1549-6024, Department of Analytical Chemistry, Faculty of Pharmacy, Ankara University, 06560 Yenimahalle, Ankara, Turkey. "" ORCID: 0000-0001-7221-0152, Department of Analytical Chemistry, Faculty of Pharmacy, Ankara University, 06560 Yenimahalle, Ankara, Turkey.

INTRODUCTION

Cardiovascular diseases occupy a central place among global health problems and are the leading cause of death and morbidity worldwide (Roth, 2018). In recent years, national and international health systems and scientific research centers have been spending great financial and economic efforts on strategies to prevent the disease and manage risk factors in cases where diabetes, cholesterol, and hypertension coexist in individuals with cardiovascular disease. Most cardiovascular diseases can be prevented by implementing social strategies and controlling behavioral risk factors (such as unhealthy diet, tobacco use, obesity, physical inactivity, and harmful alcohol use) (World Health Organization, 2024). However, in cases where it cannot be prevented, patients must take more than one medication for treatment (Asia Pacific Cohort Studies Collaboration, 2005).

Multiple studies have shown that treating hypertension and dyslipidemia together with antihypertensive drugs and statins leads to a significant and synergistic reduction in cardiovascular risk, compared to managing these conditions separately (Multiple Risk Factor Intervention Trial Research Group,1982; Sever et al., 2003; Schwalm et al., 2016). The most recent European Guidelines recommend the combined use of angiotensin receptor blockers/angiotensin-converting enzyme inhibitors plus calcium channel blockers or thiazide-like diuretic drugs hypertension management. In these guidelines, amlodipine (AML) is recognized as one of the primary blood pressure-lowering drugs and is recommended for use together with statin group drugs in patients with coexistent dyslipidemia (Williams et al., 2018). Rosuvastatin (ROS) is a member of the statin class of drugs, that reduce cholesterol levels and that are effective in preventing cardiovascular diseases and lowering high cholesterol (Mccormick et al., 2000; Olsson et al., 2001). The combined use of AML and ROS drugs not only reduces blood pressure and lipid levels but also contributes to the reduction of cardiovascular events and mortality by treating patients in their complexity (Chapman, Yeaw & Roberts, 2010; Kim et al., 2020). Moreover, this combination, offered in a single pill formulation, reduces blood pressure and lipid values more effectively than two separate drugs (Kim et al., 2020; Sarzani et al., 2022). These clinical and pharmacological results require the development of accurate, sensitive, selective, and rapid analytical methods to achieve the co-determination of the binary combination drug in tablets. The literature review indicates that various liquid chromatographic methods, including HPLC-PDA (Ashfaq et al., 2014; Kansara et al., 2020; Saurabh & Nitin, 2013; Yılmaz & Yılmaz, 2020), and HPTLC (Kansara et al., 2020), are predominantly studied for the quantitative determination of AML and ROS in drug formulations or biological fluids. However, these methods need expensive and high-tech equipment and expertise. It is also important to note that spectrophotometric methods are widely used in literature for drug analysis due to their ease of use and inexpensiveness. On the other hand, overlapping absorption spectra of multiple drug substances make it difficult to use conventional spectrophotometric methods for drug combinations.

When analyzing multiple drug substances, overlapping spectra require more sophisticated models such as classical least-squares, inverse least-squares, partial least-squares, and principal component regression with commercially available software. In contrast, bivariate and multivariate calibration models are simple and powerful choices for the quantitative analysis of mixtures due to their simple mathematical treatments.

Bivariate calibration models are based on the selection of a suitable wavelength pair to get a calibration model, explaining the relationship between the absorbance values and the concentration of analytes using Kaiser's method to find the best sensitivity. On the other hand, the multivariate calibration method of regression equations is constructed using n-wavelengths without needing a choice of suitable wave-

length pair for quantifying analytes in a mixture. Details of theoretical principles and application of the bivariate and multivariate calibration models based on the regression equations to analyze a two-component mixture can be found in Dinc, 2003.

In this work, the bivariate and multivariate calibration approaches were proposed to resolve the overlapping spectra and quantify ROS and AML in commercial tablets without a preliminary separation step.

MATERIAL AND METHODS

Instruments and software

A Shimadzu UV-160 double-beam UV-Vis spectrophotometer with Shimadzu UVPC software was used to procure the absorption spectra of the compounds and their samples in the spectral range of 200-420 nm. MATLAB 7.0 and Microsoft Excel were used for data acquisition and statistical calculations.

Chemicals and reagents

The drug standards, rosuvastatin calcium (≥98%) and amlodipine besylate (≥98%) were obtained from Sigma-Aldrich (Steinheim, Germany). For spectrophotometric analysis, the methanol, which is of HPLC grade, was used as a solvent and purchased from J.T. Baker (Netherlands). All solutions were freshly prepared daily and kept in the dark throughout the analysis to maintain the stability.

Preparation of stock standard, calibration, and validation solutions

To prepare stock solutions of ROS and AML, 0.01 grams of each compound were separately weighed and dissolved in methanol in 100 mL volumetric flasks. These stock solutions were then appropriately diluted with methanol to get calibration, and validation sample solutions would be checked with the bivariate and multivariate calibration techniques.

To apply the bivariate and multivariate calibration approaches, standard calibration solutions were prepared in the concentration range of $4.0\text{-}28.0~\mu\text{g/mL}$

for ROS and AML. The 11 synthetic mixtures containing ROS and AML in different levels within the working concentration range were prepared similarly. The standard addition samples were prepared in triplicates by adding AML and ROS standard solutions (0, 6, 14, and 22 $\mu g/$ mL) to a portion of the commercial tablet sample solution.

Preparation of Tablet Samples

Ten tablets of ROSUCOR PLUS® (Celtis İlaç Ltd. Şti.) were accurately weighed, and the quantity corresponding to one tablet (266.3 mg) was transferred to a 100 mL volumetric flask after thorough pulverization of the tablets in a mortar. The flask was filled with methanol, and the powdered sample was mixed with a mechanical stirrer for 30 minutes. Filtration was conducted through a 0.45 μ m pore size filter (Pall Industries, USA). The filtrate was diluted with methanol (1:10) to reach a concentration of 20 μ g/ mL ROS and 10 μ g/ mL AML. The diluted tablet solution was subjected to UV-VIS analysis for the application of the bivariate and multivariate calibration approaches. The declared contents of the tablet were as follows: 20 mg ROS and 10 mg AML per tablet.

RESULTS AND DISCUSSION

In traditional spectral analysis methods, the most common handicap is the overlapping of spectral bands in the solution of two or more components. To overcome this difficulty in the analysis, we applied bivariate and multivariate calibration methods which are reliable, simple, cheap, and rapid to the quantitative simultaneous determination of ROS and AML. The bivariate approach uses the four linear regression calibration equations with two calibrations for each component at two wavelengths selected (Demirbilek, Dinç & Baleanu, 2010; Dinç, Arslan & Baleanu, 2008).

Standard solutions of ROS and AML were prepared within a working concentration range of 4.0 to $28.0~\mu g/mL$. The absorption spectra of these sample solutions were recorded from 200 to 420 nm, as shown in Figure 1.

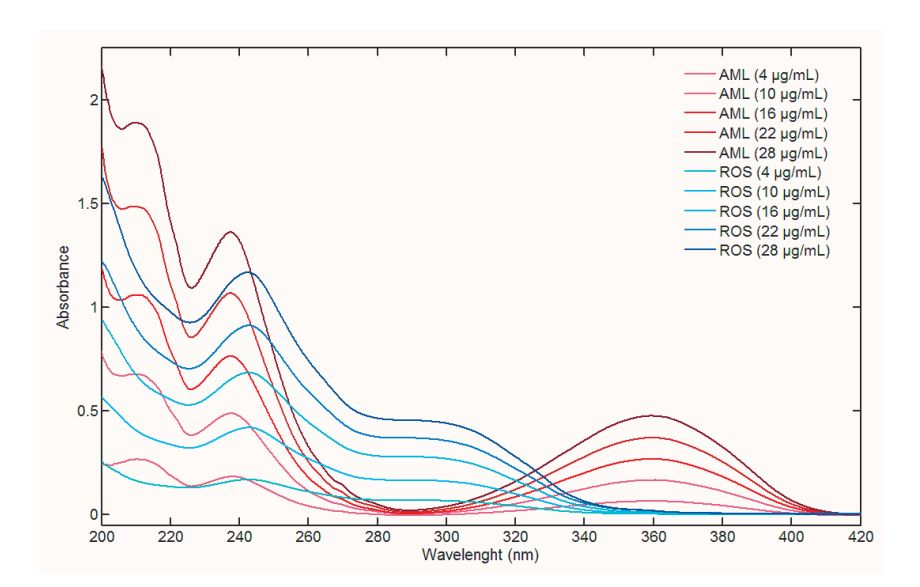


Figure 1. Absorbance spectra of ROS and AML in the working concentration range of 4.0-28.0 μg/mL

The traditional spectrophotometric method could not analyze these two drugs in their mixtures because their spectra overlap. Bivariate and multivariate calibration techniques with simple mathematical algorithms and applications were developed to simultaneously determine both ROS and AML in the same binary mixtures. To build bivariate and multivariate calibration methods, we computed 22 different re-

gression equations using known concentrations and absorbance values across various wavelengths ranging from 224 nm to 371 nm. The slope values derived from these equations were used to create sensitivity matrices. We calculated the determinants of the sensitivity matrices for each pair of wavelengths, which are illustrated in Figure 2.

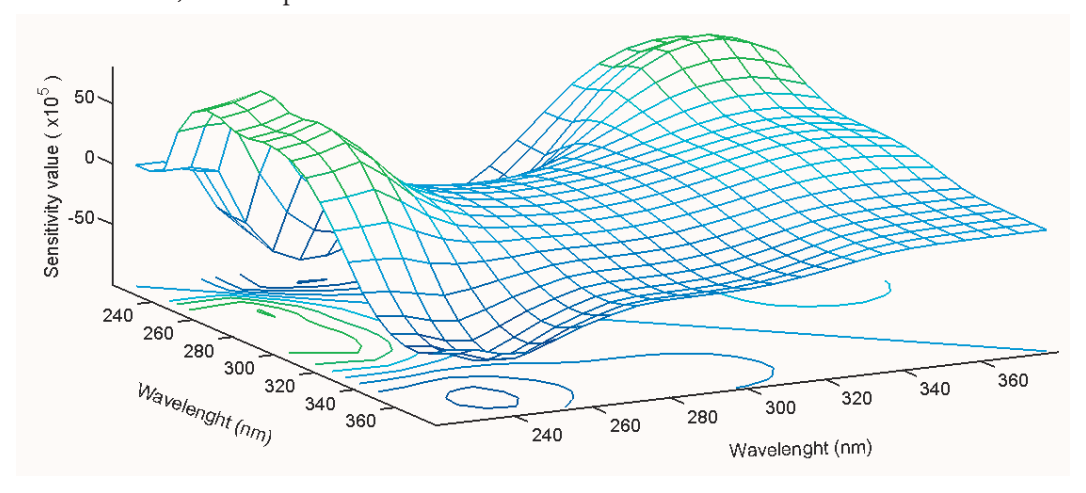


Figure 2. Three-dimensional illustration of wavelength pairs and corresponding sensitivity values.

For the bivariate calibration, an optimal pair of wavelengths were selected as 238 nm and 259 nm using Kaiser's technique. Then, an equation set was constructed using this wavelength pair to implement a bivariate calibration approach.

Unknown concentrations of AML and ROS were obtained by solving the equations constructed using the bivariate approach. Using the optimal wavelength pair, the bivariate equation system was obtained. This linear equation system in matrix format is represented below:

$$\begin{pmatrix} A_{mix_{238nm}} \\ A_{mix_{259nm}} \end{pmatrix} = \begin{pmatrix} 4.88x10^{-2} & 4.02x10^{-2} \\ 1.30x10^{-2} & 2.73x10^{-2} \end{pmatrix} x \begin{pmatrix} C_{AML} \\ C_{ROS} \end{pmatrix} + \begin{pmatrix} -4.57x10^{-3} \\ 5.27x10^{-3} \end{pmatrix}$$

The concentrations of ROS and AML in the analyzed synthetic mixtures were quantified using the linear equation above.

The multivariate calibration approach is similar to the bivariate method; however, it utilizes multiple wavelengths instead of just two [26]. In this case, a multivariate calibration technique was employed us-

ing all 22 regression equations at critical points, including the maximum, shoulder, and minimum values within the spectral range of 224-278 nm for the related compounds in the binary mixtures. The system of the 22 regression equations was represented as follows:

$$\begin{pmatrix} A_{\vec{u}} & a_{nm} \\ A_{\vec{u}} & a_{nm} \\ \ddot{u} \\ A_{\vec{u}} & a_{nm} \end{pmatrix} = \begin{pmatrix} 4.16 \vec{u} 10^{Ni} & 3.31 & 10 \\ 4.39 \vec{u} 10^{Ni} & 3.49 & 10 \\ \dots & \dots & \dots \\ \ddot{u} & \dots & \dots \\ 1.27 x 10^{Ni} & 2.55 x 10 \end{pmatrix} x \begin{pmatrix} C_{\vec{u}} \\ C_{\vec{u}} \end{pmatrix} + \begin{pmatrix} -4.52 & 10 \\ -2.05 & 10 \\ \dots & \dots \\ -4.04 x 10 \end{pmatrix}$$

Validation studies were performed using synthetic samples, and standard addition samples. The results of recovery studies as percentage average recoveries and their relative standard deviations for both bivariate and multivariate calibration methods are given in Table 1. The results were satisfactory with appropriate accuracy and precision without requiring preliminary separation step.

Table 1. Recovery results of synthetic test samples

			Biva	riate	Multiv	variate	Biva	riate	Multiv	variate
	Added	(μg/μL)	Fou	ınd	Fou	and	Recove	ry (%)	Recove	ery (%)
No.	AML	ROS	AML	ROS	AML	ROS	AML	ROS	AML	ROS
1	4	20	4.07	19.98	4.07	19.98	101.6	99.9	101.8	99.9
2	10	20	10.62	19.20	10.32	19.83	106.2	96.0	103.2	99.1
3	16	20	16.56	19.12	16.24	19.71	103.5	95.6	101.5	98.6
4	22	20	22.34	18.86	21.93	19.52	101.5	94.3	99.7	97.6
5	28	20	28.27	19.20	27.99	19.77	101.0	96.0	100.0	98.8
6	10	4	10.35	3.97	10.69	3.94	103.5	99.2	106.9	98.4
7	10	10	10.50	9.95	10.04	10.22	105.0	99.5	100.4	102.2
8	10	16	10.32	15.60	9.91	16.44	103.2	97.5	99.1	102.8
9	10	22	10.61	21.50	10.36	22.08	106.1	97.7	103.6	100.4
10	10	28	10.63	26.59	10.23	27.32	106.3	95.0	102.3	97.6
11	10	20	10.60	20.46	10.62	20.68	106.0	102.3	106.2	103.4
						Mean	104.0	97.3	102.2	99.8
			Star	ndard deviati	on		1.94	1.95	2.45	1.76
			F	Relative stand	ard deviatior	1	1.87	2.01	2.40	1.76

Standard addition samples were prepared at three distinct concentration levels for ROS and AML (6, 14, and 22 μ g/mL) and analyzed with the two proposed calibration methods. Then added recovery results for each drug were calculated. Their results (recovery value and standard deviation) are presented in Table 2. The experimental results were calculated as the mean

of triplicate measurements for each concentration level. As evidenced by the results presented in Table 2, the composition of the sample matrix did not influence the analysis of simultaneous AML and ROS. In other words, the results were found to be satisfactory for the selectivity of the proposed analytical methods.

Table 2. Quantitative results of standard addition samples

		Ado	led	Found (μg/μL)			
		$(\mu g/\mu L)$		Bivariate c	alibration	Multivariate calibration	
		AML	ROS	AML	ROS	AML	ROS
Tablet	+	6	6	6.06	5.83	5.76	6.00
Tablet	+	14	14	14.41	9.96	14.06	10.09
Tablet	+	22	22	22.88	14.47	22.21	14.94
		Recovery (%)		102.6	100.0	99.1	102.5
		RSD		0.33	0.36	0.28	0.39

RSD: Relative standard deviation

Bivariate and multivariate calibration methods were used to quantify the active drugs, AML and ROS, simultaneously in real tablet samples. The experimental results, which were calculated as an average of ten measurements (n=10) for real tablet analysis, present-

ed in Table 3, demonstrate a high degree of agreement with the labeled claims of the tablet samples. Additionally, the standard deviation and relative standard deviation values provided in Table 3 confirm the reliability and effectiveness of the proposed methods.

Table 3. Assay results of the commercial tablets.

	Bivariate calibration		Multivariat	e calibration
	AML	ROS	AML	ROS
Mean*	10.10	19.60	9.96	20.08
Standard deviation	0.13	0.45	0.11	0.31
Relative standard deviation	1.32	2.30	1.13	1.52

^{*} n = 10

(Label claim: 10 mg AML/20 mg ROS per tablet)

CONCLUSION

Two simple mathematical models, bivariate and multivariate calibration approaches based on the use of linear regression functions, were proposed to quantify ROS and AML in binary mixtures and commercial tables without a preliminary separation procedure. Both methods gave suitable results, although multivariate calibration results were slightly better (in terms of closeness to the label claim and standard deviation) When com-

paring the spectral bivariate and multivariate approaches with the HPLC method given in the literature (Ashfaq et al.), the proposed spectral methods have some advantages, such as simplicity, rapidity, ease of application, and cost-effectiveness for the quality control and routine analysis of tablets containing ROS and AML. The mentioned HPLC analysis requires expensive instrumentation, a long analysis period (e.g., long runtime, more than 20 minutes, to analyze ROS and AML), excessive

solvent conception, etc. These methods can be easily applied in routine quality control. Once the bivariate and multivariate calibration equations are constructed, the concentration of analytes in unknown solutions can be easily calculated from the absorbance values by solving these equations. Consequently, the bivariate and multivariate calibrations provided new and alternative ways to quantitatively resolve the mixtures containing the analyzed drugs with short analysis time and low cost. Assay results showed that these methods were fast, easy, cheap, and suitable for the routine analysis and quality control of tablets containing AML and ROS.

ACKNOWLEDGEMENTS

In this study, the method development and its experiment procedures were performed at the Chemometrics Laboratory of the Faculty of Pharmacy supported by Ankara University Scientific Research Fund (Project No. 10A3336001).

AUTHOR CONTRIBUTION STATEMENT

Conceptualization, Formal Analysis, Resources, Supervision, Writing-Review & Editing (ED), Investigation, Data curation, Writing-Original Draft, Writing-Review & Editing (AÜ), Data curation, Writing-Original Draft, Writing-Review & Editing (ZCE), Investigation (ÖFG)

CONFLICT OF INTEREST

Authors declare that there is no conflict of interest.

REFERENCES

- Ashfaq, M., Akhtar, T., Mustafa, G., Danish, M., Razzaq, S.N., & Nazar, M.F. (2014). Simultaneous estimation of rosuvastatin and amlodipine in pharmaceutical formulations using stability indicating HPLC method, *Brazilian Journal of Pharmaceutical Sciences*, 50(3), 629-638. http://dx.doi.org/10.1590/S1984-82502014000300023
- Asia Pacific Cohort Studies Collaboration. (2005). Joint effects of systolic blood pressure and serum cholesterol on cardiovascular disease in the Asia Pacific region. *Circulation*, 112(22), 3384-3390. doi:10.1161/circulationaha.105.537472

- Banerjee, S.K., & Vasava, N.M. (2013). Simultaneous estimation of amlodipine and rosuvastatin in combined bulk forms by RP-HPLC using ultraviolet detection, *Bulletin of Pharmaceutical Research*. *3*(1), 29-33. Retrieved from https://journal.appconnect.in/
- Chapman, R.H., Yeaw, J., & Roberts, C.S. (2010). Association between adherence to calcium-channel blocker and statin medications and likelihood of cardiovascular events among US managed care enrollees. *BMC Cardiovascular Disorders*, 10, 29. doi:10.1186/1471-2261-10-29
- Demirbilek, M.P., Dinç, E., & Baleanu, D. (2010). Spectrophotometric Simultaneous Determination of Atorvastatin-Amlodipin and Telmisartan-Hidrochlorothiazide Mixtures by Bivariate and Multivariate Calibrations, *Revista de Chimie*, 61(6), 532-540. Retrived from https://revistadechimie.ro/
- Dinç, E. (2003). Linear regression analysis and its application to the multivariate spectral calibrations for the multiresolution of a ternary mixture of caffeine, paracetamol and metamizol in tablets, *Journal of Pharmaceutical and Biomedical Analysis*, 33, 605-615. https://doi.org/10.1016/S0731-7085(03)00260-7
- Dinç, E., Arslan, F., & Baleanu, D. (2008). Spectrophotometric simultaneous Analysis of two-component mixture by bivariate and multivariate calibrations using the linear regression functions, *Revue Roumaine de Chimie*, 53(8), 607-615. Retrived from https://revroum.lew.ro/
- Kansara, D., Chhalotiya, U.K., Kachhiya, H.M., & Patel, I. (2020). Development of TLC method for simultaneous estimation of novel combination of amlodipine besylate, rosuvastatin calcium, and fimasartan potassium in synthetic mixture, *Jour*nal of Chemical Metrology, 14(2), 142-152. http:// doi.org/10.25135/jcm.45.20.07.1744

- Kansara, D.A., Chhalotiya, U.K., Kachhiya, H.M., Patel, I.M., & Shah, D.A. (2020). Simultaneous estimation of amlodipine besylate, Rosuvastatin calcium and Fimasartan potassium trihydrate combination used in the treatment of hypertension using LC method, *SN Applied Sciences*, *2*, 948. https://doi.org/10.1007/s42452-020-2758-4
- Kim, W., Chang, K., Cho, E.J., Ahn, J.C., Yu, C.W., Cho, K.I., ...Park, C.G. (2020). A randomized, double-blind clinical trial to evaluate the efficacy and safety of a fixed-dose combination of amlodipine/rosuvastatin in patients with dyslipidemia and hypertension. *The Journal of Clinical Hypertension*, 22(2), 261-269. doi:10.1111/jch.13774.
- Mccormick, A.D., Mckillop, D., Butters, C.J., Miles, G.S., Baba, T., & Touchi, A. (2000). ZD4522-an HMG-CoA reductase inhibitor free of metabolically mediated drug interactions: metabolic studies in human in vitro systems. *The Journal of Clinical Pharmacology*, 40, 1055.
- Multiple Risk Factor Intervention Trial Research Group (1982). Multiple risk factor intervention trial. Risk factor changes and mortality results. *JAMA*. 248(12), 1465-77. doi:10.1001/jama.1982.03330120023025
- Narapusetti, A., Bethanabhatla, S.S., Sockalingam, A., Repaka, N., & Saritha, V. (2015). Simultaneous determination of rosuvastatin and amlodipine in human plasma using tandem mass spectrometry: Application to disposition kinetics, *Journal of Advanced Research*, 6(6), 931-940. doi: 10.1016/j. jare.2014.08.010
- Olsson, A.G., Pears, J., Mckellar, J., Mizan, J., & Raza, A. (2001). Effect of rosuvastatin on low-density lipoprotein cholesterol in patients with hypercholesterolemia. American Journal of Cardiology, 88, 504-508.
- Roth, G. (2018). GBD 2017 Causes of Death Collaborators. Global, regional, and national age-sex-specific mortality for 282 causes of death in 195 countries and territories, 1980–2017: a systematic analysis for the Global Burden of Disease Study 2017. *Lancet*. 392(10159), 1736-88. doi:10.1016/S0140-6736(18)32203-7.

- Sarzani, R., Laureti, G., Gezzi, A., Spannella, F., & Giulietti, F. (2022). Single-pill fixed-dose drug combinations to reduce blood pressure: the right pill for the right patient. *Therapeutic Advances in Chronic Disease*. 24(13). doi:20406223221102754.
- Schwalm, J.D., McKee, M., Huffman, M.D., & Yusuf, S. (2016). Resource effective strategies to prevent and treat cardiovascular disease. *Circulation*, 133(8), 742-55. doi: 10.1161/CIRCULATIONA-HA.115.008721.
- Sever, P.S., Dahlöf, B., Poulter, N.R., Wedel, H., Beevers, G., Caulfield, M., ... Ostergren, J. (2003). Prevention of coronary and stroke events with atorvastatin in hypertensive patients who have average or lower-than-average cholesterol concentrations, in the Anglo-Scandinavian Cardiac Outcomes Trial-Lipid Lowering Arm (ASCOT-LLA): A multicentre randomised controlled trial. *The Lancet*, 361(9364), 1149–1158. doi:10.1016/S0140-6736(03)12948-0
- Williams, B., Mancia, G., Spiering, W., Agabiti, R. E., Azizi, M., Burnier, M., Desormais, I. (2018). 2018 ESC/ESH guidelines for the management of arterial hypertension. *European Heart Journal*, *39*, 3021-3104. doi:10.1093/eurheartj/ehy339.
- World Health Organization. (2017). Cardiovascular diseases fact sheet. Retrieved December 25, 2024, from https://www.who.int/news-room/fact-sheets/detail/cardiovascular-diseases-(cvds)
- Yılmaz, B., &Yılmaz, N. (2020). Simultaneous determination of rosuvastatin and amlodipine in binary mixtures by differential pulse voltammetry and HPLC methods, *Eurasian Chemical Communications*, 2(8), 881-894. doi:10.33945/sami/ecc/ecc.2020.228276.1045

Development of Innovative Microemulsion-based Gelatine Capsules of Ondansetron Hydrochloride

Sreehari S. NAIR*, Dhanashree P. SANAP***, Kisan R. JADHAV***

Development of Innovative Microemulsion-based Gelatine Capsules of Ondansetron Hydrochloride

SUMMARY

This research investigates the formulation and assessment of gelatine capsules containing a microemulsion of Ondansetron Hydrochloride (ODN) aimed at improving its bioavailability and therapeutic effectiveness. ODN, a commonly utilized antiemetic, is characterized by low oral bioavailability primarily due to significant first-pass metabolism. To mitigate this challenge, a microemulsion system was developed using a blend of oil, surfactant, and co-surfactant, which was subsequently encapsulated within gelatine capsules. The resulting capsules were analyzed for their drug - excipient interactions, drug release profile, etc., ensuring that the formulation possessed optimal characteristics for enhanced drug delivery. Findings indicated that the microemulsion-based gelatine capsules markedly enhanced the dissolution rate of ODN, indicating a viable strategy for addressing its bioavailability challenges. This study presents an innovative formulation approach that holds the potential to improve the therapeutic efficacy of ODN in clinical applications.

Key Words: Microemulsion, ondansetron hydrochloride, gelatine capsule

Ondansetron Hidroklorürün Yenilikçi Mikroemülsiyon Bazlı Jelatin Kapsüllerinin Geliştirilmesi

ÖZ

Bu araştırma, biyoyararlanımı ve terapötik etkinliği iyileştirmeyi amaçlayan Ondansetron Hidroklorürün (ODN) mikroemülsiyonu içeren jelatin kapsüllerin formülasyonu ve değerlendirilmesini incelemektedir. Yaygın olarak kullanılan bir antiemetik olan ODN, oral biyoyararlanımı düşük bir ilaçtır ve bu durum, büyük ölçüde belirgin ilk geçiş metabolizmasından kaynaklanmaktadır. Bu sorunu hafifletmek amacıyla, yağ, yüzey aktif madde ve yardımcı yüzey aktif madde karışımı kullanılarak bir mikroemülsiyon sistemi geliştirilmiş ve ardından bu sistem jelatin kapsüller içine yerleştirilmiştir. Elde edilen kapsüller, ilaç - yardımcı madde etkileşimleri, ilaç salım profili gibi özellikler açısından analiz edilerek, formülasyonun geliştirilmiş ilaç salınımı için optimum özelliklere sahip olması sağlanmıştır. Bulgular, mikroemülsiyon bazlı jelatin kapsüllerin ODN'nin çözünme hızını önemli ölçüde artırdığını ve bu durumun biyoyararlanım sorunlarını çözmeye yönelik uygulanabilir bir strateji olduğunu göstermiştir. Bu çalışma, ODN'nin klinik uygulamalardaki terapötik etkinliğini artırma potansiyeline sahip yenilikçi bir formülasyon yaklaşımı sunmaktadır.

Anahtar Kelimeler: Mikroemülsiyon, ondansetron hidroklorür, jelatin kapsül

Received: 11.12.2024 Revised: 30.03.2025 Accepted: 24.04.2025

ORCID: 0009-0009-1566-986X, Department of Quality Assurance, Bharati Vidyapeeth's College of Pharmacy, University of Mumbai, Navi Mumbai - 400614, Maharashtra, India.

[&]quot;ORCID: 0000-0002-4794-7598, Department of Pharmaceutics, Bharati Vidyapeeth's College of Pharmacy, University of Mumbai, Navi Mumbai - 400614, Maharashtra, India.

[&]quot;" ORCID: 0000-0001-7563-3935, Department of Pharmaceutics, Bharati Vidyapeeth's College of Pharmacy, University of Mumbai, Navi Mumbai - 400614, Maharashtra, India

INTRODUCTION

Ondansetron hydrochloride (ODN) is a potent and selective antagonist of the serotonin 5-HT3 receptor, renowned for its efficacy in preventing nausea and vomiting. The compound is characterized by the molecular formula C₁₈H₁₉N₃O.HCl possesses a carbazole structure that contributes to its strong receptor binding affinity. ODN is predominantly employed in the prophylaxis and treatment of nausea and vomiting associated with chemotherapy, radiation therapy, and surgical anesthesia. Its mechanism of action involves the inhibition of serotonin at the 5-HT, receptors located in both the central nervous system and the gastrointestinal tract, thereby mitigating the emetic reflex. While generally well-tolerated, it may produce side effects such as headache, constipation, and dizziness. Given its critical role in clinical practice, ODN is an essential element of supportive care, particularly in oncology and perioperative settings, providing substantial relief from the debilitating effects of nausea and vomiting (Charyulu et al., 2010; Dhanashree et al., 2022; Gullapalli et al. 2010; Gundu et al., 2020).

The administration of ODN, despite its efficacy, faces several challenges that may limit its therapeutic effectiveness. A primary issue is its relatively low oral bioavailability, which is approximately 60 %. This limitation is largely due to significant first-pass metabolism occurring in the liver, involving cytochrome P450 enzymes such as CYP3A4 and CYP2D6. This metabolic pathway not only reduces the quantity of active drug that reaches systemic circulation but also contributes to variability in patient responses to the treatment. Additionally, the poor solubility of ODN poses a challenge for formulation scientists, potentially impacting the drug's absorption and overall bioavailability (Chitneni et al. 2011; Gosai et al. 2008; Jena et al. 2010; Manavalan et al. 2009).

The oral route of drug administration is widely accepted, accounting for approximately 50-60 % of the total available dosage forms for a given medication. The popularity of solid oral dosage forms can be at-

tributed to several factors, including precise dosing, the potential for self-medication, the avoidance of pain, and, most significantly, the convenience they offer to patients (Breatnach et al., 2000; Fox et al., 1994).

The integration of ODN into a microemulsion system, followed by encapsulation in gelatine capsules, presents numerous advantages compared to traditional marketed formulations. The commonly available dosage forms include tablets, orally disintegrating tablets (ODTs), syrups, and films. Tablets, ODT, and syrups of ODN are well-established in the market, offering convenience and ease of administration for patients suffering from emesis. Films, on the other hand, provide a rapidly dissolving alternative that can be particularly beneficial for patients who experience difficulty swallowing tablets (Abruzzo et al., 2016; Ahmadi et al., 2015; Bansal et al., 2013; Canet al., 2013).

Microemulsions are noted for their thermodynamic stability, reduced droplet size, and superior solubilization capabilities, which can significantly enhance the bioavailability of poorly water-soluble compounds such as ODN. Encapsulation within gelatine capsules creates a protective matrix that mitigates drug degradation and facilitates a controlled, sustained release of the active ingredient. This innovative combination effectively overcomes the challenges associated with conventional oral formulations, which frequently experience variable absorption rates and significant first-pass metabolism, resulting in unpredictable therapeutic outcomes. By enhancing the solubility and dissolution kinetics of ODN, microemulsion-encapsulated gelatine capsules improve the drug's absorption and bioavailability, potentially leading to more effective and consistent antiemetic treatment (Anwar et al., 2020; Anwar et al., 2023).

During the formulation process, a microemulsion containing 4 mg of the drug was optimized to achieve a volume of approximately 0.15 mL (Dhanashree et al., 2024). This specific volume was essential for ensuring its accurate dosing, while also preserving the

stability and efficacy of the microemulsion. Consequently, a size 4 gelatine capsule was chosen, as it accommodates the microemulsion effectively, preventing leakage and maintaining the capsule's structural integrity. Size 4 capsules typically have a fill volume capacity of up to 0.21 mL, making them ideally suited for this formulation. This selection guarantees that each capsule delivers the precise 4 mg dose of ODN, thereby ensuring consistency in dosing and therapeutic outcomes, while also enhancing patient convenience and adherence.

MATERIALS AND METHODS

Materials

ODN was received as a gift sample from M/s ZIM Laboratories in Kalmeshwar, Nagpur, India. Lauro-glycol-90, Acconon MC 82, and Transcutol-P were also provided as gift samples by ABITEC Corporation based in Columbus, USA. Size 4 capsules were sourced from Prasadh Pharma in Chennai, India. Additionally, various other compounds and analytical grade solvents were employed in the study.

Preparation of ODN-microemulsion-loaded gelatine capsules

The formulation of the ODN microemulsion was achieved through the water titration method. The water titration method is a simple and effective technique for preparing microemulsions, particularly for drugs with low aqueous solubility like ODN. This method involves gradual addition of water to a pre-mixed combination of oil, surfactant, and co-surfactant, leading to the spontaneous formation of a thermodynamically stable microemulsion. Here, lauroglycol-90, acconon MC 82, and transcutol-P were selected as oil, surfactant and co-surfactant. Subsequently, a specified amount of drug was incorporated into the microemulsion, which was then subjected to sonication for 30 minutes. After this process, acesulfame potassium, titanium dioxide, and levomenthol were introduced, followed by an additional sonication period of 10 minutes to finalize the microemulsion. It was found that 0.15mL of this microemulsion contains 4mg of ODN. Hence size 4 gelatine capsules were selected to encapsulate the prepared ODN-microemulsion and were filled manually (Basu et al., 2012; Dhanashree et al., 2024).

Physicochemical Characterization

Weight variation test

The prepared microemulsion formulation was loaded into gelatine shells, and 20 of them were selected for examination. Each capsule was individually weighed and recorded. The average weight of the capsules was calculated, ensuring that no more than two individual weights deviated from the average (Farmer et al., 2002).

Disintegration test

The disintegration test for capsules was performed using a tablet disintegration test apparatus. Six capsules were randomly selected and placed in a disintegration apparatus containing distilled water maintained at 37 ± 2 °C. A capsule was deemed to have successfully passed the test if no drug residue remained on the No. 10 mesh screen of the tubes (United States Pharmacopeial Convention, 2010).

Drug content test

The assessment of drug content was performed through UV spectroscopy at a wavelength of 247 nm. Initially, a capsule sample was selected and weighed. The contents were then dissolved in methanol to ensure complete extraction of the active pharmaceutical ingredient (API). The solution was subsequently filtered to remove any undissolved substances and diluted to a predetermined concentration. The absorbance was measured at 247 nm, and the concentration of ODN was determined using a calibration curve. The calibration curve exhibited excellent linearity, with an R² value of 0.999, confirming a strong correlation between absorbance and drug concentration. The drug content analysis was conducted in triplicates to ensure accuracy and reproducibility (Dhanashree et al., 2024).

Content uniformity test

The content uniformity test for capsules involved random selection of 10 individual capsules from a given batch. Each capsule underwent a separate assay to quantify the API present. The extraction of the API was carried out using methanol, followed by analysis of the resultant solution through UV spectroscopy. The ODN content in each capsule was then determined and compared against the claimed amount. The test was deemed successful if the API concentration in each capsule was within the range of 85-115% of the claimed amount, allowing for a maximum of one capsule to fall outside this range, with none showing a deviation beyond 75-125% (Bedford et al., 1980).

Differential scanning calorimetry (DSC)

The weighed portion of the capsule was sealed into a DSC pan. The sample was then heated at a controlled rate under a nitrogen atmosphere. The DSC system recorded thermal events such as melting and crystallization, which provided critical insights into the thermal stability and phase behavior of the components within the capsule (Chatham et al., 1992).

Attenuated total reflectance Fourier transform infrared spectroscopy (ATR-FTIR)

After the capsule was opened, the microemulsion was poured directly onto the ATR crystal. The sample was then firmly pressed against the crystal to ensure adequate contact. The ATR-FTIR instrument subsequently acquired the infrared spectrum, which illustrated the characteristic molecular vibrations associated with the components. This approach provided

valuable information regarding the chemical composition and possible interactions occurring within the formulation (Heussen et al., 2012).

In vitro dissolution test

The *in vitro* dissolution studies of ODN micro-emulsion-loaded gelatine capsules were conducted using USP apparatus II (paddle). A dissolution medium of 500 mL 0.1 N HCl was employed. The capsules were positioned in the vessel and rotated at a speed of 50 rpm, with the temperature maintained at 37 °C ± 0.5 °C. To assess the in vitro drug release, 10 mL aliquots were extracted from each vessel at intervals of 5 min, 10 min, 20 min, and 30 min, which were subsequently filtered. The filtered samples were then analysed using a Shimadzu UV Spectrophotometer at a wavelength of 249 nm (United States Pharmacopeial Convention, 2010; U.S. Department of Health and Human Services, 2018; Newton et al., 1997).

RESULTS

Preparation of ODN-microemulsion-loaded gelatine capsules

The ODN microemulsion was successfully formulated using the water titration method, employing lauroglycol-90 as the oil phase, Acconon MC 82 as the surfactant, and Transcutol-P as the co-surfactant (Table 1). The optimized formulation was subjected to sonication to ensure homogeneity, followed by encapsulation in size 4 gelatine capsules, which were chosen based on their capacity to hold 0.15 mL of the microemulsion, equivalent to 4 mg of ODN.

Table 1. Composition of ODN Microemulsion-Loaded Gelatine (Capsules
--	----------

Components	Function	
Ondansetron Hydrochloride	Active Pharmaceutical Ingredient	
Lauroglycol-90	Oil Phase	
Acconon MC82	Surfactant	
Transcutol-P	Co-Surfactant	
Acesulfame Potassium	Sweetener	
Titanium Dioxide	Opacifier	
Levomenthol	Cooling Agent	

Physicochemical characterization Weight variation test

The average weight of the capsule was found to be 216.4 mg \pm 0.61mg. According to the pharmacopeial specifications, the acceptable limit for weight variation for capsules with specified weight range of 80 to 250 mg \pm 7.5% from the mean. All the tested capsules were within this limit, confirming that the formulation complied with the required weight uniformity standards.

Disintegration test

The average disintegration time was approximately 3 min. All capsules disintegrated within the IP specified limit of 30 min for capsules, confirming that the formulation met the required standards. No residue was observed on the mesh, indicating complete disintegration.

Drug content test

The optimized formulation exhibited a drug content of 99.04%, which falls within the acceptable limits of \pm 10% of the labeled claim for each capsule, which is established by the IP.

Content uniformity test

The average drug content was found to be 95.45% \pm 1.82% with individual contents ranging from 92.75% to 98.5%. According to the IP specifications for content uniformity, not more than two capsules may deviate from the labeled claim by more than \pm 10%, and none may deviate by more than \pm 15%. In this analysis, all capsules met these criteria, confirming the uniformity and quality of the formulation.

Differential scanning calorimetry (DSC)

DSC was employed to evaluate the thermal properties of Ondansetron HCl and the microemulsion

formulation. The thermogram of pure Ondansetron HCl exhibited an endothermic peak at 187.9°C, corresponding to its melting point. In the optimized microemulsion formulation, a broadening and slight shift in the peaks were observed. These changes are attributed to the encapsulation of the drug within the microemulsion system, which may alter the drug's physical state due to the formation of the microemulsion matrix. However, the absence of significant thermal events in the DSC thermogram indicates that the microemulsion system successfully maintained the stability of the drug during formulation. This confirms that the selected excipients did not induce any undesirable interactions that would compromise the integrity or stability of the drug (Ammar et al., 2018; Changizi et al., 2017).

Attenuated total reflectance Fourier transform infrared spectroscopy (ATR-FTIR)

ATR-FTIR was utilized to assess the compatibility of ODN with various excipients in the microemulsion formulation as shown in Figure 1. The analysis indicated that no new peaks were observed, and the disappearance of certain existing peaks suggested that there were no significant chemical interactions between the drug and the excipients. Furthermore, the characteristic peaks of ODN were still present in the infrared spectra of the formulation, confirming the stability of the drug within the microemulsion system. This stability indicates that ODN remains compatible with the selected excipients, which is crucial for ensuring the efficacy of the drug delivery system. The FTIR spectra were recorded using a SHIMAD-ZU FTIR 8400 S spectrometer, with a scanning range from 4000 cm⁻¹ to 400 cm⁻¹ at a resolution of 4 cm⁻¹, providing a comprehensive understanding of the molecular interactions within the formulation.

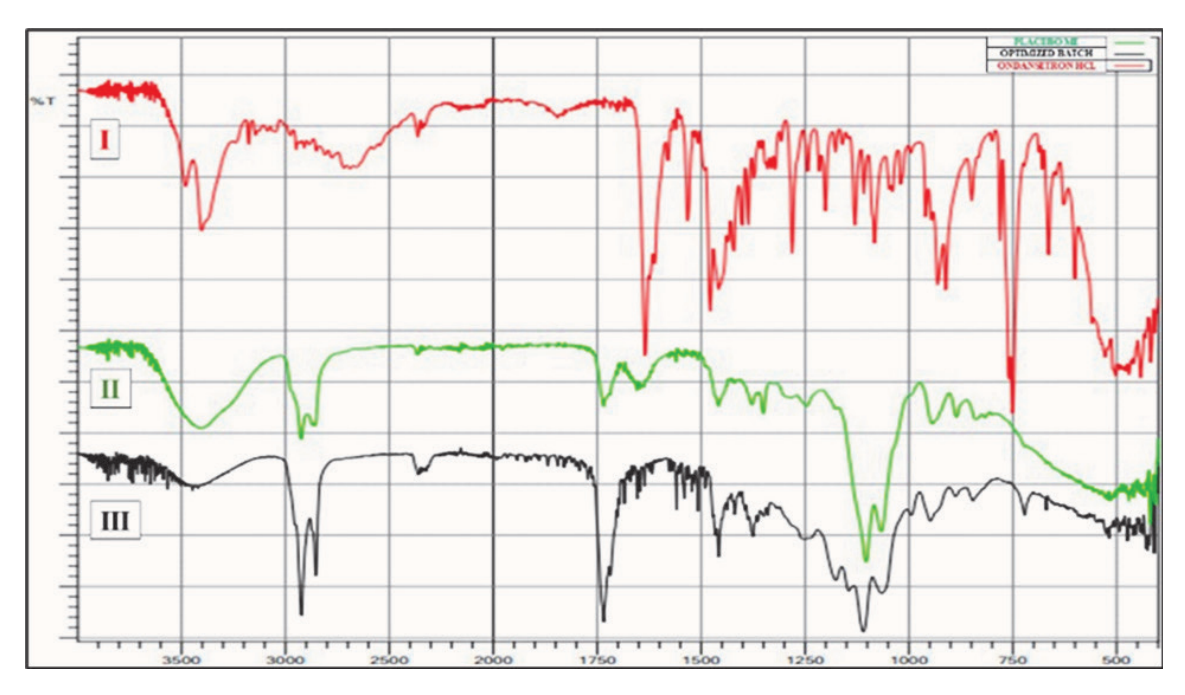


Figure 1. (I) Pure Ondansetron HCL is shown by the red peak (II) Placebo is represented by the green peak (III) Optimized batch of Microemulsion is shown by the black peak.

In vitro dissolution test

The in vitro dissolution of the ODN microemulsion-loaded gelatine capsules (Optimized Batch B2) was significantly faster than the marketed tablets (Emeset-4 and Ondem-4). As shown in Figure 2, the capsules released approximately 110% of the drug within 5 min, while the marketed tablets released around 80-90%. By 30 min, the capsules reached nearly 120% release, compared to about 98-100% release for both

marketed formulations. These results indicate that the microemulsion-loaded capsules offer superior dissolution and a faster release profile, suggesting better bioavailability and quicker therapeutic action compared to conventional tablets. To enhance the reproducibility and clarity of the results, Table 2 presents the numerical dissolution data along with the corresponding standard error (SE) values for each formulation across all time points.

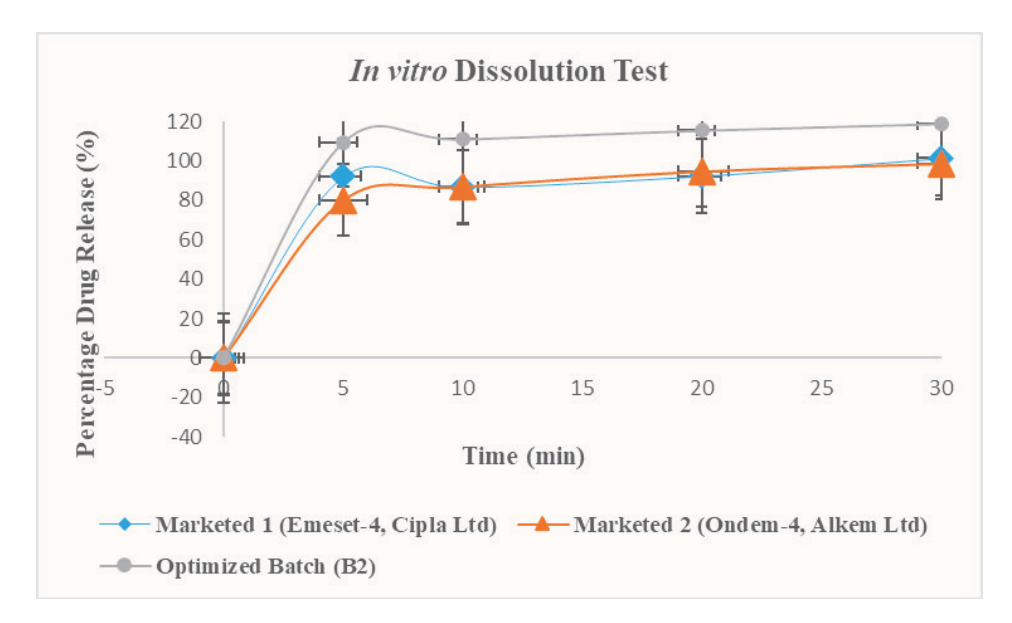


Figure 2. *In vitro* dissolution profile of ODN microemulsion-loaded gelatin capsules compared to marketed formulations.

Table 2. The dissolution data for the mentioned formulations includes the mean and standard error (SE) values.

Time (min)	Marketed 1 (Emeset-4, Cipla Ltd)	Marketed 2 (Ondem-4, Alkem Ltd)	Optimized Batch (B2)
0	0 ± 0	0 ± 0	0 ± 0
5	92.2 ± 0.61	80.18 ± 0.86	109.5 ± 0.49
10	86.8 ± 0.73	87 ± 1.02	111 ± 0.57
20	92.36 ± 0.65	94.84 ± 0.90	115.5 ± 0.61
30	101.41 ± 0.82	98.72 ± 1.14	118.9 ± 0.53

CONCLUSION

The study successfully demonstrated that the innovative formulation not only improved the dissolution rate of ODN but also ensured compatibility between the drug and the excipients used in the microemulsion system, as evidenced by the ATR-FTIR analysis which indicated no significant chemical interactions. The disintegration tests confirmed that the capsules met the required standards, with an average disintegration time of approximately 3 min, well within the specified limit of 30 min. Furthermore, the drug content analysis showed a high percentage of 99.04%, indicating that the formulation maintained its integrity and efficacy. The findings of this research highlight the potential of microemulsion systems in

overcoming the challenges associated with the low oral bioavailability of ODN, primarily due to first-pass metabolism. By utilizing a blend of oil, surfactant, and cosurfactant, the study provides a viable strategy for improving the therapeutic effectiveness of ODN in clinical settings. Overall, this innovative approach not only enhances the delivery of ODN but also opens avenues for further research into similar formulations for other poorly soluble drugs, thereby contributing to the advancement of pharmaceutical sciences and improving patient outcomes.

CONFLICT OF INTEREST

Authors declare that there is no conflict of interest.

AUTHOR CONTRIBUTION STATEMENT

Performed experiments (Nair S.), mentor, hypothesis, design, manuscript preparation, framed discussion of the manuscript (Sanap D.; Jadhav K.), writing manuscript, literature research preparing figures, writing manuscript (Nair S.).

REFERENCES

- Ahmadi, F., Alipour, S., & Akbari, S. (2015). Development and in vitro evaluation of fast-dissolving oral films of ondansetron hydrochloride, *Trends in Pharmaceutical Sciences*, *1*(1), 25- 30. https://tips.sums.ac.ir
- Abruzzo, A., Bigucci, F., Cerchiara, T., Gallucci, M. C., Luppi, B., Saladini, B., & Trastullo, R. (2016). Design and evaluation of buccal films as paediatric dosage form for transmucosal delivery of ondansetron, European Journal of Pharmaceutics and Biopharmaceutics, 105, 115-121. https://www.sciencedirect.com/journal/european-journal-of-pharmaceutics-and-biopharmaceutics
- Ammar, H. O., Fouly, A. A., Mohamed, M. I., & Tadros, M. I. (2018). Transdermal delivery of ondansetron hydrochloride via bilosomal systems: In vitro, ex vivo, and in vivo characterization studies, *AAPS PharmSciTech*, *19*(5), 2276- 2287. http://doi.org/10.1208/s12249-018-1019-y
- Anwar, D., Dhanashree, M., & Nidhi, P. (2020). Optimization, characterization and in vitro evaluation of buprenorphine microemulsion, *International Journal of Pharmaceutical Sciences Review and Research*, 60(2), 67-75. https://www.globalresearchonline.net
- Anwar, D., Dhanashree, S., & Nidhi, S. (2023). Design and characterization of microemulsion system for fentanyl citrate, *Research Journal of Pharmacy and Technology*, *16*(3), 1319- 1326. https://doi.org/10.52711/0974-360X.2023.00217

- Basu, A., & Malakar, J. (2012). Ondansetron HCl microemulsions for transdermal delivery: Formulation and in vitro skin permeation, *International Scholarly Research Notices*, 2012(1), 428396.
- Bansal, S., Gupta, V., Kumria, R., Nair, A. B., & Wadhwa, J. (2013). Oral buccoadhesive films of ondansetron: Development and evaluation, *International Journal of Pharmaceutical Investigation*, 3(2), 112. https://jpionline.org
- Bedford, K., Eaves, T., Ganley, J. A., & Walker, S. E. (1980). The filling of molten and thixotropic formulations into hard gelatin capsules, *Journal of Pharmacy and Pharmacology*, *32*(1), 389-393. https://academic.oup.com/jpp
- Breatnach, F., Daly, S. A., Hung, I. J., Leal, C., Kowalczyk, J., McKenna, C. J., Mitchell, T., Ninane, J., Smelhaus, V., White, L., & Zhestkova, N. (2000). A comparison of oral ondansetron syrup or intravenous ondansetron loading dose regimens given in combination with dexamethasone for the prevention of nausea and emesis in pediatric and adolescent patients receiving moderately/highly emetogenic chemotherapy, *Pediatric Hematology and Oncology*, 17(6), 445- 455. https://www.tandfonline.com/journals/ipho20
- Can, A. S., Erdal, M. S., Güngör, S., & Özsoy, Y. (2013).
 Optimization and characterization of chitosan films for transdermal delivery of ondansetron,
 Molecules, 18(5), 5455- 5471. https://www.mdpi.com/journal/molecules
- Charyulu, N. R., Koland, M., & Sandeep, V. P. (2010). Fast dissolving sublingual films of ondansetron hydrochloride: Effect of additives on in vitro drug release and mucosal permeation, *Journal of Young Pharmacists*, 2(3), 216- 222. https://jyoungpharm.org

- Changizi, S., Moghimipour, E., & Salimi, A. (2017). Preparation and microstructural characterization of griseofulvin microemulsions using different experimental methods: SAXS and DSC, *Advanced Pharmaceutical Bulletin*, 7(2), 281-289. http://doi.org/10.15171/apb.2017.034
- Chitneni, M., Darwis, Y., Khan, N., & Sheshala, R. (2011). Formulation and in vivo evaluation of ondansetron orally disintegrating tablets using different superdisintegrants, *Archives of Pharmacal Research*, 34, 1945- 1956. https://link.springer.com/journal/12272
- Chatham, S., Hawley, A. R., Rowley, G., & Lough, W. J. (1992). Physical and chemical characterization of thermosoftened bases for molten filled hard gelatin capsule formulations, *Drug Development and Industrial Pharmacy*, 18(16), 1719-1739. https://www.tandfonline.com/journals/iddi20
- Dhanashree, S., Kisan, J., & Prathamesh, S. (2024).

 Development and validation of a UV spectrophotometric method for determination of ondansetron hydrochloride in bulk and tablet dosage form, Research Journal of Pharmacy and Technology, 17(3), 1061-1064. https://doi.org/10.52711/0974-360X.2024.00165
- Dhanashree, S., Lokhande, K., Malusare, P., & Jadhav, K. R. (2024). Formulation and evaluation of nanostructured lipid carriers-based capsule, *Indian Drugs*. https://www.indiandrugsonline.org
- Dhanashree, S., Mrunmayi, L., Supriya, J., & Suranya, S. (2022). Ondansetron: A selective 5HT3 receptor antagonist and its advances in drug delivery system, *World Journal of Advanced Research and Reviews*, 16(3), 68-77. https://wjarr.com
- Farmer, R., Felton, L. A., & Garcia, D. I. (2002). Weight and weight uniformity of hard gelatin capsules filled with microcrystalline cellulose and silicified microcrystalline cellulose, *Drug Development and Industrial Pharmacy*, 28(4), 467- 472. https://www.tandfonline.com/journals/iddi20

- Fox, J. L., Hak, L. J., Laizure, S. C., Sanders, P. L., Stevens, R. C., & Williams, C. L. (1994). Stability of ondansetron hydrochloride in syrups compounded from tablets, *American Journal of Health-System Pharmacy*, *51*(6), 806-809. https://academic.oup.com/ajhp
- Gundu, R., Pekamwar, S., Shelke, S., Shep, S., & Kulkarni, D. (2020). Sustained release formulation of ondansetron HCl using osmotic drug delivery approach, *Drug Development and Industrial Pharmacy*, 46(3), 343-355. https://www.tandfonline.com/journals/iddi20
- Gosai, A. R., Patil, S. B., & Sawant, K. K. (2008). Formulation and evaluation of orodispersible tablets of ondansetron hydrochloride by direct compression using superdisintegrants, *International Journal of Pharmaceutical Sciences and Nanotechnology*, 26(1), 106-111. https://www.ijpsnonline.com/
- Gullapalli, R. P. (2010). Soft gelatin capsules (softgels),
 Journal of Pharmaceutical Sciences, 99(10), 4107-4148. https://www.sciencedirect.com/journal/journal-of-pharmaceutical-sciences
- Heussen, P. C., Nootenboom, P., Smit, I., Van Dalen, G., & Van Duynhoven, J. (2012). The use of ATR-FTIR imaging to study coated oil capsules, *Vibrational Spectroscopy*, 60, 118-123. https://www.sciencedirect.com/journal/vibrational-spectroscopy
- Jena, A., Kumar, K. M., Ruckmani, K., & Rajendran, P. (2010). Formulation and evaluation of taste masked orally disintegrating ondansetron hydrochloride tablet, *International Journal of Research* in Pharmaceutical Sciences, 1(3), 328. https:// www.ijrps.com
- Manavalan, R., Muthu, A. K., & Smith, A. A. (2009). Formulation development and evaluation of ondansetron hydrochloride sustained release matrix tablets, *Journal of Pharmaceutical Sciences and Research*, 1(4), 48-54. https://www.jpsr.pharmainfo.in

- Newton, J. M., & Razzo, F. N. (1977). The in vitro bioavailability of various drugs formulated as hard gelatin capsules, *Journal of Pharmacy and Pharmacology*, 29(1), 205- 208. https://academic.oup. com/jpp
- U.S. Department of Health and Human Services, Food and Drug Administration, Center for Drug Evaluation and Research (CDER) (2018): Dissolution Testing and Acceptance Criteria for Immediate-Release Solid Oral Dosage Form Drug Products Containing High Solubility Drug Substances: Guidance for Industry. Silver Spring, MD: Biopharmaceutics.

United States Pharmacopeia and National Formulary. (2010): Ondansetron. In USP 33-NF 28. Rockville, MD: United States Pharmacopeial Convention.

Antifungal Activity of Ethanol Extract of *Desmanthus* virgatus (L.) Leaves *In Silico* and *In Vitro*

Lilik FARKHIYAH*, Marshellia GHINANDA DEWISTAMARA**, Tukiran TUKIRAN***

Antifungal Activity of Ethanol Extract of Desmanthus virgatus (L.) Leaves In Silico and In Vitro

SUMMARY

Most fungal human infections are caused by Candida species, especially Candida albicans. C. albicans is a highly adaptable microorganism that can cause resistance after prolonged exposure to antifungals. C. albicans is easily transmitted therefore the discovery of new antifungal agents is very urgent. Therefore, this study aims to find antifungal agents from natural materials, namely wild tantan leaves in silico and in vitro. In the in silico test with protein 2QZX, of the 10 dominant compounds from LC-MS results, 3 compounds were obtained that had the most potential as antifungals with binding affinity values lower than ketoconazole. On the other hand, in the in vitro test with the agar diffusion method using disc paper, the average inhibition zone value was 0.01283 m and was classified as strong.

Key Words: Antifungal, wild tantan, Candida albicans, in silico, in vitro.

Desmanthus virgatus (L.) Yapraklarının Etanol Ekstresinin In Silico ve In Vitro Antifungal Aktivitesi

ÖZ

İnsanlarda görülen fungal enfeksiyonların çoğuna Candida türleri, özellikle de Candida albicans neden olmaktadır. C. albicans, antifungal ilaçlara uzun süre maruz kaldıktan sonra direnç oluşturabilen oldukça adapte edilebilir bir mikroorganizmadır. C. albicans kolaylıkla bulaşabildiğinden yeni antifungal ajanların keşfi çok acil bir ihtiyaçtır. Bu nedenle, bu çalışma doğal malzemelerden, özellikle yabani tantan yapraklarından in siliko ve in vitro olarak antifungal ajanlar bulmayı amaçlamaktadır. LC-MS sonuçlarıyla belirlenen 10 baskın bileşikten, 2QZX proteiniyle yapılan daha ileri in silico testlerde, ketokonazole göre daha düşük bağlanma afinitesi değerleri göstererek antifungal olarak en yüksek potansiyele sahip olan 3 bileşik belirlendi. Öte yandan, disk kağıdı kullanılarak agar difüzyon yöntemi ile yapılan in vitro testte ortalama inhibisyon zon değeri 0.01283 m olarak tespit edilmiş ve güçlü inhibisyon etkili olarak sınıflandırılmıştır.

Anahtar Kelimeler: Antifungal, yabani tantan, Candida albicans, in silico, in vitro.

Received: 18.11.2024 Revised: 5.04.2025 Accepted: 9.05.2025

ORCID: 0009-0007-8205-9864, Department of Chemistry, Faculty of Mathematics and Natural Science, Universitas Negeri Surabaya, Surabaya, Indonesia.

[&]quot;ORCID: 0009-0008-2554-5863, Department of Biology, Faculty of Mathematics and Natural Science, Universitas Negeri Surabaya, Surabaya, Indonesia.

[&]quot;ORCID: 0000-0001-6613-128X, Department of Chemistry, Faculty of Mathematics and Natural Science, Universitas Negeri Surabaya, Surabaya, Indonesia.

INTRODUCTION

Fungi are eukaryotic organisms (Tian et al., 2021), unicellular or multicellular, having a specific cell wall structure, and a cytoplasmic membrane made of sterols, especially ergosterol (Ivanov et al., 2022). Morphologically, fungi that cause disease in humans are yeasts, molds, and biphasic (dimorphic) fungi (Ivanov et al., 2022). Fungal diseases can often be fatal and have killed an estimated 1.6 million people per year (Richardson, 2022).

Candida species cause most human infections due to fungal pathogens (Lopes & Lionakis, 2022). Candida fungal infection causes candidiasis, a disease that affects humans (Talapko et al., 2021). Infections cause a variety of serious infectious diseases or invasive infections (Seyoum et al., 2020). Candida infections are a significant source of patient morbidity and mortality (Tran et al., 2020 & Santos et al., 2021). This infection develops into candidemia, disseminated candidiasis, endocarditis, meningitis, endophthalmitis, and other internal organ infections (Panjaitan et al., 2021). Global cases of invasive candidiasis are estimated at 700,000 annually with C. albicans classified as the main etiologic agent of these nosocomial infections (Iyer et al., 2022).

Over the past few decades, conventional antimicrobials have become increasingly ineffective in combating pathogenic microbes (Lee *et al.*, 2021). These pathogens have the potential to spread and cause systemic infectious diseases that often result in clinical death (Fan *et al.*, 2022). Overuse of fungal agents may increase opportunistic pathogen resistance (Houšt & Spížek, 2020). The issue of antimicrobial resistance is of particular concern given the scarcity of different antifungal classes for the invasive treatment of infections and the emergence of multi-drug resistance to the spread of fungal pathogens. (Lee *et al.*, 2021).

The use of antifungal drugs also has side effects such as allergies, nausea, and in some cases irritation (Makhfirah *et al.*, 2020). The presence of these side effects has made herbal remedies a trend now, as they

are proven to be safer and cause fewer side effects (Fahdi et al., 2023). Some studies suggest that natural materials have antifungal activity against the fungus *C. albicans*. Recently, Yuliati et al. (2024) revealed that the methanol extract of asam kalimbawan (*Sarcotheca diversifolia* (Miq) Hallier F.) can inhibit the growth of *C. albicans* fungi through the formation of a zone of inhibition with a medium category (Yuliati et al., 2024). Similarly, Rokhana & Nadia (2024) showed that ethanol extract of red betel leaves (*Piper crocatum*) can inhibit the growth of *C. albicans* with a strong inhibition zone category (Rokhana & Nadia, 2024).

C. albicans is a highly adaptable microorganism that can cause resistance after prolonged exposure to antifungals (Oliveira & Rodrigues, 2020). The C. albicans fungus is easily infectious so the discovery of new antifungal agents is a matter of great urgency (Heard et al., 2021). Wild tantan (Desmanthus virgatus (L.)) is one of the plants that has potential as an antifungal. D. virgatus (L.) contains secondary metabolites such as phenolics and tannins (Suybeng et al., 2021). Phenolic compounds act as Candida antifungal agents by stimulating farnesol synthesis and inhibiting hyphae formation by increasing the DPP3 gene (Teodoro et al., 2015). Tannins can act as antifungals by preventing enzymatic activity and inhibiting nucleic acid synthesis. Tannins can interfere with the synthesis of cellular systems by binding enzymes and regulating the secretion system (Huang et al., 2024). Tannic acid is a tannin compound contained in D. virgatus. According to research by Moreira et al. (2024), tannic acid showed MIC activity between 0.06 to 0.50 μg/mL against Candida sp. D. virgatus is commonly used as a source of animal feed and also a good source of protein for feed during food shortages (Olbana et al., 2023).

The absence of publications related to information on phytochemical content and the utilization of wild tantan leaves as antifungal makes this research important to do. Thus, it is necessary to conduct phytochemical and pharmaceutical tests including maceration, phytochemical identification through LC-MS

instruments, and testing of antifungal activity *in silico* and *in vitro* to determine the antifungal potential of wild tantan leaves as an effort to find antifungal drugs with lower side effects.

MATERIAL AND METHODS

Materials

The materials used for this study include wild tantan (*D. virgatus* (L.)) leaves, ethanol (98%, Merck, Germany), *C. albicans* ATCC-14053 fungal isolate, Sabouraud Dextrose Agar (SDA) media, disc paper, DMSO 5%, saffronin, lugal, carbolic gentian violet, physiological NaCl, Mc Farland standard solution, receptor protein structure (PDB ID: 2QZX) (retrieved from https://www.rcsb.org/), ligand conformers (retrieved from https://pubchem.ncbi.nlm.nih.gov/). The leaves were collected from Sidoarjo, East Java, Indonesia. The plant materials were identified at Generasi Biologi Indonesia under specimen number BT-02/0352/24 on March 22nd, 2024.

Instrumental

Equipment and instruments used in this study are beaker glass, Erlenmeyer flask, extraction chamber, spatula, Whatman filter paper, Buchner funnel, vacuum pump, Shimadzu LC-MS instrument (8040 Type, Shimadzu, Japan), hot plate (Thermo Scientific Cimarec), magnetic stirrer, petri dish, incubator (LabLine Imperial III), laminar air flow (ESCO EN 1822), microscope (Nikon ECLIPSE E100LED MV R), media refrigerator (Sanyo Medical MPR-311D(H)) and autoclave (Tomy ES-215). The docking study was performed using Windows 10, Intel®, 4.00 GB RAM, and a 64-bit operating system. The software used was Discovery Studio Client 2019, PyRx-0.8, and pyMOL 3.0.

Characterization Methods

Wild Tantan Leaf Collection and Extraction Process

Wild tantan leaf samples were collected from Sidoarjo Regency, East Java, Indonesia. The collected leaves were dried in the sun for 3 days with occasional flipping. After drying, the leaves were pulverized with a grinder until they became powder and weighed. 3.8

kg of dry powder was obtained. Wild tantan leaf powder was extracted using 2 containers, with each container containing 1.9 kg of wild tantan leaf powder and 3.4 liters of ethanol solvent. Maceration was repeated 4 times with occasional stirring. After that, filtering was carried out with a Buchner funnel assisted by a vacuum pump and obtained ethanol filtrate. The ethanol filtrate was evaporated to obtain a thick extract and weighed to obtain a thick extract of 478 grams. A total of \pm 0.5 mg of the extract was tested and analyzed for phytochemicals using the LC-MS test.

Identification of Compound Content of Wild Tantan Ethanol Extract Using LC-MS

Utilizing LC-MS equipment (Shimadzu 8040 Type) fitted with a Shimadzu Pack FC-ODS capillary column (2 mm \times 150 mm id, 3 μ m particle size) and an injection volume of 1 μ L, secondary metabolites from the ethanol extract of wild tantan leaves were identified. Capillary voltage of 3.0 kv, column chromatography temperature of 35°C, flow rate of 0.5 mL/min, methanol solvent, focused ion mode MS type [M]+, ionization utilizing ESI, isocratic mobile phase, and run time of 80 minutes are the parameters of the instrument's Electrospray Ionization (ESI) source. Secondary metabolites found in the extracts were identified using the NIST database library, retention durations, and molecular mass spectra of the compounds from the chromatograms.

In Silico Study with Protein 2QZX

The substance name and chemical structure were determined from the LC-MS test results by utilizing the PubChem web database. The potential of each of these compounds as a bioactive compound was then assessed using Lipinski's five principles for pharmacokinetics and Lipinski drug-likeness via the website http://www.scfbio-iitd.res.in/software/drugdesign/lipinski.jsp. Compounds that passed the drug-likeness and pharmacokinetic tests were tested for antifungal activity using biocomputational molecular docking analysis. The receptor used PDB ID code 2QZX. Protein sterilization is performed using PyMOL. Then, to

determine the binding affinity value, molecular docking is performed using PyRx. After docking, PyMOL and Discovery Studio are used to interact with the compounds and visualize them to ascertain the location and type of contact that occurs.

Gram Stain Identification of C. albicans

Gram staining test on *C. albicans* fungus using the method as performed by Suriany *et al.* (2024) with slight modifications. A total of 1 colony of *C. albicans* ATCC-14053 was applied to the preparation glass. Then fixed on the tongue of the flame. The fungus on the preparation glass was inundated with gentian violet carbolic, Lugol, 96% alcohol, and safranin sequentially for 1 minute each and alcohol for 20 seconds and between them rinsed using running water. After that, it was viewed under a microscope with a magnification of 10 × 10 with immersion oil.

Antifungal Activity by Agar Diffusion Method

The antifungal activity test was carried out using the agar diffusion method using disc paper as carried out by Rodiah *et al.* (2022) with slight modifications. SDA media was poured into Petri dishes and allowed to solidify. *C. albicans* fungal suspension was put into a sterile petri dish. Sterile disc paper was soaked with ethanol extract of wild tantan leaves at concentrations of 500, 250, 125, and 62.5 ppm for 15 minutes to absorb, then placed on a SDA medium. The positive control used was ketoconazole 10 ppm and the negative control used was DMSO. The disc paper was placed using sterile tweezers on the fungal culture medium. Then incubated at 35°C for 24 hours.

RESULTS AND DISCUSSION

Identification of Compound Content of Wild Tantan Ethanol Extract Using LC-MS

From the identification results using the LC-MS instrument, 160 compounds were obtained as shown in (Figure 1.) Of the 160 compounds, there are 10 dominant compounds, namely kaempferol-3-glucoside, trifolin, 3-O-(β -D-glucopyranosyl) soyasapogenol B, quercetin-7-O- β -D-glucoside, quercitrin, luteolin-7-glucoside, kaempferol-5-glucoside, kaempferol-7-O-glucoside, kaempferol-3-galactoside, and luteolin-7,3'-dimethyl ether-5-rhamnoside.

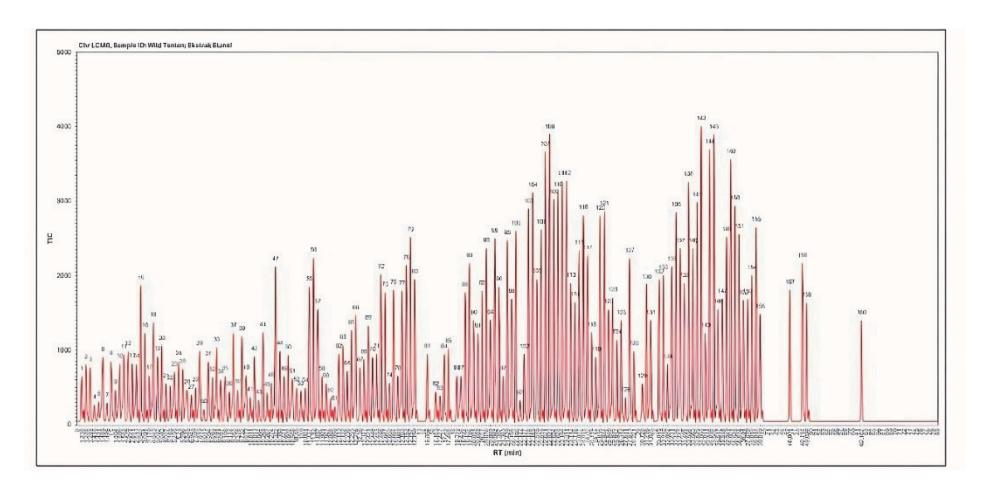


Figure 1. LC-MS chromatogram of the ethanol extract of *D. virgatus* leaves

The major compounds of the LC-MS results are flavonoids. Flavonoids have several physiological functions, such as antioxidant, antidiabetic, antiobesity, antihyperlipidemia, anti-inflammatory, antiosteoporosis, antiallergic and antithrombotic effects, hepatoprotective, neuroprotective, renoprotective,

chemopreventive and anticancer, antibacterial, antifungal, and antiviral activities (Aboody *et al.*, 2020). Flavonoids are natural products that have intrinsic antifungal properties (Nguyen *et al.*, 2021).

In Silico Study with protein 2QZX

In the *in silico* test, 10 dominant compounds were

identified through Lipinski's rule. The ideal drug compound fulfills the Lipinski rule of five (RoF). This guideline is to evaluate the drug similarity of chemical compounds with specific biological activities (Srivastava, 2021). According to RoF, a drug compound must have a molecular weight <500 g/mol, a LogP value <5 indicating its hydrophobicity, a hydrogen bond donor (HBD) <5, and a hydrogen bond acceptor (HBA) <10, and a molar refractivity between 40-130 (Stegemann *et al.*, 2023; Wandi *et al.*, 2022; &

Mohapatra *et al.*, 2021). A compound will have better pharmacokinetic properties if it meets the RoF. This rule is used for preliminary drug screening to narrow the scope of drug screening and save the cost of drug research and development (Chen *et al.*, 2020). In the Lipinski test, the compound must at least fulfill three rules as minimum requirements of a candidate drug compound (Nurlelasari *et al.*, 2023). The 10 dominant compounds all meet the minimum requirements of Lipinski, as presented in Table 1.

Table 1. Identification of 10 dominant compounds through Lipinski's rule of five.

Compound Name	Molecular mass (<500)	Log P (<5)	HBD (<5)	HBA (<10)	Molar refractivity (40-130)
Kaempferol-3-glucoside	448	-0.436	7	11	104.609
Trifolin	448	-0.444	7	11	104.609
3-O-(β-D-glucopyranosyl) soyasapogenol B	312	-0.053	5	6	77.146
Quercetin-7-O-β-D-glucoside	456	-1.540	0	12	101.324
Quercitrin	448	0.297	7	11	104.862
Luteolin-7-glucoside	448	-0.402	7	11	105.209
Kaempferol-5-glucoside	448	-0.222	7	11	105.116
Kaempferol-7-O-glucoside	447	-1.232	6	11	101.986
Kaempferol-3-galactoside	448	-0.436	7	11	104.609
Luteolin-7,3'-dimethyl ether-5-rhamnoside	460	1.232	4	10	113.571

In RoF, the LogP value is related to the lipophilicity of a compound and serves to predict drug absorption when crossing the intestinal epithelium (Srivastava, 2021), its ability to penetrate the cell barrier, and transportation to molecular targets. These properties affect pharmacokinetic processes such as absorption, distribution, metabolism, and excretion of drugs (Mlodawska et al., 2023). On the RoF for HBD less than 5 and HBA less than 10. If the HBD and HBA increase, the polarity value of the molecule will change. This causes a difference in passive diffusion at the cell membrane, which changes the absorption of molecules (Widodo et al., 2023). The relative atomic mass of the drug when >500 Da causes the ligand to diffuse through the cell membrane (Kilo et al., 2019 & Fariha et al., 2024). If the relative atomic mass of a compound is less than 500 Da, the compound diffuses more easily in the body. The molecular weight of

a compound impacts the body's ability to absorb the drug; the greater the molecular weight of the compound, the lower the body's ability to absorb the drug (Muhammad *et al.*, 2021). The range of the molar reactivity value is 40–130, indicating that the chemical would have good steric characteristics and interact with receptors with ease (Suryana *et al.*, 2022).

After RoF identification, the 10 compounds and control ketoconazole will be subjected to a molecular docking test. Generally, computational structure-based drug design methods use molecular docking methods (Stanzione *et al.*, 2021). Docking methods work by predicting the orientation of one molecule when two molecules are bound together to form a stable complex (Bharathy *et al.*, 2021). The main goal of molecular docking is to predict the bonding conformation, including position, type, and affinity (Limon *et al.*, 2022) according to bond energy (Fariha

et al., 2024). Before molecular docking, preparation is required to remove non-amino acid residues and water molecules (Pratama et al., 2021). From the mo-

lecular docking test, the binding affinity value will be generated. Binding affinity values of them are presented in Table 2.

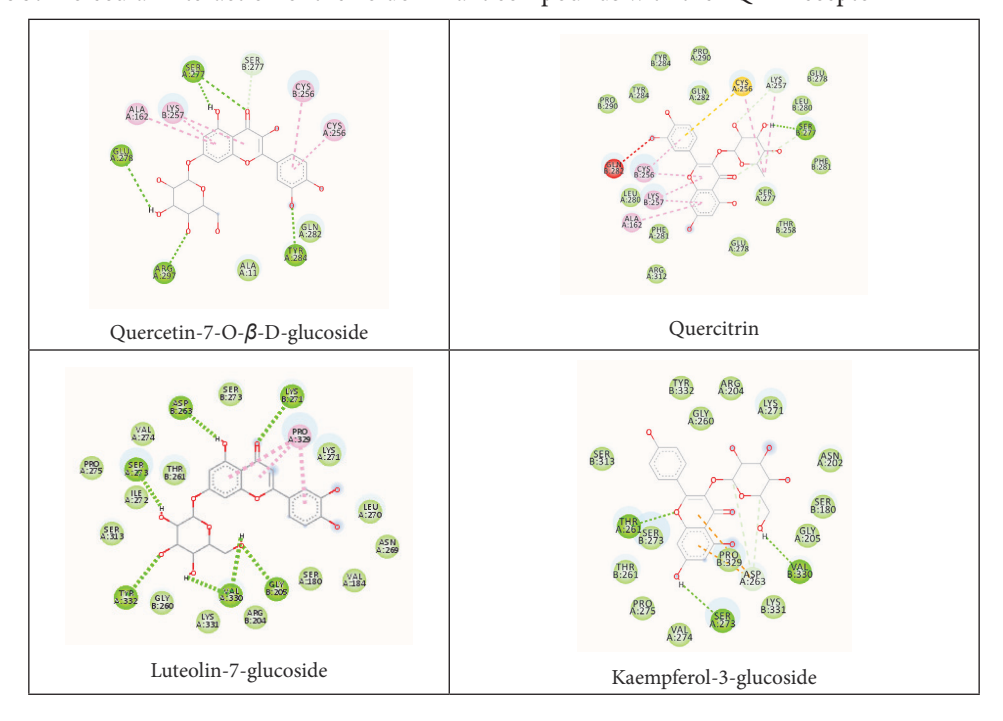
Table 2. Binding affinity values of 10 dominant compounds

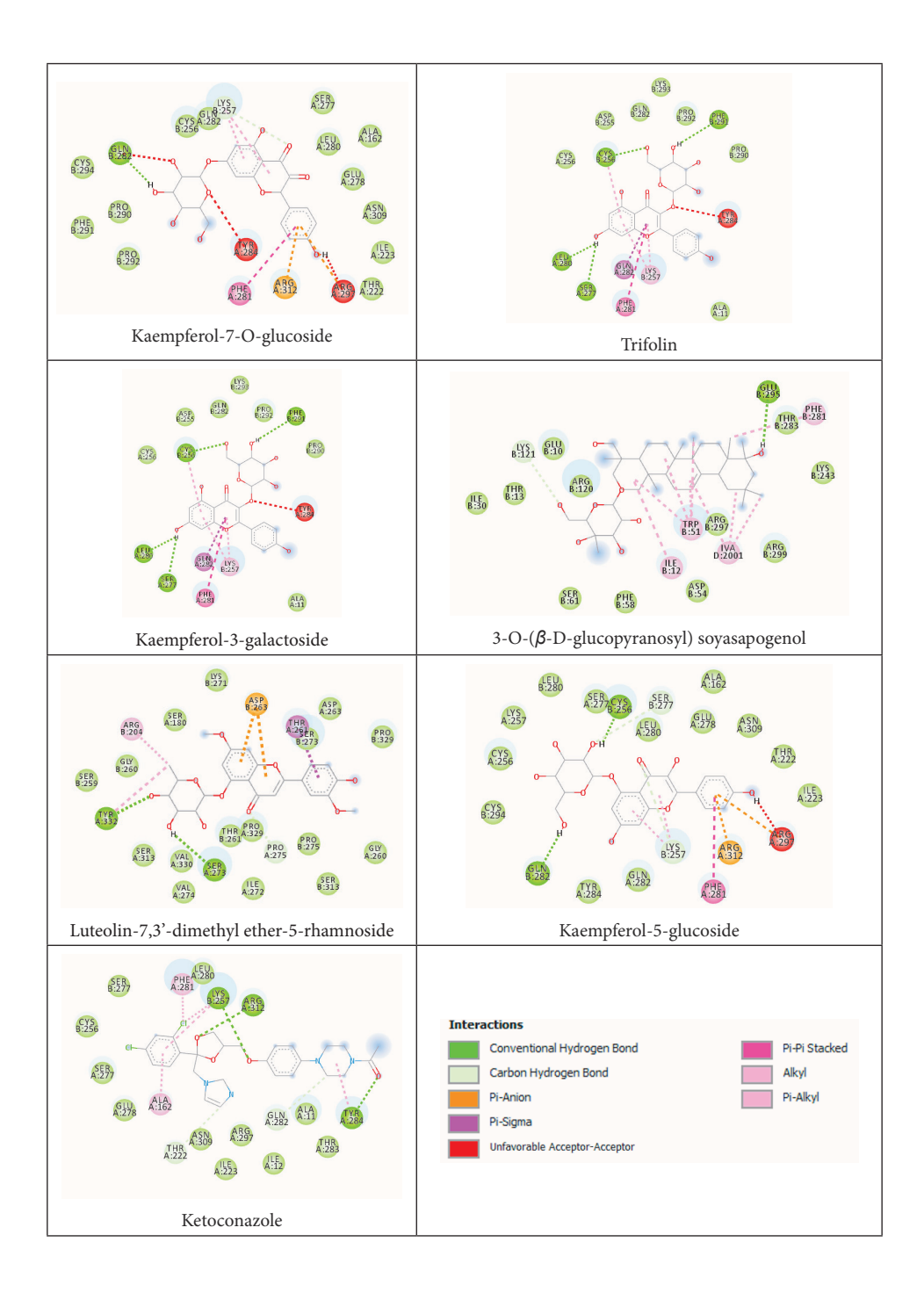
Compound Name	Binding affinity (kcal/mol).
Ketoconazole	-9.0
Kaempferol-3-glucoside	-8.1
Trifolin	-7.9
3-O-(β-D-glucopyranosyl) soyasapogenol B	-8.1
Quercetin-7-O-β-D-glucoside	-10.4
Quercitrin	-10.0
Luteolin-7-glucoside	-9.4
Kaempferol-5-glucoside	-9.5
Kaempferol-7-O-glucoside	-9.8
Kaempferol-3-galactoside	-7.9
Luteolin-7,3'-dimethyl ether-5-rhamnoside	-9.2

Apart from binding affinity, to ensure that the ligand attaches to the active side of the receptor surface, the interaction between the ligand and the receptor also needs to be considered. Discovery Studio 2019

was used to create this visual representation. Table 3 displays the results of the molecular interactions of the 10 dominant compounds and ketoconazole with the 2QZX receptor.

Table 3. Molecular interaction of the 10 dominant compounds with the 2QZX receptor





The interaction plot on ketoconazole shows that there are conventional hydrogen bonds with active site residues LYS 257, ARG 312, and TYR 284. In this case, quercetin-7-O- β -D-glucoside has similarities, namely the TYR 284 bond. In hydrophobic bonds (alkyl and Pi-alkyl), the ketoconazole control has alkyl bonds with PHE 281 and ALA 162. Luteolin-7,3'-dimethyl ether-5-rhamnoside, kaempferol-3-galactoside, kaempferol-7-O-glucoside, kaempferol-5-glucoside, and trifolin have the same bond with PHE 281. While quercetin-7-O-β-D-glucoside and quercitrin have similarities in ALA 162 bonds. In Van der Waals bond some compounds have similarities to ketoconazole, including trifolin, 3-O-(β-D-glucopyranosyl) soyasapogenol B, quercetin-7-O-β-D-glucoside, quercitrin, kaempferol-5-glucoside, kaempferol-7-O-glucoside, kaempferol-3-galactoside, and luteolin-7,3'-dimethyl ether-5-rhamnoside. Most of them have similarities that bind Van der Waals with LEU 280 and CYS 256.

Of the 10 dominant compounds, 3 compounds have the most similarities, namely luteolin-7,3'-dimethyl ether-5-rhamnoside, kaempferol-5-glucoside, and quercetin-7-O- β -D-glucoside. On the other hand, all three compounds also have lower binding affinity values than ketoconazole. It has been reported that their respective parent compounds have been known to possess antifungal activity. Luteolin and quercetin have inhibitory activity against C. albicans with MIC values of 37.5 and 75 µg/mL, respectively (Ivanov et al., 2021). Meanwhile, kaempferol has inhibitory activity against the Candida group with a minimum inhibitory concentration (MIC) of 32-128 μg/mL (Dutta & Kundu, 2021). Thus, the three compounds are potential antifungal agents. As an antimicrobial, quercetin inhibits microbial growth, including cell membrane damage, changes in membrane permeability, inhibition of nucleic acid and protein synthesis, reduction of virulence factor expression, mitochondrial dysfunction, and prevention of biofilm formation. The molecular structure of quercetin contains carbonyl groups and oxygen atoms that are alkaline so that they can form salts with acids. In addition,

there are double bonds and hydroxyl groups which are active in quercetin. The biological activity of quercetin is largely due to these active phenolic hydroxyl groups and double bonds (Nguyen & Bhattacharya, 2022). The mechanism of kaempferol and luteolin as antifungals is the same as quercetin which includes plasma membrane disruption and affects nucleic acid synthesis, and protein synthesis, and inhibits mitochondrial function (Jan *et al.*, 2022).

Gram Stain Identification of C. albicans

C. albicans is a gram-positive fungus that by gram staining can show blastospores, hyphae, or pseudohyphae (Ayu *et al.*, 2023). This purple color is due to the absorption of primary dye from carbon gentian violet by gram-positive fungi due to the presence of thick cell walls due to the peptidoglycan layer (Paray *et al.*, 2023). The existence of such a thick layer causes the absorbed color to be retained (Oigbochie *et al.*, 2022). The identification results of *C. albicans* fungus in the gram staining test produced a purple color. The results of gram staining identification are presented in Figure 2.

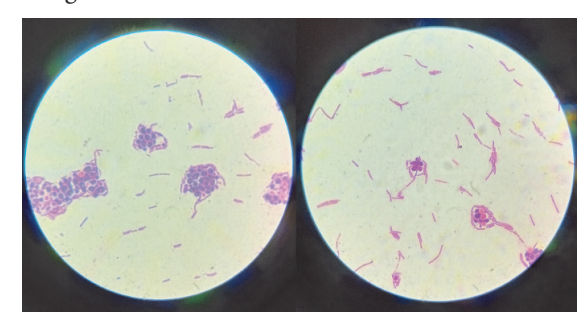


Figure 2. Gram staining results in C. albicans culture

The presence of pseudomycelia and chlamydospores can help distinguish *C. albicans*. Chlamydospores are large formations at the end of hyphae. Usually round and having thick walls, these formations have a diameter of 7-13 m (Sachivkina *et al.*, 2021). *C. albicans* has similarities with yeast-like fungal colonies (Safitri & Qurrohman, 2022). The results of microscopic observations showed that the *C. albicans* fungal colonies are round, which is a macroscopic characteristic of *C. albicans*.

Antifungal Activity by Agar Diffusion Method

In vitro assay using an agar diffusion method with paper discs. The diffusion method is used to measure the diameter of the clear zone, which indicates that an antibacterial ingredient in the extract inhibits bacterial growth (Auza et al., 2020). The working principle of the disc diffusion method is that the test material is saturated into a disc paper and placed on the surface of an agar medium that has been inoculated with test microorganisms (Putri et al., 2023). A clear zone around the paper disc indicates the presence or absence of microbial growth. During the incubation period, the test material diffuses from the paper disk into the agar medium so that a zone of inhibition is formed (Dewi et al., 2023).

The concentration of the administered substance affects the effectiveness of the antifungal agent (Andriana *et al.*, 2023). The inhibition that is formed increases as the concentration of the extract given increases because of the increase in the concentration of

bioactive components contained in the extract (Muiz *et al.*, 2021). With the increase, in extract concentration, the content of active ingredients that function as antifungals increases so that the ability to inhibit fungi is also increasing (Marbun *et al.*, 2021).

In this study, the positive control used was ketoconazole, and DMSO was a negative control. The negative control was used to determine whether the solvent used (DMSO) could affect the results of the antifungal test, while the positive control (ketoconazole, as an antifungal drug) was used to compare the inhibitory zone value of wild tantan leaf extract (Marbun et al., 2021). The results of the antifungal test can be reported that the inhibitory zone of positive control and negative control are 32 mm and no appear, respectively. Then, the antifungal test for ethanol extract of wild tantan leaves in various concentrations (500, 250, 125, and 62.5 ppm) with 3 repetitions (I, II, and III) provided an inhibitory zone with an average of 0.018; 0.014; 0.011; and 0.008 m, respectively. More details can be seen in Table 4.

Table 4. Zone of inhibition of wild tantan leaf extract by agar diffusion method

D		Concentra	tion (ppm)		Positive control Negative co	
Repetition	500	250	125	62.5	(Ketoconazole) (m)	(DMSO) (m)
I (m)	0.018	0.014	0.011	0.009		
II (m)	0.019	0.015	0.012	0.007		
III (m)	0.017	0.014	0.010	0.008	0.032	-
Average (m)	0.018	0.014	0.011	0.008		

Observation of the antifungal activity of wild tantan leaf ethanol extract against C. albicans fungus was carried out for 24 hours. The ability of ethanol extracts to diffuse into agar media is expected to inhibit fungal growth as indicated by the formation of an inhibitory zone. If the diameter of the inhibition zone is <0.005; 0.005 - 0.010; 0.010 - 0.020; and > 0.020 m, then the growth inhibition response is weak, moderate, strong and very strong, respectively. (Fitriana *et al.*, 2022). Thus, the average inhibitory response of the ethanol extract of wild tantan leaves is 0.01283 m, so it is classified as a strong category.

CONCLUSION

According to the results of an *in silico* study of 10 dominant compounds of the ethanol extract of wild tantan leaves, the three most potential compounds were obtained with lower binding affinity values and have similarities with ketoconazole, namely luteolin-7,3'-dimethyl ether-5-rhamnoside, kaempferol-5-glucoside, and quercetin-7-O- β -D-glucoside. On the other hand, *in vitro* study with the agar diffusion method using disc paper, the value of the average inhibitory zone of the ethanol extract of the plant is 0.01283 m and is classified as a strong category.

ACKNOWLEDGEMENTS

Gratitude is expressed to the Institute for Research and Community Service, Universitas Negeri Surabaya for funding support in the 2024 fiscal year through the Rector's Decree Number: B/42101/UN38.III.1/TU.00.02/2024 on 29 April 2024.

AUTHOR CONTRIBUTION STATEMENT

Writing original draft, *In silico* experiment, *In vitro* experiment, Funding acquisition (LF). *In vitro* experiment, Formal analysis, Funding acquisition (MGD). Writing review & Editing, Resources, Data curation, Supervision (TT).

CONFLICT OF INTEREST

The authors declare that there is no conflict of interest.

REFERENCES

- Aboody, M. S. Al, & Mickymaray, S. (2020). Antifungal efficacy and mechanisms of flavonoids. *Antibiotics*, *9*(45), 1–42. https://doi.org/10.3390/antibiotics9020045
- Andriana, F., Kumalasari, M. F., & Hadi, M. I. (2023).

 Aktivitas antifungi ekstrak daun kemangi (*Ocimum basilicum* L.) terhadap daya hambat *Candida albicans* secara *in vitro* pada kandidiasis. *Scripta Biologica*, 10(2), 1–5. https://doi.org/ 10.20884/1. SB.2023.10.2.1003
- Auza, F. A., Purwanti, S., Syamsu, J. A., & Natsir, A. (2020). The 2nd international conference of animal science and technology. *IOP Conference Series: Earth and Environmental Science*, 1–6. https://doi.org/10.1088/1755-1315/492/1/012024
- Ayu, I. P. E., Desi, B. N. W., Idayani, S., & Damayanti, I. A. M. (2023). Gambaran jamur *Candida albi*cans pada urin pra-menstruasi mahasiswi Stikes Wira Medika Bali. *Jurnal Riset Kesehatan Nasi*onal, 7(2), 84–90. https://doi.org/10.37294/jrkn. v7i2.499

- Bharathy, G., Christian P. J., Muthu, S., Irfan, A., Basha, A. F., Saral, A., Aayisha, S., & Niranjana D. R. (2021). Evaluation of electronic and biological interactions between *N*-[4-(ethylsulfamoyl)phenyl] acetamide and some polar liquids (IEFPCM solvation model) with Fukui function and molecular docking analysis. *Journal of Molecular Liquids*, 340(117271), 1–14. https://doi.org/10.1016/j.molliq.2021.117271
- Chen, X., Li, H., Tian, L., Li, Q., Luo, J., & Zhang, Y. (2020). Analysis of the physicochemical properties of acaricides based on Lipinski's rule of five. *Journal of Computational Biology*, 27(9), 1397–1406. https://doi.org/10.1089/cmb.2019.0323
- Dewi, L. P., Fuadiyah, W., Nirwana, L., Zulkarnain, A. R., & Faisal, F. (2023). Uji aktivitas anti bakteri eksrak daun sirsak (*Annona muricata* L.) terhadap pertumbuhan bakteri *Escherichia coli* dengan metode difusi sumuran dan paper disk. *Era Sains: Journal of Science, Engineering, and Information Systems Research*, 1(4), 8-14. Retrieved from https://jurnal.eraliterasi.com/
- Dutta, S., & Kundu, A. (2021). Macroporous resin-assisted enrichment, characterizations, antioxidant and anticandidal potential of phytochemicals from *Trachyspermum ammi. Journal of Food Biochemistry*, 46(4). https://doi.org/10.1111/jfbc.13847
- Fahdi. F, Sinaga, G. G. S., & Herviani. (2023). Ekstrak daun mimba (*Azaradiracta indica* A. Juss) sebagai antijamur *Candida albicans* dalam sediaan sampo krim antiketombe. *Journal of Biology Education, Science & Technology*, 6(2), 429–435. https://doi.org/10.30743/best.v6i2.7768
- Fan, F. M., Liu, Y., Liu, Y. Q., Lv, R. X., Sun, W., Ding, W. J., Cai, Y. X., Li, W. W., Liu, X., & Qu, W. (2022). Candida albicans biofilms: antifungal resistance, immune evasion, and emerging therapeutic strategies. International Journal of Antimicrobial Agents, 60, 1-8. https://doi.org/10.1016/j.ijantimicag.2022.106673

- Fariha, R. T., Yuhandiana, Syafa, S., Zubaidah, Fadhil, M., Pratomo, & Pertiwi, A. G. (2024). Studi *in silico* potensi antikanker pada senyawa metabolit sekunder buah Makassar. *Jurnal Ilmu Kesehatan*, *4*(3), 25–31. https://doi.org/10.5455/mnj. v1i2.644xa
- Fitriana, F., Amirah, S., & Rahman, S. (2022). Potensi antibakteri ekstrak etanol batang Wole Woe asal Halmaherah Tengah terhadap bakteri *Pseudomonas aeruginosa* dan *Bacillus subtilis* menggunakan metode difusi agar. *As-Syifaa Jurnal Farmasi*, 14(2), 155–161. https://doi.org/10.56711/jifa. v14i2.904
- Heard, S. C., Wu, G., & Winter, J. M. (2021). Antifungal natural products. *Current Opinion in Biotechnology*, 69, 232–241. https://doi.org/10.1016/j.copbio.2021.02.001
- Houšť, J., & Spížek, J.,V. H. (2020). Antifungal drugs. *Metabolites*, *10*(106), 2–16. https://doi. org/10.2165/00003495-197509060-00001
- Ivanov, M., Kannan, A., Stojković, D. S., Glamočlija, J., Calhelha, R. C., Ferreira, I. C. F. R., Sanglard, D., & Soković, M. (2021). Flavones, flavonols, and glycosylated derivatives impact on *Candida albicans* growth and virulence, expression of CDR1 and ERG11 cytotoxicity. *Pharmaceuticals*, 14(1), 1–12. https://doi.org/10.3390/ph14010027
- Ivanov, M., Ćirić, A., & Stojković, D. (2022). Emerging antifungal targets and strategies. *International Journal of Molecular Sciences*, 23(5), 1-26. https://doi.org/10.3390/ijms23052756
- Iyer, K. R., Robbins, N., & Cowen, L. E. (2022). The role of *Candida albicans* stress response pathways in antifungal tolerance and resistance. *iScience*, 25(3), 1-9. https://doi.org/10.1016/j. isci.2022.103953

- Jan, R., Khan, M., Asaf, S., Lubna, Asif, S., & Kim, K. M. (2022). Bioactivity and therapeutic potential of kaempferol and quercetin: new insights for plant and human health. *Plants*, 11(19), 1–18. https://doi.org/10.3390/plants11192623
- Jianzi, H., Madiha, Z., Yasir, S., Jallat, K., Rashid, Al-Y., Monther, S., Munawar, A., Saber, R. A., & Shuangfei Li. (2024). Tannins as antimicrobial agents: understanding toxic effects on pathogens. *Toxicon: Journal of the International Society on Toxinology,* 247(107812). https://doi.org/10.1016/j.toxicon.2024.107812
- Kilo, A. L., Aman, L. O., Sabihi, I., & Kilo, J. L. (2019). Studi potensi pirazolin tersubstitusi 1-N dari tiosemikarbazon sebagai agen antiamuba melalui uji in silico. Indonesian Journal of Chemical Research, 7(1), 9–24. https://doi.org/10.30598/ ijcr.2019.7-akr
- Lee, Y., Puumala, E., Robbins, N., & Cowen, L. E. (2021). Antifungal drug resistance: molecular mechanisms in *Candida albicans* and beyond. *Chemical Reviews*, *121*(6), 3390–3411. https://doi.org/10.1021/acs.chemrev.0c00199
- Limon, A. L., Toalá, J. E. A., & Liceaga, A. M. (2022). Integration of molecular docking analysis and molecular dynamics simulations for studying food proteins and bioactive peptides. *Journal of Agricultural and Food Chemistry*, 70(4), 934–943. https://doi.org/10.1021/acs.jafc.1c06110
- Lopes, J. P. & Lionakis, M. S. (2022). Pathogenesis and virulence of *Candida albicans*. Virulence, 13(1), 89-121. https://doi.org/10.1080/21505594.2021.2 019950
- Makhfirah, N., Fatimatuzzahra, C., Mardina, V., & Fanani H. R. (2020). Pemanfaatan bahan alami sebagai upaya penghambat *Candida albicans* pada rongga mulut. *Jurnal Jeumpa*, *7*(2), 400–413. https://doi.org/10.33059/jj.v7i2.3005

- Marbun, R. A. T. (2021). Uji aktivitas ekstrak daun pirdot (*Sauraia vulcani* Korth.) terhadap pertumbuhan *Candida albicans* secara *in vitro*. *Jurnal Bios Logos*, 11(1). https://doi.org/10.35799/jbl.11.1.2021.30564
- Młodawska, B. M. M., Jeleń, E. Martula, R., & Korlacki. (2023). Study of lipophilicity and ADME properties of *1,9-diazaphenothiazines* with anticancer action. *International Journal of Molecular Science*, *24*(8), 1–11. https://doi.org/10.3390/ijms24086970
- Mohapatra, R. K., Dhama, K., El-Arabey, A. A., Sarangi, A. K., Tiwari, R., Emran, T. Bin, Azam, M., Al-Resayes, S. I., Raval, M. K., Seidel, V., & Abdalla, M. (2021). Repurposing benzimidazole and benzothiazole derivatives as potential inhibitors of SARS-CoV-2: DFT, QSAR, molecular docking, molecular dynamics simulation, and *in silico* pharmacokinetic and toxicity studies. *Journal of King Saud University-Science*, 33(8), 1-10. https://doi.org/10.1016/j.jksus.2021.101637
- Moreira, L. E., Cabral, V. P., Rodrigues, D. S., Barbosa, A. D., Silveira, M. J., Coutinho, T. D., & Silva, C. R. (2024). Antifungal activity of tannic acid against *Candida spp.* and its mechanism of action. *Brazilian Journal of Microbiology*, 50, 3679–3690. https://doi.org/10.1007/s42770-024-01477-w
- Muhammad, F., Rahmayanti, Y., & Isfanda. (2021). Potensi fitokimia *Citrus aurantium* dalam menghambat xantin oksidase hiperurisemia secara *in silico. Jurnal Health Sains*, 2(1), 79–89. https://dx.doi.org/10.46799/jhs.v2i1.80
- Muiz, H. A., Wulandari, S., & Primadiamanti, A. (2021). Uji aktivitas antibakteri ekstrak daun patikan kebo (*Euphorbia hirta* L.) terhadap *Staphylococcus aureus* dengan metode difusi cakram. *Jurnal Analisis Farmasi*, 6(2), 84–89. https://doi.org/10.33024/jaf.v6i2.5942

- Nguyen, T. L. A., & Bhattacharya, D. (2022). Antimicrobial activity of quercetin: an approach to its mechanistic principle. *Molecules*, 27(8). https://doi.org/10.3390/molecules27082494
- Nguyen, W., Grigori, L., Just, E., Santos, C., & Seleem, D. (2021). The *in vivo* anti-*Candida albicans* activity of flavonoids. *Journal of Oral Biosciences*, 63(2), 120–128. https://doi.org/10.1016/j.job.2021.03.004
- Nurlelasari, N., Widyana, A., Julaeha, E., Hardianto, A., Huspa, D. H. P., Maharani, R., Mayanti, T., Darwati, D., Hanafi, M., & Supratman, U. (2023). Studi *in silico* aktivitas senyawa steroid terhadap antikanker payudara menggunakan estrogen alfa (ER-α). *ALCHEMY Jurnal Penelitian Kimia*, 19(1), 44-52. https://doi.org/10.20961/alchemy.19.1.62384.44-52
- Oigbochie, A. E., Otutu, I. M. M., & Odigie, E. B. (2022). The use of *Aloe barbadensis* M. (*Aloe vera*) extracts as potential stains in gram's staining technique. *Dutse Journal of Pure and Applied Sciences*, 8(2a), 47–56. https://doi.org/10.4314/dujopas. v8i2a.6
- Olbana, T., Muchugi, A., Woldemariam, Y., Hay, F. R., Ndiwa, N., & Jones, C. S. (2023). Overcoming dormancy in *Desmanthus virgatus* seeds for improved viability monitoring protocols of genebank accessions. *Seed Science and Technology*, *51*(3), 421–434. https://doi.org/10.15258/sst.2023.51.3.12
- Oliveira, C. D. S., & Rodrigues, A. G. (2020). *Candida albicans* antifungal resistance and tolerance in bloodstream infections: the triad yeast-host-antifungal. *Microorganisms*, 8(2), 1-19. https://doi.org/10.3390/microorganisms8020154
- Panjaitan, Z., Hafizah, H., Ginting, R. I., & Amrullah, A. (2021). Perbandingan metode certainty factor dan theorema Bayes dalam mendiagnosa penyakit kandidiasis pada manusia menggunakan metode perbandingan eksponensial. *Jurnal Media Informatika Budidarma*, 5(3), 1-8. https://doi.org/10.30865/mib.v5i3.3078

- Paray, A. A., Singh, M., & Amin Mir, M. (2023). Gram staining: a brief review. *International Journal of Research and Review*, 10(9), 336–341. https://doi.org/10.52403/ijrr.20230934
- Pratama, A. B., Herowati, R., & Ansory, H. M. (2021). Studi docking molekuler senyawa dalam minyak atsiri pala (*Myristica fragrans* H.) dan senyawa turunan miristisin terhadap target terapi kanker kulit. *Majalah Farmaseutik*, 17(2), 233–242. https://doi.org/10.22146/farmaseutik.v17i2.59297
- Putri, N. R., Wahidah, S. N., Hafidz, I. T. A., & Faisal. (2023). Uji daya hambat antimikroba secara difusi sumuran dan difusi paper disk. *Era Sains : Journal of Science, Engineering and Information Systems Research*, 1(4), 28-33. https://jurnal.eraliterasi.com/index.php/erasains/index
- Richardson, J. P. (2022). *Candida albicans*: a major fungal pathogen of humans. *Pathogens*, 11(4), 10-12. https://doi.org/10.3390/pathogens11040459
- Rodiah, S. A., Fifendy, M., & Indriati, G. (2022). Uji daya hambat ekstrak daun beringin (*Ficus benjamina* L.) terhadap pertumbuhan jamur *Candida albicans* secara *in vitro*. *Serambi Biologi*, 7(4), 318–325. https://doi.org/10.24036/srmb.v7i4.52
- Rokhana & Nadia, R. (2024). Uji aktivitas anti jamur ekstrak daun sirih merah (*Piper crocatum*) terhadap jamur keputihan (*Candida albicans*). *Cendekia Journal of Pharmacy*, 8(1), 98–104. https://doi.org/10.31596/cjp.v8i1.243
- Sachivkina, N., Podoprigora, I., & Bokov, D. (2021).

 Morphological characteristics of *Candida albicans*, *Candida krusei*, *Candida guilliermondii*, and *Candida glabrata* biofilms, and response to farnesol. *Veterinary World*, *14*(26), 1608–1614. https://doi.org/10.14202/vetworld.2021.1608-1614
- Safitri, A. N., & Qurrohman, M. T. (2022). Perbandingan pertumbuhan jamur *Candida albicans* pada media alami jagung, singkong dan ubi jalar kuning. *Journal of Indonesian Medical Laboratory and Science*, *3*(2), 97–107. https://doi.org/10.53699/joimedlabs.v3i2.76

- Santos, A. L. S., Silva, L. A. B., Gonçalves, D. S., Ramos, L. S., Oliveira, S. S. C., Souza, L. O. P., Oliveira, V. S., Lins, R. D., Pinto, M. R., Muñoz, J. E., Taborda, C. P., & Branquinha, M. H. (2021). Repositioning lopinavir, an HIV protease inhibitor, as a promising antifungal drug: lessons learned from *Candida albicans in silico, in vitro* and *in vivo* approaches. *Journal of Fungi*, 7(424), 1–33. https://doi.org/10.3390/jof7060424
- Seyoum, E., Bitew, A., & Mihret, A. (2020). Distribution of *Candida albicans* and non-*Candida albicans* species isolated in different clinical samples and their *in vitro* antifungal susceptibility profile in Ethiopia. *BMC Infectious Diseases*, 20(1), 1–9. https://doi.org/10.1186/s12879-020-4883-5
- Srivastava, R. (2021). Theoretical studies on the molecular properties, toxicity, and biological efficacy of 21 new chemical entities. *ACS Omega*, *6*(38), 24891–24901. https://doi.org/10.1021/acsomega.1c03736
- Stanzione, F., Giangreco, I., & Cole, J. C. (2021). Use of molecular docking computational tools in drug discovery. *Progress in Medicinal Chemistry*, *1*(60). https://doi.org/10.1016/bs.pmch.2021.01.004
- Stegemann, S., Moreton, C., Svanbäck, S., Box, K., Motte, G., & Paudel, A. (2023). Trends in oral small-molecule drug discovery and product development based on product launches before and after the rule of five. *Drug Discovery To*day, 28(2), 1-13. https://doi.org/10.1016/j.drudis.2022.103344
- Suriany, Lasmawati, A. H., & Sitepu, D. D. O. (2024). Uji ekstrak bunga mawar (*Rosa hybrida*) sebagai pengganti kristal violet pada pewarnaan gram. *Jurnal Medistra Medical*, *1*(2), 69–75. https://doi.org/10.35451/mmj.v1i2.2096

- Suryana, A. F., Aprilia, H., & Fakih, T. M. (2022). Uji aktivitas *in silico* senyawa amritoside, tinosporaside dan turunannya sebagai kanditat senyawa. *Bandung Conference Series: Pharmacy*, *2*(2), 1–10. https://doi.org/10.29313/bcsp.v2i2.4369
- Suybeng, B., Mwangi, F. W., McSweeney, C. S., Charmley, E., Gardiner, C. P., Malau-aduli, B. S., & Malau-aduli, A. E. O. (2021). Response to climate change: evaluation of methane emissions in Northern Australian beef cattle on a high-quality diet supplemented with *Desmanthus* using opencircuit respiration chambers and greenfeed emission monitoring systems. *Biology*, *10*(9). https://doi.org/10.3390/biology10090943
- Talapko, J., Juzbašić, M., Matijević, T., Pustijanac, E., Bekić, S., Kotris, I., & Škrlec, I. (2021). *Candida al-bicans* are the virulence factors and clinical manifestations of infection. *Journal of Fungi*, 7(2), 1-19. https://doi.org/10.3390/jof7020079
- Teodoro, G. R., Ellepola, K., Seneviratne, C. J., & Koga, C. Y. (2015). Potential use of phenolic acids as anti-*Candida* agents: a review. *Frontiers in Microbiology*, 6(Dec), 1–11. https://doi.org/10.3389/fmicb.2015.01420
- Tian, X., Ding, H., Ke, W., & Wang, L. (2021). Quorum sensing in fungal species. *Annual Review of Micro-biology*, 75, 449–469. https://doi.org/10.1146/an-nurev-micro-060321-045510

- Tran, H. N. H., Graham, L., & Adukwu, E. C. (2020). In vitro antifungal activity of Cinnamomum zeylanicum bark and leaf essential oils against Candida albicans and Candida auris. Applied Microbiology and Biotechnology, 104(20), 8911–8924. https://doi.org/10.1007/s00253-020-10829-z
- Wandi, I. A., Samudra, J. A., Umam, R. N. K., Asih, R. S., Nafiah, M., Jannah, S. N., & Ferniah, R. S. (2022). Eksplorasi senyawa antiretroviral dari biji tanaman *Calophyllum inophyllum* L. sebagai alternatif obat AIDS secara *in silico*. *Bioma: Berkala Ilmiah Biologi*, 24(1), 24–29. https://doi. org/10.14710/bioma.24.1.24-29
- Widodo, H. S., Ifani, M., Yusan, R. T., Subagyo, Y., & Nurus, A. (2023). Perbandingan tampilan Lipinski's rule of five peptida akibat Alel A1/A2 Gen Csn2 sapi perah pendahuluan metode dan metode penelitian. *Prosiding Seminar Nasional Teknologi dan Agribisnis Peternakan X*, 7, 27–32. Retrieved from https://jnp.fapet.unsoed.ac.id/ index.php/index
- Yuliati, Kurniatuhadi, R., & Khotimah, S. (2024). Aktivitas antifungi ekstrak metanol *Sarcotheca diversifolia* (Miq) Hallier F terhadap pertumbuhan *Candida albicans*. *Sciscitatio*, *5*(2), 76–86. https://doi.org/10.21460/sciscitatio.2024.52.180

Development and Characterization of Indomethacin Quantum Dot Loaded Hydrogel

Gamze ÇAMLIK**, Gökçe KARAOTMARLI GÜVEN**, Besa BİLAKAYA***, Emre Şefik ÇAĞLAR****, Tuğçe BORAN*****, Neslihan ÜSTÜNDAĞ OKUR******, İsmail Tuncer DEĞİM*******

Development and Characterization of Indomethacin Quantum Dot Loaded Hydrogel

SUMMARY

Inflammation occurring in the wound tissue plays an important role in wound healing. This situation can cause undesirable conditions such as pain and swelling in patients. Indomethacin (IM) is one of the most frequently preferred nonsteroidal anti-inflammatory (NSAID) active substances that suppress the inflammatory response. Indomethacin blocks prostaglandin synthesis by inhibiting the cyclooxygenase enzyme and thus helps support the wound healing process. This study includes hydrogel formulations of quantum dots (IMQDs) prepared from the indomethacin active substance for the first time. Characterization studies of the prepared IMQDs were carried out and particle sizes, % polydispersity indexes, and zeta potentials were measured as 8.53±0.096 nm, 19.49±0.550 %, -8.2±0.781 mV, respectively. Quantum yield % was calculated as 56.48%. Hydrogel formulations containing F1 (0.5%), F2 (0.75%), and F3 (1%) containing carbomer at different concentrations and F1-IMQDs, F2-IMQDs and F3-IMQDs containing 2% IMQDs were prepared. The prepared hydrogels' viscosity, pH, mechanical properties, and spreadability were measured. In vitro release studies of all formulations were performed, and it was seen that the gel drug containing IMQDs exhibited a higher release rate than traditional drugs. At the same time, the gel containing IMQDs showed fluorescent properties. Cell culture studies did not show toxicity. In line with the obtained data, the hydrogel formulations containing IMQDs prepared can be applied to dermal wound healing or antiinflammatory treatments. This study can be a source for future studies and applications.

Key Words: Indomethacin, quantum dots, hydrogel.

Received: 21.01.2025 Revised: 9.04.2025 Accepted: 9.05.2025

İndometazin Kuantum Nokta Yüklü Hidrojelin Geliştirilmesi ve Karakterizasyonu

ÖZ

Yara dokusunda meydana gelen inflamasyon, yara iyileşmesi sürecinde önemli bir rol oynamaktadır. Bu durum hastalarda ağrı ve şişlik gibi istenmeyen durumlara neden olabilmektedir. Indometazin (IM), inflamatuvar yanıtı baskılayan ve sıklıkla tercih edilen nonsteroidal anti-inflamatuvar (NSAIDs) etken maddelerin başında gelmektedir. Indometazin, siklooksijenaz enzimini inhibe ederek prostaglandin sentezini bloke etmekte ve böylece yara iyileşme sürecini desteklemeye yardımcı olmaktadır. Bu çalışma ilk defa indometazin etkin maddesinden hazırlanan KN'lerin (IMQDs) hidrojel formülasyonlarını içermektedir. Hazırlanan IMQDs'lerin karakterizasyon çalışmaları gerçekleştirilmiş olup partikül büyüklükleri, % polidispersite indeksleri ve zeta potansiyelleri sırasıyla 8.53 ± 0.096 nm, 19.49 ± 0.550 %, -8.2 ± 0.781 mV olarak ölçüldü. Kuantum verimi %56.48 olarak hesaplandı. Farklı konsantrasyonlarda karbomer içeren F1 (0.5%), F2 (0.75%) ve F3 (1%) ile %2 IMQDs içeren F1-IMQDs, F2-IMQDs ve F3-IMQDs içeren hidrojel formülasyonları hazırlandı. Hazırlanan hidrojellerin viskozite, pH, mekanik özellikleri, yayılabilirlikleri ölçüldü. Tüm formülasyonların in-vitro salım çalışmaları gerçekleştirildi ve IMQDs içeren jel ilacı geleneksel ilaçlardan daha yüksek bir salım hızı sergilediği görüldü. Aynı zamanda IMQDs içeren jel floresan özellik gösterdi. Hücre kültürü çalışmaları toksisite göstermedi. Elde edilen veriler doğrultusunda hazırlanan IMQDs içeren hidrojel formülasyonları, dermal yara iyileşmesi veya anti-inflamatuar tedavilere uygulanabilir. Bu çalışma daha sonra gerçekleştirilecek çalışmalar ve uygulamalar için bir kaynak olabilecektir.

Anahtar Kelimeler: İndometazin, kuantum noktaları, hidrojel.

^{*} ORCID: 0000-0003-3282-8307, Department of Pharmaceutical Technology, Faculty of Pharmacy, Biruni University, İstanbul, Türkiye.

[&]quot;ORCID: 0000-0001-9248-2526, Department of Pharmaceutical Technology, Faculty of Pharmacy, Biruni University, İstanbul, Türkiye. ORCID: 0000-0001-9510-4467, Department of Pharmaceutical Technology, Faculty of Pharmacy, Biruni University, İstanbul, Türkiye.

ORCID: 0000-0003-2010-4918, Department of; Pharmaceutical Biotechnology, Faculty of Pharmacy, University of Health Sciences, İstanbul, Türkiye.

ORCID: 0000-0003-4302-1947, Department of Pharmaceutical Toxicology, Faculty of Pharmacy, Cerrahpaşa University, İstanbul, Türkiye.

ORCID: 0000-0002-3210-3747, Department of Pharmaceutical Technology, Faculty of Pharmacy, University of Health Sciences, İstanbul, Türkiye.

ORCID: 0000-0002-9329-4698, Department of Pharmaceutical Technology, Faculty of Pharmacy, Biruni University, İstanbul, Türkiye.

INTRODUCTION

The skin is the largest sensory organ that protects our body from external factors. The skin consists of many layers. These layers protect our body from impact, trauma, cold, heat, etc. Wounds occur because of the disruption of the tissue integrity of the skin. Wound healing includes a series of processes carried out by our body to restore skin integrity and repair the damage. Treatments and medications are used to improve this process in wound healing (Baron, Glatz, & Proksch, 2020). Non-steroidal anti-inflammatory drugs (NSAIDs) can be an example of groups applied topically in wound healing. Indomethacin is a non-steroidal anti-inflammatory drug. It is an anti-inflammatory drug that selectively inhibits the cyclooxygenase enzyme (Augusto de Castro et al., 2023). Indomethacin (IM) also has formulations that are applied topically to the skin and eyes in wound healing.

Hydrogels are gels in which the dispersion medium is water. They are structures that can hold significant amounts of water without losing their three-dimensional network properties (Aswathy, Narendrakumar, & Manjubala, 2020). Hydrogels can be produced from polymers with various chemical and physical properties depending on their areas of use (Yan Wang, Zhang, Zhang, & Li, 2012). Many natural, synthetic, and semi-synthetic polymers such as chitosan, alginate, hyaluronic acid, cellulose derivatives, polyvinyl alcohol, and polyethylene glycol can be used in hydrogels (Divyashri et al., 2022).

Quantum dots with dimensions ranging from 1 to 10 nm are semiconductor nanocrystals discovered in the 1980s (Yunqing Wang & Chen, 2011). Their unique optical properties make them more interesting than other nanomaterials. With the development of carbon-based quantum dots in 2004, their potential for use in the health field has also begun to be investigated (Nair, Haponiuk, Thomas, & Gopi, 2020). All attempts in the literature show higher effects and better permeabilities through biological membranes. Therefore, indomethacin was prepared in quantum dots as we already noted in our other studies (Camlik,

Bilakaya, Ozsoy, & Degim, 2024).

In our study, hydrogel formulations of quantum dots synthesized from indomethacin active substances were developed. Preliminary characterization studies were completed by performing viscosity, tissue profile analyses, spreadability, *in vitro* release studies, and cellular cytotoxicity in the developed formulations.

MATERIALS AND METHODS

Materials

Indomethacin, urea, and triethanolamine were purchased from Sigma Aldrich (St. Louis, MO, USA). Carbomer was purchased from BioBasic (Canada). All pharmaceutical materials were used in analytical grade. A microwave reactor (Anton Paar Microwave 300, Anton Paar, St. Albans Hertfordshire, AL4 0LA, UK) was used to produce IMQDs. Additionally, particle size, size distribution, and zeta potential were determined using an Anton Paar LiteSizer 500. The optical properties of IMQDs were characterized using a spectrofluorometer (Model 229129, Agilent Technologies, Santa Clara, CA, USA). The formulations' pH measurement and viscosity values were performed using Mettler Toledo S220-K (Switzerland) and Brookfield DV1-LV (UK) viscosimeter, respectively. Texture analyses of the gels were completed on TAXT Plus.

Preparation of indomethacin quantum dots (IMQDs)

IMQDs were prepared by simple microwave synthesis (Monowave 300, Anton Paar, Austria) method. 0.01 g indomethacin, 0.005 g of urea, and 1 ml of distilled water were combined and allowed to react at 150 degrees for 20 minutes. The obtained quantum dots were purified using a 0.22 µm membrane filter.

Preparation of blank and loaded gel formulations

Hydrogels were prepared with various carbomer concentrations (0.5%, 0.75%, 1%). Carbomer and distilled water were added to the beaker and mixed. Cross-linking was achieved by adding 0,25 ml of triethanolamine. (Table 1) shows the formulation components and their quantities.

•						
Components	F1(%)	F1-IMQDs (%)	F2(%)	F2-IMQDs (%)	F3(%)	F3-IMQDs (%)
Carbomer	0.5	0.5	0.75	0.75	1.00	1.00
Triethanolamine	0.25	0.25	0.25	0.25	0.25	0.25
Indomethacin (IM)	2.00	-	2.00	-	2.00	-
IMQDs	-	2.00	-	2.00	-	2.00
Methyl paraben	0.015	0.015	0.015	0.015	0.015	0.015
Distilled Water (q.s.)	100	100	100	100	100	100

Table 1. Components of blank and loaded formulations

Characterization of IMQDs

Particle Size, Polydispersity Index% (PDI%) and Zeta Potential

To characterize indomethacin quantum dots, structure and morphology analysis were performed. Anton Paar Lite Sizer 500 (Austria) was used for particle size, distribution, and zeta potential measurements. Particle size measurements were performed with six replicates, and zeta potential measurements were performed with 12 replicates (Camlik et al., 2024).

Quantum yield % (QY%)

Quinine sulfate solution in 0.1 M sulfuric acid was used as a standard for calculating quantum yield. Measurements were carried out on a Shimadzu RF6000 (Japan) Spectrofluorometer. Equation (1) was used to calculate quantum yield (Alkian, Sutanto, & Hadiyanto, 2022).

QYc = QYs ×
$$\frac{Ic}{Is}$$
 × $\frac{As}{Ac}$ × $\left(\frac{\eta c}{\eta s}\right)^2$ (1)

QY% represents the yield of carbon-based quantum dots, QYs represents the quantum yield of the reference quinine sulfate (0.54), I represents the fluorescence area, A represents the absorbance intensity at 360 nm excitation wavelength, η represents the refractive index, c represents carbon-based quantum dots, and s represents quinine sulfate.

Characterization of IMQDs loaded hydrogel

pH measurements of blank and loaded formulations were carried out in triplicate at ambient conditions using a Mettler Toledo S220-K

(Switzerland) device. Viscosity measurements of the developed formulations were carried out using Brookfield DV1-LV (UK) viscosimeter.

Drug Contents

Drug content determination was performed on the Shimadzu RF6000 (Japan) device. 1 ml of gel sample was diluted in 50 ml of distilled water. The analysis was performed on a spectrofluorometer device (Chaudhary, Kohli, Amin, Rathee, & Kumar, 2011). Briefly, excitation was obtained at 560 nm, and emission was detected at 544 nm. The drug was analyzed in the gel using a calibration curve. IMQDs were sequentially diluted with distilled water across an 8-point concentration range from 9 mg/mL to 3 mg/mL. The calibration curve thus obtained had a linear response with a coefficient of determination (R²) of 0.998.

TPA analysis

Texture analysis of the gels was conducted with a TAXT Plus texture analyzer. For the determination of mechanical properties such as hardness, compressibility, adhesiveness, cohesion, and elasticity of the gels, a 25 mm diameter Perspex probe (P/25P, θ : 25 mm) was utilized. Pre-test speed was 2.00 mm/s, and test and final test speeds were both 2 mm/s with a 0.001 N trigger force. The compression depth in each process was set to 10.00 mm, and the time interval between two compressions was set to 10 seconds. The experiments were all done in triplicate at 25 \pm 0.5 °C.

Spreadability

The test sample was placed inside the female cone. The male cone was shifted towards the female cone by up to 23 mm at a rate of 3 mm/s during the test and then at 10 mm/s for the post-test. The spreadability of the gels was identified in terms of firmness, stickiness, work of shear, and work of adhesion. The testing was conducted under room conditions.

In vitro release

Franz diffusion cells and cellophane membranes were used to determine *in vitro* migration. Cellophane membranes were placed between the receptor and donor chambers of the Franz cells. Franz diffusion cells were used in triplicate for each formulation. Temperature was maintained at 37 °C, and pH 7.4 isotonic phosphate buffer solution was used as the receptor phase. 1 mL of the formulation was loaded into the donor chamber. The donor compartment's top was covered with parafilm to prevent evaporation. The receptor compartment samples were taken at 15, 30, 45, 60, 90, 120, 180, 240, and 300 minutes, and the volume taken was replaced with fresh solution to ensure sink conditions (Camlik et al., 2024).

Cellular toxicity

Cell culture

The immortalized human keratinocyte cell line (HaCaT) was grown in DMEM with 10% fetal bovine serum and 1% penicillin/streptomycin/amphotericin solution. The cell culture media was replaced every two days.

MTT cytotoxicity assay

Formulations F1, F1-IMQDs, F2, F2-IMQDs, F3, and F3-IMQDs were tested for cytotoxicity using the MTT (3-(4,5-Dimethylthiazol-2-yl)-2,5-Diphenyltetrazolium Bromide) assay. Per mL of formulation was dissolved in complete cell culture media, and $1x10^4$ cells/well in 96-well plates were incubated with the solutions at different concentrations. Following 24 h of exposure, the cell culture medium was changed, and cells were incubated with the MTT dye solution. 100 μ L of DMSO solution was added to each well to dissolve

formazan crystals generated by metabolically active cells. Optical density (OD) at 590 nm was detected using a multimode plate reader (Biotek, Agilent, USA). The absorbance of the control group was set to 100% to represent cell viability.

Stability

The prepared formulations were subjected to stability testing. F1-IMQDs formulations were stored in the refrigerator at 5 °C and at room temperature (25 °C \pm 2 °C and 60% relative humidity) for 12 months. Stability measurements were performed using the Zeta Sizer 500 (Anton Paar, Austria).

Statistical evaluation

To evaluate the results in this study, experimental mean values were accepted as mean \pm SD. A two-way ANOVA test was used for statistical analysis.

RESULTS AND DISCUSSION

IMQDs were synthesized in a microwave reactor using a bottom-up method. This method was chosen for its advantages, including high efficiency, short reaction time, simplicity, environmental compatibility, and high reproducibility (Hou et al., 2016). The initial and most rapid indication of quantum dot formation was determined through observation under 365 nm UV light (Elugoke, Uwaya, Quadri, & Ebenso, 2024). When examined under 365 nm UV light, IMQDs fluoresced yellowish green (Figure 1).



Figure 1. The physical appearance of IMQDs under UV light (365 nm).



Figure 2. Physical appereances of gels with and without IMQDs under UV light (365 nm).

This study successfully developed hydrogel formulations containing IMQDs. The hydrogel formulations were prepared using a simple method (Figure 2), and IMQDs were subsequently added. Figure 2 presents the formation of IMQDs post-synthesis and the physical appearance of IMQDs in the gel. IMQDs were prepared in a gel that can be applied to the skin for various reasons, including wound healing (Huang, Dan, Dan, & Chen, 2021).

Carbon quantum dots (CQDs) are nanocrystals with unique photochemical and photophysical properties such as particle sizes smaller than 10 nm,

continuous, long tunable emission wavelength, high fluorescence stability, low toxicity, and good biocompatibility (Smith, Gao, & Nie, 2004). Characterization studies were also carried out for IMQDs and particle size, percentage of polydispersity index (PDI%), and zeta potentials were found to be 8.53 ± 0.096 nm, 19.49 ± 0.550 %, -8.2 ± 0.781 mV, respectively. The fact that the particle size is below 10 nm further confirms quantum dot formation (Camlik et al., 2024). The value of PDI% being between 10-30 indicates a narrow size distribution, which indicates a homogeneous distribution (Luan, Zheng, Yang, Yu, & Zhai, 2015; Özkahraman, Acar, Gök, & Güçlü, 2014). The QY% of the prepared IMQDs was then calculated as 56.48%, which was accepted as high enough (Albrecht, 2008).

Hydrogel formulations F1 (0.5%), F2 (0.75%), and F3 (1%) were prepared using three different carbomer concentrations (Table 1). Figure 2 shows the image of the empty gel formulation and quantum dot-added gel formulations under UV fluorescence.

Ideal gel formulations are expected to be easy to apply and not run after application. At the same time, the pH of the preparations to be applied to the skin should be suitable for the skin pH. The viscosity and pH values of the prepared formulations are given in Table 2.

Table 2.	Viscosity	and pH	values of	formulations
----------	-----------	--------	-----------	--------------

Formulation Code	Viscosity (cP)	pH (24°C)
F1	8920±40.000	5.76± 0.044
F1-IMQDs	8026.67±23.094	5.81±0.165
F2	9333.33±23.094	5.41±0.061
F2-IMQDs	8480±40.000	5.32±0.042
F3	10426.67±23.094	4.97±0.015
F3-IMQDs	9306.67±23.094	4.98±0.084

The pH of the formulations should be in a range that will not irritate the skin and should be prepared in a way that will not alter the efficacy and stability of the drug in the formulation. IMQDs-gel formulations should be compatible with the pH of the application site and should not irritate the skin. The physiological pH of the skin is between 4.1 and 5.8 (Tottoli et al., 2020). It has been observed that the developed formulations are compatible with the skin pH. The

pH of the developed F1, F1-IMQDs, F2, F2-IMQDs, F3, and F3-IMQDs gel formulations was between 4.97 ± 0.015 and 5.81 ± 0.165 (Table 2). Viscosity is a very significant parameter in the formulation of most topical products. Failure to achieve the appropriate and desired viscosity while formulating can lead to the drug being unable to achieve the desired effect under the conditions of usage (Jin, Imran, & Mohammed, 2022).

Ideal gel formulations should be easy to apply and not run after application. Viscosity measurements were performed to determine the viscosity and flow properties of the gels. Formulations with low viscosity had a short residence time, while those with higher viscosity had a longer residence time (Binder, Mazál, Petz, Klang, & Valenta, 2019). Therefore, viscosity influences the rate of skin penetration. The developed formulations exhibited viscosities suitable for topical applications.

The viscosity values developed of the formulations were found to vary between 8480±40 cP and 10426.67±23.094 cP. The solvent mixture in all formulations is held in the three-dimensional network of the bonded polymer chains in the prepared hydrogels, and polymeric fibril content increases due to the evaporation of the solvents after the application. In addition, due to the evaporation of the solvents and their absorption into the skin layers, a dense gel network is formed. In the measurements, it is seen that the viscosity increases parallel to the carbomer concentration. Moreover, the viscosity decreases with the addition of IMQDs to the formulation. The intermolecular forces in the polymeric chain network are disrupted by IMQDs, as a result, the viscosity decreases. Depending on the pH and viscosity results, it was found that F2 and F2-IMQDs gel formulation have the appropriate viscosity and pH values (Table 2).

When the active ingredient content of the formulations is examined, it is 96.68%, 94.33%, and 96.75% for F1-IMQDs, F2-IMQDs, and F3-IMQDs, respectively.

Indomethacin-loaded hydrogel formulations were developed with increasing carbomer concentrations. When the viscosity values were examined, it was observed that the viscosity increased with increasing carbomer concentration. The hardness value of the F2-IMQDs formulation was determined to be lower than that of the other formulations. When viscosity measurements were evaluated together, it was found that the F2-IMQDs formulation had lower viscosity than the others. In addition, it can be concluded that the quantum dots added to the blank formulations reduced the viscosity of the formulation and therefore reduced the hardness of the gels. It was found that the F1-IMQDs and F2-IMQDs formulations had similar hardness.

Table 3. Results of TPA

Formulation Code	Hardness (g)	Adhesiveness (g.sec)	Cohesion	Resilience (%)	Springiness (%)
F1	-4.876±1.706	-73.877±10.760	0.894±0.019	13.652±0.006	85.129±0.003
F1-IMQDs	-5.644±0.440	-78.246±3.101	0.878±0.045	14.090±0.015	85.510±0.010
F2	-6.535±1.346	-87.906±13.969	0.922±0.037	14.600±0.012	86.214±0.007
F2-IMQDs	-7.172±0.305	-97.233±7.164	0.894±0.031	14.763±0.014	83.977±0.003
F3	-3.895±2.161	-66.800±7.067	0.925±0.027	16.862±0.018	89.157±0.024
F3-IMQDs	-5.692±2.734	-95.930±25.361	0.887±0.040	15.139±0.027	85.878±0.026

The hardness value indicates the durability of the formulation. A high hardness value is very important for the stability of the formulation. The maximum positive value in the graph indicates the hardness of the formulations. The negative regions seen in the graph indicate cohesiveness (Çağlar et al., 2025).

The mechanical properties of the prepared hydrogels, such as adhesion, cohesion, flexibility, and springiness, were evaluated with TPA (Tian et al., 348

2024). These properties were assessed by subjecting the formulations to external compressive stress and measuring their capacity to undergo reversible and irreversible deformations. Gel hardness indicates the ease of application of gels to the skin surface, while at the same time, it can indicate how long the gel will remain in the application area. The hardness of the F1, F2, and F3 formulations decreased with the addition of IMQDs, suggesting that IMQDs intercalate

within the polymer network and form a complex. A lower hardness is desirable for easy application and spreadability. Compared to the other formulations, F3 and F3-IMQDs formulations exhibited higher firmness, which suggests that gel hardness increases with carbomer concentration. All the developed formulations showed good firmness, spreading, and stickiness for topical applications.

The formulations also show that all formulations are suitable for skin applications when the adhesiveness, cohesion, flexibility, and durability results are evaluated (Carvalho et al., 2013).

The spreadability values of the developed formulations are shown in Table 4 and Figure 3.

Table 4. Results of spreadability

Formulation Code	Firmness (g)	Work of Shear (g.sec)	Stickiness (g)	Work of Adhesion (g.sec)
F1	474.63±3.920	431.03±12.470	-45.89±4.370	-138.86±3.230
F1-IMQDs	449.41±0.650	430.09±1.060	-425.68±1.190	-113.55±13.060
F2	508.01±11.140	471.84±7.860	-478.41±6.720	-130.42±9.490
F2-IMQDs	477.19±6.830	435.92±13.390	-455.69±5.640	-128.30±6.500
F3	559.79±9.670	513.94±21.060	-518.83±2.010	-144.94±4.570
F3-IMQDs	540.66±4.310	484.89±8.160	-506.55±1.850	-143.92±5.290

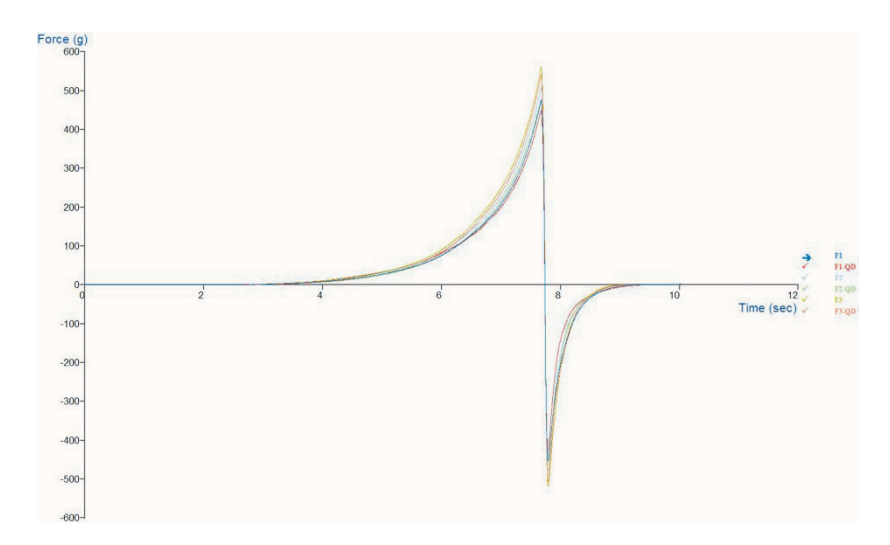


Figure 3. Graphical results of spreadability tests

Spreadability is the ease with which a gel spreads when applied to the skin. The more spreadable the product, the larger the area of skin surface covered by the product when topically applied, and therefore the larger the therapeutic effect of the active ingredient (Kashyap, Das, & Ahmed, 2020).

In vitro release of the formulations was conducted in Franz diffusion cells using phosphate buffer (pH 7.4). Cumulative drug release percentages for the formulations are shown in Figure 4.

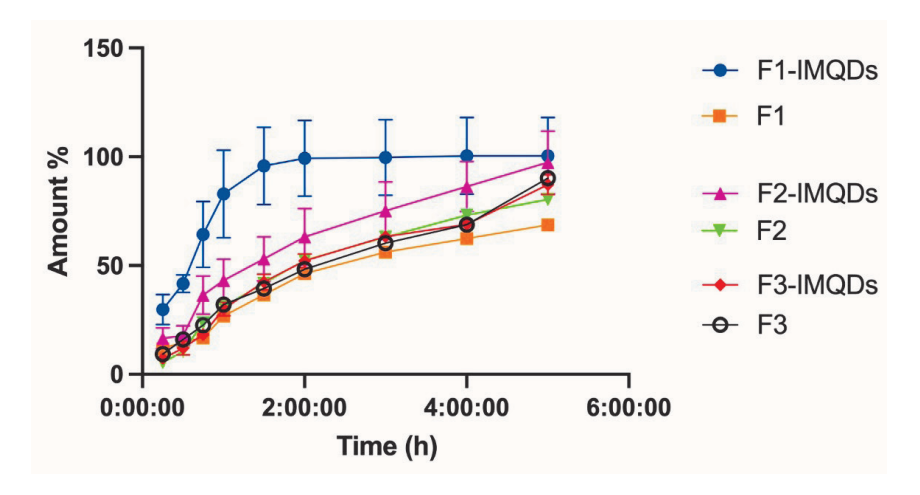


Figure 4. In vitro drug release using franz diffusion cells and cellophane membranes.

In vitro release studies are a simple and reproducible method used to examine the release characteristics of a drug from a dosage form (Shah, Elkins, & Williams, 1999). This test provides information about the *in vitro* performance of the drug and allows comparison of its equivalence with other products (Weng, Tong, & Chow, 2020).

Literature reports that indomethacin, a BCS class II NSAID, exhibits low solubility and high permeability. Our study reformed it as carbon quantum dots (CQDs) to improve its dissolution properties. The solubility was not determined because the *in vitro* dissolution properties were the first concern. Therefore, a series of experiments was conducted to assess the dissolution rate, properties, and effectiveness. The obtained dissolution profiles indicated that the CQDs formulation substantially enhanced the rate and extent of indomethacin dissolution, with the max plateau values reflecting the increased solubility.

In *in vitro* release studies, cellophane membranes are preferred because they enable to separate nanoparticles and drug molecules without representing a barrier function from the gels and the passage through the membrane is similar to biological membranes, and also provide consistency between experiments by providing a standard and reproducible barrier, while their inert structure does not interact with formulations, allowing the observed release profile to be attributed directly to the formulation;

these release studies are usually performed using a pH 7.4 buffer solution, which mimics the behavior of the drug in the body, its proximity to human physiology, are enable us to predict *in vivo* behavior of the drug and formulation stability, and offers an environment close to blood pH, especially in evaluating systemic absorption (Bhuyan, Saha, & Rabha, 2021; Makarov et al., 2022; Salamanca, Barrera-Ocampo, Lasso, Camacho, & Yarce, 2018).

In vitro release studies are critical for evaluating the safety, efficacy, and quality of the product (Çobanoğlu & Şenel, 2023). All release profiles were compared, and it was observed that the release rate slowed down as the carbomer percentage increased. It can be concluded that the F1 formulation released the drug faster than the F2 and F3 formulations; F2 and F3 released the drug about the same. Therefore, the F1 formulation was selected for further experiments.

Indomethacin was formulated as carbon quantum dots to improve its dissolution properties (Topal, Köse Özkan, & Özkan, 2023). *In vitro* dissolution experiments were conducted to assess the effectiveness of this approach. The obtained dissolution profiles indicated that the carbon quantum dot formulation led to a substantial enhancement in both the rate and extent of indomethacin dissolution, with the plateau values reflecting the increased solubility.

The IC50 value of formulations cannot be calculated, cells showed a minimum of 60% viability even at the highest concentrations.

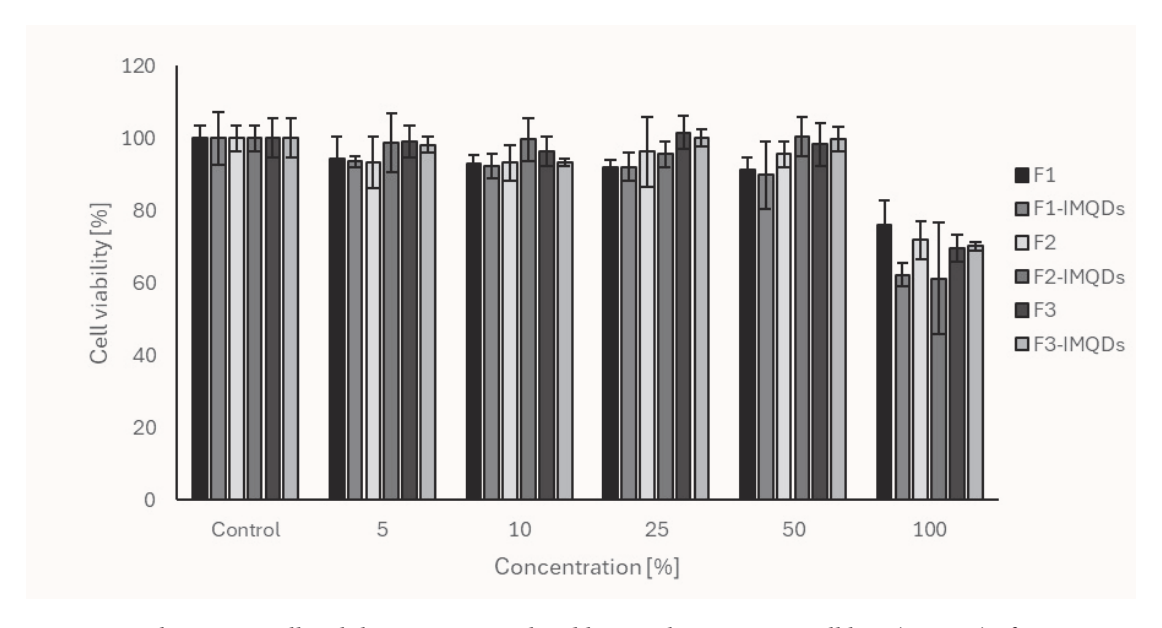


Figure 5. Changes in cell viability on immortalized human keratinocyte cell line (HaCaT) after F1, F1-IMQDs, F2, F2-IMQDs, F3, F3-IMQDs formulations exposure for 24 h.

Indomethacin is a reported NSAID active constituent with cytotoxicity in addition to its therapeutic effect (Harras et al., 2021). Cytotoxicity studies of the formulated preparations were conducted on the human keratinocyte cell line (HaCaT). The results obtained after 24 hours of exposure are shown in Figure 5. The IC50 value of the formulations cannot be calculated since the cells maintained at least 60% viability even at the maximum concentration. The graph obtained indicates the effect of indomethacinloaded F1, F2, F3, and indomethacin-quantum dotloaded F1-IMQDs, F2-IMQDs, and F3-IMQDs gel formulation on the cell viability. In Figure 5, no significant toxic effect is generally observed on the cell viability of F1, F2, and F3 formulations. However, there was a notable decline in cell viability when concentrations were greater than 50% for all formulations. It was observed that there was no

significant shift in cytotoxicity when concentrations were at 50% levels in F1-IMQDs and F1 formulations. F2-IMQDs formulation was found to be less cytotoxic than F2 formulation when concentrations were 50% or lower. F3-IMQDs formulation was found to be less cytotoxic than the F3 formulation at a 50% concentration. The results depict that quantum dots formed from the active compound are less toxic than the active compound of the same concentration.

Stability tests of F1-IMQDs were carried out in a refrigerator at 5 °C and at 25 °C \pm 2 °C and 60% relative humidity. Particle size, zeta potential, and changes in PDI values were checked. Measurements were made at 0, 3, 6, 9, and 12 months. The results showed that IMQDs were stable for 12 months (Table 5, Table 6). No significant differences were observed between the groups. The obtained results showed that the quantum dots were stable for 12 months.

Table 5. Stability test results of 25°C±2 60% relative humidity

	0 Month	3 Months	6 Months	9 Months	12 Months
Partical size	8.53±0.095	8.62±0.045	8.55±0.09	8.58±0.081	8.6±0.085
Zeta potential	-8.20±0.781	-8.24±0.201	-8.1±0.625	-8.3±0.745	-8.4±9.687
PDI%	19.49±0.55	19.58±0.25	19.55±0.48	19.62±0.68	20.05±0.72
Drug content %	96.68		96.48		96.38

Table 6. Stability test results of 5°C

	0 Month	3 Months	6 Months	9 Months	12 Months
Partical size	8.53±0.081	8.75±0.092	8.57±0.084	8.6±0.075	8.62±0.078
Zeta potential	-8.20±0.652	-8.34±0.542	-8.21±0.652	-7.56±0.794	-7.86±0.795
PDI%	19.49±0.550	19.70±0.250	19.71±0.670	19.85±0.470	19.96±0.430
Drug content %	96.68		96.50		96.32

CONCLUSION

IMQDs are the first carbon-based quantum dots prepared solely from IM in the literature. IMQDs were successfully prepared by one-step microwave synthesis and showed yellowish-green fluorescence in UV (365 nm) and very small particle sizes under 10 nm. The IMQDs-containing gel demonstrated suitability for dermal applications. This gel exhibited fluorescence and released the drug at a higher rate compared to conventional drug solutions. Cell culture studies show no toxicity, which makes it applicable to dermal wound healing or anti-inflammatory treatments. This study can be a shed for further studies and applications.

ACKNOWLEDGEMENT

There are no acknowledgements to declare.

AUTHOR CONTRIBUTION STATEMENT

Hypothesis development (NUO), (ITD), (GC), experimentation (GKG), (BB), (TB), (ESC), (GC), (NUO), preparation of the working text (GKG), (GC), text review (GKG), (GC), (ITD), analysis and interpretation of data (GC), (TB), (NU), (ITD), literature search and reference writing (GKG), (BB), (GC). All authors have read and agreed to the published version of the manuscript.

CONFLICT OF INTEREST

The authors declare that there is no conflict of interest.

REFERENCES

Albrecht, C. (2008). Joseph R. Lakowicz: Principles of fluorescence spectroscopy, 3rd Edition. *Analytical and Bioanalytical Chemistry*, 390(5), 1223–1224. Retrieved from https://doi.org/10.1007/s00216-007-1822-x

Alkian, I., Sutanto, H., & Hadiyanto. (2022). Quantum yield optimization of carbon dots using response surface methodology and its application as control of Fe ³⁺ ion levels in drinking water. *Materials Research Express*, *9*(1), 015702. Retrieved from https://doi.org/10.1088/2053-1591/ac3f60

Aswathy, S. H., Narendrakumar, U., & Manjubala, I. (2020). Commercial hydrogels for biomedical applications. *Heliyon*, *6*(4), e03719. Retrieved from https://doi.org/10.1016/j.heliyon.2020.e03719

Augusto de Castro, M., Henrique Reis, P., Fernandes, C., Geraldo de Sousa, R., Toshio Inoue, T., Ligório Fialho, S., & Silva-Cunha, A. (2023). Thermoresponsive in-situ gel containing hyaluronic acid and indomethacin for the treatment of corneal chemical burn. *International Journal of Pharmaceutics*, 631, 122468. Retrieved from https://doi.org/10.1016/j. ijpharm.2022.122468

Baron, J. M., Glatz, M., & Proksch, E. (2020). Optimal Support of Wound Healing: New Insights. *Dermatology*, 236(6), 593–600. Retrieved from https://doi.org/10.1159/000505291

- Bhuyan, C., Saha, D., & Rabha, B. (2021). A Brief Review on Topical Gels as Drug Delivery System. *Journal of Pharmaceutical Research International*, 344–357. Retrieved from https://doi.org/10.9734/jpri/2021/v33i47A33020
- Binder, L., Mazál, J., Petz, R., Klang, V., & Valenta, C. (2019). The role of viscosity on skin penetration from cellulose ether-based hydrogels. *Skin Research and Technology*, 25(5), 725–734. Retrieved from https://doi.org/10.1111/srt.12709
- Çağlar, E. Ş., Reis, R., Karadağ, A. E., Demirci, F., Sipahi, H., Aydın, A., & Üstündağ Okur, N. (2025). Preparation, characterization, and in vitro evaluation of microemulsion based cream formulations for the topical treatment of acne vulgaris. *Journal of Surfactants and Detergents*, 28(1), 13–24. Retrieved from https://doi.org/10.1002/jsde.12769
- Camlik, G., Bilakaya, B., Ozsoy, Y., & Degim, I. T. (2024). A new approach for the treatment of Alzheimer's disease: insulin-quantum dots. *Journal of Microencapsulation*, 41(1), 18–26. Retrieved from https://doi.org/10.1080/02652048 .2023.2282968
- Carvalho, F. C., Calixto, G., Hatakeyama, I. N., Luz, G. M., Gremião, M. P. D., & Chorilli, M. (2013). Rheological, mechanical, and bioadhesive behavior of hydrogels to optimize skin delivery systems. *Drug Development and Industrial Pharmacy*, 39(11), 1750–1757. Retrieved from https://doi.org/10.3109/03639045.2012.734510
- Chaudhary, H., Kohli, K., Amin, S., Rathee, P., & Kumar, V. (2011). Optimization and Formulation Design of Gels of Diclofenac and Curcumin for Transdermal Drug Delivery by Box-Behnken Statistical Design. *Journal of Pharmaceutical Sciences*, 100(2), 580–593. Retrieved from https://doi.org/10.1002/jps.22292
- Çobanoğlu, E., & Şenel, S. (2023). Nanopartiküler İlaç Taşıyıcı Sistemlerinin İncelenmesinde Kullanılan İn Vitro Salım Testi Yöntemlerine Genel Bir Bakış. *Hacettepe University Journal of the Faculty of Pharmacy*. Retrieved from https://doi.org/10.52794/hujpharm.1181365

- Divyashri, G., Badhe, R. V., Sadanandan, B., Vijayalakshmi, V., Kumari, M., Ashrit, P., ... Raghu, A. V. (2022). Applications of <scp>hydrogel-based</scp> delivery systems in wound care and treatment: An *up-to-date* review. *Polymers for Advanced Technologies*, 33(7), 2025–2043. Retrieved from https://doi.org/10.1002/pat.5661
- Elugoke, S. E., Uwaya, G. E., Quadri, T. W., & Ebenso, E. E. (2024). Carbon Quantum Dots: Basics, Properties, and Fundamentals (pp. 3–42). Retrieved from https://doi.org/10.1021/bk-2024-1465.ch001
- Harras, M. F., Sabour, R., Ammar, Y. A., Mehany, A. B. M., Farrag, A. M., & Eissa, S. I. (2021). Design synthesis and cytotoxicity studies of some novel indomethacin-based heterocycles as anticancer and apoptosis inducing agents. *Journal of Molecular Structure*, 1228, 129455. Retrieved from https://doi.org/10.1016/j.molstruc.2020.129455
- Hou, J., Li, H., Wang, L., Zhang, P., Zhou, T., Ding, H., & Ding, L. (2016). Rapid microwave-assisted synthesis of molecularly imprinted polymers on carbon quantum dots for fluorescent sensing of tetracycline in milk. *Talanta*, *146*, 34–40. Retrieved from https://doi.org/10.1016/j.talanta.2015.08.024
- Huang, Y., Dan, Y., Dan, N., & Chen, Y. (2021).
 Controlled-release of indomethacin trigged by inflammation-response for wound care. *Polymer Testing*, 97, 107129. Retrieved from https://doi.org/10.1016/j.polymertesting.2021.107129
- Jin, X., Imran, M., & Mohammed, Y. (2022). Topical Semisolid Products—Understanding the Impact of Metamorphosis on Skin Penetration and Physicochemical Properties. *Pharmaceutics*, 14(11), 2487. Retrieved from https://doi. org/10.3390/pharmaceutics14112487
- Kashyap, A., Das, A., & Ahmed, A. B. (2020).
 Formulation and Evaluation of Transdermal Topical Gel of Ibuprofen. *Journal of Drug Delivery and Therapeutics*, 10(2), 20–25. Retrieved from https://doi.org/10.22270/jddt.v10i2.3902

- Luan, J., Zheng, F., Yang, X., Yu, A., & Zhai, G. (2015).
 Nanostructured lipid carriers for oral delivery of baicalin: In vitro and in vivo evaluation. *Colloids and Surfaces A: Physicochemical and Engineering Aspects*, 466, 154–159. Retrieved from https://doi.org/10.1016/j.colsurfa.2014.11.015
- Makarov, I. S., Golova, L. K., Bondarenko, G. N., Anokhina, T. S., Dmitrieva, E. S., Levin, I. S., ... Shambilova, G. K. (2022). Structure, Morphology, and Permeability of Cellulose Films. *Membranes*, 12(3),297. Retrieved from https://doi.org/10.3390/membranes12030297
- Nair, A., Haponiuk, J. T., Thomas, S., & Gopi, S. (2020). Natural carbon-based quantum dots and their applications in drug delivery: A review. *Biomedicine & Pharmacotherapy, 132,* 110834. Retrieved from https://doi.org/10.1016/j. biopha.2020.110834
- Özkahraman, B., Acar, I., Gök, M. K., & Güçlü, G. (2014). Optimization of Synthesis Conditions of Poly(N-Vinylcaprolactam) Microgels. *Afyon Kocatepe University Journal of Sciences and Engineering*, 14(1), 13–21. Retrieved from https://doi.org/10.5578/fmbd.6637
- Salamanca, C. H., Barrera-Ocampo, A., Lasso, J. C., Camacho, N., & Yarce, C. J. (2018). Franz Diffusion Cell Approach for Pre-Formulation Characterisation of Ketoprofen Semi-Solid Dosage Forms. *Pharmaceutics*, 10(3), 148. Retrieved from https://doi.org/10.3390/pharmaceutics10030148
- Shah, V. P., Elkins, J. S., & Williams, R. L. (1999). Evaluation of the Test System Used for In Vitro Release of Drugs for Topical Dermatological Drug Products. *Pharmaceutical Development and Technology*, 4(3), 377–385. Retrieved from https://doi.org/10.1081/PDT-100101373
- Smith, A. M., Gao, X., & Nie, S. (2004). Quantum Dot Nanocrystals for *In Vivo* Molecular and Cellular Imaging. *Photochemistry and Photobiology*, 80(3), 377–385. Retrieved from https://doi.org/10.1111/j.1751-1097.2004.tb00102.x

- Tian, Z., Ai, B., Yang, Y., Zheng, X., Xiao, D., Zheng, L., ... Wang, M. (2024). Lysozyme amyloid fibril-chitosan double network hydrogel: Preparation, characterization, and application on inhibition of Nε-(carboxyethyl)lysine. *International Journal of Biological Macromolecules*, 263, 130011. Retrieved from https://doi.org/10.1016/j. ijbiomac.2024.130011
- Topal, G. R., Köse Özkan, C, & Özkan, Y. (2023). Development and optimization of indomethacin nanosuspensions using design of experiment approaches. *Ankara Universitesi Eczacilik Fakultesi Dergisi*. Retrieved from https://doi.org/10.33483/jfpau.1194470
- Tottoli, E. M., Dorati, R., Genta, I., Chiesa, E., Pisani, S., & Conti, B. (2020). Skin Wound Healing Process and New Emerging Technologies for Skin Wound Care and Regeneration. *Pharmaceutics*, 12(8), 735. Retrieved from https://doi.org/10.3390/pharmaceutics12080735
- Wang, Yan, Zhang, Q., Zhang, C., & Li, P. (2012). Characterisation and cooperative antimicrobial properties of chitosan/nano-ZnO composite nanofibrous membranes. *Food Chemistry*, 132(1), 419–427. Retrieved from https://doi.org/10.1016/j. foodchem.2011.11.015
- Wang, Yunqing, & Chen, L. (2011). Quantum dots, lighting up the research and development of nanomedicine. *Nanomedicine: Nanotechnology, Biology and Medicine, 7*(4), 385–402. Retrieved from https://doi.org/10.1016/j.nano.2010.12.006
- Weng, J., Tong, H. H. Y., & Chow, S. F. (2020). In Vitro Release Study of the Polymeric Drug Nanoparticles: Development and Validation of a Novel Method. *Pharmaceutics*, 12(8), 732. Retrieved from https:// doi.org/10.3390/pharmaceutics12080732

Comparative Evaluation of Kollidon®VA64, SoluPlus®, and Aquasolve™ Hpmcas H-L Polymers: Impacts on Oral Spray Dried Powders

Ayse Nur OKTAY **, James E. POLLI **

Comparative Evaluation of Kollidon®VA64, SoluPlus®, and Aquasolve™ Hpmcas H-L Polymers: Impacts on Oral Spray Dried Powders

SUMMARY

 ${\it Ritonavir}\,(RTV) \ is \ an \ anti-HIV \ protease \ inhibitor \ and \ antiretroviral$ $medication\ to\ treat\ HIV\ /AIDS\ and\ especially\ COVID-19\ infection.$ But it has low aqueous solubility which limits its oral bioavailability. Over the last decade, spray drying has become one of the most widely accepted solubility enhancement strategies in the pharmaceutical industry and academia. The spray drying process is a low-cost, solventbased, scalable, continuous, and consistent technique to prepare an amorphous solid dispersion (ASD) of a hydrophobic drug in a single step. Even though the spray drying process has many advantages, it is a complicated system regarding process and formulation parameters. The formulation parameters such as the composition of feed (drug, polymeric carrier, and solvent) greatly impact the physicochemical properties of the spray-dried amorphous powder. Polymer selection is very crucial to developing a physiochemically stable and highly soluble ASD. However, there is a notable lack of comprehensive studies focusing on the impact of polymer type on spray dried powders. So, the objectives of this study were to perform a comparative evaluation of the impacts of Kollidon VA64, SoluPlus, and AquaSolve HPMCAS H-L polymers on spray-dried dispersion powders (SDP) of ritonavir. Powder characterization, DSC analysis, stability, solubility, and dissolution studies were performed. Short-term chemical stability studies supported that the RTV-ASD powders were stable for three months. The solubility of the coarse RTV crystalline powder was significantly increased through the ASD powders with various polymers, compared to the physical mixtures. Dissolution studies showed that the rank order was SoluPlus®>Kollidon®VA64>A quaSolve™ HPMCAS H-L SDPs for both inlet temperatures.

Key Words: Ritonavir, soluplus[®], kollidon[®]va64, aquasolve[™] hpmcas l:h, amorphous solid dispersion

Kollidon°VA64, SoluPlus° ve Aquasolve™ Hpmcas H-L Polimerlerinin Karşılaştırmalı Değerlendirmesi: Oral Püskürtülerek Kurutulmuş Tozlar Üzerindeki Etkileri

ÖZ

Ritonavir (RTV), HIV/AIDS ve özellikle Covid-19 enfeksiyonunu tedavi etmek için kullanılan bir anti-HIV proteaz inhibitörü ve antiretroviral ilaçtır. Ancak düşük suda çözünürlüğü oral biyoyararlanımını sınırlar. Son on yılda, püskürterek kurutma ilaç endüstrisi ve akademide en yaygın kabul gören çözünürlük artırma stratejilerinden biri haline gelmiştir. Püskürterek kurutma işlemi, tek bir adımda hidrofobik bir ilacın amorf katı dispersiyonunu (ASD) hazırlamak için düşük maliyetli, çözücü bazlı, ölçeklenebilir, sürekli ve tutarlı bir tekniktir. Püskürterek kurutma işleminin birçok avantajı olmasına rağmen, işlem ve formülasyon parametreleri açısından karmaşık bir sistemdir. Beslemenin bileşimi (ilaç, polimerik taşıyıcı ve çözücü) gibi formülasyon parametreleri, püskürtülerek kurutulmuş amorf tozun fizikokimyasal özelliklerini büyük ölçüde etkiler. Polimer seçimi, fizikokimyasal olarak stabil ve yüksek oranda çözünür bir ASD geliştirmek için çok önemlidir. Ancak püskürtülerek kurutulmuş tozlar üzerinde polimer tipinin etkisine odaklanan kapsamlı çalışmaların eksikliği dikkat çekicidir. Bu çalışmanın amaçları, Kollidon VA64, SoluPlus® ve AquaSolve™ HPMCAS H-L polimerlerinin ritonavirin püskürtülerek kurutulmuş dispersiyon(SDP) tozları üzerindeki etkilerinin karşılaştırmalı değerlendirmesini yapmaktır. Toz karakterizasyonu, DSC analizi, stabilite, çözünürlük ve çözünme hızı çalışmaları yapılmıştır. Kısa süreli kimyasal stabilite çalışmaları, RTV-ASD tozlarının üç ay boyunca stabil olduğunu desteklemiştir. Kaba RTV kristal tozunun çözünürlüğü, fiziksel karışımlarla karşılaştırıldığında, çeşitli polimerlere sahip ASD tozları vasıtasıyla önemli ölçüde artmıştır. Çözünme hızı çalışmaları, her iki giriş sıcaklığı için sıralamanın SoluPlus®>Kollidon®VA64>AquaSolve™ HPMCAS H-L SDP şeklinde olduğunu göstermiştir.

Anahtar Kelimeler: Ritonavir, soluplus®, kollidon®va64, aquasolve™ hpmcas l:h, amorf katı dispersion.

Received: 20.03.2025 Revised: 24.05.2025 Accepted: 3.07.2025

ORCID ID: 0000-0002-6465-6450, Department of Pharmaceutical Technology, Gulhane Faculty of Pharmacy, University of Health Sciences, Ankara, Turkey. ORCID ID: 0000-0002-5274-4314, Department of Pharmaceutical Sciences, University of Maryland, Baltimore, U.S.A.

[°] Corresponding Author; Ayse Nur OKTAY E-mail: aysenur.oktay@sbu.edu.tr

INTRODUCTION

The spray drying method has attracted high attention in pharmaceutical drug development to overcome the solubility and dissolution challenges of oral dosage forms with low aqueous soluble drugs. Almost 40% of the top 200 or al-marketed drug products in the USA have low solubility. Moreover, 90% of new chemicals and 75% of compounds in the development pipeline of the pharmaceutical industry have low aqueous solubility (Arif Muhammed, Mohammed, Visht, & Omar Yassen, 2024; Siriwannakij, Heimbach, & Serajuddin, 2021). Amorphous solid dispersions (ASD) are solid dispersions in which the active ingredient is dispersed within an excipient matrix in a substantially amorphous form. The amorphous structure of the drug is essential for increasing its solubility and dissolution, because no energy is required to break the drug's crystal lattice. Spray drying is one method to prepare an ASD and is based on the transformation of a drug-carrier combination in a fluid state (e.g. solution, suspension, or emulsion) into dried powders, by atomizing the drug-carrier in heated air (Corrigan, 1985). Spray drying has advantages due to being energy intensive, continuous ,and commercially scalable drying process in single operation with no handling (Bhujbal et al., 2021; Mujumdar, 2006; Ogawa et al., 2018; Singh & Van den Mooter, 2016). In addition to solubility and dissolution enhancement, it provides uniform and controllable particle size. Spray drying is employed for more than half of all commercially available amorphous solid dispersion products (Jermain, Brough, & Williams III, 2018; Pandi, Bulusu, Kommineni, Khan, & Singh, 2020). Even though spray drying has advantages, the role of formulation and process parameters on the quality and reproducibility of the drug product is incompletely understood. Process parameters include inlet temperature, drying gas properties, spray gas flow, feed rate, and airflow rate. Additionally, formulation parameters include the composition of the feed such as solvent type, solid content, carrier type, and ratio. For example, the composition of the feed affects the surface tension and viscosity (Paudel, Worku, Meeus, Guns, & Van den Mooter, 2013). Polymer type and ratio are especially important due to an active substance is expected to have higher solubility in the polymeric carrier through the possibility of stronger favorable intermolecular interactions (Paudel, Van Humbeeck, & Van den Mooter, 2010). Even though the selection of the polymeric carrier is crucial to potentially developing a physicochemically stable and highly soluble formulation of a poorly soluble drug, there is a notable lack of comprehensive studies focusing on the impact of the polymer type on spraydried powders. In this study, the aim was to bridge this gap by investigating the impacts of polymers on the physicochemical properties, stability, solubility, and dissolution profiles of spray-dried powders (SDP). Ritonavir (RTV) was selected as a model drug, as it is an orally active anti-HIV protease inhibitor and antiretroviral medication to treat HIV/AIDS and especially COVID-19 infection. It is a poorly soluble drug, with its low solubility limiting oral absorption and oral bioavailability. To overcome this problem, the preparation of spray-dried powders of RTV was considered. Previously, with a focus on the systematic approach of polymer selection for ASD formulation via film casting, Kollidon VA64, SoluPlus and AquaSolve™ HPMCAS H-L combination (1:1 w/w) were selected as appropriate polymers for the spray dryer process of RTV (Oktay & Polli, 2024). Therefore, these polymers were used as carriers in spray-dried powders here, and the comparative evaluation of these polymers was performed in this study. SoluPlus' is an amphiphilic polymer due to possessing hydrophilic and lipophilic groups, and it can function as a solubility enhancer via the formation of colloidal micelles in solution (Alshahrani et al., 2015). SoluPlus is a graft copolymer of polyvinyl caprolactam-polyvinyl acetate (lipophilic) polyethylene glycol 6000 (hydrophilic) (Linn et al., 2012). Moreover, SoluPlus has low hygroscopicity which aids the stability of ASDs. Kollidon VA64 is also a copolymer composed of a chain structure of two monomers, namely N-vinylpyrrolidone and vinyl acetate (Bühler, 2008). Hypromellose acetate succinate (HPMCAS) is a cellulosic polymer, and grades of HPMCAS differ in chemical substitution of acetyl and succinoyl functional groups (Honick et al., 2019). HPMCAS has a high glass transition temperature which can prevent recrystallization and increase the stability by delayed kinetics of spraydried powders (Al-Obaidi & Buckton, 2009). Here, the impacts of these polymers on the SDP particle size, powder densities, flowabilities, moisture content %, yield %, drug content %, stability, RTV solubility, and RTV dissolution profiles from spray-dried powders were evaluated.

MATERIAL AND METHOD

Materials

Ritonavir (ChemShuttle; Blue Current Inc.; Hayward, California), polyvinylpyrrolidone-vinyl acetate (Kollidon VA64)(BASF SE; Ludwigshafen Germany), Polyvinyl caprolactam-polyvinyl acetate + polyethylene glycol graft copolymer (SoluPlus') (BASF SE; Ludwigshafen Germany), 1:1 ratio (w/w) combination of hypromellose acetate succinate (AquaSolve™ HPMCAS) H and L grades (Ashland Inc; Covington, KY) were used to prepare the spray dried powders. Solvents were in analytical grade and obtained from Fischer Scientific (Fischer Scientific; Hampton, NH) and Sigma Aldrich (Sigma-Aldrich; St. Louis, MO).

Formulation of powders by spray drying

Buchi B-290 (BUCHI Corporation; New Castle, Delaware) in closed-loop mode was used for the preparation of ritonavir (RTV) spray-dried powders (SDP). Solutions were prepared with 10% of solid content (RTV and polymer). Polymer types were determined as Kollidon VA64, SoluPlus, AquaSolve™ HPMCAS H-L (1:1 w/w ratio) (Oktay & Polli, 2024). Polymer: RTV at composition 80:20 w/w was prepared

by homogeneously dissolving in organic solvent (2:1 of dichloromethane: methanol). These solutions were pumped into the atomizer at a rate of 6 g/min, via a pump setting of 20%. The inlet temperatures were 70°C and 140°C. The atomizing N_2 gas settings were adjusted to 60 mm height at the maximum aspirator rate (100%). The produced SDPs were dried for an additional 12 hr at 40°C and stored in a desiccating cabinet (relative humidity < 5%).

Physicochemical powder characterization

Measurement of particle size

Particle size of SDPs was measured using a Master Sizer-2000 (Malvern Panalytical; Malvern, UK). Dispersive air pressure was set to 1 bar with a 50% vibrational feeding rate. The measurement time was set to 12 s, and refractive index was 1.33. The results were given the mean and standard error mean (mean±SEM) of three measurements.

Thermal analysis

Differential Scanning Calorimetry (DSC) measurements were conducted to evaluate the effect of the different polymers and two levels of the inlet temperature on the internal structure of the prepared RTV SDPs. Analysis was performed by enclosing 5-10 mg inside Tzero pans with Discovery DSC 2500 (TA Instruments; New Castle, DE) under the nitrogen flow (50 mL/min). The heat (to 200°C at 10°C/min)/ cool (to 30°C at 10°C/min)/reheat (to 200°C at 10°C/ min) method was applied. The glass transition temperatures (T_g) of polymers and SDPs were determined from the reheating cycle via TRIOS software (TA Instruments; New Castle, DE). A comparison of the T_g values of prepared SDPs with the value expected by the ideal mixing of two substances was carried out. Expected T_o values were calculated via Equation 1:

$$1/T_{g} = W_{1}/T_{g1} + W_{2}/T_{g2}$$
 Eq. 1

Where the W_1 and W_2 are the fractions of weight, and T_{g1} and T_{g2} are the T_g values of the RTV and the polymer, respectively. The T_g of amorphous RTV was given in the literature as 52.43°C (Wagner et al., 2012).

Measurements of spray-dried powder densities

Bulk and tapped densities of all RTV-SDPs were determined. The bulk density of powders was calculated by filling 1.5 g of powder into a measuring cylinder and measuring the volume of powder (V_B). The tapped density was determined by placing the measuring cylinder in a Stampf volumeter JEL STAV 2003 jolting volumeter (J. Engelsmann AG; Ludwigshafen, Germany) and by tapping 250, 500, 900, 1250 ,and 1500 times. The final volume (V_T) was recorded at certain tapped times and no further volume reduction was observed. The V_{1500} was the tapped volume (V_T) due to the difference between V_{500} and V_{1500} being less than 2 mL (United States Pharmacopeia).

Estimation of powder flowability

The compressibility index (CI) and Hausner ratio (HR) are used to predict the flowability of powders. CI and HR were calculated from Equation 2 and 3, respectively:

Compressibility Index=
$$100*((V_B-V_T)/V_B)$$
 Eq. 2
Hausner Ratio = V_B/V_T Eq. 3

Where V_B and V_T are the volume of powder prior to and after tapping. Flowability was evaluated according to the USP standard (Patel, Patel, & Shah, 2023; Pharmacopeia).

Analysis of moisture content

Loss on drying of 500 mg of SDP was measured using a Mettler-Toledo HB43 Moisture Analyzer (Mettler-Toledo; Columbus, OH). The measurements were replicated three times for each sample.

Calculation of production yield

The % production yield from spray drying was calculated from:

% yield =
$$(M/M_{\star})x100$$
 Eq. 4

where M_t is the total solid mass in the solution and M_s is the mass of obtained spray-dried powder (Pongsamart, Limwikrant, Ruktanonchai, Charoenthai, & Puttipipatkhachorn, 2022).

Short-term stability studies

After fabrication via spray drying, drug contents of the SDPs were measured on initial day, 1^{st} , 7^{th} , 14^{th} , 30^{th} days and three months of storage at $25^{\circ}\text{C} \pm 2^{\circ}\text{C}$ with $60\pm5\%$ relative humidity (RH) and $40\pm2^{\circ}\text{C}$ with $75\pm5\%$ RH. The SDPs were dissolved in methanol and then filtered using $0.22~\mu\text{m}$ membrane filter prior to HPLC analysis of drug. Percent drug content considered initial theoretical amount of RTV (i.e. 20% drug load).

Determination of saturation solubility of SDP powders of RTV with different polymers

Saturation solubility of the RTV SDPs (i.e. prepared with Kollidon VA64, SoluPlus, AquaSolve™ HPMCAS H-L) was evaluated in maleic acid buffer (50 mM) with 60 mM of polyoxyethylene 10 lauryl ether (M-PE). This media is the USP compendial dissolution media. Solubility studies were also performed with coarse RTV powder (i.e. crystalline drug powder), and a physical mixture of RTV (RTV-PM) with Kollidon VA64, SoluPlus, and AquaSolve™ HPMCAS H-L polymers (20:80% of RTV: polymer). Results were compared to RTV-SDP solubilities. An excessive amount of solid (containing an equal amount of RTV) was added to the M-PE. Samples were stirred at 500 rpm and 37°C for 24 h. Samples were filtered through a 0.22 µm membrane filter (VWR International GmbH; Darmstadt, Germany). Then, RTV in filtrate was quantified by HPLC analysis.

Dissolution of spray-dried powders

Dissolution testing was performed on the SDPs which are prepared with Kollidon VA64, SoluPlus, and AquaSolve HPMCAS H-L polymers, at inlet temperatures of 70°C and 140°C. USP II apparatus (SR8PLUS, Hanson Research; Chatsworth CA) and 900 mL of M-PE medium (50 mM maleic acid buffer including 60 mM polyoxyethylene 10 lauryl ether) were used. pH was 5.8. The temperature was 37°C, and the paddle rotation speed was 100 rpm. At predetermined time points (i.e. 0, 5, 10, 20, 30, 45, 60, 90,

120, 180, 240, and 360 min), 2 mL of the samples were taken and replaced with 2 mL of fresh M-PE medium. Samples were filtered through a 0.45 mm Millipore filter and quantified using HPLC.

High-performance liquid chromatography analysis (HPLC)

The concentration of RTV was determined using an HPLC method (Karakucuk, Celebi, & Teksin, 2016; Karakucuk, Teksin, Eroglu, & Celebi, 2019). Sample analysis was conducted with a Waters 2489 HPLC system (Waters Corporation; Milford, MA) equipped with a UV-vis detector. An isocratic mobile phase comprising 47% acetonitrile and 53% 0.05 M phosphoric acid was employed, with an injection volume of 25.0 µL and a flow rate of 1 mL/ min. Separation was achieved using a 4.6 × 150 mm Zorbax C18 column with a 5-µm particle size. The UV-vis detector was set to a wavelength of 240 nm. RTV exhibited a retention time of 9-10 minutes, and the total run time was 13 minutes. A calibration curve with RTV concentrations of 50, 25, 12.5, 6.25, 3.125, 1.56, 0.78, 0.39, 0.195, and $0.098~\mu g/m L$ was generated in triplicate for each analysis, yielding an r² value of 0.9999. For solubility studies, calibration curves were established for the M-PE medium. Standard solutions were prepared by diluting a stock solution of RTV in methanol (1 mg/mL) at a 1:9 ratio with the M-PE medium. These standard solutions were further diluted with the mobile phase to obtain final concentrations of 0.78, 1.56, 3.125, 6.25, 12.5, 25, and 50 μg/mL.

Statistical analysis

The collected data was analyzed using SPSS database Version 16 (Systat Software Inc.; San Jose, CA USA). Analysis of variance ANOVA test at the 95% confidence level, followed by Tukey's post hoc testing was used to compare multiple groups. To compare two groups, t-test was used. Results are given as mean \pm SEM (n = 3).

RESULTS AND DISCUSSION

RTV-SDPs with Kollidon*VA64, SoluPlus*, and AquaSolve™ HPMCAS H-L polymers at both 70°C and 140°C inlet temperatures were successfully prepared and characterized (i.e. stability, RTV solubility and RTV dissolution characterized).

Characterization of spray-dried powders

The powder properties were characterized, elucidating the effects of the polymer types and inlet temperatures on particle size (PS), internal structure (amorphous/crystalline), yield %, bulk density, tapped density, HR, CI, drug content %, and moisture %.

Evaluation of the polymer impacts on particle sizes

PS of SDPs is considered a critical quality bioavailability attribute. Smaller particles increase the dissolution rate (Schmitt, Baumann, & Morgen, 2022). However, the inherently small SDP size (about 5-15 μm) can cause low flowability (Yu, Nie, & Hoag, 2024). The mean PS (d_{50}) of the neat RTV powder was 36.3±10.1 μm. The d₅₀ of RTV physical mixtures with AquaSolve™ HPMCAS H-L, SoluPlus°, and Kollidon VA64 were 196.1±11.1 µm, 124.8±33.4 μm ,and 90.0±9.9 μm, respectively. Strojewski et al. indicated that the average particle size of SoluPlus' is much larger than Kollidon VA64 (Strojewski & Krupa, 2022). After spray drying, the SDP particle size was lower than the physical mixtures (PM). The d₅₀ values of the SDPs with Kollidon VA64 were 14.8±0.7 μm and 20.7±4.3 μm for 70°C and 140°C inlet temperatures, respectively. The d₅₀ values of the SDPs with SoluPlus were 16.1±0.05 µm and 20.7±4.3 μm for 70°C and 140°C, respectively. Similarly, Hofman et al. determined by microscopy that the particle size of SDP and PM with SoluPlus' were in the range of 2-35 μm and 10-100 μm, respectively, for 10% drug load (Hofmann, Harms, & Mäder, 2024). The d₅₀ values of SDPs with AquaSolve™ HPMCAS H-L polymers were 16.2±1.0 μm and 31.4±0.7 μm for 70°C and 140°C, respectively. While spray drying decreased PS significantly, higher inlet temperature

caused a larger PS (Moshe Honick et al., 2020). The PS of SDPs and PMs prepared with PVP-VA were lower than the SDPs prepared with other polymers. These results reflect the lower particle size of the PVP-VA polymer (d_{50} =53.4 µm) (Carina Hubert, 2019) than HPMCAS-L (d_{50} = 204 µm) and HPMCAS-H (d_{50} = 245.8 µm) (Moshe Honick et al., 2020). Osei-Yeboah et al. prepared celecoxib and PVP-VA amorphous solid powders which showed particle sizes in the range of 1.9 – 3.0 µm (d_{10}); 8.6 – 14.2 µm (d_{50}); 32.8 – 40.2 µm (d_{50}) (Osei-Yeboah & Sun, 2023).

Evaluation of polymer impacts on thermal analysis

Figure 1 shows the Differential Scanning Calorimetry profiles of RTV powder, polymers, and SDPs with 20% drug load. The amorphous nature of the SDPs was confirmed via DSC analyses. The effects of the polymers on the internal structure of the RTV SDPs were evaluated. The melting point of crystalline RTV powder was 128.21°C, and the glass transition temperature (T_a) value was 52.4 ± 1.2 °C. AquaSolve™ HP-MCAS H-L, Kollidon VA64 and SoluPlus polymers were in the amorphous state, and their T_{σ} values were 123.36 °C, 108.06 °C, and 66.25 °C, respectively. In the literature, the T_g of SoluPlus was 70°C, which is 30°C lower than that of Kollidon VA64 (101°C) (Strojewski & Krupa, 2022). All SDPs were completely in the amorphous state, without any apparent phase separation and RTV crystallization, which was evident from the single T_g value (Figure 1). The T_g value was 103.83 °C and 98.61 °C for RTV-AquaSolve™ HPMCAS H-L SDPs prepared using 70°C and 140°C, respectively. These values were 89.51°C and 86.20°C for RTV-Kollidon VA64 SDPs, and 64.94°C and 62.47°C for RTV-SoluPlus' SDPs. There was no significant difference $(\rho \le 0.05)$ in the T_g values of SDPs prepared from the two inlet temperatures. The estimated $T_{_{\rm g}}$ values,

which were 97.36, 89.14 ,and 65.42°C for AquaSolveTM HPMCAS H-L, Kollidon VA64 and SoluPlus were close to observed values. T_g values of SDPs were lower than the T_g value of neat polymers due to the drugin polymer lowered T_g values. This drug disposition increases the molecular mobility of the drug in the system, increasing solubility and dissolution of RTV (Siriwannakij et al., 2021).

T_g values are also important for SDP stability. It was reported that stable SDPs can be obtained if the T_g value of SDPs is more than 50°C higher than the storage temperature (Alshahrani et al., 2015; Hancock & Zografi, 1997; Li, Konecke, Wegiel, Taylor, & Edgar, 2013). Results can be interpreted that the SDPs with AquaSolve™ HPMCAS H-L and Kollidon*VA64 polymers can be stable at room temperature (25°C). Rank order SDP stability was: AquaSolve™ HPMCAS H-L > Kollidon*VA64 > SoluPlus*, in part due to AquaSolve™ HPMCAS H-L having a higher T_g value (Al-Obaidi & Buckton, 2009).

Evaluation of polymer impacts on powder densities and flowabilities

The compressibility index (CI) and the Hausner ratio (HR) are metrics concerning the flowability of bulk solids. The HR and CI were calculated by using the bulk and tapped densities to assess the effects of inlet temperature. Table 1 lists SDP density values, CI, and HR for the three polymers at 70°C and 140°C inlet temperatures. From HR and CI, the powders were classified as either 'fair' (CI and HR in the range of 16-20% and 1.19-1.25) or 'passable' (CI and HR in the range of 21-25% and 1.26-1.34) or 'poor' (CI and HR in the range of 26-31% and 1.35-1.45) or 'very poor' (CI and HR in the range of 32-37% and 1.46-1.59), according to USP (1174) (United States Pharmacopeia, 2012).

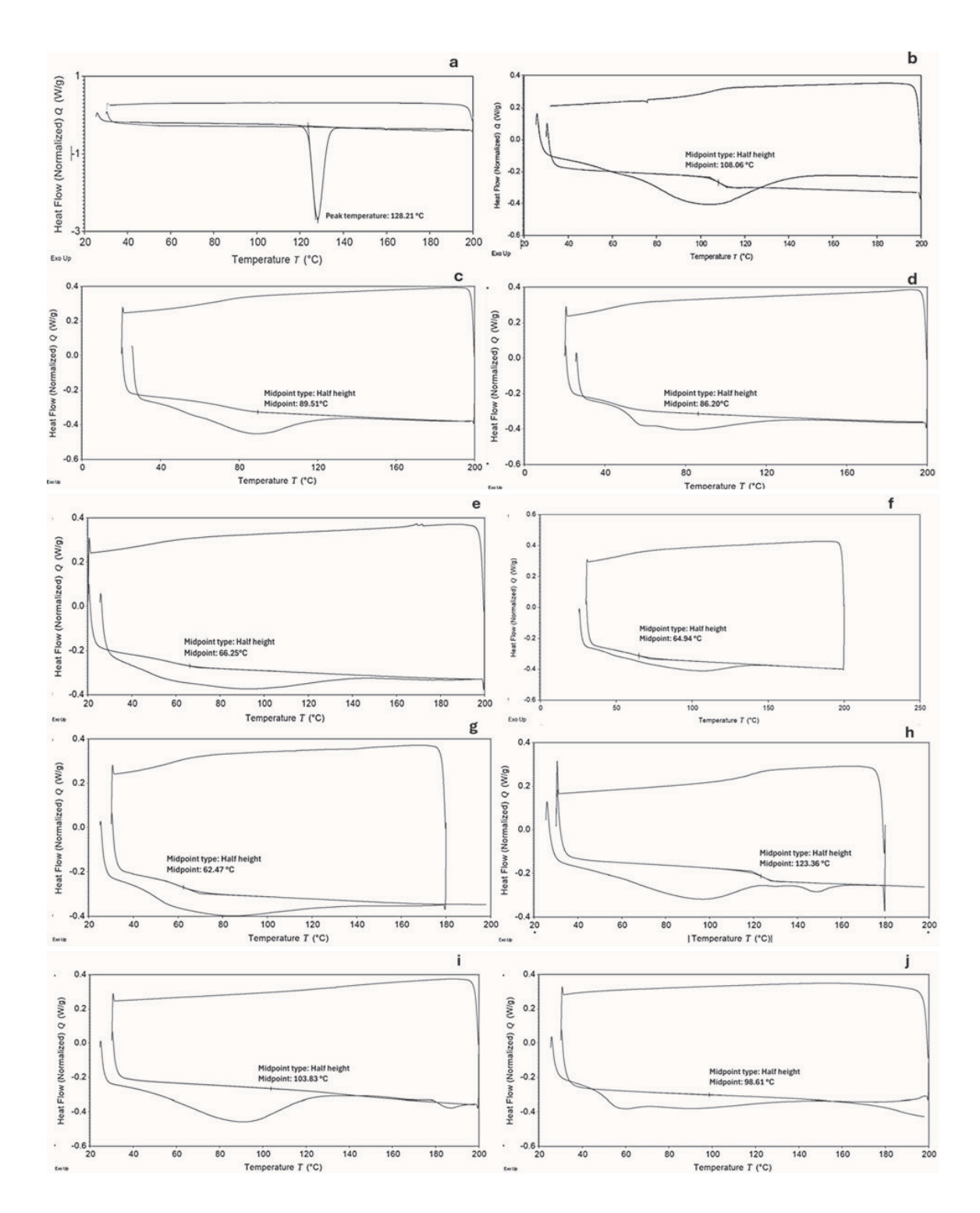


Figure 1. DSC profiles of RTV, neat polymers, and spray-dried powders of RTV and polymer. Panels are: coarse powder of RTV (a), neat Kollidon VA64 polymer (b), RTV-SDP with Kollidon VA64 polymer at 70°C (c) and 140°C (d), neat SoluPlus polymer (e), RTV-SDP with SoluPlus polymer at 70°C (f) and 140°C (g) neat AquaSolve HPMCAS H-L polymer (h), RTV-SDP with AquaSolve HPMCAS H-L polymer at 70°C (i) and 140°C (j). For all SDP, the drug load was 20% and the inlet temperature was either 70°C or 140°C.

For AquaSolve™ HPMCAS H-L polymer, the bulk density of the RTV-SDPs prepared at 140°C was 0.081±0.002 g/mL and was lower than the powder prepared at 70°C (0.252±0.005 g/mL). Similarly, the tapped density of the RTV-SDP prepared at 140°C (0.122±0.006 g/mL) was lower than the powder prepared at 70°C (0.344±0.036 g/mL). The HR were 1.364±0.116 and 1.496±0.057 for powders prepared at 70°C and 140°C, respectively. The compressibility index was 25.7±5.87% and 32.97±2.6 % for 70°C and 140°C, respectively. These values also showed that the powders with AquaSolve™ HPMCAS H-L have poor or very poor flowability.

For SoluPlus* polymer, the bulk density of the RTV-SDP prepared at 140°C (0.084±0.002 g/mL) was

lower than the powder prepared at 70°C (0.290±0.002 g/mL). Similarly, the tapped density of the RTV-SDP prepared at 140°C (0.113±0.004 g/mL) was lower than the powder prepared at 70°C (0.376±0.006 g/mL). The HR were 1.294±0.019 and 1.347±0.056 for powders prepared with 70°C and 140°C inlet temperatures, respectively. The compressibility index was 22.7±1.1 % and 25.5±3.2 % for 70°C and 140°C, respectively. So, RTV SDPs with SoluPlus* polymer showed passable and poor flowability for 70°C and 140°C, respectively. This poor flowability of SDPs with SoluPlus* and AquaSolve™ HPMCAS H-L polymers stems from the inherent characteristics of low bulk densities and the cohesive nature within spray-dried powders (Yu et al., 2024).

Table 1. The bulk, tapped, and true densities, HR, and compressibility index values of SDPs prepared with various polymers at two inlet temperatures (70°C and 140°C) (mean±SEM).

Polymer	Inlet temperature	Bulk density (gr/mL)	Tapped density (gr/mL)	Hausner Ratio	Compressibility Index (%)	Flowability
AquaSolve™ HPMCAS H-L	70 °C	0.252±0.005	0.344±0.036	1.364±0.116	25.7±5.8	Poor
AquaSolve™ HPMCAS H-L	140 °C	0.081±0.002	0.122±0.006	1.496±0.057	32.9±2.6	Very poor
Kollidon°VA64	70 °C	0.4531±0.014	0.551±0.032	1.219±0.081	17.2±5.2	Fair
Kollidon°VA64	140 °C	0.176±0.003	0.231±0.009	1.315±0.031	23.9±1.8	Passable
SoluPlus [®]	70 °C	0.290±0.002	0.376±0.006	1.294±0.019	22.7±1.1	Passable
SoluPlus [®]	140 °C	0.084±0.002	0.113±0.004	1.347±0.056	25.5±3.2	Poor

For Kollidon VA64 polymer, the flowability was better. The bulk density of the RTV-SDP prepared at 140°C (0.176±0.003 g/mL) was lower than the powder prepared at 70°C (0.4531±0.014 g/mL). Similarly, the tapped density of the RTV-SDP prepared at 140°C (0.113±0.004 g/mL) was lower than the powder prepared at 70°C (0.376±0.006 g/mL). The HR were 1.219±0.081 and 1.315±0.031 for 70°C and 140°C, respectively. The compressibility index was 17.2±5.2 % and 23.9±1.8 % for 70°C and 140°C, respectively. Even though there is no significant difference in the HR and CI values for different temperatures, 70°C inlet temperature was better than 140°C for better flowability and compressibility (Table 1). Moreover, the lowest HR and CI were observed on the RTV-SDP prepared with Kollidon VA64, indicating better

flowability than other polymers. Rank order was Kollidon VA64 > SoluPlus > AquaSolve HPMCAS

Evaluation of the polymer impacts on moisture content %

Moisture content (MC) is another factor impacting flowability, powder stability, and compressibility (Yu et al., 2024). MC, which is a measure of free water in the spray-dried powder, was determined (Table 2). For AquaSolve™ HPMCAS H-L polymer, the MC % of the powder prepared with high inlet temperature (1.217±0.067 %) was significantly lower than the low temperature (3.017±0.120 %), as expected. Similar results were observed for the Kollidon*VA64 and SoluPlus* polymers. The MC % of the SDPs with Kollidon*VA64 was 2.11±0.12 %

for high inlet temperature and 4.32±0.04 % for low inlet temperature. These values were 3.25±0.19 and 1.27±0.07% for SoluPlus polymer. Moreover, yield % and drug content % of the RTV-SDPs are listed in Table 2. The higher moisture content was observed on SDPs containing Kollidon VA64 than SoluPlus and AquaSolve™ HPMCAS polymers, which reflects polymer differences in their hygroscopicity. From the moisture content of SDPs, the rank order was: Kollidon°VA64 > SoluPlus° > AquaSolve™ HPMCAS. The relatively lower moisture content of the SoluPlus° and AquaSolve™ HPMCAS polymer was due to the low hygroscopic nature of the polymers, which promotes stability during storage. In particular, the low level of succinoyl substituent in HPMCAS-H induced a strong interaction with the hydrophobic reducing moisture uptake and inhibiting recrystallization (Alshahrani et al., 2015).

Evaluation of the polymer impacts yield and drug content %

Table 2 shows the influence of polymer and inlet temperature on powder yield and drug content %. While %yield of SDPs containing AquaSolve $^{\infty}$

HPMCAS, Kollidon VA64 and SoluPlus were 83.51±0.46 %, 80.42±0.51 % and 81.63±0.43 % for 70°C, these values were 86.15±0.93 %, 84.54±0.60 % and 85.73±0.89 % for 140°C. Higher inlet temperature also provided higher yield. Inlet temperature effect on yield correlated with the concentration of the solution and feed rate (LeClair, Cranston, Xing, & Thompson, 2016). The rank order was AquaSolve™ HPMCAS > SoluPlus' > Kollidon'VA64, independently from temperature. The effects of the polymers on yield% reflected the hygroscopicity and viscosity of the polymers. For all polymers, the % production yield exceeded 80%, showing sufficient drying at either inlet temperature. However, the drug content of powders containing AquaSolve™ HPMCAS polymer decreased from 95.3±0.5 % to 91.8±0.5 % when the inlet temperature increased from 70°C to 140°C. These values were 94.3±0.5 % and 91.0±0.3 % for Kollidon VA64, and 94.3±0.3 % and 91.8±0.2 % for SoluPlus'. Lower drug content reflected melted RTV at 140°C, resulting in sticking on the cyclone surface. For this reason, lower inlet temperature was concluded to be the preferred option to prepare the SDPs having high drug content (Table 2).

Table 2. The moisture content %, yield %, and drug content % of the spray-dried powders. Spray-dried powders were fabricated at either 70°C or 140°C inlet temperature.

Polymer	Temperature (°C)	Moisture (%)	Yield (%)	Drug content (%)
AquaSolve™ HPMCAS H- L	70	3.02±0.12	83.5±0.5	95.3±0.5
AquaSolve™ HPMCAS H-L	140	1.22±0.07	86.2±0.9	91.8±0.5
Kollidon VA64	70	4.32±0.04	80.4±0.5	94.3±0.5
Kollidon VA64	140	2.11±0.12	84.5±0.6	91.0±0.3
SoluPlus [*]	70	3.25±0.19	81.6±0.4	94.3±0.3
SoluPlus [*]	140	1.27±0.07	85.7±0.9	91.8±0.2

Evaluation of the polymer impacts on shortterm chemical stability

Drug content of SDPs over three months was investigated via short-term chemical stability. RTV content (%) of powders prepared using 70°C was 95.0±0.5, 94.1±0.5 and 93.8±0.1 % respectively for AquaSolve™ HPMCAS H-L, Kollidon VA64, and

SoluPlus after the storage at room temperature for three months. For 140°C inlet temperature, these values were 91.7±0.2, 90.8±0.1 and 91.8±0.1%, respectively (Table 3). While higher inlet temperature had lower drug content, there was no significant difference in drug content % between the initial and after 3 months.

Table 3. The drug content of the SDPs prepared with various polymers and two levels of inlet temperatures after storage at *room temperature* for three months.

	Drug content (%) after storage at room temperature						
Polymer	Inlet temperature (°C)	Initial	1 st day	7 th day	14 th day	1 st month	3 rd month
AquaSolve™ HPMCAS H-L	70°C	95.3±0.5	95.3±0.5	95.2±0.5	95.1±0.5	95.1±0.5	95.0±0.5
AquaSolve™ HPMCAS H-L	140 °C	91.8±0.5	91.8±0.5	91.8±0.5	91.7±0.5	91.7±0.1	91.7±0.2
Kollidon®VA64	70°C	94.3±0.5	94.2±0.5	94.2±0.5	94.2±0.5	94.2±0.5	94.1±0.5
Kollidon®VA64	140 °C	91.0±0.3	91.0±0.3	91.0±0.3	91.0±0.2	90.9±0.3	90.8±0.1
SoluPlus®	70 °C	94.3±0.3	94.3±0.4	94.3±0.4	94.2±0.3	93.9±0.2	93.8±0.1
SoluPlus®	140 °C	91.8±0.2	91.8±0.3	91.8±0.1	91.9±0.1	91.8±0.1	91.8±0.1

The drug content of the powders prepared with 70°C were 94.8±0.5, 93.9±0.5 and 93.7±0.2 respectively, for AquaSolve™ HPMCAS H-L, Kollidon*VA64 and SoluPlus* after the storage at 40°C

for 3 months. These values were 91.5 ± 0.1 , 90.7 ± 0.02 and 91.6 ± 0.1 respectively for 140° C (Table 4). RTV was chemically stable for three months.

Table 4. Drug contents of the SDPs prepared with various polymers and two levels of inlet temperatures after storage at 40°C for three months.

Drug content (%) after storage at 40°C							
Polymer	Inlet temperature (°C)	Initial	1 st day	7 th day	14 th day	1 st month	3 rd month
AquaSolve™ HPMCAS H-L	70°C	95.3±0.5	95.2±0.5	95.2±0.5	95.1±0.5	94.9±0.5	94.8±0.5
AquaSolve™ HPMCAS H-L	140 °C	91.8±0.5	91.8±0.5	91.8±0.5	91.7±0.4	91.6±0.4	91.5±0.1
Kollidon®VA64	70°C	94.3±0.5	94.2±0.5	94.2±0.5	94.1±0.5	94.0±0.5	93.9±0.5
Kollidon®VA64	140 °C	91.0±0.3	91.0±0.3	91.0±0.3	90.9±0.2	90.8±0.2	90.7±0.1
SoluPlus®	70 °C	94.3±0.3	94.3±0.3	94.2±0.3	94.2±0.3	93.8±0.2	93.7±0.2
SoluPlus®	140 °C	91.8±0.2	91.8±0.2	91.9±0.1	91.7±0.1	91.7±0.1	91.6±0.1

Similar to the results here, Liu et al. indicated that the aprepitant ASD with SoluPlus was stable for 3 months at 40°C and 60% RH by confirming that there was no recrystallization of the amorphous aprepitant (Liu et al., 2015). The high stability of carbamazepine amorphous solid dispersion was also provided via HPMCAS-H polymer. This stability reflects the low level of succinoyl groups of polymer increased the hydrophobic interaction with the drug and decreased the recrystallization (Ueda, Higashi, Yamamoto, & Moribe, 2013). Moreover, the high T_g of HPMCAS-H and its hydrophobic nature inhibited the molecular

mobility of the drug within the solid dispersion, preventing crystallization growth (Alshahrani et al., 2015). Kollidon VA64 polymer was also confirmed as stable for ASDs, in part due to the polymer having a high $T_{\rm g}$ value. In the literature, copovidone was found to effectively protect amorphous indomethacin from recrystallization during storage in a stability chamber for 3 months at various temperatures, from 5 to 50°C (Sarode, Sandhu, Shah, Malick, & Zia, 2013). Findings here demonstrated that all three polymers were suitable and promising to provide stable RTV spray dried powders at 25°C and 40°C for 3 months.

Evaluation of the polymer impacts on saturation solubility

The effect of polymer type on RTV solubility was evaluated in the M-PE medium. Solubility studies were performed with coarse RTV powder and with SDPs from the three polymers at two inlet temperatures. Results are given in Table 5. While the saturation solubility of RTV in M-PE medium was 201.8 μ g/mL, the solubility of SDPs with AquaSolve HPMCAS H-L were 2521.2 and 2982.3 μ g/mL for

140°C and 70°C, respectively. The solubility of SDPs with SoluPlus were 1879.3 and 2163.8 μ g/mL for 140°C and 70°C, respectively. The solubility of SDPs with Kollidon VA64 were 1645.0 and 2093.9 μ g/mL for 140°C and 70°C, respectively. While there was no significant impact of inlet temperature on solubility from SDPs, a significant improvement (10-15 fold increase) was observed with spray-dried powders compared to the RTV coarse powder. A 1.2-1.4 fold increase was observed with the physical mixture.

Table 5. Solubility of the coarse powder of RTV, physical mixtures (PMs), and spray-dried powders (SDPs)

Sample	Solubility in M-PE
	(μg/mL, mean ±SEM)
RTV coarse powder	201.8±2.4
RTV- AquaSolve™ HPMCAS H-L PM	258.4+4.2
RTV- AquaSolve™ HPMCAS H-L SDP – 70°C	2982.3±11.8
RTV- AquaSolve™ HPMCAS H-L SDP – 140°C	2521.2±70.1
RTV-SoluPlus® PM	273.7+20.1
RTV- SoluPlus® SDP – 70°C	2163.8±106.7
RTV- SoluPlus® SDP – 140°C	1879.3±20.0
RTV- Kollidon®VA64 PM	229.3+19.0
RTV- Kollidon®VA64 SDP – 70°C	2093.9 ±17.9
RTV- Kollidon®VA64 SDP – 140°C	1645.0±113.5

The highest solubility increase was with HPMCAS polymer. Rank order was: AquaSolve™ HPMCAS H-L > SoluPlus' > Kollidon'VA64. This result may reflect the lower hygroscopic nature of AquaSolve™ HPMCAS and SoluPlus polymers than Kollidon VA64, which was confirmed by moisture content analysis and inhibited recrystallization to maintain supersaturation (Alshahrani et al., 2015). Kollidon VA64 is a copolymer composed of a chain structure of N-vinylpyrrolidone and vinyl acetate (Bühler, 2008). In contrast to Kollidon VA64, SoluPlus is a graft copolymer consisting of PEG 6000, polyvinyl caprolactam, and polyvinyl acetate, and is an amphiphilic polymer and serves as a surfactant (70-100 nm diameter micelles) to increase drug solubility (Oktay & Polli, 2024; Strojewski & Krupa, 2022). Even though copovidone does not have an amphiphilic structure, its ability to increase the solubility of hydrophobic drugs was confirmed by several studies (Strojewski & Krupa, 2022). Moreover, Alshahrani et al. indicated that the intensity of the hydrogen bond

in the FTIR spectrum of carbamazepine is increased by adding HPMCAS-HF, which is a sign of the hydrogen bond formation with the hydroxyl group of HPMCAS-HF. The hydrogen bond formation worked synergistically with Soluplus to enhance the solubility and stability of the formulations (Alshahrani et al., 2015; Rumondor, Stanford, & Taylor, 2009).

Evaluation of the polymer impacts on the dissolution of spray-dried powders

The dissolution profiles of the SDPs were determined in the M-PE medium and plotted in Figure 2. Graphs 'a' and 'b' refer to dissolution profiles of SDPs prepared with low and high inlet temperatures, respectively. The rank order was SoluPlus' > Kollidon VA64 > AquaSolve™ HPMCAS H-L for both inlet temperatures. At the end of the 360 min, SDP powder prepared using Kollidon VA64 polymer releases 89.2% and 88.0% for 70°C and 140°C, respectively. For SoluPlus', they were 99.3% and 93.5%. For AquaSolve™ HPMCAS H-L, they were 84.0% and 80.5% respectively.

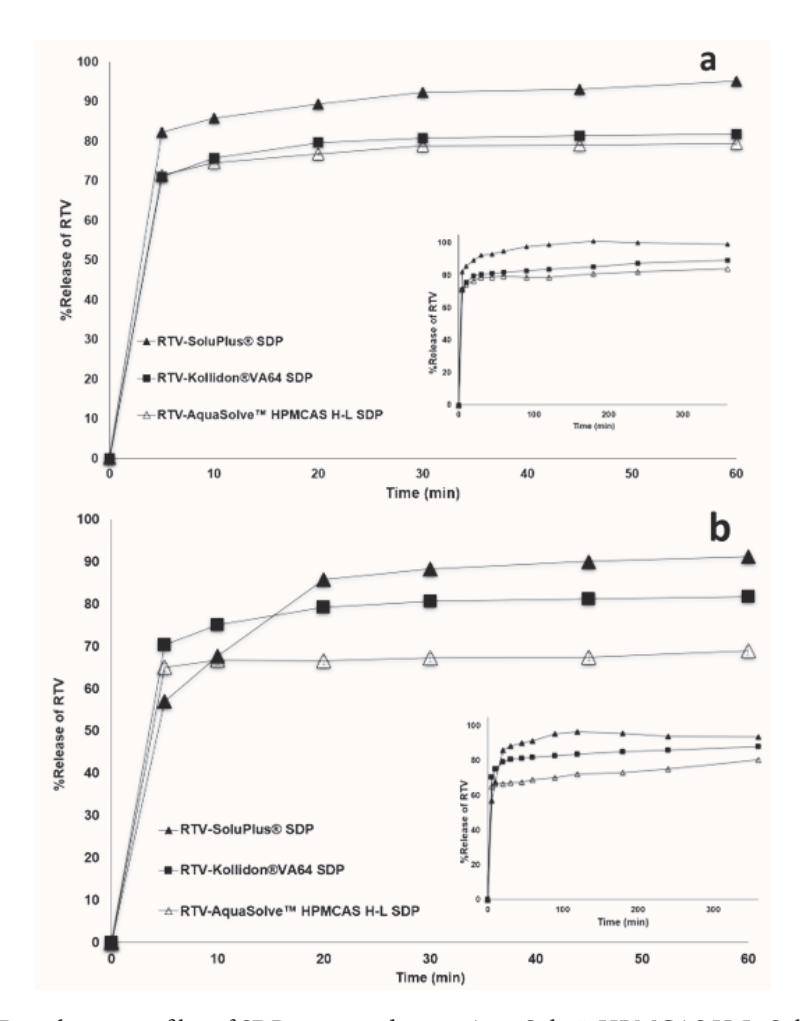


Figure 2. Dissolution profiles of SDPs prepared using AquaSolve™ HPMCAS H-L, SoluPlus˚ and Kollidon˚VA64 polymers. Panels are: a) SDPs prepared with 70°C inlet temperature, and b) SDPs prepared with 140°C inlet temperature.

After the first 10 min, drug release was 75.7%, 85.8% and 74.6% for Kollidon VA64, SoluPlus and AquaSolve™ HPMCAS H-L with 70°C. They were 75.1%, 67.7%, and 66.8% for 140°C. The dissolution profiles of the SDPs from 70°C were higher than from 140°C, reflecting that 140°C is higher than the melting point of ritonavir, yielding a sticky, melted drug caused delayed dissolution profile. While there was no significant difference on dissolution profiles of SDPs containing Kollidon VA64 and AquaSolve™ HPMCAS H-L for 70 °C, Kollidon VA64 showed better profile than AquaSolve™ HPMCAS H-L for 140°C inlet temperature. Similar results were observed on the indomethacin ASD tablets prepared with HPMCAS and PVP polymers (Yu et al., 2024). AUC values of 366

the dissolution profiles are given in Table 6. AUC values have been used to characterize the rate and extent of dissolution (Maghsoodi & Shahi, 2019; Ruiz & Volonté, 2014). The highest dissolution profile and AUC values were observed on the SDPs containing SoluPlus*. It can be related to the amphiphilic nature of SoluPlus*, which stabilizes the amorphous form and maintains the supersaturation leading to higher dissolution of RTV. Moreover, SoluPlus* acts as a surfactant which helps the micelle formation and increases the wettability and dispersibility of RTV in the medium (Strojewski & Krupa, 2022). Smaller particle sizes of the micelles (70-100 nm) provide a larger surface area and so it increases the dissolution rate of RTV.

	`	,		
Powder	Inlet	AUC _{0-20 min}	AUC _{0-60 min}	AUC _{0-120 min}
	temperature (°C)	$(\mu g.min/mL)$	$(\mu g.min/mL)$	$(\mu g.min/mL)$
RTV- SoluPlus SDP	70	1672±329	4003±789	8040±1629
RTV- SoluPlus SDP	140	1531±291	3878±758	7988±1550
RTV- Kollidon VA64 SDP	70	1469±298	3436±696	7028±1394
RTV- Kollidon VA64 SDP	140	1465±298	3432±696	7009±1390
RTV- AquaSolve™ HPMCAS H-L SDP	70	1427±281	3303±677	6647±1351
RTV- AquaSolve™ HPMCAS H-L SDP	140	1236±243	2886±574	6022±1187

Table 6. AUC values of dissolution profiles (mean±SEM, n=3).

CONCLUSION

Characterization studies, along with the ability to successfully form spray-dried powders of RTV with various polymers using spray-drying method, showed that all three polymers were suitable for spray-dried amorphous powders with lower moisture content, better flowability, lower particle size, and high %yield. SDP was also stable and highly soluble. The saturation solubility of the coarse RTV was significantly increased through the ASD powders with various polymers compared to the physical mixtures. Dissolution studies showed that the rank order was SoluPlus[®] SDP > Kollidon[®]VA64 SDP > AquaSolve[™] HPMCAS H-L SDP for both inlet temperatures. Short-term chemical stability studies supported that the RTV-ASD powders were stable for all polymers for three months. Results indicate the high potential of these polymers for the development of stable spraydried amorphous powders with hydrophobic drugs such as RTV.

ACKNOWLEDGEMENTS

This research was supported by the Scientific and Technological Research Council of Turkey (BIDEB 2219 (Project code: 1059B192000617)).

AUTHOR CONTRIBUTION STATEMENT

Writing – review & editing, Writing – original draft, Methodology, Investigation, Funding acquisition, Conceptualization (A.N.O). Writing – review & editing, Resources, Conceptualization (J.E.P).

CONFLICT OF INTEREST

The authors declare that there is no conflict of interest.

REFERENCES

Al-Obaidi, H., & Buckton, G. (2009). Evaluation of griseofulvin binary and ternary solid dispersions with HPMCAS. AAPS PharmSciTech, 10, 1172-1177.

Alshahrani, S. M., Lu, W., Park, J.-B., Morott, J. T., Alsulays, B. B., Majumdar, S., . . . Repka, M. A. (2015). Stability-enhanced hot-melt extruded amorphous solid dispersions via combinations of Soluplus* and HPMCAS-HF. *AAPS PharmSciTech*, *16*, 824-834.

Arif Muhammed, R., Mohammed, S., Visht, S., & Omar Yassen, A. (2024). A review on development of colon targeted drug delivery system. *International Journal of Applied Pharmaceutics*, 16(2), 12-27.

Bhujbal, S. V., Mitra, B., Jain, U., Gong, Y., Agrawal, A., Karki, S., . . . Zhou, Q. T. (2021). Pharmaceutical amorphous solid dispersion: A review of manufacturing strategies. *Acta Pharmaceutica Sinica B*, 11(8), 2505-2536.

Bühler, V. (2008). *Kollidon: Polyvinylpyrrolidone* excipients for the pharmaceutical industry: BASF-The Chemical Company.

Carina Hubert, T. C., Verena Geiselhart, Nils Rottmann (2019). Influence of the particle size of copovidone and crospovidone on tablet characteristics. https://www.pharmaexcipients.com/wp-content/uploads/2019/08/Influence-of-the-particle-size-of-copovidone-and-crospovidone-on-tablet-characteristics.pdf, (accessed 25 November 2024)

- Corrigan, O. I. (1985). Mechanisms of dissolution of fast release solid dispersions. *Drug Development and Industrial Pharmacy*, 11(2-3), 697-724.
- Hancock, B. C., & Zografi, G. (1997). Characteristics and significance of the amorphous state in pharmaceutical systems. *Journal of Pharmaceutical Sciences*, 86(1), 1-12.
- Hofmann, N., Harms, M., & Mäder, K. (2024). ASDs of PROTACs: Spray-dried solid dispersions as enabling formulations. *International Journal of Pharmaceutics*, 650, 123725.
- Honick, M., Das, S., Hoag, S. W., Muller, F. X., Alayoubi, A., Feng, X., . . . Polli, J. E. (2020). The effects of spray drying, HPMCAS grade, and compression speed on the compaction properties of itraconazole-HPMCAS spray dried dispersions. *European Journal of Pharmaceutical Sciences*, 155, 105556.
- Honick, M., Sarpal, K., Alayoubi, A., Zidan, A., Hoag, S. W., Hollenbeck, R. G., . . . Polli, J. E. (2019). Utility of Films to Anticipate Effect of Drug Load and Polymer on Dissolution Performance from Tablets of Amorphous Itraconazole Spray-Dried Dispersions. *AAPS PharmSciTech*, 20(8), 331. doi:10.1208/s12249-019-1541-6
- Jermain, S. V., Brough, C., & Williams III, R. O. (2018). Amorphous solid dispersions and nanocrystal technologies for poorly water-soluble drug delivery–an update. *International Journal of Pharmaceutics*, 535(1-2), 379-392.
- Karakucuk, A., Celebi, N., & Teksin, Z. S. (2016).
 Preparation of ritonavir nanosuspensions by microfluidization using polymeric stabilizers: I. A Design of Experiment approach. *European Journal of Pharmaceutical Sciences*, 95, 111-121.
- Karakucuk, A., Teksin, Z. S., Eroglu, H., & Celebi, N. (2019). Evaluation of improved oral bioavailability of ritonavir nanosuspension. *European Journal of Pharmaceutical Sciences*, 131, 153-158.

- LeClair, D. A., Cranston, E. D., Xing, Z., & Thompson, M. R. (2016). Optimization of spray drying conditions for yield, particle size and biological activity of thermally stable viral vectors. *Pharmaceutical Research*, *33*, 2763-2776.
- Li, B., Konecke, S., Wegiel, L. A., Taylor, L. S., & Edgar, K. J. (2013). Both solubility and chemical stability of curcumin are enhanced by solid dispersion in cellulose derivative matrices. *Carbohydrate Polymers*, 98(1), 1108-1116.
- Linn, M., Collnot, E.-M., Djuric, D., Hempel, K., Fabian, E., Kolter, K., & Lehr, C.-M. (2012). Soluplus[®] as an effective absorption enhancer of poorly soluble drugs in vitro and in vivo. *European Journal of Pharmaceutical Sciences*, 45(3), 336-343.
- Liu, J., Zou, M., Piao, H., Liu, Y., Tang, B., Gao, Y., . . . Cheng, G. (2015). Characterization and pharmacokinetic study of aprepitant solid dispersions with soluplus. *Molecules*, 20(6), 11345-11356.
- Maghsoodi, M., & Shahi, F. (2019). Combined Use of Polymers and Porous Materials to Enhance Cinnarizine Dissolution. *Pharmaceutical Sciences*, 25(4), 331-337.
- Mujumdar, A. S. (2006). *Handbook of Industrial Drying*: CRC press.
- Ogawa, N., Hiramatsu, T., Suzuki, R., Okamoto, R., Shibagaki, K., Fujita, K., . . . Yamamoto, H. (2018). Improvement in the water solubility of drugs with a solid dispersion system by spray drying and hot-melt extrusion with using the amphiphilic polyvinyl caprolactam-polyvinyl acetate-polyethylene glycol graft copolymer and d-mannitol. *European Journal of Pharmaceutical Sciences*, 111, 205-214.
- Oktay, A. N., & Polli, J. E. (2024). Screening of Polymers for Oral Ritonavir Amorphous Solid Dispersions by Film Casting. *Pharmaceutics*, *16*(11), 1373.

- Osei-Yeboah, F., & Sun, C. C. (2023). Effect of drug loading and relative humidity on the mechanical properties and tableting performance of Celecoxib–PVP/VA 64 amorphous solid dispersions. *International Journal of Pharmaceutics*, 644, 123337.
- Pandi, P., Bulusu, R., Kommineni, N., Khan, W., & Singh, M. (2020). Amorphous solid dispersions: An update for preparation, characterization, mechanism on bioavailability, stability, regulatory considerations and marketed products. *International Journal of Pharmaceutics*, 586, 119560.
- Patel, K., Patel, J., & Shah, S. (2023). Development of Delayed Release Oral Formulation Comprising Esomeprazole Spray Dried Dispersion Utilizing Design of Experiment As An Optimization Strategy. AAPS PharmSciTech, 24(7), 186.
- Paudel, A., Van Humbeeck, J., & Van den Mooter, G. (2010). Theoretical and experimental investigation on the solid solubility and miscibility of naproxen in poly (vinylpyrrolidone). *Molecular Pharmaceutics*, 7(4), 1133-1148.
- Paudel, A., Worku, Z. A., Meeus, J., Guns, S., & Van den Mooter, G. (2013). Manufacturing of solid dispersions of poorly water soluble drugs by spray drying: formulation and process considerations. *International Journal of Pharmaceutics*, 453(1), 253-284.
- Pharmacopeia, U. S. <1174>PowderFlow. https://www.usp.org/sites/default/files/ usp/document/harmonization/genchapter/20230428HSm99885.pdf, (accessed 25 November 2024)
- Pongsamart, K., Limwikrant, W., Ruktanonchai, U. R., Charoenthai, N., & Puttipipatkhachorn, S. (2022). Preparation, characterization and antimalarial activity of dihydroartemisinin/β-cyclodextrin spray-dried powder. *Journal of Drug Delivery Science and Technology*, 103434.

- Ruiz, M. E., & Volonté, M. G. (2014). Biopharmaceutical relevance of the comparison of dissolution profiles: proposal of a combined approach.
- Rumondor, A. C., Stanford, L. A., & Taylor, L. S. (2009). Effects of polymer type and storage relative humidity on the kinetics of felodipine crystallization from amorphous solid dispersions. *Pharmaceutical Research*, 26, 2599-2606.
- Sarode, A. L., Sandhu, H., Shah, N., Malick, W., & Zia, H. (2013). Hot melt extrusion for amorphous solid dispersions: temperature and moisture activated drug-polymer interactions for enhanced stability. *Molecular Pharmaceutics*, 10(10), 3665-3675.
- Schmitt, J. M., Baumann, J. M., & Morgen, M. M. (2022). Predicting spray dried dispersion particle size via machine learning regression methods. *Pharmaceutical Research*, *39*(12), 3223-3239.
- Singh, A., & Van den Mooter, G. (2016). Spray drying formulation of amorphous solid dispersions. Advanced Drug Delivery Reviews, 100, 27-50.
- Siriwannakij, N., Heimbach, T., & Serajuddin, A. T. (2021). Aqueous dissolution and dispersion behavior of polyvinylpyrrolidone vinyl acetate-based amorphous solid dispersion of ritonavir prepared by hot-melt extrusion with and without added surfactants. *Journal of Pharmaceutical Sciences*, 110(4), 1480-1494.
- Strojewski, D., & Krupa, A. (2022). Kollidon® VA 64 and Soluplus® as modern polymeric carriers for amorphous solid dispersions. *Polymers in Medicine*, 52(1), 19-29.
- Ueda, K., Higashi, K., Yamamoto, K., & Moribe, K. (2013). Inhibitory effect of hydroxypropyl methylcellulose acetate succinate on drug recrystallization from a supersaturated solution assessed using nuclear magnetic resonance measurements. *Molecular Pharmaceutics*, 10(10), 3801-3811.

- United States Pharmacopeia. <616>Bulk Density of Powder., https://www.usp.org/sites/default/files/usp/document/our-work/reference-standards/20240927HSm99375.pdf (accessed 25 November 2024)
- United States Pharmacopeia. (2012). <1174>Powder Flow. The United States Pharmacopeia 35. https://www.drugfuture.com/pharmacopoeia/usp35/PDF/0801-0804%20%5B1174%5D%20 POWDER%20FLOW.pdf, (accessed 01 March 2025).
- Wagner, C., Jantratid, E., Kesisoglou, F., Vertzoni, M., Reppas, C., & Dressman, J. B. (2012). Predicting the oral absorption of a poorly soluble, poorly permeable weak base using biorelevant dissolution and transfer model tests coupled with a physiologically based pharmacokinetic model. European Journal of Pharmaceutics and Biopharmaceutics, 82(1), 127-138.
- Yu, D., Nie, H., & Hoag, S. W. (2024). Comprehensive evaluation of polymer types and ratios in Spray-Dried Dispersions: Compaction, Dissolution, and physical stability. *International Journal of Pharmaceutics*, 650, 123674.

Quantitative Estimation of Dexketoprofen and Paracetamol in Effervescent Tablets by Chemometrics-Assisted Spectrophotometry

Zehra Ceren ERTEKİN**, Erdal DİNÇ**

Quantitative Estimation of Dexketoprofen and Paracetamol in Effervescent Tablets by Chemometrics-Assisted Spectrophotometry Kemometri Destekli Spektrofotometri ile Efervesan Tabletlerdeki Deksketoprofen ve Parasetamolün Kantitatif Tayini

SUMMARY

Dexketoprofen (DEX) and paracetamol (PAR), a common drug pair in multimodal analgesia, exhibit overlapping absorbance spectra, making conventional UV-Vis spectroscopy unsuitable for their simultaneous quantification. The objective of this work was to develop and validate chemometrics-assisted spectrophotometric methods for the simultaneous quantification of these drugs in effervescent tablet formulations, despite their overlapping spectra. UV-Vis spectrophotometry was combined with Principal Component Regression (PCR) and Partial Least Squares (PLS) regression to develop predictive models. A calibration set of 25 binary mixtures, with concentration ranges of 3–18 µg/mL for DEX and 5-25 µg/mL for PAR, was used to develop the chemometric models. The models were built using the concentration data set and the spectral data between 220 and 320 nm ($\Delta\lambda$ =0.1 nm). The accuracy and precision of the proposed chemometric methods were assessed by analyzing a set of independent test samples as well as intra-day and inter-day samples. The PCR and PLS models provided accurate and precise quantification, with mean recovery values and relative standard deviations within acceptable limits. Commercial effervescent tablet samples were analyzed to evaluate the applicability, and assay results showed good agreement with label claims. The proposed PCR and PLS methods offer reliable and cost-effective alternatives to HPLC for the simultaneous analysis of DEX and PAR in pharmaceutical formulations. These methods are suitable for routine quality control, reducing analysis time and solvent consumption.

Key Words: Dexketoprofen, paracetamol, PCR, PLS, UV-Vis spectroscopy

ÖZ

Deksketoprofen (DEX) ve parasetamol (PAR), multimodal analjezide yaygın olarak kullanılan iki ilaçtır. Ancak, UV bölgesinde örtüşen spektrumları nedeniyle geleneksel UV-GB spektroskopisi ile bu bileşiklerin eş zamanlı kantitatif tayini mümkün değildir. Bu çalışmanın amacı, spektral örtüşmeye rağmen DEX ve PAR etken maddelerinin aynı anda analizini sağlayan kemometri destekli spektrofotometrik yöntemler geliştirmek, valide etmek ve bu yöntemleri efervesan tablet formülasyonlarının analizine uygulamaktır. Bu doğrultuda, birincil bileşen regresyonu (PCR) ve kısmi en küçük kareler (PLS) regresyonu modellerinin UV-GB spektroskopisi ile beraber kullanılımlı iki farklı miktar tayini yöntemi geliştirilmiştir. Modellerin oluşturulması için 3-18 μg/mL DEX ve 5-25 μg/mL PAR konsantrasyon aralığında hazırlanan 25 adet ikili karışımdan oluşan bir kalibrasyon seti hazırlanmıştır. Bu setin 220–320 nm ($\Delta\lambda$ = 0.1 nm) arasındaki spektral verileri ve konsantrasyon değerleri arasındaki ilişki PCR ve PLS yöntemleri ile modellenmiştir. Önerilen kemometrik yöntemlerin doğruluğu ve kesinliği, bağımsız test örnekleri ile birlikte gün içi ve günler arası analizlerle değerlendirilmiştir. PCR ve PLS modelleri, kabul edilebilir sınırlar içinde geri kazanım yüzdeleri ve bağıl standart sapma değerleriyle doğru ve hassas sonuçlar vermiştir. Geliştirilen ve valide edilen bu yöntemler, ticari efervesan tablet örneklerinin analizine uygulanmış ve elde edilen sonuçlar, etiket değerleriyle büyük ölçüde uyumlu bulunmuştur. Geliştirilen PCR ve PLS yöntemlerinin, HPLC'ye maliyet açısından avantajlı, güvenilir bir alternatif sunarak rutin kalite kontrol analizleri için uygun olduğu belirlenmiştir. Bu yöntemler, rutin kalite kontrol için uygun olup, analiz süresini ve solvent tüketimini azaltır.

Anahtar Kelimeler: Deksketoprofen, parasetamol, PCR, PLS, UV-GB spektroskopisi

Received: 25.03.2025 Revised: 5.06.2025 Accepted: 7.07.2025

ORCID: 0000-0002-1549-6024, Department of Analytical Chemistry, Faculty of Pharmacy, Ankara University, Ankara, Türkiye.

[&]quot;ORCID: 0000-0001-6326-1441, Department of Analytical Chemistry, Faculty of Pharmacy, Ankara University, Ankara, Türkiye.

INTRODUCTION

Multimodal analgesia, the simultaneous use of multiple analgesic drugs with different mechanisms of action, is a pharmacologic approach designed to provide superior pain control with reduced side effects (O'Neill & Lirk, 2022; Yerebakan et al., 2024). Dexketoprofen (DEX), the active enantiomer of ketoprofen, is a non-steroidal anti-inflammatory drug prescribed for short-term treatment of moderate pain, particularly musculoskeletal pain, dental pain, and dysmenorrhea (Kuczyńska et al., 2022). Paracetamol (PAR) is one of the most popular and widely used drugs in pain management. It has a central analgesic effect and is primarily used for treating headaches, minor aches, and moderate pain (Ayoub, 2021). As these drugs reduce pain through different mechanisms, they are a common pair in multimodal pain strategies. Combining DEX and PAR leads to more effective analgesia while lowering the required doses of each drug and reducing side effects. This has led to the development of pharmaceutical formulations containing DEX and PAR for acute pain management, including musculoskeletal and post-operative pain, and for arthritis (López Navarro et al., 2019). Additionally, this combination has been used for the treatment of post-COVID-19 symptoms, including myalgia and headache (Medhat et al., 2024).

Developing new and effective analytical methods is crucial to ensure the quality, efficacy, and safety of drugs and pharmaceutical dosage forms. UV-Vis spectrophotometry offers several advantages as an analytical technique, including simplicity, accessibility, minimal sample preparation, and rapid analysis. The simplicity and low-cost equipment of spectrophotometry make it the method of choice for many laboratories. However, classical spectrophotometric methods may fail when analyzing dosage forms containing more than one active ingredient with overlapping spectra, such as DEX and PAR. In these cases, the researchers choose high-performance liquid chromatography (HPLC), despite the disadvantages,

which include high costs, extensive maintenance, time-consuming procedures, higher solvent use, and less environmentally friendly operations. A literature review shows that the simultaneous determination of DEX and PAR has primarily been conducted using HPLC (Medhat et al., 2024; Mulla et al., 2011; Pokharkar et al., 2011; Rao et al., 2011).

On the other hand, there are less labor-intensive and more feasible options to overcome these challenges, such as chemometrics-assisted UV-Vis spectrophotometry. Chemometric methods allow the extraction of relevant information from complex datasets, including overlapping spectral data. Principal component regression (PCR) and partial least squares (PLS) are multivariate chemometric techniques commonly used in combination drug analysis to handle complex, multicomponent systems. Chemometric techniques, especially PCR and PLS, play an essential role in overcoming the challenges of analyzing combination drugs with overlapping spectral data. These methods provide the accuracy needed for quality control in the pharmaceutical industry, ensuring safe and effective medications reach the market.

PCR and PLS are well-established tools in pharmaceutical analysis and they are extensively documented in the chemometric literature for their high predictive power, robustness to noise, and flexibility in handling collinear and overlapping data. Recent studies continue to demonstrate their effectiveness in the quantification of multicomponent mixtures in both pharmaceutical and biological matrices (Aktas & Sahin, 2021; Çolak, 2024; Demirkaya Miloğlu & Karagöl, 2023; Ertokus, 2022; Gandhi et al., 2021; Michael et al., 2024; Pekcan, 2024; Sayed et al., 2021; Sebaiy et al., 2023). These methods not only improve analytical sensitivity and selectivity but also streamline method development by reducing reliance on expensive instrumentation and solvent-intensive protocols.

To date, the only spectrophotometric quantification study reported in the literature for this combination (Kothapalli et al., 2011) employed classical spectrophotometric methods, specifically the simultaneous equation method and the Q-absorbance ratio method. In these approaches, concentrations are determined by solving simultaneous equations derived from absorptivity coefficients at selected wavelengths. While these methods are simple, rapid, and cost-effective, they depend heavily on the careful selection of wavelengths, such as isosbestic points or regions with significant absorbance differences, which limits their applicability. These univariate techniques are generally effective when spectral overlap between analytes is minimal or well-characterized, but tend to be less reliable in cases of substantial spectral overlap and often result in lower sensitivity and selectivity.

In contrast, chemometrics-assisted methods, such as PCR and PLS, utilize the full spectral dataset to model latent variables that correlate with analyte concentrations. These multivariate approaches do not require prior selection of discrete wavelengths and can accurately resolve overlapping spectra without physical separation of analytes. As a result, they offer improved sensitivity, robustness, and analytical performance, particularly in complex mixtures or formulations.

In this work, two chemometrics-assisted spectrophotometric methods were developed to simultaneously quantify PAR and DEX in spite of their overlapping spectra. PCR and PLS methods were developed and validated by employing training and test sets containing both drugs in their linear concentration range. Intra-day and inter-day measurements were also performed for the validation of the analytical methods. Finally, the chemometric methods were applied to the quantitative estimation of PAR and DEX in effervescent tablet samples.

MATERIAL AND METHODS

Instruments and Software

A Shimadzu UV-2550 double-beam UV-VIS spectrophotometer (Kyoto, Japan) with UVProbe Software (Shimadzu, Kyoto, Japan) was used to record absorption spectra of samples. A quartz cuvette with a 1 cm light path was used, and the slit width was set to 2 nm. Spectra were recorded over the wavelength range of 200–340 nm with an increment of 0.05 nm. The spectra were transferred to an Excel sheet as column vectors. Absorbance data between 220 and 320 nm ($\Delta\lambda$ =0.1 nm), along with the nominal concentration data, were used to model and validate the PCR and PLS methods using MATLAB software (MathWorks, USA).

Chemicals and reagents

The standard materials of paracetamol and dexketoprofen trometamol were kindly gifted by a national pharmaceutical manufacturer Deva (Tekirdağ, Türkiye). Methanol of analytical grade supplied by Carlo Erba (Milan, Italy). The commercial sample, as an effervescent tablet preparation, was procured from a local pharmacy. It was produced by Neutec Pharmaceuticals, with a label claim of 50 mg DEX and 300 mg PAR per effervescent tablet.

Standard solutions

Individual stock solutions of PAR and DEX were prepared by dissolving 10 mg standard paracetamol and 14.8 mg standard dexketoprofen trometamol (equivalent to dexketoprofen) in 100 mL methanol. A calibration set of 25 solutions (planned by 5^2 a factorial design, 5 levels and 2 analytes) was prepared by mixing appropriate amounts of stock solutions and diluting them in methanol. The working concentration ranges were 3-18 μ g/mL for DEX and 5-25 μ g/mL for PAR. The concentrations of DEX and PAR in each calibration sample are shown in Table 1.

	μg/mL			μg/mL			
Sample code	DEX	PAR	Sample code	DEX	PAR		
C1	3	5	C14	10	20		
C2	3	10	C15	10	25		
C3	3	15	C16	14	5		
C4	3	20	C17	14	10		
C5	3	25	C18	14	15		
C6	6	5	C19	14	20		
C7	6	10	C20	14	25		
C8	6	15	C21	18	5		
С9	6	20	C22	18	10		
C10	6	25	C23	18	15		
C11	10	5	C24	18	20		
C12	10	10	C25	18	25		
C13	10	15					

To evaluate the performance of the chemometric models, a set of 11 independent test samples containing both drugs at various concentration levels was prepared in the same manner. The test set included: (i) five DEX concentrations from the calibration range with a fixed PAR concentration matching that of the commercial formulation; (ii) five PAR concentrations from the calibration range with a fixed DEX concentration matching the commercial level; and (iii) one sample containing both PAR and DEX at concentrations equivalent to those in the commercial product. This design ensured that all validation samples, listed in Table 3, were distinct from those used in calibration. Additionally, as a part of the validation studies, synthetic samples at three different concentration levels (Table 4) were prepared in triplicate to assess intra-day and inter-day precision.

Effervescent tablet sample solutions

Five effervescent tablets were ground into a fine powder using a dry mortar. A portion equivalent to the mass of 0.1 tablet was transferred into a 50 mL volumetric flask. Approximately 20 mL of methanol was added, and the mixture was allowed to stand until foaming stopped, with occasional manual shaking. The flask was then filled to volume with methanol. To ensure complete dissolution of the drugs, the solution

was magnetically stirred for 15 minutes and subsequently filtered. A 0.4 mL aliquot of the filtrate was diluted to 10 mL and subjected to spectrophotometric analysis. This procedure was repeated 10 times.

RESULTS AND DISCUSSION

In preliminary experiments, the spectra of individual standard solutions of PAR and DEX at increasing concentrations were recorded between 200-340 nm. The spectra of these solutions are shown in Figure 1, where red represents DEX and blue represents PAR. DEX exhibits a prominent absorption band with a maximum around 255 nm, while PAR shows strong absorbance near 248.4 nm. As can be seen in this figure, significant spectral overlap between DEX and PAR in the UV region makes direct univariate spectrophotometric quantification unsuitable for their mixtures due to signal interference. Figure 1 also displays the UV absorption spectra of their binary mixture (containing 18 µg/mL DEX and 20 µg/mL PAR) in green. The binary mixture spectrum reflects the additive absorbance of both drugs, yet due to the overlapping nature and possible matrix effects in commercial formulations, the resulting profile may not be a straightforward superposition. This overlap underscores the necessity of multivariate calibration methods such as PCR and PLS, which can deconvolute the

mixed spectral information and extract concentration data for each analyte by modeling the latent structure in the dataset. Linear concentration ranges were investigated by plotting the absorbance values at 255 nm for DEX and 248.4 nm for PAR against the corresponding concentrations. The appropriate working ranges were decided as $3-18 \,\mu g/mL$ for DEX and $5-25 \,\mu g/mL$ for PAR.

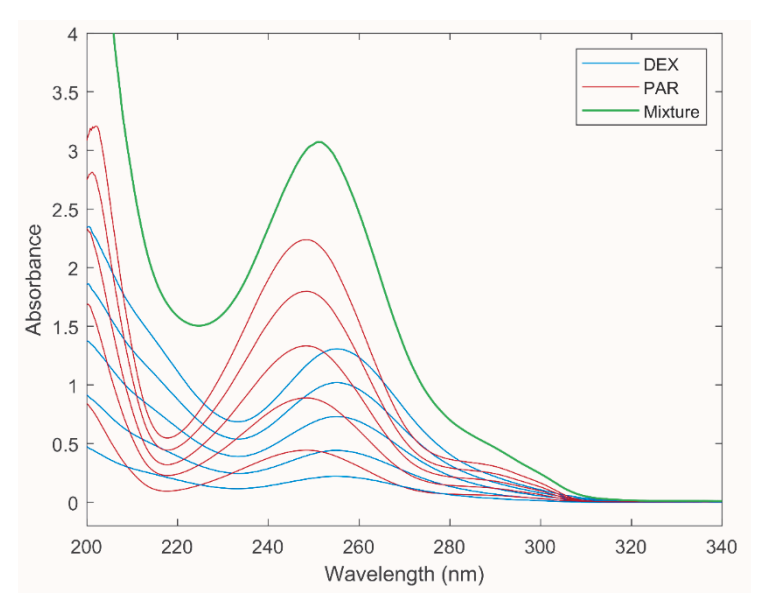


Figure 1. UV absorption spectra of 3.0-18 μg/mL DEX (— blue), 5.0-25.0 μg/mL PAR (— red), and their binary mixture consisting of 18 μg/mL DEX and 20 μg/mL PAR (— green).

Application of chemometric regression methods

Principal component regression (PCR) is a technique that combines principal component analysis (PCA) and multilinear regression. The absorbance data matrix is decomposed by PCA to extract the latent variables (eigenvectors and their corresponding eigenvalues). Then, a multilinear regression is applied in an inverse least-squares manner to construct the PCR calibration using the selected eigenvectors and the mean-centered concentration data (Olivieri, 2018c).

In this study, the PCR model was implemented by calculating the loadings, q, using the equation $q=D\times T^T\times A$, where D is the diagonal matrix containing the inverse of the selected eigenvalues, T is the score matrix, and A is the absorbance matrix of the calibration samples. Then, the regression coefficient, b, was calculated as $b=P\times q$, where P is the matrix of eigenvectors. The predicted concentration matrix, C_{pred} was obtained using the equation $C_{pred}=b\times A_{sample}$, where A_{sample} is the absorbance matrix of the samples (Dinç et al., 2006; Dinç, 2007). In this work, the absorbance

matrix was constructed as absorbance values between 220-320 nm with an increment of 0.1 nm, and was mean-centered.

The optimal number of principal components (i.e., eigenvector–eigenvalue pairs) was determined using the leave-one-out cross-validation technique. In this approach, multiple PCR models are constructed by sequentially excluding one sample from the calibration set, calibrating the model with the remaining samples, and predicting the excluded sample. This process begins with a model containing a single principal component, and the corresponding prediction error is calculated. The excluded sample is then reintegrated into the dataset, and the procedure is repeated for each sample in turn. This entire process is performed iteratively for an increasing number of principal components, up to a maximum of 10 in this study.

For each number of components, cross-validation statistics, including the prediction error sum of squares (PRESS), root mean squared error of cross-validation (RMSECV), and explained variance, were calculated.

Table 2 presents the cross-validation results, while Figure 2 illustrates the RMSECV as a function of the number of principal components. As shown in Figure 2, adding up to three principal components resulted in a significant reduction in prediction error. This finding is further supported by the data in Table 2, which indicates that three principal components ac-

count for more than 99.99% of the variance in both compounds. Including additional components yielded minimal improvement, offering little relevant information and posing a risk of overfitting. Therefore, the final PCR model was constructed using three principal components, with the remaining components excluded (Dinç et al., 2005; Olivieri, 2018a).

Table 2. Statistical results of cross-validation

		PR	ESS	RMS	ECV	E	V	
	PC number	DEX	PAR	DEX	PAR	DEX	PAR	
	1	642.549	505.821	5.174	4.591	97.499	97.499	
PCR	2	11.022	15.263	0.678	0.797	99.966	99.966	
PCR	3	0.889	1.320	0.192	0.234	99.992	99.992	
	4	1.004	0.541	0.204	0.150	99.998	99.998	
	5	1.030	0.550	0.207	0.151	99.999	99.999	
		PR	ESS	RMS	RMSECV		EV	
	LV number	DEX	PAR	DEX	PAR	DEX	PAR	
	1	551.068	436.490	4.792	4.265	97.495	54.123	
DI C	2	2.766	3.527	0.339	0.383	99.966	99.771	
PLS	3	0.193	0.431	0.090	0.134	99.992	99.958	
	4	0.616	1.325	0.160	0.235	99.998	99.979	
	5	0.421	0.623	0.132	0.161	100.000	99.982	

PCR: principal component regression, PLS: partial least squares, PC: principal component, LV: latent variable, PRESS: prediction error sum of squares, RMSECV: root mean squared error of cross-validation, EV: explained variance

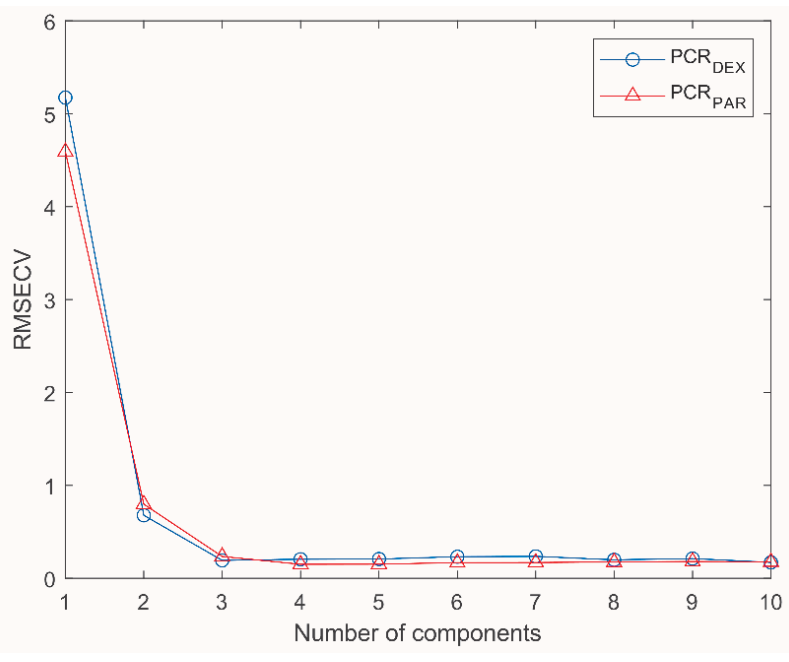


Figure 2. Number of components versus the root mean squared error of cross-validation during cross-validation of the PCR model.

Unlike PCR, PLS uses both absorbance data and concentration data in the decomposition process to estimate the latent variables. It means that the latent variables (principal components) in PCR are analyte-independent, whereas PLS latent variables are analyte-dependent (Olivieri, 2018b; Üstündağ et al., 2015). In the calibration step of PLS, absorbance data A and calibration data C are decomposed into scores and loadings by the following equations, called outer relation (Dinc et al., 2010):

$$A = TP^{T} + E \tag{1}$$

$$C=UQ^{T}+F$$
 (2)

here, and denote score matrices, and represent the loading matrices, and and are the residuals associated with absorbance and concentration data, respectively. PLS minimizes the F while keeping the correlation between A and C using the inner relation U=TD, where D is a diagonal matrix that ensures the relationship between T and U.

In the regression step, the vector of PLS regression coefficients, B, is calculated by the equation $B=W \times (P^T \times W)^{-1} \times Q$, where W is a matrix of weights. Finally, the concentration of the samples, C_{pred} , was com-

puted using the equation $C_{pred} = B \times A_{sample}$ (Dinç, 2007).

As in the PCR method, the absorbance matrix, between 220-320 nm with $\Delta\lambda$ =0.1 nm, was used after mean-centering during PLS implementation. Similarly, the optimal number of latent variables in the PLS method was determined by leave-one-out cross-validation. For a maximum of 10 latent variables, PRESS, RMSECV, and explained variance values were calculated. Table 2 presents the cross-validation results, while Figure 3 illustrates RMSECV values as a function of the number of latent variables. As shown in the figure, the inclusion of more than three latent variables results in a slight increase in prediction error. This observation is also supported by Table 2, where the minimum PRESS value was obtained with a PLS model using three latent variables, achieving an explained variance greater than 99.9% for both analytes. Although models with more latent variables accounted for slightly higher variance, they were deemed unsuitable due to the potential risk of overfitting. Consequently, a PLS model with three latent variables was selected as the most appropriate for modeling the calibration data.

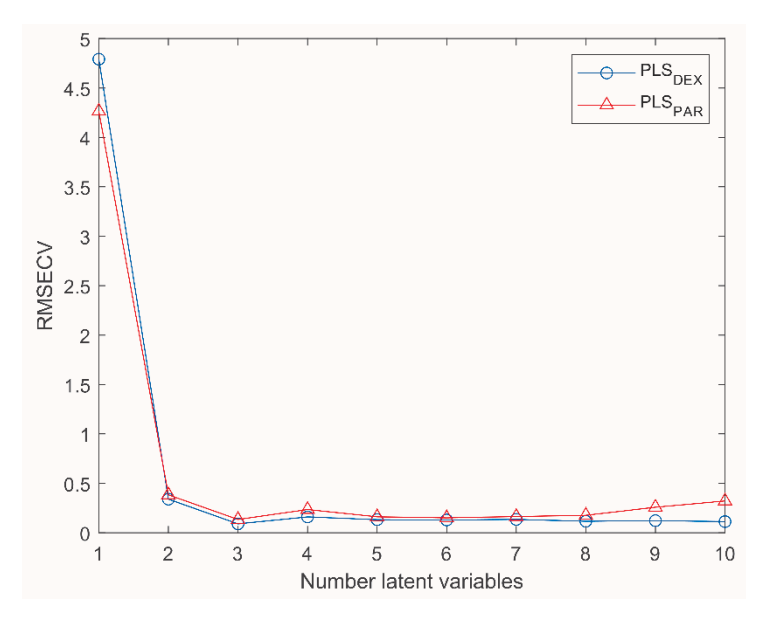


Figure 3. Number of latent variables versus root mean squared error of cross-validation in the PLS method

Analytical validation of the developed methods

The analytical performance of the developed PCR and PLS methods was evaluated by analyzing several validation samples. A set of 11 independent test samples, containing DEX and PAR in several concentration levels different from the levels used in the calibration set, was used for this purpose. The predicted concentrations of DEX and PAR in these samples by

PCR and PLS models are listed in Table 3. This table also depicts the percentage recovery of the samples as well as the average and standard deviation of the recovery values. The mean recovery, standard deviation, and relative standard deviation values were found to be appropriate, indicating the suitability of the method for the simultaneous analysis of the mentioned drugs in their mixtures.

Table 3. Recovery results of independent test samples by PCR and PLS methods

A	Added (μg/mL)			Found (µg/mL)			Recovery (%)			
			PO	CR	P:	LS	PCR		PLS	
Code	DEX	PAR	DEX	PAR	DEX	PAR	DEX	PAR	DEX	PAR
M1	3	24	2.92	23.96	2.84	24.08	97.36	99.83	94.76	100.34
M2	6	24	5.69	23.93	5.61	24.06	94.88	99.72	93.55	100.24
M3	10	24	10.09	24.08	10.01	24.21	100.91	100.32	100.06	100.85
M4	14	24	13.84	24.07	13.76	24.20	98.84	100.31	98.26	100.83
M5	18	24	18.05	23.86	17.97	23.99	100.28	99.41	99.81	99.95
M6	4	5	3.98	4.96	3.90	5.09	99.61	99.26	97.49	101.90
M7	4	10	4.07	9.76	3.99	9.89	101.74	97.60	99.67	98.90
M8	4	15	3.94	14.72	3.86	14.85	98.62	98.12	96.56	98.97
M9	4	20	3.94	20.11	3.86	20.23	98.48	100.54	96.48	101.16
M10	4	25	4.02	25.05	3.94	25.18	100.47	100.21	98.39	100.71
M11	4	24	3.99	23.96	3.91	24.09	99.71	99.85	97.65	100.38
						Mean	99.17	99.56	97.52	100.38
					Standar	d deviation	1.89	0.94	2.07	0.89
				Relative standard deviation			1.90	0.94	2.13	0.88

Additionally, the precision and accuracy of the methods were evaluated by the inter-day (n=3) and intra-day (n = 3) analyses at three concentration levels (5 μ g/mL, 10 μ g/mL, 15 μ g/mL for DEX and 8 μ g/mL, 16 μ g/mL, 24 μ g/mL for PAR). The predict-

ed concentration values were calculated by applying PCR and PLS methods, and the corresponding results (expressed as mean percent recovery, relative standard deviation, and percent relative error values) are summarized in Table 4.

Table 4. Analysis results of intra-day and inter-day samples (n=3)

	Added (μg/mL)			Found (μg/mL)			
			PO	CR	PI	LS.	
Code	DEX	PAR	DEX	PAR	DEX	PAR	
ay	5	8	5.21	7.94	5.12	8.07	
Inter-day	10	16	9.72	16.22	9.63	16.34	
In	15	24	14.73	24.36	14.64	24.49	
lay	5	8	5.09	8.10	5.00	8.23	
Intra-day	10	16	9.97	16.52	9.89	16.65	
- I	15	24	15.27	24.59	15.18	24.73	
				Mean rec	overy (%)		
			PO	CR	PI	LS	
			DEX	PAR	DEX	PAR	
κ̂ι			104.16	99.22	102.32	100.89	
Inter-day			97.18	101.35	96.34	102.15	
Int			98.18	101.50	97.62	102.04	
ay			101.85	101.25	100.03	102.92	
Intra-day			99.70	103.26	98.85	104.06	
In			101.83	102.48	101.21	103.05	
				Relative Stand	lard Deviation		
			PO	CR	PI	LS	
			DEX	PAR	DEX	PAR	
*			1.00	0.64	1.01	0.63	
Inter-day			0.16	0.40	0.16	0.40	
Inte			1.19	0.81	1.19	0.80	
>			3.87	2.03	3.74	2.09	
Intra-day			1.32	0.45	1.31	0.44	
Intr			0.40	1.11	0.42	1.09	
			0.10	Relative		1.07	
			Po	CR	PI	.S	
			DEX	PAR	DEX	PAR	
			4.16	-0.78	2.32	0.89	
Inter-day			-2.82	1.35	-3.66	2.15	
Intel							
			-1.82	1.50	-2.38	2.04	
-day			1.85	1.25	0.03	2.92	
Intra-day			-0.30	3.26	-1.15	4.06	
			1.83	2.48	1.21	3.05	

The limit of quantification (LOQ) values for both DEX and PAR were calculated using a residual-based approach. Unlike univariate calibration, where LOQ is typically defined using the slope of a calibration curve, multivariate models such as PLS and PCR do not produce a single, well-defined slope. This is because predictions are based on a combination of correlated spectral variables and latent variables, making the direct application of univariate formulas inappropriate. To address this, we applied a residual-based method, consistent with established practices in the chemometric literature (Allegrini & Olivieri, 2014; Felmy et al., 2024; Parastar & Kirsanov, 2020). Specifically, LOQ was calculated using the formula: LOQ = $10.\sigma$ /S, where σ is the standard deviation of the residuals between the measured and predicted concentrations for each analyte in the calibration set, and S represents the model sensitivity, defined as the Euclidean norm of the regression coefficient vector for each analyte. This approach incorporates the prediction error to quantify noise and employs the regression vector norm as a surrogate for sensitivity, thereby providing a performance-based and model-consistent estimate of LOQ. The computed LOQ values of DEX and PAR were 0.51 μ g/mL and 0.50 μ g/mL for PCR model, and 0.02 μ g/mL and 0.02 μ g/mL for the PLS model.

Assay results of effervescent tablet solutions

The absorbance matrix of effervescent tablet solutions was subjected to the prediction step of PCR and PLS methods. The predicted concentration of the sample solutions was multiplied by the dilution factor of 12.5, to calculate the DEX and PAR content as milligrams per effervescent tablet. The assay results are summarized in Table 5, indicating a good agreement with the label claim of 50 mg DEX and 300 mg PAR per tablet. F-test and t-test were used to compare the assay results obtained by applying PCR and PLS. As can be seen in Table 5, the computed F- and t-statistics were smaller than the critical values, indicating comparable results in terms of variance and mean. For both drugs, there was no significant difference between the analysis results, provided by PCR and PLS methods.

Table 5. Assay results of commercial effervescent tablets by proposed PCR and PLS methods

	mg/tablet ^a				
		PCR		PLS	
Sample code	DEX	PAR	DEX	PAR	
E1	53.47	296.43	52.38	298.05	
E2	50.01	295.57	48.97	297.13	
E3	48.96	295.83	47.90	297.41	
E4	50.81	304.56	49.73	306.16	
E5	51.10	305.93	50.01	307.55	
E6	51.12	295.49	50.05	297.08	
E7	49.96	295.60	48.91	297.19	
E8	49.93	298.21	48.88	299.79	
E9	51.26	302.98	50.20	304.55	
E10	48.87	296.20	47.81	297.78	
Mean	50.55	298.68	49.48	300.27	
Standard deviation	1.34	4.14	1.33	4.15	
Relative standard deviation	2.65	1.39	2.68	1.38	
F-stat	1.02	1.00	F-crit =3.18 (p=0.05)		
t-stat	1.79	0.86	t-crit =2.10 (p=0.05)		

^aLabel claim: 50 mg DEX, 300 mg PAR per tablet

CONCLUSION

This study introduces two novel chemometrics-assisted UV/Vis spectrophotometric methods-PCR and PLS-for the simultaneous determination of DEX and PAR in commercial effervescent tablets. Both models used three latent variables and demonstrated strong predictive performance across 11 independent validation samples, with mean recoveries ranging from 97.5% to 100.4% and relative standard deviations below 2.2%, confirming their accuracy and precision. Intra-day and inter-day analyses further supported the methods' robustness, with low relative errors and RSD values. The assay results for commercial tablets closely matched label claims (50 mg DEX and 300 mg PAR), with no significant differences between PCR and PLS outcomes. These methods effectively resolved spectral overlap without requiring separation or complex sample preparation and offer a rapid, cost-efficient alternative to chromatographic

techniques. Their strong analytical performance and practical advantages make them promising tools for routine pharmaceutical quality control.

AUTHOR CONTRIBUTION STATEMENT

Conception and design (ZCE, ED), literature search (ZCE), sources (ED), data collection (ZCE), data analysis and interpretation (ZCE, ED), preparing the study text (ZCE), reviewing the text (ZCE, ED)

CONFLICT OF INTEREST

The authors declare that there is no conflict of interest.

REFERENCES

Aktas, A. H., & Sahin, H. O. (2021). A speedy method for simultaneous determination in tablet active content by nir and uv-vis spectrophotometry: Comparison of PLS-1 and ICA-ANN models. *Gazi University Journal of Science*, 34(2), 370-379. doi:10.35378/gujs.752042

- Allegrini, F., & Olivieri, A. C. (2014). IUPAC-Consistent Approach to the Limit of Detection in Partial Least-Squares Calibration. *Analytical Chemistry*, 86(15), 7858-7866. doi:10.1021/ac501786u
- Ayoub, S. S. (2021). Paracetamol (acetaminophen): A familiar drug with an unexplained mechanism of action. *Temperature (Austin)*, 8(4), 351-371. doi:1 0.1080/23328940.2021.1886392
- Çolak, S. (2024). Discrimination of some expired and unexpired drugs under different conditions using Fourier Transform Infrared-Attenuated Total Reflectance. *Spectroscopy Letters*, *57*(8), 469-482. doi:10.1080/00387010.2024.2383189
- Demirkaya Miloğlu, F., & Karagöl, N. (2023). Simultaneous Spectrophotometric Determination of Dexketoprofen Trometamol and Thiocolchicoside by Using Principal Component Regression Multivariate Calibration Model in Combined Pharmaceutical Formulation. *Pharmata*, *3*(4), 99-104. doi:10.5152/Pharmata.2023.23017
- Dinç, E. (2007). Kemometri Çok Değişkenli Kalibrasyon Yöntemleri. *Hacettepe* Üniversitesi *Eczacılık Fakültesi Dergisi*, 27(1), 61-92.
- Dinç, E., Aktaş, A. H., Baleanu, D., & Üstünda, Ö. (2006). Simultaneous determination of tartrazine and allura red in commercial preparation by chemometric HPLC method. *Journal of Food and Drug Analysis*, 14(3), 284-291. doi:10.38212/2224-6614.2467
- Dinç, E., Aktaş, A. H., & Üstündağ, Ö. (2005). New liquid chromatographic-chemometric approach for the determination of sunset yellow and tartrazine in commercial preparation. *Journal of AOAC INTERNATIONAL*, 88(6), 1748-1755. doi:10.1093/jaoac/88.6.1748

- Dinç, E., Üstündağ, Ö., & Baleanu, D. (2010). Simultaneous chemometric determination of pyridoxine hydrochloride and isoniazid in tablets by multivariate regression methods. *Drug Testing and Analysis*, 2(8), 383-387. doi:10.1002/dta.145
- Ertokus, G. P. (2022). Chemometric determination of common cold infection drugs in human urine. *Reviews in Analytical Chemistry*, 41(1), 158-167. doi:10.1515/revac-2022-0040
- Felmy, H. M., Cox, R. M., Espley, A. F., Campbell, E. L., Kersten, B. R., Lackey, H. E., . . . Lines, A. M. (2024). Quantification of Hydrogen Isotopes Utilizing Raman Spectroscopy Paired with Chemometric Analysis for Application across Multiple Systems. *Analytical Chemistry*, 96(18), 7220-7230. doi:10.1021/acs.analchem.4c00802
- Gandhi, S. V., Patil, D., & Baravkar, A. A. (2021). Comparison of Chemometric assisted UV Spectrophotometric and RP-HPLC Method for the simultaneous determination of Ofloxacin and Tinidazole in their Combined dosage form. *Research Journal of Pharmacy and Technology*, 14(11), 5713-5718. doi:10.52711/0974-360X.2021.00993
- Kothapalli, L. P., Karape, A. K., Thomas, A. B., Nanda, R. K., Gaidhani, P., & Choudhari, M. E. (2011). Simultaneous spectrophotometric estimation of paracetamol and dexketoprofen trometamol in pharmaceutical dosage form. *Der Pharma Chemica*, *3*(1), 365-371.
- Kuczyńska, J., Pawlak, A., & Nieradko-Iwanicka, B. (2022). The comparison of dexketoprofen and other painkilling medications (review from 2018 to 2021). *Biomedicine & Pharmacotherapy*, 149, 112819. doi:10.1016/j.biopha.2022.112819

- López Navarro, A. Á., Martínez Gómez, M. A., Gras Colomer, E., Campillos, P., & Climente Martí, M. (2019). Physicochemical stability of binary admixtures of paracetamol and dexketoprofen-trometamol for patient-controlled analgesia use. *European Journal of Hospital Pharmacy*, 26(6), 308-313. doi:10.1136/ejhpharm-2018-001535
- Medhat, P. M., Fouad, M. M., Monir, H. H., & Ghoniem, N. S. (2024). A sustainable and green HPLC-PDA technique for the simultaneous estimation of Post-COVID-19 syndrome co-administered drugs with greenness and whiteness assessment. *Scientific Reports*, *14*(1). doi:10.1038/s41598-024-75216-4
- Michael, A. M., Lotfy, H. M., Rezk, M. R., & Nessim, C. K. (2024). Development and Evaluation of Chemometric Models for the Estimation of Sumatriptan in the Presence of Naproxen and a Degradation Product Using UV Spectrophotometry. *Journal of AOAC International*, 107(5), 749-760. doi:10.1093/jaoacint/qsae041
- Mulla, T. S., Rao, J. R., Yadav, S. S., Bharekar, V. V., & Rajput, M. P. (2011). Development and Validation of HPLC Method for Simultaneous Quantitation of Paracetamol and Dexketoprofen Trometamol in Bulk Drug and Formulation. *Pharmacie Globale* : *International Journal of Comprehensive Pharmacy*, 7(9).
- O'Neill, A., & Lirk, P. (2022). Multimodal Analgesia. *Anesthesiol Clin*, 40(3), 455-468. doi:10.1016/j.an-clin.2022.04.002
- Olivieri, A. C. (2018a). The Optimum Number of Latent Variables. In A. C. Olivieri (Ed.), *Introduction to Multivariate Calibration: A Practical Approach* (pp. 87-101). Cham: Springer International Publishing.

- Olivieri, A. C. (2018b). The Partial Least-Squares Model. In A. C. Olivieri (Ed.), *Introduction to Multivariate Calibration: A Practical Approach* (pp. 103-121). Cham: Springer International Publishing.
- Olivieri, A. C. (2018c). Principal Component Regression. In A. C. Olivieri (Ed.), Introduction to Multivariate Calibration: A Practical Approach (pp. 73-86). Cham: Springer International Publishing.
- Parastar, H., & Kirsanov, D. (2020). Analytical Figures of Merit for Multisensor Arrays. *ACS Sensors*, 5(2), 580-587. doi:10.1021/acssensors.9b02531
- Pekcan, G. (2024). Determination of Alzheimer's Drugs in a Human Urine Sample by Different Chemometric Methods. *International Journal of Analytical Chemistry*, 2024. doi:10.1155/2024/5535816
- Pokharkar, D., Korhale, R., Jadhav, S., Birdar, N., Puri, D., & Wani, P. (2011). Stability indicating RP-HPLC-PDA method for simultaneous determination of dexketoprofen trometamol and paracetamol from tablet dosage form. *Der Pharmacia Letter*, 3, 49-57.
- Rao, J. R., Mulla, T. S., Bharekar, V. V., Yadav, S. S., & Rajput, M. P. (2011). Simultaneous HPTLC Determination of Paracetamol and Dexketoprofen trometamol in pharmaceutical dosage form. *Der Pharma Chemica*, 3(3), 32-38.
- Sayed, R. A., Ibrahim, A. E., & Sharaf, Y. A. (2021). Chemometry-assisted UV-spectrophotmetric methods for the simultaneous determination of paritaprevir, ritonavir, and ombitasvir in their combined tablet dosage forms: A comparative study. *Journal of Chemometrics*, 35(5). doi:10.1002/cem.3339

Sebaiy, M. M., El-Adl, S. M., Nafea, A., Aljazzar, S. O., Elkaeed, E. B., Mattar, A. A., & Elbaramawi, S. S. (2023). Different methods for resolving overlapping UV spectra of combination medicinal dose forms of ciprofloxacin and metronidazole. *BMC Chem*, *17*(1), 137. doi:10.1186/s13065-023-01007-z

Üstündağ, Ö., Dinç, E., Özdemir, N., & Tilkan, M. G. (2015). Comparative application of PLS and PCR methods to simultaneous quantitative estimation and simultaneous dissolution test of zidovudine - Lamivudine tablets. *Acta Chimica Slovenica*, 62(2), 437-444. doi:10.17344/acsi.2014.1071

Yerebakan, F. C., Kurt, F., Çınbay, K., & Alkış, N. (2024). Multimodal Analgesia for Perioperative Pain Management. *Ankara* Üniversitesi Tıp *Fakültesi Mecmuası*, *77*(2), 122-127. doi:10.4274/atfm.galenos.2024.54871

Clinical Pharmacist in Palliative Care Unit: A Retrospective Study

Özgenur GERİDÖNMEZ *,****, Kamer TECEN ***

Clinical Pharmacist in Palliative Care Unit: A Retrospective Study

Palyatif Bakım Ünitesinde Klinik Eczacı: Bir Retrospektif Çalışma

SUMMARY

In palliative care, the goal of medication therapy is to improve the quality of life and lessen the burden of symptoms. However, comorbidities, polypharmacy, or general vulnerability may cause drug-related problems (DRPs) in palliative care patients. Clinical pharmacists are crucial members of a hospital multidisciplinary team who identify DRPs and offer recommendations and interventions. The objective of this study was to categorize and define the pharmacist interventions and DRPs in the palliative care unit. A retrospective study was conducted in a palliative care unit at a Turkish state hospital. Details like the DRP's identification, possible causes, planned intervention, acceptance of the intervention, and status were filled in by the clinical pharmacist through regular in-person interactions with patients or caregivers. The PCNE(V9.1) classification was used to classify all DRPs. A total of 130 patients were evaluated, with an average of 1.9 DRPs per patient. The most common problems were "treatment effectiveness" and followed by "treatment safety". The primary cause of DRPs was "drug selection", followed by "patient related" and "dose selection". Clinical pharmacists performed 235(97.1%) interventions, a total of 132(55.0%) interventions were accepted, and 118(48.8%) problems were solved. In palliative units the implementation of a team member who specializes in drug therapy, like a clinical pharmacist, may be advantageous in mitigating potential complications. This is the first time clinical pharmacists have been involved in our center. Therefore, as the adaptation process progresses, it is anticipated that intervention and acceptance rates will rise. Treatment outcomes will be enhanced by multidisciplinary healthcare teams.

Key Words: Clinical pharmacist, Palliative care, Drug-related problems.

ÖZ

Palyatif bakımda ilaç tedavisinin amacı, yaşam kalitesini artırmak ve semptom yükünü azaltmaktır. Ancak, eşlik eden hastalıklar, polifarmasi veya genel kırılganlık, palyatif bakım hastalarında ilaçla ilişkili sorun (İLİS) meydana getirebilir. Klinik eczacılar, hastane multidisipliner ekibinin önemli üyeleri olup İLİS'leri belirleyerek öneriler ve müdahalelerde bulunurlar. Bu çalışmanın amacı, bir devlet hastanesinin palyatif bakım ünitesinde klinik eczacı müdahalelerini ve İLİS'leri sınıflandırmak ve tanımlamaktır. Bu çalışma, Türkiye'deki bir devlet hastanesinde palyatif bakım ünitesinde retrospektif olarak gerçekleştirilmiştir. Klinik eczacı, hastalar veya bakım verenlerle düzenli yüz yüze görüşmeler yaparak İLİS'in tespiti, olası nedenleri, planlanan müdahale, müdahalenin kabulü ve durumu gibi bilgileri doldurmuştur. Tüm İLİS'ler PCNE(V9.1) sınıflandırmasına göre kategorize edilmiştir. Çalışmaya toplam 130 hasta dahil edilmiş, hasta başına ortalama 1.9 İLİS kaydedilmiştir. En yaygın problemler "tedavi etkinliği" olup bunu "tedavi güvenliği" takip etmiştir. İLİS'lerin başlıca nedeni "ilaç seçimi" olup, bunu "hastaya bağlı nedenler" ve "doz seçimi" izlemiştir. Klinik eczacılar toplam 235 (%97,1) müdahale gerçekleştirmiş, bunların 132'si (%55,0) kabul edilmiş ve 118'i (%48,8) tamamen çözülmüştür. Palyatif bakım ünitelerinde, ilaç tedavisi konusunda uzmanlaşmış bir ekip üyesinin, örneğin klinik eczacının, görevlendirilmesi olası komplikasyonları azaltmada faydalı olabilir. Merkezimizde ilk kez klinik eczacılar bu sürece dahil edilmiştir. Bu nedenle, adaptasyon süreci ilerledikçe müdahale ve kabul oranlarının artacağı öngörülmektedir. Multidisipliner sağlık ekipleri sayesinde tedavi sonuçları iyileştirilecektir.

Anahtar Kelimeler: Klinik eczacı, Palyatif bakım, İlaçla ilişkili problemler

Received: 16.06.2025 Revised: 9.07.2025 Accepted: 9.07.2025

^{*} ORCID:0000-0002-8223-2723: Hacettepe Üniversitesi, Eczacılık Fakültesi, Klinik Eczacılık Anabilim Dalı, 06100, Ankara, Türkiye

[&]quot; ORCID: 0000-0002-5381-0950: Anadolu Üniversitesi, Eczacılık Fakültesi, Klinik Eczacılık Anabilim Dalı, 26470, Eskişehir, Türkiye

INTRODUCTION

Palliative care medication therapy attempts to improve patients' quality of life and lessen their symptom burden. However, end-of-life drugs require a delicate balance of factors (Tatum & Mills, 2020). Palliative care patients receive an average of 7.0 – 7.8 drugs daily (Wernli et al., 2023). Drug-related problems (DRPs), primarily include insufficient drug treatment, adverse drug reactions, drug-drug interactions, inappropriate dosages, low adherence, and medication errors (Krishnaswami et al., 2019), which can arise as a result of the patients' general fragility, comorbidities, and the high frequency of polypharmacy, all of which are common among palliative care patients (Hailu, Berhe, Gudina, Gidey & Detachew, 2020; Abunahlah, Elawaisi, Velibeyoğlu & Sancar, 2018).

Clinical pharmacists are important in identifying DRPs and making recommendations and interventions in a hospital multidisciplinary team. Several studies have indicated that pharmacists benefit from resolving and avoiding DRPs in outpatient clinics and inpatient acute care (Viktil & Blix, 2008). Studies have also indicated that having a pharmacist on the multidisciplinary healthcare team can enhance outcomes and reduce mortality and readmissions associated with drugs in elderly patients (Selcuk, Sancar, Okuyan, Demirtunc & Izzettin, 2015; Cortejoso, Dietz, Hofmann, Gosch & Sattler, 2016). However, clinical pharmacists' roles in palliative care units are limited. Although further studies are needed, Remi et al. concluded that the care of palliative care patients by pharmacists could lead to a sustained increase in the safety of medication therapy by continuously reducing medication risks (Krumm, Bausewein & Remi, 2023).

Clinical pharmacy is based on pharmaceutical care, which is the pharmacist's contribution to the patient's care to maximize medication use and enhance health outcomes. The last ten years have seen modifications to undergraduate pharmacy education and new rules in the Turkish healthcare system, which

have demonstrated a greater recognition of pharmaceutical care practice. Nonetheless, clinical pharmaceutical services remain a comparatively novel concept.

Among the numerous classification methods employed globally to describe DRPs (Basger, Moles & Chen, 2015), the Pharmaceutical Care Network Europe (PCNE) classification system is frequently used in clinical practice and demonstrates internal consistency due to its frequent updates and revisions. The PCNE classification for DRPs V9.1 is a verified system that has undergone numerous revisions to effectively categorize DRPs across various situations (Ayhan, Karakurt & Sancar, 2022; Europe Pharmaceutical Care Network, 2020; Lampert, Kraehenbuehl & Hug, 2008). It distinguishes itself from other systems by differentiating between issues and their underlying causes.

Numerous studies indicate the beneficial impact of pharmacy services on patients with chronic illnesses across various settings, with some findings endorsing the proactive engagement of pharmacists to enhance medication management (Kara, Kelleci Çakır, Sancar & Demirkan, 2021). To the authors' knowledge, this is the first study evaluating DRPs and intervention acceptance in palliative care patients in Turkey using the PCNE classification system. The purpose of this study was to categorize and define the DRPs and pharmacist interventions in a Turkish public hospital's palliative care unit.

MATERIAL AND METHOD

Study design, setting, and participants

This retrospective study was conducted in a 60-bed palliative care unit at a state hospital in Eskise-hir, Türkiye. In this palliative care unit, two clinical pharmacists accompany the physician on patient visits three days a week to identify drug-related issues and deliver clinical pharmacy services. They advised physicians on these matters.

This study included patients aged 18 and older

who received over 24 hours of palliative care in the hospital from October 1, 2022, to April 1, 2023, while undergoing polypharmacy. Individuals who didn't meet the inclusion criteria for the study were excluded. Utilizing PCNE version 9.1 (Pharmaceutical Care Network, 2020), validated in Turkish, the medications in the patient files of individuals hospitalized during the study period were analyzed, and the issues regarding the medications communicated by clinical pharmacists to the physician were identified and categorized.

No sample size calculation was made for the study, including all volunteers between the determined dates. The study intended to show the actual conditions rather than to compare differences or impacts, assuming any exist.

Classification and identification

In this study, we categorized all DRPs according to the PCNE classification (V9.1), which included five components: problems (P), causes (C), planned interventions (I), intervention acceptance (A), and status of the DRPs (O). Even though a single issue may have several root causes and different solutions, there is only one result. The patient's physician or caregivers were informed of every intervention. Interventions requiring prescription adjustment were sent to the physicians. While interventions related to incorrect medication administration were communicated to the caregivers. Accepted interventions were characterized by the consensus of physicians on the suggestions, which were completely executed, leading to the total resolution of DRPs. All DRPs were identified and classified by two clinical pharmacists, with the involvement of an experienced physician. The recorded DRPs were coded consecutively by including them in the class that best described them.

Data collection

All data for the study were collected from electronic health records, patient files, and clinical pharmacist visit notes. Patient files were searched for medical history, demographic information, diagnoses, comorbidities, laboratory results, past medication history, and daily medication list. In addition, visit notes from 1 October 2022 to 1 April 2023 obtained by the clinical pharmacist through routine face-to-face conversations with patients or caregivers were used to fill in the details, such as identification of the DRP, their potential causes, planned intervention, intervention acceptance, and status of DRP. Using guidelines, published literature, and databases like Lexicomp*, Micromedex*, and Sanford Guide*, DRPs and their potential causes were identified. Clinical pharmacists' interventions to diagnose DRPs were documented, including the types and causes of DRPs that were explored.

Data analysis

Medians are used to express non-descriptive data, while numbers and percentages are used to express descriptive statistics. IBM SPSS v.23.0 software was used to evaluate the data. For all tests, p<0.05 was considered statistically significant.

Ethics committee approval

This study was approved by the Anadolu University Scientific Research and Publication Ethics Committee (Protocol number: 515938).

RESULTS AND DISCUSSION

Patients characteristics

This study included 130 patients in total. The mean age of the patients was 78 years \pm 14 (range 22-100), and 60% (n = 78) were women. Common comorbidities are hypertension (36.19%), dementia (28.49%), and diabetes mellitus (25.41%), respectively (Table 1). All patients stayed in the palliative care ward for at least one night and had their medications reviewed by the clinical pharmacists.

Table 1. Patients' Demographics

Characteristics		Total N=130 (%)
C 1	Male	52 (40.00)
Gender	Female	78 (60.00)
A ()	Mean ± SD	78 years ± 14
Age (years)	Range	22 - 100
	Hypertension	47 (36.19)
C C l : l:4:	Dementia	37 (28.49)
Common Comorbidities	Diabetes mellitus	33 (25.41)
	Previous cerebrovascular accident	27 (20.79)

Details on the DRPs

After clinical pharmacists' investigation, a total of 242 DRPs were documented, with an average rate of 1.9 per patient (min: 1, max: 9). The PCNE classification system indicated that "treatment effectiveness" (61.6%, n = 149) and "treatment safety" (38%, n = 93)

were the most prevalent issues.

The majority of DRPs related to treatment effectiveness were related to "the effect of drug treatment not optimal" (47%, n=113). All the problems related to "treatment safety" were linked to "adverse drug event (possibly) occurring" (38%, n=93) (Table 2).

Table 2. The types of problems and causes of DRPs according to PCNE Classification V9.1

Code	Classification	Total n=242(%)	Examples
Problems			
P1	Treatment effectiveness	149 (61.6)	
P1.1	No effect of drug treatment despite correct use	15 (6.2)	The patient is taking thyroid medication and has no current blood values (TSH, T3, or T4), despite having a previous TSH value that was outside the normal range.
P1.2	The effect of drug treatment not optimal	113 (47.0)	Piperacillin-tazobactam is administered in 3x4.5g doses instead of the recommended 4x4.5g dose in the patient.
P1.3	Untreated symptoms or indications	21 (8.7)	There is no use of anticoagulants for the risk of deep vein thrombosis in the high-risk patient with prolonged hospitalization.
P2	Treatment safety	93 (38.0)	
P2.1	Adverse drug event (possibly) occurring	93 (38.0)	Low potassium due to furosemide use
Causes			
C1	Drug Selection	111 (46.3)	
C1.3	Inappropriate combination of drugs, or drugs and herbal medications, or drugs and dietary supplements	91 (38.0)	There is an X-level potential drug-drug interaction between rivastigmine and metoprolol.
C1.5	No or incomplete drug treatment despite existing indication	20 (8.3)	The unknown presence of or incompletely treated infection before admission
C3	Dose Selection	41 (16.9)	
C3.1	The drug dose is too low	1 (0.4)	Insufficient dose of meropenem in a patient whose GFR value has improved
C3.2	The drug dose of a single active ingredient is too high	9 (3.7)	Although the patient's GFR was below 30mL/min/1,73m², meropenem dose was not adjusted according to renal function.
C3.3	The dosage regimen is not frequent enough	15 (6.2)	Piperacillin-tazobactam is administered in 3x4.5g doses instead of the recommended 4x4.5g dose in the patient.
C3.4	The dosage regimen is too frequent	16 (6.6)	The dose of ceftriaxone that should be given at once was given by dividing it.
C7	Patient related	74 (31.0)	
C7.8	Patient unintentionally administers/ uses the drug in the wrong way	74 (31.0)	The caregiver was incorrectly administering medications that should have been administered through a nasogastric tube.
C9	Other	16 (6.6)	
C9.1	No or inappropriate outcome monitoring (incl. TDM)	16 (6.6)	Theophylline blood level was not monitored in the patient.

Causes of DRPs

As shown in Table 2, the primary cause of DRPs was "drug selection" (46.3%, n=111), followed by "patient related" (31%, n=74) and "dose selection" (16.9%, n=41). The most frequently observed cause related to drug selection is "inappropriate combination of drugs, or drugs and herbal medications, or drugs and dietary supplements". The most common cause for DRP classified under subheading is "inappropriate combination of drugs, or drugs and herbal medications, or drugs and dietary supplements" (38.0%, n=91), followed by "patient unintentionally

administers/uses the drug in the wrong way" (31.0%, n=31).

Interventions and acceptance

Clinical pharmacists performed 235 (97.1%) interventions in total; for 7 (2.9%) of the DRPs, no intervention was made. The majority of interventions were at "the prescriber level" (43.2%, 106), and it was followed by "the patient level" (31.0%, 74) and "spoken to family member/caregiver" (31.0%, 74), respectively (Table 3). Outcomes of the interventions according to PNCE V9.1 classifications were shown in Figure 1.

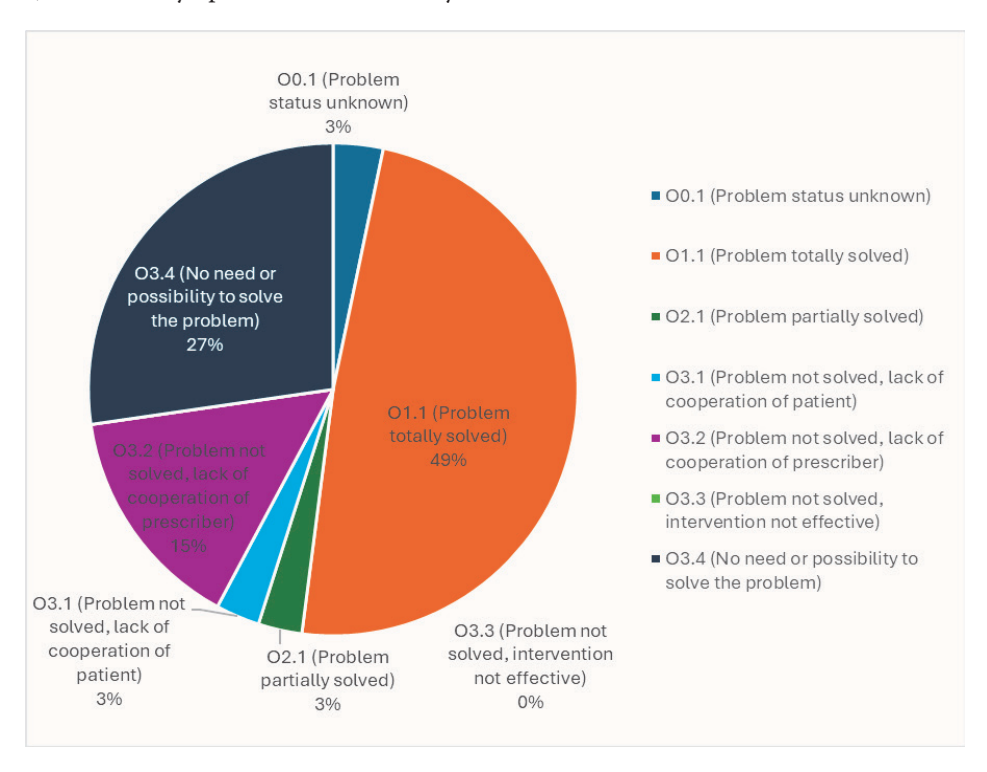


Figure 1. Outcomes of the interventions according to PNCE V9.1 classifications

A total of 132 (55.0%) interventions were accepted, and 115 (48.0%) of them were coded as A1.1 "intervention accepted and fully implemented". However, 52 (21.2%) interventions were not accepted, and 15 (6.2%) of them were coded as "A2.1 intervention not accepted: not feasible", and 37 (15.0%) DRPs were coded as "A2.2 intervention not accepted: no agreement". Finally, 58 (24.0%) DRP interventions were not proposed (A3.2) (Table 3). According to the details of the PCNE V9.1 intervention categories, their accep-

tance rates were shown in Figure 2.

Status of DRPs

Looking at the final status of DRPs, 8 (3.3%) problems are status unknown, 118 (48.8%) problems are totally solved, 7 (2.9%) problems are partially solved, and 109 (45.1%) problems are not solved. Causes of not solved problems are, respectively, "no need or possibility to solve the problem" (27.3%, 66), "lack of cooperation of prescriber" (14.9%, 36), and "lack of cooperation of the patient" (2.9%, 7) (Table 3).

Table 3. The types of interventions, acceptance, and status of DRPs according to PCNE Classification V9.1

Planned 1	interventions	N (%)
I0	No intervention	7 (2.9)
I0.1	No Intervention	7 (2.9)
I1	At the prescriber level	106 (43.2)
I1.1	The prescriber informed only	19 (7.9)
I1.2	The prescriber asked for information	35 (14)
I1.3	Intervention proposed to prescriber	20 (8.3)
I1.4	Intervention discussed with prescriber	32 (13)
I2	At the patient level	74 (31.0)
I2.4	Spoke to a family member/caregiver	74 (31.0)
I3	At drug level	55 (22.9)
I3.2	Dosage changed to	6 (2.5)
I3.5	The drug was paused or stopped	36 (15.0)
I3.6	Drug started	13 (5.4)
Intervent	ion Acceptance	<u>'</u>
A1	Intervention accepted	132 (55.0)
A1.1	Intervention accepted and fully implemented	115 (48.0)
A1.2	Intervention accepted, partially implemented	11 (4.5)
A1.4	Intervention accepted, implementation unknown	6 (2.5)
A2	Intervention not accepted	52 (21.2)
A2.1	Intervention not accepted: not feasible	15 (6.2)
A2.2	Intervention not accepted: no agreement	37 (15.0)
A3	Other	58 (24.0)
A3.2	Intervention not proposed	58 (24.0)
Status of	the DRP	
O0	Problem status unknown	8 (3.3)
O0.1	Problem status unknown	8 (3.3)
O1	Problem solved	118 (48.8)
O1.1	Problem totally solved	118 (48.8)
O2	Problem partially solved	7 (2.9)
O2.1	Problem partially solved	7 (2.9)
O3	Problem not solved	109 (45.1)
O3.1	The problem was not solved, a lack of cooperation from the patient	7 (2.9)
O3.2	The problem was not solved, a lack of cooperation from the prescriber	36 (14.9)
O3.4	No need or possibility to solve the problem	66 (27.3)

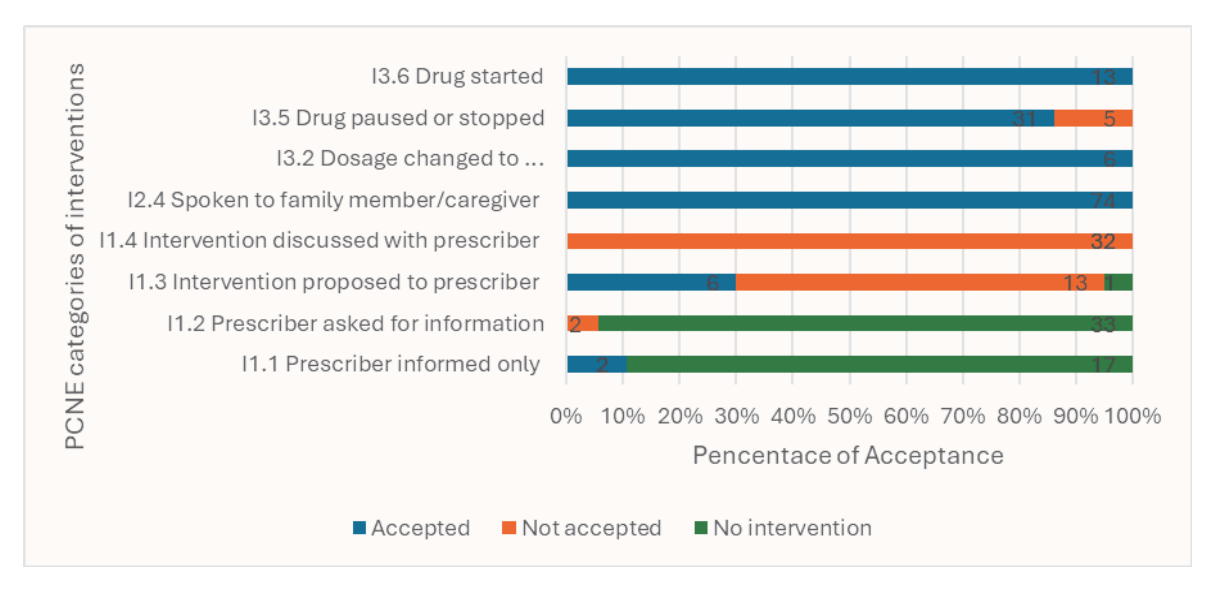


Figure 2. The details of the PCNE V9.1 intervention categories, their acceptance rate

CONCLUSION

Drug-related problems include inherent risks for both patients and prescribers, particularly in palliative care settings where patients are severely ill and time constraints are significant. DRPs may result from a patient's comorbidities, general vulnerability, and high prevalence of polypharmacy. To avoid potential harm from DRPs, rational and appropriate prescribing must be enabled, prescribing errors reduced, and potential DRPs identified (Wernli et al., 2023). Therefore, medication reviews conducted by clinical pharmacists and their recommendations about DRPs are important. This study illustrates that DRPs in a palliative care unit can be identified and resolved through pharmacist-led monitoring of the medication process. This may enhance the efficacy and safety of pharmacological treatment.

Pharmacists play a variety of roles in palliative care, including reviews and reconciliations of medications, medication counseling, education and training, administrative duties, direct patient care, and contributions to scholarship and education (Wernli et al., 2023). Pharmacists have been shown to be valuable in these roles in a variety of contexts, but there is still a dearth of evidence regarding palliative care.

In this study, an average of 1.9 DRPs could be recorded for each palliative care patient through DRP evaluation. In other studies, the number of DRPs per patient is probably higher because the patients were treated for a longer period of time than in the study that was presented. Major problems of DRPs are treatment effectiveness and adverse drug events, and DRPs main reasons are drug selection or patient-related issues in this study. Rami et al. also reported the detection and classification of DRPs in palliative care patients in Germany. During their 12-month period, 207 DRPs were documented for 41 patients; the problems and causes of these DRPs are similar to the current study (Rémi, Bauer, Krumm & Bausewein, 2022). In another study about geriatric patients' DRPs (Hailu et al., 2020), 200 patients were included, and 380 DRPs (1.90 per patient) were identified. Treatment effectiveness is the most common reason for DRPs and followed by treatment safety (adverse drug event), as in our study. The inclusion of a pharmacist in the home care setting, as demonstrated in a study by Hussainy et al. (2011), resulted in the identification of numerous drug-related problems (120 DRPs across 46 patients). The current study and others (Hailu et al., 2020; Remi et al., 2022) offered the majority of the interventions at the prescriber level.

Higher acceptance rates are seen at the patient/caregiver level and drug level. At the prescriber level, generally there is no need for intervention, or the prescriber was informed only. But almost half of the total interventions are accepted, and problems are totally solved. Other studies (Remi et al., 2022; Cheng et al., 2022) may have higher acceptance and solved problems rates, but in our center, this is the first time clinical pharmacists are involved. Therefore, an increase in these rates is expected as the adaptation process continues. In addition, many of the interventions that cannot be fully resolved or accepted are due to the low life expectancy of the patients and the aim to alleviate more symptomatic findings.

The knowledge of pharmacists regarding medications contributes to the reduction of medication errors, enhances symptom management, and increases the team's awareness of drug utilization. The pharmacist's knowledge of pertinent medication therapies benefits patients and the palliative care team. Working in palliative care units with clinical pharmacists generally resulted in better coordination of identification and mitigation of potential harms like drug interactions, inappropriate dosing, or abnormal drug-taking behaviors, and optimized medication regimens with improved adherence (Atayee, Sam, & Edmonds, 2018; Hanley, Spargo, Brown & Magee, 2021). This study anticipates that these favorable outcomes will improve due to the collaboration among physicians, healthcare professionals, caregivers, and clinical pharmacists. The findings indicate that DRPs in palliative care create a significant issue. Specialized professionals in drug therapy, such as clinical pharmacists, are essential in palliative care units as well as other hospital settings. In palliative units with elderly populations with polypharmacy and various comorbidities, the inclusion of a team member specializing in drug therapy may be beneficial in minimizing potential issues.

The pharmacist's notes, which combined written and in-person interactions with the caregiver or palliative care team, were used in this study. The pharmacist recognized the drug-related problem and determined the appropriate intervention based on the associated risk level. Issues were addressed by physicians or caregivers. Relevant information regarding the DRP or the associated intervention was documented in the patient record to ensure dissemination among the physicians. Manifest DRPs necessitating intervention (e.g., dosages substantially above the authorized range, severe adverse effects, etc.) were thoroughly addressed with the physician during ward rounds. The combination of in-person discussions and written material allows for the clear emphasis of the intervention's clinical relevance and the clarification of any possible questions. The intervention's acceptance or non-acceptance was promptly acknowledged. In instances of non-acceptance, justification was readily available, allowing the pharmacist to propose a potential alternative.

There are some limitations in this study. This study emphasizes the significance of the clinical pharmacist in identifying and addressing DRPs in a palliative care unit at a hospital that previously did not provide normal clinical pharmacy services. This study is constrained by its brief length and the small patient sample size. The lack of a clinical pharmacist on staff to consult during training is a considerable constraint. Executing research with a greater cohort of residents, over an extended duration, and involving a clinical pharmacy specialist would more accurately represent the effects of proposed solutions and clinical pharmacy interventions for DRPs. The findings of this study, done in a single center, cannot be applied to other internal medicine wards. The patients' low life expectancy and the aim to alleviate more symptomatic findings have led to a lower acceptance rate of the proposals compared to other studies.

This study identified a minimum of 1.9 DRPs per patient admitted to the palliative care unit. The predominant issues and origins of DRPs were treatment effectiveness and drug selection, respectively. The majority of the interventions were implemented at the prescriber level. The healthcare team's accep-

tance rate for these interventions was lower than that documented in the literature. Nonetheless, given that clinical pharmacy services were not regularly offered at this hospital, this acceptance can be regarded as a successful initial benchmark. Clinical pharmacists and other healthcare providers must collaborate to reduce drug-related problems while providing pharmaceutical care. Multidisciplinary patient care teams will enhance therapeutic outcomes. This research takes a position among the few studies in the literature addressing the detection, resolution, and prevention of DRPs in palliative care units.

AUTHOR CONTRIBUTION STATEMENT

Concept: Ö.G., K.T.; Design: Ö.G., K.T.; Supervision: K.T.; Resources: Ö.G., K.T.; Data Collection and/or Processing: Ö.G.; Analysis and/or Interpretation: Ö.G., K.T.; Literature Review: Ö.G., K.T.; Writing the Article: Ö.G.; Critical Review: K.T.

CONFLICT OF INTERESTS

The authors declare that there is no conflict of interest.

REFERENCES

- Abunahlah, N., Elawaisi, A., Velibeyoglu, F. M., & Sancar, M. (2018). Drug-related problems identified by clinical pharmacist at the internal medicine ward in Turkey. *International Journal of Clinical Pharmacy*, 40(2), 360–367. https://doi.org/10.1007/s11096-018-0596-3
- Atayee, R. S., Sam, A. M., & Edmonds, K. P. (2018). Patterns of palliative care pharmacist interventions and outcomes as part of inpatient palliative care consult service. *Journal of Palliative Medicine*, 21(12), 1781–1787. https://doi.org/10.1089/jpm.2018.0276
- Ayhan, Y. E., Karakurt, S., & Sancar, M. (2022). The effect of the clinical pharmacist in minimizing drug-related problems and related costs in the intensive care unit in Turkey: A non-randomized controlled study. *Journal of Clinical Pharmacy and Therapeutics*, 47(11), 1867–1874. https://doi.org/10.1111/jcpt.13718

- Basger, B. J., Moles, R. J., & Chen, T. F. (2015). Development of an aggregated system for classifying causes of drug-related problems. *Annals of Pharmacotherapy*, 49(4), 405–418. https://doi.org/10.1177/1060028014568005
- Cheng, H. T., Zhao, M., Liu, H. T., Shen, G. L., Zhao, T., & Feng, Z. E. (2022). The prevalence of chronic medication therapy problems and pharmacists' interventions among hospitalized perioperative patients: A retrospective observational study. *BMC Health Services Research*, 22(1), 1483. https://doi.org/10.1186/s12913-022-08948-7
- Cortejoso, L., Dietz, R. A., Hofmann, G., Gosch, M., & Sattler, A. (2016). Impact of pharmacist interventions in older patients: A prospective study in a tertiary hospital in Germany. *Clinical Interventions in Aging, 11*, 1343–1350. https://doi. org/10.2147/CIA.S114580
- Europe Pharmaceutical Care Network. (2020). The PCNE classification V 9.1. Retrieved from https://www.pcne.org/upload/files/417_PCNE_classification_V9-1_final.pdf
- Hailu, B. Y., Berhe, D. F., Gudina, E. K., Gidey, K., & Getachew, M. (2020). Drug-related problems in admitted geriatric patients: The impact of clinical pharmacist interventions. *BMC Geriatrics*, 20(1), 13. https://doi.org/10.1186/s12877-020-1425-7
- Hanley, J., Spargo, M., Brown, J., & Magee, J. (2021). The development of an enhanced palliative care pharmacy service during the initial COVID-19 surge. *Pharmacy (Basel)*, 9(4), Article 209. https://doi.org/10.3390/pharmacy9040209
- Hussainy, S. Y., Box, M., & Scholes, S. (2011). Piloting the role of a pharmacist in a community palliative care multidisciplinary team: An Australian experience. *BMC Palliative Care*, *10*, 16. https://doi.org/10.1186/1472-684X-10-16

- Kara, E., Kelleci Çakır, B., Sancar, M., & Demirkan, K. (2021). Impact of clinical pharmacist-led interventions in Turkey. *Turkish Journal of Pharmaceutical Sciences*, 18(4), 517–526. https://doi. org/10.4274/tjps.galenos.2021.98167
- Krishnaswami, A., Steinman, M. A., Goyal, P., Zullo, A. R., Anderson, T. S., Birtcher, K. K., ... Tjia, J. (2019). Deprescribing in older adults with cardiovascular disease. Journal of the *American College of Cardiology*, 73(20), 2584–2595. https://doi.org/10.1016/j.jacc.2019.03.467
- Krumm, L., Bausewein, C., & Rémi, C. (2023). Drug therapy safety in palliative care-pharmaceutical analysis of medication processes in palliative care. *Pharmacy (Basel)*, *11*(5), Article 138. https://doi.org/10.3390/pharmacy11050138
- Lampert, M. L., Kraehenbuehl, S., & Hug, B. L. (2008). Drug-related problems: Evaluation of a classification system in the daily practice of a Swiss university hospital. *Pharmacy World & Science*, 30(6), 768–776. https://doi.org/10.1007/s11096-008-9236-1

- Rémi, C., Bauer, D., Krumm, L., & Bausewein, C. (2022). Drug-related problems on a palliative care unit. *Journal of Pain & Palliative Care Pharmacotherapy*, *35*(4), 264–272. https://doi.org/10.1080/15360288.2022.2128393
- Selcuk, A., Sancar, M., Okuyan, B., Demirtunc, R., & Izzettin, F. V. (2015). The potential role of clinical pharmacists in elderly patients during hospital admission. *Pharmazie*, 70(8), 559–562.
- Tatum, P. E., & Mills, S. S. (2020). Hospice and palliative care: An overview. *Medical Clinics of North America*, 104(3), 359–373. https://doi.org/10.1016/j.mcna.2019.12.007
- Viktil, K. K., & Blix, H. S. (2008). The impact of clinical pharmacists on drug-related problems and clinical outcomes. *Basic & Clinical Pharmacology & Toxicology*, 102(3), 275–280. https://doi.org/10.1111/j.1742-7843.2007.00191.x
- Wernli, U., Hisciher, D., Meier, C. R., Jean-Petit-Matile, S., Kobleder, A., & Mayer-Massetti, C. (2023). Pharmacists' clinical roles and activities in inpatient hospice and palliative care: A scoping review. *International Journal of Clinical Pharmacy*, 45(3), 577–586. https://doi.org/10.1007/s11096-022-01493-w

Development and Validation of an UPLC-MS/MS Method for Quantification of Glyphosate in Urine

Göksel KOÇ MORGİL*, Ismet ÇOK ***

Development and Validation of an UPLC-MS/MS Method for Quantification of Glyphosate in Urine

SUMMARY

For the last four decades, the herbicide glyphosate has been the most widely used herbicide worldwide, including in Turkey, with the assumption that it has insignificant effects on the human and environmental health. However, particularly for the last decade, global concerns have escalated about the potential direct and indirect health risks it may pose to humans and ecosystems due to its high-volume use. Due to these increasing health concerns, especially cancer, the development of methods to detect traces of this herbicide in biological materials is of great importance for the protection of public health. To assess glyphosate exposure levels, it is crucial to have a selective, sensitive, and precise analytical procedure that can determine low glyphosate concentrations, especially in complex biological matrices. In the presented study, we developed and validated an Ultra-performance chromatography-mass spectrometry (UPLC-MS/MS) procedure for the accurate and sensitive determination of glyphosate levels in urine. It is based on the "dilute and shoot" technique with no derivatization procedure and is quantitatively determined by UPLC-MS/MS. The advantages of this methodology are simplicity, minimal analyte loss, and high sample yield. The calibration curve for glyphosate was linear in the concentration range of 0.1-50 ng/ mL. The limit of quantification (LOQ) for glyphosate was 0.1 ng/ mL. This validated method can be applied very quickly and easily in the analysis of spot urine samples collected from healthy people.

Key Words: Glyphosate, herbicide, urine, UPLC-MS/MS

İdrarda Glifosatın Kantitatif Analizi için bir UPLC-MS/MS Yönteminin Geliştirilmesi ve Doğrulanması

ÖZ

Son 40 yıldır, Glifosat, çevre ve insan sağlığı üzerinde ihmal edilebilir etkileri olduğu varsayımıyla Türkiye de dahil olmak üzere tüm dünyada en yaygın kullanılan herbisittir. Ancak, özellikle son on yılda, glifosatın yüksek miktarlarda kullanımı nedeniyle insan sağlığı ve ekosistemler üzerindeki potansiyel doğrudan ve dolaylı etkileri konusunda küresel olarak endişeler artmıştır. Başta kanser olmak üzere, artmış sağlık endişeleri nedeniyle insan biyolojik örneklerinde bu herbisitin kalıntılarını tespit etmeye yönelik yöntemlerin geliştirilmesi halk sağlığının korunması açısından büyük önem taşımaktadır. Glifosat maruziyet düzeylerini değerlendirmek için, özellikle karmaşık örnek matrislerinde düşük glifosat konsantrasyonlarını tespit edebilen seçici, hassas ve doğru bir analitik yönteme sahip olmak önemlidir. Sunulan çalışmada, idrardaki glifosat seviyelerinin doğru ve hassas bir şekilde belirlenmesi için ÜPLC-MS/MS yöntemi geliştirilmiş ve valide edilmiştir. Hiçbir türevlendirme prosedürü olmayan ve ultra performanslı sıvı kromatografisi-tandem kütle spektrometrisi ile kantitatif olarak belirlenen, "seyrelt ve enjekte et" tekniğine dayanmaktadır. Bu metodolojinin avantajları basitlik, minimum analit kaybı ve yüksek numune verimidir. Glifosata ait kalibrasyon eğrisi 0.1- 50 ng/mL konsantrasyon aralığında doğrusaldı. Glifosat için tayin limiti (LOQ) 0,1 ng/mL dir. Valide edilmiş/doğrulanmış bu yöntem, sağlıklı kişilerden toplanan spot idrar örneklerinin analizinde çok hızlı ve kolay bir şekilde uygulanabilme özelliğindedir.

Anahtar Kelimeler: : Glifosat, Herbisit, İdrar, UPLC-MS/MS.

Received: 7.04.2025 Revised: 16.06.2025 Accepted: 17.07.2025

ORCID: 0000-0001-8614-9671, Minister of Health, General Directorate of Public Health, Department of Consumer Safety and Public Health Laboratories, Toxicology Laboratory, Sihhiye, Ankara, Turkey

[&]quot;ORCID: 0000-0003-3128-677X, Gazi University, Faculty of Pharmacy, Department of Toxicology, 06330, Hipodrom, Ankara, Turkey

INTRODUCTION

The ever-increasing human population and decreasing agricultural lands require the development of new strategies for effective crop management. At the forefront of these strategies are herbicide applications, which aim to eliminate small plants and weeds that cause serious losses in agriculture. Glyphosate (N-(phosphonomethyl) glycine) (C3H8NO5P) is the active ingredient developed by Monsanto under the name Roundup in the 1970s. It quickly became one of the most widely used herbicides in many communities and regions of the World. It is the most popular organophosphate herbicide and has become indispensable in the agricultural sector in more than 140 countries and regions due to its non-selectiveness, high efficiency, and compatibility with genetically modified agricultural products (Jiang et al., 2025). Today, it is an herbicide with widespread post-emergence application in Türkiye to control grass and broadleaf weed species both in agricultural and non-agricultural areas such as gardens, parks, etc.

Humans are exposed to this herbicide through several routes, including oral, dermal, and inhalation, as well as through the food chain, soil, air, water, and surrounding fauna and flora. For example, dust ingestion is a significant exposure route, especially in indoor environments near agricultural regions (Galli et al., 2024; Ben Khadda et al., 2025).

There is a great debate both in the scientific community and among various health authorities regarding the toxic effects of exposure to glyphosate in humans. Studies conducted in recent years in particular, have reported that glyphosate exposure may cause atherosclerosis, neurological effects, and alterations in the intestinal microbiome. Furthermore, links have also been found for increased risks of allergic respiratory symptoms and follicular lymphoma. Thus, both in the scientific community and in the general population, glyphosate is suspected to act as a mutagenic, carcinogenic, and a neurotoxic substance (Van Brug-

gen et al., 2018). The International Agency for Research on Cancer (IARC) (IARC, 2016) has classified glyphosate as "probably carcinogenic to humans" in Group 2A. However, the European Chemicals Agency (ECHA) and the European Food Safety Authority (EFSA) have classified glyphosate as "non-carcinogenic to humans" (ECHA, 2017; EFSA, 2015), and the U.S. Environmental Protection Agency (EPA) has classified it as Category IV, meaning practically non-toxic and non-irritating (EPA, 2016). In 2017, the European Commission (EC) permitted the use of glyphosate for another five years. The EC's decision on the continued use of glyphosate was suspended in 2022. Later, in November 2023, the Commission approved the use of glyphosate in herbicide applications until 2033 (EC, 2023). However, member states are allowed to implement different rules at the national level. While no EU country has currently banned glyphosate entirely, some, such as Austria, France, the Netherlands, Belgium, Luxembourg, and Germany, have introduced partial bans that prohibit its use in certain regions. In addition, the risk of glyphosate causing soil and water pollution increases, especially if applied incorrectly. Therefore, exposure to glyphosate residue levels through environmental routes such as drinking water, surface water, and groundwater can pose a significant threat to human health and ecosystems. For example, information is increasing on the negative effects of glyphosate on marine organisms in the aquatic ecosystem, including fish and mollusks (Parlapiano et al., 2021; Ames, Miragem, Cordeiro, Cerezer & Loro, 2022).

The accumulating evidence of the adverse effects of glyphosate on both ecosystem integrity and human health highlights that the use of this herbicide is becoming a serious public health crisis not only locally but also globally. Recent scientific findings, in particular, suggest that strict restrictions on the use of this chemical and, ultimately, its ban are critical steps

that must be taken without delay. For these reasons, there is a need for sensitive, rapid, and reliable analysis methods that can facilitate the biomonitoring of human exposure to glyphosate and assess the health risks that may develop due to exposure. In the presented study, an improved UPLC-MS/MS analysis procedure with the specified features has been developed for this need.

MATERIALS AND METHODS

Chemicals

Glyphosate and 1,2-¹³C₂ ¹⁵N-Glyphosate were obtained from HPC Standards GmbH. Methanol, acetonitrile, formic acid, and ultrapure water were obtained from Sigma Aldrich. All solvents used in this study were HPLC grade. The representative chemical structures of the target compounds are presented in Figure 1.

Figure 1. The representative chemical structures of glyphosate and 1,2-13C, 15N-Glyphosate

Instrumentation

Identification and quantification of the target analytes were carried out using a liquid chromatography triple quadrupole/trap mass spectrometer, QTRAP 5500 (Applied Biosystem, SCIEX, Singapore).

Sample preparation

1,2- 13 C $_2$ 15 N-Glyphosate (≥ 95%) was used as an internal standard (IS) for glyphosate determination and was added to the samples at the beginning of the analysis. The urine samples (900 μ L) were mixed with water containing 5 μ g/mL 1,2- 13 C $_2$ 15 N-Glyphosate (100 μ l) as an IS before vortex mixing. After that, the sample was diluted 1:10 with water. It was transferred to a polypropylene vial, and a 10 μ L aliquot was used for the UPLC-MS/MS application.

Analytical conditions

The liquid chromatography operating conditions established for this study were as follows: A Torus DEA (Waters Corporation, Milford, MA, USA; 2.1 mm x 100 mm; 1.7 μ m) column was preferred to separate the analytes from matrix components while the

column oven was held at 40 °C. The mobile phase A consisted of water with 1.2% formic acid. The mobile phase B consisted of acetonitrile with 0.6% formic acid. The analysis for glyphosate was performed using the following gradient (%B) program at a flow rate of 0.5 mL/min: 0 min, 90%; 0.5 min, 90%; 1.5 min, 20%; 4.5 min, 10%; 17.5 min, 10%; and 17.6 min, 90%. The re-equilibration of the column to the initial conditions lasted 6 min. The total run time was 24 min.

The mass spectrometry conditions were as follows: A Mass spectrometer coupled with electrospray ionization (ESI) interfaces was used in a negative ion mode. Nitrogen (N_2) was used as a nebulizer gas (55 psi). The source temperature and ion spray voltage were fixed at 550 °C and 4000 V, respectively. Optimization results for each analyte in multiple reaction monitoring scan mode are presented in Table 1. Glyphosate and 1,2- $^{13}C_2$ ^{15}N -Glyphosate were assayed by quantifying the multiple reaction monitoring transition of the [M + H]- ion of glyphosate at m/z 167.9 \rightarrow 63.0 and 1,2- ^{15}N -Glyphosate at m/z 170.9 \rightarrow 63.0 (Table 1).

I	1	71	I J .	71	,	- 2	1
Compounds	Precursor ion (m/z)	Product ion (m/z)	Declustering potential [V]	Entrance potential [V]	Collision energy [V]	Cell exit potential [V]	Dwell time [ms]
Glyphosate Quantifier Io 11	167.9	63.0	85	10	-32.0	-9.0	500
Glyphosate Qualifier Ion	167.9	150.0	85	10	-14.0	-11.0	500
1,2-13C,15N-Glyphosate	170.9	63.0	85	10	-32.0	-9.0	500

Table 1. Optimal mass spectrometry parameters provided for the Glyphosate and 1,2-13C₂15N-Glyphosate

RESULTS

Method validation

The method was validated according to the US FDA guidelines for bioanalytical methods (FDA, 2018). Due to the lack of a matrix, the method validation was carried out with the help of synthetic urine. The synthetic urine used in our study was prepared following the guidelines of the Centers for Disease Control and Prevention (CDC). One liter of synthetic urine was prepared by adding 24.5 g urea, 8.5 g sodium chloride, 3.8 g potassium chloride, 1.4 g creatinine, 1.03 g citric acid, 1.18 g potassium phosphate, 0.64 g sodium hydroxide, 0.47 g sodium bicarbonate, 0.34 g ascorbic acid, and 0.28 mL sulfuric acid in deionized water (NCEH, 2010).

Standard solutions, calibration standards, and quality control samples

The standard stock solution of glyphosate was prepared in water (1 mg/mL). The working solutions of glyphosate were prepared by proper dilution of these stock solutions in synthetic urine with 0.1 % formic

acid, which included 2 ng/mL $1,2^{-13}C_2^{-15}N$ -Glyphosate (1 mL). The calibration standards, quality control (QC) samples (at low, medium, and high concentrations), samples at the lower limit of quantification (LOQ), and limit of detection (LOD), were prepared by spiking the synthetic urine with a known quantity of compounds. The set of concentrations of the analytes in the quality control samples and of calibration curve are shown in Table 2.

A calibration curve was prepared for glyphosate to enable quantitative analyses. For this purpose, glyphosate standards were added to synthetic urine samples corresponding to concentrations of 0.1, 0.5, 1, 5, 10, 25, and 50 ng/mL. These concentrations were injected into the LC-MS/MS device three times to achieve the best possible values. Concentration-dependent responses were calculated from glyphosate standards prepared in synthetic urine and measured with a 7-point calibration curve having a linear range of 0.1–50 ng/mL. The regression equation for glyphosate was obtained as y = 0.23774x - 0.01121 ($R^2 = 0.9934$).

Table 2. *Selected concentrations of analytes in quality control samples and calibration curve ranges (ng/mL).*

	Calibration	Lower limit of	Limit of	Low-quality	Medium-quality	High-quality
	range	quantification	detection	control	control	control
		(LOQ)	(LOD)	(QC1)	(QC2)	(QC3)
Glyphosate	0.1-50	0.1	0.03	1	10	50

For intraday and interday precision, QC samples and LOQ were prepared by spiking the synthetic urine with a known quantity of analyte standards. Each sample was analyzed ten times to determine intraday precision. Each sample was analyzed once on five separate days within 2 months for interday precision.

The precision and accuracy of the LOQ and QC samples obtained in this method development study are presented in Table 3. The intraday accuracy ranged from 98.60 to 100.81%, whereas the interday accuracy ranged from 96.67 to 100.38%. The precision was expressed as a CV% that varied depending on the con-

centration. It was determined that intraday precision varied between 1.06% and 2.49%, while interday precision varied between 2.01% and 3.58%.

Glyphosate chromatograms shown for blank samples (synthetic urine), synthetic urine spiked with the

LOQ level (0.1 ng/mL), and synthetic urine spiked with 1 ng/mL are shown in Figure 2 and Figure 3. The internal standard, $1,2^{-13}C_2^{-15}N$ -Glyphosate (2 ng/mL) (m/z 170.9 \rightarrow 63), was used in the analysis.

Table 3. *Intraday and interday accuracy and precision were obtained for the analytes in synthetic urine.*

	Lower limit of quantification (LOQ)	Low-quality control (QC1)	Medium-quality control (QC2)	High-quality control (QC3)
Intraday accuracy [%]				
Glyphosate	98.60	100.33	100.37	100.81
Intraday precision [%]				
Glyphosate	2.35	2.49	1.06	1.67
Interday accuracy [%]				
Glyphosate	96.67	100.14	100.07	100.38
Interday precision [%]				
Glyphosate	3.58	2.85	2.01	2.02

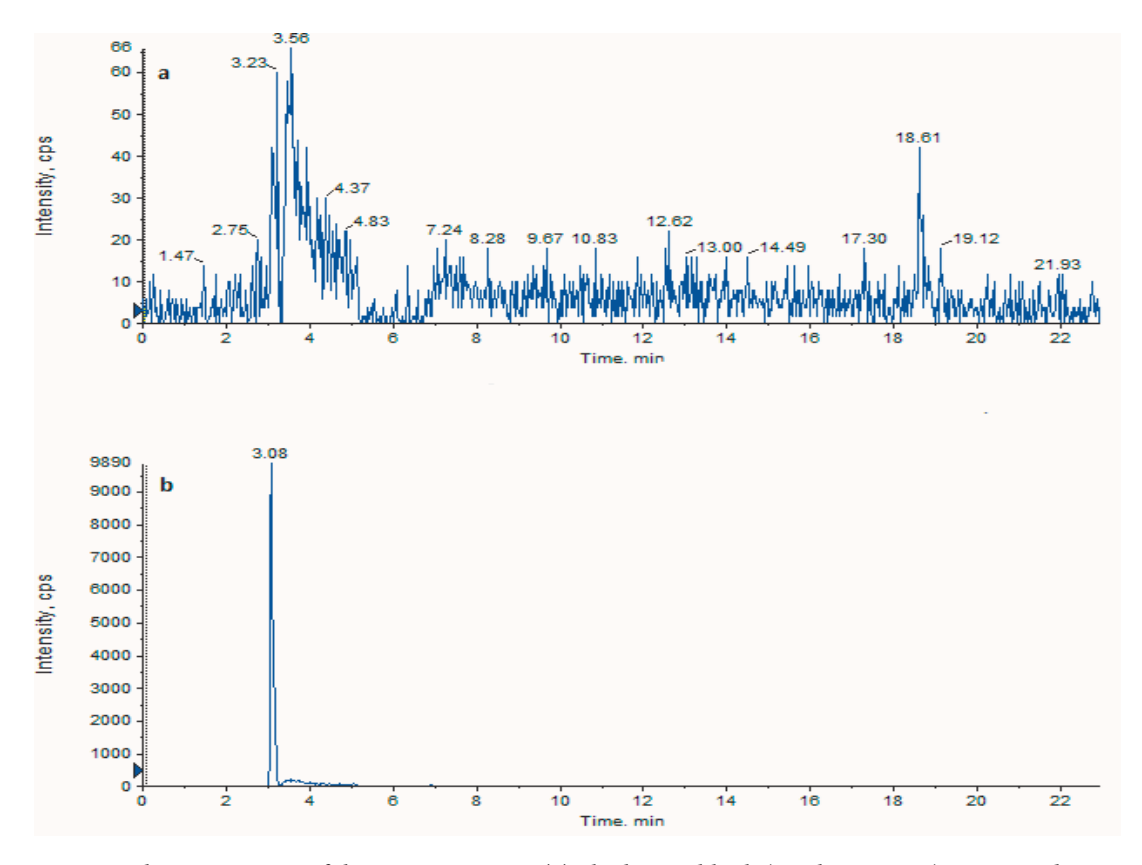


Figure 2. Chromatograms of the ion transitions: **(a)** glyphosate blank (synthetic urine) monitored at m/z 167.9→63, **(b)** 1,2-13C2 15N-Glyphosate (IS) (2 ng/mL) monitored at m/z 170.9→63.

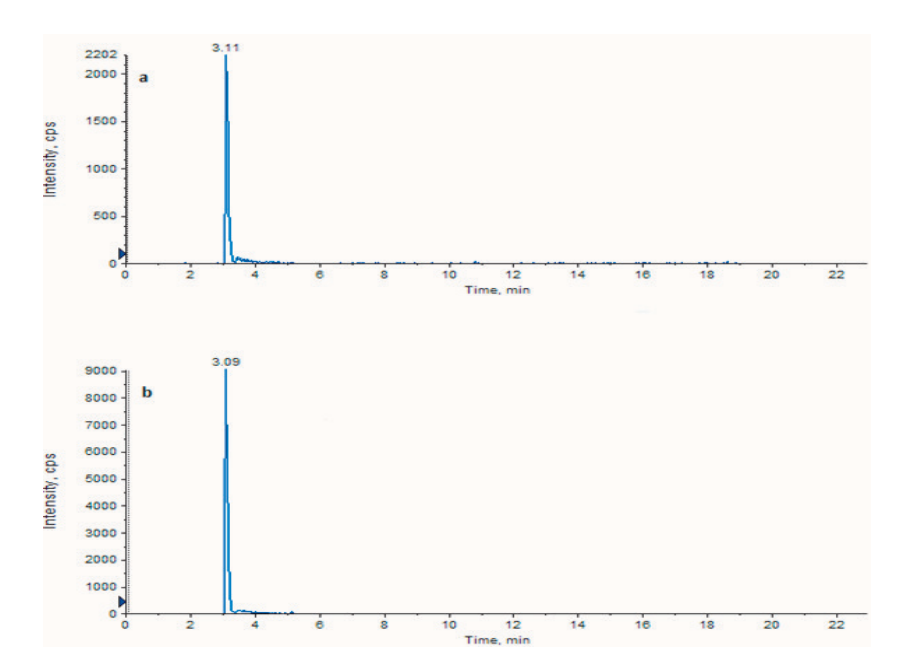


Figure 3. Chromatograms of the ion transitions: (a) for 1ng/ml glyphosate monitored at m/z 167.9→63, (b) 1,2-13C2 15N-Glyphosate (I.S) (2 ng/mL) monitored at m/z 170.9→63.

DISCUSSION

Pesticides are chemicals developed to control or eliminate pests primarily in agricultural areas and are the most important chemicals used to increase the yield of agricultural products. Herbicides are a group of pesticides used most widely and in large volumes in all societies. Due to this widespread use, unwanted/ unexpected risks may occur to humans and the environment due to exposure from application areas or residues in the product obtained. Glyphosate, which is used as an herbicide in many countries, is currently the highest volume herbicide used globally in both agricultural applications and non-agricultural areas to control invasive weeds.

Concerns about various health risks caused by glyphosate are increasingly disturbing societies. Therefore, in this presented study, a fast UPLC-MS/MS analytical procedure was developed and characterized for the quick separation and quantification of glyphosate in urine for routine applications for assessment of exposure levels. Quantification of xenobiotics such as pesticides themselves or their metabolites in biological samples such as urine or blood (i.e., biomoni-

toring) allows for the assessment of exposure levels to these chemicals and the health risks that may arise at these levels (Barr, 2008).

Glyphosate does not undergo extensive biotransformation in the human body and, the parent compound can be detected in urine. Glyphosate is one of the polar pesticides. The high water solubility of glyphosate and its low affinity for organic matter (Log Kow < 3.4) (Acquavella et al., 2004) make urine the most widely used biological material for monitoring human exposure to glyphosate. In order to determine human exposure to this herbicide, glyphosate and its major degradation product, aminomethylphosphonic acid (AMPA), can also be detected in other biological materials, such as blood/serum, breast milk, and meconium. AMPA has a level of toxicity comparable to glyphosate and is therefore considered to be of similar toxicological importance (EFSA, 2022). Glyphosate is excreted in both urine and feces as an unchanged compound in greater amounts than its parent metabolite AMPA (Leblanc, Breton, Léveillé, Tessier, & Pelletier, 2024; Peillex & Pelletier, 2020). The number of studies providing quantitative data on the AMPA metabolite is quite scarce.

Regardless of the analytical strategy followed, the most critical step is method validation. Validation is the entirety of the processes performed to demonstrate that the success of a device, method, or system complies with the specified conditions. It is a test and measurement process performed according to a set of variables to determine the performance of a method. Many decisions in various fields are made based on the results of the measurements made. To make the right decision, it is desired that the analytical measurement result is accurate and reliable (repeatable) (FDA, 2018). In this step, a wide range of experiments should be performed to obtain appropriate selectivity, sensitivity, accuracy, recovery, and precision. In our study, we tried to contribute to the most reliable results that can be obtained in human biomonitoring studies of glyphosate by performing these steps for method validation.

Different methods are used for extraction in glyphosate determination studies in urine. For example, while some studies performed liquid-liquid extraction for pretreatment, many studies preferred solid phase extraction (SPE) in method development. In addition to the methods that use a derivatization process, some studies perform the analysis with dilution methods. There are also studies utilizing immunoassay methodology, which is considered a less reliable method for measuring glyphosate levels due to lower sensitivity and higher false positive rates, and the LOD in these studies ranged from 0.9 to 7.5 ng/mL (Acquavella et al., 2004; Curwin et al., 2007).

Other studies have performed glyphosate analysis in urine with low LOD values (0.15-2.0 ng/ml) using the more sensitive GC-MS or HPLC/MS techniques. The analytical methods that have been developed for the detection of glyphosate were reviewed and discussed by Wei et al. (2024). Among these different methods, MS analysis quickly provides accurate results. Being selective, sensitive, and accurate at even trace amounts of glyphosate concentrations and requiring no derivatization in the method, LC-MS/MS is the primary used LC technique for specifying

glyphosate and for glyphosate-related evaluation of biological samples. On the other hand, electrospray ionization (ESI), one of the ionization modes used to determine the fragmentation patterns of ions and among the modern analysis techniques used today, is one of the most sensitive techniques for mass spectrometry detection and one of the most successful interfaces used in LC-MS configurations. Configuration of LC-MS with ESI represents fragmentation data for structural verification and provides an effective method for the analysis of complex systems (Kumar, Dinesh, & Rini, 2016).

In the present study, the sample preparation process was realized by dilution. The "dilute and shoot" method is based on simple sample dilution instead of extraction, and the biological sample is diluted with an IS-containing solution before being injected into the Torus DEA column. It is suitable for liquid samples containing low amounts of protein, such as urine and saliva. The dilution method provides superiority over the methods reported above because it is easy, faster, and more cost-effective to perform analyses.

The LOQ value in this work was calculated as 0.1 ng/mL for glyphosate. The values obtained with the methods we developed in this study are more sensitive than the results of many other studies reported previously. For example, in two studies where the dilution method was used and analysis was performed with LC-MS/MS (Jaikwang et al., 2020; Trasande et al., 2020), similar to this study, the LOQ values were 0.33 ng/mL and 5 ng/mL. On the other hand, in three separate studies that attempted to determine the amount of glyphosate in urine, the LOQ level of 0.1 ng/ml that we obtained in our study was reached. In these studies, unlike the present study, solid-phase extraction and liquid-liquid extraction techniques were used in sample preparation processes. However, in the study, we used the dilution method, which is much simpler, less time-consuming, and more cost-effective for the same LOQ value. On the other hand, the LOQ values of five studies in the literature were lower than in the present study (Fagan, Bohlen, Patton, & Klein, 2020; Nova, Calheiros, & Silva, 2020; Soukup et al., 2020), but the recovery and precision data of these methods were not specified. All of the LOQ, recovery, and reproducibility data obtained in the method used in the study reveal that it was more sensitive and reliable when compared with studies using urine as biological material.

CONCLUSIONS

The findings obtained from this study show that the presence of glyphosate at very low concentrations in urine samples can be detected with the help of the dilution method we used and the UPLC-ESI MS/MS method. In this method developed for glyphosate analysis in urine, sensitivity, linearity, and, recovery were evaluated and all of these parameters meet the criteria in the literature. We believe that by using the method we developed, determination of glyphosate exposure in urine will be easier, cost less, and save time. It is considered that this method we developed will make significant contributions by facilitating glyphosate biomonitoring studies.

AUTHOR CONTRIBUTION RATE STATE-MENT

Concept and Design (\dot{I} Ç), Data Collection (GKM), Analysis (GKM), Interpretation (GKM, \dot{I} Ç), Writing (\dot{I} Ç).

CONFLICT OF INTEREST

The authors declare that there is no conflict of interest.

REFERENCES

- Acquavella, J. F., Alexander, B. H., Mandel, J. S., Gustin, C., Baker, B., Chapman, P., & Bleeke, M. (2004). Glyphosate biomonitoring for farmers and their families: results from the Farm Family Exposure Study. *Environmental Health Perspectives*, 112, 321-326. doi: 10.1289/ehp.6667
- Ames, J., Miragem, A. A., Cordeiro, M. F., Cerezer, F. O., & Loro, V. L. (2022). Effects of glyphosate on zebrafish: a systematic review and meta-analysis. *Ecotoxicology*, *31*(8), 1189-1204. doi: 10.1007/s10646-022-02581-z

- Barr, D. B. (2008). Biomonitoring of exposure to pesticides. *Journal of Chemical Health and Safety*, 15, 20-29. doi:10.1016/j.jchas.2008.07.001
- Ben Khadda, Z., Bungau, S.G., El Balkhi, S., Ezrari, S., Radu, A.F., Houssaini, T.S., & Achour, S.(2025). Urinary biomonitoring of exposure to glyphosate and its metabolite amino-methyl phosphonic acid among farmers and non-farmers in Morocco. *Environmental Toxicology and Pharmacology*, 113:104620. doi: 10.1016/j.etap.2024.104620
- Curwin, B. D., Hein, M. J., Sanderson, W. T., Striley, C., Heederik, D., Kromhout, H., ...Alavanja, M. C. (2007). Pesticide dose estimates for children of Iowa farmers and non-farmers. *Environmental Research*, 105, 307-315. doi: 10.1016/j.envres.2007.06.001
- EC. (2023). Commission Implementing Regulation (EU). 2023/2660 of 28 November 2023 renewing the approval of the active substance glyphosate in accordance with Regulation (EC) No 1107/2009 of the European Parliament and of the Council and amending Commission Implementing Regulation (EU) No 540/2011. Official Journal of the European Union. 2023. https://eur-lex.europa.eu/eli/reg_impl/2023/2660 (accessed on 6 March 2025).
- ECHA. (2017). European Chemicals Agency Glyphosate Not Classified as a Carcinogen by ECHA. https:// echa.europa.eu/-/glyphosate-not-classified-as-a-carcinogen-by-echa. (accessed on 6 March 2025).
- EFSA. (2015). European Food Safety Authority Conclusion on the peer review of the pesticide risk assessment of the active substance glyphosate. EFSA Journal, 13, 4302. doi: 10.2903/j.efsa.2015.4302
- EFSA. (2022). European Food Safety Authority Report of Pesticide Peer Review TC 80 Glyphosate. https://www.efsa.europa.eu/sites/default/files/2023-01/glyphosate-peer-review-minutes-nov-dec-2022.pdf (accessed on 6 March 2025).

- EPA. (2016). U.S. Environmental Protection Agency Glyphosate issue paper: evaluation of carcinogenic potential. https://www.epa.gov/sites/default/files/2016-09/documents/glyphosate_issue_paper_evaluation_of_carcincogenic_potential.pdf (accessed on 6 March 2024).
- Fagan, J., Bohlen, L., Patton, S., & Klein, K. (2020).
 Organic diet intervention significantly reduces urinary glyphosate levels in US children and adults. *Environmental Research*, 189, 109898. doi: 10.1016/j.envres.2020.109898
- FDA. (2018). U.S. Department of Health and Human Services Food and Drug Administration Guidance for Industry, Bioanalytical Method Validation https://www.fda.gov/files/drugs/published/Bioanalytical-Method-Validation-Guidance-for-Industry.pdf (accessed on 6 March 2025).
- Galli, F.S., Mollari, M., Tassinari, V., Alimonti, C., Ubaldi, A., Cuva, C., & Marcoccia, D.(2024). Overview of human health effects related to glyphosate exposure. *Frontiers in Toxicology*, 6,1474792. doi: 10.3389/ftox.2024.1474792
- IARC. (2016). *IARC Monographs on the Evaluation of Carcinogenic Risks to Humans Glyphosate (second ed.*). http://monographs.iarc.fr/ENG/Monographs/vol112/mono112-10.pdf. (accessed on 6 March 2025).
- Jaikwang, P., Junkuy, A., Sapbamrer, R., Seesen, M., Khacha-ananda, S., Mueangkhiao, P., & Wunnapuk, K. (2020). A dilute-and-shoot LC–MS/MS method for urinary glyphosate and AMPA. *Chro*matographia, 83, 467-475. doi: 10.1007/s10337-019-03853-3
- Jiang, Y., He, Y., Pei, R., Chen, L., Liu, Q., & Hu, Z. (2025). Ecotoxicological mechanism of glyphosate on Moerella iridescens: Evidence from enzyme, histology and metabolome. *Marine Pollu*tion Bulletin, 213, 117680. doi: 10.1016/j.marpolbul.2025.117680

- Kumar, P., Dinesh, S., & Rini, R. (2016). LCMS—a review and a recent update. *Journal of Pharmacy and Pharmaceutical Sciences*, 5, 377-391. doi:10.20959/wjpps20165-6656
- Leblanc, P.-O., Breton, Y., Léveillé, F., Tessier, P. A., & Pelletier, M. (2024). The impact of the herbicide glyphosate and its metabolites AMPA and MPA on the metabolism and functions of human blood neutrophils and their sex-dependent effects on reactive oxygen species and CXCL8/IL-8 production. *Environmental Research*, 252, 118831. doi: 10.1016/j.envres.2024.118831
- NCEH. (2010). National Center for Environmental Health (NCEH) Laboratory Procedure Manual Bisphenol A and Other Environmental Phenols in Urine NHANES 2007–2008, Organic Analytical Toxicology, Branch Division of Laboratory Sciences. https://www.cdc.gov/nchs/data/nhanes/nhanes_07_08/pp_e_met_phenols.pdf (accessed on 6 March 2025).
- Nova, P., Calheiros, C. S., & Silva, M. (2020). Glyphosate in Portuguese adults–a pilot study. *Environmental Toxicology and Pharmacology*, 80, 103462. doi: 10.1016/j.etap.2020.103462
- Parlapiano, I., Biandolino, F., Grattagliano, A., Ruscito, A., Libralato, G., & Prato, E. (2021). Effects of commercial formulations of glyphosate on marine crustaceans and implications for risk assessment under temperature changes. *Ecotoxicology and Environmental Safety*, 213, 112068. doi: 10.1016/j. ecoenv.2021.112068
- Peillex, C., & Pelletier, M. (2020). The impact and toxicity of glyphosate and glyphosate-based herbicides on health and immunity. *Journal of Immunotoxicology*, 17, 163-174. doi: 10.1080/1547691X.2020.1804492

- Soukup, S. T., Merz, B., Bub, A., Hoffmann, I., Watzl, B., Steinberg, P., & Kulling, S. E. (2020). Glyphosate and AMPA levels in human urine samples and their correlation with food consumption: results of the cross-sectional KarMeN study in Germany. *Archives of Toxicology*, *94*, 1575-1584. doi: 10.1007/s00204-020-02704-7
- Trasande, L., Aldana, S. I., Trachtman, H., Kannan, K., Morrison, D., Christakis, D. A., ...Karthikraj, R. (2020). Glyphosate exposures and kidney injury biomarkers in infants and young children. *Environmental Pollution*, 256, 113334. doi: 10.1016/j. envpol.2019.113334
- Van Bruggen, A. H., He, M. M., Shin, K., Mai, V., Jeong, K., Finckh, M., & Morris Jr, J. (2018). Environmental and health effects of the herbicide glyphosate. *Science of the Total Environment*, *616*, 255-268. doi: 10.1016/j.scitotenv.2017.10.309
- Wei, X., Pan, Y., Zhang, Z., Cui, J., Yin, R., Li, H., ...Qiu, R. (2024). Biomonitoring of glyphosate and aminomethylphosphonic acid: Current insights and future perspectives. *Journal of Hazardous Materials*, 463, 132814. doi: 10.1016/j.jhazmat.2023.132814

Evaluation of Antioxidant and Enzyme Inhibitory Activities of Some Daphne Species

Semih BULUT**, Hüseyin FAKİR**

Evaluation of Antioxidant and Enzyme Inhibitory Activities of Some Daphne Species

SUMMARY

Daphne species are distributed in many parts of the world and are traditionally used in the treatment of various diseases. This study was carried out to investigate the antioxidant, antiobesity, and antidiabetic activities of leaf and branch extracts of Daphne gnidioides Jaub. & Spach, D. oleoides Schreb. and D. sericea Vahl. In vitro antidiabetic (α -glucosidase and α -amylase inhibitory effects) and antiobesity (pancreatic lipase inhibitory effects) activities of D. oleoides and D. sericea were reported for the first time in this study. Antioxidant effect was evaluated by DPPH and ABTS radical scavenging activity, total antioxidant capacity, and ferric reducing power tests. The total flavonoid content of the extracts ranged from 11.26 ± 0.55 to 81.97 ± 1.84 QE/g extract. D. oleoides leaf extract was found to have the highest ferric reducing power absorbance value (0.406 ± 0.02). D. oleoides branch extract (90.05 ± 0.57%) was found to have the strongest DPPH radical scavenging activity and this result was similar to the reference substance ascorbic acid at the same concentration. The analysed Daphne species showed either weak or no effect on the pancreatic lipase enzyme. Among the tested extracts, D. oleoides branch extract was found to have the strongest α -glucosidase inhibitory activity (IC50 = 28.53 ± 1.35 μ g/mL). Similarly, D. oleoides branch extract inhibited α -amylase enzyme at the highest rate (52.09 ± 1.91%). In conclusion, D. oleoides branch extract was found to have high antioxidant activity and remarkable antidiabetic activity in experiments with different mechanisms.

Key Words: Daphne, antioxidant, antidiabetic, pancreatic lipase.

Bazı Daphne Türlerinin Antioksidan ve Enzim İnhibitör Aktivitelerinin Değerlendirilmesi

ÖZ

Daphne türleri dünyanın birçok bölgesinde dağılım göstermekte ve çeşitli hastalıkların tedavisinde geleneksel olarak kullanılmaktadır. Bu çalışma Daphne gnidioides Jaub. & Spach, D. oleoides Schreb. ve D. sericea Vahl'ın yaprak ve dal ekstrelerinin antioksidan, antiobezite ve antidiyabetik aktivitelerinin araştırılması amacıyla gerçekleştirilmiştir. D. oleoides ve D. sericea'nın in vitro antidiyabetik (α-glukozidaz ve α-amilaz inhibitör etkileri) ve anti-obezite (pankreatik lipaz inhibitör etkileri) aktiviteleri ilk kez bu çalışmada rapor edilmiştir. Antioksidan etki DPPH ve ABTS radikal süpürücü aktivite, total antioksidan kapasite ve demir indirgeme gücü testleri ile değerlendirilmiştir. Ekstrelerin total flavonoit içeriği 11,26 ± 0,55 ile 81,97 ± 1,84 QE/g ekstre aralığında bulunmuştur. D. oleoides yaprak ekstresinin en yüksek demir indirgeme gücü absorbans değerine (0,406 ± 0,02) sahip olduğu bulunmuştur. D. oleoides dal ekstresinin (%90,05 ± 0,57) en güçlü DPPH radikal süpürücü aktiviteye sahip olduğu ve bu sonucun aynı konsantrasyonda referans madde olan askorbik asit ile benzer olduğu görülmüştür. İncelenen Daphne türleri pankreatik lipaz enzimi üzerinde ya zayıf etki göstermiş ya da hiç etki göstermemiştir. Test edilen ekstrelerinden en güçlü α-glukozidaz inhibitör aktiviteye D. oleoides dal ekstresinin sahip olduğu bulunmuştur (IC50 = 28,53 ± 1,35 µg/mL). Benzer şekilde D. oleoides dal ekstresi α-amilaz enzimini en yüksek oranda (%52,09 ± 1,91) inhibe etmiştir. Sonuç olarak D. oleoides dal ekstresinin farklı mekanizmalar ile gerçekleştirilen deneylerde yüksek antioksidan aktiviteye ve dikkate değer antidiyabetik aktiviteye sahip olduğu bulunmuştur.

Anahtar Kelimeler: Daphne, antioksidan, antidiyabetik, pankreatik lipaz.

Received: 5.02.2025 Revised: 30.06.2025 Accepted: 30.07.2025

ORCID: 0000-0002-4098-0221, Department of Pharmacognosy, Faculty of Pharmacy, Suleyman Demirel University, Isparta, Turkey

[&]quot;ORCID: 0000-0002-6606-8011, Department of Forest Botany, Faculty of Forestry, Isparta University of Applied Sciences, Isparta, Turkey

INTRODUCTION

People have been using plants against various diseases for centuries (Nwozo, Effiong, Aja, & Awuchi, 2023). Fruits, roots, flowers, seeds, and leaves of plants contain bioactive compounds. Medicinal plants and herbal products are advantageous because they are easily accessible, inexpensive and have fewer side effects/toxicity and contraindications compared to synthetic drugs (Petrovska, 2012; Sun & Shahrajabian, 2023). In recent years, the number of studies on plants and plant-derived active compounds in new drug discovery has increased (Miller, 2001; Parasuraman, 2018). Although the mechanisms of action of plants on diseases are not fully understood, many of them have antioxidant activity. Thanks to this activity, plants and plant-derived compounds are effective in diabetes, atherosclerosis, cardiovascular diseases, cancer, and memory problems (Karimi, Majlesi, & Rafieian-Kopaei, 2015).

Diabetes mellitus is a disease caused by problems in the secretion or action of insulin and characterised by hyperglycaemia. It is reported that more than 360 million people worldwide will be affected by diabetes by 2030 (Patel, Kumar, Laloo, & Hemalatha, 2012). In the treatment of diabetes, insulin, insulin analogs, oral hypoglycaemic and genetic agents are prescribed. These drugs cause stability problems, bioavailability problems, and various side effects in oral use (Zhao et al., 2020). Therefore, the number of studies on medicinal plants in the management of Type 2 diabetes has increased (Unuofin & Lebelo, 2020). In this context, reducing glucose absorption by inhibiting α -amylase and α -glucosidase is desired in the treatment of diabetes (Cardullo et al., 2020). Moreover, obesity or overweight is also effective in the progression of Type 2 diabetes. In this context, diabetic patients should not be overweight (Chandrasekaran & Weiskirchen, 2024). Pancreatic lipase has a particularly active role in lipid absorption and digestion. Therefore, improvement in obesity can be achieved by inhibiting the pancreatic lipase enzyme (Hou, Qin, Hou, Tang, & Ge, 2022).

The genus Daphne belongs to the Thymelaeaceae family and has about 100 species. This genus is distributed in Europe, Asia and Africa, and species of the genus are traditionally used in the treatment of various diseases (Moshiashvili, Tabatadze, & Mshvildadze, 2020). When literature data is examined, it has been reported that these species are generally used internally and externally against rheumatic diseases, stomach disorders, hypertension, skin diseases, malaria and gonorrhea (Moshiashvili et al., 2020; Suntar et al., 2012). However, when these plants are consumed internally by humans, various toxic and side effects are observed (Tongur, Erkan, & Ayranci, 2018; Tosun, 2006). Plants belonging to this genus have been reported to have antioxidant, anti-inflammatory, anti-HIV, antiproliferative, antifungal and antibacterial effects in various activity studies (Kupeli, Tosun, & Yesilada, 2007; Grubešić, Kremer, Končić, Rodríguez, & Randić, 2012; Hajji et al., 2017; Tundis, Loizzo, Bonesi, Peruzzi, & Efferth, 2019; Lutfullah, Shah, Ahmad, & Haider, 2019; Tang et al., 2021; Tan et al., 2022; Muzammil et al., 2023).

To our knowledge, there is no report on the *in vitro* antidiabetic (α -glucosidase and α -amylase inhibitory effect) and antiobesity (pancreatic lipase inhibitory effect) activities of *Daphne oleoides* Schreb., and *D. sericea* Vahl. In this study, antioxidant, anti-obesity and antidiabetic effects of three *Daphne* species (*D. oleoides*, *D. sericea* and *D. gnidioides* Jaub. & Spach) distributed in Türkiye were reported.

MATERIAL AND METHODS

Plant material and extraction method

The three *Daphne* species used in this study were collected and identified by Prof. Dr. Hüseyin Fakir (Department of Forest Botany, Isparta University of Applied Sciences, Türkiye) and voucher specimens were preserved in the GUL herbarium (Isparta, Türkiye) (Table 1). After the plant samples were dried, the leaf and branch parts were separated and ground. Plant parts (leaf and branch, 10 g) were extracted using 80% ethanol (200 mL) for 18 h and filtered at the end of the time. Crude extracts were then obtained using a rotary evaporator (Heidolph) and these extracts were stored in glass vials at 2-8°C for use in activity assays.

Plant name	Herbarium no	Collection sites and dates
D. gnidioides	GUL 97/1/6-1	Isparta, Eğirdir, Aşağıgökdere village, <i>Pinus</i> brutia Forest, October 2023
D. oleoides	GUL 97/1/5-1	Isparta, Sütçüler, Mount Tota, <i>P. nigra</i> Forest, October 2023
D. sericea	GUL 97/1/4-1	Isparta, Eğirdir, Aşağıgökdere village, <i>P. brutia</i> Forest, October 2023

Determination of total phenols

The total phenol content of leaf and branch extracts was determined using the Folin-Ciocalteu technique. In this experiment, Folin-Ciocalteau (10%) reagent prepared by dissolving in distilled water was added to the extracts (1mg/mL) in the microplate. After the extract-Folin mixture was kept for 5 minutes, sodium carbonate prepared by dissolving in distilled water was transferred to the mixture. At the end of half an hour, the absorbance of the mixture was measured at 735 nm. All of these procedures were also applied to the gallic acid solutions used to establish the calibration curve equation (Zongo et al., 2010).

Determination of total flavonoids

Total flavonoid content of leaf and branch extracts was investigated using the total flavonoid determination method of Kosalec et al. (Kosalec, Bakmaz, Pepeljnjak, & Vladimir-Knezevic, 2004). CH₃COONa, ethanol (95%), AlCl₃, and sodium acetate were transferred to the sample and the final volume of the mixture was completed to 1 mL with distilled water. After half an hour of incubation, the absorbance of leaf and branch extracts was read at 415 nm. All these procedures were also applied to quercetin solutions.

Antioxidant activity assays

Total antioxidant capacity

Firstly, the molybdate reagent was prepared in the experiment. To prepare this reagent, sulfuric acid, so-dium phosphate monobasic, ammonium molybdate were dissolved in distilled water to a total volume of 10 ml and then the reagent and extract (100 μ L) were mixed. The extract-reagent mixture was incubated at 90°C for 90 min, and the absorbance was measured at

695 nm. All of these procedures were also applied to the ascorbic acid solutions used to establish the calibration curve equation (Prieto, Pineda, & Aguilar, 1999).

Ferric reducing power

Branch and leaf samples were reacted with potassium ferricyanide and phosphate buffer at 37° C. The reaction was completed after 1 h and $C_2HCl_3O_2$ (10%) solution was transferred to the mixture. After measuring the absorbance of the mixture, iron (III) chloride (0.01%) was added and the absorbance was measured again at 700 nm (Orhan, Deliorman Orhan, Gokbulut, Aslan, & Ergun, 2017). The reference substance was quercetin. The extract and reference substance concentrations used in this experiment were the same as in other antioxidant activity tests.

ABTS radical scavenging activity

Firstly, the reference substance (gallic acid) and extracts were prepared at concentrations of 0.5, 1 and 2 mg/mL. In this experiment, 2,2'-azino-bis(3-ethylbenzothiazoline-6-sulfonate) (ABTS) and potassium peroxodisulfate solutions were prepared with distilled water at 7 mM and 2.45 mM, respectively. These two prepared reagents were mixed and the final volume was completed to 7.5 mL with distilled water. This mixture was kept in a dark cabinet at room temperature for 16 hours and then phosphate buffer (pH 7.4) was added. The final mixture was added to the branch and leaf extracts (10 μ L) and absorbance values were read at 734 nm after 6 min (Orhan et al., 2017).

DPPH radical scavenging activity

In this test, the extract and reference substance (ascorbic acid) were prepared in 80% ethanol at 0.5,

1 and 2 mg/mL concentration. 1 mM 2,2-Diphenyl-1-picrylhydrazyl (DPPH) reagent was prepared and transferred to references and plant extracts (80 μ L). After the mixture was kept in a dark cabinet, absorbance was measured at 520 nm (Jung et al., 2011).

Enzyme assays

α-Amylase enzyme inhibitory activity

This experiment was performed with minor modifications to the α -amylase inhibitory activity test method of Ali et al. (Ali, Houghton, & Soumyanath, 2006). Sodium potassium tartrate solution (5.31 M) was prepared using sodium hydroxide solution (2 M). Then, DNS solution (96 mM) was prepared by dissolving 3,5-dinitrosalicylic acid (DNS) in distilled water and mixed with the 5.31 M solution. This final mixture was called color reagent. Phosphate buffer adjusted to pH=6.9 and 4 U/mL α -amylase (Type I-A, Sigma) enzyme were added to the leaf and branch extracts and potato starch (0.5%) was added to the mixture after 5 min. Incubation was carried out for 15 min and at the color reagent the was transferred at the end of the time. Then, the mixture was kept at 80°C for 40 min and 75 μ L of cold distilled water was added to the mixture at the end of the time. The change in absorbance (A) due to the mixture and maltose was measured at 540 nm. The same procedure was applied for acarbose (reference substance).

 $A_{\text{extract, control}} = A_{\text{Sample}} - A_{\text{Blank}};$ Inhibition % = [1-(X/Y)] × 100; X: Mean maltose in acarbose and extract; Y: Mean maltose in control

α-Glucosidase enzyme inhibitory activity

 α -glucosidase enzyme (*Bacillus stearothermophilus*, Type IV) purchased from Sigma was prepared in pH=6.5 phosphate buffer, and phosphate buffer and enzyme were added to the extracts transferred to the microplate. The resulting mixture was heated in an oven at 37°C for 15 min and 10 μ l of 4-Nitrophenyl α -D-glucopyranoside (20 mM, substrate) was transferred to the mixture at the end of the time. Then, the microplate was kept in the oven at 37°C for 35 min and the absorbance was read at 405 nm. The same

procedure was applied for acarbose (reference substance) (Lam, Chen, Kang, Chen, & Lee, 2008).

Inhibitory activity $\% = [1-(B-b/C-c)] \times 100$; B: Activity with inhibitor; b: Negative control with inhibitor; C: Activity without inhibitor; c: Negative control without inhibitor

Pancreatic lipase enzyme inhibitory activity

The method of Lee et al. (2012) was used to evaluate the enzyme inhibitory activity of the samples (Lee et al., 2012). Tris HCl (100 mM Tris-HCl, 5 mM CaCl_2) and pH=6.8, morpholinepropanesulfonic acid (mops) buffers were prepared to be used in this enzyme inhibition test and stored at room temperature. Lipase enzyme was transferred to the samples. Then, Tris HCl buffer (150 μ L) and mops buffer were added to the mixture and the microplate was kept at 37°C for 15 min. To each well in the microplate, 10 mM substrate (*p*-nitrophenylbutyrate) prepared with acetonitrile was added and the mixture was reacted at 37°C for 30 min. At the end of the time, absorbance was measured at 405 nm and the same procedure was applied for orlistat (reference substance).

Inhibition $\% = [1-(B-b/C-c)] \times 100$; B: Activity with inhibitor; b: Negative control with inhibitor; C: Activity without inhibitor; c: Negative control without inhibitor

Statistical analysis

All experimental procedures were repeated three times. The values found in this study were shown as mean \pm standard deviation (SD). GraphPad Prism and Microsoft Excel programs were used to determine activity results and IC₅₀ values. The difference in the experimental results at P<0.05 level was considered statistically significant.

RESULTS AND DISCUSSION

Total phenolic contents of the extracts were determined according to the calibration curve equation (y = 6.8205 x - 0.1166 and coefficient of determination $R^2 = 0.9924$) generated from different dilutions of gallic acid. Although the investigated extracts gave similar total phenolic content results, *D. oleoides* leaf

extract had the highest phenolic content (142.01 ± 1.02 mg/gallic acid equivalent (GAE) g extract).

Total flavonoid contents of the extracts were determined according to the calibration curve equation (y = 2.1336x - 0.042) and coefficient of determination $R^2 = 0.9977$) generated from different dilutions of quercetin. The total flavonoid contents of the extracts ranged from 11.26 ± 0.55 to 81.97 ± 1.84 mg quercetin equivalents (QE)/g extract and the leaf extracts of all three species had higher flavonoid content than the branch extracts.

Total antioxidant capacity results of the tested samples were expressed as mg ascorbic acid equivalent (AAE)/g extract. The highest total antioxidant capacity was found in D. oleoides branch extract (216.47 ± 6.18 AAE/g extract) and the lowest antioxidant capacity was found in D. gnidioides leaf extract (65.55 ± 2.88 AAE/g extract). Total phenol, flavonoid contents, and total antioxidant capacity test results of the extracts are shown in Table 2.

Table 2. Total phenol, flavonoid content, and total antioxidant capacity assay results

Plant	Used parts	Total Phenolic Content ^a (Mean ± SD)	Total Flavonoid Content ^b (Mean ± SD)	Total Antioxidant Capacity ^c (Mean ± SD)	
D 1: .: 1	Branch	118.26 ± 1.45	14.13 ± 1.15	164.90 ± 9.89	
D. gnidioides	Leaf	109.02 ± 0.83	29.54 ± 2.90	65.55 ± 2.88	
5 1 11	Branch	124.66 ± 3.64	11.26 ± 0.55	216.47 ± 6.18	
D. oleoides	Leaf	142.01 ± 1.02	62.74 ± 0.95	82.16 ± 3.30	
D. sericea	Branch	108.19 ± 8.53	27.15 ± 1.49	213.46 ± 3.21	
	Leaf	107.04 ± 6.95	81.97 ± 1.84	130.23 ± 7.83	

amg GAE/g extract, bmg QE/g extract, cmg AAE/g extract

All leaf and branch extracts analysed showed strong DPPH radical scavenging antioxidant activity with over 80% inhibition. The highest DPPH radical scavenging activity was found in D. oleoides branch extract (90.05 ± 0.57%) and this result was similar to ascorbic acid $(91.80 \pm 0.71\%)$ at the same concentration. Both leaf and branch extracts of D. oleoides had the highest ABTS radical scavenging activity (78.97 \pm 1.61%, 98.77 ± 1.42%, respectively). All leaf and branch extracts had weaker ABTS radical scavenging activity (<40%) at 0.5 mg/mL concentration and the weakest activity was found in D. sericea branch extract. The absorbance values of the extracts and quercetin were compared at three different concentrations while evaluating the re-

sults of ferric reducing power activity. At all concentrations examined (0.5, 1 and 2 mg/mL) D. oleoides leaf extract had the highest absorbance values (0.310 \pm 0.00, 0.374 ± 0.02 , and 0.406 ± 0.02 , respectively). In the ferric reducing power experiment, D. oleoides leaf extract (0.406 ± 0.02) had a similar absorbance value to quercetin (0.570 \pm 0.05). In all extracts (leaf and branch), the absorbance value of reducing power increased with increasing concentration. Antioxidant activity test results of the extracts are shown below (Table 3).

Table 3. Antioxidant activity test results

				Antioxidant activity tests	
Plant	Used parts	Concentration (mg/mL)	DPPH radical scavenging activity inhibition % ± SD	ABTS radical scavenging activity inhibition % ± SD	Ferric reducing power absorbance ± SD
		0.5	85.12 ± 0.33***	36.15 ± 0.43***	0.223 ± 0.02***
	Branch	1	87.26 ± 0.20***	47.56 ± 2.16***	0.260 ± 0.01***
D. midiaidae		2	88.05 ± 0.20***	79.84 ± 1.24***	0.302 ± 0.02***
D. gnidioides		0.5	83.77 ± 1.93***	34.32 ± 0.43***	0.231 ± 0.00***
	Leaf	1	86.78 ± 1.12***	38.09 ± 3.17***	0.293 ± 0.01***
		2	87.22 ± 0.08***	43.69 ± 3.89***	0.304 ± 0.01***
		0.5	82.90 ± 0.20***	37.21 ± 1.82***	0.224 ± 0.01***
	Branch	1	87.30 ± 0.45***	58.17 ± 0.89***	0.290 ± 0.01***
D. oleoides		2	90.05 ± 0.57***	78.97 ± 1.61***	0.297 ± 0.02***
D. oleotaes		0.5	85.21 ± 0.35***	32.08 ± 1.58***	0.310 ± 0.00***
	Leaf	1	87.13 ± 0.15***	60.96 ± 2.04***	0.374 ± 0.02***
		2	87.61 ± 0.84***	98.77 ± 1.42***	0.406 ± 0.02***
		0.5	86.08 ± 0.20***	18.90 ± 1.11**	0.233 ± 0.01***
	Branch	1	87.17 ± 0.23***	23.34 ± 1.52***	0.270 ± 0.01***
D. sericea		2	88.09 ± 0.23***	77.33 ± 1.35***	0.307 ± 0.02***
D. sericea		0.5	86.04 ± 0.40***	31.10 ± 0.63***	0.245 ± 0.01***
	Leaf	1	86.61 ± 0.87***	48.92 ± 0.85***	0.301 ± 0.03***
		2	87.65 ± 2.46***	68.75 ± 2.39***	0.332 ± 0.02***
	AA	0.5	91.54 ± 0.41***	98.88 ± 0.22***	0.416 ± 0.01***
Reference	GA	1	89.95 ± 1.05***	99.25 ± 0.13***	0.437 ± 0.05***
	QU	2	91.80 ± 0.71***	99.93 ± 0.26***	0.570 ± 0.05***

DPPH test reference: Ascorbic acid (AA); ABTS test reference: Gallic acid (GA); Ferric reducing power test reference: Quercetin (QU); **p<0.01; ***p<0.001

In this study, the effects of three *Daphne* species on obesity and diabetes were investigated by *in vitro* enzyme assays. The antidiabetic effect was tested using hibitory effect, only *D. oleoides* branch extract inhibation are discovered as a state of the enzyme at IC_{50} values below 200 μ g/mL. The inhibitory effect of the investigated extracts on α -amenzyme.

Among the leaf and branch extracts tested, D. oleoides branch extract showed the strongest α -glucosidase inhibitory activity and inhibited the α -glucosidase enzyme with an IC $_{50}$ value of $28.53 \pm 1.35 \ \mu g/mL$. After this extract, D. sericea leaf and branch extracts highly inhibited α -glucosidase enzyme (IC $_{50}$ values: 48.46 ± 1.28 and $49.74 \pm 0.95 \ \mu g/mL$, respectively). None of the extracts inhibited the α -glucosidase enzyme as potently as acarbose (IC $_{50}$ = $0.58 \pm 0.02 \ \mu g/mL$). Among the extracts analysed for α -amylase in-

hibitory effect, only D. oleoides branch extract inhibited the enzyme at IC_{50} values below 200 µg/mL. The inhibitory effect of the investigated extracts on α -amylase was extremely low compared to acarbose. In the pancreatic lipase inhibitory activity test in which the anti-obesity effect of the extracts was evaluated, none of the extracts had an IC_{50} value below 200 µg/mL. Additionally, D. sericea branch extract did not show inhibitory effect on the pancreatic lipase enzyme. The activity of the extracts acting on the pancreatic lipase enzyme was found to be extremely weak compared to orlistat. The α -glucosidase, α -amylase, and pancreatic lipase enzyme inhibitory activity test results of the extracts are shown in Table 4.

Plant	Used parts	200 μg/ml	nL ± S.D)		
		α-amylase	α-glucosidase	Pancreatic lipase	
	Branch	4.51 ± 1.91 ^{ns}	89.74 ± 1.13*** (IC ₅₀ =96.86 ± 0.22)	12.86 ± 3.27*	
D. gnidioides	Leaf	16.20 ± 3.82*	$61.96 \pm 1.60^{**}$ ($IC_{50} = 138.67 \pm 3.23$)	22.62 ± 1.80***	
D. oleoides	Branch	$52.09 \pm 1.91^{***}$ (IC ₅₀ = 186.36 ± 4.30)	96.99 ± 0.82*** (IC ₅₀ = 28.53 ± 1.35)	25.95 ± 0.82***	
	Leaf	18.29 ± 2.61**	86.54 ± 0.45*** (IC ₅₀ =83.75 ± 1.04)	12.86 ± 1.43*	
Danie	Branch	26.37 ± 3.24**	88.94 ± 1.37*** (IC ₅₀ =49.74 ± 0.95)	-	
D. sericea	Leaf	27.05 ± 2.61***	87.32 ± 2.47*** (IC ₅₀ =48.46 ± 1.28)	40.71 ± 3.03***	
Reference Acarbose Orlistat		94.48 ± 2.80***b (IC ₅₀ =4.41 ± 0.02)	$99.55 \pm 0.01^{***b}$ (IC ₅₀ = 0.58 ± 0.02)	$76.09 \pm 3.28^{***c}$ (IC ₅₀ =11.49 ± 0.09)	

Table 4. Enzyme inhibitory activity test results of extracts

During extraction, 80% ethanol with medium polarity is generally preferred to reveal active phytochemicals (Al Jaafreh, 2024). Extraction with hydro-alcoholic solvents dissolves many phytochemicals and solvents of this polarity have the highest extraction yield and total phytochemical (phenol and flavonoid) content (Kabubii, Mbaria, Mathiu, Wanjohi, & Nyaboga, 2023). Based on this information, we preferred 80% ethanol for the extraction of plant parts.

The total phenol and flavonoid contents of the ethanol extract obtained from aerial parts of D. sericea (collected from Italy) were 34.1 ± 2.8 tannic acid equivalents $\mu g/mg$ extract and 8.4 ± 0.9 QE $\mu g/mg$ extract, respectively. It has been reported that the extract has antioxidant effects with its DPPH, ABTS radical scavenging activity, and ferric ion chelating properties (Frezza et al., 2021). In a different study, Tongur et al. investigated the antioxidant activity of D. gnidioides and D. sericea leaf methanol extracts and the results showed that D. gnidioides methanol extract had the highest ABTS radical scavenging activity (IC₅₀= 147.2 ± 0.4) while D. sericea methanol extract had the highest DPPH radical scavenging power (IC₅₀ = 61.6 ± 0.1). The total flavonoid content of *D. gnidioides* methanol extract was 244.5 ± 19.5 mg rutin/g extract, while the flavonoid content of D. sericea methanol extract was 121.3 ± 19.7 mg rutin/g extract (Tongur et al., 2018). In contrast to Tongur et al., in our study, *D. sericea* leaf extract had stronger ABTS radical scavenging activity than *D. gnidioides* leaf extract and both leaf extracts had similar DPPH radical scavenging activity. This may be related to the varying phytochemical contents of plants.

In a different study, the antioxidant activity and chemical content of hexane, ethyl acetate, methanol and ethanol extracts prepared from the aerial parts of D. oleoides subsp. oleoides (collected from Konya, Türkiye) were evaluated. The highest phenolic content $(391.970 \pm 1.286 \text{ mg GAE/g extract})$ was found in the ethanol extract, while the lowest content (3.182 ± 1.814) mg GAE/g extract) was found in the hexane extract. Ethyl acetate extract had the strongest DPPH radical scavenging activity and ferric reducing power (IC₅₀= 65.481 \pm 0.613 µg/mL, EC $_{50}$ = 160.676 \pm 6.013 µg/mL, respectively) (Zengin, Arkan, Aktumsek, Guler, & Cakmak, 2013). The antioxidant activity of the extract (methanol) and its fractions (hexane, dichloromethane, ethyl acetate, n-butanol, water) prepared from the aerial parts of *D. oleoides* subsp. *oleoides* (collected from Karaman, Türkiye) was evaluated. The authors found the highest DPPH radical scavenging activity and reducing power in the ethyl acetate extract and attributed this to the high phenolic substance content of the extract (Balkan et al., 2017). Similar to the study

^a: Final concentration; ^b: Acarbose; ^c: Orlistat; ^{ns}: Not statistically significant; -: No activity; *p<0.05, **p<0.01; ***p<0.001

by Balkan et al., we found that *D. oleoides* leaf extract had the strongest reducing power and ABTS radical scavenging activity. At the same time, we revealed that this extract had the highest phenolic content.

There are very few reports on the effect of *Daphne* species on diabetes. The α -amylase activity of stem, root, and leaf extracts prepared from D. gnidioides was investigated. As a result of the study, it was seen that all three extracts had close inhibitory activity. When a-glucosidase inhibitory activity results were analysed, it was found that root extracts had no effect on the enzyme. Stem and leaf extracts showed 3.87 \pm 0.06 and 2.56 \pm 0.01 mmol acarbose equivalent/g inhibition on α-glucosidase enzyme, respectively (Can et al., 2020). In another study, the in vivo hypoglycemic effects of methanol extract prepared from D. oleoides roots were evaluated and it was found that the antidiabetic effect of *D. oleoides* extract (191.50 \pm 0.48 mg/dL) was less than that of metformin (111.58 \pm 1.30 mg/dL) used as standard substance (Muddassir, Batool, Miana, & Zafar, 2022). Similar to the literature results, we found that the in vitro antidiabetic enzyme inhibitory activity of Daphne species was lower than that of the standard substance (acarbose). D. oleoides branch extract showed stronger inhibitory activity in terms of both α -glucosidase and α -amylase inhibitory activity compared to other extracts. In this study, the α-glucosidase inhibitory activity of *D. oleoides* branch extract was remarkable.

Four compounds (luteolin-7,3',4'-trimethyl ether, β -sitosterol, 5-hydroxy-7,4'-dimethoxyflavone, 5,3'-dihydroxy-7,4'-dimethoxyflavone) isolated from the barks of *Aquilaria subintegra* (Thymelaeaceae) showed pancreatic lipase inhibitory activity in the range of 6% to 53% (Ibrahim, Abdul Azziz, Wong, Bakri, & Abdullah, 2020). In another study, dichloromethane extract of *A. malaccensis* barks had significant inhibition (0.065 \pm 0.147 U/mL) on pancreatic lipase (Ibrahim et al., 2018). Chloroform extract of *Thymelaea hirsute* (Thymelaeaceae) roots was reported to have 61% inhibition on pancreatic lipase at a concentration of 1 mg/mL (Abdallah, Hammoda,

El-Gazzar, Ibrahim, & Sallam, 2023). To our knowledge, the anti-obesity activity of *Daphne* species has not been previously investigated. In this study, no extract had an IC_{50} value below 200 µg/mL. Therefore, the analysed *Daphne* species did not have a significant pancreatic lipase inhibitory effect.

The chemical composition of Daphne species may vary depending on the species or plant parts. This situation has also been reported for the species we investigated. Balkan et al. reported that the *n*-hexane extract prepared from the aerial parts of *D*. oleoides subsp. oleoides was rich in hexadecanoic acid and 9,15- octodecadienoic acid (Balkan et al., 2017). Oxygenated sesquiterpenes (43.0%) and nootkatone (18.5%) were found to be dominant in D. oleoides subsp. oleoides essential oil (Uysal et al., 2017). D. gnidioides, was reported to have high amounts of apigenin-6,8-diglucoside and syringic acid in leaf extracts (Tongur et al., 2018; Can et al., 2020). 3-O-p-coumaroyl-5-O-caffeoylquinic acid was detected in the root and stem extract of this plant (Can et al., 2020). The activities shown by Daphne species may be related to their rich chemical contents.

CONCLUSION

In this study, antioxidant, antidiabetic and anti-obesity effects of six extracts of three *Daphne* species were investigated. Although extracts of *Daphne* species had strong antioxidant activity, they showed either weak or no effect on pancreatic lipase enzyme. Our results show that these plants are important sources of antioxidants. Our findings revealed that *Daphne* species have significant α -glucosidase inhibitory activity. In this context, the branch extract of *D. oleoides* showed stronger antidiabetic effect than other extracts. As a result, *Daphne* species can be important resources for the pharmaceutical industry. Therefore, further studies should be conducted on these species.

AUTHOR CONTRIBUTION STATEMENT

Concept: SB, HF; Design: SB; Control: SB; Sources: SB, HF; Materials: SB, HF; Data Collection and/or processing: SB, HF; Analysis and/or interpretation:

SB, HF; Literature review: SB; Manuscript writing: SB, HF; Critical review: SB, HF; Other: SB

CONFLICT OF INTEREST

The authors declare that there is no conflict of interest.

REFERENCES

- Abdallah, R. M., Hammoda, H. M., El-Gazzar, N. S., Ibrahim, R. S., & Sallam, S. M. (2023). Exploring the anti-obesity bioactive compounds of *Thymelaea hirsuta* and *Ziziphus spina-christi* through integration of lipase inhibition screening and molecular docking analysis. *RSC Advances*, *13*, 27167-27173. doi:10.1039/d3ra05826c
- Al Jaafreh, A. M. (2024). Investigation of the phytochemical profiling and antioxidant, anti-diabetic, anti-inflammatory, and MDA-MB-231 cell line antiproliferative potentials of extracts from *Ephedra alata Decne*. *Scientific Reports*, *14*, 18240. doi:10.1038/s41598-024-65561-9
- Ali, H., Houghton, P. J., & Soumyanath, A. (2006). alpha-Amylase inhibitory activity of some Malaysian plants used to treat diabetes; with particular reference to *Phyllanthus amarus*. *Journal of Ethnopharmacology*, *107*(3), 449-455. doi:10.1016/j. jep.2006.04.004
- Balkan, İ. A., Taşkın, T., Doğan, H. T., Deniz, İ., Akaydın, G., & Yesilada, E. (2017). A comparative investigation on the *in vitro* anti-inflammatory, antioxidant and antimicrobial potentials of subextracts from the aerial parts of *Daphne oleoides* Schreb. subsp. *oleoides*. *Industrial Crops and Products*, 95, 695-703.

- Can, T. H., Tufekci, E. F., Altunoglu, Y. C., Baloglu, M. C., Llorent-Martínez, E. J., Stefanucci, A., . . . Zengin, G. (2020). Chemical characterization, computational analysis and biological views on *Daphne gnidioides* Jaub. & Spach extracts: Can a new raw material be provided for biopharmaceutical applications? *Computational Biology and Chemistry*, 87, 107273.
- Cardullo, N., Muccilli, V., Pulvirenti, L., Cornu, A., Pouységu, L., Deffieux, D., . . . Tringali, C. (2020).
 C-glucosidic ellagitannins and galloylated glucoses as potential functional food ingredients with anti-diabetic properties: A study of α-glucosidase and α-amylase inhibition. *Food Chemistry*, 313, 126099. doi: 10.1016/j.foodchem.2019.126099
- Chandrasekaran, P., & Weiskirchen, R. (2024). The Role of Obesity in Type 2 *Diabetes Mellitus*-An Overview. *International Journal of Molecular Sciences*, 25(3), 1882. doi:10.3390/ijms25031882
- Frezza, C., Venditti, A., De Vita, D., Sciubba, F., Tomai, P., Franceschin, M., . . . Bianco, A. (2021). Phytochemical Analysis and Biological Activities of the Ethanolic Extract of *Daphne sericea* Vahl Flowering Aerial Parts Collected in Central Italy. *Biomolecules*, 11(3), 379. doi:10.3390/biom11030379
- Grubešić, R. J., Kremer, D., Končić, M. Z., Rodríguez, J. V., & Randić, M. (2012). Quantitative analysis of polyphenols and antioxidant activity in four *Daphne L.* species. *Central European Journal of Biology*, 7, 1092-1100.
- Hajji, H., El Makhfi, F., Abdennebi, E., Fatima, E., Laila, O., & Aicha, E. (2017). *In vitro* evaluation of antifungal activity of *Daphne gnidium* extracts against six human pathogenic fungi. *Journal of Chemical and Pharmaceutical Sciences*, 10, 6.

- Hou, X. D., Qin, X. Y., Hou, J., Tang, H., & Ge, G. B. (2022). The potential of natural sources for pancreatic lipase inhibitors: a solution of the obesity crisis? *Expert Opinion on Drug Discovery*, 17(12), 1295-1298. doi:10.1080/17460441.2023.2156499
- Ibrahim, M., Abdul Azziz, S. S. S., Wong, C. F., Bakri, Y. M., & Abdullah, F. (2020). Interactions of flavone and steroid from *A. subintegra* as potential inhibitors for porcine pancreatic lipase. *Current Computer Aided Drug Design*, *16*(6), 698-706. do i:10.2174/1573409915666191015112320
- Ibrahim, M., Syed Abdul Azziz, S. S., Wong, C. F., Wan Mohamad Din, W. N. I., Wan Mahamod, W. R., Bakri, Y. M., . . . Salleh, W. M. N. H. W. (2018). Evaluation of anti-lipase activity of leaf and bark extracts from *Aquilaria subintegra* and *A. malaccensis*. *Marmara Pharmaceutical Journal*, 22(1), 91-95. doi:10.12991/mpj.2018.46
- Jung, H. A., Jin, S. E., Choi, R. J., Manh, H. T., Kim, Y. S., Min, B. S., . . . Choi, J. S. (2011). Anti-tumorigenic activity of sophoflavescenol against Lewis lung carcinoma in vitro and in vivo. Archives of Pharmacal Research, 34(12), 2087-2099. doi:10.1007/s12272-011-1212-y
- Kabubii, Z. N., Mbaria, J. M., Mathiu, M. P., Wanjohi, J. M., & Nyaboga, E. N. (2023). Evaluation of seasonal variation, effect of extraction solvent on phytochemicals and antioxidant activity on *Rosmarinus officinalis* grown in different agro-ecological zones of Kiambu County, Kenya. *CABI Agriculture and Bioscience*, 4, 1. doi:10.1186/s43170-023-00141-x
- Karimi, A., Majlesi, M., & Rafieian-Kopaei, M. (2015).
 Herbal versus synthetic drugs; beliefs and facts.
 Journal of Nephropharmacology, 4(1), 27-30. Retrieved from https://www.ncbi.nlm.nih.gov/pubmed/28197471

- Kosalec, I., Bakmaz, M., Pepeljnjak, S., & Vladimir-Knezevic, S. (2004). Quantitative analysis of the flavonoids in raw propolis from northern Croatia. *Acta Pharmaceutica*, *54*(1), 65-72. Retrieved from https://www.ncbi.nlm.nih.gov/pubmed/15050046
- Kupeli, E., Tosun, A., & Yesilada, E. (2007). Assessment of anti-inflammatory and antinociceptive activities of *Daphne pontica* L. (Thymelaeaceae). *Journal of Ethnopharmacology*, 113(2), 332-337. doi:10.1016/j.jep.2007.06.018
- Lam, S. H., Chen, J. M., Kang, C. J., Chen, C. H., & Lee, S. S. (2008). alpha-Glucosidase inhibitors from the seeds of *Syagrus romanzoffiana*. *Phyto-chemistry*, 69(5), 1173-1178. doi:10.1016/j.phyto-chem.2007.12.004
- Lee, Y. M., Kim, Y. S., Lee, Y., Kim, J., Sun, H., Kim, J. H., & Kim, J. S. (2012). Inhibitory activities of pancreatic lipase and phosphodiesterase from Korean medicinal plant extracts. *Phytotherapy Research*, 26(5), 778-782. doi:10.1002/ptr.3644
- Lutfullah, G., Shah, A., Ahmad, K., & Haider, J. (2019). Phytochemical screening, antioxidant and antibacterial properties of *Daphne mucronata*. *Journal of Traditional Chinese Medicine*, 39(6).
- Miller, J. S. (2001). The global importance of plants as sources of medicines and the future potential of Chinese plants. In *Drug Discovery and Traditional Chinese Medicine: Science, Regulation, and Globalization* (pp. 33-42): Springer.
- Moshiashvili, G., Tabatadze, N., & Mshvildadze, V. (2020). The genus *Daphne*: A review of its traditional uses, phytochemistry and pharmacology. *Fitoterapia*, 143, 104540. doi:10.1016/j.fitote.2020.104540

- Muddassir, M., Batool, A., Miana, G. A., & Zafar, S. (2022). Comparative studies of anticancer, antimicrobial, antidiabetic, antioxidant activities of *Daphne oleoides* and *Berberis baluchistanica* extracts native to Pakistan. *Pakistan Journal of Pharmaceutical Sciences*, 35(2(Special)), 649-656. Retrieved from https://www.ncbi.nlm.nih.gov/pubmed/35668566
- Muzammil, K., Kzar, M. H., Mohammed, F., Mohammed, Z. I., Hamood, S. A., Hussein, T. K., ... Alsalamy, A. (2023). Methanol extract of Iraqi Kurdistan Region *Daphne mucronata* as a potent source of antioxidant, antimicrobial, and anticancer agents for the synthesis of novel and bioactive polyvinylpyrrolidone nanofibers. *Frontiers in Chemistry*, 11, 1287870. https://doi.org/10.3389/fchem.2023.1287870. doi:10.3389/fchem.2023.1287870
- Nwozo, O. S., Effiong, E. M., Aja, P. M., & Awuchi, C. G. (2023). Antioxidant, phytochemical, and therapeutic properties of medicinal plants: A review. *International Journal of Food Properties*, 26(1), 359-388.
- Orhan, N., Deliorman Orhan, D., Gokbulut, A., Aslan, M., & Ergun, F. (2017). Comparative Analysis of Chemical Profile, Antioxidant, In-vitro and In-vivo Antidiabetic Activities of *Juniperus foetidissima* Willd. and *Juniperus sabina* L. *Iranian Journal of Pharmaceutical Research*, 16(Suppl), 64-74. Retrieved from https://www.ncbi.nlm.nih.gov/pubmed/29844777
- Parasuraman, S. (2018). Herbal drug discovery: challenges and perspectives. Current Pharmacogenomics and Personalized Medicine (Formerly Current Pharmacogenomics), 16(1), 63-68.
- Patel, D. K., Kumar, R., Laloo, D., & Hemalatha, S. (2012). *Diabetes mellitus*: an overview on its pharmacological aspects and reported medicinal plants having antidiabetic activity. *Asian Pacific Journal of Tropical Biomedicine*, 2(5), 411-420. doi:10.1016/S2221-1691(12)60067-7.

- Petrovska, B. B. (2012). Historical review of medicinal plants' usage. *Pharmacognosy Reviews*, 6(11), 1-5. doi:10.4103/0973-7847.95849
- Prieto, P., Pineda, M., & Aguilar, M. (1999). Spectrophotometric quantitation of antioxidant capacity through the formation of a phosphomolybdenum complex: specific application to the determination of vitamin E. *Analytical Biochemistry*, 269(2), 337-341. doi:10.1006/abio.1999.4019
- Sun, W., & Shahrajabian, M. H. (2023). Therapeutic Potential of Phenolic Compounds in Medicinal Plants-Natural Health Products for Human Health. *Molecules*, 28(4), 1845. doi:10.3390/molecules28041845
- Suntar, I., Kupeli Akkol, E., Keles, H., Yesilada, E., Sarker, S. D., Arroo, R., & Baykal, T. (2012). Efficacy of *Daphne oleoides* subsp. *kurdica* used for wound healing: identification of active compounds through bioassay guided isolation technique. *Journal of Ethnopharmacology*, 141(3), 1058-1070. doi:10.1016/j.jep.2012.04.001
- Tan, L., Otsuki, K., Zhang, M., Kikuchi, T., Okayasu, M., Azumaya, I., . . . Li, W. (2022). Daphnepedunins A-F, Anti-HIV Macrocyclic Daphnane Orthoester Diterpenoids from *Daphne pedunculata*. *Journal of Natural Products*, 85(12), 2856-2864. doi:10.1021/acs.jnatprod.2c00894
- Tang, Z.-Y., Fan, R.-Z., Yin, A.-P., Tang, D.-K., Ahmed, A., Cao, J., . . . Tang, G.-H. (2021). Flavonoids with anti-inflammatory activities from *Daphne giral-dii*. *Arabian Journal of Chemistry*, *14*(2), 102962. doi:10.1016/j.arabjc.2020.102962
- Tongur, T., Erkan, N., & Ayranci, E. (2018). Investigation of the composition and antioxidant activity of acetone and methanol extracts of *Daphne sericea* L. and *Daphne gnidioides* L. *Journal of Food Science and Technology*, 55(4), 1396-1406. doi:10.1007/s13197-018-3054-9

- Tosun, A. (2006). *Daphne* L. türlerinin kimyasal içeriği ve biyolojik aktiviteleri. *Ankara Eczacılık. Fak*ültesi *Dergisi.* 35, 43-68.
- Tundis, R., Loizzo, M. R., Bonesi, M., Peruzzi, L., & Efferth, T. (2019). *Daphne striata* Tratt. and *D. mezereum* L.: a study of anti-proliferative activity towards human cancer cells and antioxidant properties. *Natural Product Research*, 33(12), 1809-1812. doi:10.1080/14786419.2018.1437432
- Unuofin, J. O., & Lebelo, S. L. (2020). Antioxidant Effects and Mechanisms of Medicinal Plants and Their Bioactive Compounds for the Prevention and Treatment of Type 2 Diabetes: An Updated Review. Oxidative Medicine and Cellular Longevity, 2020(1), 1356893. doi:10.1155/2020/1356893
- Uysal, A., Zengin, G., Aktumsek, A., Rigano, D., Senatore, F., & Sanda, M. A. (2017). *Daphne oleoides*: An alternative source of important sesquiterpenes. *International Journal of Food Properties*, 20(3), 549-559.

- Zengin, G., Arkan, T., Aktumsek, A., Guler, G. O., & Cakmak, Y. S. (2013). A study on antioxidant capacities and fatty acid compositions of two *Daphne* species from Turkey: new sources of antioxidants and essential fatty acids. *Journal of Food Biochemistry*, 37(6), 646-653.
- Zhao, R., Lu, Z., Yang, J., Zhang, L., Li, Y., & Zhang, X. (2020). Drug Delivery System in the Treatment of Diabetes Mellitus. Frontiers in Bioengineering and Biotechnology, 8, 880. doi:10.3389/ fbioe.2020.00880
- Zongo, C., Savadogo, A., Ouattara, L., Bassole, I., Ouattara, C., Ouattara, A., . . . Traore, A. (2010). Polyphenols content, antioxidant and antimicrobial activities of *Ampelocissus grantii* (Baker) Planch.(Vitaceae): a medicinal plant from Burkina Faso. *International Journal of Pharmacology*, 6(6), 880–887. doi: 10.3923/ijp.2010.880.887

In Vitro and Bioinformatic Studies on The Phytochemical Constituent of Selected Zingiberaceae Plants Targeting Inhibitor Lipoxygenase (LOX)

Nur Amalia CHOIRONI*, Asep Gana SUGANDA**, Kusnandar ANGGADIREDJA***

In Vitro and Bioinformatic Studies on The Phytochemical Constituent of Selected Zingiberaceae Plants Targeting Inhibitor Lipoxygenase (LOX)

SUMMARY

Lipoxygenase (LOX) is an enzyme essential for forming leukotriene, an endogenous substance involved in inflammatory pathological conditions, including asthma and rheumatoid arthritis. Plants that belong to the Zingiberaceae family have been empirically used as drugs in Indonesia. However, previous research has not spesifically identified the potential of this plant in inhibiting the lipoxygenase enzyme. This study aimed to screen the LOX-inhibiting activity of 18 plants from the Zingiberaceae family. The compounds of Curcuma zedoaria ((Chritsm.) Roscoe.) essential oil exhibiting the highest activity were identified for bioinformatic studies. Bioinformatics analysis to reveal and confirm the gene target of the active compound was acquired from the STITCH, STRING, and Swiss Target Prediction databases. The research result showed that the ethanol extract of C. zedoaria at 100 ppm had the highest inhibiting activity compared to other extracts, with a value of 54.8% and the IC50 value is 86.03 ppm. The further test also showed that the essential oil of C. zedoaria (EOCZ) in the selected plants was better than the extracts and their fractions. Based on GC-MS identification, the main components are longiverbenone, germacrene A, and α-pinene. The bioinformatics study showed that the potential target of EOCZ is MAPK3, MPO, HMOX1, ACE, PARP1, PPARĞ, ALOX 5 (5-LOX), PTGS1, PTGES, ESR, and NOS2. And one of the potential targets of EOCZ is 5-LOX. 5-LOX is essential in inflammatory reactions, and EOCZ, by inhibiting 5-LOX, may have the potential as an adjunct therapy for respiratory disorders.

Key Words: Lipoxygenase, Zingiberaceae, Curcuma zedoaria.

Seçilmiş Zingiberaceae Bitkilerinin İnhibitör Lipoksijenazı (LOX) Hedefleyen Fitokimyasal Bileşeni Üzerine İn Vitro ve Biyoinformatik Çalışmalar

ÖZ

Lipoksijenaz (LOX), astım ve romatoid artrit dahil olmak üzere iltihaplı patolojik durumlarda rol oynayan endojen bir madde olan lökotrien oluşumu için gerekli bir enzimdir. Zingiberaceae ailesine ait bitkiler Endonezya'da deneysel olarak ilaç olarak kullanılmıştır. Ancak daha önce yapılan araştırmalarda bu bitkinin lipoksijenaz enzimini inhibe etme potansiyeli özel olarak belirlenmemiştir. Bu çalışma, Zingiberaceae ailesinden 18 bitkinin LOX inhibe edici aktivitesini taramayı amaçlamıştır. En yüksek aktivite sergileyen Curcuma Zedoaria ((Chritsm.) Roscoe.) uçucu yağının bileşikleri, biyoinformatik çalışmalara devam etmek için tanımlanmıştır. Aktif bileşiğin gen hedefini ortaya çıkarmak ve doğrulamak için biyoenformatik analizi STITCH, STRING ve Swiss Target Prediction veritabanlarından elde edilmiştir. Araştırma sonucu, C. zedoaria türünün 100 ppm'deki etanol özütünün %54,8'lik bir değerle diğer özütlere kıyasla en yüksek inhibe edici aktiviteye sahip olduğunu ve IC50 değerinin 86,03 ppm olduğunu göstermiştir. Ayrıca, daha ileri test için seçilen bitkilerden C. zedoaria'nın (EOCZ) uçucu yağının, özütlerden ve fraksiyonlarından daha iyi olduğunu göstermiştir. GC-MS kullanılarak yapılan tanımlamaya göre ana bileşenler longiverbenon, germakren A ve α-pinendir. Biyoenformatik çalışması, EOCZ'nin potansiyel hedefinin MAPK3, MPO, HMOX1, ACE, PARP1, PPARG, ALOX 5 (5-LOX), PTGS1, PTGES, ESR ve NOS2 olduğunu EOCZ'nin den önce ve EOCZ'nin potansiyel hedeflerinden birinin 5-LOX olduğunu göstermiştir. 5-LOX, inflamatuar reaksiyonlarda önemli bir enzimdir ve EOCZ, 5-LOX'u inhibe ederek solunum yolu hastalıklarına yönelik yardımcı tedavi potansiyeline sahip olabilir.

Anahtar Kelimeler: Lipoksijenaz, Zingiberaceae, Curcuma zedoaria.

Received: 24.11.2024 Revised: 05.07.2025 Accepted: 14.08.2025

^{*} ORCID: 0000-0003-3399-5019, Department of Pharmacy, Jenderal Soedirman University, Purwokerto, Indonesia

^{*} ORCID: 0000-0003-3399-5019, Research Centre of Rural Health, Jenderal Soedirman University, Purwokerto, Indonesia.

[&]quot;ORCID: 0000-0003-0523-129X, School of Pharmacy, Bandung Institute of Technology, Bandung, Indonesia.

ORCID: 0000-0001-9879-6112, School of Pharmacy, Bandung Institute of Technology, Bandung, Indonesia.

INTRODUCTION

LOX is an enzyme that catalyzes the oxygenation of arachidonic acid and converts hydroperoxyeicosatetraenoic acid (HPETE) into leukotriene-A₄ (LTA₄). Other leukotrienes formed include LTB4, LTC₄, LTD4, and LTE₄. Leukotrienes are involved in the mediation of various inflammatory disorders, including asthma (Hafner, Kahnt, & Steinhilber, 2019). The inflammatory response involves a biosynthetic pathway known as the arachidonic acid cascade. Cyclooxygenase (COX) and lipoxygenase (LOX) are two enzymes particularly important in the cascade. While there have been many studies on COX, only a few studies have been conducted to investigate LOX, let alone studies on enzyme-inhibiting substances (Leuti et al., 2020).

Lipoxygenases in the human body contribute significantly to the stimulation of inflammatory responses. Reactive oxygen species are key inflammatory disorders signaling molecules that trigger cytokine production and LOX activation. Illnesses, including asthma, cancer, stroke, cardiovascular and neurological diseases, associated with inflammation. LOXs produce prostaglandins and leukotrienes. They are linked to the emergence of diseases, and preventing them is a step in preventing the disease. Linoleic, linolenic, and arachidonic acid are three polyunsaturated fatty acids (PUFAs) oxidized by lipoxygenases (LOXs), a class of monomeric proteins, to create hydroperoxides. LOXs are widely distributed in the kingdoms of cyanobacteria, plants, and animals. Additionally, 9-LOX and 13-LOX are plant LOXs that catalyze the oxygenation of linoleic and linolenic acid, whereas 5-LOX is pervasive in mammals and oxygenates carbon-5 on arachidonic acid (Leuti et al., 2020). The enzyme 5-lipoxygenase (5-LOX), also known as Arachidonate 5-lipoxygenase (ALOX5), oxidizes arachidonic acid, which interacts with eicosapentaenoic acid to generate inflammationcausing leukotrienes. Drugs that inhibit 5-LOX are thought to prevent the production of inflammatory mediators from the arachidonic acid pathway, as 5-LOX plays a crucial role in the production of leukotrienes. Thus, it has been determined that inhibiting 5-LOX enzymes is a sensible strategy for antiinflammatory medications, especially for asthma. Zileuton, a synthetic inhibitor of 5-LOX, demonstrates hepatotoxic effects, similar to other synthetic medicines. This possible limitation, it is necessary to create inhibitory alternatives to 5-LOX (Loncaric et al., 2021). Due to the undesirable elements of the LOX pathway, research on lipoxygenase inhibition was conducted.

Plant phytochemicals have a significant protective function that may help prevent diseases brought on by oxidative stress. For thousands of years, several plants have been used as medicine. Plants which belong to the Zingiberaceae family, including Amomum compactum, Zingiber amaricans, Curcuma zedoaria, Curcuma xanthorriza, Kaempferia galanga, and Maranta galanga, have been empirically used in Indonesia to relieve pain, swelling, and asthma (Kloppenburg, 1983). Several in vivo pharmacological have demonstrated antiinflammatory activity of plants from the Zingiberaceae family (Leelarungrayub, Manorsoi, & Manorsoi, 2017; Karungkaran & Sadanandan, 2019). Early data from studies on Zingiber purpureum, Zingiber officinale, Kaempferia galanga, Curcuma domestica, Zingiber zerumbet, Alpinia galanga, Curcuma xanthoriza, Curcuma aeruginosa, and Curcuma zedoaria have so far been available (Wahuni, Sufiawati, Nittayanannta, & Levita, 2022; Iweala et al., 2023; Reanmongkol et al., 2011; Singh et al., 2012; Cahyono, Suzery, & Amalina, 2023; Rahaman et al., 2020). However, the study did not specifically determine the potential of Zingiberaceae plants in inhibiting the lipoxygenase enzyme. Therefore, further research is needed to determine its activity and the target protein that inhibits the enzyme. Based on this background, this study aims to verify the best LOX inhibitory activity

of several Zingiberaceae plant extracts and confirm the prediction of its molecular target.

MATERIAL AND METHODS

Preparation of Plant Material

Rhizomes and semen from 18 species of Zingiberaceae were selected based on ethnobotanical literature (Cumming et al., 2019; Kloppenburg, 1983). Plants used in this research were obtained from Manoko Garden, and their identification was carried out at Herbarium Bandungense, School of Life Sciences and Technology, ITB, Bandung, West Java, Indonesia. They were the rhizomes of Curcuma manga, Kaempferia galangal, Curcuma xanthorrhiza, Zingiber officinale, Boesenbergia pandurata, Zingiber purpureum, Zingiber ottensii, Curcuma zedoaria, Curcuma aeruginosa, Zingiber aromaticum, Amomum zingiber, Alpinia galanga, Maranta galanga, Zingiber zerumbet, Zingiber amaricans, Curcuma domestica, Curcuma heyneana, and the seed of Amomum compactum.

Extraction and Fractionation

The samples of 300 g were extracted by maceration using ethanol 95 % (in a 1:5 sample-to-solvent ratio) for 24 hours, followed by filtration. Residues were re-extracted twice with the same method and solvent. Ethanol extracts were concentrated using a rotavapor and dried using a freeze dryer. The extract with the highest inhibition activity, C. zedoaria, was fractionated using liquid-liquid extraction. The extract of C. zedoaria is dissolved in hot water at a ratio of 1:10. The aqueous solution is extracted using n-hexane solvent, then extracted with ethyl acetate solvent. The ratio between the aqueous solution and the solvent is 1:1. Three fractions were obtained: the n-hexane fraction, the ethyl acetate fraction, and the water fraction. The fractionation results were concentrated using a rotary vacuum evaporator and dried using a freeze dryer.

LOX-inhibiting Activity of Extracts

Assay of LOX inhibiting activity was adopted from Khan et al. (2012) with minor modifications.

Test solution (100 ppm for extract and seven ppm for baicalein) 10 μ L was pipetted into 1000 μ L linoleic acid solution and 1690 μ L of 0.2 M borate buffer solution. The solution was pre-incubated at 25 °C for 10 minutes. Three hundred microliters of 10000U/ml LOX were added, and the solution was then incubated for 5 minutes. After the second incubation, the formed HPETE can be measured for its absorbance at 234 nm using a UV spectrophotometer. Each sample was analysed in triplicate. The absorbance of the reference substance baicalein was used as a control. The percent of inhibition was calculated using the formula:

% \in hibition = Absorbance of control absorbance of test subtance \times 100% absorbance of control

The ${\rm IC}_{50}$ value represented the inhibiting activity for the highest activity; subsequently will be continued for fractionated and destillated. The lipoxygenase inhibition activity test on the fractions and essential oil of C. zedoaria was conducted using the same procedure as the test on the extract. Ethanol extract, n-hexane fraction, ethyl acetate fraction, water fraction, and essential oil of C. zedoaria were prepared into solutions with concentrations of 50 ppm, 100 ppm, 150 ppm, 200 ppm, and 250 ppm to determine the ${\rm IC}_{50}$ value for lipoxygenase inhibition. For the positive control, baicalein, solutions were made with one ppm, three ppm, five ppm, and seven ppm.

Distillation and Identification of Essential Oils

The essential oil of *C. zedoaria* (EOCZ) was obtained through hydrodistillation using a modified apparatus. 2 kg of *C. zedoaria* produced 4,2 mL of 100% concentrated essential oil. The essential oil was stored in a brown glass bottle at 0–4°C after being dried using anhydrous sodium sulfate. Gas chromatography-mass spectrometry (GC-MS) examined the essential oil composition. The gas chromatograph is equipped with a split-splitless injector and 5% difenil-95% methylpolysiloxane, 30 m, 0.25 mm, 0.25 µm film thickness capillary column RTX5. Gas chromatography conditions include a temperature range of 60 to 290°C at 8°C/min, with a

solvent delay of 2 min. The injector was maintained at a temperature of 280°C. The inert gas was helium at a flow of 1.31 mL/min, and the injected volume in the splitless mode was 0.20 μ L. The qualitative analysis was based on the percent area of each peak of the sample compounds. The mass spectrum of each compound was compared with the mass spectrum from the Wiley 7 and *National Institute of Standards and Technology* (NIST) databases.

Bioinformatics Analysis

This study involved a bioinformatic analysis to identify the gene targets of the active compound of EOCZ on asthma (Figure 1). The databases used

included: NCBI to analyze gene expression in asthma (https://www.ncbi.nlm.nih.gov/), Swiss Target Prediction to identify the direct or indirect protein targets of EOCZ (http://www.swisstargetprediction. ch/) (Daina, Michielin, & Zoete, 2019), and Venny 2.1 for analyzing the overlap of EOCZ targets as an anti-asthma agent. STRING was used to analyze the protein-protein interaction network based on Venny 2.1 results (https://string-db.org/) (Szklarczyk et al., 2023), and WEBGESTALT was used to analyze GO and KEGG pathways (http://www.webgestalt.org/) (Elizarraras et al., 2024). Their results were visualized as a bar graph.

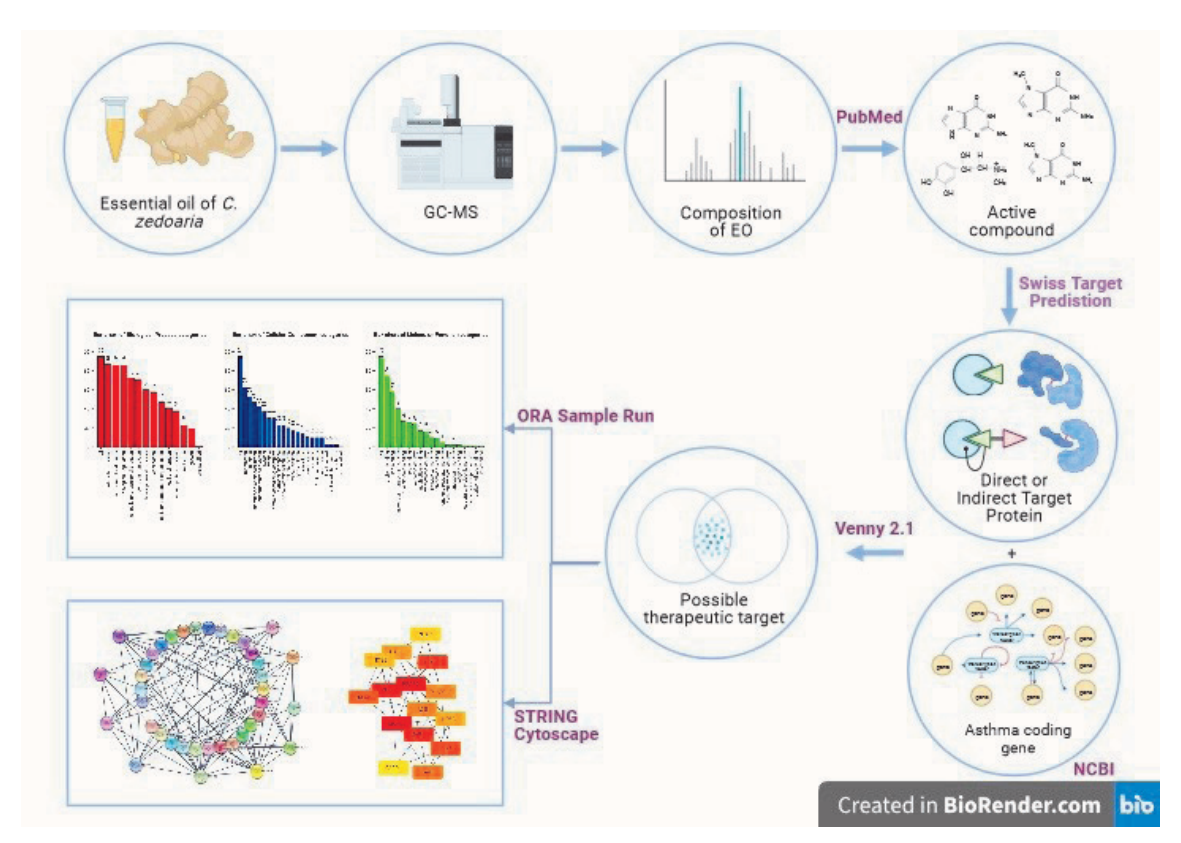


Figure 1. Scheme of bioinformatics analyses

RESULTS AND DISCUSSION

LOX-inhibiting Activity of Zingiberaceae Plant

The current study was carried out to screen plant extracts with lipoxygenase-inhibiting activity. Results

showed that the ethanol extract of *Curcuma zedoaria* at 100 ppm had the highest inhibiting activity compared to the other extracts, with a value of 54.8% (Table 1).

Table 1. Inhibition activity of LOX of the Zingiberaceae species and baicalein

Species	Vern name	Part of the plant	Yield (%)	Inhibition (%)
Curcuma manga	Temu manga	Rhizomes	5.00	7.17 ± 1.55
Curcuma xanthorrhiza	Temulawak	Rhizomes	5.45	10.54 ± 2.63
Amomum zingiber	Jahe merah	Rhizomes	10.35	11.64 ± 2.52
Zingiber officinale	Jahe	Rhizomes	5.60	12.08 ± 1.26
Alpinia galanga	Lengkuas	Rhizomes	10.55	12.29 ± 1.71
Zingiber ottensii	Bangle hantu	Rhizomes	7.00	13.07 ± 3.41
Zingiber purpureum	Bangle	Rhizomes	6.45	13.52 ± 1.90
Boesenbergia pandurata	Temu kunci	Rhizomes	6.35	15.10 ± 4.27
Amomum compactum	Kapulaga	Seed	2.05	15.48 ± 6.86
Zingiber amaricans	Lempuyang emprit	Rhizomes	11.50	16.37 ± 1.55
Kaempferia galanga	Kencur	Rhizomes	5.10	16.94 ± 3.92
Curcuma domestica	Kunyit	Rhizomes	12.50	21.50 ± 1.37
Zingiber aromaticum	Lempuyang wangi	Rhizomes	8.75	40.98 ± 6.19
Maranta galanga	Laos merah	Rhizomes	10.80	42.46 ± 6.28
Curcuma heyneana	Temu giring	Rhizomes	12.55	47.92 ± 3.70
Zingiber zerumbet	Lempuyang gajah	Rhizomes	11.35	51.62 ± 1.17
Curcuma aeruginosa	Temu hitam	Rhizomes	7.35	52.71 ± 4.98
Curcuma zedoaria	Temu putih	Rhizomes	7.25	54.58 ± 1.02
Baicalein	-	-	-	54.90 ± 1.16

Subsequently, the highest activity is fractionated and distilled. ${\rm IC}_{50}$ was determined for the ethanol extract, n-hexane fraction, ethyl acetate fraction, water fraction, and essential oil of C. zedoaria (EOCZ). The inhibition value of C. zedoaria extract was 86.03 ppm, and the reference substance baicalein was 6.59 ppm (Table 2). LOX inhibiting activity was determined by comparing the absorbance of hydroperoxyeicosatetranoate (HPETE) formed in the presence or absence of the extracts. As the substrate of LOX, linoleic acid was used in the current study, as this is due to the structural similarity between linoleic acid and arachidonic acid. Both substrates are

unsaturated fatty acids with methylene units between two double bonds. Both substrates are unsaturated fatty acids with methylene units between two double bonds. The mechanism of the LOX reaction consists of four steps. The LOX reaction's initial step is removing the hydrogen atom from the methylene unit between the double bonds in the substrate fatty acid, and the resulting electron is picked up by the ferric non-heme iron, which is reduced to the ferrous form. The second step is radical rearrangement, then oxygen insertion and peroxy radical reduction. The iron is reoxidized to its ferric form, and the peroxy anion is protonated (Cumming et al., 2019; Ivanov et al., 2010).

Table 2. LOX-inhibiting activity of *C. zedoaria* samples

Species	Yield (%)	IC ₅₀	
Ethanol extract	7.25	86.03 ± 2.15	
Fraction of n-hexane	15.07	49.60 ± 2.78	
Fraction of ethyl acetate	33.73	40.91 ± 3.14	
Fraction of water	7.20	44.36 ± 2.97	
Essential oil	0.21	17.03 ± 6.02	
Baicalein (7 ppm)	-	6.59 ± 2.23	

Phytochemicals naturally occur in plants with defense mechanisms and disease protection (Dosoky & Setzer, 2018). Phytochemical screening showed that the ethanol extract of C. zedoaria contained alkaloids, quinones, flavonoids, phenols, and steroid/ triterpenoids is consistent with several studies that flavonoids and triterpenoids contribution to lipoxygenase-inhibiting activity (Eissa et al., 2020). An earlier study by Dosoky and Setzer showed that the ethanol extract of C. zedoaria had inflammatory activity in vivo (Dosoky and Setzer, 2018). C. zedoaria belongs to the family of Zingiberaceae, which has been reported to contain curcuminoids, flavonoids, and essential oils. Curcuminoid (constituted by curcumin, demethoxycurcumin, and bisdemethoxycurcumin) was shown to have a role in inhibiting the enzyme lipoxygenase (Yang et al., 2017). Work by Sroka et al. (Sroka, Sowa, & Drys, 2017) demonstrated that flavonoids also had lipoxygenase-inhibiting activity.

Identification of EOCZ

This study showed that the essential oil had better lipoxygenase inhibition than the extract and its three fractions. This shows that compounds that play a role in the lipoxygenase inhibition process are more abundant in essential oils than others. The identification of essential oil components (Table 3) using GC-MS shows that there are 26 peaks (Figure 2) and compares the mass spectrum with the Wiley 7 and National Institute of Standards and Technology (NIST) databases. In the study of Servi et al. (Servi, Sen, Servi, & Dogan, 2021) proposed that the presence of α-pinene, elemicin, and estragole, possibly synergistic action for the antiinflammatory effect. Corroborating these findings, Albano et al. (2012) showed the enzyme-inhibiting activity of essential oil, which terpenoid group containing α -thujene, α -pinene, camphene, sabine, β -pinene, 1,8-cineole, p-cymene, β -myrcene, α -phellandrene, limonene, α-terpinol, γ-terpinene, camphor, trans-linalool oxide, trans-anetol, carvacrol, and eucalyptol.

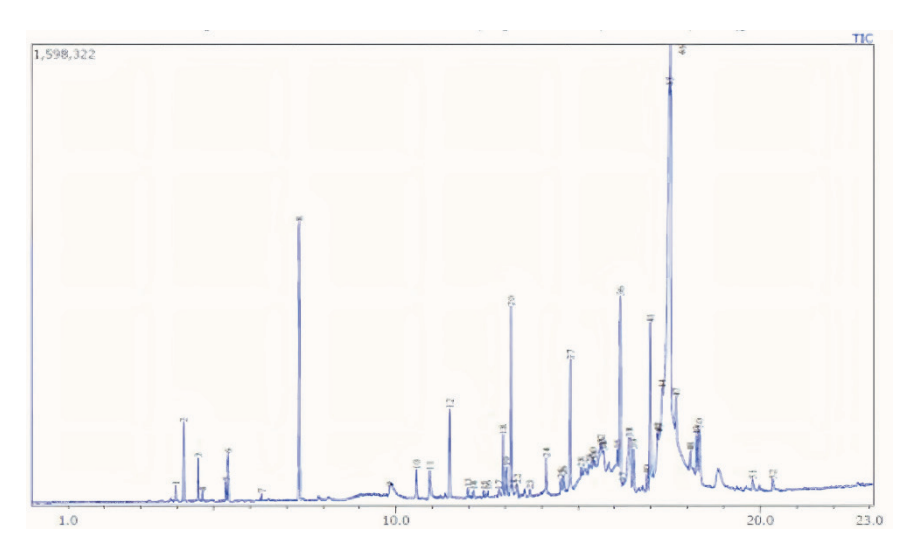


Figure 2. GC-MS Chromatogram of EOCZ

Juergens also hypothesized that 1,8-cineol inhibits 5-LOX and COXs to stop the production of inflammatory arachidonic acid metabolites such as LTB4 and PGE2 (Juergens, 2014). The camphoraceous oil

of *Rosmarinus officinalis* showed the most remarkable ability to inhibit LOX in vitro (Cutillas, 2018). The inhibition of 5-LOX by α -pinene was also suggested by Kohoude et al. (Kohoude et al., 2017)..

Table 3. Chemical constituent of EOCZ

Retention time	Area	m/z	Constituent	RIcalc	RIdb
3.953	4.25	136	α-pinene	931	931
4.175	1.37	136	Camphene	944	948
4.572	0.77	136	β-pinene	976	978
4.692	0.15	136	β-myrcene	989	989
5.331	0.37	136	Limonen	1026	1028
5.390	0.91	154	Eucalyptol	1030	1030
6.309	0.13	142	2-nonanon	1088	1090
7.348	6.80	152	Camphor	1145	1145
11.476	1.92	204	β-elemene	1281	1281
11.977	0.17	204	Cariophyllene	1418	1418
12.132	0.16	204	Cyclohexane	1470	1471
12.518	0.18	204	α-humulen	1454	1454
12.942	1.47	204	Germacrene-D	1462	1463
13.330	0.59	204	β-elemene	1471	1471
14.126	0.75	204	Germacrene B	1558	1560
14.792	3.57	286	Boldenon	1561	1561
15.083	0.24	190	Triquinasen	1565	1565
15.455	0.74	220	Isobutyric acid	1566	1566
16.085	0.37	216	Furanodiena	1884	1886
16.160	5.21	204	Germacrene A	1885	1885
16.400	3.63	214	Azulene	1892	1892
16.523	1.00	204	Delta selinene	1897	1898
16.887	0.38	218	2,3,3-Trimethyl-2-(3-methylbuta-1,3-dienil)-6-methylencyclohexanone	1888	1899
17.181	2.35	176	Cycloloheptatriene	1898	1900
17.311	4.14	214	1-(1-Methylamino-2-hydroxy-3-propyl)-dibenzo(b,e)-Bicyclo(2,2,2) octadiene Hydrochloride	1921	1921
17.539	12.29	218	Longiverbenon	1998	1998

 RI_{calc} : Retention index determined concerning homologous series of n-alkanes, RI_{db} : Retention index from the database (Poudel et al., 2022; Quemel et al., 2021; Satyal, 2015)

Bioinformatics Analysis

To determine the mechanism of action of compounds in EOCZ (Figure 3), a bioinformatic study was carried out on the four dominant compounds in EOCZ, namely longiverbenon, camphor, α-pinene, and germacrene A (Table 3). The result showed that the potential target of these compounds was related to the expression of genes for asthma. Based on Venny's analysis, these four compounds affected 38 target genes encoding asthma. The protein-protein interaction network of EOCZ was analyzed using the STRING database. EOCZ interacted with proteins, namely MAPK3, MPO, HMOX1, ACE, PARP1, PPARG, ALOX 5 (5-LOX), PTGS1, PTGES, ESR,

and NOS2 (Figure 3). In addition, ALOX5 has an impact on asthma activity. Swiss target analysis shows that longiverbenon, germacrene A, and α-pinene interaction with 5-LOX. The result of KEGG pathway analysis represents the inflammatory process. The KEGG pathway analysis indicates that there are pathways related to inflammation processes, such as prostaglandin receptor, GPCR, prostaglandin E receptor, eicosanoid receptor binding, and MAP kinase activity (Figure 4). KEGG pathway analysis described the interaction pathways that occur from proteins obtained by the STRING analysis. The enrichment ratio level represents the evidence-related pathways.

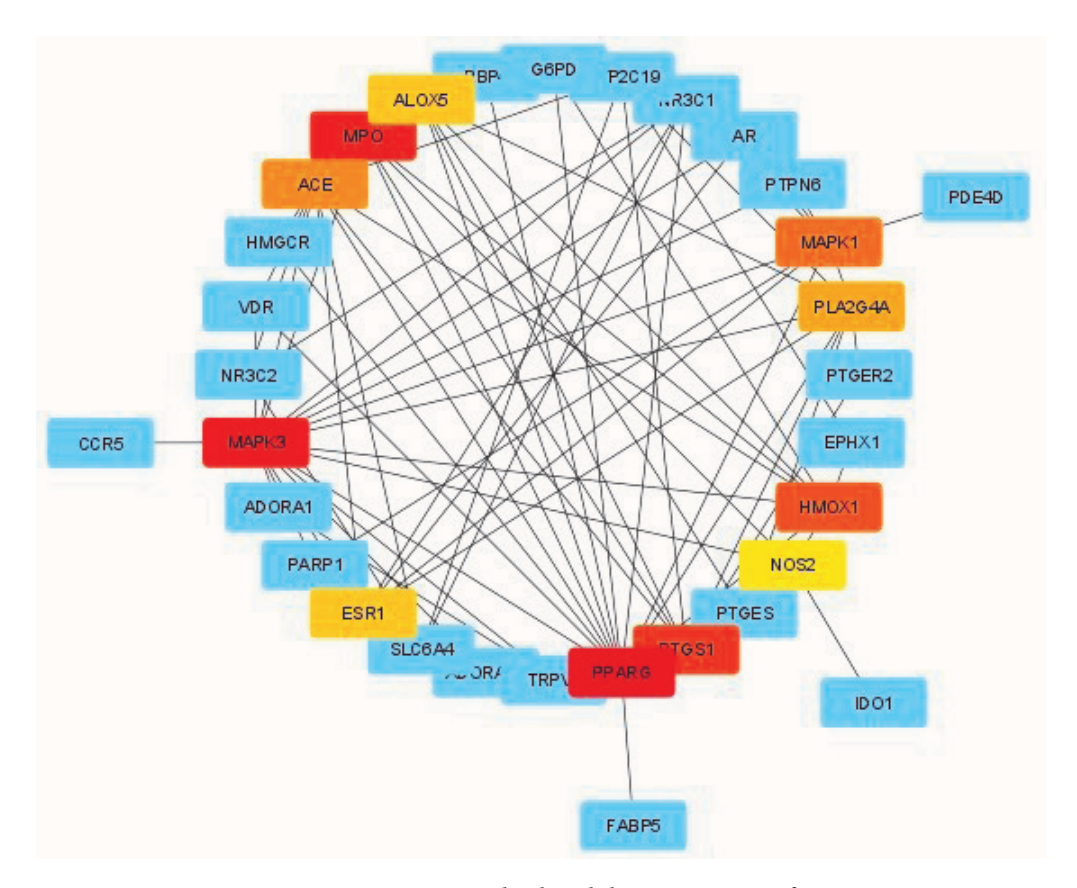


Figure 3. Top top-scoring displayed the target genes of EOCZ

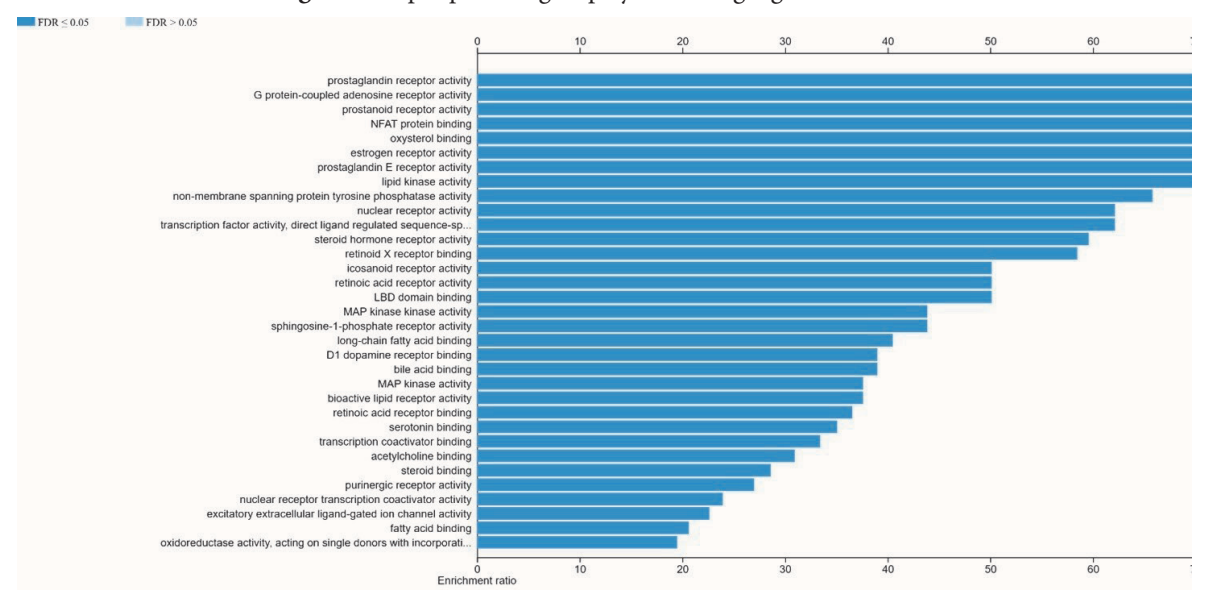


Figure 4. KEGG pathway of EOCZ

The GO analysis described the characteristics of a gene are biological process (BP), cellular component (CC), and molecular function (MF) (Figure 5). The analysis of KEGG pathway and gene ontology (GO) using the WEBGESTALT database was carried out to identify the involvement and role of these proteins, derived explicitly from wide-ranging molecular datasets

generated by genome sequencing and other highthroughput experimental methods. The BP analysis showed the metabolic process, biological regulation, cell communication, and cell proliferation process. CC analysis describes the identified protein's localization sites at the membrane, nucleus, mitochondria, extracellular matrix, and Golgi apparatus.

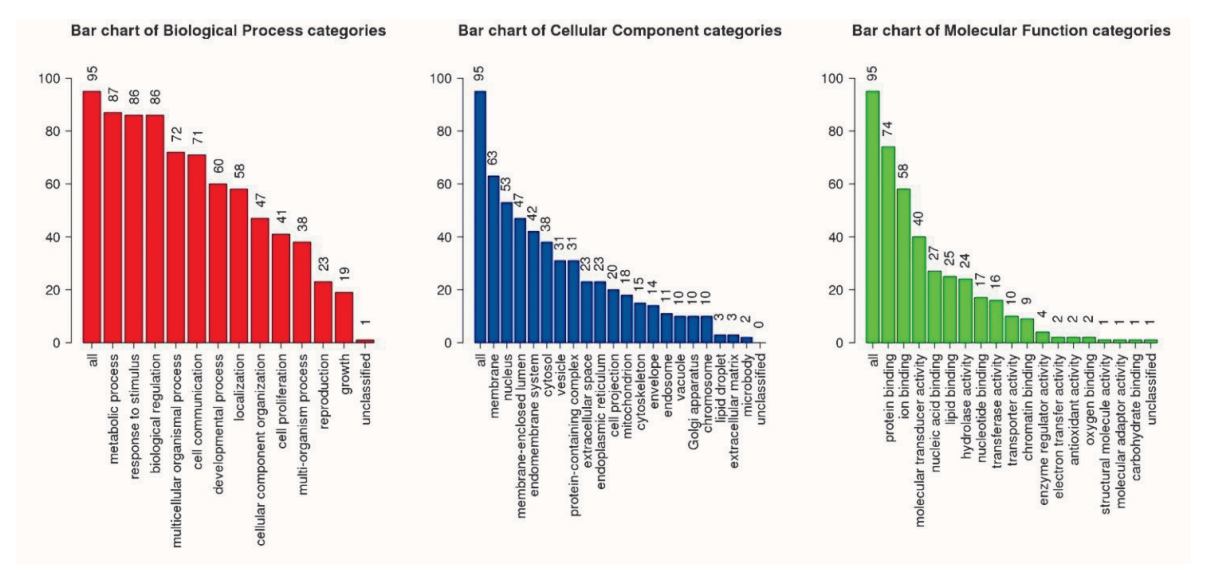


Figure 5. Gene ontology of EOCZ

The MF analysis reflects the molecular functions related to enzyme regulator activity and antioxidant activity (Figure 5). 5-LOX, which is found on chromosome 10q11.21, encodes 5-Lipoxygenase. The 5-LOX gene is located on chromosome 10q.11.21 and codes for an enzyme expressed in bone marrowderived inflammatory cells. This enzyme catalyzes the conversion of arachidonic acid to LTA4, which is then converted by other enzymes in the LT pathway to LTB4 and the cysLTs (LTC4, LTD4, and LTE4). Asthma, atherosclerosis, and pulmonary hypertension are only a few of the inflammatory disorders that have been linked to 5-LOX function. Others have investigated the role of 5-LOX in predicting the phenotype of asthma and how well it responds to treatment. The association between 5-LOX expression and a patient's reaction to an anti-5-LOX drug was originally demonstrated. The impact of 5-LOX Sp1 promoter genotypes on leukotriene production and asthma outcomes may

be influenced by other polymorphisms in 5-LOX, or leukotriene pathway genes like LTC4S and LTA4H. The powerful 5-LOX inhibitor prevents a significant percentage of cysteinyl leukotriene synthesis. Patients with bronchiolar asthma have been found to have the genetic E254K (760G4A) mutation in 5-LOX, despite the low incidence (Mashima & Torayuki, 2015; Mougey et al., 2013; Cai et al., 2019).

CONCLUSION

The current study's results show that the essential oil of *C. zedoaria* had the highest LOX-inhibiting activity among the tested plant extracts. The potential targets of EOCZ are 5-LOX, MAPK3, MPO, HMOX1, ACE, PARP1, PPARG, PTGS1, PTGES, ESR, and NOS2. 5-LOX is essential in inflammatory reactions and might be a potential adjunct therapy for this disease and respiratory disorder. Further research is needed to analyze its interaction with target receptors through molecular docking and dynamics.

AUTHOR CONTRIBUTION STATEMENT

Concept (NAC, AGS, KA), Design (NAC, AGS, KA), Supervision (AGS, KA), Resources (NAC, AGS), Materials (NAC, AGS), Data Collection and/or Processing (NAC), Analysis and/or Interpretation (NAC, AGS), Literature Search (NAC), Writing (NAC), Critical Reviews and proofreading (KA).

CONFLICT OF INTEREST

The authors declared no conflict of interest in this manuscript.

REFERENCES

- Albano, S. M., Lima, A. S., Miguel, M. G., Pedro, L. G., Barosso, J. G., & Figuieirido, A.C. (2012). Antioxidant, anti-5-lipoxygenase, and antiacetylcholinesterase activities of essential oils and decoction waters of some aromatic plants. *Records of Natural Products*, 6, 35-48. Retrieved from: https://www.acgpubs.org/doc/201808061907144-RNP-1011-389.pdf
- Cahyono, B., Suzery, M., & Amalina, N. D. (2023). Antiinflammatory effect of *Alpinia galanga* extract on acute inflammatory cell model of peripheral blood mononuclear cells stimulated with TNF-α. *Medicinski Glasnik*, 20(2), 207-213. https://doi.org/10.1016/j.prmcm.2023.100222
- Cai, C., Xiqing, B., Mingshan, X., Xiaoqing L., Haisheng, H., Jingxian, W.,...Jian-Lin W. (2019). Eicosanoid metabolized through LOX distinguishes asthma-COPD overlap from COPD by metabolomics study. *International Journal of Chronic Obstructive Pulmonary Disease*, 14, 1769-1778. https://doi.org/10.2147%2FCOPD.S207023
- Cumming, M., Massey, K. A., Mappa, G., Wilkinson, N., Hutson, R., Munot, S.,...Orsi, N. M. (2019). Integrated eicosanoid lipidomics and gene expression reveal decreased prostaglandin catabolism and increased 5-lipoxygenase expression in aggressive subtypes of endometrial cancer. *The Journal of Pathology*, 274(1), 21-34. https://doi.org/10.1002/path.5160

- Cutillas, A. B., Carrasco, A., Martinez, R., Tomas, V., & Tudela, J. (2018). *Rosmarinus officinalis* L. essential oils from Spain: composition, antioxidant capacity, lipoxygenase and acetylcholinesterase inhibitory capacities, and antimicrobial activities. *Plant Biosystems*, *3504*, 1–11. https://doi.org/10.10 80/11263504.2018.1445129
- Daina, A., Michielin, O., & Zoete, V. (2019). Swiss Target Prediction: updated data and new features for efficient prediction of protein targets of small molecules. *Nucleic Acids Research*, 47(W1), W357–W364. http://www.swisstargetprediction.ch/
- Dosoky, N. S., & Setzer, W. N. (2018). Chemical composition and biological activities of essential oils of *Curcuma* species. *Nutrients*, *10*(9), 1-42. https://doi.org/10.3390/nu10091196
- Eissa, M. A., Yumi, Z. H., Dina, M. E., Saripah, S. A., Hamzah, M. S., Isa, M. L., & Nor, M. A. W. (2020). Metabolite profiling of *Aquilaria malaccensis* leaf extract using liquid chromatography-Q-TOF-mass spectrometry and investigation of its potential antilipoxygenase activity in vitro. *Processes*, 8(2), 202. https://doi.org/10.3390/pr8020202
- Elizarraras, J. E., Yuxing, L., Zhiao, S., Qian, Z., Alexander, R. P., & Bing, Z. (2024). WebGestalt: faster gene set analysis and new support for metabolomics and multi-omics. *Nucleic Acids Research*, 456.
- Hafner, A. K., Kahnt, A. S., & Steinhilber, D. (2019). Beyond leukotriene, the noncanonical functions of 5-lipoxygenase. *Prostaglandins and Other Lipid Mediators*, 142, 24-32. https://doi.org/10.1016/j.prostaglandins.2019.03.003
- Ivanov, I., Heydeck, D., Hofheinz, K., Roffeis, J., Valerie, B., Donnel,...Walther M. (2010). Molecular Enzymology of Lipoxygenases. Archives of Biochemistry and Biophysics, 503, 161-174. https://doi.org/10.1016/j.abb.2010.08.016

- Iweala, E. J., Uche, M. E., Dike, E. D., Etumnu, L. R., Dokunmu, T. M., Oluwapelumi, A. E.,... Ugbogu, E. A. (2023). Curcuma longa (Turmeric): ethnomedicinal uses, phytochemistry, pharmacological activities and toxicity profiles-a review. Pharmacological Research-Modern Chinese Medicine, 5, 7-23. https://doi.org/10.1016/j.prmcm.2023.100222
- Juergens, U. (2014). Antiinflammatory properties of the monoterpene 1.8-cineole: current evidence for co-medication in inflammatory airway diseases. *Drug Research*, 64, 638–646. https://doi. org/10.1055/s-0034-1372609
- Karungkaran, R., & Sadanandan, S. P. (2019). Zingiber officinale: Antiinflammatory actions and potential usage for arthritic conditions. In: Bioactive food as dietary interventions for arthritis and related inflammatory diseases (second edition). Elsevier Inc., Newyork, 2019, pp. 234-244.
- Khan, H., Khan, M. A., Naveed, M., Nadeem, A., Farah, G., & Tariq, S. A. (2012). Antiinflammatory and antioxidant activity of Joshanda is partially mediated through inhibition of lipoxygenase. *Phytopharmacology*, *3*, 19-28. Retrieved from: https://scispace.com/pdf/anti-inflammatory-and-antioxidant-activity-of-joshanda-l3snq4pwot.pdf
- Kloppenburg, V. (1983). Properties and ingredients about plants in Indonesia as traditional medicine, Yayasan Dana Sejahtera, Yogyakarta, Indonesia.
- Kohoude, M. J., Gbaguidi, F., Agbani, P., Ayedoun, M. A., Cazaux, S., & Bouajila, J. (2017). Chemical composition and biological activities of extracts and essential oil of Boswellia dalzielii leaves. *Pharmaceutical Biology*, 55, 33–42. https://doi.org /10.1080%2F13880209.2016.1226356
- Leelarungrayub, J., Manorsoi, J., & Manorsoi, A. (2017). Antiinflammatory activity of niosomes entrapped with plai oil (*Zingiber cassumunar* Roxb.) by therapeutic ultrasound in a rat model. *International Journal of Nanomedicine*, 29(12), 2469-2476. https://doi.org/10.2147/IJN.S129131

- Leuti, A., Fazio, D., Fava, M., Piccoli, A., Oddi, S., & Maccarrone, M. (2020). Bioactive lipids, inflammation, and chronic disease. *Advanced Drug Delivery Reviews*, 159, 140-153. https://doi. org/10.1016/j.addr.2020.06.028
- Loncaric, M., Strelec, I., Moslavac, T., Subaric, D., Pavic, V., & Molnar M. (2021). Review: Lipoxygenase Inhibition by Plant Extracts. *Biomolecules*, 469(3), 743-747. https://doi.org/10.3390/biom11020152
- Mashima, R., & Torayuki, O. (2015). The role of lipoxygenase in pathophysiology: new insights and future perspectives. *Redox Biology*, *6*, 297-310. https://doi.org/10.1016/j.redox.2015.08.006
- Mougey, E., Jason, E., Hooman, A., Gerald, T., Allen, J., Robert, A., & John J. (2013). ALOX5 polymorphism associates with increased leukotriene production and reduced lung function and asthma control in children with poorly controlled asthma. *Clinical and Experimental Allergy*, 43, 512-520. https://doi.org/10.1111%2Fcea.12076
- Poudel, D. K., Pawan, K. O., Anil, R., Rakesh, S., Prabodh, S., & William, N. S. (2022). Analysis of volatile constituents in Curcuma species, viz. *C. aeruginosa, C. zedoaria*, and *C. longa*, from Nepal. *Plants*, *11*, 1-12. https://doi.org/10.3390/plants11151932
- Quemel, F. S., Dantas, A. P., Sanches, L., Viana, A. C. G. A., Silva, E. S., Monteiro, E. R.,...Lopes, A. D. (2021). Chemotypes of turmeric (*Curcuma longa* L.) essential oil from four states of Brazil, *Australian Journal of Crop Science*, 15(07), 1035-1042. https://doi.org/10.21475/ajcs.21.15.07. p3146
- Rahaman, M. M., Rakib, A., Mitra, S., Tareq, A. M., Emran, T. B., Daula, A. E. M.,...Gandara, J. S. (2020). The genus *Curcuma* and inflammation: Overview of the pharmacological perspective. *Plants*, 10(1),1-19. https://doi.org/10.3390/plants10010063

- Reanmongkol, W., Subhadhirasakul, S., Khaisombat, N., Fuengnawakit, P., Jantasila, S., & Khamjun, A. (2011). Investigation the antinociceptive, antipyretic, and antiinflammatory activities of *Curcumaaeruginosa* Roxb.extractsin experimental animals. *Journal of Science and Technology, 28* (5), 999-1008. Retrieved from: https://www.researchgate.net/publication/288595398_Investigation_the_antinociceptive_antipyretic_and_anti-inflammatory_activities_of_Curcuma_aeruginosa_Roxb_extracts_in_experimental_animals
- Satyal, P. (2015). Development of a GC-MS Database of essential oil components by analyzing natural essential oils and synthetic compounds and discovering biologically active novel chemotypes in essential oils. *Ph.D. Thesis*, University of Alabama in Huntsville, Huntsville, AL, USA.
- Servi, H., Sen, A., Servi, E. Y., & Dogan, A. (2021). Chemical composition and biological activities of essential oils of Foeniculum vulgare Mill. And *Daucus carota* L. growing wild in Turkey. *Journal of Research in Pharmacy*, 25(2), 142-152. https://dx.doi.org/10.29228/jrp.5
- Singh, C. B., Nongalleima, K., Brojendrosingh, S., Ningombam, S., Lokendrajit, N., & Singh, L. W. (2012). Biological and chemical properties of *Zingiber zerumbet* Smith. *Phytochem Reviews*, 11, 113-125. Retrieved from: https://link.springer. com/article/10.1007/s11101-011-9222-4

- Szklarczyk, D., Kirsch, R., Koutrouli, M., Nastou, K., Mehryary, F., Hachilif, R.,...& Mering C[‡]. (2023). The STRING database 2023 will contain protein– protein association networks and functional enrichment analyses for any sequenced genome of interest. *Nucleic Acids Res*, 6(51): 638-646.
- Sroka, Z., Sowa, A., & Drys, A. (2017). Inhibition of lipoxygenase and peroxidase reaction by some flavonols and flavones: the structure-activity relationship. *Natural Product Communications*, 12(11),1705-1708. Retrieved from: https://journals. sagepub.com/doi/10.1177/1934578X1701201111
- Wahuni, I. S., Sufiawati, I., Nittayanannta, W., & Levita, J. (2022). Antiinflammatory activity and wound healing effect of *Kaempferia galanga* L. rhizome on the chemical-induced oral mucosal ulcer in Wistar rats. *Journal of Inflammation Research*, 15, 2281-2294. https://doi.org/10.2147/JIR.S359042
- Wang, J., Duncan, D., Shi, Z., & Zhang, B. (2013). Webbased Gene Set Analysis Toolkit (WebGestalt): update 2013. Nucleic Acids Res, 41 (Web Server issue), W77-83. http://www.webgestalt.org/
- Yang, H., Du, Z., Wang, W., Song, M., Sanidad, K., Sukamtoh, E.,...Zhang, G. (2017). Structure-activity relationship of curcumin: role of the methoxy group in antiinflammatory and anticolitis effects of curcumin. *Agricultural and Food Chemistry*, 65(22), 4509-4515. https://doi.org/10.1021/acs.jafc.7b01792

Bioavailability File: Bicalutamide

Nihal Tugce OZAKSUN**, Tuba INCECAYIR**

Bioavailability File: Bicalutamide

SUMMARY

The non-steroidal antiandrogen drug bicalutamide (BIC) is used in the treatment of prostate cancer. It blocks the stimulatory effects of androgens on the growth of prostate cancer cells by blocking binding to androgen receptors in the prostate gland. BIC is a racemic mixture, and the (R)-enantiomer exhibits the main effect. It has been reported that BIC provides the targeted antiandrogenic impact due to its high selectivity, but its adverse effects should be carefully monitored. (R)-BIC is slowly absorbed after oral administration, and its absorption is dose-dependent. The drug is extensively metabolized in the liver, while elimination is largely achieved by renal and hepatic pathways. BIC and its metabolites are found in almost equal amounts in urine and feces. This review comprehensively covers the physicochemical properties, analytical methods, pharmacokinetics, bioavailability, and pharmacology of BIC.

Key Words: Bicalutamide, bioavailability, pharmacokinetics, pharmacology, physicochemical properties.

Biyoyararlanım Dosyası: Bikalutamid

ÖZ

Bikalutamid (BIC) prostat kanseri tedavisinde kullanılan steroidal olmayan bir anti-androjen ilaçtır. Prostat bezindeki androjen reseptörlerine bağlanmayı engelleyerek androjenlerin prostat kanseri hücrelerinin büyümesi üzerindeki uyarıcı etkilerini bloke eder. BIC rasemik bir karışımdır ve esas etkiyi (R)-enantiyomeri sergiler. BIC'nin yüksek selektivitesi sayesinde hedeflenen antiandrojenik etkiyi sağladığı, ancak advers etkilerinin dikkatli izlenmesi gerektiği belirtilmiştir. (R)-BIC, oral uygulama sonrası yavaş bir şekilde emilir ve emilimi doza bağlıdır. İlacın metabolizasyonu karaciğerde yoğun olarak gerçekleşirken, eliminasyon büyük ölçüde renal ve hepatik yollarla sağlanır. BIC ve metabolitleri idrar ve dışkıda neredeyse eşit oranda bulunur. Bu derleme BIC'nin fizikokimyasal özellikleri, analitik yöntemleri, farmakokinetiği, biyoyararlanımı ve farmakolojisini kapsamlı bir şekilde ele almıştır.

Anahtar Kelimeler: Bikalutamid, biyoyararlanım, farmakokinetik, farmakoloji, fizikokimyasal özellikler.

Received: 13.01.2025 Revised: 22.04.2025 Accepted: 27.05.2025

ORCID: 0000-0001-6276-9227, Department of Pharmaceutical Technology, Faculty of Pharmacy, Gazi University, Ankara, Turkiye

[&]quot;ORCID: 0000-0002-7106-7929, Department of Pharmaceutical Technology, Faculty of Pharmacy, Gazi University, Ankara, Turkiye

INTRODUCTION

Bicalutamide (BIC) (CAS 90357-06-5) is a non-steroidal antiandrogen drug used to treat prostate cancer. Also known as N-[4-cyano-3-(trifluoromethyl)phenyl]-3-(4-fluorophenyl)sulfonyl-2-hy-

droxy-2-methylpropanamide; its molecular formula is $C_{18}H_{14}F_4N_2O_4S$ (Bhise et al. 2009). The chemical structure of BIC is shown in Figure 1 (Bhise et al. 2009; NCBI, 2025).

Figure 1. The chemical structure of BIC.

This article aims to provide an extensive review of the bioavailability of BIC, including its pharmacokinetic profile, absorption, distribution, metabolism, and elimination. We also aim to investigate the effects of BIC's physicochemical properties on the bioavailability of the drug and highlight the key issues for the beneficial clinical usage and effective formulation development strategies.

Physicochemical Properties

BIC, with the molecular formula $C_{18}H_{14}F_4N_2O_4S$, is characterized by a complex structure that includes a fluorinated phenyl ring linked to a cyano group and a trifluoromethyl group, as well as a fluorophenyl ring attached to a hydroxy-2-methylpropanamide group (Tucker & Chesterson, 1988). Incorporating

these fluorinated groups significantly influences its physicochemical properties and pharmacological activities by introducing a blend of electrostatic, steric, and lipophilic effects that impact the drug's molecular structure and its binding affinity to the androgen receptor (Pertusati et al., 2019).

BIC is chiral; there are two enantiomers: (R)-BIC and (S)-BIC. The (R)-enantiomer demonstrates significant pharmacological efficacy by competitively inhibiting the binding of dihydrotestosterone to the androgen receptor, thereby playing a crucial role in the therapeutic management of androgen-dependent conditions, such as prostate cancer. In contrast, the (S)-enantiomer exhibits negligible antiandrogenic activity (Wellington & Keam, 2006). The stereochemistry of BIC is shown in Figure 2.

S (+)-enantiomer **Figure 2.** Stereochemistry of BIC.

BIC appears as a white or off-white crystalline powder. BIC is commercially available as Casodex, the original brand product, in the form of oval, biconvex, film-coated oral tablets, typically marked with a logo and the dosage (50 or 150 mg) (Casodex 50 mg, 2025; Casodex 150 mg, 2025).

The physicochemical parameters of BIC include a log P value of 2.92 and a pKa of 11.49 (De Gaetano et al., 2022; Volkova et al., 2022), with a melting point range of 192-198 °C, indicating thermal stability (Vega et al., 2007; Ren et al., 2006; Patil et al., 2008). The molecular weight of BIC is approximately 430.4 g/mol (De Gaetano et al., 2022). It exhibits extremely low water solubility, measured at less than 5 mg/L, which presents the main challenge to improving the bioavailability and efficacy of BIC (Cockshott, 2004). The high pKa indicates that BIC's solubility is relatively independent of the pH in a biological environment, and it exhibits higher solubility in certain organic solvents as opposed to water (Volkova et al., 2022).

Du et al. examined the solubility of BIC in various solvents, including methanol, ethanol, n-propanol, isopropanol, 1-butanol, isobutanol, toluene, acetonitrile, ethyl acetate, n-propyl acetate, cyclohexane, and n-hexane. The solubility values, arranged from highest to lowest, are as follows: n-propyl acetate, acetonitrile, ethyl acetate, methanol, ethanol. 1-butanol. n-propanol, isopropanol, isobutanol, toluene, cyclohexane, and n-hexane (Du et al., 2023). BIC is classified as a class II drug within the Biopharmaceutics Classification System (BCS), by its high permeability and low solubility features. Therefore, it has restricted solubility in water and consequently has reduced absorption when taken orally (Pokharkar et al., 2013).

Analytical Methods

BIC has been quantitatively determined using a range of analytical techniques, including UV spectrophotometry, high-performance liquid chromatography (HPLC), ultra-performance liquid chromatography (UPLC), liquid chromatographytandem mass spectrometry (LC-MS/MS), and electrochemical methods (Gomes & Garcia, 2012; Nanduri et al., 2012; Nageswara Rao et al., 2006; Nageswara Rao et al., 2008; Pandit et al., 2015; Ramarao et al., 2013; Sancheti et al., 2008a; Sharma et al., 2012; Subramanian et al., 2009). The literature on BIC quantification has been systematically categorized to offer a structured overview of the analytical methods.

Analysis of BIC and Related Impurities

Stability-indicating and quantitative HPLC methods have been extensively developed for the identification of degradation products and process-related impurities under stress conditions (Nanduri et al., 2012; Nageswara Rao et al., 2006).

Nanduri et al. reported HPLC and UPLC techniques using Zorbax SB phenyl and HSS T3 columns, with limits of quantification (LOQ) as low as 0.02-0.03%, demonstrating high sensitivity and suitability for stability and impurity profiling. The validated methods exhibited recoveries between 90% and 100% for purity and 98% and 102% for assay, confirming their high accuracy and reliability (Nanduri et al., 2012).

A gradient RP-HPLC method developed by Nageswara Rao et al. achieved excellent separation of BIC from its degradation products, with linearity ($r^2 \ge 0.9999$) in the 10-250 µg/mL range, and limits of detection (LOD) was found to be 2.4 and 3.0 x 10⁻⁸ g/mL for (S)-BIC and (R)-BIC, respectively, and LOQ was found to be 7.6 and 9.3 × 10⁻⁸ g/mL for (S)-BIC and (R)-BIC, respectively (Nageswara Rao et al., 2006).

Nageswara Rao et al. also developed an isocratic RP-HPLC method for impurity profiling of BIC using a Symmetry *C18 column and a mobile phase of 0.01 M KH₂PO₄ and acetonitrile. The method enabled the identification of degradation products and unknown impurities using Electrospray tandem mass spectrometry (ESI-MS/MS), Proton nuclear magnetic resonance (¹H NMR), and Fourier transform infrared spectroscopy (FTIR), with LOD and LOQ ranging

from 0.0165-0.074 $\mu g/mL$ and 0.20-0.48 $\mu g/mL$, respectively (Nageswara Rao et al., 2008).

Gomes and Garcia proposed a simultaneous determination method for BIC and structurally related compounds using a Symmetry C8 column and a mobile phase of acetonitrile and water containing 0.18% N, N-dimethyloctylamine (46.5:53.5, v/v). Although the method demonstrated a good linearity ($r^2 > 0.99$) and LOD and LOQ values of 2.61 µg/mL and 8.72 µg/mL, respectively (Gomes & Garcia, 2012).

BIC Determination in Pharmaceutical Formulations

UV spectrophotometry is frequently used for its simplicity, speed, cost-effectiveness, and accuracy. Sancheti et al. developed a UV spectrophotometric method to analyze BIC in distilled water containing 1% sodium lauryl sulphate (SLS) with an absorbance peak at 272 nm. The method provided LOQ and LOD of 0.4 μ g/mL and 0.1 μ g/mL, respectively (Sancheti et al., 2008a). UV spectrophotometry is also widely used for solubility studies and *in vitro* release experiments (Danquah et al., 2009; Kumbhar & Pokharkar, 2013; Li et al., 2011; Ray et al., 2016; Ren et al., 2006;).

BIC Determination in Biological Fluids

A rapid and sensitive LC-MS/MS method was developed by Sharma et al. to quantify BIC in mouse plasma using electrospray ionization (ESI) in negative-ion mode. The separation was carried out using an Atlantis dC-18 column using a mobile phase of 0.2% formic acid and acetonitrile (35:65, v/v). The ion transitions were m/z 428.9 \Rightarrow 254.7 for BIC and m/z 269.0 \Rightarrow 169.6 for the internal standard (tolbutamide). The LOQ was 1.04 ng/mL with a linearity range of 1.04-1877 ng/mL (Sharma et al., 2012).

Ramarao et al. reported an LC-MS/MS method for the quantification of (R)-BIC in human plasma using an isocratic mobile phase of acetonitrile and 0.1% formic acid buffer (50:50, v/v). The method exhibited an excellent linearity over 20-3200 ng/mL ($r^2 \ge 0.9990$) and a recovery rate of 98.56% (Ramarao et al., 2013).

Alternative Analytical Techniques

Electrochemical methods such as cyclic voltammetry and Differential Pulse Voltammetry (DPV) have been explored for BIC analysis. Pandit et al. developed a sensitive electrochemical method using a Single-Walled Carbon Nanotube (SWCNT) Carbon Paste Electrode (CPE). The method showed excellent performance under optimized experimental conditions, with an LOD of $5.20 \times 10^{-8} \, \mathrm{M}$ and an LOQ of $1.74 \times 10^{-6} \, \mathrm{M}$ (Pandit et al., 2015).

Subramanian et al. suggested a high-performance thin-layer chromatographic (HPTLC) method for analyzing BIC in liposomal formulations. The method utilized silica gel 60F-254 plates with a toluene-ethyl acetate (4.5:5.5, v/v) mobile phase, and densitometric detection at 273 nm. It demonstrated high sensitivity, precision, and specificity for BIC (Subramanian et al., 2009).

Pharmacology

Mechanism of Action

BIC is a non-steroidal antiandrogen that exerts its therapeutic effect by competitively inhibiting the binding of androgens, such as testosterone, to androgen receptors in target tissues, particularly the prostate. This antagonism impairs androgen signaling pathways that contribute to the proliferation and survival of prostate cancer cells, as schematically illustrated in Figure 3. Unlike the therapies that lower systemic testosterone levels, BIC acts at the receptor level, providing selective inhibition while preserving circulating androgen concentrations (Cereda et al., 2022).

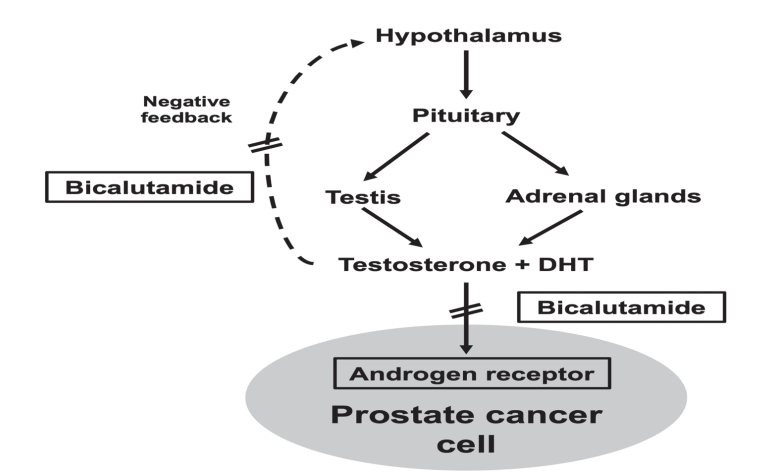


Figure 3. BIC mechanism of action. The figure was redrawn from the literature (Cereda et al., 2022).

Usage and Administration

BIC is administered orally in tablet form. The recommended dosage is 50 mg once daily for adult males, including the elderly. The drug can be consumed with or without food, as there is no clinically relevant effect of food on its bioavailability (eMC, 2023). Patients with metastatic prostate cancer are often treated with BIC and a luteinizing hormone-releasing hormone (LHRH) analogue. This combination therapy starts BIC with the LHRH analog or a few weeks later (Beebe-Dimmer et al., 2018; Grundmark et al., 2012).

In addition to its primary use in the prostate cancer treatment, it has also been investigated for its efficacy in treating androgenetic alopecia, commonly referred to as male pattern hair loss. Studies on BIC's potential to treat androgenic alopecia have shown positive findings, indicating that it may reduce the adverse impacts of androgens on hair follicles (Carvalho et al., 2022; Gomez-Zubiaur et al., 2023).

Also, a study was conducted on the use of BIC to treat hypertrichosis caused by minoxidil, a hair loss treatment. While minoxidil is generally safe, hypertrichosis has been reported in 24% of people consuming it. Oral BIC has been proven to improve patients' minoxidil-induced hypertrichosis. However, the study's limitations were a small number of patients,

a lack of a control arm, a retrospective design, and a lack of official hypertrichosis rating (Moussa et al., 2022).

BIC's anti-androgenic properties have prompted an investigation into its ability to treat hirsutism by blocking androgen receptor-mediated effects on hair follicles. Investigations have been carried out into the efficacy of low-dose (25 mg/day) BIC in the management of hirsutism, a condition characterized by excessive hair growth, particularly in women. BIC at a dose of 25 mg/day is an effective medication to treat people with hirsutism (Müderris et al., 2002).

Precautions and Adverse Effects

Breast pain, tenderness, and gynecomastia are the most common side effects of antiandrogen drugs like BIC. These complications are more common than castration. Gynecomastia, specifically, is prevalent among patients undergoing BIC treatment due to the drug's inhibition of androgen receptors, which subsequently increases estrogen levels (Ghadjar et al., 2020). A study investigating the side effects of BIC monotherapy revealed that gynecomastia affected 49.4% of participants, while breast pain was reported by 40.1% after an average follow-up of 6.3 years. However, only 1.3% of patients stopped treatment due to these side effects, indicating that the drug is well tolerated (Iversen et al., 2000).

Hot flashes are the typical side effect of androgen deprivation therapy, significantly decreasing the quality of life for men undergoing antiandrogen treatment. Hot flashes were reported by 80% of patients who were receiving antiandrogen therapy, with 27% of patients describing this symptom as the most unpleasant side effect. It is hypothesized that hot flashes result from a disruption in the hypothalamic thermoregulatory mechanisms caused by testosterone deficiency (Sakai et al., 2009).

BIC is a nonsteroidal antiandrogen with a relatively favorable safety and tolerability profile compared to flutamide and nilutamide. It is administered once daily due to its long half-life and is generally better tolerated, particularly in terms of gastrointestinal side effects. Unlike nilutamide, BIC is not associated with adverse effects such as visual disturbances, alcohol intolerance, or interstitial pneumonitis. Although no direct comparative trials between BIC and nilutamide were available in the literature, BIC was considered a more favorable option based on its adverse effect profile (Dole & Holdsworth, 1997).

A retrospective study evaluated the safety of BIC in 316 patients diagnosed with female pattern hair loss. The average duration of therapy was 6.21 months, with a range of 2 to 69 months. BIC was administered in combination with oral minoxidil to 308 patients and with spironolactone to 172 patients, while six patients received BIC as monotherapy. The most frequently reported side effect was a mild increase in liver transaminases, occurring in nine patients (2.85%). This change was asymptomatic in every case and ended in four of the nine patients without any dose adjustment, while in two patients, liver enzyme levels improved following a dose reduction. However, three patients who chose to discontinue BIC experienced persistent liver enzyme elevation. In total, 13 patients stopped treatment, with some cases potentially attributed to the adverse effects of minoxidil rather than BIC. Two patients who had previously stopped flutamide from colitis were able to tolerate BIC without experiencing a relapse (Ismail et al., 2020).

Drug Interactions

Nonsteroidal antiandrogens have the potential to interact with the other medications because of their high plasma protein binding capacity. The free serum concentration of highly protein-bound drugs, such as warfarin, phenytoin, or theophylline, may increase when antiandrogens are given to patients who use these drugs. Consequently, this increase may enhance the therapeutic or adverse effects associated with these medications (Wirth et al., 2007).

BIC can interact with coumarin anticoagulants, including warfarin and aspirin. It may cause these drugs to dissociate from plasma binding proteins, especially albumin, which may result in an increased anticoagulant effect. Consequently, when BIC is coadministered with these agents, it is essential to closely monitor prothrombin time and adjust the dosage as necessary (Hebenstreit et al., 2020).

LHRH agonists, such as leuprolide acetate and goserelin acetate, are combined with BIC to treat combined androgen blockade (CAB). In a comparative study assessing the clinical efficacy of BIC against flutamide, the mean concentration of (R)-BIC at week 12 among patients undergoing CAB was measured at 8.93 ± 3.48 mg/L (n=40). The concentration is comparable to that observed within monotherapy at the same dose level (8.53 \pm 2.93 mg/L; n=27), and aligns closely with the geometric mean steady-state concentration (C) of 8.85 mg/L derived from a larger cohort (n=116). Furthermore, after 3 months of CAB treatment, the mean serum testosterone levels were below the assay detection limit (< 0.69 nmol/L), with the upper limit recorded at 1.66 nmol/L, remaining within the defined castration range (<1.73 nmol/L) for CAB patients. These findings indicate no significant pharmacokinetic or pharmacodynamic interactions between BIC and LHRH agonists. These results are similar to the (R)-BIC concentration recorded for Japanese patients treated with 80 mg/day of BIC monotherapy (Cockshott, 2004).

BIC, as part of androgen deprivation therapy, may contribute to QT interval prolongation, particularly when co-administered with other QT-prolonging agents such as psychotropic drugs. Heitzmann et al. reported a clinical case in which long-term treatment with BIC and goserelin, combined with psychotropics like clozapine and trazodone, led to a significant increase in QTc values. The QT interval improved after discontinuation of these agents, suggesting a potential additive effect on cardiac repolarization (Heitzmann et al., 2017).

BIC is primarily metabolized by the CYP3A4 enzyme, and its co-administration with other drugs metabolized via the same pathway may result in pharmacokinetic interactions. While the daily doses of 150 mg or less have not been associated with clinically significant drug interactions when combined with CYP inhibitors or inducers (Wellington & Keam, 2006), caution is still advised. In particular, concomitant use with drugs such as cyclosporine or calcium channel blockers may increase the plasma drug concentrations of these agents. Therefore, the dose adjustment and close clinical monitoring may be necessary during the initiation or withdrawal of bicalutamide therapy (Casodex 150 mg, 2025).

BIC may inhibit CYP3A4 and, to a lesser extent, CYP2C9, CYP2C19, and CYP2D6. Nevertheless, with 150 mg of BIC, no clinically meaningful inhibition was seen *in vivo* utilizing midazolam as a specific CYP3A4 marker. The treatment effect on the area under the plasma drug concentration-time curve (AUC) was a 27% increase, and on the peak plasma concentration (C_{max}) was a 13% increase. While BIC is

known to activate CYP in laboratory animals, doses of 150 mg/day or less did not reveal any signs of enzyme induction in humans (Cockshott, 2004).

Pharmacokinetics and Bioavailability Absorption

The absolute bioavailability of BIC remains uncertain. However, it is characterized by a gradual and effective absorption profile following oral administration. This absorption is not influenced by food intake (eMC, 2023). The extent of absorption is dose and formulation-dependent; experimental animal studies have demonstrated that bioavailability is high at low doses but decreases at higher doses (Cockshott et al., 1991).

In a study assessing the absorption of BIC and its enantiomers in healthy male volunteers, a single 50 mg dosage was administered. Plasma concentration profiles of the enantiomers differed significantly (Figure 4). (S)-BIC was found to undergo extensive first-pass elimination, while (R)-BIC showed slow absorption with a mean absorption half-life of 6 hours. The peak plasma concentration for (R)-BIC was observed between 15 and 48 hours post-dose, with an average 4.2-day half-life. (S)-BIC reached its peak plasma concentration within 2 to 5 hours, subsequently decreased exponentially with an average 19-hour half-life (Cockshott, 2004; McKillop et al., 1993). The pharmacokinetic parameters for BIC and its enantiomers are summarized in Table 1 following the administration of a 50 mg single oral dose of 14C-(R, S)-BIC to healthy male volunteers (McKillop et al., 1993).

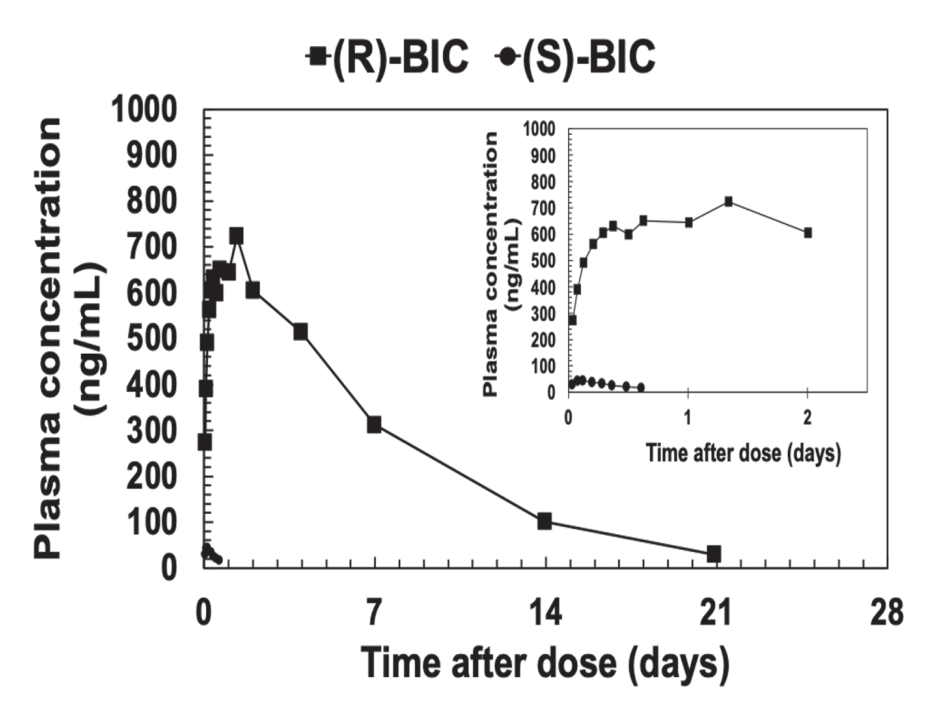


Figure 4. Mean plasma concentrations of (R)-BIC and (S)-BIC following the administration of a 50 mg single oral dose of ¹⁴C-(R, S)-BIC to healthy male volunteers. The plasma concentration data were obtained from the literature (McKillop et al., 1993) using the Automeris.io Version V5 plot digitizer.

Table 1. The pharmacokinetic parameters for (R)-BIC, (S)-BIC, and (R, S)-BIC following the administration of a 50 mg single oral dose of 14 C-(R, S)-BIC to healthy male volunteers. The data were derived from the literature (McKillop et al., 1993). a k_a = Absorption rate constant (1/h), b k_d = Elimination rate constant (1/day), c AUC $_\infty$ = The area under the plasma drug concentration-time curve (μ g.h/L), d SE = Standard error.

	(R)-BIC			(S)-BIC		(R,S)-BIC		
Subject	" k _a (1/h)	^b k _d (1/day)	'AUC _∞ (μg.h/mL)	^b k _d (1/h)	' AUC _∞ (μg.h/mL)	" k _a (1/h)	^b k _d (1/day)	' AUC _∞ (μg.h/mL)
1	0.06	0.20	92	0.01	2.07	0.05	0.22	98.4
2	0.17	0.14	177	0.03	1.65	0.25	0.14	181
3	0.08	0.17	143	0.09	0.67	0.03	0.20	157
4	0.36	0.21	121	0.15	0.50	0.61	0.18	123
5	0.21	0.14	190	0.11	0.58	0.29	0.14	196
Mean	0.17	0.17	145	0.08	1.09	0.25	0.17	151
^d SE	0.12	0.03	18	0.06	0.32	0.23	0.04	18

The effect of food on BIC absorption was evaluated by administering a 50 mg dose to healthy male volunteers before and after meals (Cockshott et al., 1997). Plasma levels of (R)-BIC were significantly higher compared to (S)-BIC following fasting (Figure 5). The time to peak drug concentration (t_{max}) values for (R)-BIC and (S)-BIC are 19 and 3 hours, respectively. Although food intake significantly increased the C_{max} values, food did not substantially affect AUC, t_{max} , and the elimination half-life ($t_{1/2}$) for either enantiomer. These results indicate that Casodex can be administered regardless of meal timing (Cockshott et al., 1997).

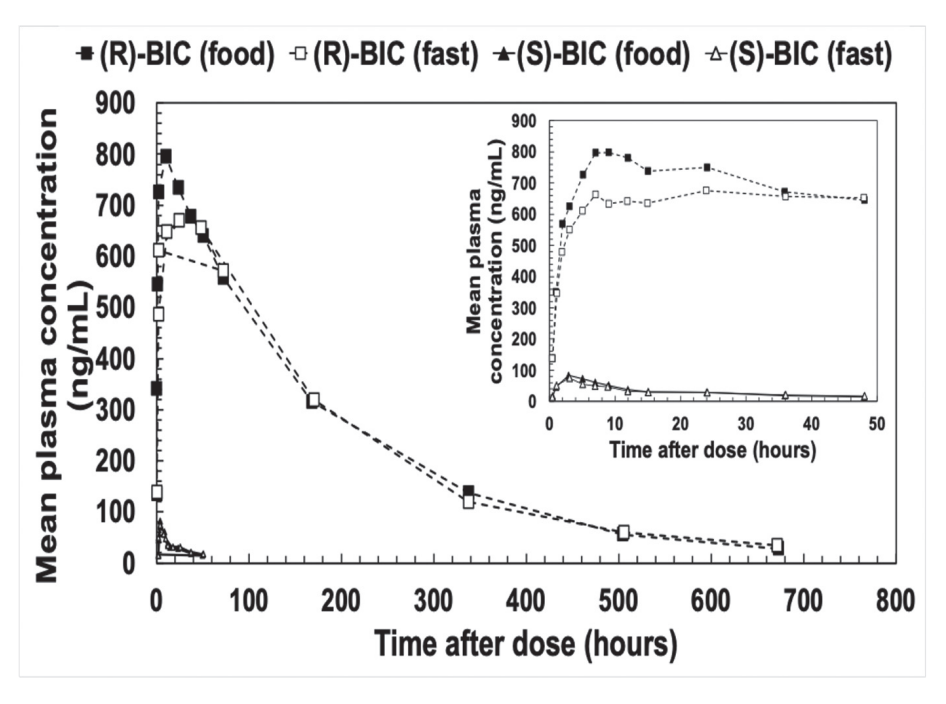


Figure 5. Plasma concentration profile of (R)-BIC and (S)-BIC following a single 50 mg oral dose of Casodex in healthy male volunteers under fasting and fed conditions. The plasma concentration data were obtained from the literature (Cockshott et al., 1997) using the Automeris.io Version V5 plot digitizer.

Distribution

An *in vitro* assessment was conducted to investigate the binding of BIC in human plasma. The binding affinity is $96.1\% \pm 0.4\%$, and there is no observable pattern of binding at concentrations ranging from 0.5 to 202 mg/L. Studies indicate that BIC has a strong affinity for albumin. Plasma samples were obtained 24 hours after administering a 150 mg dose of BIC to 14 volunteers with normal kidney and liver functioning. The average binding of $99.6\% \pm 0.15\%$ was much higher than the *in vitro* binding of the racemate, indicating notable enantioselectivity in protein binding (Cockshott, 2004).

Metabolization

BIC undergoes metabolism in the liver by oxidation and glucuronidation. The (R)-enantiomer makes up the majority of BIC, which is eliminated by metabolism. The drug is metabolized in the liver through oxidation and glucuronidation. (R)-BIC's main metabolic pathway is glucuronidation, and

it is driven by cytochrome P450 (CYP); however, oxidation is required before glucuronidation. (S)-BIC undergoes direct glucuronidation (McKillop et al., 1993).

BIC disappears in urine (36%) and feces (42%) within 9 days after a single dose is administered (Wellington & Keam, 2006). BIC and its metabolites are eliminated almost equally in urine and feces, with little of the first drug found in urine. Urine contains glucuronide conjugates of BIC hydroxybicalutamide. These compounds are believed to hydrolyze in the colon and accumulate as glucuronides in the bile. Plasma concentrations are dominated by the main drug (Cockshott, 2004; McKillop et al., 1993).

CYP3A4 enzyme metabolizes (R)-BIC mostly by hydroxylation into (R)-hydroxybicalutamide. Also, it is exposed to glucuronidation by the enzyme known as UDP-glucuronyltransferase UGT1A9. (R)hydroxybicalutamide is converted into (R)-hydroxy bicalutamide glucuronide in this way. (R)-hydroxy bicalutamide is metabolized by glucuronidation and eliminated from the body. Grosse et al.'s studies demonstrated the successful use of UGT2B7, UGT1A8, and UGT1A9 isoforms in metabolizing BIC (Grosse et al., 2013).

Elimination

BIC has a long plasma elimination half-life of a week and increases around ten times in plasma with daily treatment. BIC is primarily metabolized in the liver, with (R)-BIC metabolism being predominantly mediated by CYP3A4, while (S)-BIC undergoes glucuronidation as the main pathway. The metabolites are excreted almost equally in urine (36%) and feces (42%), while unchanged BIC is not detected in significant amounts in urine. The steady-state plasma concentrations (C_{ss}) of (R)-BIC exhibit a nonlinear increase with higher doses, indicating that absorption mechanisms seem to reach saturation at doses over 300 mg/day. However, there are no dose-dependent changes in elimination kinetics. The elimination half-life of (R)-BIC is substantially prolonged (approximately 1.75-fold) in individuals with mild to moderate hepatic impairment, suggesting the significance of hepatic metabolism in its clearance. Significant hepatic impairment may further reduce the drug's elimination capacity (Cockshott, 2004).

Alternative Formulation Types

BIC, a nonsteroidal antiandrogen used in the treatment of prostate cancer, exhibits poor aqueous solubility and high permeability, classifying it as a BCS Class II compound. These physicochemical limitations significantly reduce its oral bioavailability. Therefore, advanced drug delivery systems have been explored to increase the solubility, dissolution rate, permeability, and ultimately, the bioavailability of BIC.

Nanocarrier systems, particularly polymeric micelles and poly (lactic-co-glycolic acid) (PLGA) based nanoparticles, have demonstrated significant enhancements in the biopharmaceutical performance of BIC. PLGA nanoparticles demonstrated enhanced

cellular uptake and cytotoxicity in prostate cancer cell lines, while providing sustained drug release (Ray et al., 2016; Guo et al., 2015). Functionalization with folic acid-conjugated chitosan further enhanced the cellular internalization and therapeutic efficacy (Dhas et al., 2015; Kudarha et al., 2015).

Polymeric micelles have also been extensively studied to improve the delivery and therapeutic efficacy of BIC. Danquah et al. developed a series of polymeric micelle systems using different block copolymers to enhance the delivery and therapeutic efficacy of BIC. Initial studies employed PEG-PLA-based micelles for the co-delivery of BIC and embelin, yielding improved solubility and synergistic anticancer activity (Danquah et al., 2009). Subsequent formulations utilized methoxy poly(ethylene glycol)-b-poly(carbonate-colactide) and crosslinked carbonate-lactide copolymers to achieve sustained drug release, enhanced tumor growth inhibition, and greater micelle stability under physiological conditions (Danquah et al., 2010; Danquah et al., 2013).

Solid dispersion strategies using hydrophilic carriers such as polyvinylpyrrolidone (PVP), poloxamers, and PEG 6000 have been employed to reduce BIC crystallinity and enhance wettability, leading to increased dissolution rates. Optimized formulations preserved the amorphous state for prolonged durations (Ren et al., 2006; Sancheti et al., 2008b; Szafraniec et al., 2018; Szczurek et al., 2017). Pokharkar et al. reported a nanocrystal formulation using Soluplus, enhanced aqueous solubility up to 5-fold compared to the pure drug. In vivo pharmacokinetic studies revealed a substantial improvement in oral bioavailability. The nanocrystal formulation achieved a C_{max} of 17.6 \pm 2.57 $\mu g/$ mL, significantly higher than the 4.9 \pm 2.09 $\mu g/mL$ observed for pure BIC. Similarly, AUC increased from 87.21 \pm 11.49 $\mu g.h/mL$ to 275.54 \pm 29.22 $\mu g.h/$ mL, corresponding to a approximately 3.2-fold enhancement. The t_{max} was also reduced from 10 to 8 hours, indicating faster absorption (Pokharkar et al., 2013).

Lipid-based systems, including self-emulsifying drug delivery systems (SMEDDS and SNEDDS) and nanostructured lipid carriers (NLCs), have been studied to enhance the oral bioavailability of BIC via improved solubilization and potential lymphatic uptake. BIC-loaded SMEDDS formulation administered or ally at 25 mg/kg in rats resulted in a C_{max} of 12.04 \pm 1.57 $\mu g/mL$ and an AUC $_{\!_{m}}$ of 464.62 \pm 69.22 μ g.h/mL, compared to 4.21 \pm 2.09 μ g/mL and 229.33 \pm 27.03 µg.h/mL for the suspension. This corresponds to a 2.1-fold increase in AUC and 2.86-fold in C_{max} , indicating enhanced bioavailability (Singh et al., 2009). Arya et al. developed an SNEDDS formulation co-loaded with hesperetin, which achieved an AUC of 181,985.75 \pm 2810.40 h.ng/mL and a C_{max} of 4315 \pm 289.91 ng/mL, compared to 143,063.94 \pm 9583.68 h.ng/mL and 3465 \pm 417.19 ng/mL for the aqueous suspension. These results represent an increase in systemic exposure and peak plasma concentration, indicating improved oral bioavailability (Arya et al., 2017). Kumbhar and Pokharkar developed BICloaded NLCs and sustained release over 24 hours (Kumbhar & Pokharkar, 2013).

Cyclodextrin complexation with hydroxypropyl- β -cyclodextrin (HP- β -CyD), sulfobutylether-(SBE- β -CyD), β-cyclodextrin and acetylated β-cyclodextrin (Ac-β-CD) significantly enhanced BIC solubility and dissolution performance. Inclusion complexes showed improved antiproliferative activity in prostate cancer cell lines (De Gaetano et al., 2022), while the use of hydroxypropyl methylcellulose (HPMC) as a precipitation inhibitor in Ac-β-CD complexes led to high permeability and apparent supersaturation (Volkova et al., 2022).

Amorphous and co-amorphous formulations have also proven to be effective in enhancing the biopharmaceutical properties of BIC. Bohr et al. developed a co-amorphous system consisting of bicalutamide and docetaxel (DTX) at a 1:1 molar ratio. In this formulation, BIC functioned both as an active drug and a co-former with P-glycoprotein inhibitory activity, which enhanced the permeability of docetaxel. The

co-amorphous system exhibited faster dissolution, achieved a 1.9-fold supersaturation for DTX. *In vivo* pharmacokinetic studies demonstrated that, compared to the crystalline form, the co-amorphous formulation resulted in a 15-fold increase in AUC (2188 \pm 264 vs. 185 \pm 29 ng.h/mL) and a 9-fold increase in $C_{\rm max}$ (132 vs. 15 ng/mL) for DTX. Similarly, for BIC, the co-amorphous formulation provided a 3.2-fold increase in AUC (138.72 \pm 11.12 vs. 43.06 \pm 4.79 µg.h/mL) and a 3.3-fold increase in $C_{\rm max}$ (5542 vs. 1664 ng/mL), clearly indicating a substantial improvement in oral bioavailability for both compounds (Bohr et al., 2019).

In a separate study, Pacult et al. prepared a ternary amorphous solid dispersion containing flutamide, BIC, and polyvinylpyrrolidone (PVP). This system was designed to overcome the crystallization tendencies observed in binary drug combinations. The inclusion of PVP successfully stabilized the amorphous state for at least 182 days and led to a 7-fold increase in BIC's aqueous solubility and dissolution rate compared to its crystalline form (Pacult et al., 2019).

Additionally, Essa et al. demonstrated that cocrystallization of BIC with sucralose significantly enhanced its dissolution rate. The optimized 1:4 molar ratio co-crystals were formulated into fastdisintegrating tablets with disintegration times below 20 seconds and maintained physicochemical stability for 12 weeks. This approach offers a patient-friendly dosage form with improved dissolution, particularly suitable for elderly prostate cancer patients (Essa et al., 2019)

Several emerging formulation strategies have explored site-specific or alternative-route delivery systems to enhance the clinical performance of BIC. Yang et al. developed a protein-based formulation by complexing BIC with bovine serum albumin (BSA), which led to the formation of a metastable polymorph with improved thermal properties and rapid dissolution characteristics (Yang et al., 2017). Kesch et al. designed an injectable PLGA-based in situ forming paste containing both BIC and docetaxel

for the localized treatment of prostate cancer. This formulation enabled sustained intratumoral release, reduced tumor volume and PSA levels in orthotopic xenograft models, and demonstrated a safer alternative to systemic chemotherapy (Kesch et al., 2020). Zalcman et al. reported a novel water-soluble formulation, BIC-sol, which achieved over 1000-fold enhancement in aqueous solubility and significantly increased brain AUC in intracranial glioblastoma models, showing therapeutic superiority over conventional BIC and enzalutamide (Zalcman et al., 2023). Ghasemiyeh et al. developed dual-drug-loaded niosomal vesicles for topical delivery of BIC and tretinoin, which effectively targeted pilosebaceous units and improved local drug retention for the treatment of acne (Ghasemiyeh et al., 2023).

While direct comparisons between formulation strategies are limited by variations in study design, experimental models, and evaluation criteria, some general observations can be made. Nanocarrier systems, particularly polymeric micelles and PLGAbased nanoparticles, have frequently demonstrated notable improvements in solubility, dissolution, and systemic exposure. Solid dispersions and coamorphous systems offer promising results in terms of stability and manufacturability, though their performance is more formulation-dependent. Cyclodextrin complexes and lipid-based systems contribute significantly to solubility enhancement but may require further optimization to achieve consistent in vivo performance. Overall, the most effective strategies appear to be those that combine solubility enhancement with sustained or site-specific release while maintaining stability and clinical feasibility.

Future research should focus on developing multifunctional delivery systems that not only enhance solubility but also improve tissue targeting, overcome biological barriers, and demonstrate robust pharmacokinetic performance to support clinical translation of BIC-based therapies.

CONCLUSION

BIC is a commonly used antiandrogen with a favorable safety profile for treating prostate cancer that has been thoroughly investigated in clinical trials. The drug's absorption is influenced by its dose and formulation and differs between enantiomers. Absorption is independent of food consumption. It has a strong affinity for plasma proteins, with a primary binding to albumin. BIC is metabolized in the liver by oxidation and glucuronidation pathways. The medicine is released primarily through urine and feces, with most of it being digested and removed. Novel formulations of BIC have been created to enhance solubility, bioavailability, and therapeutic efficacy. The BIC formulations are designed to enhance drug delivery and selectively target certain tissues to improve treatment outcomes. Commonly utilized analytical techniques like HPLC, LC-MS/MS, and UV spectrophotometry are employed for the detection and quantification of BIC in formulations and biological Understanding the pharmacokinetics, bioavailability, and various formulation approaches of BIC is crucial for improving its therapeutic use and outcomes in prostate cancer.

AUTHOR CONTRIBUTION STATEMENT

Writing-review & editing, Writing-original draft, Visualization, Validation, Resources (NTO), Writing-review & editing, Writing-original draft, Visualization, Validation, Supervision (TI)

CONFLICT OF INTEREST

Authors declare that there is no conflict of interest.

REFERENCES

Arya, A., Ahmad, H., Tulsankar, S., Agrawal, S., Mittapelly, N., Boda, R., Dwivedi, A. K. (2017). Bioflavonoid hesperetin overcome bicalutamide induced toxicity by co-delivery in novel SNEDDS formulations: Optimization, *in vivo* evaluation and uptake mechanism. *Materials Science and Engineering*: C, 71, 954–964. https://doi.org/10.1016/j.msec.2016.11.006

Beebe-Dimmer, J. L., Ruterbusch, J. J., Bylsma, L. C.,

- Gillezeau, C., Fryzek, J., Schultz, N. M., & Quek, R. G. (2018). Patterns of bicalutamide use in prostate cancer treatment: a US real-world analysis using the SEER-Medicare database. *Advances in Therapy*, *35*, 1438-1451. https://doi.org/10.1007/s12325-018-0738-5
- Bhise, N. B., Sathe, D. G., Radhakrishanan, T., & Deore, R. (2009). Synthesis of potential impurities of bicalutamide. *Synthetic Communications**, 39(9), 1516-1526. https://doi.org/10.1080/00397910802519208
- Bohr, A., Nascimento, T. L., Harmankaya, N., Weisser, J. J., Wang, Y., Grohganz, H., & Löbmann, K. (2019). Efflux inhibitor bicalutamide increases oral bioavailability of the poorly soluble efflux substrate docetaxel in co-amorphous anti-cancer combination therapy. *Molecules*, 24(2), 266. https://doi.org/10.3390/molecules24020266
- Carvalho, R. de M., Santos, L. D. N., Ramos, P. M., Machado, C. J., Acioly, P., Frattini, S. C., Melo, D. F. (2022). Bicalutamide and the new perspectives for female pattern hair loss treatment: What dermatologists should know. *Journal of Cosmetic Dermatology*, 21(10), 4171-4175. https://doi.org/10.1111/jocd.14773
- Casodex 150 mg film tablet. Retrieved January 13, 2025, from https://www.astrazeneca.com.tr/content/dam/az-tr/medicine/PDF/Casodex%20 150mg%20KT_11.06.2019.pdf
- Casodex 50 mg film tablet. Retrieved January 13, 2025, from https://www.astrazeneca.com.tr/content/dam/az-tr/medicine/PDF/newpdfs09062017/1312-KT-Temiz%20 Kopya_50%20mg-09.05.2017.pdf

- Cereda, V., Falbo, P. T., Manna, G., Iannace, A., Menghi, A., Corona, M., & Lanzetta, G. (2022). Hormonal prostate cancer therapies and cardiovascular disease: a systematic review. *Heart Failure Reviews*, *27*(1), 119-134. https://doi.org/10.1007/s10741-020-09984-2
- Cockshott, I. D. (2004). Bicalutamide: clinical pharmacokinetics and metabolism. *Clinical Pharmacokinetics*, 43, 855-878. https://doi.org/10.2165/00003088-200443130-00003
- Cockshott, I. D., Oliver, S. D., Young, J. J., Cooper, K. J., & Jones, D. C. (1997). The effect of food on the pharmacokinetics of the bicalutamide ('Casodex') enantiomers. Biopharmaceutics & Drug Disposition, 18(6), 499-507. https://doi.org/10.1002/(SICI)1099-081X(199708)18:6<499::AID-BDD37>3.0.CO;2-J
- Cockshott, I. D., Plummer, G. F., Cooper, K. J., & Warwick, M. J. (1991). The pharmacokinetics of Casodex in laboratory animals. *Xenobiotica*, 21(10), 1347-1355. https://doi.org/10.3109/00498259109043209
- Danquah, M., Fujiwara, T., & Mahato, R. I. (2010). Self-assembling methoxypoly (ethylene glycol)b-poly (carbonate-co-L-lactide) block copolymers for drug delivery. *Biomaterials*, 31(8), 2358-2370. https://doi.org/10.1016/j.biomaterials.2009.11.081
- Danquah, M., Fujiwara, T., & Mahato, R. I. (2013). Lactic acid-and carbonate-based crosslinked polymeric micelles for drug delivery. *Journal of Polymer Science Part A: Polymer Chemistry*, *51*(2), 347-362. https://doi.org/10.1002/pola.26392
- Danquah, M., Li, F., Duke, C. B., Miller, D. D., & Mahato, R. I. (2009). Micellar delivery of bicalutamide and embelin for treating prostate cancer. *Pharmaceutical Research*, 26, 2081-2092. https://doi.org/10.1007/s11095-009-9903-5

- De Gaetano, F., Cristiano, M. C., Paolino, D., Celesti, C., Iannazzo, D., Pistarà, V., & Ventura, C. A. (2022). Bicalutamide anticancer activity enhancement by formulation of soluble inclusion complexes with cyclodextrins. *Biomolecules*, *12*(11), 1716. https://doi.org/10.3390/biom12111716
- Dhas, N. L., Ige, P. P., & Kudarha, R. R. (2015). Design, optimization and in-vitro study of folic acid conjugated-chitosan functionalized PLGA nanoparticle for delivery of bicalutamide in prostate cancer. *Powder Technology*, 283, 234-245. https://doi.org/10.1016/j.powtec.2015.04.053
- Dole, E. J., & Holdsworth, M. T. (1997). Nilutamide: an antiandrogen for the treatment of prostate cancer. *Annals of Pharmacotherapy*, *31*(1), 65-75. https://doi.org/10.1177/10600280970310011
- Du, D., Wang, G., & Lian, S. (2023). Solubility Profile and Intermolecular Force Analysis of Bicalutamide Form I in Mono Solvents at Several Temperatures. *Journal of Chemical & Engineering Data*, 68(8), 2066-2072. https://doi.org/10.1021/acs.jced.3c00149
- electronic Medicines Compendium (eMC). (2023).

 Casodex 50 mg film-coated tablets Summary of
 Product Characteristics (SmPC). AstraZeneca UK
 Limited. Retrieved April 20, 2025, from https://
 www.medicines.org.uk/emc/product/949/smpc
- Essa, E. A., Elbasuony, A. R., Abdelaziz, A. E., & El Maghraby, G. M. (2019). Co-crystallization for enhanced dissolution rate of bicalutamide: preparation and evaluation of rapidly disintegrating tablets. *Drug Development and Industrial Pharmacy*. https://doi.org/10.1080/036 39045.2019.1571504

- Ghadjar, P., Aebersold, D.M., Albrecht, C., Böhmer, D., Flentje, M., Ganswindt, U., & Wiegel, T. (2020). Treatment strategies to prevent and reduce gynecomastia and/or breast pain caused by antiandrogen therapy for prostate cancer. *Strahlentherapie und Onkologie 196*, 589–597. https://doi.org/10.1007/s00066-020-01598-9
- Ghasemiyeh, P., Moradishooli, F., Daneshamouz, S., Heidari, R., Niroumand, U., & Mohammadi-Samani, S. (2023). Optimization, characterization, and follicular targeting assessment of tretinoin and bicalutamide loaded niosomes. *Scientific Reports*, 13(1), 20023. https://doi.org/10.1038/s41598-023-47302-6
- Gomes, F. P., & Garcia, P. L. (2012). Development and validation of a simple and sensitive high performance liquid chromatographic method for the simultaneous determination of anastrozole, bicalutamide, tamoxifen, and their synthetic impurities. *Talanta*, *101*, 495-503. https://doi.org/10.1016/j.talanta.2012.10.004
- Gomez-Zubiaur, A., Andres-Lencina, J. J., Cabezas, V., Corredera, C., di Brisco, F., Ferrer, B., & Ricart, J. M. (2023). Mesotherapy with Bicalutamide: A New Treatment for Androgenetic Alopecia. *International Journal of Trichology*, 15(1), 39-40. https://doi.org/10.4103/ijt.ijt_78_21
- Grosse, L., Campeau, A. S., Caron, S., Morin, F. A., Meunier, K., Trottier, J., & Barbier, O. (2013). Enantiomer selective glucuronidation of the non-steroidal pure anti-androgen bicalutamide by human liver and kidney: Role of the human UDP-glucuronosyltransferase (UGT) 1A9 enzyme. *Basic & Clinical Pharmacology & Toxicology*, 113(2), 92-102. https://doi.org/10.1111/bcpt.12071

- Grundmark, B., Garmo, H., Zethelius, B., Stattin, P., Lambe, M., & Holmberg, L. (2012). Antiandrogen prescribing patterns, patient treatment adherence and influencing factors; results from the nationwide PCBaSe Sweden. *European Journal of Clinical Pharmacology*, 68, 1619-1630. https://doi.org/10.1007/s00228-012-1290-x
- Guo, J., Wu, S. H., Ren, W. G., Wang, X. L., & Yang, A. Q. (2015). Anticancer activity of bicalutamide-loaded PLGA nanoparticles in prostate cancers. *Experimental and Therapeutic Medicine*, 10(6), 2305-2310. https://doi.org/10.3892/etm.2015.2796
- Hebenstreit, D., Pichler, R., & Heidegger, I. (2020). Drug-drug interactions in prostate cancer treatment. *Clinical Genitourinary Cancer*, *18*(2), e71-e82. https://doi.org/10.1016/j.clgc.2019.05.016
- Heitzmann, E., Muller, C., Tebacher, M., Michel, B., &, & Javelot, H. (2017). Augmentation de l'intervalle QT imputable à un traitement antiandrogénique, majorée par les psychotropes: à propos d'un cas [Increased QT interval due to antiandrogenic therapy, majorated by psychotropic drugs. *Therapies*, 72, 701–703. https://doi.org/10.1016/j. therap.2017.05.003
- Ismail, F. F., Meah, N., de Carvalho, L. T., Bhoyrul, B., Wall, D., & Sinclair, R. (2020). Safety of oral bicalutamide in female pattern hair loss: a retrospective review of 316 patients. *Journal of the American Academy of Dermatology*, 83(5), 1478-1479.
- Iversen, P., Tyrrell, C. J., Kaisary, A. V., Anderson, J. B., Van Poppel, H., Tammela, T. L., & Melezinek, I. (2000). Bicalutamide monotherapy compared with castration in patients with nonmetastatic locally advanced prostate cancer: 6.3 years of followup. *The Journal of Urology*, 164(5), 1579-1582. https://doi.org/10.1016/S0022-5347(05)67032-2

- Kesch, C., Schmitt, V., Bidnur, S., Thi, M., Beraldi, E., Moskalev, I., & Gleave, M. E. (2020). A polymeric paste-drug formulation for intratumoral treatment of prostate cancer. *Prostate Cancer and Prostatic Diseases*, 23(2), 324-332. https://doi.org/10.1038/ s41391-019-0190-x
- Kudarha, R., Dhas, N. L., Pandey, A., Belgamwar, V. S., & Ige, P. P. (2015). Box–Behnken study design for optimization of bicalutamideloaded nanostructured lipid carrier: Stability assessment. *Pharmaceutical Development and Technology*, 20(5), 608-618. https://doi.org/10.310 9/10837450.2014.908305
- Kumbhar, D. D., & Pokharkar, V. B. (2013). Engineering of a nanostructured lipid carrier for the poorly water-soluble drug, bicalutamide: physicochemical investigations. *Colloids and Surfaces A: Physicochemical and Engineering Aspects*, 416, 32-42. https://doi.org/10.1016/j.colsurfa.2012.10.031
- Li, C., Li, C., Le, Y., & Chen, J. F. (2011). Formation of bicalutamide nanodispersion for dissolution rate enhancement. *International Journal of Pharmaceutics*, 404(1-2), 257-263. https://doi.org/10.1016/j.ijpharm.2010.11.015
- McKillop, D., Boyle, G. W., Cockshott, I. D., Jones, D. C., Phillips, P. J., & Yates, R. A. (1993). Metabolism and enantioselective pharmacokinetics of Casodex in man. *Xenobiotica*, 23(11), 1241-1253. https://doi.org/10.3109/00498259309059435
- Moussa, A., Kazmi, A., Bokhari, L., & Sinclair, R. D. (2022). Bicalutamide improves minoxidil-induced hypertrichosis in female pattern hair loss: a retrospective review of 35 patients. *Journal of the American Academy of Dermatology*, 87(2), 488-490.

- Müderris, I. I., Bayram, F., Özçelik, B., & Güven, M. (2002). New alternative treatment in hirsutism: bicalutamide 25 mg/day. *Gynecological Endocrinology*, 16(1), 63-66. https://doi.org/10.1080/gye.16.1.63.66
- Nageswara Rao, R., Narasa Raju, A., & Nagaraju, D. (2006). An improved and validated LC method for resolution of bicalutamide enantiomers using amylose tris-(3,5-dimethylphenylcarbamate) as a chiral stationary phase. *Journal of Pharmaceutical and Biomedical Analysis*, 42(3), 347-353. https://doi.org/10.1016/j.jpba.2006.04.014
- Nageswara Rao, R., Narasa Raju, A., & Narsimha, R. (2008). Isolation and characterization of process related impurities and degradation products of bicalutamide and development of RP-HPLC method for impurity profile study. *Journal of Pharmaceutical and Biomedical Analysis*, 46(3), 505-519. https://doi.org/10.1016/j.jpba.2007.11.015
- Nanduri, V. R., Adapa, V. P., & Kura, R. R. (2012). Development and validation of stability-indicating HPLC and UPLC methods for the determination of bicalutamide. *Journal of Chromatographic Science*, 50(4), 316-323. https://doi.org/10.1093/chromsci/bms010
- National Center for Biotechnology Information (2025). PubChem Compound Summary for CID 2375, Bicalutamide. Retrieved April 20, 2025, from https://pubchem.ncbi.nlm.nih.gov/compound/Bicalutamide.
- Pacult, J., Rams-Baron, M., Chmiel, K., Jurkiewicz, K., Antosik, A., Szafraniec, J., & Paluch, M. (2019). How can we improve the physical stability of co-amorphous system containing flutamide and bicalutamide? The case of ternary amorphous solid dispersions. European Journal of Pharmaceutical Sciences, 136, 104947. https://doi.org/10.1016/j.ejps.2020.105697

- Pandit, U. J., Khan, I., Wankar, S., Raj, K. K., & Limaye, S. N. (2015). Development of an electrochemical method for the determination of bicalutamide at the SWCNT/CPE in pharmaceutical preparations and human biological fluids. *Analytical Methods*, 7(24), 10192-10198. https://doi.org/10.1039/c5ay02025e
- Patil, A. L., Pore, Y. V., Kuchekar, B. S., & Late, S. G. (2008). Solid-state characterization and dissolution properties of bicalutamide-β-cyclodextrin inclusion complex. *Die Pharmazie-An International Journal of Pharmaceutical Sciences*, 63(4), 282-285. https://doi.org/10.1691/ph.2008.7260
- Pertusati, F., Ferla, S., Bassetto, M., Brancale, A., Khandil, S., Westwell, A. D., & McGuigan, C. (2019). A new series of bicalutamide, enzalutamide and enobosarm derivatives carrying pentafluorosulfanyl (SF5) and pentafluoroethyl (C2F5) substituents: Improved antiproliferative agents against prostate cancer. *European Journal of Medicinal Chemistry*, 180, 1-14. https://doi.org/10.1016/j.ejmech.2019.07.001
- Pokharkar, V. B., Malhi, T., & Mandpe, L. (2013). Bicalutamide nanocrystals with improved oral bioavailability: in vitro and *in vivo* evaluation. *Pharmaceutical Development and Technology*, *18*(3), 660-666. https://doi.org/10.3109/10837450.2012.663391
- Ramarao, N., Vidyadhara, S., Sasidhar, R., Deepti, B., & Yadav, R. (2013). Development and Validation of LC-MS/MS Method for the Quantification of Chiral Separated R-Bicalutamide in Human Plasma. *American Journal of Analytical Chemistry*, 4, 63-76. DOI:10.4236/ajac.2013.42009

- Ray, S., Ghosh, S., & Mandal, S. (2016). Development of bicalutamide-loaded PLGA nanoparticles: preparation, characterization and in-vitro evaluation for the treatment of prostate cancer. *Artificial Cells, Nanomedicine, and Biotechnology*, 45(5), 944-954. https://doi.org/10.1080/21691401.2016.1196457
- Ren, F., Jing, Q., Tang, Y., Shen, Y., Chen, J., Gao, F., & Cui, J. (2006). Characteristics of bicalutamide solid dispersions and improvement of the dissolution. *Drug Development and Industrial Pharmacy*, 32(8), 967-972. https://doi.org/10.1080/03639040600637606
- Sakai, H., Igawa, T., Tsurusaki, T., Yura, M., Kusaba, Y., Hayashi, M., & Kanetake, H. (2009). Hot Flashes During Androgen Deprivation Therapy With Luteinizing Hormone-Releasing Hormone Agonist Combined With Steroidal or Nonsteroidal Antiandrogen for Prostate Cancer. *Urology*, 73(3), 635-640. https://doi.org/10.1016/j.urology.2008.09.013
- Sancheti, P. P., Vyas, V. M., Shah, M., Karekar, P., & Pore, Y. V. (2008a). Spectrophotometric estimation of bicalutamide in tablets. *Indian Journal of Pharmaceutical Sciences*, 70(6), 810. doi: 10.4103/0250-474X.49131
- Sancheti, P. P., Vyas, V. M., Shah, M., Karekar, P., & Pore, Y. V. (2008b). Development and characterization of bicalutamide-poloxamer F68 solid dispersion systems. *Die Pharmazie-An International Journal of Pharmaceutical Sciences*, 63(8), 571-575. https://doi: 10.1691/ph.2008.8061
- Sharma, K., Pawar, G. V., Giri, S., Rajagopal, S., & Mullangi, R. (2012). Development and validation of a highly sensitive LC-MS/MS-ESI method for the determination of bicalutamide in mouse plasma: application to a pharmacokinetic study. *Biomedical Chromatography*, 26(12), 1589-1595. https://doi.org/10.1002/bmc.2736

- Singh, A. K., Chaurasiya, A., Jain, G. K., Awasthi, A., Asati, D., Mishra, G., & Mukherjee, R. (2009). High performance liquid chromatography method for the pharmacokinetic study of bicalutamide SMEDDS and suspension formulations after oral administration to rats. *Talanta*, 78(4-5), 1310-1314. https://doi.org/10.1016/j.talanta.2009.01.058
- Subramanian, G. S., Karthik, A., Baliga, A., Musmade, P., & Kini, S. (2009). High-performance thin-layer chromatographic analysis of bicalutamide in bulk drug and liposomes. *JPC-Journal of Planar Chromatography–Modern TLC*, 22, 273-276. https://doi.org/10.1556/JPC.22.2009.4.6
- Szafraniec, J., Antosik, A., Knapik-Kowalczuk, J., Chmiel, K., Kurek, M., Gawlak, K., & Jachowicz, R. (2018). Enhanced dissolution of solid dispersions containing bicalutamide subjected to mechanical stress. *International Journal of Pharmaceutics*, 542(1-2), 18-26. https://doi.org/10.1016/j.ijpharm.2018.02.040
- Szczurek, J., Rams-Baron, M., Knapik-Kowalczuk, J., Antosik, A., Szafraniec, J., Jamróz, W., & Paluch, M. (2017). Molecular dynamics, recrystallization behavior, and water solubility of the amorphous anticancer agent bicalutamide and its polyvinylpyrrolidone mixtures. *Molecular Pharmaceutics*, 14(4), 1071-1081. https://doi.org/10.1021/acs.molpharmaceut.6b01007
- Tucker, H., & Chesterson, G. J. (1988). Resolution of the non steroidal antiandrogen 4'-cyano-3-[(4-fluorophenyl) sulfonyl]-2-hydroxy-2-methyl-3'-(trifluoromethyl) propionanilide and the determination of the absolute configuration of the active enantiomer. *Journal of Medicinal Chemistry*, 31(4), 885-887.

- Vega, D. R., Polla, G., Martinez, A., Mendioroz, E., & Reinoso, M. (2007). Conformational polymorphism in bicalutamide. *International Journal of Pharmaceutics*, 328(2), 112-118. https://doi.org/10.1016/j.ijpharm.2006.08.001
- Volkova, T. V., Simonova, O. R., & Perlovich, G. L. (2022). Another Move towards Bicalutamide Dissolution and Permeability Improvement with Acetylated β-Cyclodextrin Solid Dispersion. *Pharmaceutics*, 14(7), 1472. https://doi.org/10.3390/pharmaceutics14071472
- Wellington, K., & Keam, S. J. (2006). Bicalutamide 150mg: a review of its use in the treatment of locally advanced prostate cancer. *Drugs*, 66, 837-850. https://doi.org/10.2165/00003495-200666060-00007

- Wirth, M. P., Hakenberg, O. W., & Froehner, M. (2007). Antiandrogens in the treatment of prostate cancer. *European Urology*, *51*(2), 306-314. https://doi.org/10.1016/j.eururo.2006.08.043
- Yang, C., Di, P., Fu, J., Xiong, H., Jing, Q., Ren, G., & Ren, F. (2017). Improving the physicochemical properties of bicalutamide by complex formation with bovine serum albumin. *European Journal of Pharmaceutical Sciences*, *106*, 381-392. https://doi.org/10.1016/j.ejps.2017.05.059
- Zalcman, N., Larush, L., Ovadia, H., Charbit, H., Magdassi, S., & Lavon, I. (2023). Intracranial Assessment of Androgen Receptor Antagonists in Mice Bearing Human Glioblastoma Implants. *International Journal of Molecular Sciences*, 25(1), 332. https://doi.org/10.3390/ ijms25010332

A Comprehensive Review on The Phytochemical Profile, Ethnobotanical Uses and Pharmacological Activities of Cuscuta reflexa Roxb.: An Asiatic Parasitic Vine

Rosy AHMED*, Akramul ANSARY**, Abhilash BHARADWAJ***, Koushik Nandan DUTTA****, Bhargab Jyoti SAHARIAH*****, Nilutpal Sharma BORA*******

A Comprehensive Review on The Phytochemical Profile, Ethnobotanical Uses and Pharmacological Activities of Cuscuta reflexa Roxb.: An Asiatic Parasitic Vine

SUMMARY

Cuscuta reflexa Roxb., commonly called dodder, represents a distinctive parasitic plant within the Convolvulaceae family, notable for its remarkable absence of roots and leaves. Beyond its botanical peculiarities, Cuscuta reflexa holds significant medicinal value, featuring prominently in numerous therapeutic formulations esteemed for their efficacy in addressing a diverse spectrum of ailments, including migraines, headaches, constipation, chronic catarrh, epilepsy, prolonged fever, amnesia, and itching, among others. This review endeavors to present a comprehensive synthesis of the botanical, taxonomical, pharmacological, and phytochemical attributes of Cuscuta reflexa. Employing a meticulous literature survey encompassing research articles published between 2010 and 2024, sourced from electronic databases the medicinal potential of Cuscuta reflexa emerges as multifaceted. Approximately 25 bioactive compounds have been identified and isolated from various anatomical components of the plant, showcasing significant pharmacological promise. However, despite the promising findings, a comprehensive understanding of the therapeutic mechanisms underlying Cuscuta reflexa's medicinal attributes necessitates further in vivo pharmacological and toxicological investigations. These endeavors are indispensable for unlocking the full therapeutic potential of the plant and its isolated chemical constituents, facilitating their clinical use. Continued research on Cuscuta reflexa is needed to understand its full healing potential. By delving deeper into the intricacies of its pharmacological profile, we can aspire to leverage Cuscuta reflexa's medicinal virtues more effectively, thereby advancing the frontiers of medical science and enhancing healthcare outcomes for diverse populations.

Key Words: Cuscuta reflexa, Dodder, Ethnobotany, Pharmacological, Phytochemistry.

Cuscuta reflexa Roxb.'nin Fitokimyasal Profili, Etnobotanik Kullanımları ve Farmakolojik Aktiviteleri Üzerine Kapsamlı İnceleme: Asya Parazit Sarmaşığı

ÖZ

Yaygın olarak küsküt olarak adlandırılan Cuscuta reflexa Roxb. Convolvulaceae familyası içinde özgün bir parazitik bitkiyi temsil eder ve kayda değer kök ve yaprak yokluğuyla dikkat çeker. Botanik özelliklerinin ötesinde, Cuscuta reflexa önemli bir tıbbi değere sahiptir ve migren, baş ağrısı, konstipasyon, kronik nezle, epilepsi, uzun süreli ateş, amnezi ve kaşıntı gibi çeşitli rahatsızlıkların giderilmesindeki etkinliği nedeniyle çok sayıda terapötik formülasyonda öne çıkmaktadır. Bu derleme, Cuscuta reflexa'nın botanik, taksonomik, farmakolojik ve fitokimyasal özelliklerinin kapsamlı bir sentezini sunmaktadır. Elektronik veri tabanlarından elde edilen ve 2010 ile 2024 yılları arasında yayınlanan araştırma makalelerini kapsayan titiz bir literatür taramasıyla, Cuscuta reflexa'nın tıbbi potansiyeli çok yönlü olarak karşımıza çıkmaktadır. Bitkinin çeşitli anatomik bileşenlerinden izole edilen ve tanımlanan yaklaşık 25 biyoaktif bileşik önemli farmakolojik potansiyel vaat etmektedir. Ancak, umut verici bulgulara rağmen, Cuscuta reflexa'nın tıbbi özelliklerinin altında yatan terapötik mekanizmaların kapsamlı bir şekilde anlaşılması için daha fazla in vivo farmakolojik ve toksikolojik araştırma yapılması gerekmektedir. Bu çabalar, bitkinin ve izole edilmiş kimyasal bileşenlerinin tüm terapötik potansiyelini ortaya çıkarmak ve klinik kullanımlarını kolaylaştırmak için elzemdir. Cuscuta reflexa'nın tüm iyileştirme potansiyelini anlamak için üzerinde daha fazla araştırma yapılması gerekmektedir. Farmakolojik profilinin inceliklerinin derinlemesine incelemesiyle, Cuscuta reflexa'nın tıbbi faydalarından daha etkin bir şekilde yararlanmak, böylece tıp biliminin sınırlarını genişletmek ve çeşitli popülasyonlar için sağlık sonuçlarını iyileştirmek hedeflenmektedir.

Anahtar Kelimeler: Küsküt, Cuscuta reflexa, Etnobotanik, Fitokimya, Farmakolojik.

Received: 29.10.2024 Revised: 5.05.2025 Accepted: 9.07.2025

^{*} ORCID: 0009-0001-0973-2756, Rahman Institute of Pharmaceutical Sciences and Research, Tepesia, Kamarkuchi, Kamrup(M), Assam. Pin-782402

^{**} ORCID: 0009-0004-7568-8812, NETES Institute of Pharmaceutical Science, NEMCARE Group of Institutions, Mirza, Kamrup, Assam, India, PIN – 781125.

^{***}ORCID: 0009-0009-4980-8397, NETES Institute of Pharmaceutical Science, NEMCARE Group of Institutions, Mirza, Kamrup, Assam, India, PIN – 781125.

^{*****} ORCID: 0000-0003-3555-9480, NETES Institute of Pharmaceutical Science, NEMCARE Group of Institutions, Mirza, Kamrup, Assam, India, PIN – 781125.

****** ORCID: 0000-0003-0440-6983, NETES Institute of Pharmaceutical Science, NEMCARE Group of Institutions, Mirza, Kamrup, Assam, India, PIN – 781125.

^{******} ORCID: 0000-0001-8648-0823, NETES Institute of Pharmaceutical Science, NEMCARE Group of Institutions, Mirza, Kamrup, Assam, India, PIN – 781125.

[°] Corresponding Author; Dr. Nilutpal Sharma Bora, Associate Professor E-mail: nilutpalsharma3@gmail.com

INTRODUCTION

Cuscuta reflexa recognized colloquially as devil's hair and alternatively referred to as a dodder plant, is an atypical parasitic botanical specimen within the Convolvulaceae family (Ahmad et al., 2022; Nadeem et al., 2020). Cuscuta reflexa, distinguished by its characteristic absence of roots as well as leaves, boasts a distinctive green-yellow hue. This peculiar parasitic vine thrives by intricately weaving its stems around host plants, a strategy it employs prolifically across the tropical and subtropical landscapes of South Asia. Its habitat spans regions of India, Afghanistan, Bangladesh, China, Sri Lanka, Indonesia, Malaysia, Nepal, Myanmar, Pakistan, Bhutan and Thailand (Figure 1), typically flourishing at altitudes ranging from 900 to 2800 meters above sea level (Islam, Rahman, & Rahman, 2015; Paudel, Satyal, Maharjan, Shrestha, & Setzer, 2014; Shailajan, Joshi, & Tiwari, 2014). In various regions across the globe, the plant is bestowed with different names that reflect its cultural significance. Referred to as Akashabela or Amarabela in Hindi and known as Akakhilata in Assamese, these vernacular appellations underscore the diverse linguistic tapestry through which the plant is recognized and revered (Adnan et al., 2020). In the Kannada language, the plant is identified as Swarnalatha (Lingaraju, Sudarshana, & Rajashekar, 2013). In the Udham district of Jammu and Kashmir, it is recognized as Aandal-Kaandal (Bhatia, Manhas, Kumar, & Magotra, 2014), while in Bengali, it is referred to as Sornolota or Swarnalata (Choudhury et al., 2015; Vineeta, Shukla, Bhat, & Chakravarty, 2022). In the Budgam district of Jammu and Kashmir, it is known as Kuklipot (Mir, Jan, & Khare, 2021), while in Tripura, it goes by the names Sannalata and Kuchilalata (Choudhury et al., 2015; Sen, Chakraborty, De, & Devanna, 2011). Nepali and Bhutia cultures denote it as Binajarhi, Akashveli and Rubeyshepo respectively (Tamang, Singh, Bussmann, Shukla, & Nautiyal, 2023), whereas in the Khasi community, it is

identified as Jawieh and Sonalu lata (Bhat et al., 2023). In Sri Lanka, it carries the name Ala binthamburu (Dharmadasa, Akalanka, Muthukumarana, & Wijesekara, 2016) and additionally, it is recognized as Nilatar in certain contexts (Saqib et al., 2014). These diverse names reflect the intricate tapestry of regional languages and cultural associations surrounding the plant.

Cuscuta reflexa finds its place as a key component in numerous medicinal formulations renowned for their efficacy in addressing a spectrum of ailments. These include treatments for migraines, expectorants, headaches, constipation, chronic catarrh, epilepsy, prolonged fever, amnesia and itching. Its utilization underscores its valued contribution to traditional medicinal practices, offering relief for various health conditions across different cultures and communities (Raza, Mukhtar, & Danish, 2015). Cuscuta reflexa exhibits a spectrum of pharmacological activities, including anticonvulsant as well as antiviral properties and effects on bradycardia, anti-steroidogenic, antispasmodic activity, as well as hemodynamic effects. Additionally, the seeds of Cuscuta reflexa are noted for their sweet taste and are traditionally employed in treating diverse disorders affecting the liver and kidneys. Furthermore, when combined with other medicinal plants, they are utilized in managing various diseases, underscoring their role in traditional healing practices across cultures (Ahmad et al., 2022). Furthermore, Cuscuta reflexa is employed in the treatment of conditions such as sperm leakage, impotence, tinnitus, premature ejaculation, lower back pain, knee discomfort, frequent urination, leucorrhoea or white vaginal discharge, eye fatigue, itching, blurred vision and dry eyes. These traditional uses underscore the plant's versatility in addressing various health concerns, reflecting its valued role in holistic healing practices embraced by various communities (Islam et al., 2015).

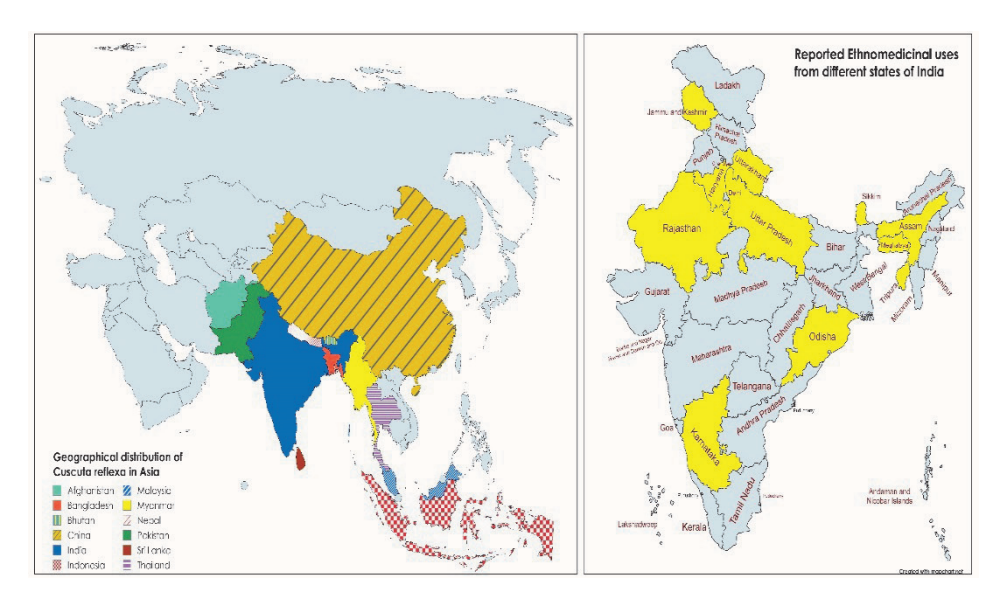


Figure 1. Geographical distribution of *Cuscuta reflexa* Roxb. in Asia and reported ethnomedicinal uses from different states of India

The initial investigations indicate promising therapeutic prospects for *Cuscuta reflexa* due to its rich array of active constituents. Despite some existing reviews touching upon certain facets of *Cuscuta reflexa*, a comprehensive review elucidating the potential therapeutic advantages of this plant remains conspicuously absent in scholarly literature. Therefore, the present review endeavors to fill this gap by offering a comprehensive overview encompassing the taxonomy, ethnobotanical uses, phytochemical composition and pharmacological activities associated with *Cuscuta reflexa*. By providing a robust evidence base, this review aims to stimulate further research endeavors aimed at harnessing the therapeutic potential of this botanical species.

MATERIALS AND METHODS

Databases, keyword searches and software

A thorough exploration of existing literature was undertaken to assemble pertinent information concerning *Cuscuta reflexa*. This involved meticulous searches across prominent electronic databases such as PubMed, Google Scholar, Scopus, SpringerLink and ScienceDirect. A wealth of studies published in esteemed peer-reviewed journals, including

Natural Product Research, Food Chemistry, Current Research in Pharmacology and Drug Discovery, International Journal of Molecular Sciences, Journal of Ethnopharmacology and Journal of Science in Food and Agriculture and various others, were meticulously gathered, encompassing a diverse array of perspectives and insights on the subject matter. Specific keywords like "Cuscuta reflexa," "pharmacological activities," "ethnobotany," "Dodder," and "phytochemistry" were strategically employed to navigate the expansive realm of scholarly literature. Only research articles published within the timeframe of 2010 to 2024 were included in the review process. Initially, a total of 2309 studies were identified and through a series of rigorous screening phases, 106 studies were ultimately selected for inclusion in the review. Adhering to the structure outlined by PRISMA guidelines (depicted in Figure 2), the article was systematically organized into distinct sections. This meticulous approach ensured the gathering of a wealth of knowledge encompassing diverse perspectives and facets of inquiry surrounding this botanical entity. Furthermore, to enrich the investigation, IUPAC names and chemical structures were incorporated via PubChem. This methodical integration of chemical information enhances the depth of analysis. Additionally, Mendeley software was employed to manage as well as organize the studies until the completion of the draft, ensuring a systematic approach to our research process.

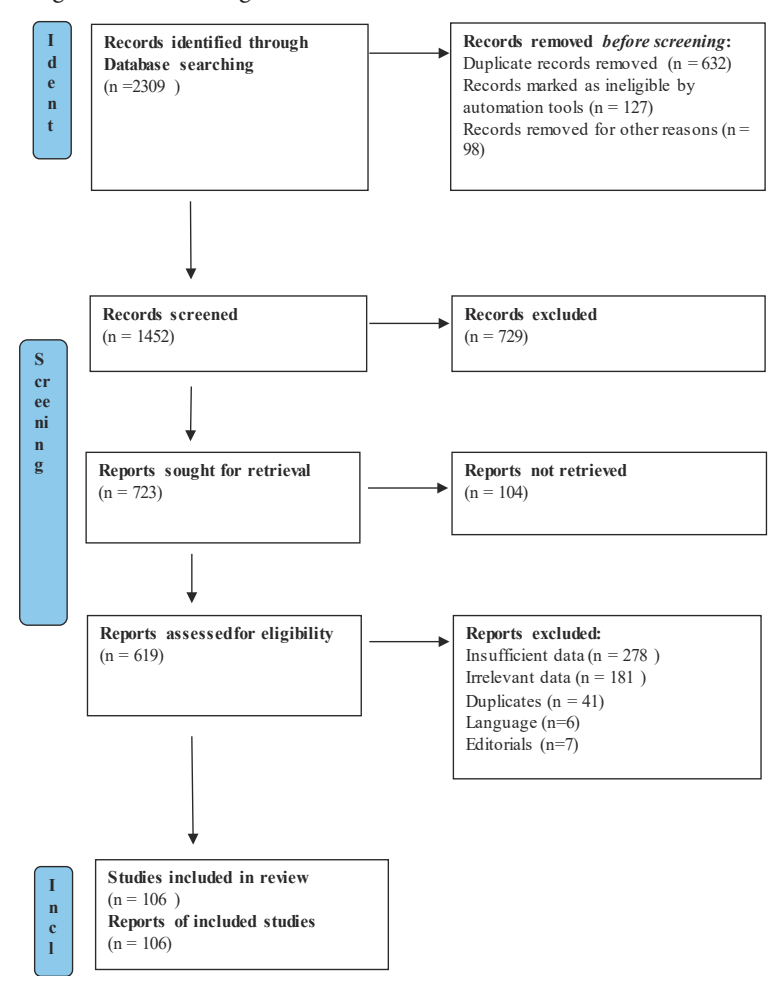


Figure 2. PRISMA outline followed for literature search

Botanical Characteristics

Cuscuta reflexa is a member of the Cuscuta genus, which encompasses approximately 170–200 species of parasitic vines within the Convolvulaceae family. Plants within the Cuscuta genus stand apart from other genera in the Convolvulaceae family due to their distinct characteristics. These include the presence of haustoria, the absence of leaves and an

acotyledonous embryo. Additionally, their flowers are typically arranged in clusters or short racemes, with the corolla featuring five-fimbriate scales, contributing to their unique botanical identity (Park et al., 2019). *Cuscuta reflexa* is a species native to the tropical regions of Asia (Masanga et al., 2022) and exhibits complete chloroplast genomes, adding to its botanical significance (Park et al., 2019). Figure 3 depicts *Cuscuta reflexa*.

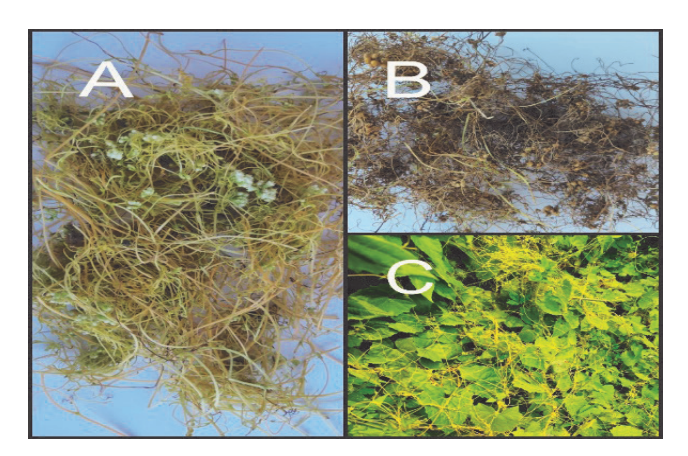


Figure 3. (A) Fresh Cuscuta reflexa stem along with flowers (B) Dried Cuscuta reflexa and (C) Habitat

Phytochemistry

The chemical composition of Cuscuta reflexa has consistently aroused the interest of researchers, leading to the isolation and identification of numerous compounds across various parts of the plant. Table 1 summarizes the bioactive compounds found in Cuscuta reflexa along with their associated pharmacological activities. These constituents encompass a diverse array of chemical classes, including alkaloids, phenols, flavonoids, tannins, coumarins, saponins, terpenoids, phytosterols, glycosides and carbohydrates (Akhtar, Ihsan-ul-Haq, & Mirza, 2018; Sharma, Kumar, & Gupta, 2021). In addition to the isolated compounds of Cuscuta reflexa, several other bioactive compounds have been identified through

various chromatographic techniques such as LC-MS and HPTLC. These include piperitone, caryophyllene, elemol, α-selinene, α-humulene, β-elemene, thujone, bergamotene, juniper camphor, bopindolol, doxylamine, isoproterenol, N6,N6dimethyladenosine, octadecatetraenoic acid, oxolinic acid and primidone (Ahmed et al., 2025; Islam et al., 2015). The compounds derived from Cuscuta reflexa showcase remarkable pharmacological properties, spanning a spectrum of beneficial effects including anticancer, antipyretic, antiaging, anti-inflammatory, hepatoprotective and various other therapeutic attributes, largely attributed to their diverse phytoconstituents.

Table 1. Isolated chemical compounds from Cuscuta reflexa

References	(Aung et al., 2020)	(Aung et al., 2020)	(Aung et al., 2020)	(Versiani, Kanwal, Faizi, & Farooq, 2017)
Pharmacological Activity	Antiobesity activity, porcine pancreatic lipase (PPL), antiplatelet aggregation activity	Antiobesity activity, porcine pancreatic lipase (PPL), antiplatelet aggregation activity	Antiobesity activity, porcine pancreatic lipase (PPL), antiplatelet aggregation activity	Anti-cancer activity
Chemical Structure	δ	\$ 0	\$ must	2
Intervention mechanism	Inhibits platelet aggregation	Inhibits platelet aggregation	Reduces fat absorption in the gut	Na ⁺ /K ⁺ -ATPase inhibition raises intracellular calcium, inducing apoptosis
Isolated Chemical Compounds	Cuscutarosides A	Cuscutarosides B	7β-methoxy-β-sitosterol 3-O-β-glucopyranoside	Odoroside H
Part of the Plant	Whole	Whole	Whole	Whole plant
Serial No	-1	7	С	4

(Versiani et al., 2017)	(Versiani et al., 2017)	(Versiani et al., 2017)	(Gao et al., 2019; Jiang, Yu, & Wang, 2015; Thangnipon et al., 2012; Versiani et al., 2017)	(Caroli et al., 2023; J. Li, Wang, Fan, Hu, & Guo, 2022; Mhiri et al., 2020; Versiani et al., 2017)
Anti-cancer activity	Anti-cancer activity	Cardioprotective activity	Antioxidant, Neuroprotective and Anticancer activities	Antioxidant, Antiproliferative, Anti- Hyperuricemia and Anticancer activities
	TIME TO THE TOTAL THE TOTAL TO THE TOTAL TO THE TOTAL TO THE TOTAL TOT	δ = -5 δ	\$ 0 P	£
Na ⁻ /K ⁻ -ATPase inhibition raises intracellular calcium, inducing apoptosis	Na ⁻ /K ⁻ -ATPase inhibition raises intracellular calcium, inducing apoptosis	Na ⁻ /K ⁻ -ATPase inhibition raises intracellular calcium	Neutralizes free radicals, reduces oxidative stress and induces dosedependent apoptosis in HepG2 cells.	Suppresses inflammatory mediators by downregulating iNOS and COX-2 via AP-1/ JNK pathways and scavenging ROS
Neritaloside	Strospeside	16-β-hydroxydigitoxin	N-Trans-feruloyltramine	N-Cis-feruloyltramine
Whole	Whole plant	Whole	Whole	Whole plant
r	9	7	∞	6

(Lee et al., 2014; Versiani et al., 2017; Xu, Zuo, Guo, & Wan, 2017)	(Nayeli et al., 2020; Son, Lee, Oh, Lee, & Choi, 2015)	(Bacanlı, Başaran, & Başaran, 2017; Samsonowicz, Kalinowska, & Gryko, 2021; Shao et al., 2011; Versiani et al., 2017; Wang et al., 2020; Wolska, Grudniak, Fiecek, Kraczkiewicz- Dowjat, & Kurek, 2010)	(Choi et al., 2012; Versiani et al., 2017; Vikram, Jayaprakasha, Uckoo, & Patil, 2013; Vo, Ta, Chu, Nguyen, & Vo, 2020)
Anti-inflammatory activity, Anticancer, Anti-arthritic.	Gastroprotective, Anti-inflammatory, Antioxidant,	Anti-inflammatory, Antioxidant, Antimicrobial, Antigenotoxic and Anticancer	Anti-inflammatory, Antioxidative, Antimicrobial, Hepato-protective, Anticancer
○ P			T IIIIII
Neutralizes free radicals, reduces oxidative stress and induces dosedependent apoptosis in HepG2 cells	Stimulates gastric mucus secretion; Suppresses inflammatory mediators	Suppresses inflammatory mediators, Modulates NF-kB/NLRP3 inflammasome pathway	Na ⁺ /K ⁺ -ATPase inhibition raises intracellular calcium, inducing apoptosis; suppresses lipopolysacchaide (LPS); Reduces secretion of pro- inflammatory cytokines TNF-α and IL-1β
Ethyl caffeate	Trimethoxycoumarin	Ursolic Acid	eta-sitosterol glucoside
hole plant	hole plant	Whole plant	Whole
0	11	12	13

(Ivanova et al., 2017; Korbecki & Bajdak- Rusinek, 2019)	(Lerata et al., 2020)	(Singh, Arya, Sharma, Dobhal, & Gupta, 2015; Viet, Xuan, & Anh, 2021)	(Caporali et al., 2022; Ganai et al., 2021; Luo, Shang, & Li, 2017; Qian et al., 2020)
Antibacterial and antiinflammatory	Antimicrobial, Antidepressant and Anticancer activity	Antioxidant, Hepatoprotective and Anxiolytic	Anti-inflammatory, Antimicrobial, Cardioprotective and Anticancer activities
	o 		5 J
Exert mechanical stress on the bacterial cell membrane; Suppresses inflammatory mediators	Reduces oxidative stress and enhances the production of anti-inflammatory cytokines	Inhibits xanthine oxidase (XO)	Modulates key molecular pathways and signaling mechanisms, reduces ROS production and increases levels of the pro-apoptotic protein Bax
Palmitic acid	Stearic acid	α-amyrin	Luteolin
Leaves	Leaves	Whole	Seed
14	15	16	17

(Liu et al., 2024)	(Li et al., 2021; Lu et al., 2018)	(Ekinci Akdemir, Albayrak, Çalik, Bayir, & Gülçin, 2017; Shen et al., 2019)	(Mallu, Vemula, & Kante, 2019)	(Kleemann et al., 2011; Lesjak et al., 2018)
Antiepileptic and whitening effect	Anti-cancer and anti-inflammatory activity	Anti-cancer, Antioxidant, Hepatoprotective, Antiangiogenic and Anti-hyperlipidemic	Anti-cancer activity	Anti-inflammatory, Anti-proliferative, Antioxidant and Anti-atherosclerotic
HO OH OH		O HO		HO HO HO
Downregulates tyrosinase- related proteins, including TYR, TRP-2 and MITF (Microphthalmia- associated Transcription Factor)	Inhibits cancer cell proliferation, migration and invasion and induces cell cycle arrest and apoptosis via the PI3K/Akt pathway	Inhibits oxidative stress	Exhibits inhibition of PRAD1 expression (Parathyroid adenoma 1)	Reduced NF-ĸB transcriptional activity in human hepatocytes and decreased cytokine-induced cell surface expression
Cuscutin	Scoparone	p-Coumaric acid	Stigmastan-3,5-diene	Quercetin
Stem	Whole	Whole	Whole	Whole
18	19	20	21	22

(Kaushik, Aeri, Showkat, & Ali, 2017)	(Gu, Huang, Huang, Sun, & Xu, 2019; Mach et al., 2017)	(Mala & Sofi, 2017)
Antidiabetic	Diuretic activity, reduction of intracranial pressure	Antioxidant, Cytoprotective and Anticancer
	HO HO HO	PO PO P
Enhances cellular glucose uptake and promotes pancreatic beta-cell regeneration	Increases urination	Stabilizing effect on mast cells
Coccinoside B	Mannitol	Myrecetin
Whole	Whole	Whole
23	24	25

Ethnobotany

Cuscuta reflexa, known for its diverse ethnobotanical applications, holds significance across various communities worldwide. Among these, the tribal inhabitants of Kodagu district in Karnataka employ the entire plant to address epilepsy. Their traditional remedy involves preparing a paste from the whole plant, which is then mixed with a teaspoonful of honey and administered orally once daily for three days (Lingaraju et al., 2013). Similarly, indigenous groups residing in the sub-Himalayan region of Uttarakhand utilize the stem of Cuscuta reflexa in the treatment of epilepsy (Sharma, Gairola, Gaur, Painuli, & Siddiqi, 2013).

The Saperas community, residing in Khetawas, Jhajjar District, Haryana, has long relied on the medicinal properties of the plant for fever management (Panghal, Arya, Yadav, Kumar, & Parkash Yadav, 2010). Similarly, indigenous populations in the Sub-Himalayan region of Uttarakhand have traditionally utilized the decoction derived from the entire plant to alleviate jaundice (J. Sharma, Gairola, Gaur, & Painuli, 2012). Moreover, it finds application in mitigating liver swelling (S. Akhtar et al., 2023). In Southern Assam, Cuscuta reflexa is employed to combat digestive system disorders (Choudhury et al., 2015). Meanwhile, among the Jaintia tribes residing in the North Cachar Hills district of Assam, northeast India, this botanical remedy is cherished for its ability to stave off premature hair loss, prevent graying of hair and manage dandruff (Sajem & Gosai, 2006). In the region of Harighal, Pakistan, Cuscuta reflexa holds significance in addressing both jaundice and dandruff (Amjad et al., 2020). Furthermore, among the ethnic communities inhabiting the West and South districts of Tripura, this plant is revered for its efficacy in treating viral infections, cough, as well as alleviating itchy skin conditions (Sen et al., 2011). The people of East Sikkim have long employed Cuscuta reflexa to address liver ailments, including jaundice (Tamang et al., 2023). Similarly, in Eastern Rajasthan, the paste derived from this plant is applied topically to alleviate muscular and rheumatic pain (Upadhyay, Parveen, Dhaker, & Kumar, 2010). Meanwhile, in Odisha, the stem juice of *Cuscuta reflexa* is harnessed for the treatment of malaria (Panda, 2014). The indigenous communities residing in the Kalahandi district of Odisha have long relied upon the medicinal properties of *Cuscuta reflexa* in addressing a spectrum of health concerns. Among these, ailments such as diarrhea, dysentery, rheumatism, swellings and joint pain are notably treated using this traditional remedy (Swain & Padhy, 2015).

Additionally, in the Budgam district of Jammu and Kashmir, the plant is utilized to alleviate joint pain (Mir et al., 2021). These diverse applications extend to the treatment of jaundice and paralysis, with the plant also exhibiting purgative properties (Saqib et al., 2014). In the district of Udham Singh Nagar, Uttarakhand, the Tharu community has historically utilized a paste derived from the entire plant of Cuscuta reflexa to address eczema through topical application. Additionally, this paste is employed on the scalp to mitigate dandruff (Sharma, Gairola, Sharma, & Gaur, 2014). In Uttarakhand, the comprehensive utilization of the entire Cuscuta reflexa plant extends to the treatment of respiratory diseases (Kala, 2020). Meanwhile, in North Tripura, this botanical resource is valued for its versatility in addressing a spectrum of ailments, including gastric issues, jaundice, ear pain and urinary troubles (Choudhury et al., 2015). Nepal stands as a vibrant hub of ecological and cultural richness, where the traditional knowledge of its people intertwines with the natural bounty of the land. Within Nepalese communities, Cuscuta reflexa finds application in the treatment of paralysis. A customary remedy involves preparing a mixture of pastes derived from the stems of Cuscuta reflexa and the stems and leaves of Tinospora sinensis. This concoction is consumed three times a day until the ailment is alleviated (De Rus Jacquet, Subedi, Ghimire, & Rochet, 2014). In the Chenab riverine area of Punjab province, Pakistan, Cuscuta reflexa serves as a versatile remedy for a variety of ailments.

Local inhabitants rely on it to address headaches and urinary disorders, as well as to alleviate symptoms of constipation (Umair, Altaf, Bussmann, & Abbasi, 2019). Additionally, the powdered form and extract derived from the entire plant are utilized to alleviate toothache (Fatima et al., 2018). It is also employed to alleviate bronchitis (Kayani et al., 2014).

The entire *Cuscuta reflexa* plant material is used in traditional medicinal practices to address hematological irregularities. Infusions prepared by boiling the whole plants are employed to alleviate symptoms associated with liver inflammation and fibrosis. Additionally, the whole plants are subjected to crushing and subsequent pasting to alleviate conditions such as pruritus and dermatological conditions such as rashes (Zhang et al., 2021). These traditional practices underscore the intimate connection between the local populace and their natural environment, where botanical resources are harnessed to provide relief from common health concerns, reflecting a longstanding tradition of holistic healing passed down through generations.

Cuscuta reflexa also exhibits ethnoveterinary significance, being employed across diverse communities to address various ailments afflicting livestock. Its utilization spans multiple regions as well as cultures, reflecting the profound relationship between humans and animals. From traditional knowledge passed down through generations, communities have discovered the plant's efficacy in treating livestock diseases, underscoring the intricate web of interconnectedness between humanity and the natural world. This practice illuminates the holistic approach to animal welfare, where botanical resources play a vital role in maintaining well-being and the health of valuable livestock populations.

In the East Khasi Hills district of Meghalaya, located in North East India, local inhabitants utilize the paste derived from *Cuscuta reflexa* to address various health concerns among their cattle. This includes the treatment of indigestion, bone fractures, foot and

mouth disease (Bhat et al., 2023). The Tharu tribal community residing in Uttar Pradesh, India, employs a traditional method involving the application of warmed paste derived from Cuscuta reflexa externally onto livestock to alleviate swelling (Kumar, Pandey, & Tewari, 2012). In the war-affected region of northwest Pakistan, the indigenous population employs a traditional method involving the grinding of Cuscuta reflexa in sufficient quantity. Subsequently, the plant material is cooked in oil to create a topical application for its analgesic properties as well as wound care (Adnan et al., 2014). The application of whole plant paste as a galactagogue is documented (Mehmood Abbasi et al., 2013). Additionally, Cuscuta reflexa finds application in the treatment of arthralgia and arthritis in horses, also as an abortifacient (Ullah et al., 2014). Among the Garo tribal practitioners residing in the Mymensingh district of Bangladesh, stem juice of Cuscuta reflexa is employed for the management of diabetes (Rahmatullah et al., 2012). Furthermore, within the Tamang communities of the Nepal Himalayas, this botanical resource is utilized as a poultice to address wounds and as a tonic to alleviate hematuria in bulls (O'Neill & Rana, 2016).

Pharmacology

Antidiabetic activity

Rath et al. conducted a study to assess the potential anti-diabetic effects of methanol and aqueous extracts derived from the aerial parts of *Cuscuta reflexa* Roxb. in both normal and diabetic rats induced by glucose and Streptozotocin (STZ). These effects were compared against those of Metformin and a solvent control. The findings revealed that administration of both methanol and aqueous extracts of *Cuscuta reflexa* (at a dosage of 400 mg/kg) resulted in a noteworthy reduction in blood glucose levels during the Oral Glucose Tolerance Test (OGTT) in diabetic rats, particularly at the 3-hour mark. Furthermore, a single oral dose of either aqueous or methanol extracts at 400 mg/kg led to a significant decrease (p < 0.05) in blood glucose levels, reaching 55.39%

and 61.90% reduction respectively, compared to the Metformin group (which exhibited a 68.32% reduction) at the 8-hour mark. Moreover, continuous administration of methanol extract of *Cuscuta reflexa* at a dosage of 400 mg/kg for 30 days to diabetic rats demonstrated a substantial decrease (p < 0.01) in blood glucose levels, with a reduction of 60.00% compared to other experimental groups. Importantly, the histopathological examination did not reveal any evident injury; instead, regeneration of beta cells was observed in diabetic rats treated with the extracts (Rath, Kar, Panigrahi, & Maharana, 2016).

In a separate investigation, the anti-diabetic potential of Cuscuta reflexa leaves methanol extract (CRME) was examined utilizing alloxan-induced diabetes in Wistar albino rats. Administered orally, methanol extract of Cuscuta reflexa at doses of 100, 200, as well as 400 mg/kg/day, along with a standard comparator (gliclazide, 10 mg/kg/day), commenced from the onset of diabetes induction and persisted for 45 days. Results indicated a noteworthy reduction in blood glucose levels with Cuscuta reflexa methanol extract treatment at all doses (137.1 \pm 5.8, 125.9 ± 6.5 and 109.5 ± 5.4 mg/dL at doses of 100, 200 and 400 mg/kg, respectively) compared to the diabetic control (249.7 \pm 7.3 mg/dL), with statistical significance observed (p < 0.01). Additionally, at the highest dosage, CRME exhibited a decline in HbA1C levels and enhancement in insulin levels (3.96% and 11 ng/ml, respectively) in contrast to the diabetic control group (7.55% and 6.5 ng/ml, respectively). Consequently, the study concludes that CRME holds promise as a substantial anti-diabetic agent with potential organ-protective properties, thus warranting further exploration of its role in diabetes management (Mostofa et al., 2020).

Antiemetic

Muhammad et al. conducted a study to investigate the antiemetic properties of aqueous, as well as methanolic extract and also juice of *Cuscuta reflexa* in pigeons. Emesis was induced using gastrointestinal irritants such as copper sulfate (100 mg/kg, PO), ampicillin (300 mg/kg, IM), cisplatin (a 5-HT3 receptor stimulator) (6 mg/kg, IM) and concentrated sodium chloride solution (1600 mg/kg, PO). 2 mg/kg, intramuscular, Dimenhydrinate served as the positive control. Administered intramuscularly aqueous and methanolic extract at various doses (50, 100 and 200 mg/kg), juice of CR (at concentrations of 1% and 2%), were evaluated in terms of their ability to reduce the total number of vomiting episodes, vomiting weight, as well as jerks, in each pigeon. The findings suggest that the aqueous, methanolic extracts and juice of C. reflexa possess significant antiemetic potential. These extracts contain pharmacologically active constituents that interfere with emetic mediators by acting on gastrointestinal irritation as well as 5-HT3 receptor stimulation pathways (Muhammad et al., 2020).

Antidiarrheal

A study on the antidiarrheal effects of *Cuscuta reflexa* was conducted using pigeons, with diarrhea induced by various substances including ampicillin and castor oil. Loperamide served as a positive control. The pigeons received intramuscular injections of *C. reflexa* juice at 1% and 2% concentrations, along with aqueous (CRAE) and methanol (CRME) extracts at doses of 50, 100 and 200 mg/kg. Results indicated that *C. reflexa* extracts exhibited significant antidiarrheal properties, demonstrating notable anti-secretory and anti-motility effects. This suggests potential therapeutic applications for gastrointestinal health (Muhammad et al., 2021).

Antipyretic

Bhattacharya et al. conducted a study to assess the antipyretic properties of ethanol as well as aqueous extracts derived from *Cuscuta reflexa* Roxb. employing Brewer's yeast-induced pyrexia in rats. Administered at a dose of 400 mg/kg body weight, the ethanol and aqueous extracts exhibited reductions of 83.8% and 79% respectively in elevated rectal temperature compared to the reference drug

paracetamol (96.5%) after 6 hours of treatment. The findings suggest that both extracts of C. *reflexa* demonstrate antipyretic activity, with the ethanol extract showing slightly greater potency than the aqueous extract (Bhattacharya & Roy, 2010).

Wound-healing

The wound healing capabilities of ethanolic as well as water extracts derived from the stem of *Cuscuta reflexa* Roxb were investigated utilizing the Excision wound model, with 5% Povidone-iodine ointment serving as the standard comparator. The study findings suggest that the stems of *Cuscuta reflexa* Roxb exhibit significant therapeutic potential in promoting wound healing. In essence, the research highlights the promising ability of *Cuscuta reflexa* Roxb stem extracts to facilitate the recovery process of wounds (Gautam, Gautam, Keservani, & Sharma, 2015).

In a separate investigation, the wound-healing effects of the aqueous methanolic extract of *Cuscuta reflexa* (Cs.Cr) on contact frostbite in rats. Thirty rats were divided into five groups: three treatment groups receiving increasing doses of Cs.Cr, one group treated with acetylsalicylic acid as a standard and a control group exposed to frostbite using a metal bar cooled to -79°C. The healing process was monitored alongside malondialdehyde levels and hematological parameters. Results showed that Cs.Cr significantly accelerated healing and reduced malondialdehyde levels in a dose-dependent manner, indicating its potential as an effective therapeutic agent for frostbite injuries (Hassan et al., 2020).

Anti-inflammatory

The initial assessment of the anti-inflammatory potential of the parasitic plant *Cuscuta reflexa* was conducted through the examination of its human red blood cell stabilizing activity. The findings of the study indicated that both the methanolic extract of *Cuscuta reflexa* (MECR) and its ethyl acetate soluble fraction (EAMECR) exhibited notable anti-inflammatory effects. This activity is believed to be attributed to

the presence of flavonoids, phenols and polyphenols within the plant extract (Udavant, Satyanarayana, & Upasani, 2012).

Another study was conducted to explore the anti-inflammatory properties of *Cuscuta reflexa* seed essential oil. They induced inflammation in mice using TPA as the inducing agent and assessed oxidative stress and various biochemical parameters by analyzing the homogenate of the mice's ear pinna. The results indicated that the essential oil from *Cuscuta reflexa* seeds effectively mitigated inflammation by modulating inflammatory mediators, particularly cytokines (Nooreen et al., 2023).

Antioxidant

Spectrophotometric techniques were employed to quantify the total phenolic as well as flavonoid contents, while the DPPH radical scavenging method was utilized to assess the *in vitro* antioxidant activity. Among the various fractions analyzed, the ethyl acetate fraction exhibited the highest concentrations of total phenolic content (46.272±2.77 mg/g GAE) as well as total flavonoid content (32.970±2.37 mg/g RE). Additionally, the ethyl acetate fraction demonstrated the most potent radical scavenging activity with an IC_{50} value of 15.70±1.82 µg/ml using the DPPH method. These findings underscore the significance of *Cuscuta reflexa* as a valuable source of bioactive compounds with notable antioxidant properties (Sharma et al., 2021).

Singh et al. assessed the biodynamic properties of extracts from *Cocculus hirsutus* (CHP) and *Cuscuta reflexa* (CRA). They evaluated free radical scavenging activity using DPPH and ABTS assays, as well as intracellular reactive oxygen species (ROS) scavenging in RAW 264.7 cells. Chromatographic analysis confirmed the presence of polyphenols in both extracts. Results showed that CRA-K had lower free radical scavenging activity than CHP-K, but CRA-K exhibited a higher intracellular ROS scavenging potential (84%) compared to CHP-K (50%) and the LPS control. This study highlights the

antioxidant properties of both extracts, linked to their polyphenolic content (A. Singh, Singh, Ananthan, & Kumar, 2022).

Antimicrobial

The antibacterial efficacy of extracts derived from *Cuscuta reflexa* plant specimens was examined through the disc diffusion assay against a panel of bacterial strains, including *Sarcina lutea* IFO 3232, *Bacillus subtilis* IFO 3026, *Xanthomonas campestris* IAM 1671, Proteus vulgaris MTCC 321, *Klebsiella pneumoniae* ATCC 10031, *Pseudomonas denitrificans* KACC 32026 and *Escherichia coli* IFO 3007. Notably, the dichloromethane and petroleum ether extracts of *C. reflexa* demonstrated substantial antibacterial activity against all bacterial strains tested. The observed minimum inhibitory concentration values across various extracts exhibited a range of 16 to 512 µg/mL (Islam et al., 2015).

The agar well diffusion technique assessed the antimicrobial potential of extracts from Acacia arabica and Zizyphus jujube against various bacterial and fungal strains, including Staphylococcus epidermidis, Staphylococcus aureus, Escherichia coli, Pseudomonas aeruginosa and Aspergillus niger. Ethanol and methanol extracts of Cuscuta reflexa showed significant inhibitory effects on most tested gram-positive and gram-negative bacteria. However, the aqueous extract from Cuscuta reflexa (arabica) exhibited no antimicrobial activity and that from Cuscuta reflexa (jujube) showed only slight effectiveness. The study suggests that Cuscuta reflexa growing on Zizyphus jujube may be a promising natural source of antimicrobial agents (Summit, Jatin, Pradeep, & Yogesh, 2010).

Cuscuta reflexa, along with three other plant species, underwent testing against a spectrum of microbial strains, encompassing two grampositive bacteria (Staphylococcus aureus as well as Staphylococcus epidermidis), three gram-negative bacteria (Klebsiella pneumoniae Escherichia coli and Pseudomonas sp.) and two pathogenic fungal strains

(Penicillium sp. And Fusarium oxysporum). The antibacterial activity was evaluated using the agar well diffusion method, while the agar tube dilution method was employed for assessing antifungal activity. Among the extracts tested, the chloroform extract of Cuscuta reflexa demonstrated notable inhibitory effects against all bacterial strains, with the most significant inhibition zone observed against Klebsiella pneumoniae, measuring up to 21 mm. This highlights the potential antimicrobial properties of Cuscuta reflexa, particularly its chloroform extract, against a broad spectrum of bacterial pathogens (Bibi, Naeem, Zahara, Arshad, & Qayyum, 2018).

Upon conducting biological screening, it was observed that the essential oil extracted from the parasitic vine *Cuscuta reflexa* Roxb. did not demonstrate significant antimicrobial activity against both Gram-positive bacteria such as *Staphylococcus aureus* and *Bacillus cereus*, as well as Gram-negative bacteria including *Escherichia coli* and *Pseudomonas aeruginosa*. However, there was a slight activity noted against *Aspergillus niger*, at a marginal level, with a minimum inhibitory concentration of 313 mg/mL (Paudel et al., 2014).

Anticancer

The anti-cancer potential of *Cuscuta reflexa* (CR) water extract was assessed on Hep3B cells through various analyses including MTT assay, annexin V staining, DAPI staining, as well as SQ-RT PCR analysis targeting key apoptotic regulators including Bcl-2, BAX, survivin and p53. The results indicated that the CR water extract exhibited notable effects on Hep3B cells by upregulating pro-apoptotic factors such as BAX as well as p53, while concurrently downregulating anti-apoptotic factors like survivin and Bcl-2. This modulation in gene expression profile suggested the induction of apoptosis in Hep3B cells, facilitated by the upregulation of BAX as well as p53, alongside the downregulation of survivin as well as Bcl-2 (Suresh, Sruthi, Padmaja, & Asha, 2011).

In a separate study, the anticancer effects of the

ethanolic extract of *Cuscuta reflexa* were investigated against 1, 2-Dimethyl hydrazine (DMH)-induced animals using various assessment methods including colonoscopy, Aberrant crypt foci (ACF) studies and barium enema X-ray. The results indicated a significant reduction in Disease Activity Indexing (DAI) levels and ACF counts upon treatment with *C. reflexa* extract, comparable to the effects observed with the standard drug 5-Fluorouracil (5-FU). Furthermore, the extract demonstrated potential hepatoprotective properties, suggesting its potential utility in the management of colon or colorectal cancer (Mishra et al., 2022).

The cytotoxicity and antitumor potential were evaluated utilizing the Sulforhodamine B (SRB) assay against human breast cancer cell lines (MCF-7), colon cancer cell lines (HT-29), liver (Hep-2) and lung cancer cell lines (A 549) and murine models, respectively. A range of extracts, including 95% alcoholic, 50% hydro-alcoholic and aqueous extracts, as well as four fractions (n-hexane, chloroform, n-butanol and aqueous) were examined. Among these, the alcoholic extract and its chloroform fraction exhibited the highest levels of cytotoxicity and demonstrated significant inhibition of tumor growth. The alcoholic extract exhibited notable tumor growth inhibition at 40 mg/kg, with reductions of 42.62% and 25.96% observed in the Ehrlich tumor and Sarcoma-180 solid tumor models, respectively. Similarly, the chloroform fraction of the alcoholic extract demonstrated significant tumor growth inhibition of 48.98% and 44.11% in the Ehrlich tumor and Sarcoma-180 solid tumor models at 10 mg/kg, respectively (Bhagat, Arora, & Saxena, 2013).

Hepatoprotective

The hepatoprotective potential of aqueous and alcoholic extracts derived from *Cuscuta reflexa* was examined in rats subjected to hepatotoxicity induced by carbon tetrachloride (CCl₄). Following intoxication with CCl₄, the rats were administered the aqueous and alcoholic extracts of *Cuscuta reflexa*.

Subsequent treatment with the extracts resulted in the restoration of liver profile parameters to normal levels. The findings of the study suggest that both aqueous and alcoholic extracts of *Cuscuta reflexa* exhibit therapeutic efficacy in ameliorating liver dysfunction induced by CCl₄ intoxication (Ranjan, Kumar, Kumar, & Sinha, 2020).

Anti-obesity

Kaur A et.al. investigated the potential anti-obesity effects of the ethanolic extract of Cuscuta reflexa in Wistar rats with high-fat diet (HFD)-induced obesity. Male Wistar rats were administered varying doses of Cuscuta reflexa extract (200 and 100 mg/kg/day) for 6 weeks alongside the high-fat diet. Orlistat (30 mg/kg/day) served as the standard comparator. Results demonstrated a significant, dose-dependent reduction in body mass index (BMI), body weight, feed intake (in kcal) and Lee's index, compared to rats solely on the high-fat diet. Furthermore, oral administration of graded doses of Cuscuta reflexa extract led to reductions in triglycerides (TG), serum total cholesterol (TC), glucose levels, low-density lipoprotein (LDL) and very low-density lipoprotein (VLDL), while simultaneously enhancing high-density lipoprotein (HDL) levels compared to the group fed with the high-fat diet alone (Kaur, Behl, Makkar, & Goyal, 2019). The findings suggest promising antiobesity effects of Cuscuta reflexa extract, indicating its potential as a therapeutic intervention for combating obesity-related health concerns, with implications for human health and well-being.

Hair growth

Cuscuta reflexa holds significant promise as a natural remedy for addressing androgenic alopecia. Extracts derived from C. reflexa exhibit the ability to regulate the apoptosis of hair cells and mitigate testosterone-induced alopecia. In vivo experiments have revealed that treatment with petroleum ether extract (PTE), ethanolic extract (ETE) of C.reflexa and SGTA (Stigmast-5-en-3-O-glucopyranosidetriacetate-51-ol), an isolate leads

to an increase in rat follicular density and anagen/telogen (A/T) ratio compared to untreated control groups. Histological analysis of skin samples further demonstrates that PTE, ETE, as well as SGTA-treated groups exhibit enhancements in both the morphology and number of hair follicles, as well as an increase in the anagen/telogen ratio of follicles, in comparison to both finasteride-treated and control groups. Overall, these findings highlight the potential of *Cuscuta reflexa* extracts, particularly PTE, ETE and SGTA, in mitigating androgenic alopecia and promoting hair growth (Patel, Nag, Sharma, Chauhan, & Dixit, 2014).

Hair oils derived from Cuscuta reflexa from various host plants demonstrated efficacy in promoting hair growth, controlling dandruff and reducing hair loss. A comparative analysis between herbal hair oils and mustard oil was conducted by administering the oils to human volunteers experiencing hair fall and dandruff issues. Additionally, the promotion of hair growth activity was assessed using rat models. The experimental oils derived from Cuscuta reflexa demonstrated efficacy in enhancing hair growth, mitigating hair fall occurrences and managing dandruff. Patients treated with Cuscuta reflexa hair oil exhibited a highly significant reduction in the score of white scale formation, dropping from 2.5891 and 2.5997 to 1.00 and 1.012, respectively. Furthermore, animals administered with the formulated hair oils displayed a noteworthy increase in hair length. Throughout the experimentation period, the maximum reduction in hair fall, ranging from 15 to 82 hairs per combing, was observed on the 60th day. Notably, the employment of Cuscuta hair oil

resulted in a remarkable 96.38% reduction in hair fall, surpassing the control (mustard oil) users, where the reduction was merely 14.38% (Anjum, Bukhari, Shahid, Bokhari, & Talpur, 2014).

Polycystic syndrome

A research investigation explored the therapeutic potential of hydroalcoholic extracts from *Cuscuta reflexa* Roxb (CRE) and *Peucedanum grande* C.B. Clarke (PGE) in addressing letrozole-induced polycystic ovary syndrome (PCOS) in female Wistar albino rats. PCOS-afflicted rats received treatment with CRE (280 mg/kg), PGE (140 mg/kg), or a combination of CRE + PGE orally over 3 weeks. Various parameters including vaginal smears for determining the estrous cycle phase, lipid profile, serum levels of sex androgens, oxidative stress markers, as well as histopathological analysis of ovarian tissues were assessed.

The findings underscored that both CRE and PGE, independently or in combination, significantly mitigate PCOS symptoms in rat models induced by letrozole. Administration of hydroalcoholic extract of Cuscuta reflexa (CRE), Peucedanum grande (PGE), or their combination led to a notable decrease (p < 0.05) in the duration of the diestrous phase in comparison to the negative control group. There was no statistically significant increase noted in the diameter, weight, or organ index of ovarian tissues.

This suggests promising therapeutic implications for managing the reproductive as well as metabolic complications associated with PCOS (Kausar et al., 2021).

 Table 2. Scientifically established pharmacological activities of Cuscuta reflexa

SI No.	Activities	Part of plant	Model	Formulation/Dosage/ Extract	Control	Results	References
	Antidiabetic	Aerial parts	Rats (in vivo)	200 and 400 mg/kg Aqueous and methanolic extract of C. <i>reflexa</i> .	Positive control: P.O.: 250 mg/kg Metformin	Both the aqueous (AECR) and methanol (MECR) extracts of <i>Cuscuta reflexa</i> , given at 400 mg/kg, significantly reduced blood glucose levels. Additionally, treatment with both extracts led to improvements in body weight, decreased HbA1c levels and restored lipid profiles.	(Mostofa et al., 2020;
		Leaves	Rats (in vivo)	100, 200 and 400 mg/kg/ day methanolic extract.	Positive control: P.O. Gliclazide at the dose of 10 mg/ kg, once daily.	The administration of Cuscuta reflexa methanol extract (CRME) resulted in a significant reduction in blood glucose levels. Additionally, CRME demonstrated marked enhancements in liver function and lipid profile parameters.	Katir et at., 2010)
2	Antiemetic	Whole plant	Pigeons (in vivo)	Juice of C. reflexa (1% and 2%). I.M Aqueous and methanolic extract of Cuscuta reflexa (At 50, 100 and 200 mg/kg doses)	Positive control: Dimenhydrinate (2 mg/kg; I.M)	Juice, aqueous extract and methanolic extract of Cuscuta reflexa demonstrated significant antiemetic effects, reducing both the frequency and onset of vomiting.	(Muhammad et al., 2020)
e	Antidiarrheal	Whole plant	Pigeons (<i>in vivo</i>)	Juice of C. reflexa (1% and 2%). I.M Aqueous and methanolic extract of Cuscuta reflexa (At 50, 100 and 200 mg/kg doses)	Positive control: 2mg/kg loperamide (I.M)	The juice, aqueous extract and methanol extract of Cuscuta reflexa display significant anti-motility and anti-secretory properties.	(Rath et al., 2016)
4	Antipyretic	Whole plant	Rat (in vivo)	Aqueous and ethanolic extracts at a dose 200 and 400 mg/kg body weight	Positive control: Paracetamol, 150mg/kg body weight orally	The extracts of Cuscuta reflexa exhibited antipyretic activity, with the ethanol extract showing slightly greater potency compared to the aqueous extract.	(Bhattacharya & Roy, n.d.)

(Gautam et al., 2015;	Hassan et al., 2020)	(Nooreen et al., 2023; Udavant et al., 2012)		(Sharma et al., 2021; A. Singh et al., 2022)	
Cuscuta reflexa Roxb shows notable analgesic and wound-healing effects.	The extract of Cuscuta reflexa significantly reduced the wound area in a dose- and timedependent manner.	Methanolic extract of Cuscuta reflexa (MECR) and its ethyl acetate soluble fraction (EAMECR) show significant anti- inflammatory activities.	CREO significantly reduces inflammation by inhibiting pro-inflammatory cytokines (IL-1b, IL-6 and TNF-a)	Ethyl acetate fraction showed highest radical scavenging. Order of antioxidant activity in terms of IC ₅₀ was ethyl acetate fraction >crude methanolic extract >aqueous fraction >n-hexane fraction >chloroform fraction.	CRA-K demonstrated the highest inhibitory potential (84%) in contrast to another plant extract <i>Cocculus hirsutus</i> CHP-K (50%).
Positive control: 5% Povidone- iodine ointment.	Positive control: 50mg/kg Acetylsalicylic acid	Positive control: Diclofenac Sodium at doses 50,100,150,200 and 250 (µg).	Positive control: Applied Indomethacin Vehicle control: Applied acetone	Positive control: Ascorbic acid	Positive control: Ascorbic acid
Water and ethanolic extract at 200 and 400mg/kg.	200, 400 and 800 mg/ kg aqueous methanolic extract of <i>Cuscuta</i> reflexa.	Petroleum ether, Chloroformic, Methanolic and Ethylacetate fraction of Methanolic extract of Cuscuta reflexa (50,100,150,200 and 250 (μg)).	Applied C. <i>reflexa</i> essential oil (CREO) 1,2 and 5%.	Methanolic extract of Cuscuta reflexa and its fractions.	Cuscuta reflexa Kwath, CRAK (Traditional formulation),
Rats (in vivo)	Rats (in vivo)	In vitro (HRBC Stabilization)	Mice (In vivo)	In vitro (IC ₅₀)	In vitro (IC ₅₀)
Stem	Stem	Stem	Seeds	Stem	Aerial part
Wound healing		Anti- inflammatory		Antioxidant	
rv)	v			

	(Bibi et al., 2018;	Faudel et al., 2014; Summit et al., 2010)	
Both the dichloromethane and petroleum ether extracts of Cuscuta reflexa exhibited significant antibacterial activity against all tested bacterial strains.	Ethanol and methanol extracts derived from Cuscuta reflexa showed significant antimicrobial activity against a majority of the tested grampositive and gram-negative bacteria. However, the aqueous extract of Cuscuta reflexa did not exhibit any discernible antimicrobial activity.	The chloroform extract of Cuscuta reflexa Sa demonstrated notable inhibitory effects against all bacterial strains, with the most significant inhibition zone observed against Klebsiella pneumoniae, measuring up to 21 mm.	Cuscuta reflexa Roxb. showed no significant antimicrobial activity against Gram-positive bacteria like Staphylococcus aureus and Bacillus cereus, or Gram-negative bacteria such as Escherichia coli and Pseudomonas aeruginosa. However, minimal activity was observed against Aspergillus niger, with a minimum inhibitory concentration of 313 mg/mL.
Positive control: Nalidixic acid (15µg/disc).	Positive control: Streptomycin, Tetracycline, Clotrimazole, Fluconazole, Ampicillin, Ketoconazole and Penicillin.	Positive control: Cefotaxime	Positive control: Gentamicin
300µg Methanolic, Ethanolic, Ethyl acetate, n-hexane, Dichloromethane and Petroleum ether extract of Cuscuta reflexa.	100µL Ethanol, Methanol, Benzene, Acetone and aqueous extract of <i>Cuscuta</i> <i>reflexa</i> .	100 μL of polar and non- polar solvent extract of Cuscuta reflexa.	50 mL of 1% w/w solutions of crude essential oil
In vitro (disc diffusion method)	<i>In vitro</i> (Bacteria and fungi)	In vitro (agar well diffusion and agar tube dilutions	In vitro (micro broth dilution technique)
Whole plant	Whole plant	Leafless Stem	Essential oil of the Whole plant of Cuscuta reflexa
	Antimicrobial		
	∞		

	(Mishra et al., 2022; Suresh et al., 2011) (Bhagat et al., 2013)	
The extract reduced the elevated levels of TNF-α and COX-2 caused by LPS in RAW264.7 cells. It inhibited NF-κB binding to its motifs and triggered apoptosis in Hep3B cells. Moreover, the extract enhanced the expression of pro-apoptotic factors BAX and p53, while decreasing the levels of anti-apoptotic factors Bcl-2 and survivin.	Cuscuta reflexa significantly decreased Disease Activity Index (DAI) levels and aberrant cryptfoci (ACF) counts, demonstrating comparable efficacy to the standard drug 5-Fluorouracil (5-FU). Additionally, C. reflexa effectively restored hemoglobin levels, RBC count, packed cell volume (PCV), mean cell hemoglobin (MCH), mean cell hemoglobin concentration (MCHC), mean corpuscular volume (MCV) and mean corpuscular hemoglobin concentration.	Among the three extracts and four fractions of the alcoholic extract, the alcoholic extract and its chloroform fraction exhibited the highest potency. They demonstrated maximum cytotoxicity against human breast (MCF-7) cancer cell lines. Furthermore, the alcoholic extract significantly inhibited tumor growth, as did the chloroform fraction of the alcoholic extract.
Positive control: Silymarin (50 µg/ ml).	Positive control: 1 mM EDTA Negative control: 1, 2- Dimethyl hydrazine (DMH)	Positive control: Mitomycin C (1 mM), Paclitaxel (10 mM) and Adriamycin (1 mM) for <i>in vitro</i> . I.p.5-Fluorouracil (22 mg/kg) for <i>in vitro</i>
Water extract of Cuscuta reflexa (at doses 25, 50, and 100 µg/ml).	200 mg/kg and 400 mg/kg ethanolic extract of Cuscuta reflexa.	10 µg/ml, 30 µg/ml and 100 µg/ml of three extracts (95% alcoholic, 50% hydro-alcoholic and aqueous) along with four fractions (n-hexane, chloroform, n-butanol and aqueous) extracts of C. reflexa for in vitro cytotoxicity studies. For in viro, antitumor injected i.p. C. reflexa suspension in 1% gum acacia.
In vitro	In vivo (Rats)	Both In vitro (sulforhodamine-B assay) and in vivo (mice)
Whole plant	Whole plant	Whole plant
	Anticancer	
	0	

				Alcoholic and agueous			
10	Hepatoprotective	Stem	In vivo (Rats)	extract of Cuscuta reflexa	Negative control: CCl ₄ solution orally.	Following treatment with the extracts, the liver profile parameters returned to normal levels.	(Ranjan et al., 2020)
Ξ	Anti-obesity	Whole plant	In vivo (Rats)	Ethanolic C <i>uscuta</i> reflexa extract (100 and 200 mg/kg/day p.o.)	Positive control: Orlistat (30mg/kg/ day p.o.)	The ethanolic extract of Cuscuta reflexa demonstrated a significant, dose-dependent reduction in BMI, body weight, Lee's index and feed intake. It led to decreased levels of triglycerides (TG), serum total cholesterol (TC), low-density lipoprotein (UDL), very low-density lipoprotein (VLDL) and glucose compared to the high-fat diet (HFD) fed group. Additionally, it enhanced the levels of high-density lipoprotein (HDL).	(Kaur et al., 2019)
12	Hair growth	Stem	In vivo (Rats)	2% Petroleum ether extract and ethanolic extract of Cuscuta reflexa. And 0.5 % of Isolate suspension (SGTA); topically	Positive control: 2% Finasteride solution (Topically)	The rat follicular density and anagen/ telogen (A/T) ratio exhibited an elevation in groups treated with PTE, ETE and SGTA in comparison to the control group. SGTA and extract administration demonstrated efficacy in regulating hair cell apoptosis and mitigating testosterone-induced alopecia.	(Anjum et al., 2014; Patel et al., 2014)
		Stem	In vivo (Rats) and Human volunteers	Applied 15µL (rats) and 6 ml (human) / application of hair oil prepared from Cuscuta reflexa.	Positive control: Mustard oil	White scale formation dropped from 2.5891 and 2.5997 to 1.00 and 1.012, respectively. Cuscuta reflexa hair oil resulted in a remarkable 96.38% reduction in hair fall and a noteworthy increase in hair length.	
13	Polycystic syndrome	Whole plant	In vivo (Rats)	112 mg/kg hydroalcoholic extract of Cuscuta reflexa Roxb (CRE) and Peucedanum grande	Positive control: Metformin 50 mg/ kg	Extracts of CRE, PGE, or in combination notably decrease (p < 0.05) the duration of the diestrous phase. There was no increase in diameter, weight, or organ index of ovarian tissues.	(Kausar et al., 2021)

Toxicity studies related to Cuscuta reflexa

Cuscuta reflexa underwent acute oral toxicity assessment following the OECD-425 guidelines. The study findings revealed no indication of toxicity or mortality, even at the highest administered dose of 2000 mg/kg (Mishra et al., 2022). This observation underscores the plant's favorable safety profile and suggests its potential as a safe botanical remedy. Toxicological investigations into Cuscuta reflexa have been relatively limited, though several studies have explored its safety and pharmacological effects. An in vivo study assessed the methanol extract of C. reflexa stem (MECR) on mice, revealing that low doses (25 mg/kg) did not significantly alter hematological or hepatorenal parameters. However, moderate to high doses (50-75 mg/kg) led to elevated liver enzymes (SGOT, SGPT), increased plasma cholesterol and raised creatinine levels, indicating potential hepatic and renal toxicity at higher concentrations (Mazumder et al., 2003).

Conversely, other studies have highlighted the plant's hepatoprotective properties. Ethanolic and aqueous stem extracts demonstrated significant protection against thioacetamide-induced liver damage in rats, with no mortality observed at doses up to 2000 mg/kg, suggesting a favorable safety profile at these levels. Similarly, aqueous extracts showed hepatoprotective effects against paracetamolinduced hepatotoxicity, with biochemical and histopathological improvements noted (Katiyar et al., 2015). In vitro analyses have as well been conducted. A study using murine macrophage cell lines found that C. reflexa water extract inhibited inflammatory markers like TNF-α and COX-2 and suppressed NF-κB activation. Additionally, the extract induced apoptosis in Hep3B liver cancer cells, indicating potential anti-inflammatory and anticancer properties (Suresh et al., 2011).

While these studies provide insights into the pharmacological and toxicological aspects of *C. reflexa*, comprehensive toxicological evaluations, including chronic toxicity, genotoxicity and clinical

trials, remain sparse. Further research is essential to fully elucidate the safety profile of this traditionally used medicinal plant.

CONCLUSION

The present review provides a comprehensive overview of the botanical, phytochemical, pharmacological and toxicological dimensions of Cuscuta reflexa, offering critical insights into the reported findings. Analysis of the data suggests that C. reflexa harbors significant therapeutic potential attributable to its rich phytoconstituent profile. In vitro and in vivo studies have corroborated various ethnomedicinal uses and demonstrated diverse pharmacological activities, affirming the plant's efficacy across a spectrum of ailments. Extracts and chemical components of Cuscuta reflexa exhibit notable antiinflammatory, analgesic, antipyretic, antioxidant and immune-modulating properties, along with potential benefits in hepatic, cardiovascular and dermatological conditions. It was also found to be effective in delaying aging processes, enhancing physical well-being and disease conditions such PCOS.

However, it's noteworthy that much of the existing research has primarily focused on extract-based investigations, warranting further exploration into the specific pharmacological and biological effects of individual plant constituents. The review underscores the need for future studies to delve into the bioavailability, mechanisms of action and pharmacokinetics of C. reflexa compounds, thus deepening our understanding of their therapeutic mechanisms and clinical potential. Despite the considerable medical promise of Cuscuta reflexa, the absence of clinical trials remains conspicuous, with the majority of studies confined to preclinical investigations. Clinical research serves as a pivotal gateway for transitioning novel therapeutics from laboratory discovery to real-world application, emphasizing the urgent need for clinical studies to advance the development of pharmaceuticals derived from this plant. Furthermore, the limited exploration of bioassay-guided extraction and isolation of

phytochemicals underscores the importance of future research efforts in validating the traditional uses of C. reflexa through focused drug development approaches. The majority of Cuscuta reflexa studies are confined to preclinical research, such as in vitro and animal models, which prove its antioxidant, hepatoprotective and neuroprotective effects (Verma & Yadav., 2018). Until strict clinical trials are conducted, however, its pharmacological advantages are speculative for human use. Recent reviews point to the necessity of randomized controlled trials (RCTs) to determine its bioavailability, dosage and possible side effects (Gangarde et al., 2025). Though ethnopharmacological accounts validate its folk uses, the lack of clinical data precludes its integration into evidence-based practice. Future studies must prioritize human trials to fill this lacuna and delineate its therapeutic potential in a thorough manner.

Toxicological research on C. reflexa has received insufficient attention and remains incompletely addressed, necessitating comprehensive investigations into its long-term in vivo toxicity. Systemic toxicity as well as safety assessments warrant further scrutiny to ensure the plant's overall safety profile. Moreover, with the majority of C. reflexa's chemical constituents still unidentified, leveraging modern analytical techniques such as LC-MS is essential for ongoing characterization and isolation efforts. These endeavors are pivotal not only for elucidating the pharmacological activities and mechanisms of action of C. reflexa constituents but also for uncovering their potential therapeutic value.

In light of these considerations, additional *in vivo* pharmacological as well as toxicological studies, focusing on both *C. reflexa* extracts and isolated chemical constituents, are recommended to expand our understanding of their practical applications and safety profile in clinical settings. Such concerted research efforts hold the key to unlocking the full therapeutic potential of *Cuscuta reflexa* and harnessing its benefits for human health and wellbeing.

ACKNOWLEDGMENTS

The administration and management of the NEMCARE Group of Institutions is acknowledged for providing the basic facilities to carry out the systematic review work.

Plant details

This work is a comprehensive review article of the plant *Cuscuta reflexa* Roxb. Therefore, neither permission nor a license is deemed necessary.

AUTHOR CONTRIBUTION STATEMENT

RA was involved in drafting the original manuscript, data collection, and investigating; AA was involved in revision; AB was involved in editing, KND was responsible for formal analysis; BJS was responsible for supervision; NSB was involved in conceptualization and methodology.

CONFLICT OF INTEREST

The authors declare that there is no conflict of interest.

REFERENCES

Adnan, M., Chy, M. N. U., Kamal, A. T. M. M., Chowdhury, M. R., Islam, M. S., Hossain, M. A., Tareq, A. M., Bhuiyan, M. I. H., Uddin, M. N., Tahamina, A., Azad, M. O. K., Lim, Y. S., & Cho, D. H. (2020). Unveiling Pharmacological Responses and Potential Targets Insights of Identified Bioactive Constituents of Cuscuta reflexa Roxb. Leaves through *In Vivo* and *In Silico* Approaches. Pharmaceuticals, 13(3), 50. https://doi.org/10.3390/ph13030050

Adnan, Muhammad, Ullah, I., Tariq, A., Murad, W., Azizullah, A., Khan, A. L., & Ali, N. (2014). Ethnomedicine use in the war affected region of northwest Pakistan. *Journal of Ethnobiology and Ethnomedicine*, 10(1). https://doi.org/10.1186/1746-4269-10-16

- Ahmad, N., Khan, P., Khan, A., Usman, M., Ali, M., Fazal, H., ... Abbasi, B. H. (2022). Elicitation of submerged adventitious root cultures of stevia rebaudiana with cuscuta reflexa for production of biomass and secondary metabolites. *Molecules*, 27(1). https://doi.org/10.3390/molecules27010014
- Ahmed, R., Bhattacharya, K., Nandan Dutta, K., Das, D., Sahariah, B. J., Deka, S., & Bora, N. S. (2025). Harnessing the anti-inflammatory potential of Cuscuta reflexa Roxb.: a comprehensive study on a leafless parasitic weed using chromatographic, in silico and in vitro methods. *Natural Product Research*, 1–7.
- Akhtar, N., Ihsan-ul-Haq, & Mirza, B. (2018). Phytochemical analysis and comprehensive evaluation of antimicrobial and antioxidant properties of 61 medicinal plant species. *Arabian Journal of Chemistry*, *11*(8), 1223–1235. https://doi.org/10.1016/j.arabjc.2015.01.013
- Akhtar, S., Hayat, M. Q., Ghaffar, S., Naseem, M., Abbas, N., & Jabeen, S. (2023). Plants used against liver disorders by autochthonous practitioners of Multan, Pakistan. *Heliyon*, *9*(3). https://doi.org/10.1016/j.heliyon.2023.e14068
- Amjad, M. S., Zahoor, U., Bussmann, R. W., Altaf, M., Gardazi, S. M. H., & Abbasi, A. M. (2020). Ethnobotanical survey of the medicinal flora of Harighal, Azad Jammu & Kashmir, Pakistan. *Journal of Ethnobiology and Ethnomedicine*, 16(1). https://doi.org/10.1186/s13002-020-00417-w
- Anjum, F., Bukhari, S. A., Shahid, M., Bokhari, T. H., & Talpur, M. M. A. (2014). Exploration of nutraceutical potential of herbal oil formulated from parasitic plant. African Journal of Traditional, Complementary and Alternative Medicines: AJTCAM / African Networks on Ethnomedicines, 11(1), 78–86. https://doi.org/10.4314/ajtcam.v11i1.11

- Aung, T. T. T., Xia, M. Y., Hein, P. P., Tang, R., Zhang,
 D. D., Yang, J., ... Wang, Y. H. (2020). Chemical
 Constituents from the Whole Plant of Cuscuta reflexa. *Natural Products and Bioprospecting*, 10(5), 337–344. https://doi.org/10.1007/s13659-020-00265-x
- Bacanlı, M., Başaran, A. A., & Başaran, N. (2017). The antioxidant, cytotoxic and antigenotoxic effects of galangin, puerarin and ursolic acid in mammalian cells. *Drug and Chemical Toxicology*, 40(3), 256–262.
- Bhagat, M., Arora, J. S., & Saxena, A. K. (2013). *In vitro* and *in vivo* antiproliferative potential of Cuscuta reflexa Roxb. *Journal of Pharmacy Research*, 6(7), 690–695. https://doi.org/10.1016/j.jopr.2013.06.005
- Bhat, N. A., Jeri, L., Karmakar, D., Mipun, P., Bharali, P., Sheikh, N., ... Kumar, Y. (2023). Ethnoveterinary practises of medicinal plants used for the treatment of different cattle diseases: A case study in East Khasi Hill district of Meghalaya, North East India. *Heliyon*, 9(7). https://doi.org/10.1016/j. heliyon.2023.e18214
- Bhatia, H., Manhas, R. K., Kumar, K., & Magotra, R. (2014). Traditional knowledge on poisonous plants of Udhampur district of Jammu and Kashmir, India. *Journal of Ethnopharmacology*, *152*(1), 207–216. https://doi.org/10.1016/j.jep.2013.12.058
- Bhattacharya, S., & Roy, B. (2010). 83 Preliminary Investigation On Antipyretic Activity Of Cuscuta Reflexa In Rats. *Journal of Advanced Pharmaceutical Technology & Research*, 1(1). 83-87.
- Bibi, Y., Naeem, J., Zahara, K., Arshad, M., & Qayyum, A. (2018). In Vitro Antimicrobial Assessment of Selected Plant Extracts from Pakistan. *Iranian Journal of Science and Technology, Transaction A:* Science, 42(1), 267–272. https://doi.org/10.1007/ s40995-018-0498-8

- Caporali, S., De Stefano, A., Calabrese, C., Giovannelli, A., Pieri, M., Savini, I., ... Terrinoni, A. (2022). Anti-inflammatory and active biological properties of the plant-derived bioactive compounds luteolin and luteolin 7-glucoside. *Nutrients*, 14(6), 1155.
- Caroli, C., Brighenti, V., Cattivelli, A., Salamone, S., Pollastro, F., Tagliazucchi, D., & Pellati, F. (2023). Identification of phenolic compounds from inflorescences of non-psychoactive Cannabis sativa L. by UHPLC-HRMS and in vitro assessment of the antiproliferative activity against colorectal cancer. *Journal of Pharmaceutical and Biomedical Analysis*, 236, 115723.
- Choi, J. N., Choi, Y.-H., Lee, J.-M., Noh, I. C., Park, J. W., Choi, W. S., & Choi, J. H. (2012). Anti-inflammatory effects of β-sitosterol-β-Dglucoside from Trachelospermum jasminoides (Apocynaceae) in lipopolysaccharide-stimulated RAW 264.7 murine macrophages. *Natural Product Research*, 26(24), 2340–2343.
- Choudhury, P. R., Choudhury, M. D., Ningthoujam, S. S., Mitra, A., Nath, D., & Talukdar, A. Das. (2015). Plant utilization against digestive system disorder in Southern Assam, India. *Journal of Ethnopharmacology*, *175*, 192–197. https://doi.org/10.1016/j.jep.2015.09.020
- Choudhury, P. R., Choudhury, M.D., Ningthoujam, S. S., Das, D., Nath, D., & Das Talukdar, A. (2015). Ethnomedicinal plants used by traditional healers of North Tripura district, Tripura, North East India. Journal of Ethnopharmacology, 166, 135–148. https://doi.org/10.1016/j.jep.2015.03.026
- De Rus Jacquet, A., Subedi, R., Ghimire, S. K., & Rochet, J. C. (2014). Nepalese traditional medicine and symptoms related to Parkinsons disease and other disorders: Patterns of the usage of plant resources along the Himalayan altitudinal range. *Journal of Ethnopharmacology*, 153(1), 178–189. https://doi.org/10.1016/j.jep.2014.02.016

- Dharmadasa, R. M., Akalanka, G. C., Muthukumarana, P. R. M., & Wijesekara, R. G. S. (2016). Ethnopharmacological survey on medicinal plants used in snakebite treatments in Western and Sabaragamuwa provinces in Sri Lanka. *Journal of Ethnopharmacology*, 179, 110–127. https://doi.org/10.1016/j.jep.2015.12.041
- Ekinci Akdemir, F. N., Albayrak, M., Çalik, M., Bayir, Y., & Gülçin, İ. (2017). The protective effects of p-coumaric acid on acute liver and kidney damages induced by cisplatin. *Biomedicines*, *5*(2), 18.
- Fatima, A., Ahmad, M., Zafar, M., Yaseen, G., Zada Khan, M. P., Butt, M. A., & Sultana, S. (2018). Ethnopharmacological relevance of medicinal plants used for the treatment of oral diseases in Central Punjab-Pakistan. *Journal of Herbal Medicine*, 12, 88–110. https://doi.org/10.1016/j. hermed.2017.09.004
- Ganai, S. A., Sheikh, F. A., Baba, Z. A., Mir, M. A., Mantoo, M. A., & Yatoo, M. A. (2021). Anticancer activity of the plant flavonoid luteolin against preclinical models of various cancers and insights on different signalling mechanisms modulated. *Phytotherapy Research*, 35(7), 3509–3532.
- Gangarde, P., Bhatt, S., & Pujari, R. (2025). Assessment of Neuroprotective Potential of Cuscuta reflexa in Aluminium Chloride-Induced Experimental Model of Alzheimer's Disease: *In Vitro* and *In Vivo* Studies. *Journal of Trace Elements in Medicine and Biology*, 127612.
- Gao, X., Wang, C., Chen, Z., Chen, Y., Santhanam, R. K., Xue, Z., ... Zhang, M. (2019). Effects of N-trans-feruloyltyramine isolated from laba garlic on antioxidant, cytotoxic activities and H2O2-induced oxidative damage in HepG2 and L02 cells. *Food and Chemical Toxicology*, 130, 130–141.

- Gautam, T., Gautam, S. P., Keservani, R. K., & Sharma, A. K. (2015). Phytochemical screening and wound healing potential of Cuscuta reflexa. *Journal of Chinese Pharmaceutical Sciences*, 24(5), 292–302. https://doi.org/10.5246/jcps.2015.05.038
- Gu, J., Huang, H., Huang, Y., Sun, H., & Xu, H. (2019). Hypertonic saline or mannitol for treating elevated intracranial pressure in traumatic brain injury: a meta-analysis of randomized controlled trials. *Neurosurgical Review*, 42, 499–509.
- Hassan, W., Buabeid, M. A., Kalsoom, U., Bakht, S., Akhtar, I., Iqbal, F., & Arafa, E. S. A. (2020). Cuscuta reflexa Roxb. Expedites the Healing Process in Contact Frostbite. *BioMed Research International*, 2020. https://doi.org/10.1155/2020/4327651
- Islam, R., Rahman, M. S., & Rahman, S. M. (2015).
 GC-MS analysis and antibacterial activity of Cuscuta reflexa against bacterial pathogens. *Asian Pacific Journal of Tropical Disease*, 5(5), 399–403. https://doi.org/10.1016/S2222-1808(14)60804-5
- Ivanova, E. P., Nguyen, S. H., Guo, Y., Baulin, V. A., Webb, H. K., Truong, V. K., ... Mainwaring, D. E. (2017). Bactericidal activity of self-assembled palmitic and stearic fatty acid crystals on highly ordered pyrolytic graphite. *Acta Biomaterialia*, 59, 148–157.
- Jiang, Y., Yu, L., & Wang, M.-H. (2015). N-transferuloyltyramine inhibits LPS-induced NO and PGE2 production in RAW 264.7 macrophages: involvement of AP-1 and MAP kinase signalling pathways. *Chemico-Biological Interactions*, 235, 56–62.
- Kala, C. P. (2020). Medicinal plants used for the treatment of respiratory diseases in Uttarakhand state of India. Studies on Ethno-Medicine, 14(1-2), 1-8. https://doi. org/10.31901/24566772.2020/14.1-2.597

- Katiyar, N. S., Singh, A. P., Gangwar, A. K., & Rao, N. V. (2015). Evaluation of hepatoprotective activity of stem extracts of Cuscuta reflexa (roxb) on thioacetamide induced liver damage in rats. World Journal of Pharmaceutical Sciences, 872-877.
- Kaur, A., Behl, T., Makkar, R., & Goyal, A. (2019).
 Effect of ethanolic extract of Cuscuta reflexa on high fat diet- induced obesity in Wistar rats.
 Obesity Medicine, 14. https://doi.org/10.1016/j.
 obmed.2019.02.001
- Kausar, F., Rather, M. A., Bashir, S. M., Alsaffar, R. M., Nabi, S. ul, Ali, S. I., ... Wali, A. F. (2021). Ameliorative effects of Cuscuta reflexa and Peucedanum grande on letrozole induced polycystic ovary syndrome in Wistar rats. *Redox Report*, 26(1), 94–104. https://doi.org/10.1080/135 10002.2021.1927396
- Kaushik, U., Aeri, V., Showkat, R. M., & Ali, M. (2017).
 Cucurbitane-type triterpenoids from the blood glucose-lowering extracts of Coccinia indica and Momordica balsamina fruits. *Pharmacognosy Magazine*, 13(Suppl 1), S115.
- Kayani, S., Ahmad, M., Zafar, M., Sultana, S., Khan, M. P. Z., Ashraf, M. A., ... Yaseen, G. (2014). Ethnobotanical uses of medicinal plants for respiratory disorders among the inhabitants of Gallies Abbottabad, Northern Pakistan. *Journal of Ethnopharmacology*, 156, 47–60. https://doi.org/10.1016/j.jep.2014.08.005
- Kleemann, R., Verschuren, L., Morrison, M., Zadelaar, S., van Erk, M. J., Wielinga, P. Y., & Kooistra, T. (2011). Anti-inflammatory, anti-proliferative and anti-atherosclerotic effects of quercetin in human in vitro and in vivo models. Atherosclerosis, 218(1), 44–52.
- Korbecki, J., & Bajdak-Rusinek, K. (2019). The effect of palmitic acid on inflammatory response in macrophages: an overview of molecular mechanisms. *Inflammation Research*, 68, 915–932.

- Kumar, A., Pandey, V. C., & Tewari, D. D. (2012). Documentation and determination of consensus about phytotherapeutic veterinary practices among the Tharu tribal community of Uttar Pradesh, India. *Tropical Animal Health and Production*, 44(4), 863–872. https://doi.org/10.1007/s11250-011-9979-x
- Lee, H. N., Kim, J.-K., Kim, J. H., Lee, S.-J., Ahn, E.-K., Oh, J. S., & Seo, D.-W. (2014). A mechanistic study on the anti-cancer activity of ethyl caffeate in human ovarian cancer SKOV-3 cells. *Chemico-Biological Interactions*, 219, 151–158.
- Lerata, M. S., D'Souza, S., Sibuyi, N. R. S., Dube, A., Meyer, M., Samaai, T., ... Beukes, D. R. (2020). Encapsulation of variabilin in stearic acid solid lipid nanoparticles enhances its anticancer activity in vitro. *Molecules*, 25(4), 830.
- Lesjak, M., Beara, I., Simin, N., Pintać, D., Majkić, T., Bekvalac, K., ... Mimica-Dukić, N. (2018). Antioxidant and anti-inflammatory activities of quercetin and its derivatives. *Journal of Functional Foods*, 40, 68–75.
- Li, J., Wang, Z., Fan, M., Hu, G., & Guo, M. (2022).

 Potential Antioxidative and Anti-Hyperuricemic

 Components Targeting Superoxide Dismutase and

 Xanthine Oxidase Explored from Polygonatum

 Sibiricum Red. *Antioxidants*, 11(9), 1651.
- Li, N., Yang, F., Liu, D.-Y., Guo, J.-T., Ge, N., & Sun, S.-Y. (2021). Scoparone inhibits pancreatic cancer through PI3K/Akt signaling pathway. World Journal of Gastrointestinal Oncology, 13(9), 1164.
- Lingaraju, D. P., Sudarshana, M. S., & Rajashekar, N. (2013). Ethnopharmacological survey of traditional medicinal plants in tribal areas of Kodagu district, Karnataka, India. *Journal of Pharmacy Research*, 6(2), 284–297. https://doi. org/10.1016/j.jopr.2013.02.012

- Liu, Y.-Y., Zhang, Y., Jiang, L., Lu, Q.-Y., Ye, R.-H., Guo, Z.-Y., ... Luo, X.-D. (2024). The whitening effect of cuscutin responsible for traditional use of Bergenia purpurascens. *Journal of Ethnopharmacology*, *326*, 117933.
- Lu, C., Li, Y., Hu, S., Cai, Y., Yang, Z., & Peng, K. (2018). Scoparone prevents IL-1β-induced inflammatory response in human osteoarthritis chondrocytes through the PI3K/Akt/NF-κB pathway. *Biomedicine & Pharmacotherapy*, 106, 1169–1174.
- Luo, Y., Shang, P., & Li, D. (2017). Luteolin: a flavonoid that has multiple cardio-protective effects and its molecular mechanisms. *Frontiers in Pharmacology*, *8*, 295438.
- Mach, C. M., Kha, C., Nguyen, D., Shumway, J., Meaders, K. M., Ludwig, M., ... Anderson, M. L. (2017). A retrospective evaluation of furosemide and mannitol for prevention of cisplatin-induced nephrotoxicity. *Journal of Clinical Pharmacy and Therapeutics*, 42(3), 286–291.
- Mala, F. A., & Sofi, M. A. (2017). Evaluation of antihistaminic Activity of herbal drug isolated from Cuscuta reflexa Roxb. *Annals of Plant Sciences*, *6*(11), 1807–1810. https://doi.org/10.21746/aps.2017.11.15
- Mallu, M. R., Vemula, S., & Kante, R. K. (2019). Molecular docking studies of bioactive compounds from Stevia rebaudiana for its anti-cancer activity. *Journal of Pharmaceutical Sciences and Research*, 11(5), 2016–2018.
- Masanga, J., Oduor, R., Alakonya, A., Ngugi, M., Ojola, P., Bellis, E. S., & Runo, S. (2022). Comparative phylogeographic analysis of Cuscuta campestris and Cuscuta reflexa in Kenya: Implications for management of highly invasive vines. *Plants People Planet*, 4(2), 182–193. https://doi.org/10.1002/ppp3.10236

- Mazumder, U. K., Gupta, M., Pal, D., & Bhattacharya, S. (2003). Chemical and toxicological evaluation of methanol extract of Cuscuta reflexa Roxb. stem and Corchorus olitorius Linn. seed on hematological parameters and hepatorenal functions in mice. Acta Poloniae Pharmaceutica, 60(4), 317-324.
- Mehmood Abbasi, A., Mulk Khan, S., Ahmad, M., Ajab Khan, M., Leah Quave, C., & Pieroni, A. (2013). Botanical ethnoveterinary therapies in three districts of the Lesser Himalayas of Pakistan. In *Journal of Ethnobiology and Ethnomedicine* (Vol. 9). Retrieved from http://www.ethnobiomed.com/content/9/1/84
- Mhiri, R., Koubaa, I., Chawech, R., Auberon, F., Allouche, N., & Michel, T. (2020). New isoflavones with antioxidant activity isolated from Cornulaca monacantha. *Chemistry & Biodiversity*, *17*(12), e2000758.
- Mir, T. A., Jan, M., & Khare, R. K. (2021). Ethnomedicinal application of plants in Doodhganga forest range of district Budgam, Jammu and Kashmir, India. *European Journal of Integrative Medicine*, 46. https://doi.org/10.1016/j.eujim.2021.101366
- Mishra, S., Alhodieb, F. S., Barkat, M. A., Hassan, M. Z., Barkat, H. A., Ali, R., ... Alam, O. (2022). Antitumor and hepatoprotective effect of Cuscuta reflexa Roxb. in a murine model of colon cancer. *Journal of Ethnopharmacology*, 282. https://doi.org/10.1016/j.jep.2021.114597
- Mostofa, R., Begum, R., Wang, H., Begum, Mst. M., Karim, R., Begum, T., ... Nova, T. T. (2020). Promising anitidiabetic potential of Cuscuta reflexa leaves methanol extract in alloxan-induced diabetic rats. *Clinical Phytoscience*, *6*(1). https://doi.org/10.1186/s40816-020-00169-w

- Muhammad, N., Ullah, S., Abu-Izneid, T., Rauf, A., Shehzad, O., Atif, M., ... Uddin, M. S. (2020). The pharmacological basis of Cuscuta reflexa whole plant as an antiemetic agent in pigeons. *Toxicology Reports*, 7, 1305–1310. https://doi.org/10.1016/j.toxrep.2020.09.009
- Muhammad, N., Ullah, S., Rauf, A., Atif, M., Patel, S., Israr, M., ... Mubarak, M. S. (2021). Evaluation of the anti-diarrheal effects of the whole plant extracts of Cuscuta reflexa Roxb in pigeons. *Toxicology Reports*, 8, 395–404. https://doi.org/10.1016/j.toxrep.2021.02.013
- Nadeem, M., Mumtaz, M. W., Danish, M., Rashid, U., Mukhtar, H., Irfan, A., ... Saari, N. (2020). UHPLC-QTOF-MS/MS metabolites profiling and antioxidant/antidiabetic attributes of Cuscuta reflexa grown on Casearia tomentosa: exploring phytochemicals role via molecular docking. *International Journal of Food Properties*, 23(1), 918–940. https://doi.org/10.1080/10942912.2020. 1764578
- Nayeli, M.-B., Maribel, H.-R., Enrique, J.-F., Rafael, B.-P., Margarita, A.-F., Macrina, F.-M., ... Manasés, G.-C. (2020). Anti-inflammatory activity of coumarins isolated from Tagetes lucida Cav. *Natural Product Research*, 34(22), 3244–3248.
- Nooreen, Z., Siddiqui, N. A., Wal, P., Shukla, A., Verma, R. S., Ahmad, A., ... Mohammad, A. (2023). Evaluation of Cuscuta reflexa seed essential oil on TPA-induced inflammation in mice. *Journal of King Saud University Science*, *35*(5). https://doi.org/10.1016/j.jksus.2023.102711
- O'Neill, A. R., & Rana, S. K. (2016). An ethnobotanical analysis of parasitic plants (Parijibi) in the Nepal Himalaya. *Journal of Ethnobiology and Ethnomedicine*, 12(1). https://doi.org/10.1186/s13002-016-0086-y

- Panda, S. K. (2014). Ethno-medicinal uses and screening of plants for antibacterial activity from Similipal Biosphere Reserve, Odisha, India. *Journal of Ethnopharmacology*, *151*(1), 158–175. https://doi.org/10.1016/j.jep.2013.10.004
- Panghal, M., Arya, V., Yadav, S., Kumar, S., & Parkash Yadav, J. (2010). *Indigenous knowledge of medicinal plants used by Saperas community of Khetawas, Jhajjar District, Haryana, India*. Retrieved from http://www.ethnobiomed.com/content/6/1/4
- Park, I., Song, J. H., Yang, S., Kim, W. J., Choi, G., & Moon, B. C. (2019). Cuscuta species identification based on the morphology of reproductive organs and complete chloroplast genome sequences. *International Journal of Molecular Sciences*, 20(11). https://doi.org/10.3390/ijms20112726
- Patel, S., Nag, M. K., Sharma, V., Chauhan, N. S., & Dixit, V. K. (2014). A comparative *in vivo* and *in vitro* evaluation of hair growth potential of extracts and an isolate from petroleum ether extract of Cuscuta reflexa Roxb. *Beni-Suef University Journal of Basic and Applied Sciences*, *3*(3), 165–171. https://doi.org/10.1016/j.bjbas.2014.10.002
- Paudel, P., Satyal, P., Maharjan, S., Shrestha, N., & Setzer, W. N. (2014). Volatile analysis and antimicrobial screening of the parasitic plant Cuscuta reflexa Roxb. from Nepal. *Natural Product Research*, 28(2), 106–110. https://doi.org/10.1080/ 14786419.2013.847440
- Qian, W., Liu, M., Fu, Y., Zhang, J., Liu, W., Li, J., ... Wang, T. (2020). Antimicrobial mechanism of luteolin against Staphylococcus aureus and Listeria monocytogenes and its antibiofilm properties. *Microbial Pathogenesis*, 142, 104056.
- Rahmatullah, M., Azam, M. N. K., Khatun, Z., Seraj, S., Islam, F., Rahman, M. A., ... Aziz, M. S. (2012). Medicinal plants used for treatment of diabetes

- by the Marakh sect of the Garo tribe living in Mymensingh district, Bangladesh. *African Journal of Traditional, Complementary and Alternative Medicines*, 9(3), 380–385. https://doi.org/10.4314/ajtcam.v9i3.12
- RANJAN, R., KUMAR, M., KUMAR, A., & SINHA, M. P. (2020). Hepatoprotective activity of Cuscuta reflexa aqueous and alcoholic extracts against CCl4 induced toxicity in rats. *Balneo Research Journal*, (Vol.11, 4), 463–466. https://doi.org/10.12680/balneo.2020.379
- Rath, D., Kar, D. M., Panigrahi, S. K., & Maharana, L. (2016). Antidiabetic effects of Cuscuta reflexa Roxb. in streptozotocin induced diabetic rats. *Journal of Ethnopharmacology*, 192, 442–449. https://doi.org/10.1016/j.jep.2016.09.026
- Raza, M. A., Mukhtar, F., & Danish, M. (2015). Cuscuta reflexa and Carthamus Oxyacantha: potent sources of alternative and complimentary drug. *SpringerPlus*, 4(1). https://doi.org/10.1186/s40064-015-0854-5
- Sajem, A. L., & Gosai, K. (2006). Traditional use of medicinal plants by the Jaintia tribes in North Cachar Hills district of Assam, northeast India. *Journal of Ethnobiology and Ethnomedicine*, 2. https://doi.org/10.1186/1746-4269-2-33
- Samsonowicz, M., Kalinowska, M., & Gryko, K. (2021). Enhanced antioxidant activity of ursolic acid by complexation with copper (II): Experimental and theoretical study. *Materials*, 14(2), 264.
- Saqib, Z., Mahmood, A., Naseem Malik, R., Mahmood, A., Hussian Syed, J., & Ahmad, T. (2014). Indigenous knowledge of medicinal plants in Kotli Sattian, Rawalpindi district, Pakistan. *Journal of Ethnopharmacology*, 151(2), 820–828. https://doi.org/10.1016/j.jep.2013.11.034

- Sen, S., Chakraborty, R., De, B., & Devanna, N. (2011).

 An ethnobotanical survey of medicinal plants used by ethnic people in West and South district of Tripura, India. *Journal of Forestry Research*, 22(3), 417–426. https://doi.org/10.1007/s11676-011-0184-6
- Shailajan, S., Joshi, H., & Tiwari, B. (2014). A comparative estimation of quercetin content from Cuscuta reflexa Roxb.using validated HPTLC and HPLC techniques. *Journal of Applied Pharmaceutical Science*, 4(7), 123–128. https://doi.org/10.7324/JAPS.2014.40721
- Shao, J.-W., Dai, Y.-C., Xue, J.-P., Wang, J.-C., Lin, F.-P., & Guo, Y.-H. (2011). *In vitro* and *in vivo* anticancer activity evaluation of ursolic acid derivatives. *European Journal of Medicinal Chemistry*, 46(7), 2652–2661.
- Sharma, J., Gairola, S., Gaur, R. D., & Painuli, R. M. (2012). The treatment of jaundice with medicinal plants in indigenous communities of the Sub-Himalayan region of Uttarakhand, India. *Journal of Ethnopharmacology*, *143*(1), 262–291. https://doi.org/10.1016/j.jep.2012.06.034
- Sharma, J., Gairola, S., Gaur, R. D., Painuli, R. M., & Siddiqi, T. O. (2013). Ethnomedicinal plants used for treating epilepsy by indigenous communities of sub-Himalayan region of Uttarakhand, India. *Journal of Ethnopharmacology*, *150*(1), 353–370. https://doi.org/10.1016/j.jep.2013.08.052
- Sharma, J., Gairola, S., Sharma, Y. P., & Gaur, R. D. (2014). Ethnomedicinal plants used to treat skin diseases by Tharu community of district Udham Singh Nagar, Uttarakhand, India. *Journal of Ethnopharmacology*, 158(PART A), 140–206. https://doi.org/10.1016/j.jep.2014.10.004

- Sharma, N., Kumar, V., & Gupta, N. (2021). Phytochemical analysis, antimicrobial and antioxidant activity of methanolic extract of Cuscuta reflexa stem and its fractions. *Vegetos*, *34*(4), 876–881. https://doi.org/10.1007/s42535-021-00249-3
- Shen, Y., Song, X., Li, L., Sun, J., Jaiswal, Y., Huang, J., ... Zhang, H. (2019). Protective effects of p-coumaric acid against oxidant and hyperlipidemia-an *in vitro* and *in vivo* evaluation. *Biomedicine & Pharmacotherapy*, 111, 579–587.
- Singh, A., Singh, V., Ananthan, R., & Kumar, B. D. (2022). Evaluation of immunomodulatory and antioxidants properties of Kwath, conventional extracts in plants Cocculus hirsutus and Cuscuta reflexa in vitro & ex vivo studies. *Journal of Ayurveda and Integrative Medicine*, *13*(1). https://doi.org/10.1016/j.jaim.2021.100537
- Singh, D., Arya, P. V, Sharma, A., Dobhal, M. P., & Gupta, R. S. (2015). Modulatory potential of α-amyrin against hepatic oxidative stress through antioxidant status in wistar albino rats. *Journal of Ethnopharmacology*, *161*, 186–193.
- Son, D. J., Lee, G. R., Oh, S., Lee, S. E., & Choi, W. S. (2015). Gastroprotective efficacy and safety evaluation of scoparone derivatives on experimentally induced gastric lesions in rodents. *Nutrients*, 7(3), 1945–1964.
- Summit, C., Jatin, T., Pradeep, K., & Yogesh, P. (2010).
 Comparative evaluation of antimicrobial potential of different extracts of Cuscuta reflexa growing on Acacia arabica and Zizyphus jujuba. *Pharmacognosy Journal*, 2(9), 293–296. https://doi.org/10.1016/S0975-3575(10)80119-1
- Suresh, V., Sruthi, V., Padmaja, B., & Asha, V. V. (2011). In vitro anti-inflammatory and anti-cancer activities of Cuscuta reflexa Roxb. *Journal of Ethnopharma-cology*, 134(3), 872–877. https://doi.org/10.1016/j. jep.2011.01.043

- Swain, S. S., & Padhy, R. N. (2015). In vitro antibacterial efficacy of plants used by an Indian aboriginal tribe against pathogenic bacteria isolated from clinical samples. *Journal of Taibah University Medical Sciences*, 10(4), 379–390. https://doi.org/10.1016/j.jtumed.2015.08.006
- Tamang, S., Singh, A., Bussmann, R. W., Shukla, V., & Nautiyal, M. C. (2023). Ethno-medicinal plants of tribal people: A case study in Pakyong subdivision of East Sikkim, India. *Acta Ecologica Sinica*, 43(1), 34–46. https://doi.org/10.1016/j.chnaes.2021.08.013
- Thangnipon, W., Suwanna, N., Kitiyanant, N., Soi-Ampornkul, R., Tuchinda, P., Munyoo, B., & Nobsathian, S. (2012). Protective role of N-trans-feruloyltyramine against β-amyloid peptide-induced neurotoxicity in rat cultured cortical neurons. *Neuroscience Letters*, 513(2), 229–232.
- Udavant, P. B., Satyanarayana, S. V., & Upasani, C. D. (2012). Preliminary screening of Cuscuta reflexa stems for Anti inflammatory and cytotoxic activity. Asian Pacific Journal of Tropical Biomedicine, 2(3 SUP-PL.). https://doi.org/10.1016/S2221-1691(12)60405-5
- Ullah, S., Rashid Khan, M., Ali Shah, N., Afzal Shah, S., Majid, M., & Asad Farooq, M. (2014). Ethnomedicinal plant use value in the Lakki Marwat District of Pakistan. *Journal of Ethnopharmacology*, 158(PartA), 412–422. https://doi.org/10.1016/j.jep.2014.09.048
- Umair, M., Altaf, M., Bussmann, R. W., & Abbasi, A. M. (2019). Ethnomedicinal uses of the local flora in Chenab riverine area, Punjab province Pakistan. *Journal of Ethnobiology and Ethnomedicine*, 15(1). https://doi.org/10.1186/s13002-019-0285-4
- Upadhyay, B., Parveen, Dhaker, A. K., & Kumar, A. (2010). Ethnomedicinal and ethnopharmacostatistical studies of Eastern Rajasthan, India. *Journal of Ethnopharmacology*, 129(1), 64–86. https://doi.org/10.1016/j.jep.2010.02.026

- Verma, N., & Yadav, R. K. (2018). Cuscuta reflexa: a paracitic medicinal plant. *Plant Arch*, *18*(2), 1938-1942.
- Versiani, M. A., Kanwal, A., Faizi, S., & Farooq, A. D. (2017). Cytotoxic Cardiac Glycoside from the Parasitic Plant Cuscuta reflexa. *Chemistry of Natural Compounds*, *53*(5), 915–922. https://doi.org/10.1007/s10600-017-2154-5
- Viet, T. D., Xuan, T. D., & Anh, L. H. (2021). α -amyrin and β -amyrin isolated from Celastrus hindsii leaves and their antioxidant, anti-xanthine oxidase and anti-tyrosinase potentials. *Molecules*, 26(23), 7248.
- Vikram, A., Jayaprakasha, G. K., Uckoo, R. M., & Patil, B. S. (2013). Inhibition of Escherichia coli O157: H7 motility and biofilm by β-sitosterol glucoside. *Biochimica et Biophysica Acta (BBA)-General Subjects*, 1830(11), 5219–5228.
- Vineeta, Shukla, G., Bhat, J. A., & Chakravarty, S. (2022). Species richness and folk therapeutic uses of ethnomedicinal plants in West Bengal, India A meta-analysis. *Phytomedicine Plus*, *2*(1). https://doi.org/10.1016/j.phyplu.2021.100158
- Vo, T. K., Ta, Q. T. H., Chu, Q. T., Nguyen, T. T., & Vo, V. G. (2020). Anti-hepatocellular-cancer activity exerted by β -sitosterol and β -sitosterol-glucoside from Indigofera zollingeriana Miq. *Molecules*, 25(13), 3021.
- Wang, C., Gao, Y., Zhang, Z., Chen, C., Chi, Q., Xu, K., & Yang, L. (2020). Ursolic acid protects chondrocytes, exhibits anti-inflammatory properties via regulation of the NF-κB/NLRP3 inflammasome pathway and ameliorates osteoarthritis. *Biomedicine & Pharmacotherapy*, 130, 110568.

- Wolska, K. I., Grudniak, A. M., Fiecek, B., Kraczkiewicz-Dowjat, A., & Kurek, A. (2010). Antibacterial activity of oleanolic and ursolic acids and their derivatives. *Central European Journal of Biology*, 5, 543–553.
- Xu, S., Zuo, A., Guo, Z., & Wan, C. (2017). Ethyl caffeate ameliorates collagen-induced arthritis by suppressing Th1 immune response. *Journal of Immunology Research*, 2017.
- Zhang, D., Arunachalam, K., Wang, Y., Zhang, Y., Yang, J., Hein, P. P., ... Yang, X. (2021). Evaluation on Antidiabetic Properties of Medicinal Plants from Myanmar. *Scientific World Journal*, 2021. https://doi.org/10.1155/2021/1424675

Nuclear Imaging Modalities and Radiopharmaceuticals in Veterinary Medicine

Elif Tugce SARCAN*, Asuman Yekta ÖZER**°

Nuclear Imaging Modalities and Radiopharmaceuticals in Veterinary Medicine

SUMMARY

Nuclear imaging modalities are based on radiopharmaceutical accumulation in organs and are imaged by a scintillation gamma camera and these radiopharmaceuticals consist of radionuclidic and pharmaceutical parts. Compared with other imaging modalities such as computed tomography (CT), nuclear imaging provides pathophysiological and morphological information. These applications as positron emission tomography (PET) and single photon emission computed tomography (SPECT) in veterinary medicine have been gaining attention for several decades, although some disadvantages, such as a lack of equipment and staff in veterinary science and high costs. This may be due to the pet industry's growth, the number of pet owners, and developed technologies. In this review, nuclear imaging techniques in veterinary medicine were examined and frequently used radiopharmaceuticals were included. Apart from preclinical studies, it has been observed how important the research in this field is relatively new, especially considering that the use of nuclear medicine applications in clinical veterinary.

Key Words: Radiopharmaceuticals, veterinary nuclear medicine, positron emission tomography, Technetium-99m, scintigraphy, nuclear imaging modalities.

Veteriner Hekimliğinde Nükleer Görüntüleme Yöntemleri ve Radyofarmasötikler

ÖZ

Nükleer görüntüleme yöntemleri, organlarda radyofarmasötik birikimine ve organların bir sintilasyon gama kamerasıyla görüntülenmesine dayanmaktadır. Bu radyofarmasötikler radyonüklidik ve farmasötik parçalardan oluşur. Bilgisayarlı Tomografi (BT) gibi diğer görüntüleme yöntemleriyle karşılaştırıldığında nükleer görüntüleme patofizyolojik ve morfolojik bilgiler sağlar. Veteriner hekimliğindeki bu uygulamaların (pozitron emisyon tomografisi (PET) ve tek foton emisyon bilgisayarlı tomografisi (SPECT)) kullanımı, ekipman ve personel eksikliği, yüksek maliyetler gibi bazı dezavantajları olmasına rağmen son yıllarda giderek artmaktadır. Bunun nedeni evcil hayvan endüstrisinin büyümesi, evcil hayvan sahiplerinin sayısı ve geliştirilen teknolojiler olarak sıralanabilir. Bu derlemede, veteriner hekimliğinde nükleer görüntüleme teknikleri incelenmiş ve sıklıkla kullanılan radyofarmasötikler dahil edilmiştir. Klinik öncesi çalışmalar dışında, özellikle klinik veterinerlikte nükleer tıp uygulamalarının kullanımının, bu alandaki araştırmaların nispeten yeni olması nedeniyle ne kadar önemli olduğu görülmüştür.

Anahtar Kelimeler: Radyofarmasötikler, veterinerlikte nükleer tıp, pozitron emisyon tomografisi, teknesyum-99m, sintigrafi, nükleer görüntüleme yöntemleri.

Received: 2.01.2025 Revised: 1.07.2025 Accepted: 14.07.2025

ORCID: 0000-0002-7323-6044, Hacettepe University, Faculty of Pharmacy, Department of Radiopharmacy, 06100-Ankara, Turkey.

[&]quot; ORCID: 0000-0001-6707-247X, Hacettepe University, Faculty of Pharmacy, Department of Radiopharmacy, 06100-Ankara, Turkey.

INTRODUCTION

Nuclear imaging modalities are not commonly used in veterinary medicine due to high costs and strict regulations (Greco, Meomartino, Gnudi, Brunetti, & Di Giancamillo, 2023). However, they (PET, SPECT and their combinations with CT) show increasing usage in veterinary medicine research and clinics (Rowe et al., 2013). Nuclear medicine in veterinary science follows the development and trends in human medicine and it is rapidly developing.

Regulations and protocols in nuclear medicine in veterinary are governed by the rules of the International Atomic Energy Agency (IAEA) and should follow published protocols and regulations by national authorities as in human nuclear medicine applications (Milardovic, 2021). IAEA also published a report entitled "Radiation Protection and Safety in Veterinary Medicine," which explains general requirements and principles of nuclear imaging in veterinary medicine and radiation protection for practitioners (IAEA, 2021).

Nuclear imaging modalities are considered safe, non-invasive and highly sensitive for early detection of diseases. However, regulations and protocols published by IAEA or other authorities should be followed for the safety of animals, owners and practitioners. Nuclear imaging modalities are mostly used for clinical purposes/diagnosis of diseases in large-sized animals, while used for disease research/ preclinical purposes for small-sized animals. After a radiopharmaceutical application, animals' urine, feces, sweat and saliva become radioactive due to the excretion/elimination of radiopharmaceuticals. Small animals can be removed after the imaging process, and they are generally controlled by their owners/ handlers, unlike larger animals such as horses. Bigger animals should be followed 24 hours after the imaging process (Lattimer, 2022; Milardovic, 2021). Clinically, thyroid glands, bones, kidneys and livers were the most imaged organs in veterinary medicine (Milardovic, 2021).

The most common usage of scintigraphy in veterinary is bone scintigraphy, especially for horses. Bone damage in racehorses can easily be detected with these imaging methods. Scintigraphy in veterinary medicine provides many advantages over traditional diagnostic modalities: 1. More sensitive for bone damage than radiographs; 2. Gamma cameras can be located anywhere on the horse's body; so any part of the body can be imaged; 3. Subtle lameness can be detected with gamma cameras, while only visible lameness can be detected with other traditional methods; 4. Blood flow can be traceable to the distal limb which is very helpful for some of the injuries and time lost for blood supply can be detected. Thyroid, portal, renal scintigraphies and glomerular filtration rate (GFR) determinations are the other common nuclear imaging procedures in veterinary medicine (Centre).

PET IMAGING

PET imaging plays an important role in diagnosing, monitoring, staging and therapy planning of diseases. It provides functional information besides the structural information (Yitbarek & Dagnaw, 2022). Although PET imaging applications focused on oncology, it has also been used for nononcologic diseases such as neurology, inflammation detection, and lameness evaluation in veterinary medicine (Yitbarek & Dagnaw, 2022).

PET is based on two 511 keV photons detected by a scanner. PET radionuclides emit positrons, and this positron is annihilated with an electron after its travel. Then, two 511 keV photons with opposite directions occur. These photons are detected by two detectors, and data is collected from many angles around the body (Saha, 2018; Sharp & Welch, 2005).

The first PET/CT scanning was started to use in 2001, and the number of PET/CT centers around the world has increased rapidly since then. Some of these facilities are trying to provide these techniques to veterinary medicine as well as human medicine with little differences (Table 1) (Figure 1) (Lawrence, Rohren, & Provenzale, 2010).



Figure 1. A dog undergoing PET/CT scaning (Reproduced with permission from Lawrence et al., 2010) (Lawrence et al., 2010).

PET imaging modality, especially the combination of PET and CT in veterinary medicine, shows increased popularity nowadays. The increasing number of people with pets, caused development in technology leading to the increase in to applications and developments in veterinary medicine (Martinez et al., 2012).

Table 1. Comparison of nuclear imaging in veterinary and human medicine.

Nuclear imaging in veterinary medicine	Nuclear imaging in human medicine
Animals are mostly required to be anesthetized.	Patients do not need to be anesthetized.
There is no standartized PET/CT protocols.	There are standartized PET/CT protocols.
High cost.	Relatively high cost.
Veterinary staff are exposed to radiation for longer	Staff are exposed to radiation for shorter
periods.	periods.
Used both in preclinical and clinical studies.	Used both in preclinical and clinical studies.
After imaging process, animals have to be	No need to be hospitalized.
hospitalized to avoid radiation exposure.	
Same rules and regulations should be followed.	

Radiopharmaceuticals Used for Veterinary Medicine

¹⁸F-fluorodeoxyglucose (FDG)

¹⁸F-FDG is the common radiopharmaceutical used in human medicine to detect cells with high metabolic activity such as tumours, inflamed cells, heart and brain while used for tumour detection, cardiac and neuroimaging in veterinary medicine. It is a glucose analogue and transported into the cells via glu-

cose transporter-1 (GLUT-1) and GLUT-6 which are transporter proteins (Lawrence et al., 2010). Adenocarcinoma, lung tumours, lymphoma, melanoma etc. can also be detected and staged in veterinary medicine by using a PET/CT agent like ¹⁸F-FDG due to their increasing glucose consumption (Greco et al., 2023).

The standardized uptake value (SUV) is the measurement value of radiopharmaceutical uptake in tissues/organs and shows tracer activity. It is a com-

mon parameter and helpful guide in clinical decisions (Rohren, Turkington, & Coleman, 2004). SUVs of osteosarcoma, lymphoma, blastomycosis, pulmonary carcinoma and soft tissue carcinoma in healthy dogs have been calculated in several studies. Also, SUVs of parenchymal organs were found similar in healthy humans and dogs by LeBlanc and co-workers (LeBanc, Jakoby, Townsend, & Daniel, 2008). However, some differences were determined in the SUV of healthy cats from healthy dogs and humans. Lower average hepatic and renal uptake was found compared with dogs and humans. Also, higher cardiac uptake was observed in cats rather than dogs and humans after 12-18 hours of fasting (LeBlanc et al., 2009).

¹⁸F-Sodium Fluoride (NaF)

Orthopedic imaging is getting increased usage in veterinary nuclear medicine. ¹⁸F-NaF provides bone remodeling, bone tumours detection in veterinary medicine and horse lameness imaging (Yitbarek & Dagnaw, 2022). ¹⁸F-NaF was a common skeletal imaging agent in the 60's. However, it is considered as an alternative radiopharmaceutical to Technetium-99m (^{99m}Tc)- methylene diphosphonate (MDP) when high spatial resolution and higher sensitivity are required due to the cost and availability. Currently, it has become popular in bone imaging again because

of the developments in technology with PET/CT (Li, Schiepers, Lake, Dadparvar, & Berenji, 2012; Valdés-Martínez et al., 2012). Moreover, ¹⁸F-NaF provides higher and faster bone uptake with a rapid clearance which causes a high bone/background ratio (Lawrence et al., 2010).

¹⁸F-3'-Deoxy-3'-Fluorothymidine (¹⁸F-FLT)

¹⁸F-FLT is a thymidine analog, and plays a role in DNA synthesis as a thymidine substrate. 18F-FLT is trapped in cells due to phosphorylation by thymidine kinase 1; thus PET images are obtained. The early preclinical studies, for veterinary usage of ¹⁸F-FLT, showed promising results in the characterization of neoplastic diseases and the evaluation of therapeutic responses in dogs (Rowe et al., 2013; Shields et al., 2002). Besides, ¹⁸F-FLT is also very useful for neoplastic lesion detection, and therapy monitoring in dogs with lymphoma, sarcoma and carcinoma. Based on this information, ¹⁸F-FLT was also investigated by Rowe and co-workers in healthy cats to provide information for potential clinical applications in a cat species (Rowe et al., 2013). 18F-FLT is a promising agent for also dogs with lymphoma for monitoring the therapy protocol (Figure 2) (Lawrence et al., 2009).

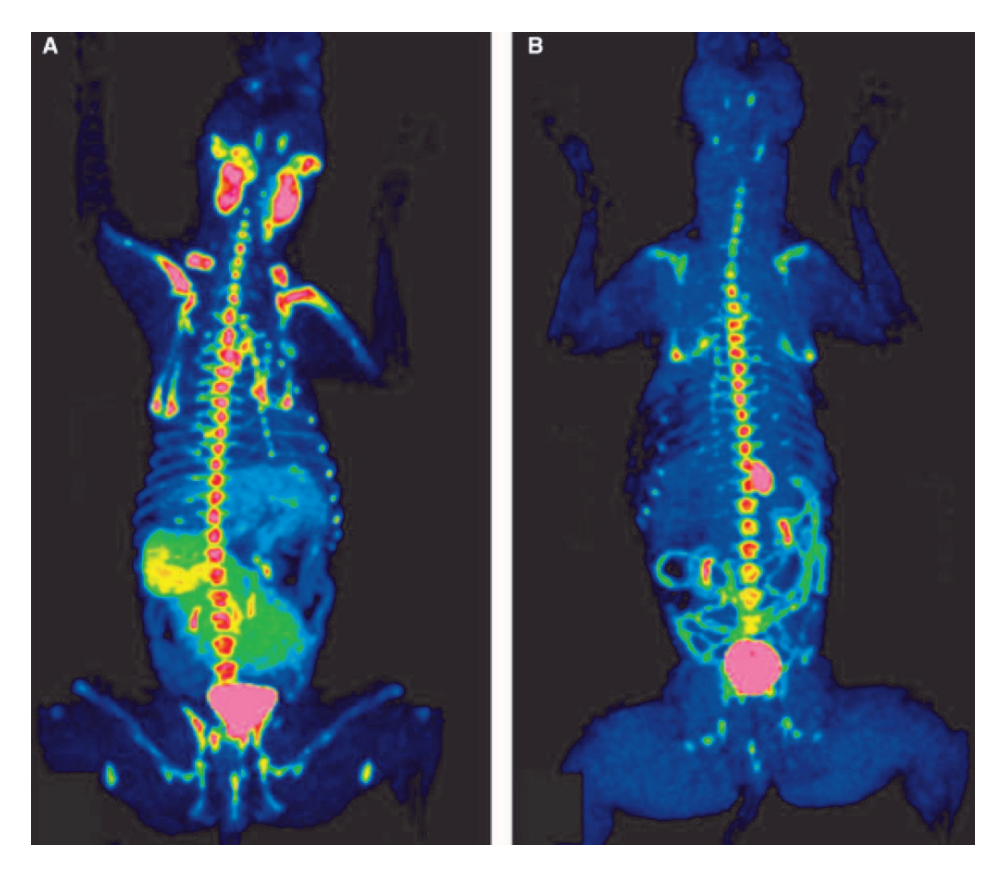


Figure 2. ¹⁸F-FLT PET/CT images of a Golden Retriever with Non-Hodgkin's Lymphoma; (A) before therapy (B) after 3 weeks of chemotherapy (Reused with permission from Lawrence et al., 2009) (Lawrence et al., 2009).

¹⁸F-FLT also showed higher specificity in cancer types -metastatic to lymph nodes- or caused by an inflammatory response- compared with ¹⁸F-FDG (LeBlanc & Peremans, 2014).

Copper-64 (⁶⁴Cu)-diacetyl-bis-N4-methylthiosemicarbazone (ATSM)

It is the other PET radiopharmaceutical used for hypoxia and an effective marker to depict hypoxic tissue (Black, McJames, Rust, & Kadrmas, 2008). It shows high trapping in hypoxic tissues while rapid clearance in normal tissues (Hansen et al., 2012; Hetrick, Kraft, & Johnson, 2015).

NUCLEAR SCINTIGRAPHY and SPECT IMAGING

The planar imaging system is a two-dimensional imaging modality that consists of a collimator filter, scintillator crystal and photomultiplier tubes, and a 2D gamma camera (Mattoon & Bryan, 2013). Even though planar imaging modalities have been used for years in veterinary medicine. Scintigraphy is the most sensitive imaging technique for detecting rib fractures in horses (Spriet & Vandenberghe, 2024).

SPECT is a three-dimensional imaging modality that is acquired with a gamma camera and reconstruction of a three-dimensional image volume. Multiple cameras rotate around the patients and provide information about the uptake of radiopharmaceuticals. The most common SPECT radionuclide is ^{99m}Tc in both human and veterinary medicine (Sarcan & ÖZer, 2023). SPECT imaging is only used for lameness diagnosis in horses and several diseases of small animals (Figure 3) (Yitbarek & Dagnaw, 2022). However, SPECT has an increasing interest in veterinary clinical settings (Yitbarek & Dagnaw, 2022).



Figure 3. A dog underwent SPECT scan [Reused from Greco et al. 2023 under CC-BY-NC-ND] (Greco et al., 2023).

Renal Imaging

The earlier SPECT application in veterinary medicine is renal morphologic imaging. 99mTc radiolabelled diethylenetriaminepentaacetic acid (DTPA), glucoheptonate (GH), dimercaptosuccinic acid (DMSA), and mercaptoacetyltriglycine (MAG3) are used for renal morphologic imaging (Balogh et al., 1999). These agents provide dynamic images to assess renal flow, the function of renal parenchyma and real-time GFR (Milardovic, 2021). GFR determination with imaging procedure, is one of the best ways to estimate renal function and early kidney diseases in dogs and cats. Renal scintigraphy also provides individual and total kidney function in dogs and cats, which makes it more advantageous than other imaging modalities (Peterson).

^{99m}Tc-DTPA is used in various animal species; however, GFR measurement could be changed according to the animal species; because plasma protein binding affects the GFR measurements. If the ^{99m}Tc-DTPA binds the plasma proteins, GFR could be reduced and falsely measured (Tyson & Daniel, 2014). Among these renal imaging SPECT agents, ^{99m}Tc-DMSA was detected earlier for renal tubular damage caused by gentamicin in dogs, compared with ^{99m}Tc-DTPA and ^{99m}Tc-MAG3 (Lora-Michiels, Anzola, Amaya, & Solano, 2001).

Liver Imaging

Portal scintigraphy is another modality frequently used in veterinary medicine, especially in diagnosing portosystemic shunt (Figure 4) (Morandi, 2014). It has also been used for liver function quantification and biliary tract assessment in dogs and cats.

Studies proved that hepatobiliary scintigraphy showed high sensitivity (83%) and specificity (94%) for extrahepatic biliary obstruction in veterinary practice (Kozat & Sepehrizadeh, 2017). Portal circulation is blood flow from blood vessels to the stomach, intestines and ends with the liver and heart. Portosystemic shunt is the abnormal portal circulation and commonly seen in dogs, cats, pigs, foals and calves. 99mTc-sulfur-colloid is one of the first radiopharmaceuticals used for a portosystemic shunt in dogs in the early 80s. 99mTc-pertechnetate, 99mTc-iminodiacetic acid (IDA) derivatives, 99mTc-mebrofenin and 99mTc-disofenin have been investigated as portal scintigraphy agents. In comparison of two, 99mTc-mebrofenin provides better morphologic images than 99mTc-disofenin (Morandi, 2014).

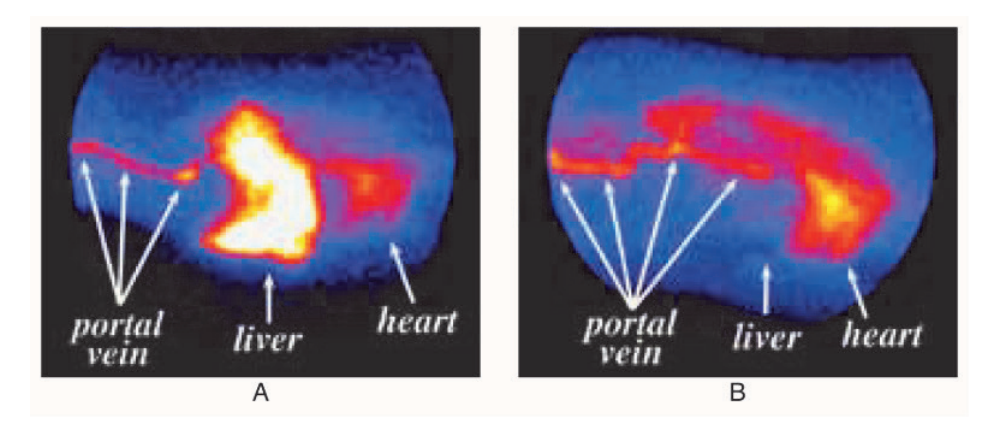


Figure 4. Portal scintigraphy of (A) a healthy dog (B) a dog with a portosystemic shunt [Reused from the document on website] (Peterson).

Lung Imaging

Lung tumours and lymph node metastasis are hardly prognosed and defined in dogs. Intrathoracic biopsy of lymph nodes is recommended; however, there is no specific guide for it. For this purpose, ^{99m}Tc-sulfur colloid has been investigated as a SPECT agent for mapping thoracic lymphadenectomy in dogs (Tuohy & Worley, 2014).

Thyroid Imaging

Thyroid scintigraphy is frequently performed in veterinary nuclear medicine because thyroid diseases are common in dogs and cats and are also reported in other animal species (Daniel & Neelis, 2014; Kintzer & Peterson, 1994). Immune-mediated thyroiditis and idiopathic atrophy are commonly seen in dogs, while adenomatous hyperplasia and hyperthyroidism are

common in cats (Rand, Behrend, Gunn-Moore, & Campbell-Ward, 2013).

Hyperthyroidism is one of the most common endocrine disorders in aging cats, and generally, thyroid adenoma and/or adenomatous hyperplasia are seen (Figure 5). Thyroid scintigraphy is mostly performed in cats and it is considered as a gold standard for the diagnosis of hyperthyroidism (Lim, Lee, Cho, & Nam, 2021). ^{99m}Tc-pertechnetate is the first choice in veterinary nuclear imaging for diagnosing thyroid diseases rather than radioiodine due to availability and low cost (LeBlanc & Peremans, 2014). However, ¹²³I provides a higher target/background ratio compared with ^{99m}Tc-pertechnetate. Thyroid images are taken after 20 minutes of radiopharmaceutical administration, and because of the short scanning process (approx. 3 minutes) sedation is not required (Peterson).

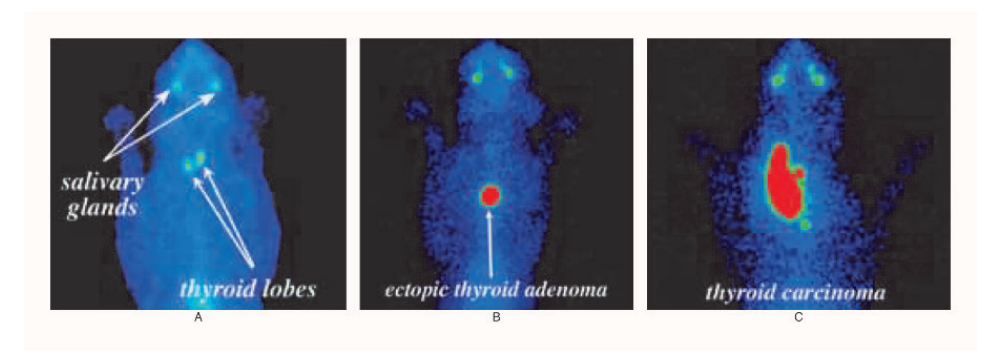


Figure 5. Thyroid scintigraphy of (A) healthy cat (B) hyperthyroid cat with thyroid adenoma (C) hyperthyroid cat with thyroid carcinoma [Reused from the document on the website] (Peterson).

Most thyroid tumours in dogs do not cause hyperthyroidism, so, quantitative imaging is required for hyperthyroidism in dogs.

Thyroid scintigraphy is considered the best imaging technique for dogs compared to other techniques and shows the size of the primary tumour and metastases location in %65 of dogs (Peterson). Moreover, it provides much information about thyroid gland functions, detection, and localization of thyroid tissues (Huaijantung, 2015).

Skeletal Imaging

Bone scintigraphy is a common procedure for infection, tumour and arthritis diagnosis in veterinary medicine (Huaijantung, 2015). It also shows high sensitivity for the diagnosis of bone injury due to the ability of osteoblastic activity detection (Trope, Anderson, & Whitton, 2011).

^{99m}Tc-MDP (Geissbuhler, Busato, & Ueltschi, 1998) and ^{99m}Tc-hydroxymethylene diphosphonate (HDP) (Levine, Ross, Ross, Richardson, & Martin, 2007) are common agents for scintigraphy of horses

(especially racehorses) (Figure 6A) and dogs (Figure 6B) and provide accurate images of the upper limb, pelvis and vertebral column in stress fractures and bone injuries (Cook & Cook, 2009). Besides bone injury, bone infection may also be detected in the early stages by using bone scintigraphy.

Bone scintigraphy is performed in 3 phases:

Phase I (Vascular Phase): arteries and veins are seen right after the administration of radiopharmaceuticals;

Phase II (Soft Tissue Phase): also known as the soft tissue phase, is the biodistribution of radiopharmaceuticals in the extracellular space of tissues;

Phase III (Bone phase): the detection phase of bone abnormalities/damages.

Three-phase scintigraphy may provide more information about the muscle in addition to the bone. Bone scintigraphy is also a very useful procedure for primary and metastatic bone tumours due to the osteoblastic activity of bone (Drost, Cummings, Mathew, Panciera, & Ko, 2003; Trope et al., 2011).

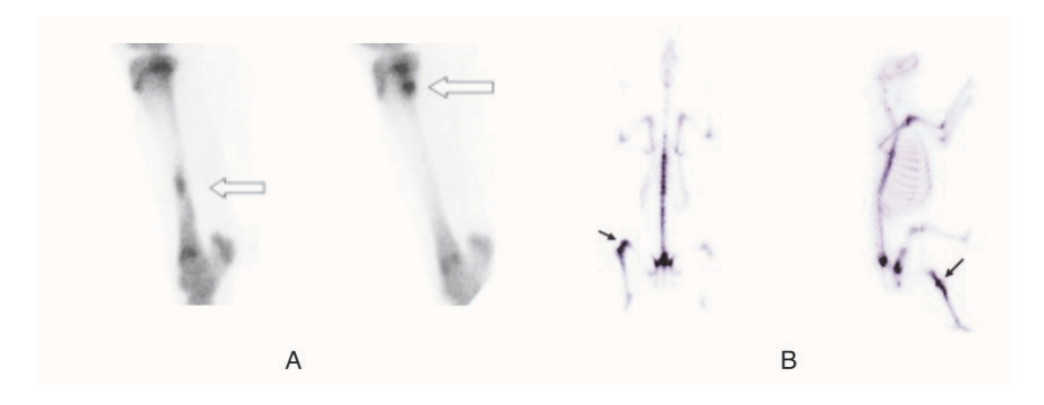


Figure 6. Bone scintigraphy (A) of a racehorse (spot views, hot spots: tibial stress fracture), (B) of a dog (total body, primary osteosarcoma in left knee) [Adapted from Milardovic, 2021 under CC BY 4.0] (Milardovic, 2021).

For the first time in literature, ^{99m}Tc-MDP was studied to detect early bone lesions and their time frame of onset of the infection in *Hepatozoon Americanum* infected dogs. Bone scintigraphy was found to be a viable option for detecting *H. Americanum* bone lesions by researchers due to the characteristics of *H. Americanum* bone lesions with polyostotic, high-intensity lesions(Drost et al., 2003).

Brain Imaging

^{99m}Tc-hexamethylpropylenamine oxime (HM-PAO) and ^{99m}Tc-ethyl cysteinatedimer (ECD) are the brain perfusion imaging agents that can be used in dogs' brain imaging. When the regional cerebral blood flow of ^{99m}Tc-ECD and ^{99m}Tc-HMPAO was compared, the tracers' regional distributions were found to

be different which means direct comparison of these tracers is not possible in dogs like humans. Besides, ^{99m}Tc-ECD uptake and washout rate were found to be more rapid than ^{99m}Tc-HMPAO in dogs and provided better quality images (Waelbers, Peremans, Vermeire, Piron, & Polis, 2012). In addition, ^{99m}Tc-DTPA, ^{99m}Tc-GH and ^{99m}Tc-pertechnetate are common agents for brain imaging in veterinary medicine due to their lower price (Balogh et al., 1999)

CONCLUSION

Nuclear medicine, one of the most frequently used and crucial imaging methods in human medicine, is becoming more widely used in veterinary medicine. It has been used limitedly in veterinary medicine because of high cost, lack of equipment and lack of trained personnel. However, due to developing technologies, growing pet industry, and increasing pet owner numbers, nuclear imaging methods have become widespread in veterinary medicine. In particular, high sensitivity, high resolution, and the availability of static imaging (a snapshot of the radiopharmaceutical distribution within a part of the body) as well as dynamic imaging (the imaging which administration of radiopharmaceuticals to patient over a specific period during nuclear imaging test) opportunities provide a significant advantage in this regard.

Although preclinical studies are frequently performed, the clinical usage of PET, SPECT in veterinary medicine is still limited. Although the high cost of new radiopharmaceuticals usage in nuclear imaging in veterinary, "old" radiopharmaceuticals (99m*Tc-pertechnetate, 99m*Tc-ECD, 99m*Tc-HDP, 99m*Tc-MDP, 99m*Tc-GH) are widely used. It is expected that these techniques will be used more frequently as the prices of radiopharmaceuticals and the costs of nuclear imaging methods decrease with developing technologies and opportunities. It is essential to conduct more studies in this field and to evaluate the results obtained by applying radiopharmaceuticals used in humans to veterinary medicine.

ACKNOWLEDGEMENTS

This work is not funded by any organization.

AUTHOR CONTRIBUTION RATE STATE-MENT

Conception (AYÖ), Literature research and writing (ETS), Reviewing the text (AYÖ, ETS), Supervision (AYÖ).

CONFLICT OF INTEREST

The authors declare that there is no conflict of interest.

REFERENCES

- Balogh, L., Andocs, G., Thuroczy, J., Nemeth, T., Lang, J., Bodoi, K., & Janoki, G. A. (1999). Veterinary Nuclear Medicine. Scintigraphical Examinations -A Review Acta Vet Brno, 68, 231-239.
- Black, N. F., McJames, S., Rust, T. C., & Kadrmas, D. J. (2008). Evaluation of rapid dual-tracer 62Cu-PTSM + 62Cu-ATSM PET in dogs with spontaneously occurring tumors. *Physics in Medicine & Biology*, 53(1), 217. doi:10.1088/0031-9155/53/1/015
- Centre, A. E. M. a. S. Equine Nuclear Scintigraphy.

 Retrieved from https://azequine.com/nucle-ar-scintigraphy/
- Cook, C. R., & Cook, J. L. (2009). Diagnostic imaging of canine elbow dysplasia: a review. *Vet Surg*, *38*(2), 144-153. doi:10.1111/j.1532-950X.2008.00481.x
- Daniel, G. B., & Neelis, D. A. (2014). Thyroid scintigraphy in veterinary medicine. *Semin Nucl Med*, 44(1), 24-34. doi:10.1053/j.semnuclmed.2013.08.007
- Drost, W. T., Cummings, C. A., Mathew, J. S., Panciera, R. J., & Ko, J. C. (2003). Determination of time of onset and location of early skeletal lesions in young dogs experimentally infected with Hepatozoon americanum using bone scintigraphy. *Vet Radiol Ultrasound*, 44(1), 86-91. doi:10.1111/j.1740-8261.2003.tb01455.x

- Geissbuhler, U., Busato, A., & Ueltschi, G. (1998). Abnormal bone scan findings of the equine ischial tuberosity and third trochanter. *Vet Radiol Ultrasound*, 39(6), 572-577. doi:10.1111/j.1740-8261.1998.tb01654.x
- Greco, A., Meomartino, L., Gnudi, G., Brunetti, A., & Di Giancamillo, M. (2023). Imaging techniques in veterinary medicine. Part II: Computed tomography, magnetic resonance imaging, nuclear medicine. *Eur J Radiol Open, 10*, 100467. doi:10.1016/j. ejro.2022.100467
- Hansen, A. E., Kristensen, A. T., Jørgensen, J. T., McEvoy, F. J., Busk, M., van der Kogel, A. J., . . . Kjær, A. (2012). 64Cu-ATSM and 18FDG PET uptake and 64Cu-ATSM autoradiography in spontaneous canine tumors: comparison with pimonidazole hypoxia immunohistochemistry. *Radiation Oncology*, 7(1), 89. doi:10.1186/1748-717X-7-89
- Hetrick, L. D., Kraft, S. L., & Johnson, T. E. (2015).

 Occupational Exposure to Veterinary Workers from the Positron Emission Tomography Imaging Agent 64Cu-ATSM. *Health Phys*, 109(3 Suppl 3), S219-223. doi:10.1097/hp.0000000000000363
- Huaijantung, S. (2015). Nuclear Scintigraphic Examination in Veterinary Medicine. *Journal of Applied Animal Science*, 8, 9-16.
- IAEA. (2021). Radiation Protection and Safety Veterinary Medicine. Retrieved from Vienna:
- Kintzer, P. P., & Peterson, M. E. (1994). Nuclear medicine of the thyroid gland. Scintigraphy and radioiodine therapy. *Vet Clin North Am Small Anim Pract*, 24(3), 587-605. doi:10.1016/s0195-5616(94)50061-5
- Kozat, S., & Sepehrizadeh, E. (2017). Methods of Diagnosing in Liver Diseases for Dog and Cats. *Turkish Journal of Scientific Reviews*, 10, 36-46.

- Lattimer, J. C. (2022). Nuclear Medicine Imaging in Animals Retrieved from https://www.msdvetmanual.com/clinical-pathology-and-procedures/ diagnostic-imaging/nuclear-medicine-imaging-in-animals?query=nuclear%20imaging
- Lawrence, J., Rohren, E., & Provenzale, J. (2010). PET/CT today and tomorrow in veterinary cancer diagnosis and monitoring: fundamentals, early results and future perspectives. *Vet Comp Oncol*, 8(3), 163-187. doi:10.1111/j.1476-5829.2010.00218.x
- Lawrence, J., Vanderhoek, M., Barbee, D., Jeraj, R., Tumas, D. B., & Vail, D. M. (2009). Use of 3'-deoxy-3'-[18F]fluorothymidine PET/CT for evaluating response to cytotoxic chemotherapy in dogs with non-Hodgkin's lymphoma. *Vet Radiol Ultrasound*, 50(6), 660-668. doi:10.1111/j.1740-8261.2009.01612.x
- LeBanc, A. K., Jakoby, B., Townsend, D. W., & Daniel, G. B. (2008). Thoracic and abdominal organ uptake of 2-deoxy-2-[18F]fluoro-D-glucose (18FDG) with positron emission tomography in the normal dog. *Vet Radiol Ultrasound*, 49(2), 182-188. doi:10.1111/j.1740-8261.2008.00348.x
- LeBlanc, A. K., & Peremans, K. (2014). PET and SPECT imaging in veterinary medicine. *Semin Nucl Med*, 44(1), 47-56. doi:10.1053/j.semnuclmed.2013.08.004
- LeBlanc, A. K., Wall, J. S., Morandi, F., Kennel, S. J., Stuckey, A., Jakoby, B., . . . Daniel, G. B. (2009). Normal thoracic and abdominal distribution of 2-deoxy-2-[18F]fluoro-D-glucose (18FDG) in adult cats. *Vet Radiol Ultrasound*, 50(4), 436-441. doi:10.1111/j.1740-8261.2009.01562.x
- Levine, D. G., Ross, B. M., Ross, M. W., Richardson, D. W., & Martin, B. B. (2007). Decreased radiopharmaceutical uptake (photopenia) in delayed phase scintigraphic images in three horses. *Vet Radiol Ultrasound*, 48(5), 467-470. doi:10.1111/j.1740-8261.2007.00280.x

- Li, Y., Schiepers, C., Lake, R., Dadparvar, S., & Berenji, G. R. (2012). Clinical utility of 18F-fluoride PET/CT in benign and malignant bone diseases. *Bone*, 50(1), 128-139. doi:https://doi.org/10.1016/j. bone.2011.09.053
- Lim, J. C., Lee, S. Y., Cho, E. H., & Nam, S. S. (2021). Veterinary Use of Radiopharmaceuticals. Paper presented at the Transactions of the Korean Nuclear Society Virtual Autumn Meeting.
- Lora-Michiels, M., Anzola, K., Amaya, G., & Solano, M. (2001). Quantitative and qualitative scintigraphic measurement of renal function in dogs exposed to toxic doses of Gentamicin. *Vet Radiol Ultrasound*, 42(6), 553-561. doi:10.1111/j.1740-8261.2001. tb00986.x
- Martinez, N. E., Kraft, S. L., Gibbons, D. S., Arceneaux, B. K., Stewart, J. A., Mama, K. R., & Johnson, T. E. (2012). Occupational per-patient radiation dose from a conservative protocol for veterinary (18) F-fluorodeoxyglucose positron emission tomography. *Vet Radiol Ultrasound*, *53*(5), 591-597. doi:10.1111/j.1740-8261.2012.01958.x
- Mattoon, J. S., & Bryan, J. N. (2013). The future of imaging in veterinary oncology: learning from human medicine. *Vet J*, 197(3), 541-552. doi:10.1016/j.tvjl.2013.05.022
- Milardovic, R. (2021). Veterinary Nuclear Medicine: A Look into the Future. *Veterinaria*, 70(2), 157-168. doi:10.51607/22331360.2021.70.2.157
- Morandi, F. (2014). Liver scintigraphy in veterinary medicine. *Semin Nucl Med*, 44(1), 15-23. doi:10.1053/j.semnuclmed.2013.08.002
- Peterson, M. E. Nuclear Imaging for Animals. Retrieved from https://www.animalendocrine.com/wp-content/uploads/2011/02/AEC_NuclearImaging.pdf?phpMyAdmin=pyzhyvp4yXZsgH-cwle5ITsJbEe8
- Rand, J., Behrend, E., Gunn-Moore, D., & Campbell-Ward, M. (2013). *Clinical endocrinology of companion animals*: John Wiley & Sons.

- Rohren, E. M., Turkington, T. G., & Coleman, R. E. (2004). Clinical applications of PET in oncology. *Radiology*, 231(2), 305-332. doi:10.1148/radiol.2312021185
- Rowe, J. A., Morandi, F., Wall, J. S., Akula, M., Kennel, S. J., Osborne, D., . . . LeBlanc, A. K. (2013). Whole-body biodistribution of 3'-deoxy-3'-[(18) f]fluorothymidine ((18) FLT) in healthy adult cats. *Vet Radiol Ultrasound*, *54*(3), 299-306. doi:10.1111/yru.12024
- Saha, G. B. (2018). Instruments for Radiation Detection and Measurement. In G. B. Saha (Ed.), *Fundamentals of Nuclear Pharmacy* (pp. 33-47). Cham: Springer International Publishing.
- Sarcan, E. T., & ÖZer, Y. (2023). Monoclonal Antibodies and Immuno-PET Imaging: An Overview. Fabad Journal of Pharmaceutical Sciences. doi:10.55262/fabadeczacilik.1172020
- Sharp, P. F., & Welch, A. (2005). Positron Emission
 Tomography. In P. F. Sharp, H. G. Gemmell, & A.
 D. Murray (Eds.), *Practical Nuclear Medicine* (pp. 35-48). London: Springer London.
- Shields, A. F., Grierson, J. R., Muzik, O., Stayanoff, J. C., Lawhorn-Crews, J. M., Obradovich, J. E., & Mangner, T. J. (2002). Kinetics of 3 -Deoxy-3 -[F-18]Fluorothymidine Uptake and Retention in Dogs. *Molecular Imaging & Biology*, 4(1), 83-89. doi:https://doi.org/10.1016/S1095-0397(01)00070-X
- Spriet, M., & Vandenberghe, F. (2024). Equine Nuclear Medicine in 2024: Use and Value of Scintigraphy and PET in Equine Lameness Diagnosis. *Animals (Basel)*, 14(17). doi:10.3390/ani14172499
- Trope, G. D., Anderson, G. A., & Whitton, R. C. (2011). Patterns of scintigraphic uptake in the fetlock joint of Thoroughbred racehorses and the effect of increased radiopharmaceutical uptake in the distal metacarpal/tarsal condyle on performance. *Equine Vet J*, 43(5), 509-515. doi:10.1111/j.2042-3306.2010.00316.x

- Tuohy, J. L., & Worley, D. R. (2014). Pulmonary lymph node charting in normal dogs with blue dye and scintigraphic lymphatic mapping. *Res Vet Sci*, 97(1), 148-155. doi:10.1016/j.rvsc.2014.07.002
- Tyson, R., & Daniel, G. B. (2014). Renal scintigraphy in veterinary medicine. *Semin Nucl Med*, 44(1), 35-46. doi:10.1053/j.semnuclmed.2013.08.005
- Valdés-Martínez, A., Kraft, S. L., Brundage, C. M., Arceneaux, B. K., Stewart, J. A., & Gibbons, D. S. (2012). Assessment of blood pool, soft tissue, and skeletal uptake of sodium fluoride F 18 with positron emission tomography–computed tomography in four clinically normal dogs. *American Journal of Veterinary Research*, 73(10), 1589-1595. doi:10.2460/ajvr.73.10.1589
- Waelbers, T., Peremans, K., Vermeire, S., Piron, K., & Polis, I. (2012). Regional distribution of technetium-99m-ECD in the canine brain: Optimal injection–acquisition interval in adult beagles. *Journal of Veterinary Behavior*, 7(5), 261-267. doi:https://doi.org/10.1016/j.jveb.2012.05.001
- Yitbarek, D., & Dagnaw, G. G. (2022). Application of Advanced Imaging Modalities in Veterinary Medicine: A Review. *Vet Med (Auckl)*, 13, 117-130. doi:10.2147/VMRR.S367040

A New Perspective on The Treatment of Brain Diseases: Plant-Derived Exosome-Like Nanovesicles

Meric A. ESMEKAYA*, Burhan ERTEKIN**°

A New Perspective on The Treatment of Brain Diseases: Plant-Derived Exosome-Like Nanovesicles

SUMMARY

The incidence of neurological illnesses has recently escalated globally, posing significant challenges for both individuals and their families. The ineffectiveness of the majority of existing chemical medications for treating these ailments has prompted researchers to explore other therapeutic approaches. Recently, plant-derived exosome-like nanovesicles (PELNs) have garnered attention from researchers owing to their industrial applicability, low cellular toxicity, excellent biocompatibility, and acceptance by the immune system. This paper presents an overview of PELNs and discusses their isolation and characterization methodologies. The mechanisms of action of PELNs in both in vivo and in vitro brain illness models will be examined. Ultimately, we will present information on the obstacles linked to the utilization of PELNs and their prospective positioning concerning neurological disorders.

Key Words: Extracellular vesicles, exosome, plant-derived-exosome-like nanovesicles, PELNs, brain disease

Beyin Hastalıklarının Tedavisine Yeni Bir Bakış Açısı: Bitki Kaynaklı Eksozom Benzeri Nanoveziküller

ÖZ

Beyinle ilgili rahatsızlıkların yaygınlığı son zamanlarda dünya çapında artmakta olup, bu durum hem birey hem de kişinin yakınları için büyük zorluklar yaratmaktadır. Bu hastalıkların tedavisinde kullanılan mevcut kimyasal ilaçların çoğunun etkilerinin istenilen düzeyde olmaması araştırmacıları yeni tedavi yöntemleri aramaya yöneltmiştir. Son zamanlarda bitki kaynaklı eksozom benzeri nanoveziküller (BEBN), endüstriyel uygulamaları için uygun olması, minimal hücresel toksisitesi, yüksek derecede biyouyumluluğa sahip olması ve immün sistem tarafından kabul görme gibi avantajları dolayısıyla araştırmacıların ilgi odağı haline gelmiştir. Bu derleme öncelikle BEBN'e genel bir bakış sağlamayı, izolasyon ve karakterizasyon tekniklerini ele almayı amaçlamaktadır. Ardından, BEBN'nin in vivo ve in vitro oluşturulan beyin hastalığı modellerinde etki mekanizmalarını tartışılacaktır. Son olarak, BEBN'in kullanımıyla ilişkili zorluklar ve beyin hastalıkları açısından gelecekte nasıl konumlandırılacakları hakkında bilgi vereceğiz.

Anahtar Kelimeler: Hücre dışı veziküller, eksozom, bitki kaynaklı-eksozom benzeri nanoveziküller, BEBN, beyin hastalığı

Received: 5.02.2025 Revised: 12.07.2025 Accepted: 21.07.2025

ORCID: 0000-0003-0469-4954 Faculty of Medicine, Department of Biophysics, Gazi University, Ankara, Turkey

[&]quot;ORCID: 0000-0003-2804-047X, Faculty of Medicine, Department of Biophysics, Tokat Gaziosmanpasa University, Tokat, Turkey

INTRODUCTION

More than half of the world's population suffers from neurological disorders [Alzheimer's and other dementias, Parkinson's disease, etc.] (Thakur et al., 2016), and they should be provided with more social and economic support (WHO, 2006). Additionally, taking precautions against neurological disorders is urgent, creating a healthy population/society. Molecular-based targeted therapeutic techniques have been developed significantly over the last decade.

As one of the therapeutic treatments, the nano-sized exosome (30-150 nm) isolated from bacteria, plants, and mammal cells with DNA, lipids, proteins, non-coding RNA, etc., provides an opportunity for intercellular communication (Mu et al., 2023, Omrani et al., 2024; Zhao et al., 2024).

Moreover, studies available in the literature have shown that exosomes have many remarkable and beneficial contributions to intercellular communications, being a safe medical delivery system and a suitable biological indicator.

Despite their benefits, they also have some limitations; for example,

i. Immune activators and immunosuppressive factors together may cause a reduction in the host resistance against pathogens.

ii. The highly sensitive and difficult stages of exosome extraction with low purity may lead to an increase in the cost of research.

The discovery and treatment of plant-derived exosome-like nanovesicles (PELNs) were made to overcome the limitations mentioned above (Mu et al., 2023; Bai et al., 2024). Isolation processes of PELNs, such as ultracentrifugation, size exclusion chromatography, and precipitation techniques, have been developed to date. There are a lot of advantages to their bio-molecular structures involved in the intercellular communication, the lipid membrane. PELNs, as a biomolecular vehicle with a phospholipid-rich characteristic, particularly have a protective coating for

external factors, which tend to degrade the activities of PELNs' composition. It's worthwhile to add that they can pass through the blood-brain barrier and the placenta. PELNs have been accepted for their suitability in industrial processes owing to their benefits, including biocompatibility, reliability, and immunological validation.

Bio-molecular targeted medicine with PELNs can be achieved by investigating the contents and functions of cargo elements, especially the bioactive components (Jin et al., 2018; Sarasati et al., 2023). Research has shown in the literature that the development of the trans-Golgi network and early endosome indicates the debut of PELNs secretion and biogenesis. As natural nanocarriers, these constituents also exhibit distinct morphological and compositional properties (Barzin et al., 2023).

In this review, the various contributions of PELNs in the blood-brain barrier-based treatment of central nervous system (CNS) disorders were summarized. Their neuroprotective, anti-inflammatory properties and their ability to increase cell-cell communication are discussed.

Therapeutic studies on various central nervous system disorders, such as Alzheimer's disease (AD) and Parkinson's disease (PD), and brain tumors showed that molecular-based techniques with PELNs would have potential for early disease identification and observation, being novel treatment alternatives. The crucial role of PELNs in CNS communication is reviewed, and their advantages and sensitivities for comprehending, identifying, and treating brain disorders are highlighted (Sharma et al., 2024).

CONTENT OF PELNs

PELNs, similar to mamalian-derived exosomes, consist of several components, including lipids, proteins, microRNA, mRNA, and distinctive bioactive substances according to their source (Figure 1). PELNs consist of membrane and cytosolic proteins. They encompass a diverse array of validated proteins, including defense proteins, transmembrane proteins

(such as proteolysis, actin, chloride channel proteins, and aquaporin), heat shock proteins (notably CD9 and CD63), acknowledged as exosome markers, and additional proteins linked to the plasmalemma. Research has established that citrus fruit-derived exosome-like nanovesicles encompass proteins with diverse activities, such as PTL3 and clathrin-3 for cellular growth and division, fructose bisphosphate for glycolysis, and PTL39 and HSP80 for protein folding and transport. Antioxidants and enzymes were also identified. PELNs exhibit a reduced protein concentration compared to mammalian exosomes (Sarasati et al., 2023).

Lipids constitute the fundamental components of PELNs and are crucial for their development and functionality. Phosphatidylcholine, phosphatidic acid, phosphatidylglycerol, phosphatidylinositol, and phosphatidylethanolamine are the principal lipids identified in PELNs, as substantiated by multiple studies. Certain research has performed lipidomic analyses of PELN lipids derived from tomato fruit, grapes, grapefruit, and tea. Purified PELNs are lipid-rich, and these five lipids

are the primary components, notwithstanding the variability in the overall lipid content of PELNs from different sources (Sha et al., 2024).

Multiple studies have confirmed that miRNA, a small RNA molecule usually consisting of fewer than 30 nucleotides, is found in PELNs. It has been suggested that plant miRNA, a short, single-stranded non-coding RNA, is protected from degradation during transport due to its association with micro or nanocapsules. Upon the introduction of nanovesicles into people or animals, PELNs are essential for regulating relevant pathophysiological responses alongside the defensive mechanisms of plants. Studies have shown that PELNs specifically target an organism's gastrointestinal system and may utilize microRNAs to regulate physiological activities. A study has proposed that PELNs may enhance communication between the intestinal microbiota and the human immune system, as well as modify the makeup of the intestinal microbiota through the transport of diverse short RNAs (Liu et al., 2024).

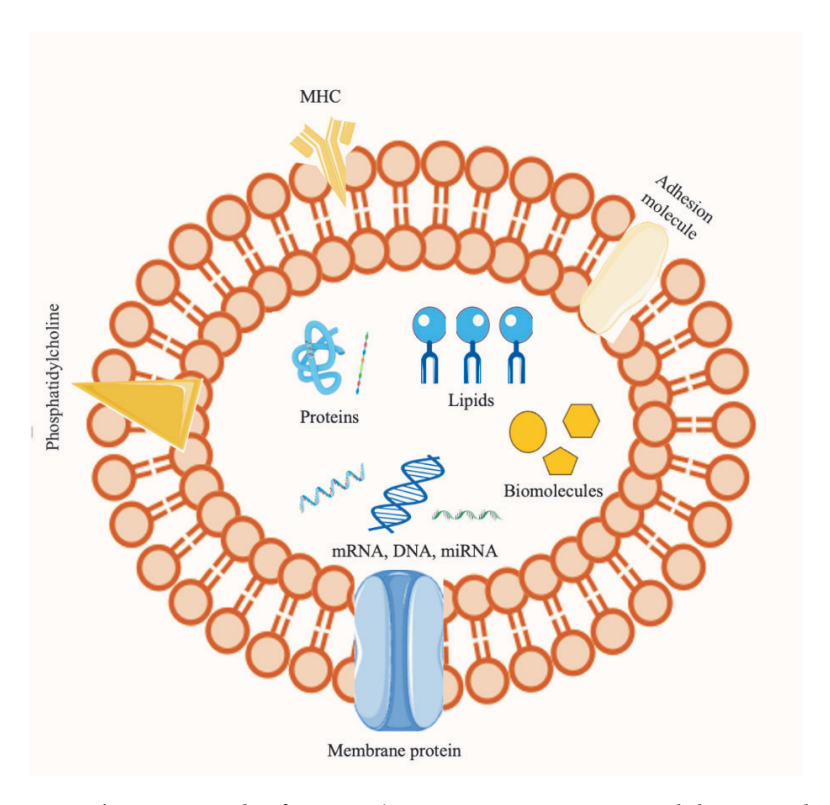


Figure 1. The compounds of PELNs. (MHC: Major Histocompatibility Complex).

ISOLATION METHODS OF PELNs

The isolation techniques employed in the synthesis of PELNs are typically as follows (Figure 2).

Ultracentrifugation

Ultracentrifugation (UC) is the segregation of particles based on their buoyant density. To enhance the enrichment of PELNs, various UC techniques are typically conducted. Cells (300–400 x g), cellular debris (2000 x g), biopolymer aggregates, apoptotic bodies, and other entities with a density above that of extracellular vesicles are the initial particles with

elevated buoyant density to be sedimented. A PELNs pellet is generated by ultracentrifuging the resulting supernatant containing extracellular vesicles for two hours at over 100,000 x g. While ultracentrifugation (UC) may isolate PELNs from a substantial number of samples, it is subject to several drawbacks, including prolonged isolation times (140–600 minutes), the presence of non-exosomal impurities, limited reproducibility of results, and efficiency that fluctuates according on the applied force, sample type, and rotor type (Zhao, Wijerathne, Godwin, & Soper, 2021).

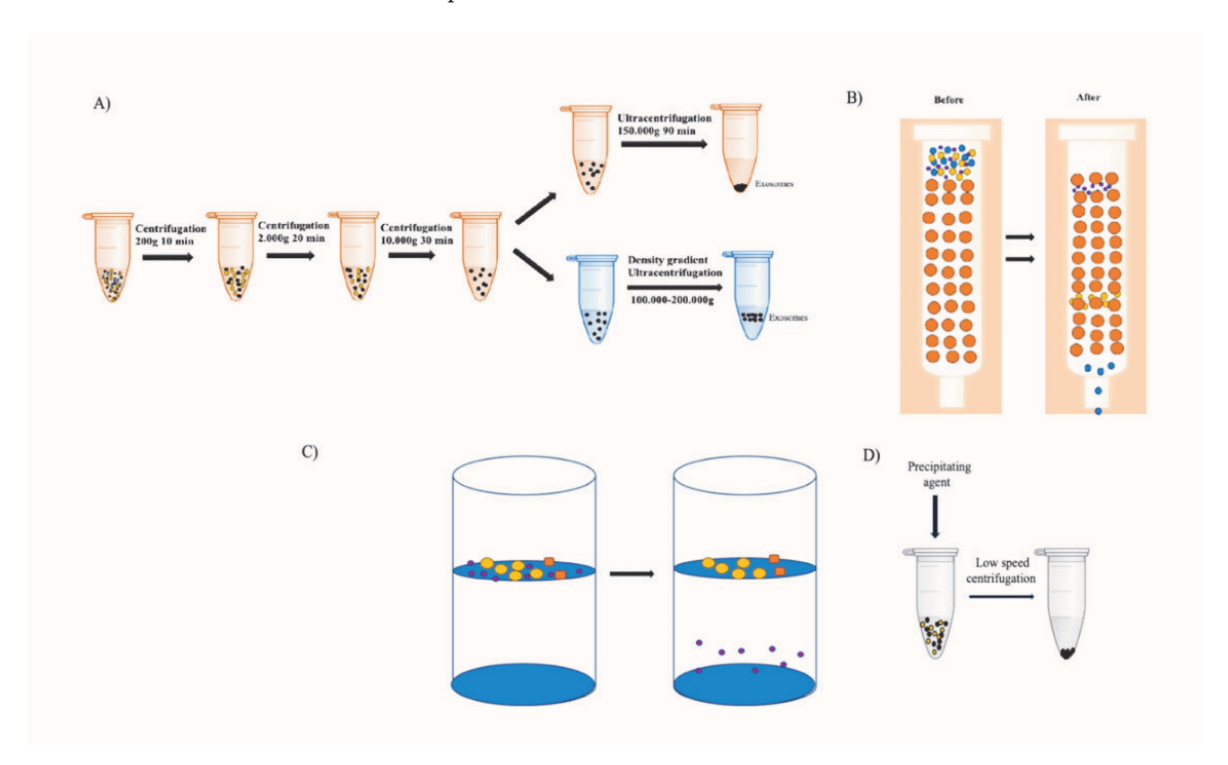


Figure 2. Isolation methods of PELNs. A) Ultracentrifugation and Density gradient ultracentrifugation (Adapted from: Li et al., 2017) B) Size-Exclusion Chromatography (SEC) C) Ultrafiltration D) Precipitation

Density gradient ultracentrifugation

A refined separation technique, utilizing ultracentrifugation, is density gradient centrifugation. Density gradient centrifugation, in contrast to ultracentrifugation, utilizes two or more separating medium with differing densities, such as sucrose and iodixanol. The sample is positioned above the separating medium for ultracentrifugation, after the removal of primary pollutants using low-speed centrifugation. This method's

benefit is its superior isolation purity. Regrettably, its clinical usefulness is constrained by the necessity for pre-preparation, intricate operation, and protracted centrifugation duration (>16 h) (Chen et al., 2022).

Size-Exclusion Chromatography (SEC)

Another size-based isolation technique, Size-Exclusion Chromatography (SEC) (gel filtration), employs a stationary phase composed of polymeric porous beads with a defined pore size to segregate par-

ticles of varying radii (Fekete, Beck, Veuthey, & Guillarme, 2014; Hong, Koza, & Bouvier, 2012). Complex components cannot traverse the pores and navigate among the porous beads; nevertheless, smaller particles can penetrate the pores, resulting in subsequent elution, contingent upon the sizes of the particles and pores. This approach provides numerous benefits, including preservation of the exosomes' inherent structure and morphology, cost-effectiveness, ease of use, and generation of uniformly sized exosomes. Nonetheless, SEC is typically impeded by the transit of particles of comparable size, extended turnaround times, and restricted sample processing volume, necessitating supplementary purification techniques (Shirejini, & Inci, 2022).

Ultrafiltration

This approach is classified as a size-based isolation strategy. It entails the passage of liquids through a filter with holes of a predetermined size.

Exosome separation protocols involve a series of consecutive filtration steps utilizing filters with pore sizes of 0.22, 0.45, 0.8, and occasionally 0.1 µm. This technique progressively removes particles larger than the pore size from the filtered liquid. The ultrafiltration approach offers advantages such as user-friend-liness, negating the necessity for specialist equipment and expertise, rapid purification capabilities that facilitate the swift processing of multiple samples, and the absence of alternative chemicals that could compromise exosome integrity. This method has drawbacks, including the possibility of exosome deformation and contamination by fluid components smaller than the filter's pore size (Yakubovich, Polischouk, & Evtushenko, 2022).

Precipitation

The process of polyethylene glycol (PEG) precipitation involves adding hydrophilic PEG to a sample at a specific concentration of salt. Exosome condensation and precipitation occur when low-speed centrifugation is used because the mixing of water molecules decreases the solute's solubility. This technique allows

for the mass isolation of exosomes without requiring sophisticated, costly equipment and without affecting biological activity. However, contaminants such as protein polymers might be present in the exosomes that are separated using this technique. The PEG separation process is distinguished by its simplicity, low cost, and high efficiency (Jiang, Liu, & Li, 2024).

CHARACTERIZATION OF PELNs

Nanoparticle Tracking Analysis (NTA)

Exosomes are quantified and analyzed with data derived from the Brownian motion of light molecules and particles in Nanoparticle Tracking Analysis (NTA). Particles suspended in liquid are lit by reflected laser light, and the apparatus captures the dispersed light from the particles utilizing a light-sensitive CCD camera. The software thereafter monitors the movement of vesicles varying in size from 10 to 1000 nm and employs the Stokes-Einstein equation to ascertain their dimensions. While NTA is regarded as the benchmark for exosome characterization, contamination from diluents is unavoidable, and such diluents (distilled water or buffering agents) or other substances are necessary for sample preparation (Zhang et al., 2018).

Transmission Electron Microscopy (TEM) and Scanning Electron Microscopy (SEM)

TEM is the most effective instrument for examining the form and structure of exosomes, as it can detect exosomes as small as one micron. The negative staining technique is straightforward and expedient, necessitating merely a few hours, with a transmission electron microscopy resolution of around 1 nm. Exosomes can be analyzed using conventional TEM to confirm their presence in solution, estimate their quality, and evaluate their morphology. The widely employed TEM technique may also analyze the morphology, dimensions, and architecture of individual exosomes and identify impurities.

SEM examines samples via a focused point beam, in contrast to TEM's broad beam. SEM offers a three-dimensional representation of exosomes by concentrating on the material's surface, in contrast to the two-dimensional perspective of TEM. SEM revealed spherical, protruding exosomes devoid of core indentation, in contrast to the cup-shaped morphology observed via TEM (Dilsiz, 2024).

Atomic Force Microscopy (AFM)

AFM represents an innovative method for analyzing exosomes, apart from laser and electron beam diffraction techniques. It quantifies and documents the relationships between a probing point and the sample surface, demonstrating reliability as a method. A key aspect of this technique is its capacity to analyze materials in their native state, requiring minimal sample preparation and employing a non-destructive operational mode. AFM is a nanoscale method for examining the quantity, morphology, biomechanics, and biomolecular composition of exosomes. This technique has effectively elucidated the biophysical, structural, and biomolecular characteristics of diverse subcellular structures, such as membrane proteins, DNA, and nanovesicles, while also enhancing our understanding of exosomes at both the subvesicular and single-vesicle levels (Gurunathan, Kang, Jeyaraj, Qasim, & Kim, 2019).

Flow Cytometry

A flow cytometer is a widely utilized technology for exosome analysis because of its capacity to evaluate multiple parameters simultaneously. Microvesicles and apoptotic bodies can be identified by the instrument's capacity to enumerate particles above 500 nm in size. Conventional cytometers may overlook particles smaller than 300 nm due to limitations in side detection. Consequently, multi-angle lasers in advanced flow cytometers can enhance particle resolution. Exosomes fall outside the detection capabilities of flow cytometry; therefore, they must be coupled to beads coated with specific antibodies targeting antigens present on the exosomal membrane. After binding to secondary fluorophore-conjugated antibodies, these counting beads are suspended in liquid and traversed

through the center of a detection cell in a narrow, single-particle flow regulated by a sheath fluid (Kurian, Banik, Gopal, Chakrabarti, & Mazumder, 2021).

Dynamic Light Scattering

Dynamic light scattering (DLS) is an optical measurement method employed to assess dispersed systems. The approach identifies high-frequency variations in scattered light that indicate the dynamics of microstructural processes, including elastic vibrations in gels, sol-gel transformation, and particle agglomeration. DLS is mostly employed to assess the Brownian motion of individual nanovesicles in liquids to ascertain vesicle diameter. The primary result of this work is an intensity-weighted distribution of the hydrodynamic equivalent size (or hydrodynamic diameter) of the nanovesicles. "Hydrodynamic diameter" refers to the dimensions of independently moving entities, encompassing individual particles as well as particle aggregation or agglomeration. It often denotes external dimensions; however, it has little relation to the dimensions of the constituent particles within an aggregate or agglomeration (Babick, 2020).

Zeta Potential

Zeta potential (ZP) is an indicator of colloidal stability that depends on surface charge and can be measured through the electrophoretic mobility of a suspension. Electrically charged particles exist in dispersed systems, including suspensions, emulsions, and colloidal dispersions. In dispersed systems, the ZP denotes the net charge of nanovesicles at their surface, which affects the stability of interactions between particles and between particles and the medium, including particle aggregation. Consequently, ZP is among the most effective tools for investigating the collective behavior of PELNs, including colloidal stability akin to extracellular vesicles (EVs) in dispersed systems, thereby illustrating its potential for analyzing EV function in natural processes. (Midekessa et al., 2020).

THERAPEUTIC USE OF PELNs IN BRAIN DISEASE

The blood-brain barrier (BBB) is a complex and dynamic structure that separates the brain from the peripheral circulation. This mechanism regulates the influx of substances into the brain, maintaining CNS homeostasis and a stable regional ionic microenvironment crucial for neurological function (Wood, O' Loughlin, & Lakhal, 2011). The BBB governs the transport and influx of molecules into the CNS, serving to shield it from bacteria, neurotoxins, and chemical substances. The blood-brain barrier comprises a complex system that selectively facilitates the transport of compounds. The passage of molecules across the blood-brain barrier is influenced by factors such as size, chemical composition, surface characteristics, and additional variables. Only small lipophilic compounds with a molecular weight less than 400 Da are capable of crossing the blood-brain barrier (Salarpour, Barani, Pardakhty, Khatami, & Chauhan, 2022). Hydrophilic compounds generally cannot traverse the BBB because of the tight junctions between brain endothelial cells, which restrict paracellular movement. The barrier function of the BBB presents a significant therapeutic challenge in neurodegenerative diseases, despite alterations in its structure and function under these conditions (Niu, Chen, & Gao, 2019).

Recently, researchers have focused their efforts on PELNs, nanoscale structures engineered for drug loading and traversing the blood-brain barrier, to address this challenge. The recognition of PELNs as natural carriers for biomolecules such as DNA, RNA, lipids, peptides, and proteins has enhanced the comprehension of their potential uses in the delivery of exogenous chemicals and medicinal agents. PELNs

demonstrate therapeutic potential for central nervous system disorders owing to their unique characteristics, including biodegradability, ability to encapsulate endogenous physiologically active molecules, lower toxicity relative to synthetic lipid-based nanovesicles, capacity to cross the blood-brain barrier (Figure 3), and suitability for large-scale production (Shinge, Xiao, Xia, Liang, & Duan, 2022; Wang et al., 2023). This has been demonstrated by several investigations.

In a study, Yoon et al. showed that green onion-derived exosome-like nanovesicles (GoPELN) effectively inhibited glutamate-induced Ca2+ influx and lipid peroxidation to prevent ferroptotic cell death in HT-22 mouse hippocampal cells. They explained this by suggesting that GoPELNs keep the prospect of operating as bioactive agents against glutamate-induced neuronal cell death, such as ferroptosis, by regulating various biological pathways after crossing the bloodbrain barrier (Yoon, Won, Lee, & Seo, 2024).

Liu et al. revealed in another study that intravenous administration of ginger-derived exosome-like nanovesicles (GELNs) exhibits therapeutic potential compared to medications that cannot penetrate the blood-brain barrier for the treatment of neurological disorders (Liu et al., 2025).

Cui et al. assessed the efficacy of Temozolomide (TMZ) encapsulated in citrus limon-derived exosome-like nanovesicles (CLELNs), characterized by limited blood-brain barrier permeability, fast disintegration, and systemic toxicity, on glioblastoma cell lines. Consequently, they demonstrated that CLELNs effectively traversed the blood-brain barrier while maintaining endothelial integrity, mitigating oxidative stress, and diminishing TMZ-induced toxicity (Cui et al., 2025).

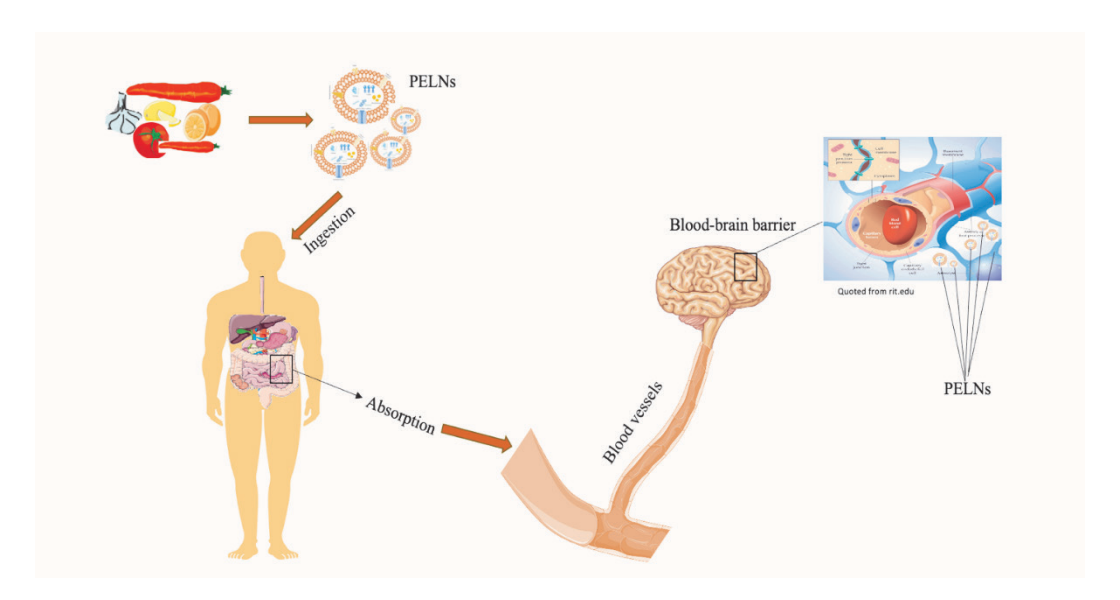


Figure 3. Schematic representation of the uptake of plant-derived exosome-like nanovesicles into the human body and the BBB crossing

Alzheimer's Disease

AD is among the most prevalent and lethal neurodegenerative disorders globally. It is estimated that about 50 million individuals globally experience cognitive impairment. AD accounts for almost 90% of all dementia cases globally (Iqbal et al., 2024). AD is marked by the extracellular deposition of Amyloid beta (AB) plaques and the intracellular presence of neuronal fibrillary tangles composed of hyperphosphorylated Tau (Lei et al., 2024). AD modifies various molecular mechanisms and intracellular signaling pathways, encompassing amyloid-beta and tau, inflammatory immune responses, neuroplasticity, synaptic equilibrium, and oxidative stress. These disorders arise from genetic, environmental, and biological factors. Furthermore, mounting data indicate an imbalance in the epigenetic pathways that underlie the aberrant synaptic plasticity and memory-associated genes in AD. (Greeny et al., 2024).

The Food and Drug Administration (FDA) has sanctioned two classes of medications for the management of AD. Cholinesterase inhibitors (ChEIs) are employed to reduce the degradation of acetylcholine during the initial phases of the disease. AChE inhibitors may be co-administered with an N-methyl-D-as-

partate (NMDA) receptor antagonist to enhance illness progression in moderate to severe instances. While these medications can postpone disease progression, their effectiveness is suboptimal (Singh, Day, Abdella, & Garg, 2024).

The inadequacy of conventional AD treatment methods to effectively alleviate patients' symptoms has prompted researchers to investigate PELN-based studies, a novel approach to AD treatment. Several studies have been undertaken, yielding promising outcomes for the future.

Zhang et al. evaluated the efficiency of *Lycium ruthenicum* Murray-derived exosome-like nanovesicles (LRELNs) using an A β -induced transgenic Caenorhabditis worm in vivo model. Their findings demonstrated that LRELNs decreased the amounts of A β oligomers and monomers through the DAF-16 pathway. LRELNs were discovered to suppress acetylcholinesterase activity, thereby mitigating cholinergic dysfunction, restoring mitochondrial membrane potential and adenosine triphosphate generation, and ameliorating mitochondrial malfunction (Zhang et al., 2025).

In a separate study, Dolma et al. applied *in vitro* research to assess the potential application of citrus-limon juice-derived exosome-like nanovesicles

(CLELNs) in safeguarding against AD-related neurodegeneration. An in vitro artificial membrane permeability assay validated the capacity of CLELNs to traverse the lipid bilayer and indicated the potential to access the brain for the treatment of neurological disorders. CLELNs demonstrated a neuroprotective effect by suppressing Aβ-induced neurotoxicity in SH-SY5Y cells, hence preventing Aβ-induced damage. (Dolma et al., 2024). Esmekaya and Ertekin investigated coffee-derived exosome-like nanovesicles (CELNs) as a prospective therapeutic or prophylactic treatment for Aβ-induced Alzheimer's disease. Aβ-induced toxicity (HT-22) was employed to produce AD in vitro in mouse hippocampal neuronal cells. Cells subjected to $A\beta_{\scriptscriptstyle (1\text{-}42)}$ were administered different concentrations of CELN (1-50 µg/ml). The results demonstrated that CELNs safeguard cells from $A\beta_{(1)}$ 42)-induced neurotoxicity via rectifying mitochondrial malfunction (Esmekaya, & Ertekin, 2024).

In 2024, Etxebeste-Mitxeltorena et al. showed that exosomes derived from Tomafran at concentrations of 25 and 50 μ g/mL safeguarded SH-SY5Y cells from damage induced by okadaic acid. Exosomes derived from Tomafran showed neuroprotective properties against okadaic acid-induced toxicity through tau phosphorylation. The research demonstrated that exosomes can traverse the blood-brain barrier, highlighting the significance of these nanovesicles for drug administration (Etxebeste-Mitxeltorena et al., 2024).

Parkinson's Disease

PD is a prevalent neurodegenerative disorder that leads to considerable disability related to cognitive, motor, and non-motor symptoms, constituting an increasing global public health challenge (Bhore et al., 2024, Morris, Spillantini, Sue, & Williams-Gray, 2024). Parkinsonian synucleinopathy is characterized by the presence of misfolded α -synuclein, Lewy bodies, and neurites. Neuropathological findings have elucidated the differences between PD and other synucleinopathies, such as multiple system atrophy. The presence of elevated lipid levels and many membranes, along with abnormal organelles including dysmorphic mi-

tochondria and vesicular structures, characterizes this Lewy disease (Bloem, Okun, & Klein, 2021). The primary pharmaceutical intervention for PD motor symptoms primarily aims to enhance central dopamine receptor activation. Dopamine agonists, levodopa, and monoamine oxidase-B (MAO-B) inhibitors, including Selegiline and Rasagiline, constitute excellent first-line therapies. Despite a comprehensive understanding of the fundamental physiology of PD for decades and the advent of levodopa as an effective treatment for motor symptoms due to dopaminergic deficiencies, no intervention has had a meaningful impact on disease progression (Wang & Shih, 2023).

Kim and Rhee found that the application of elevated concentrations of carrot-derived nanovesicles to cells resulted in minimal cytotoxicity in SH-SY5Y neuroblastoma cells subjected to 6-OHDA to create an *in vitro* PD model. Researchers discovered that nanovesicles produced from carrots hindered the generation of reactive oxygen species (ROS) by downregulating the expression of antioxidant molecules such as Nrf-2, HO-1, and NQO-1, and markedly suppressed apoptosis by efficiently obstructing caspase-3 activation. Collectively, these findings indicate that nanovesicles sourced from carrots represent a viable pharmacological approach for the management of PD (Kim, & Rhee, 2021).

A further study was done in 2024 by Xu et al. Transferring *Pueraria lobata*-derived exosome-like nanovesicles (PLELNs) into PD pathological SH-SY5Y cells demonstrated that PLELNs significantly improved mitochondrial dysfunction in affected dopaminergic neurons by regulating PINK1-Parkin-mediated mitophagy and maintaining the functionality of mitochondrial respiratory chain complexes I and V (Xu et al., 2024).

Cui et al. (2024) posited that the microbiota-gut-brain axis (MGBA) is intricately linked to the etiology and progression of PD and may serve as a viable treatment target. They developed ginger-derived exosome-like nanovesicles (GELNs) incorporating Tetrahedral framework nucleic acids (tFNAs) to modulate the microbiota and immune response, enhanced with acid-resistant and antimicrobial peptides (AMPs). Exo@tacs was administered to C57BL/6 male mice, designated as a PD model, via gavage at a volume of 200 μ L each administration, three times daily for 60 days, resulting in a considerable amelioration of Parkinson's disease symptoms (Cui et al., 2024).

Encouraging outcomes from in vivo and in vitro research suggest that PELNs may provide a novel option to conventional pharmacotherapy for PD in the future.

Brain Ischemia

Ischemic brain damage, commonly referred to as stroke, is the leading cause of neurological morbidity and mortality globally. Recent statistics indicate that ischemic stroke constitutes 86.8% of all strokes and ranks as the second leading cause of mortality globally (Zhang et al., 2024). In patients with significant arterial atherosclerosis and cardiogenic embolic infarction, cerebral blood flow is disrupted, leading to symptoms including paralysis and speech impairments (Wang et al., 2024). Researchers in this domain persist in developing efficacious pharmaceuticals for stroke prevention and treatment; nonetheless, the majority of preclinical medications do not succeed. An important exception is tissue plasminogen activator (tPA), which the FDA has sanctioned as a thrombolytic agent for the management of acute ischemic stroke. Nonetheless, its brief half-life and related hemorrhagic risk hinder its extensive application (Ma et al., 2020).

Researchers recently employed PELNs to acquire novel insights on the management of this severe disease.

Li et al. revealed that *Panax notoginseng* exosome-like nanovesicles (PNELNs) extracted from fresh roots of *Panax notoginseng* might mitigate cerebral ischemic injury in a rat model of transient middle cerebral artery occlusion. PNELNs mitigated cerebral ischemia injury by modifying microglial polariza-

tion, enhancing behavioral outcomes, and preserving blood-brain barrier integrity (Li, Kaslan, Lee, Yao, & Gao, 2023).

Cai et al. demonstrated the neuroprotective benefits of *Momordica charantia*-derived exosome-like nanovesicles (MCELNs) against brain ischemic injury by suppressing matrix metalloproteinase 9 (MMP-9) and activating the AKT/GSK-3 β signaling pathway. They demonstrated that MCELNs could traverse the blood-brain barrier to the infarct site,Mpreserve blood-brain barrier integrity, and mitigate cerebral ischemia injury. Given this knowledge, MCELNs may represent a novel pharmacological option for the treatment of ischemic stroke (Cai et al., 2022).

Brain Tumor

Brain tumors are atypical cellular proliferations or masses located in the central nervous system or brain (Isla Talukder, Uddin, Akhter, & Khalid, 2024). Brain tumors are classified into two categories: benign and malignant. Brain tumors are categorized as primary or secondary. Primary brain tumors originate within the brain, encompassing the meninges, cranial nerves, pituitary gland, and pineal gland. Conversely, secondary brain tumors, which are more prevalent, arise when cancer cells metastasize to the brain from other regions of the body (Khan, Iftikhar, Anwar, & Ramay, 2024).

Inhibiting tumor proliferation and enhancing immune responses inside the tumor microenvironment are critical considerations for advancing cancer therapy. Nevertheless, efficient nanomedicines for glioma treatment face restricted access to the brain owing to the blood-brain barrier.

Luo et al. reported that *Garcinia mangostana* L.-derived exosome-like nanovesicles were internalized by GL261 glioma and BV2 microglial cells, induced apoptosis in tumor cells, and inhibited their proliferation through the suppression of the PI3K-Akt signaling pathway, indicating a potential therapeutic strategy for glioma (Luo et al., 2025).

Kim et al. examined the anti-tumor immune responses in T cells and Tregs to nanosized ginseng-derived exosome-like nanovesicles (GiELNs), composed of phospholipids with diverse bioactive constituents that inhibit tumor growth. They found that GiELNs' enhanced targeting capability to the blood-brain barrier and glioblastoma produced a substantial therapeutic impact and demonstrated notable effectiveness in promoting M1 macrophage production within the tumor microenvironment. They demonstrated that GiELNs possess a significant capacity to inhibit glioma proliferation and modulate tumor-associated macrophages, successfully addressing glioblastoma both *in vitro* and *in vivo* (Kim et al., 2023).

A separate study conducted in 2016 further evidenced the brain tumor activity of PELNs. Zhuang et al. revealed that grapefruit-derived exosome-like nanovesicles (GNVs), which inherently enclose tiny RNA and proteins, may transport miR17 for the treatment of animal brain cancers. Folic acid-coated GNVs (FA-GNVs) were developed to specifically target folate receptor-positive GL-26 brain tumors. Moreover, they found that polyethylenimine coated with FA-GNVs (FA-pGNVs) not only improved RNA transport efficacy but also mitigated the toxicity of polyethylenimine associated with GNVs. The intranasal administration of miR17 through FA-pGNVs facilitated fast delivery of miR17 to the brain and preferential absorption by GL-26 tumor cells. Consequently, the proliferation of brain tumors was postponed in mice administered intranasally with FApGNV/miR17. The research indicated that this technique may offer a non-invasive therapeutic option for intranasal therapies targeting neurological disorders (Zhuang et al., 2016).

Brain Inflammation

Neuroinflammation is regulated by neurons, astrocytes, mast cells, T-cells, neutrophils, microglia—the resident macrophages of the brain—and the inflammatory mediators generated by these cells. In contrast to other cells, neurons in the central nervous system

cannot be repaired or reproduced following damage or degradation. Neuroinflammation serves as a protective response in the brain; nevertheless, excessive inflammation is detrimental and hinders neuronal renewal. Chronic neuroinflammation greatly contributes to the progression and development of neurodegenerative diseases such as Alzheimer's, Parkinson's, and Multiple Sclerosis (Kempuraj et al., 2016).

The positive results of PELNs in brain inflammation have been noted in some studies.

In 2023, Ishida et al. gave *Allium tuberosum*-derived exosome-like nanovesicles (ALELNs) to MG-6 cells and BV-2 microglia sourced from C57/BL6 mice, supplemented with lipopolysaccharide (LPS), and subsequently assessed the levels of inflammatory factors. To evaluate the drug delivery potential, scientists integrated ALELNs with the anti-inflammatory agent dexamethasone to make dexamethasone-embedded ALELNs (Dex-ALELNs). ALELNs significantly decreased LPS-induced nitric oxide (NO) and inflammatory cytokine levels in BV-2 and MG-6 cells. Dex-ALELN, formulated as a pharmaceutical agent, demonstrated a more powerful inhibition of NO generation in BV-2 cells compared to both ALELNs and dexamethasone (Ishida et al., 2023).

Consumption of a high-fat diet (HFD) stimulates the production of several inflammatory cytokines, such as TNF-α and IFN-γ, which contribute to neuronal cell death and cerebral inflammation. Sundaram et al. demonstrated that microglial cells efficiently internalized garlic-derived exosome-like nanovesicles (GaELNs), resulting in the suppression of various inflammatory cytokines, including IFN-γ and TNF-α. Thus, they established that GaELNs suppressed microglial cell activation and enhanced memory performance in mice subjected to a high-fat diet. The findings indicated that, alongside the anti-neuroinflammatory properties of GaELNs, GaELNs may serve as a therapeutic agent in the distribution system for the treatment of microglial-associated brain diseases (Sundaram et al., 2022).

CHALLENGES

Remarkable features of PELNs

- Membrane stability,
- Low immunogenicity,
- Acceptable biodistribution,
- Enhanced loading efficiency and target specificity,
- The surface features and capacity of PELNs can be altered depending on the recipient cell activity (Man et al., 2020).

PELNs in drug administration

Because of their small size, capacity to transport across the BBB, be absorbed by the gastrointestinal system, and penetrate the layers of skin (Barzin et al., 2023). Although PELNs have been used in the mentioned above and have potential use in the future, there are many challenges that researchers face in this field:

- The collection of PELNs and the improvement of their production efficiency.
- O Differential ultracentrifugation, which is currently utilised for gold extraction, is unsuitable for large-scale manufacturing, and the efficiency and stability of alternate extraction technologies should be researched further. Therefore, present extraction and separation techniques need to be further enhanced if PELNs are to be manufactured on a large scale in the future.
- o Improving the efficacy of PELNs detection is necessary since the only way to differentiate PELNs membrane surface indicators that have not yet been identified is through ultramicroscopic structure and particle size detection. The development of PELN technology that is easy to use, affordable, and has a high separation purity, as well as the advancement of identification technology, are currently major problems that need to be resolved. PELNs can have many different forms and come from a wide range of sources. Standardizing the

source of PELNs is beneficial for future study and use because the size and content of PELNs from different plant sources differ (Sha et al., 2024).

Despite the fact that PELNs have demonstrated numerous benefits in the prevention and treatment of a variety of illnesses in both in vitro and in vivo investigations, there are still certain challenges to be addressed to fully investigate the potential of their clinical applications.

As nanocarriers, PELNs are unable to hold large quantities of medication. It could be possible to combine PELNs with synthetic liposomes using the membrane fusion process to boost the cargo loading capacity. Moreover, it is uncertain how PELNs are absorbed by mammalian cells. The processes that promote PELNs internalization in mammalian cells must be identified to investigate the possibility of clinical application further (Zhang et al.,2022).

In the iterature, it has not been achieve the clinical treatment of PELNs for brain disorders. However, there are some clinical studies, for example;

- A completed clinical trial (NCT04879810) has investigated the ginger-derived exosome-like nanovesicles (GELNs) with and without curcumin in Inflammatory bowel disease (IBD) treatment, and we will know the safety and tolerability of GELNs in patients once the results are published (Liu et al., 2025).
- There are also corresponding clinical trials in progress. NCT03493984 aims to confirm that GELNs and *Aloe vera*-derived exosome-like nanovesicles can be used in Polycystic Ovary Syndrome (PCOS) patients to improve their reproductive function, but this clinical trial is still not approved, so there is still a long way to go before they can be applied in the clinic (Bai et al., 2024).

PELNs stability

One obstacle for the clinical use of PELNs is their decreased stability after purification, resulting in restricted storage time. This is a major barrier to commercial acceptance for applications based on PELNs. Pharmaceutical companies have shown that solid medication formulations are consistently more stable than liquid ones. Freeze-drying is a popular method for treating solid formulations, making it excellent for long-term storage of PELNs (Li et al., 2017). Freeze-drying PELNs can accelerate research and provide long-term stability, which is a critical step toward their use as medicines. Additionally, lyophilizates provide additional routes of administration, such as pulmonary distribution. However, unless the right stabilisers are included, lyophilisation increases stress during freezing and drying, which can cause EV damage (Trenkenschuh et al. 2021). Frank et al. performed that the first comprehensive stability assessment of different commonly available EV types during various storage conditions, including -80°C, 4°C, room temperature, and freeze-drying (lyophilization). They demonstrated that the intrinsic stability of PELNs is enhanced by cryoprotectants upon lyophilization (Frank et al. 2018). The use of a suitable lyoprotectant is crucial for the successful lyophilization of biological materials, including PELNs. Numerous earlier studies have used other kinds of disaccharides, like sucrose and trehalose, as lyoprotectant compositions to create a glassy state that promotes the development of amorphous ice during the freezing process and increases viscosity and inhibits ice crystallization. The lyoprotectant solution gets glassier as the concentration rises during the drying process, preventing non-covalently coupled chains of biomolecules from moving and maintaining the biological samples' original physicochemical characteristics and architecture (Li et al., 2017).

 One of the biggest challenges to overcome is the storage and stability of the produced PELNs. A study has indicated that the preservation of the integrity and size of PELNs is largely dependent on storage conditions. While PELNs' population decreases when stored at 4 °C for 24 hours, their operational and structural features are maintained for 28 days at -80 °C (Sivanantham, & Jin, 2022). General evaluations have demonstrated that PELNs maintain their physical and functional properties for 6 months at -80 °C. However, several freeze-thaw processes after creating this temperature condition can damage the structure of PELNs. This will lead to a loss of functionality. Conducting stability examinations for storing PELNs in applicable and easy-to-create conditions will lead to more effective and efficient studies in the future.

CONCLUSION AND FUTURE PERSPECTIVE

Before these promising PELNs can be applied clinically, several factors must be thoroughly investigated. The safety of PELNs is essential for their translational potential. Although current studies suggest that PELNs exhibit low immunogenicity and minimal cytotoxicity in preclinical models—largely due to their natural origin and biocompatible composition—they also possess unique biological properties and functions, despite sharing common features such as shape and size. Notably, their absorption times, biodistribution, and pharmacological effects can vary significantly (Mun, Song, Kee, & Han, 2025).

There are several problems that must be fixed. First, the advancement of PELN research is significantly hampered by the absence of standardisation in the identification and isolation techniques. Second, the biological roles of PELNs have been the focus of most research efforts, with relatively little investigation into the processes that underlie these roles. Third, the process of cultivating plants is time-consuming and labour-intensive, even while the expense of removing PELNs from fresh plants is not high. In order to generate sufficient quantities of PELNs from the culture broth, it is crucial to research tissue culture. Fourth, because of their potential therapeutic signifi-

cance, PELNs made from medicinal plants should be further explored and developed. Fifth, it's important to develop analytical methods that can help us better understand PELNs. For example, the advancement of bioinformatics allows us to perform systematic analyses and predict relationships between biomolecules using huge data (An et al., 2025).

According to current research, the mechanisms of action of PELNs made from plant components are yet unknown. To prove PELNs' effectiveness and safety in treating diseases, future studies should concentrate on figuring out which signalling pathways they affect. Furthermore, the vesicle damage brought on by highspeed centrifugation during isolation results in a noticeably low yield of PELNs from plant materials. Using different isolation methods, like ultrafiltration and low-speed centrifugation, could reduce vesicle damage and increase productivity. Certain plant components can to cytotoxically and immunogenically affect healthy, normal cells. To identify possible hazards and guarantee biocompatibility, thorough preclinical and clinical safety assessments, including dose-response studies, will be required. To properly utilise PELNs' therapeutic effects in healthcare applications, these challenges must be resolved (Sah et al., 2025).

PELNs can be altered by fusing liposomes or other vesicles with vesicle indications utilizing membrane fusion technology, as they do not contain any medications on their own. Because of their small size and capacity to pass through a variety of biological barriers, this enhances the vesicles' performance and drug-carrying capacity and can lead to a notable boost in their loading and transportation efficiency. Numerous natural active compounds are present in PELNs, and altering the vesicles through membrane fusion technology enhances the nanovesicles' killing ability, causing an interaction between the exogenous medicine and the natural active ingredients they contain. Recently, piggyback medication delivery to receptor cells has emerged as a novel therapeutic approach due to PELNs' ability to orchestrate targeted cellular communication (Jin et al., 2024). Extracellular vesicles produced from plants have recently been frequently used in treating brain diseases because of their capacity to penetrate the BBB, their high biocompatibility, and their targeting capacity. These nano-sized biocarriers have low toxicity and immunogenicity compared to inorganic and polymeric nanovesicles frequently used in synthetic drug delivery techniques due to their physicochemical structures. Although numerous studies have been conducted on PELNs, there are great difficulties in standardization, yield, stability, and storage in their production. In this context, cooperating with the International Organization for Standardization to encourage the standardization of PELNs and thus establishing across the world recognized standards is considered a feasible approach for the standardization of PELNs. Optimizing isolation techniques, enhancing separation methods, and automating production for scale-up are seen as one of the strategies to increase the purity and yield of PELNs. (Wu et al., 2024). One of the biggest challenges to overcome is the storage and stability of the produced PELNs. Currently, PELNs are only isolated from certain plants. More PELNs generated from medicinal plants should be taken into consideration for research, given the wide range and quantity of available medicinal plants. The PELNs found in medicinal plants can include specialized proteins, phytochemicals, and nucleic acids that might provide additional therapeutic choices compared to the synthetic and protein medications now on the market. Additionally, recent studies have not clearly stated whether PELNs isolated from various sections of the plant vary in terms of content, neuroprotective properties, and drug transport abilities (Lian et al., 2022). The targeting ability and safety of PELNs are one of the challenges to their use in therapeutic applications. Improving their targeting ability, like by targeting ligands or membrane-derived vesicles, may increase their efficacy in intracellular delivery, especially when administered intravenously. Furthermore, the safety of PELNs should be carefully evaluated. Though most methods of delivery of PELNs have not revealed any

harmful effects in previous studies, some studies, especially with intravenous injection, have shown safety issues, which pose limitations to their therapeutic applications (Zhao *et al.*, 2024. It is seen in the literature that the antioxidant, anti-inflammatory, and anticancer properties of PELNs are frequently investigated. As can be seen above, it is clear that PELNs have anti-neurotoxic and neuroprotective effects against brain-related diseases. In this context, further studies should be conducted to investigate the effectiveness of PELNs that have therapeutic compounds that can treat such diseases, and the support of existing studies with in vivo and clinical studies will allow PELNs to be proven as a powerful therapeutic agent to be used in the treatment of these diseases.

CONFLICT OF INTEREST

The authors declare that there is no conflict of interest.

AUTHOR CONTRIBUTION STATEMENT

Literature search and preparation of the manuscript (BE), conceptualization, review and final drafting/editing of the review (MAE).

REFERENCES

- An, Y., Sun, J. X., Ma, S. Y., Xu, M. Y., Xu, J. Z., Liu, C. Q.,...Xia, Q. D. (2025). From plant based therapy to plant-derived vesicle-like nanoparticles for cancer treatment: past, present and future. *International Journal of Nanomedicine*, 3471-349. doi: 10.2147/IJN.S499893.
- Babick, F. (2020). Dynamic light scattering (DLS). In Characterization of nanoparticles. *Elsevier*, 137-172. doi: 10.1016/B978-0-12-814182- 3.00010-9
- Bai, C., Zhang, X., Li, Y., Qin, Q., Song, H., Yuan, C., & Huang, Z. (2024). Research status and challenges of plant-derived exosome-like nanoparticles. *Biomedicine Pharmacotherapy*, 174, 116543. doi: 10.1016/j.biopha.2024.116543

- Barzin, M., Bagheri, A. M., Ohadi, M., Abhaji, A. M., Salarpour, S., & Dehghannoudeh, G. (2023). Application of plant-derived exosome-like nanoparticles in drug delivery. *Pharmaceutical Development and Technology*, 28(5), 383-402. doi: doi: 10.1080/10837450.2023.22022
- Bhore, N., Bogacki, E. C., O'Callaghan, B., Plun-Favreau, H., Lewis, P. A., & Herbst, S. (2024). Common genetic risk for Parkinson's disease and dysfunction of the endo-lysosomal system. *Philosophical Transactions of the Royal Society B*, 379(1899), 20220517. doi: 10.1098/rstb.2022.0517
- Bloem, B. R., Okun, M. S., & Klein, C. (2021). Parkinson's disease. *The Lancet*, *397*(10291), 2284-2303. doi: 10.1016/S0140-6736(21)00218-X
- Cai, H., Huang, L. Y., Hong, R., Song, J. X., Guo, X. J., Zhou, W.,...Shen, J. G., & Qi, S. H. (2022). Momordica charantia exosome-like nanoparticles exert neuroprotective effects against ischemic brain injury via inhibiting matrix metalloproteinase 9 and activating the AKT/GSK3β signaling pathway. Frontiers in pharmacology, 13, 908830. doi: 10.3389/fphar.2022.908830
- Cui, L., Perini, G., Minopoli, A., Palmieri, V., De Spirito, M., & Papi, M. (2025). Plant-derived extracellular vesicles as a natural drug delivery platform for glioblastoma therapy: A dual role in preserving endothelial integrity while modulating the tumor microenvironment. *International Journal of Pharmaceutics: X*, 100349. doi: 10.1016/j. ijpx.2025.100349
- Cui, W., Guo, Z., Chen, X., Yan, R., Ma, W., Yang, X., & Lin, Y. (2024). Targeting modulation of intestinal flora through oral route by an antimicrobial nucleic acid-loaded exosome-like nanovesicles to improve Parkinson's disease. *Science Bulletin*, 69(24), 3925-3935. doi: 10.1016/j.scib.2024.10.027

- Chen, J., Li, P., Zhang, T., Xu, Z., Huang, X., Wang, R., & Du, L. (2022). Review on strategies and technologies for exosome isolation and purification. Frontiers in bioengineering and biotechnology, 9, 811971. doi: 10.3389/fbioe.2021.811971
- Dilsiz, N. (2024). A comprehensive review on recent advances in exosome isolation and characterization: Toward clinical applications. *Translational Oncology*, *50*, 102121. 102121. doi: 10.1016/j.tranon.2024.102121
- Dolma, L., Damodaran, A., Panonnummal, R., & Nair, S. C. (2024). Exosomes isolated from citrus lemon: a promising candidate for the treatment of Alzheimer's disease. *Therapeutic Delivery*, 1-13. doi: 10.1080/20415990.2024.2354119
- Esmekaya, M. A., & Ertekin, B. (2024). Neuroprotective effects of coffee-derived exosome-like nanoparticles against Aβ-induced neurotoxicity. *General Physiology Biophysics*, *43*(6). doi: 10.4149/gpb_2024025
- Etxebeste-Mitxeltorena, M., Niza, E., Fajardo, C. M., Gil, C., Gómez-Gómez, L., Martinez, A., & Ahrazem, O. (2024). Neuroprotective properties of exosomes and chitosan nanoparticles of Tomafran, a bioengineered tomato enriched in crocins. *Natural Products and Bioprospecting*, *14*(*1*), 9. doi: 10.1007/s13659023004259
- Fekete, S., Beck, A., Veuthey, J. L., & Guiilarme, D. (2014). Theory and practice of size exclusion chromatography for the analysis of protein aggregates. J Pharm Biomed Anal., 101, 161-173. doi: 10.1016/j.jpba.2014.04.011.
- Frank, J., Richter, M., de Rossi, C., Lehr, C. M., Fuhrmann, K., & Fuhrmann, G. (2018). Extracellular vesicles protect glucuronidase model enzymes during freeze-drying. *Scientific reports*, *8*(1), 12377. doi: 10.1038/s41598-018-30786-y.

- Greeny, A., Nair, A., Sadanandan, P., Satarker, S., Famurewa, A. C., & Nampoothiri, M. (2024). Epigenetic Alterations in Alzheimer's Disease: Impact on Insulin Signaling and Advanced Drug Delivery Systems. *Biology*, *13*(*3*), 157. doi: 10.3390/biology13030157
- Gurunathan, S., Kang, M. H., Jeyaraj, M., Qasim, M., & Kim, J. H. (2019). Review of the isolation, characterization, biological function, and multifarious therapeutic approaches of exosomes. *Cells*, *8*(*4*), 307. doi: 10.3390/cells8040307
- Hong, P., Koza, S., & Bouvier, E. S. P. (2012). Size-Exclusion Chromatography for the Analysis of Protein Biotherapeutics and their Aggregates. J Liq Chromatogr Relat Technol. 35(20), 2923-2950. doi: 10.1080/10826076.2012.743724.
- Iqbal, I., Saqib, F., Mubarak, Z., Latif, M. F., Wahid, M., Nasir, B.,...Mubarak, M. S. (2024). Alzheimer's disease and drug delivery across the blood-brain barrier: approaches and challenges. *European Journal of Medical Research*, 29(1), 313. doi: 10.1186/s40001-024-01915-3
- Ishida, T., Kawada, K., Jobu, K., Morisawa, S., Kawazoe, T., Nishimura, S.,...Miyamura, M. (2023). Exosome-like nanoparticles derived from Allium tuberosum prevent neuroinflammation in microglia-like cells. *Journal of Pharmacy and Pharmacology*, 75(10), 1322-1331. doi: 10.1093/jpp/rgad062
- Islam, M. M., Talukder, M. A., Uddin, M. A., Akhter, A., & Khalid, M. (2024). Brainnet: precision brain tumor classification with optimized efficientnet architecture. *International Journal of Intelligent Systems*, 2024(1), 3583612. doi: 10.1155/2024/3583612
- Jin, Z., Na, J., Lin, X., Jiao, R., Liu, X., & Huang, Y. (2024). Plant-derived exosome-like nanovesicles: A novel nanotool for disease therapy. *Heliyon*, 10 (9), e30630. doi: 10.1016/j.heliyon.2024.e30630.

- Jiang, Z., Liu, G., & Li, J. (2020). Recent progress on the isolation and detection methods of exosomes. *Chemistry–An Asian Journal*, 15(23), 3973-3982. doi: 10.1002/asia.202000873
- Kempuraj, D., Thangavel, R., Natteru, P. A., Selvakumar, G. P., Saeed, D., Zahoor, H.,...Zaheer, A. (2016). Neuroinflammation induces neurodegeneration. *Journal of neurology, neurosurgery and* spine, 1(1).
- Khan, M. F., Iftikhar, A., Anwar, H., & Ramay, S. A. (2024). Brain tumor segmentation and classification using optimized deep learning. *Journal of Computing Biomedical Informatics*, 7(01), 632-640. doi: 10.56979
- Kim, D. K., & Rhee, W. J. (2021). Antioxidative effects of carrot-derived nanovesicles in cardiomyoblast and neuroblastoma cells. *Pharmaceutics*, *13*(8), 1203. doi: 10.3390/pharmaceutics13081203
- Kim, J., Zhu, Y., Chen, S., Wang, D., Zhang, S., Xia, J.,...Wang, J. (2023). Anti-glioma effect of ginseng-derived exosomes-like nanoparticles by active blood–brain-barrier penetration and tumor microenvironment modulation. *Journal of nanobiotechnology*, *21*(1), 253. doi: 10.1186/s12951-023-02006-x
- Kurian, T. K., Banik, S., Gopal, D., Chakrabarti, S., & Mazumder, N. (2021). Elucidating methods for isolation and quantification of exosomes: a review. *Molecular biotechnology*, 63, 249-266. doi: 10.1007/s12033-021-00300-3
- Lee, R. H., Lee, M. H., Wu, C. Y., e Silva, A. C., Possoit, H. E., Hsieh, T. H.,...Lin, H. W. (2018). Cerebral ischemia and neuroregeneration. *Neural regeneration research*, *13*(3), 373-385. doi: 10.4103/1673-5374.228711
- Lei, T., Yang, Z., Li, H., Qin, M., & Gao, H. (2024). Interactions between nanoparticles and pathological changes of vascular in Alzheimer's disease. Advanced Drug Delivery Reviews, 115219. doi: 10.1016/j.addr.2024.115219

- Li, P., Kaslan, M., Lee, S. H., Yao, J., & Gao, Z. (2017). Progress in exosome isolation techniques. *Theranostics*, 7(3), 789. doi: 10.7150/thno.18133
- Li, S., Zhang, R., Wang, A., Li, Y., Zhang, M., Kim, J., Zhu, Y.,...Wang, J. (2023). Panax notoginseng: derived exosome-like nanoparticles attenuate ischemia reperfusion injury via altering microglia polarization. *Journal of nanobiotechnology*, *21*(1), 416. doi: 10.1186/s12951-023-02161-1
- Lian, M. Q., Chng, W. H., Liang, J., Yeo, H. Q., Lee, C. K., Belaid, M.,...Pastorin, G. (2022). Plant-derived extracellular vesicles: Recent advancements and current challenges on their use for biomedical applications. *Journal of extracellular vesicles*, 11(12), 12283. doi: 10.1002/jev2.12283
- Luo, X., Zhang, X., Xu, A., Yang, Y., Xu, W., Cai, M.,... Li, K. (2025). Mechanistic Insights into the Anti-Glioma Effects of Exosome-Like Nanoparticles Derived from Garcinia Mangostana L.: A Metabolomics, Network Pharmacology, and Experimental Study. *International Journal of Nanomedicine*, 5407-5427. doi: 10.2147/IJN.S514930
- Liu, Y., Xiao, S., Wang, D., Qin, C., Wei, H., & Li, D. (2024). A review on separation and application of plant-derived exosome-like nanoparticles. *Journal of Separation Science*, 47(8), 2300669. doi: 10.1002/jssc.202300669
- Liu, H., Deng, Y., Li, J., Lin, W., Liu, C., Yang, X.,... Jiang, Y. (2025). Ginger-derived exosome-like nanoparticles: a representative of plant-based natural nanostructured drug delivery system. *Frontiers in Bioengineering and Biotechnology*, 13, 1569889. doi: 10.3389/fbioe.2025.1569889
- Ma, R., Xie, Q., Li, Y., Chen, Z., Ren, M., Chen, H.,... Wang, J. (2020). Animal models of cerebral ischemia: A review. *Biomedicine Pharmacotherapy*, 131, 110686. doi: 10.1016/j.biopha.2020.110686

- Midekessa, G., Godakumara, K., Ord, J., Viil, J., Lattekivi, F., Dissanayake, K.,...Fazeli, A. (2020). Zeta potential of extracellular vesicles: toward understanding the attributes that d etermine colloidal stability. ACS omega, *5*(*27*), 16701-16710. doi: 10.1021/acsomega.0c01582
- Morris, H. R., Spillantini, M. G., Sue, C. M., & Williams-Gray, C. H. (2024). The pathogenesis of Parkinson's disease. *The Lancet*, 403(10423), 293-304. doi: 10.1016/S0140-6736(23)01478-2
- Mu, N., Li, J., Zeng, L., You, J., Li, R., Qin, A.,...Zhou, Z. (2023). Plant-derived exosome-like nanovesicles: current progress and prospects. International Journal of Nanomedicine, 4987-5009. doi: 10.2147/IJN.S420748
- Mun, J. G., Song, D. H., Kee, J. Y., & Han, Y. (2025). Recent advances in the isolation strategies of plant-derived exosomes and their therapeutic applications. *Current Issues in Molecular Biology*, 47(3), 144. doi: 10.3390/cimb47030144
- Niu, X., Chen, J., & Gao, J. (2019). Nanocarriers as a powerful vehicle to overcome blood-brain barrier in treating neurodegenerative diseases: Focus on recent advances. *Asian journal of pharmaceutical sciences*, *14*(5), 480-496. doi: 10.1016/j. ajps.2018.09.005
- Omrani, M., Beyrampour-Basmenj, H., Jahanban-Esfahlan, R., Talebi, M., Raeisi, M., Serej, Z. A.,... Ebrahimi-Kalan, A. (2024). Global trend in exosome isolation and application: an update concept in management of diseases. *Molecular and Cellular Biochemistry*, 479(3), 679-691. doi: 10.1007/s11010-023-04756-6
- Sah, N. K., Arora, S., Sahu, R. C., Kumar, D., & Agrawal, A. K. (2025). Plant-based exosome-like extracellular vesicles as encapsulation vehicles for enhanced bioavailability and breast cancer therapy: recent advances and challenges. *Medical Oncology*, 42(6), 1-19. doi: 10.1007/s12032-025-02720-6

- Salarpour, S., Barani, M., Pardakhty, A., Khatami, M., & Chauhan, N. P. S. (2022). The application of exosomes and exosome-nanoparticle in treating brain disorders. *Journal of Molecular Liquids*, 350, 118549. doi: 10.1016/j.molliq.2022.118549
- Sarasati, A., Syahruddin, M. H., Nuryanti, A., Ana, I. D., Barlian, A., Wijaya, C. H.,...Takemori, H. (2023). Plant-derived exosome-like nanoparticles for biomedical applications and regenerative therapy. *Biomedicines*, *11*(*4*), 1053. doi: 10.3390/biomedicines11041053
- Sha, A., Luo, Y., Xiao, W., He, J., Chen, X., Xiong, Z.,...Li, Q. (2024). Plant-Derived Exosome-like Nanoparticles: A Comprehensive Overview of Their Composition, Biogenesis, Isolation, and Biological Applications. *International Journal of Molecular Sciences*, 25(22), 12092. doi: 10.3390/ijms252212092
- Sharma, H., Rachamalla, H. K., Mishra, N., Chandra, P., Pathak, R., & Ashique, S. (2024). Introduction to exosome and its role in brain disorders. *Exo*somes Based Drug Delivery Strategies for Brain Disorders, 1-35.
- Sharif, M., Tanvir, U., Munir, E. U., Khan, M. A., & Yasmin, M. (2024). Brain tumor segmentation and classification by improved binomial thresholding and multi-features selection. *Journal of ambient intelligence and humanized computing*, 1-20. doi: 10.1007/s12652-018-1075-x
- Shinge, S. A. U., Xiao, Y., Xia, J., Liang, Y., & Duan, L. (2022). New insights of engineering plant exosome-like nanovesicles as a nanoplatform for therapeutics and drug delivery. Extracellular Vesicles and Circulating Nucleic Acids, 3(2), 150. doi: 10.20517/evcna.2021.25
- Shirejini, S. Z., & Inci, F. (2022). The Yin and Yang of exosome isolation methods: conventional practice, microfluidics, and commercial kits. *Biotech*nology Advances, 54, 107814. doi: 10.1016/j.biotechadv.2021.107814

- Singh, B., Day, C. M., Abdella, S., & Garg, S. (2024). Alzheimer's disease current therapies, novel drug delivery systems and future directions for better disease management. *Journal of Controlled Release*, 367, 402-424. doi: 10.1016/j.jconrel.2024.01.047
- Sivanantham, A., & Jin, Y. (2022). Impact of storage conditions on EV integrity/surface markers and cargos. *Life*, 12(5), 697. doi: 10.3390/life12050697
- Sundaram, K., Mu, J., Kumar, A., Behera, J., Lei, C., Sriwastva, M. K.,...Zhang, H. G. (2022). Garlic exosome-like nanoparticles reverse high-fat diet induced obesity via the gut/brain axis. *Theranostics*, 12(3), 1220. doi: 10.7150/thno.65427.
- Suharta, S., Barlian, A., Hidajah, A. C., Notobroto, H. B., Ana, I. D., Indariani, S.,...Wijaya, C. H. (2021). Plant-derived exosome-like nanoparticles: A concise review on its extraction methods, content, bioactivities, and potential as functional food ingredient. *Journal of food science*, 86(7), 2838-2850. doi: 10.1111/1750-3841.15787
- Thakur, T., Albanese, E., Giannakopoulos, P., Jette, N., Linde, M., Prince, M. J.,...Medina-Mora, E. M. (2016). Neurological Disorders. *The International Bank for Reconstruction and Development / The World Bank*, 14, 6
- Trenkenschuh, E., Richter, M., Heinrich, E., Koch, M., Fuhrmann, G., & Friess, W. (2022). Enhancing the stabilization potential of lyophilization for extracellular vesicles. *Advanced healthcare materials*, *11*(5), 2100538. doi: 10.1002/adhm.202100538
- Wang, R., & Shih, L. C. (2023). Parkinson's disease–current treatment. *Current Opinion in Neurology*, 36(4), 302-308. doi: 10.1097/WCO.0000000000001166
- Wang, R., Zhang, Y., Guo, Y., Zeng, W., Li, J., Wu, J.,... Cao, P. (2023). Plant-derived nanovesicles: Promising therapeutics and drug delivery nanoplat-forms for brain disorders. *Fundamental Research*. *5*(2), 830-850. doi: 10.1016/j.fmre.2023.09.007

- Wang, Q., Yang, F., Duo, K., Liu, Y., Yu, J., Wu, Q., & Cai, Z. (2024). The role of necroptosis in cerebral ischemic stroke. *Molecular Neurobiology*, 61(7), 3882-3898. doi: 10.1007/s12035-023-03728-7
- Wood, M. J., O 'Loughlin, A. J., & Lakhal, S. (2011). Exosomes and the blood-brain barrier: implications for neurological diseases. *Therapeutic delivery*, *2*(9), 1095-1099. doi: 10.4155/tde.11.83
- Wu, W., Zhang, B., Wang, W., Bu, Q., Li, Y., Zhang, P., & Zeng, L. (2024). Plant-Derived Exosome-Like Nanovesicles in Chronic Wound Healing. *International Journal of Nanomedicine*, 11293-11303. doi: 10.2147/IJN.S485441
- Xu, Y., Yan, G., Zhao, J., Ren, Y., Xiao, Q., Tan, M., & Peng, L. (2024). Plant-derived exosomes as cell homogeneous nanoplatforms for brain biomacromolecules delivery ameliorate mitochondrial dysfunction against Parkinson's disease. *Nano Today*, 58, 102438. doi: 10.3390/ijms252212092
- Yakubovich, E. I., Polischouk, A. G., & Evtushenko, V. I. (2022). Principles and problems of exosome isolation from biological fluids. *Biochemistry (Moscow), Supplement Series A: Membrane and Cell Biology, 16(2),* 115-126. doi: 10.1134/ S1990747822030096
- Yoon, H. J., Won, J. P., Lee, H. G., & Seo, H. G. (2024). Green Onion-Derived Exosome-like Nanoparticles Prevent Ferroptotic Cell Death Triggered by Glutamate: Implication for GPX4 Expression. *Nutrients*, 16(19), 3257. doi: 10.3390/nu16193257
- Zhang, M., Jin, K., Gao, L., Zhang, Z., Li, F., Zhou, F., & Zhang, L. (2018). Methods and technologies for exosome isolation and characterization. *Small Methods*, 2(9), 1800021. doi: 10.1002/smtd.201800021. doi: 10.1016/j.ijbiomac.2025.140758.

- Zhang, Y., Zhang, X., Zhou, J., Li, Y., Kai, T., & Zhang, L. (2025). Lycium ruthenicum Murray exosome-like nanovesicles alleviated Alzheimer's disease–like symptoms induced by Aβ protein in transgenic Caenorhabditis elegans through the DAF-16 pathway. *International Journal of Biological Macromolecules*, 140758
- Zhang, Z., Yu, Y., Zhu, G., Zeng, L., Xu, S., Cheng, H., Ouyang, Z.,...Yu, L. (2022). The emerging role of plant-derived exosomes-like nanoparticles in immune regulation and periodontitis treatment. *Frontiers in immunology*, 13, 896745. doi: 10.3389/fimmu.2022.896745.
- Zhang, W., Liu, Y., Wang, Z., He, S., Liu, W., Wu, Y.,... Wang, Y. (2024). Remodeling brain pathological microenvironment to lessen cerebral ischemia injury by multifunctional injectable hydrogels. *Journal of Controlled Release*, 369, 591-603. doi: 10.1016/j.jconrel.2024.03.050

- Zhao, B., Lin, H., Jiang, X., Li, W., Gao, Y., Li, M.,... Gao, J. (2024). Exosome-like nanoparticles derived from fruits, vegetables, and herbs: Innovative strategies of therapeutic and drug delivery. *Theranostics*, 14(12), 4598. doi: 10.7150/thno.97096
- Zhao, Z., Wijerathne, H., Godwin, A. K., & Soper, S. A. (2021). Isolation and analysis methods of extracellular vesicles (EVs). Extracellular vesicles and circulating nucleic acids, 2, 80. doi: 10.20517/evcna.2021.07
- Zhuang, X., Teng, Y., Samykutty, A., Mu, J., Deng, Z., Zhang, L.,...Zhang, H. G. (2016). Grapefruit-derived nanovectors delivering therapeutic miR17 through an intranasal route inhibit brain tumor progression. *Molecular Therapy*, 24(1), 96-105. doi: 10.1038/mt.2015.188